KARST HYDROGEOLOGY OF

VALLES-SAN LUIS POTOSI REGION, MEXICO

KARST HYDROGEOLOGY AND GEOMORPHOLOGY OF THE SIERRA DE EL ABRA AND THE VALLES-SAN LUIS POTOSI REGION, MEXICO

BY

JOHNNIE EDWARD FISH, B.A., M.A.

A Thesis

Submitted to the School of Graduate Studies

in Partial Fulfillment of the Requirements

for the Degree

Doctor of Philosophy

McMaster University

1977

© JOHNNIE EDWARD FISH 1977

DOCTOR OF PHILOSOPHY (1977)
(Geology)

McMASTER UNIVERSITY
Hamilton, Ontario

TITLE: Karst Hydrogeology and Geomorphology of the Sierra de El Abra and the Valles-San Luis Potosí Region, México

AUTHOR: Johnnie Edward Fish, B.A. (Kansas State Teachers College, at Emporia)

M.A. (University of Texas in Austin)

SUPERVISOR: Professor Derek C. Ford

NUMBER OF PAGES: xvii, 469

ABSTRACT

The general objective of this work was to develop a basic understanding of the karst hydrology, the nature and origin of the caves, the water chemistry, the surface geomorphology, and relationships among these aspects for a high relief tropical karst region having a thick section of limestone. The Valles-San Luis Potosí region of northeástern México, and in particular, the Sierra de El Abra, was selected for the study. A Cretaceous Platform approximately 200 km wide and 300 km long (N-S) delimits the region of interest. A thick Lower Cretaceous deposit of gypsum and anydrite, and probably surrounded by Lower Cretaceous limestone facies, is overlain by more than 1000 m of the thick-bedded middle Cretaceous El Abra limestone, which has a thick platform-margin reef. The Sierra de El Abra is a greatly elongated range along the eastern margin of the Platform. During the late Cretaceous, the region was covered by thick deposits of impermeable rocks. During the early Tertiary, the area was folded, uplifted, and subjected to erosion. A high relief karst having a wide variety of geomorphic forms controlled by climate and structure has developed. Rainfall in the region varies from 250-2500 mm and is strongly concentrated in the months June-October, when very large rainfalls often occur.

A number of specific investigations were made to meet the general objective given above, with special emphasis on those that provide information concerning the nature of ground-water flow systems in the region. Most of the runoff from the region passes through the karstic subsurface.

Large portions of the region have no surface runoff whatsoever. The El Abra Formation is continuous over nearly the whole Platform, and it defines a region of very active ground-water circulation. Discharge from the aquifer occurs at a number of large and many small springs. Two of them, the Coy and the Frío springs group, are among the largest springs in the world with average discharges of approximately 24 m^3/sec and 28 m^3/sec respectively. Most of the dry season regional discharge is from a few large springs at low elevations along the eastern margin of the Platform. The flow systems give extremely dynamic responses to large precipitation events; floods at springs usually crest roughly one day after the causal rainfall and most springs have discharge variations (Q_{max}/Q_{min}) of 25-100 times. These facts indicate well-developed conduit flow systems.

The hydrochemical and hydrologic evidence in combination with the hydrogeologic setting demonstrate the existence of regional ground-water flow to several of the large eastern springs. Hydrochemical mixing-model calculations show that the amount of regional flow is at least 12 m^3/sec, that it has an approximately constant flux, and that the local flow systems provide the extremely variable component of spring discharge. The chemical and physical properties of the springs are explained in terms of local and regional flow systems.

Local studies carried out in the Sierra de El Abra show that large conduits have developed, and that large fluctuations of the water table occur. The large fossil caves in the range were part of great deep phreatic flow systems which circulated at least 300 m below ancient water tables and which discharged onto ancient coastal plains much higher than

the present one. The western margin swallet caves are of the floodwater type. The caves are structurally controlled.

Knowledge gained in this study should provide a basis for planning future research, and in particular for water resource development. The aquifer has great potential for water supply, but little of that potential is presently used.

ACKNOWLEDGEMENTS

A large number of persons and organizations have assisted this research. Their contributions are considered invaluable, and the author wishes to thank the following:

Prof. Derek C. Ford for acting as supervisor, and for his encouragement and patience;

Prof. G.V. Middleton and Prof. Brian McCann for their guidance and helpful criticisms as members of the thesis committee; and to Prof. James R. Kramer for discussion of the hydrochemistry;

Sandra Patrick, my wife, for the great amount of assistance she offered in the field, typing, drafting, editing, and discussing the thesis, and for her spiritual support;

Ing. Francisco Lavín Ortiz of the Tampico office of the Secretaría de Recursos Hidráulicos who provided a large amount of unpublished hydrologic and climatic data;

Ing. Diego A. Cordoba, director of the Instituto de Geología, who provided assistance in many ways, and Prof. Ernesto Lopez Ramos of the same organization for providing helpful geologic information;

The help and companionship in the field of many cavers, especially Don Broussard who was my field assistant, Steve Bittinger, Neal Morris who also has provided some maps, Craig Bittinger, Robert Hemperley, Logan McNatt, Skip and Kathy Roy, and William H. Russell;

Fellow graduate students Julian Coward, Peter Thompson, Melvin Gascoyne, Ralph Ewers, and John Drake for assistance, discussion of thesis and other matters of interest, and for friendship;

The foreman of Rancho Florida for granting access to the Choy spring;

Señor Gloria, owner of the Restaurant Condesa in Cd. Valles, for help with many matters;

Robert Bignell, who printed the photographs;

Martha Nixon, for typing the final manuscript.

TABLE OF CONTENTS

			Page
CHAPTER I		INTRODUCTION	1
CHAPTER II		GEOLOGY AND ENVIRONMENT OF THE FIELD AREA	10
2.1		Introduction and Location	10
2.2		Geologic History	13
2.3		Stratigraphy and Lithology	16
2.4		Structure and Physiography	32
2.5		The Environment	36
	2.5.1	Climate and Vegetation	36
	2.5.2	Culture	41
CHAPTER III		GEOMORPHIC FEATURES OF THE SURFACE	43
3.1		The Sierra de El Abra	43
	3.1.1	The East Face and the Coastal Plain	48
	3.1.2	The Crest of the Range	55
	3.1.3	The Western Flank and the Valles or Antiguo Morelos Valley	61
	3.1.4	Passes in the El Abra Range	69
	3.1.5	Origin of the Escarpment of the Sierra de El Abra	71
3.2		Karst Geomorphic Features in the Region	76
3.3		Summary	80
CHAPTER IV		HYDROLOGY AND HYDROGEOLOGY	83
4.1		Introduction	83
	4.1.1	Hydrogeology	83
	4.1.2	The Drainage Basins and Gauging Stations	88
	4.1.3	Distribution of Precipitation	92
	4.1.4	Springs	98
4.2		Temporal Aspects of the Hydrology	98
	4.2.1	Long Term Trends at El Choy Spring	98
	4.2.2	Seasonal Pattern	101
	4.2.3	Short Duration Events	105
	4.2.4	Flood Exceedance; Major Events	115
	4.2.5	Flow Duration	119
4.3		Spatial Distribution of Runoff; Basin Yield	121
	4.3.1	Low Flows	121
	4.3.2	Average Flows	127
	4.3.3	Basin Yield	134

4.4		Ground Water in the Sierra de El Abra	139
	4.4.1	Distribution of Ground Water; Storage	139
	4.4.2	Ground-Water Level Fluctuations	144
	4.4.3	Water Tracing	155
4.5		Summary	156
CHAPTER V		HYDROGEOCHEMISTRY	160
5.1		Introduction	160
5.2		Chemistry and Environment of the Karst Waters	164
5.3		Flood Pulse Behavior of the Springs	184
5.4		Summary	200
CHAPTER VI		THE CAVES	202
6.1		Introduction	202
6.2		Caves of the East Face of the Sierra de El Abra	205
	6.2.1	Cueva del Nacimiento del Río Choy	205
	6.2.2	Las Cuevas de Taninul Numeros 1 and 2	211
	6.2.3	Grutas de Quintero	216
	6.2.4	Cueva de las Cuates	222
	6.2.5	Cueva de la Ceiba	224
	6.2.6	Ventana Jabalí	226
	6.2.7	Other East Face Caves	234
6.3		Caves on the Crest of the Sierra de El Abra	235
	6.3.1	Sótano de la Escalera	235
	6.3.2	Cueva Pinta	235
	6.3.3	Sótano de la Cuesta	239
	6.3.4	Sótano de los Loros	241
	6.3.5	Cueva de Taninul Number 4	243
	6.3.6	La Cueva de Tanchipa	245
	6.3.7	La Hoya de Zimapán	248
	6.3.8	Sótano and Cueva de los Monos	254
	6.3.9	Other Caves on the Crest	259
6.4		Caves on the Western Flank and the Western Margin of the Sierra de El Abra	260
	6.4.1	Sótano de Soyate	261
	6.4.2	Cueva del Prieto	265
	6.4.3	Sótano de Japonés	268
	6.4.4	Sótano de Jos	273
	6.4.5	El Sistema de los Sabinos	277
	6.4.5.1	Cueva de los Sabinos	277
	6.4.5.2	El Sótano del Arroyo	282
	6.4.5.3	Sótano (Cueva) de la Tinaja	291
	6.4.5.4	The System	300
	6.4.6	Other Caves	303
6.5		Caves in Other Parts of the Region	306

	6.5.1	The Coy Caves and Spring	306
	6.5.2	Other Caves in the Region	309
CHAPTER VII		ANALYSIS AND SYNTHESIS	311
7.1		Hydrochemical Analysis	311
	7.1.1	Review of Hydrochemical Data and Interpretations	312
	7.1.2	The Geochemical Model	316
	7.1.3	Mixing Model Calculations	330
	7.1.4	Summary and Comparison of the Hydrochemistry with Other Regions	343
7.2		The Ground-Water Hydrology of the Region	359
	7.2.1	Geology and Hydrogeology	361
	7.2.2	Spatial Variation of Runoff	364
	7.2.3	Base Flow and Flood Flow	369
	7.2.4	The Ground-Water System	371
	7.2.5	Ground-Water Temperature	382
	7.2.6	Discussion	387
7.3		Hydrology of the Sierra de El Abra	393
	7.3.1	Water Budget and Distribution of Discharge of the Sierra de El Abra	393
	7.3.2	Analysis and Discussion of the Ground-Water Systems	398
7.4		Morphology and Origin of the Caves of the Sierra de El Abra	421
	7.4.1	Character and Origin of the East Face Caves	422
	7.4.2	Character and Origin of the Crest Caves	429
	7.4.3	Character and Origin of the Western Flank and Western Margin Caves	435
	7.4.4	Discussion	443
7.5		Summary and Conclusions	446
APPENDIX I		ANALYTICAL METHODS AND SAMPLING PROCEDURES	454
APPENDIX II		CAVE MAP SYMBOLS	456
BIBLIOGRAPHY			460

LIST OF FIGURES

		Page
1.1	Geography and physiography of the Valles-San Luis Potosí region	2
2.1	Middle Cretaceous reef trend around Gulf of Mexico and Valles-San Luis Potosí Platform	11
2.2	Geologic cross section of the Valles-San Luis Potosí Platform during the Cretaceous	21
2.3	Gross carbonate facies distribution on the Valles-S.L.P. Platform	23
2.4	Platform limits during the Cretaceous	29
2.5	Structural map of the Valles-S.L.P. Platform	33
3.1	Sierra de El Abra and surrounding area	44
3.2	Geomorphic and hydrologic map of southern Sierra de El Abra	47
3.3	Geomorphology of North El Abra Pass area	58
3.4	Map of Caldera, a large collapse sinkhole	63
4.1	Hydrogeologic map of Valles-S.L.P. Platform	84
4.2	Drainage basins and gauging stations of the region	89
4.3	Annual rainfall in the region	94
4.4	Annual flow of Choy spring compared with rainfall for 1960-1971	99
4.5	Monthly average, standard deviation, and coefficient of variation of discharge and precipitation at El Choy station for 1960-1971	102
4.6	Monthly average and coefficient of variation of discharge of Río Coy (Estacion Ballesmí) and Río Tampaón (Estacion El Pujal), for 1960-1971	104
4.7	Choy and Coy hydrographs and rainfall for Jan. 1, 1971-June 30, 1973	107
4.8	October 1966 flood events - Hurrican Inez	109
4.9	Hydrographs of Río Mante and Frío springs in 1951	111

Figure		Page
4.10	Río Santa Clara hydrograph, June-October for 1972, 1973	114
4.11	Magnitude of flooding of springs and rivers as shown by flood exceedance	117
4.12	Flow duration graph of Choy spring for 1960-1971	120
4.13	Soyate and Jos cave-lake hydrographs compared with rainfall and Choy discharge, July and August, 1971	146
4.14	Soyate cave-lake hydrograph and correlation with rainfall and Choy discharge, June, 1972	148
4.15	Flood events at Jos, Soyate, and Choy, September, 1971	150
4.16	Relationship between Soyate cave lake stage and Choy discharge	154
5.1	Hydrochemical environments in the Sierra de El Abra	161
5.2	Comparison of chemistry of water samples from various environments in the Sierra de El Abra	170
5.3	Ca/Mg against SO_4 for El Abra region karst water	174
5.4	Temperature regime of springs in the region	180
5.5	Trilinear plot of samples from 6 springs	182
5.6	Effect of flooding on chemistry of Choy spring, June-August, 1971	186
5.7	Effect of flooding on chemistry of Choy and Coy springs, May-June, 1972	189
5.8	Relationship between Mg and SO_4 for Choy, Coy, and Mante during flooding	191
5.9	Relationship between T (°C) and SO_4 for Choy, Coy, and Mante during flooding	191
5.10	Effect of flooding on degree of saturation with respect to calcite, dolomite, and gypsum at Choy and Coy, May-July, 1972	194
5.11	Effect of flooding on chemistry of Taninul Sulfur Pool, June-July, 1971	197
6.1	Map of Cueva del Nacimiento del Río Choy	206
6.2	Maps of Cuevas de Taninul No. 1 and 2 and the Taninul springs	212
6.3	Profile of Cuevas de Taninul No. 1 and 2	213

Figure		Page
6.4	Map of Grutas de Quintero	218
6.5	Map of Cueva de las Cuates	223
6.6	Map of Cueva de la Ceiba	225
6.7	Map of Ventana Jabalí	229
6.8	Profile of Ventana Jabalí	230
6.9	Map of Sótano de Escalera	236
6.10	Map of Cueva Pinta	237
6.11	Map of Sótano de la Cuesta (provided by Neal Morris)	240
6.12	Map of Sótano de los Loros (provided by Neal Morris)	242
6.13	Map of Cueva de Taninul No. 4	244
6.14	Map of Cueva de Tanchipa (provided by Neal Morris)	246
6.15	Map of La Hoya de Zimapán (provided by Neal Morris)	250
6.16	Map of La Cueva and Sótano de los Monos	255
6.17	Map of Sótano de Soyate	262
6.18	Map of Cueva del Prieto	267
6.19	Map of Sótano de Japonés	269
6.20	Map of Sótano de Jos	275
6.21	Map of El Sistema de los Sabinos	278
6.22	Map of Cueva de los Sabinos	279
6.23	Map of Sótano de Arroyo	285
6.24	Map of Sótano de la Tinaja	293
6.25	Profile of part of Sótano de la Tinaja	294
6.26	Maps of Las Cuevas y El Nacimiento del Río Coy	308
7.1	Plot of Mg against SO_4 for best base flow analysis of 13 springs	314
7.2	Two-source mixing model for the Choy and Coy springs	315
7.3	The hydrochemical model	318
7.4	Evolutionary calcite solution diagram, HCO_3 against pH	321
7.5	Ca against SO_4, and Ca + Mg against SO_4 for springs and the theoretical models of type B ground water	328

Figure		Page
7.6	Mixing curves of type A with type B ground water	328
7.7	Plot of Ca^{++} against T (°C) for various geographical regions from Harmon et al. (1973), with a new Mexico point from this study	354
7.8	Calcite saturation index (SI_c) versus negative logarithm of partial pressure of carbon dioxide (pP_{CO_2}) for region springs	375
7.9	Regional E-W hydrogeologic cross section showing hypothesized local and regional ground-water flow systems	362
7.10	Map summarizing spatial distribution of runoff in the region, possible directions of ground-water flow, base flow chemistry, discharge and elevation of the major springs	365
7.11	Hypothesized regional dry season potentiometric surface	375
7.12	N-S cross section of front ranges of Sierra Madre Oriental	376
7.13	Comparison of elevation of cave lakes and deepest point known in caves with radial distance to and elevation of El Choy rise pool	401
7.14	Hypothesized N-S dry season ground-water profile in the Sierra de El Abra	408
7.15	Hydrographs in February, 1957, of Frío springs, Mante, and Río Guayalejo showing an unusual, isolated dry season flood	412
7.16	Comparison of Mante, Santa Clara, and Río Comandante hydrographs and precipitation for July-August, 1972	415
7.17	E-W cross sections showing relationships of geology, hydrology, topography, and caves in the Sierra de El Abra	425
7.18	Models of the east face caves	426

LIST OF TABLES

Table		Page
1.1	Translation of Spanish Words	9
2.1	Correlation of Stratigraphic Units	17
2.2	Mean Monthly and Annual Air Temperatures (°C)	38
2.3	Daily Maximum and Minimum Temperatures at Estación Santa Rosa (Cd. Valles)	39
3.1	Drainage Area of the Swallet Caves	68
4.1	Gauging Stations in the Valles-S.L.P. Region	90-91
4.2	Selected Climatology Stations in the Region	93
4.3	Longer Term Rainfall Compared with Base Period Averages	96
4.4	Monthly Distribution of Gulf Coastal Zone Hurricanes, 1921-61	105
4.5	1951 Rainfall (mm)	112
4.6	Low Flows and Low Flow Budget	122
4.7	Special Gaugings	125
4.8	Indirect Calculations of Flow of Smaller Frío Springs	125
4.9	Runoff from Basins, 1961-1968	128
4.10	Annual Regional Runoff	131
4.11	Runoff of Full Record Compared with 1961-1968 Average	133
4.12	Unitary Discharges of Various Basins	138
5.1	Chemical Analyses and Derived Geochemical Measures	
	a - Best Analyses	165
	b - Other Analyses	166-68
5.2	Analyses for Na, K, and Cl	169
5.3	CO_2 of Soil and Cave Air	176

Table		Page
7.1	Equilibrium Constant Functions	322
7.2	Possible Theoretical Compositions of Type B Ground Water	325-6
7.3	Mixing Model Calculations for the Choy and Coy Springs	334
7.4	Dry Season Regional Flow (Q_B)	339
7.5	Flood Dilution Mixing Model Calculations	341
7.6	Equilibrium Model with Greater K_d	349
7.7	Some Published Data for Comparison with the Geochemical Model	351
7.8	Ratio of Minimum to Average Flows for Basins	370
7.9	Data Used to Construct the Potentiometric Map	374
7.10	Calculated Temperatures for Type B (Regional) Water	386
7.11	Drainage Area of the Sierra de El Abra "Basin"	396
7.12	Cave Survey Data and Elevations for Water-Level Profile	403
7.13	Base-Level Points of the Sierra de El Abra	409

LIST OF PLATES

Plate		Page
2.1 a,b	Two views of the thick-bedded El Abra limestone	26
3.1	Aerial view of the Gulf coastal plain and Sierra de El Abra	45
3.2	Flat-Topped hills: remnants of an older coastal plain surface	49
3.3	Typical relief on the coastal plain near the El Abra range	49
3.4	The eastern escarpment of the El Abra range in the high central zone	51
3.5	The Mante spring	51
3.6	Fracture-controlled recesses in the east face	54
3.7	The surface of the crest of the El Abra range	54
3.8	The Caldera, a giant collapse doline on the crest of the El Abra	62
3.9	Stream capture along the western margin of the range	66
3.10	The spectacular Xilitla-Aquismón area karst	78
6.1	The Choy spring at base flow	208
6.2	The Choy in moderate flood	208
6.3	View from inside Choy cave looking out the lower or Resurgence Entrance	209
6.4	El Choy ceiling showing phreatic pocketing and domes	210
6.5	The Entrance Passage of Grutas de Quintero	219
6.6	The Main Passage of Quintero	219
6.7	View out of the entrance of Ventana Jabalí	227
6.8	The immense chamber of Ventana Jabalí	231
6.9	The high dome and bedrock natural bridge in Ventana Jabalí	232
6.10	The rear portion of Ventana Jabalí	233
6.11	A 5 m sediment section exposed in a test pit near the entrance of Ventana Jabalí	233

Plate		Page
6.12	The entrance to Cueva Pinta	238
6.13	View toward the entrance in Cueva Pinta from near the test pit in sediments	238
6.14	Phreatic fissure in Tanchipa	247
6.15	The entrance to La Hoya de Zimapán	247
6.16	The nearly circular entrance passage of Zimapán	249
6.17	The stalagmite barrier across the end of the entrance passage in Zimapán	249
6.18	The Zimapán Room	252
6.19	Large stalagmites in Zimapán that have undergone "phreatic" re-solution	253
6.20	Partially redissolved stalagmite and solution features in the Zimapán Room	253
6.21	A pocket dissolved by a "phreatic" re-solution phase in Zimapán	256
6.22	Entrance to Cueva de los Sabinos	280
6.23	The entrance pit of Sótano del Arroyo	283
6.24	View out Main Passage of Sótano del Arroyo into the entrance sink	284
6.25	Main Passage in Sótano del Arroyo	287
6.26	A log in Main Passage in Arroyo	287
6.27	Entrance to Sótano de la Tinaja	292
6.28	Entrance Passage in Tinaja just above Cabble Ladder Drop	292
6.29	Part of the Sandy Floored Passage in Tinaja	297
6.30	An old fill in the Sandy Floored Passage	297
6.31	The slot-like entrance to Sótano de Yerbaniz	305

CHAPTER I

INTRODUCTION

There has been exploration and utilization of caves and springs for at least several millennia. A classic example is the use of cenotes in Yucatan by the Mayas (John Lloyd Stephens, 1842; Back and Hanshaw, 1974). There were occasional astute observations, but more commonly there were myths or expressions of curiosity concerning these features as well as the exotic karst landforms in some regions. The scientific study of karst did not begin in earnest until about one century ago (Roglić, 1972). Some of the work was prompted by water-supply or engineering activities such as railroad building. Other studies of a broader nature were made by physical geographers and geologists, essentially concurrent with the growth of geomorphology as a science.

As a result of the past century of exploration and study, the karsts of Europe and the United States have become famous even among the general public. Many conflicting theories of origin or process have been given, and there has been much debate about the relative importance of various factors such as climate and rock structure in the development of karst features, and about the nature of karst ground-water circulation. It appears that the study of karst requires the integration of knowledge and techniques from as many "separate" disciplines as any subject in geology (to place it in a category). For example, hydrology, aqueous and isotope geochemistry, geomorphology, climatology, petrology and sedi-

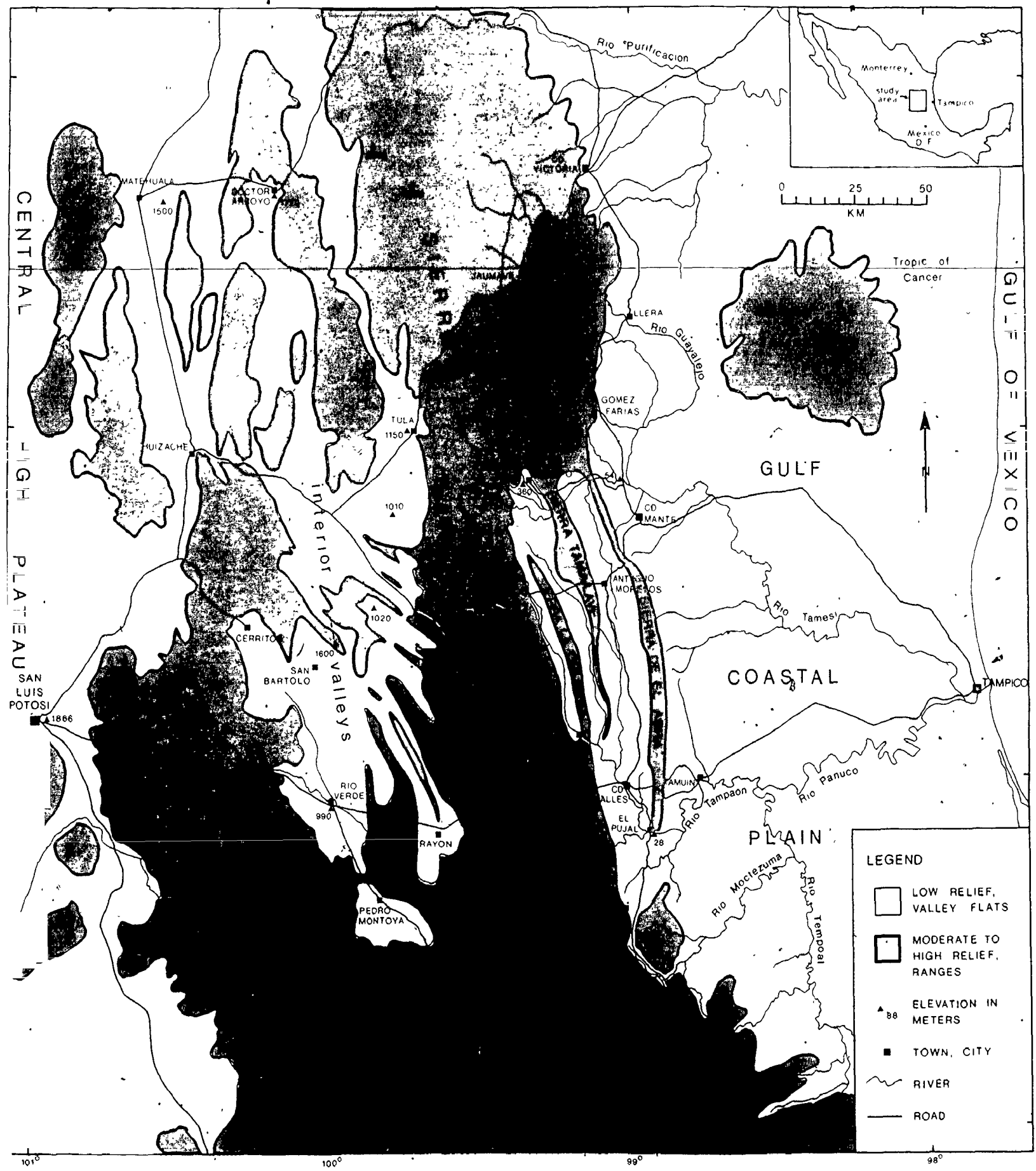

Figure 11 Geography and physiography of the Valles - San Luis Potosí region

mentary processes, structural geology, and fluid mechanics all have an important bearing on karst studies. Modern work has a very strong emphasis on karst hydrology and related fields, not merely for academic enlightenment, but for development of water resources and control of environmental problems such as pollution of carbonate aquifers. The great preponderance of research has been conducted in the middle latitudes, although carbonate rocks form a significant portion of the sedimentary rock column in most parts of the world. Although there have been many significant contributions, work in tropical karsts has been limited; most of it has been largely descriptive and much of it has dealt primarily with surface landforms. It was a general goal of this dissertation research to study in as great a depth as possible one tropical karst area, emphasizing the hydrogeology and hydrology, the development of caves, and the relationship of the surface geomorphology to the first three subjects.

It was especially desirable that such studies be undertaken in an area having a thick, well karstified carbonate-rock section and high relief, because so much of the work done in the United States has been conducted where the relief is low to moderate and the section of carbonate rocks seldom exceeds 200 m. Personal familiarity with many karst areas in México indicated that they were of scientific and practical importance. Excepting the Yucatan Peninsula, most of the rest of the Mexican karst lies in extremely rugged mountainous terrain posing severe logistic problems, and is thus poorly known. The area selected, the Sierra de El Abra in northeastern México (Figure 1.1), offered caves in a variety of geologic and geomorphic settings (although not many were actually surveyed when the

research was begun), some very large springs and many smaller ones, relatively high relief, a thick carbonate rock section extending below base level, a long erosional history so that the paleohydrology could be examined, and perhaps the most reasonable access (although still difficult) of any of the Mexican karst areas. Some geologic information was available because the karstic limestone that outcrops there is a prolific oil producer where buried in other parts of México. Also, there were extensive runoff and climatic data published for the much larger surrounding region, although there was little information concerning individual springs. Aside from some early work on cave fauna in the region, F. Bonet (1953a) conducted the first speleologic and karst morphologic investigations in the Sierra de El Abra, where he examined part or all of 15-20 horizontal caves, and in the nearby Xilitla karst area (1953b). In the 1960's, the Association for Mexican Cave Studies (based in Austin, Texas) began exploring and surveying caves in México; it has published two bulletins (Russell and Raines, 1967; and Raines, ed., 1968) which briefly describe a number of caves in the El Abra range and in other parts of the Sierra Madre Oriental in northeastern México. A recently published study of blind fish caves in the El Abra (Mitchell, Russell, and Elliott, 1977) utilizes a large amount of their independent work plus information from this research and other members of the Association for Mexican Cave Studies. The observations and ideas contained in these reports as well as some comparisons with other areas will be referred to in appropriate discussions in later chapters.

Initially, it was planned to confine the study to the Sierra de El Abra, with only a minor discussion of the regional hydrology and geomorphology. However, it became clear from the first results of the water

chemistry, from observations of the hydrology, and from analysis of the geologic relationships that a much broader regional treatment was both desirable and in fact necessary to solve many of the fundamental problems of the El Abra. Based on the geology and the hydrology, it was ultimately judged that the area of interest was a paleocarbonate platform measuring about 200 x 300 kms (Carrillo Bravo, 1971) that extends from Tamuín to San Luis Potosí and from Jalpan as far north as Cd. Victoria (Figure 1.1). This region includes parts of the states of San Luis Potosí, Tamaulipas, Querétaro, Guanajuato, Hidalgo, and Nuevo León. It was decided that the research would comprise two levels of study: the Sierra de El Abra would be studied extensively in the field to develop a detailed understanding of its hydrology, cave development, geomorphology, and water chemistry; and the regional hydrology and hydrogeology would be analyzed from gauging station data, the published geologic literature, and from reconnaissance hydrologic and geomorphic observations and water sampling. Specifically, the thesis objectives are:

1) for the region
   a) to determine the hydrogeologic units, and the regional hydrogeologic framework including geomorphic relationships;
   b) to analyse quantitatively the hydrology including regional and local runoff, magnitude and importance of karst springs to the total runoff, flow behavior (temporal variations) especially of the springs, and character of the regional ground-water body;
   c) to conduct a hydrochemical survey of springs for flow system analysis and comparison with other regions;

2) for the Sierra de El Abra

a) to study in detail the contemporary hydrology including the water budget, ground-water levels, calculation of hydraulic gradients, distribution of ground water, and dynamics of the aquifer;

b) to make detailed surveys, descriptions, and morphologic analyses of caves in all geomorphic positions across the range, to analyse the role of caves in the contemporary or paleohydrology, and to place the caves in the general theory of cavern genesis and karst ground-water circulation;

c) to describe the geomorphic features and their relationship to the caves and the hydrology;

d) to establish the place of the Sierra de El Abra in the region.

To attain the above goals, support was obtained from agencies of the Mexican government. The Instituto de Geología (geological survey) directed by Ing. Diego A. Córdoba provided geologic maps and reports, air photos of the El Abra range, a pickup truck for some of the more rugged field work, and other assistances as well. The Sectretaría de Recursos Hidráulicos provided two bulletins of published hydrologic and climatologic data for the Panuco basin which includes all of the region of interest, and their Tampico office directed by Ing. Francisco Lavín Ortiz made available a large quantity of unpublished discharge and rainfall data. A major hindrance to this and other geologic field studies was the lack of good topographic maps. The old 1:100,000 maps have only a 50 m contour

interval, cover only part of the region, and are often grossly in error. Presently, the Mexican government is producing a good quality new series at 1:50,000 having a contour interval of 10 or 20 m; unfortunately, they were begun after fhe field work for this project was completed. Most of the Sierra de El Abra is not yet available, but about 80% of the region of interest is now covered. Air photos were used for study of surface features, for guidance in the field, and for preparation of some maps. The majority of the field work was accomplished during the 1971 and 1972 summer field seasons; three other trips were made, including one during December 1971-January 1972 to obtain some early dry season data, and conduct some cave surveys when there was less danger of flooding. On each trip, a base of operations was established in Ciudad Valles to protect the voluminous equipment, set up a laboratory, and provide refuge.

The results of this study are reported in the following pages. Each chapter from II through VI will concern a separate subject area, presenting considerable information and analysis. Chapter II gives the geologic background and some aspects of the environment. Chapter III focuses on the geomorphic features of the El Abra range and surrounding area, and briefly describes karst development in other parts of the region. Chapter IV establishes the regional hydrogeologic framework; provides a quantitative treatment of spatial and temporal characteristics of the regional hydrology, emphasizing karst springs; and discusses some aspects of ground water in the Sierra de El Abra. In Chapter V, the chemistry of various karst waters is examined, and variations in concentrations that occur in some springs during flood pulses are described. Chapter VI gives maps, descrip-

tions, and morphologic interpretations of the caves as individual entities. In Chapter VII, data and interpretations from previous chapters are summarized, further analyzed, and synthesized into models and speculative discussions of the karst ground-water systems and the caves. Also given are a summary and conclusions.

Mexican geographic names are generally used in this thesis; Table 1.1 provides a translation.

TABLE 1.1

Translation of Spanish Words

cañon	canyon
ciudad	city, town
cueva	cave, usually with a horizontal or sloping entrance
estación	station, such as Estación Ballesmí (gauging station)
gruta	cavern
manantial	spring, fountain
municipio	municipality, township
nacimiento	spring, source (of river)
pozo	well
presa	dam
río	river
sierra	mountain range
sótano	pit

CHAPTER II

GEOLOGY AND ENVIRONMENT OF THE FIELD AREA

2.1 Introduction and Location

The purpose of this chapter is to provide the geological framework for the data and interpretations of subsequent chapters. This section will locate and identify the region of interest. It will be followed by a brief geologic history, stratigraphic and lithologic descriptions, the regional structure and physiography, and some environmental considerations. The stratigraphy section is lengthy because important recent knowledge is not covered in the English literature. A general location map of the region is given as Figure 1.1, and a more detailed map of the Sierra de El Abra and environs is given in Chapter III as Figure 3.1.

The area considered is the Valles-San Luis Potosí Platform (Carrillo Bravo, 1971; Figure 2.1), and in particular the Sierra de El Abra which lies along its eastern margin. It is part of a great Cretaceous carbonate complex that nearly encircles the Gulf of Mexico. In México along the west-central portion of the complex, there has been extensive uplift, deformation and erosion that has led to the development of high relief karsts which contrast with the low relief karst plains of the Yucatan and Florida peninsulas (Fish, 1977). Certain aspects of the field area, particularly the hydrology and water chemistry cannot be fully understood except in the broader context of the whole Platform. Thus, some parts of this study will deal with a large portion of the Platform, while the remainder will focus on

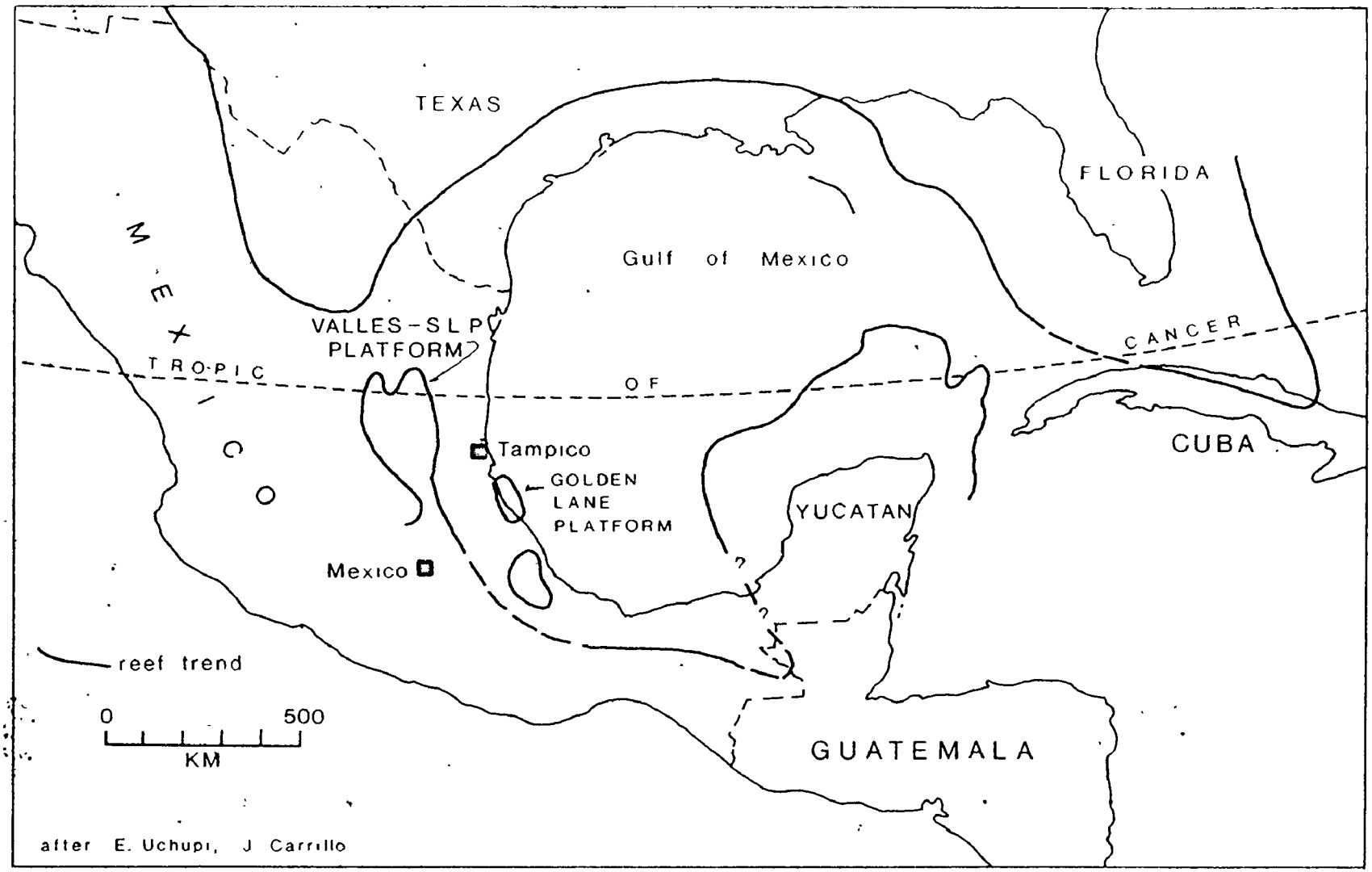

Figure 2.1 Middle Cretaceous reef trend around Gulf of Mexico and Valles-San Luis Potosí Platform.

the Sierra de El Abra.

Several studies in recent years especially by Pemex geologists have considerably clarified the picture of the Cretaceous system in northeastern México, although much remains to be done. Enos (1974) has provided a good general description of the carbonate complex. He distinguishes three major facies and paleoenvironments: 1) fine-grained cherty basinal limestones, 2) platform limestones and dolomites (El Abra Formation in the middle Cretaceous) and 3) basin margin carbonate debris surrounding platforms. The three principal platforms in the region were the large Valles-San Luis Potosí Platform, the Golden Lane Platform south of Tampico (which has been Mexico's most prolific oil producer), and the El Doctor Platform, south of the Valles-S.L.P. Platform (it should be remembered that these were paleoplatforms and the names are used to denote the area of interest, even though tectonism has since altered their character). Enos (1974, pp. 801-802) succinctly summarizes the character of the margins as follows:

> Several lines of evidence indicate that the middle Cretaceous platforms were bounded by steep edges, probably as the result of rapid vertical accretion of the platform-margin facies (reefs). Seismic reflection profiles (Rockwell and Garcia Rojas, 1953) and structural contour maps (Guzman, 1967, Fig. 7; Viniegra and Castillo-Tejero, 1970, Fig. 5) of the Golden Lane platform indicate relief of about 1000 m at the platform edge by the close of the middle Cretaceous. The east edges of the El Doctor platform and of the Valles platform north of Valles form prominent escarpments which appear to reflect depositional topography, although the relations in both are complicated by faulting. Well records (Viniegra and Castillo-Tejero, 1970, Figs. 6,7) and isopach maps (courtesy of Petróles Mexicanos) of the middle Cretaceous rocks along the west side of the Golden Lane platform show that the platform facies is about 1000 m thicker than the basinal facies. Finally, the sedimentary facies show abrupt changes at the platform edges and indicate very little lateral migration with time.

The great difference in thickness, the structure contour map and the change of facies are critical evidence that the basin margin carbonates (Tamabra Limestone of the Poza Rica trend near the Golden Lane) are forereef and turbidite deposits rather than down-faulted or down-folded true reef rocks (Coogan et al., 1972, advocate that they are the "true reef" rocks of the El Abra complex).

The Sierra de El Abra is the classic area for studying the middle Cretaceous reef trends in outcrop and several reports have been written about it as well as about the other "front ranges" of the Sierra Madre Oriental. However, there was little information concerning the central and western portions of the Platform until the regional synthesis of studies by Pemex and others was published by Carrillo Bravo (1971). Indeed, this was the report that first identified the Platform, and the geologic information that follows relies heavily on it.

2.2 Geologic History

The geologic history of the region, largely adapted from Carrillo Bravo (1971), is summarized as follows:

1) During the late Precambrian, a regional diastrophism produced the majority of the metamorphic rocks found in the subsurface.

2) In the early Paleozoic, an intercontinental geosyncline began to form in the region of the Mexican high plains (or plateaus) and the Sierra Madre Oriental (Figure 1.1). Considerable subsidence occurred during the Carboniferous and the Permian and a large volume of orogenic-type terrigenous rocks was deposited. In the closing stages of the

Paleozoic or the beginning of the Triassic the region emerged and was strongly folded.

3) All of the region remained emergent in the Triassic and through the middle Jurassic. Erosion was great in some places and thick continental red beds were deposited in others. Along the western and southern margins, marine basins developed. At the end of the early Jurassic, vertical movements and faulting occurred.

4) A regional marine transgression began in the late Jurassic. Large areas remained emergent; other areas may have received a thin section of sediments. To the west, the Mesozoic Basin of central México was formed. The "Platform" was a stable unit during the Triassic and Jurrassic, receiving almost exclusively continental red bed deposits, whereas numerous basins had formed on the margins. By the close of the Jurassic, the inundation was nearly complete, setting the stage for the Cretaceous.

5) The Cretaceous was the time of development of the great carbonate platforms in the Gulf region, continuing to the present on the Yucatan Platform. On the Valles-S.L.P. Platform, it began with a thin section of clay, sand, and calcareous sediments in the early Neocomian. From the geology, it is inferred (but not adequately confirmed as yet by drilling) that large reef growths developed on the margins of the Platform from the middle Neocomian through the Aptian. Within the Platform (lagoon?) a thick evaporitic sequence, principally of sulfate rocks, was deposited. A slight influx of argillaceous sediment deposited in the deeper water surrounding the Platform marks the

beginning of more rapid subsidence at the close of the Aptian.

6) During the Albian-Cenomanian (middle Cretaceous) maximum reef-platform development and platform-margin relief occurred. This gave rise to the Sierra de El Abra reef, the Cerro Ladron bank, the Jacala bank and other reefs. In the central zone, a thick section of backreef or platform carbonates was deposited.

7) In the Turonian, most of the Platform was emergent. A transgression began on the margins, depositing pelagic limestones and calcareous shales in the east and north; and clay, sand and calcareous sediments in the south and west. Platform carbonate deposition occurred in the central region during the Senonian-Maestrichtian, while progressively siltier and shalier limestone and finally a thick section of calcareous shales were deposited on the margins. Transgressive and regressive movements near the end of the Cretaceous covered the central and western portions of the Platform with a thick section of clay and sand, and signaled a new period of instability.

8) At the beginning of the Tertiary, the sea withdrew permanently and the area became affected by the Laramide Orogeny. Carbonate deposition ceased entirely and early Tertiary terrigenous deposits in the paleo Gulf of Mexico (east of the Platform) record the accelerating diastrophism in the Sierra Madre Oriental. Some granite bodies were emplaced. The Tertiary and Quaternary were times of uplift, erosion and some terrestrial deposition. Extensive rhyolitic outpourings occurred in the southwestern portion of the region during the middle Tertiary. There are some remnants of Pliocene-Pleistocene basalt

flows in valleys of the central and eastern portion of the Platform and basalt-capped mesas on the coastal plain to the northeast.

2.3 Stratigraphy and Lithology

This section describes the stratigraphy and lithology of the sedimentary rocks that occur in the region, and briefly indicates the minor occurrences of igneous rocks. The age and correlation of the sedimentary units may be seen in Table 2.1.

Sedimentary Rocks

Triassic

Huizachal (La Boca) Formation

The Huizachal Formation (redbeds) in the Huizachal-Peregrina anticline consists of a sequence, locally more than 2000 m thick, of red, gray and green shale, sandstone and conglomerate. The formation contains Upper Triassic and Lower Jurassic flora, including silicified tree trunks. It is also exposed in the Miquihuana arch and has been reached by wells on the Platform.

Jurassic

La Joya Formation

The La Joya Formation west of Cd. Victoria generally consists of less than 65 m of red beds made up of a poorly sorted basal conglomerate, overlain by thin limestones, mudstones and sandstones of about middle

TABLE 2.1

Correlation of Stratigraphic Units*

SYSTEM	Series		European Stage	Western to central portion of Valles-S.L.P Platform Formation	Eastern Platform margin and Tamalihuale No. 1 Well Formation	Western margin ancient Gulf of Mexico Formation	Agua Nueva No. 1 Well Formation	Northern Platform and Cd. Victoria area Formation
QUATERNARY	RECENT			Alluvium			Alluvium	
	PLEISTOCENE			La Borreguita / Santo Domingo ?			Santo Domingo	
TERTIARY	PLIOCENE							
	MIOCENE							
	OLIGOCENE							
	EOCENE					Chicontepec Group		Chicontepec-Velasco
	PALEOCENE							
CRETACEOUS	UPPER	GULFIAN	MAESTRICHTIAN	Cárdenas	Méndez	Méndez		Méndez
			SENONIAN	Tamasopo	San Felipe	San Felipe		San Felipe
			TURONIAN	Soyatal ?	Agua Nueva	Agua Nueva		Agua Nueva
	MIDDLE		CENOMANIAN	El Abra (reef to backreef)	El Abra (reef and backreef)	El Abra (fore-reef) / Cuesta del Cura	El Abra (backreef)	El Abra / Cuesta del Cura
		COMANCHEAN	ALBIAN					
	LOWER	COAHUILA	APTIAN	reef limestone / Guaxcamá	?	Upper Tamaulipas / Otates	Guaxcamá	Upper Tamaulipas / Otates
			NEOCOMIAN		Lower Tamaulipas	Lower Tamaulipas	**	Lower Tamaulipas
JURASSIC	UPPER	SABINIAN	TITHONIAN		Pimienta (?)	Pimienta	La Casita	La Casita
			KIMMERIDGIAN		Taman (mixed)	Tamán		Olvido
			OXFORDIAN					Zuloaga
			CALLOVIAN			Tepexic		La Joya
	MIDDLE		BATHONIAN			Cahuasas		
			BAJOCIAN					
	LOWER		TOARCIAN			Huayacocotla		
			PLIENSBACHIAN					
			SINEMURIAN					
			HETTANGIAN					
TRIASSIC	UPPER					Huizachal	Huizachal (?)	Huizachal
	MIDDLE							
	LOWER							

no outcrop not deposited **"Platform limestone without formal nomenclature"

*after Carrillo Bravo (1971) and D.R. Boyd et al. (1963)

Jurassic age (Mixon, 1963).

Olvido Formation

The Olvido Formation in northern San Luis Potosí, Tamaulipas, Nueve León, and Coahuila is a late Jurassic sequence of approximately 150 m of anhydrite, gypsum, limestone and shale (Carrillo Bravo, 1963).

Tamán Formation (Mixed Facies)

The Mixed Facies of the Tamán Formation is found in wells along the east margin of the Platform and designates the interdigitation of basin and platform rocks. This late Jurassic unit has a basal conglomerate of quartz fragments and clay overlain by up to 200 m of fine-grained microcrystalline limestone with frequent layers of oolitic limestone and calcarenite. Some dolerite intrusions were encountered in the Tamalihuale No. 1 well (locations of wells are shown in Figures 2.2 and 2.3).

Pimienta Formation

Twenty-eight meters of this dark compact argillaceous limestone was found in Tamalihuale No. 1, concordantly above the Tamán and below the Lower Tamaulipas (Carrillo Bravo, 1971). This late Jurassic formation crops out south of Tamazunchale as a black cherty limestone and shale.

La Casita Formation

The La Casita Formation is a series of shale, siltstone, sandstone,

conglomerate and limestone of late Jurassic age that forms a thin transgressive unit over the Platform.

Cretaceous

Lower Tamaulipas Formation

The Lower Cretaceous Lower Tamaulipas Formation refers to a dense dark, stylolitic cherty lime mudstone considered to have formed as an open-sea basin deposit in the Tampico Embayment (that part of the ancient Gulf of Mexico east of the Valles-S.L.P. Platform). About 30 m has been found in wells in the El Abra region, where it is coarser grained, includes some quartz grains, and is partially dolomitized. Outcrops are known on the western and northern margins of the Platform.

"Platform Limestone without Formal Nomenclature"

This unnamed Lower Cretaceous unit consists of 300 m of platform calcareous sediments in medium to thick beds that crop out in the axial portion of the Valle de Guadalupe anticline. A thinner section of somewhat similar rocks, with bentonites, and of the same age was penetrated by the Agua Nueva No. 1 well (Carrillo Bravo, 1971).

Guaxcamá Formation

A thick Lower Cretaceous sequence of evaporites, mostly anhydrite and gypsum, but with a substantial content of limestone and fractured dolomite beds, composes the Guaxcamá Formation. Some red terrigenous sediments and silicified conglomerate have been found, but no salt has been

recorded. The Guaxcamá crops out in an area approximately 35 by 10 km in the central portion of the Santa Domingo and Guaxcamá anticlines near the western margin of the Platform. It appears to concordantly underlie the El Abra Formation over much of the interior of the Platform, but its true thickness is difficult to determine because of plastic deformation. In the Agua Nueva No. 1 well, 1987 m was penetrated, and 3009 m (not including 500 m eroded from the top) was cut by the Guaxcamá No. 1 (Carrillo Bravo, 1971). These sections are probably exaggerated by folding. The geology of the Platform and small sections of backreef and reef facies cut in the Guaxcamá No. 1 suggest that a massive Lower Cretaceous reef developed as shown in Figure 2.2, forming a shallow lagoon for evaporite deposition. The exact structure, distribution, and thickness of the Lower Cretaceous reef trend is not yet known. Anhydrite with similar stratigraphic relationships has been found in wells in the central portion of the middle Cretaceous Golden Lane Platform (Boyd, 1963; see especially his Figure 2). The distribution of the evaporite facies is not well known on either platform.

El Abra Formation

Investigation of the middle and Upper Cretaceous limestone of northeastern Mexico has had a stormy history concerning almost every possible aspect, including nomenclature. The terminology given here is that of Carrillo Bravo (1971) in his recent regional synthesis. The name El Abra Formation is applied to the calcareous complex principally of Albian-Cenomanian age that is found over the Valles-S.L.P. and Golden Lane Platforms.

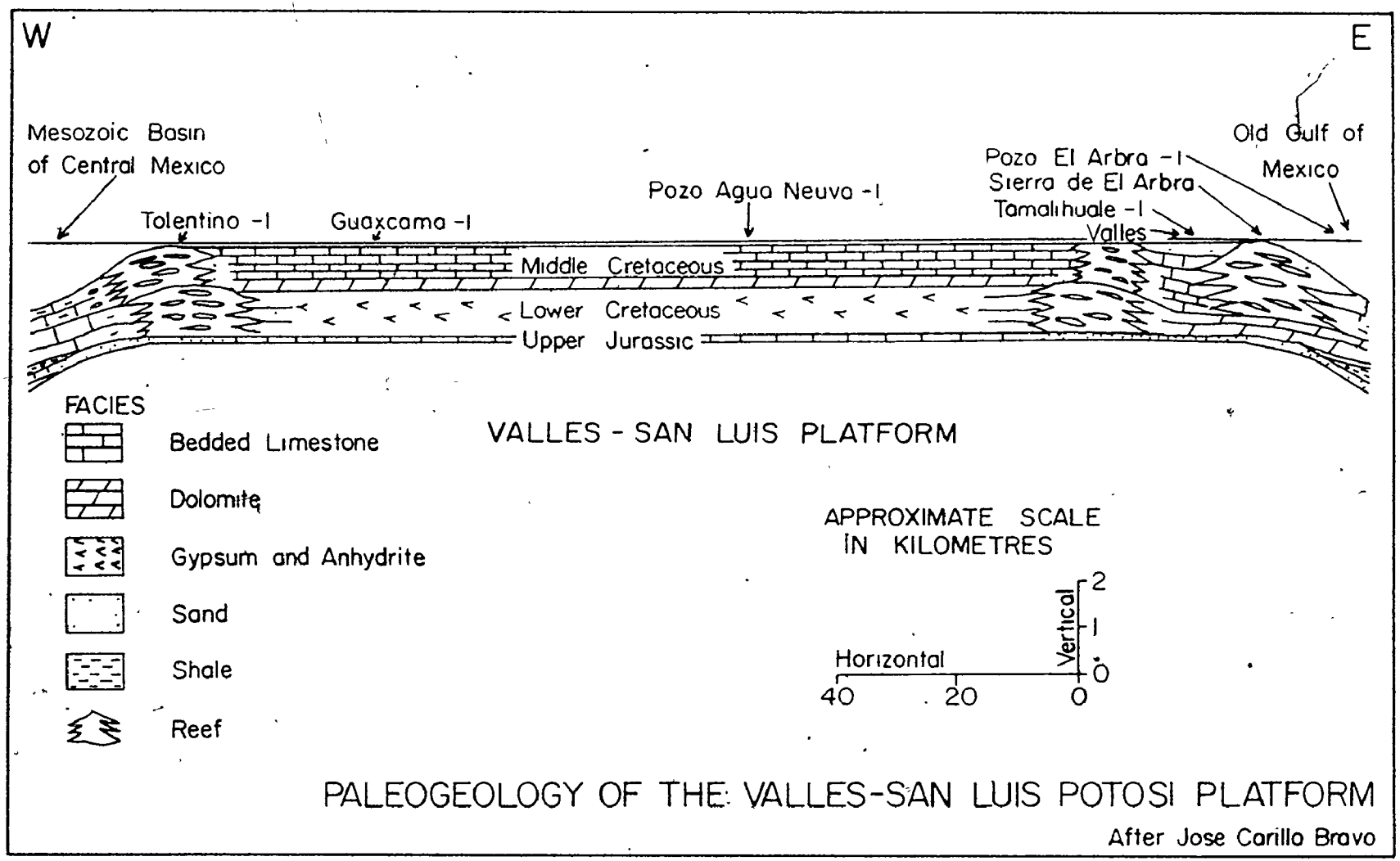

Figure 2.2 Geologic cross section of the Valles-San Luis Potosí Platform during the Cretaceous.

Previously, the name El Doctor Formation or Group was applied to the middle Cretaceous limestones west of Valles, and the name El Abra Formation was restricted to the reef and adjacent backreef facies of the Sierra de El Abra and Golden Lane. The El Abra formation is now subdivided into 3 contemporaneous gross facies (see Figures 2.2 and 2.3):

1) forereef facies (previously the Tamabra Formation or member)
2) reef facies (Taninul facies or member)
3) backreef and platform facies (including the El Abra facies and El Doctor limestone of older classifications).

The forereef facies is a "mixed" rock unit a few hundred meters thick found around the margin of the Platform and is transitional to the basin facies (Cuesta del Cura Fm.). It consists of porous dolomitized calcarenites and breccias derived from the reef, and dark lime mudstone and wackestone with chert lenses typical of the basin limestone. Relative proportions of the lithologies vary around the region and with distance from the reef.

The "reef" facies (Taninul facies) is not strictly a reef analogous to modern coral reefs. Bonet (1952, 1963) has extensively described this facies in the Sierra de El Abra and compared it with various modern carbonate models. It is composed of muddy rudist banks (tabular bioherms) together with the volumetrically much more abundant interreef bioclastic debris and mud. The rudist reefs are tabular in form, measuring a few hundred meters long and a few tens of meters thick. They are composed of abundant whole rudists, many in growth position, weakly bound by stromatoporids and coralline

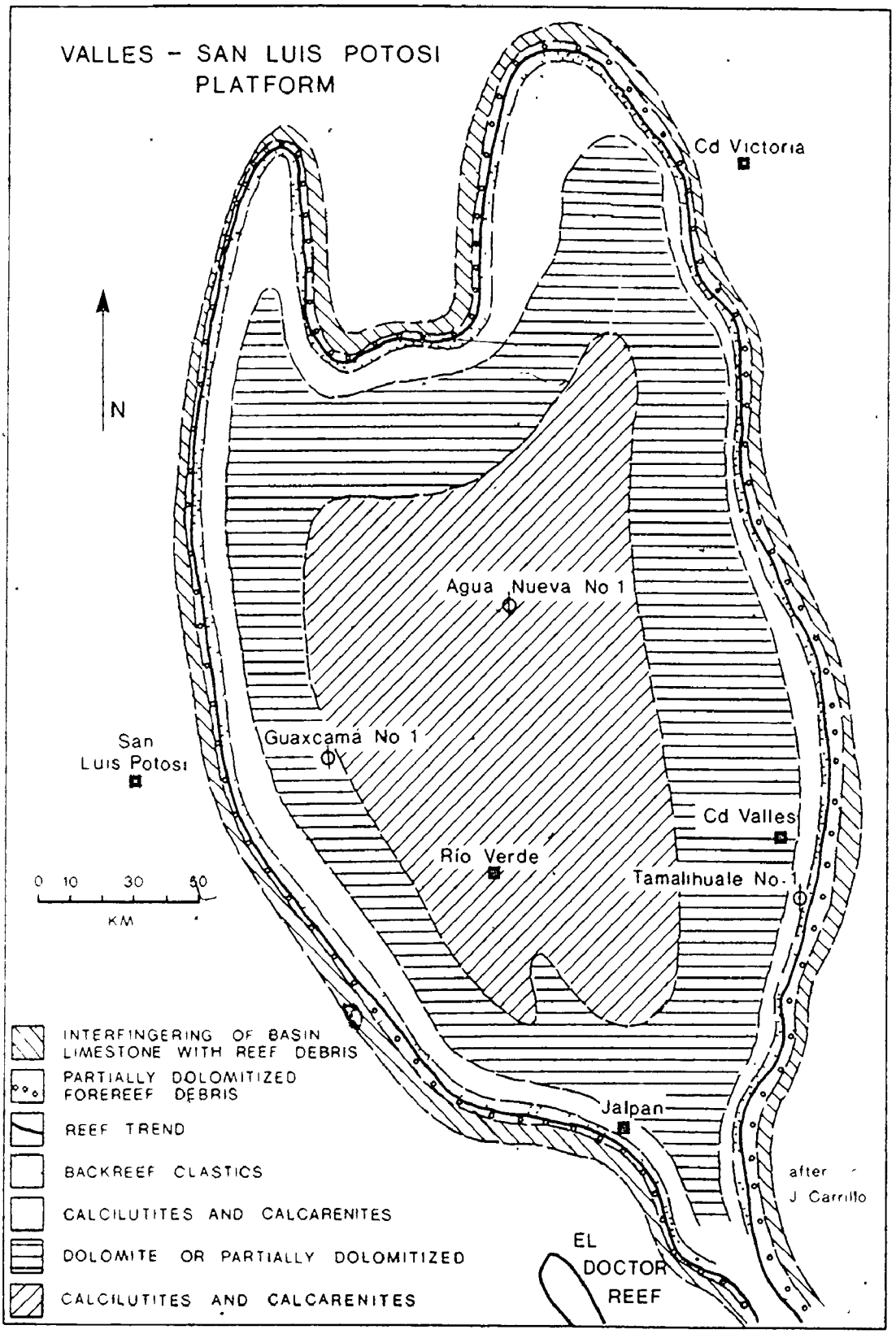

Figure 2.3 Gross carbonate facies distribution on the Valles-S.L.P. Platform.

algae in a matrix of lime mud and skeletal sand. These reefs tended to form complexes of individual reefs and to grow along the margin of the Platform. The interreef and immediate backreef areas were filled with reef debris forming massive, coarse skeletal grainstones and packstones to skeletal siltite. The skeletal sand and reef facies display very little bedding and grade almost imperceptibly into each other. According to Griffith, et al. (1969), the complex Taninul facies can be divided into just 3 subfacies: skeletal siltite, skeletal sand, and organic reef facies. They form what has been called a "calcareous bank". Sparry calcite cement has eliminated all porosity except some cavities left by fossils and a system of massive fractures. Carrillo Bravo (1971) suggests the total thickness of the reef may exceed 2000 m, but 800+ m is apparently the largest outcrop. In the Sierra de El Abra, the width of the reef zone is usually 600 m or less, but about 2 or 3 times this width is known at Gómez Farías in the Sierra de Guatemala.

Over the interior of the Platform, a wide variety of lithofacies make up the "backreef" or platform facies of the El Abra Formation. Carrillo Bravo (1971) outlines the following gross distribution and types (Figure 2.3): 1) backreef clastic unit bordering the reef zone; 2) unit of calcilutites and calcarenites with miliolids and <u>toucasia</u> biostromes in a belt encircled by the clastic zone; 3) unit of fine to medium grained dolomite and partially dolomitized limestone, with some beds similar to lithofacies 2; 4) unit of calcilutites and calcarenites with miliolids and <u>toucasias</u> and of sporadic dolomite horizons, which covers more than 15,000 km^2 in the central portion of the Platform; and 5) basal dolomite

zone, in thick beds, apparently covering the entire Platform at the base of the El Abra Formation. Types 1-4 occur in a bull's eye pattern overlying type 5. The total thickness of the backreef facies is 1000 to 1500 m in the central region, including about 100 m of the basal dolomite, and up to 2000 m nearer the margins. The Tamalihuale No. 1 well, located about 4 km west of the reef and southeast of Cd. Valles on the Sierra de El Abra, penetrated about 1450 m of lithofacies 2 above, and 350 m of basal dolomite which was described as having frequent small and irregularly distributed caverns. On the outcrop at the south El Abra pass, the backreef facies is predominately light cream to gray lime mudstone and wackestone with some asphaltic stains. Exposure surfaces marked by thin dolomite layers, flat-pebble conglomerate and dessication structures are present. Some beds contain abundant stylolites. Bedding varies from one-half to four meters, with a few prominent shale partings up to 4 cm thick (Plate 2.1). Near the reef, the bedding is indistinct and massive, and the shale partings and the thin dolomite layers are absent; all these features become more abundant with increasing distance from the reef. Numerous small solution openings are found in the pass, but the rocks are very compact. Rose (1963) reports that only one of the 30 outcrop samples from the Southern El Abra pass had a measurable permeability (0.6 millidarcy) and the average porosity was 2.4% with extremes of 6.7% to 0.3% (measurements by Shell Oil).

Most of the upper surface of the El Abra Formation on the Platform is an unconformity. In the Valles area, the Agua Nueva, San Felipe and Méndez Formations directly overlie the El Abra at different places (Heim, 1940). The top of the El Abra limestone is now exposed and eroded in the

(a)

Plate 2.1 Two views of the thick-bedded El Abra limestone. These sections occur in a quarry in the south El Abra Pass, about 1½ km west of the reef facies. There are a few thin shale partings here that become slightly thicker farther west. Note the numerous solution openings in (a), and the thin to spotty soil cover in both photos.

(b)

Sierra de El Abra, hence it is not directly proven that it was ever covered. Since this has important implications on development of permeability and karstification, evidence bearing on this problem will be analyzed in a later section.

Agua Nueva Formation (Xilitla Flags)

The Agua Nueva consists principally of fine to medium grained black argillaceous flaggy limestone in thin to medium beds alternating with brown to black shale. A basal conglomerate is often present. On the western flank of the Sierra de El Abra near Los Sabinos, the Agua Nueva is not so "dirty" and appears as a thin band of white limestone circling hills (W. Russell, personal communication; caution must be exercised because some beds in the El Abra limestone also show up as "white bands".) Its thickness varies from 0-30 m in the Sierra de El Abra and about 50 m in the Sierra la Colmena. It is also found on the southeastern and northern margins of the Platform in thin units and in wells throughout the coastal plain.

Soyatal Formation

The Soyatal Formation was deposited over the western margin of the Platform and over a broad area in the deeper water basin to the south and west. It is quite variable in thickness, ranging up to about 1000 m. It is transitional from thin to medium bedded dark gray limestones with thin, often reddish shale partings and chert at the base to a middle and upper section consisting predominantly of gray shales with interbeds of sandstone and shaley limestone. The Soyatal is thought to be equivalent

to the Agua Nueva.

San Felipe Formation

The San Felipe Formation on the eastern margin of the Platform is a thin Upper Cretaceous body of fine grained argillaceous limestone, with intercalations of olive gray shale and green bentonite. This thin-bedded finely-jointed unit concordantly overlies the Agua Nueva and in some places discordantly overlies the El Abra Formation. It is found in a narrow belt along the base of the eastern scarp of the Sierra de El Abra, in the synclincal valley and anticlincal Sierra Tamalave to the west (4 to 50 m), in the Xilitla and Gómez Farías areas, and under the coastal plain (several hundred m). At least three small patches of San Felipe occur on top of the El Abra southwest of Quintero, and numerous tiny patches cap hills southeast of Los Sabinos on the dissected western flank of the range. It weathers to shades of yellow and brown.

Tamasopo Formation

The Tamasopo Formation of Turonian-Senonian age designates about 200 m of reef and backreef limestones that cover (or covered) a large portion of the Platform (see reef trend in Figure 2.4). These rocks are similar to the El Abra Formation and represent the continuation of shallow water conditions in the central region as the margins subsided and received terrigenous sediments.

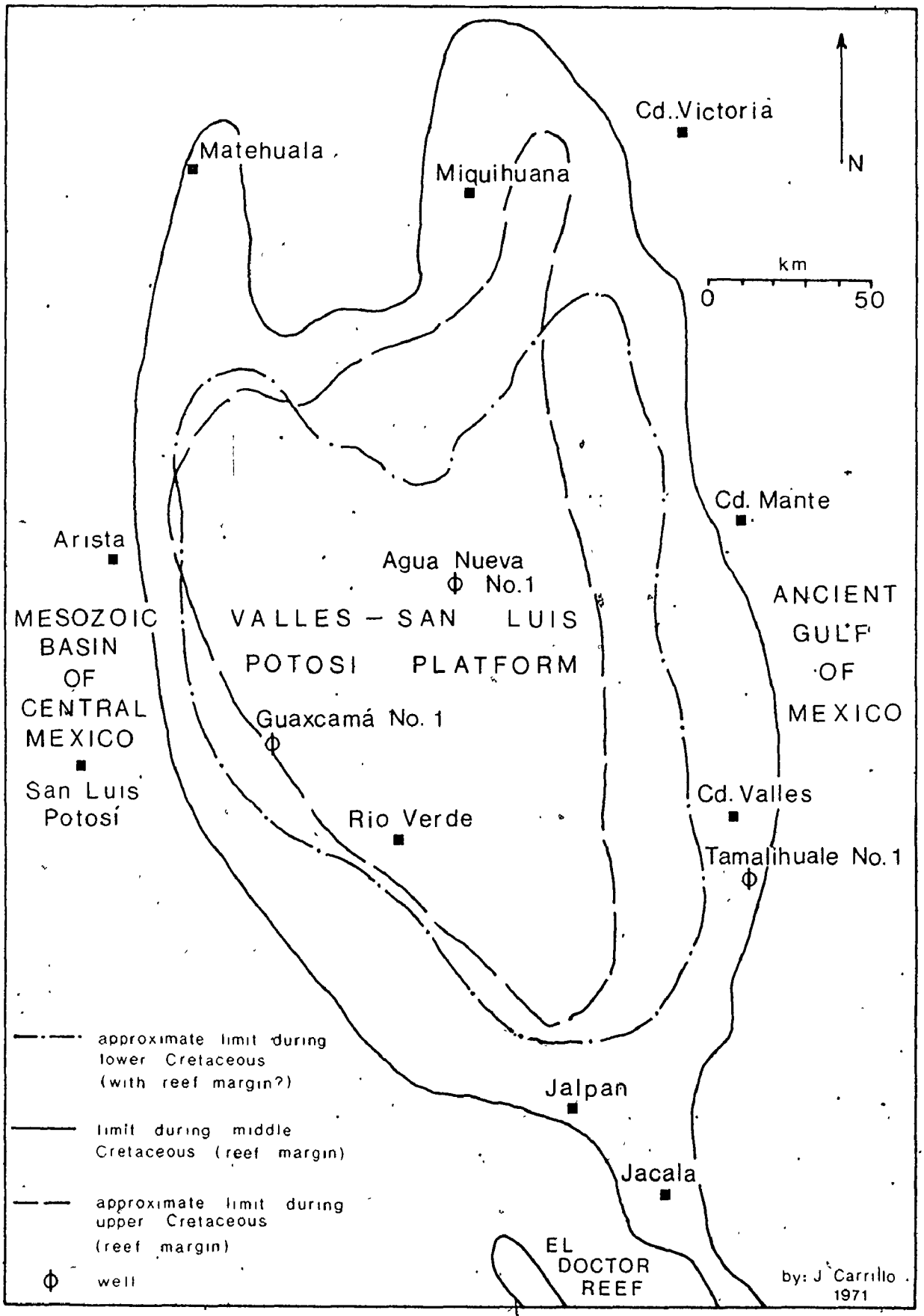

Figure 2.4 Valles-S.L.P. Platform limits during the Cretaceous.

Méndez Formation

The Méndez consists of monotonous gray, greenish gray and brown calcareous shale and marl with some sandy beds and frequent thin beds of white bentonite. Because it is easily eroded, it is now found only in synclinal valleys along the east front of the Sierra Madre Oriental and on the coastal plain east of the El Abra range. Up to 300 m remain in the Valles valley and over 1000 m southeast of Aquismón. It is Campanian-Maestrichtian in age and conformably overlies the San Felipe.

Cárdenas Formation

A suite of calcareous shale, siltstone and sandstone, sometimes exceeding 1000 m in thickness covers the central portion of the Platform. It correlates with the Méndez Formation and generally unconformably overlies the Tamasopo. The top of the Cárdenas is usually eroded and often covered with alluvial material and sometimes by volcanic flows.

Tertiary-Quaternary

Santo Domingo Formation

The Santo Domingo Formation (Carrillo Bravo, 1971) designates a thin unit of fluvial and laucustrine terrigenous sediments of Pliocene-Pleistocene (?) age. Fragments of Cretaceous limestone, chert and basalt occur in conglomeratic horizons. The formation is found in the San Bartolo-Cd. Maiz-El Huizache region. In many places, it is covered by basalt flows.

La Borreguita Formation

The La Borreguita Formation (Carrillo Bravo, 1971) is proposed for up to 30 m of finely banded gypsum of lacustrine origin that probably correlates with the Santo Domingo Formation. It occurs in the broad Río Verde valley and was likely washed down from higher exposures of the Guaxcamá to the West. Another important occurrence of gypsum, not mentioned by Carrillo Bravo, and of undetermined age and thickness, lies in the valley from Matehuala to Huizache. The upper 10 m is weathered, but bedding is beautifully exposed in numerous caves developed in the gypsum.

Alluvium

In the west and central areas, recent fluvial sediments are found in many valleys. Alluvium is relatively thin and patchy in the eastern part of the Platform. Immediately east of the Sierra de El Abra, there are isolated occurrences of lacustrine (?) limestone (capping a hill south of Quintero) and calichefied conglomerates (about 2 m capping hills of Méndez shale east of the Choy spring).

Igneous Rocks

Intrusive igneous rocks are rare on the Platform. Some were emplaced during the early Tertiary orogeny.

Extrusive igneous rocks are of local importance in the region. Tertiary rhyolite is found in the southwestern portion of the Platform

and extensively in the central Mexican plateau. Numerous small basalt flows are found in the central, southern and eastern zones. Many of the flows were "basalt rivers" in river valleys. In some places, they overlie lacustrine deposits containing Pliocene-Pleistocene pollen (Carrillo Bravo, personal communication). East of the Platform between Cd. Mante and Cd. Victoria, there are large basalt capped mesas between 400-500 m elevation.

2.4 Structure and Physiography

During the late Cretaceous, tectonic movements began to occur in the region, as shown by the shifting sedimentary facies. The Laramide movements culminated during Paleocene and Eocene times with uplift and intense folding. No marine Tertiary rocks are known on the Platform -- the depocenter (ancient Gulf shoreline) moved eastward with time as the region emerged.

Nearly all the large structural features of the Platform are folds having as much as 2 km of structural relief. The structural trend varies from NW-SE to N-S and is discordant with the pre-Mesozoic fold trend (Carrillo Bravo, 1971). Four broad arches and 2 large anticlines, all with numerous associated folds, are shown in Figure 2.5. In a belt of intense folding in the eastern half of the Platform, the anticlines are generally narrower and asymmetric or overturned to the east. Carrillo Bravo (1971) believes that rocks principally from Upper Jurassic to Upper Cretaceous are involved, and that the structures were formed by a sub-

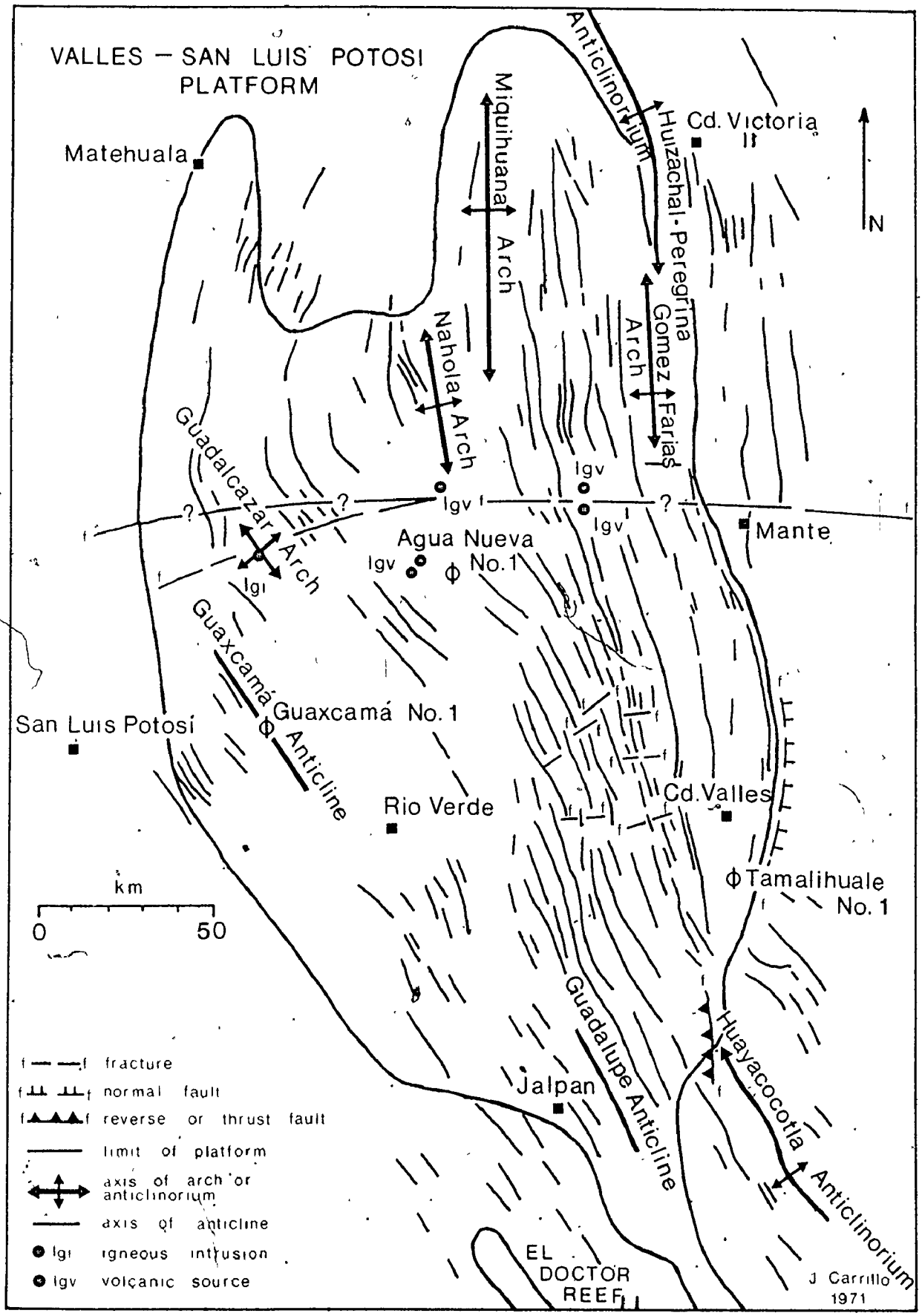

Figure 2.5 Structural map of the Valles-San Luis Potosí Platform.

siding basement to the east causing gravitational gliding of rigid strata over Lower Cretaceous evaporites. He believes that many of the folds are injection folds. Along the eastern margins of the Platform in the Valles area, the folds have less relief and are separated by broad synclinal valleys.

Faults seem to be of lesser importance than folds on the Platform. Many of the anticlines have longitudinal faults along their eastern side, and may have tear faults at their terminations, as well as other transverse shearing within the structure. The Xilitla overthrust which has many kilometers of displacement is the largest fault structure in the area; several other overthrusts have been described by Russell (1968) in the adjacent Aquismón area. Undoubtedly, there are countless small faults, but mapping has not been carried out in this detail.

Intense deformation of the rigid carbonate rock has produced massive fractures. Joints in the El Abra Formation normally pass through several beds; fractures that extend vertically for over 100 m and sometimes much more without observable offset are known. Later, it will be shown that these fractures are very important to the circulation of ground water.

The uplift and subsequent erosion of all of central México has created 3 main physiographic provinces in the region: 1) the coastal plain of terrigenous rocks extending 110 km from Tampico to the Sierra de El Abra, and at less than 120 m elevation; 2) the Sierra Madre Oriental foldbelt of carbonate rocks, having high local relief and elevations mostly between 400-2500 m, but reaching over 3000 m in places; and 3) the Central Mexican Plateau or highlands of sedimentary and volcanic rocks, having more moderate

local relief and elevations ranging from 1500-3000 m (Figure 1.1 shows the general regional physiography). Another large regional feature is a broad down-warped zone west of the main fold belt that stretches from Río Verde to Tula (and beyond) where there is now a broad valley or system of wide intermontane valleys at about 1000 m elevation. They contain alluvial, lacustrine and bolson deposits and have been leveled by sedimentary processes. Erosional processes began to work on the Platform probably in the early Tertiary, but it must have taken a long time to establish a regional fluvial system. The southern half of the Platform is drained by the Río Tampaón which now extends to the city of San Luis Potosí. Most of the northeastern quadrant is drained by the Río Guayalejo. The entire northwestern quadrant lacks a fluvial network. The stratigraphy of Tertiary continental rocks and late Tertiary-Quaternary erosion terraces suggest that there has been intermittent uplift since the early Tertiary.

Although most of the Platform is now a karst area, the largest scale physiographic features within it were formed by the fluvial erosion of less resistant Upper Cretaceous shales and thin bedded limestones from the tops and sides of structural highs of the El Abra and Tamasopo formations. Hence, these features are the result of structural relief and erosional processes. An excellent example is the Sierra de Guatemala which has over two kilometers of structural and topographic relief. Another example is a large anticline southwest of Ayutla that has about 1 km of structural relief and a width of several kilometers. Previously overlying shales have been stripped off the top and about three-fourths of the way down the flanks; shale remains on the lower flanks and in the valley. The crestal limestones having had the longest exposure are the most inten-

sively karstified. Most of the positive structures are anticlines; therefore, ridges of varying complexity are the dominant positive form, except in the Xilitla area where a thrust block has formed a karst plateau. West of the Sierra la Colmena, most of the shale has been removed, exposing a broad belt of folded limestone to karst processes. The largest purely erosional features are the transverse valleys, or water gaps crossing the structures, which were formed by the major drainage channels. Some of the water-gap canyons are 1000 m deep.

The Sierra de El Abra is a long ridge of resistant El Abra limestone at the eastern central margin of the Platform. The range is much lower in elevation than the nearby high sierras. Its geomorphology and structure will be examined in Chapter III. A broad synclinal valley floored with the Méndez and San Felipe formations on the western side of the range is referred to as the Valles valley, or sometimes in its northern end as the Antiguo Morelos valley. This valley connects directly with the coastal plain around the southern end of the range. Two small domes which expose the El Abra limestone occur along the slightly curving strike of the El Abra range structure beyond its southern limits. One is called the Tantobal dome and the other is called the Salsipuedes or Coy dome, the latter having a very large spring. There are many smaller folds in the El Abra area that often significantly affect local geomorphic features and drainage.

2.5 The Environment

2.5.1 Climate and Vegetatión

The climate of the region varies greatly, both temporally and spatially.

In terms of precipitation, the year is normally divided into wet and dry seasons. During the months November through May, there is very little precipitation in any part of the region; most of the rainfall occurs during the months June through October. Moisture is brought into the region by warm summer winds from the Gulf of Mexico; occasionally, there are hurricanes. The mean annual rainfall may exceed 2500 mm in the wettest localities along the eastern flanks of the high sierras such as the Xilitla area, and is as low as 300 mm in the semiarid western half of the region, which is in the rain shadow of the Sierra Madre Oriental (Figure 1.1). The Sierra de El Abra receives about 1200-1400 mm per year. A more detailed discussion of precipitation in the region is given in Chapter IV.

Seasonal temperatures are related to both solar cycles and precipitation. The coldest months are December and January, early in the dry season (Table 2.2). Gradual warming occurs through the spring to the hot, dry days of April-May, when the daily maximum occasionally exceeds 40°C in the Valles area (Table 2.3); the vegetation on the Sierra de El Abra usually appears to be a parched brown at this time. Usually the rains begin modestly in May and come heavily sometime in June. During the rainy season, the relative humidity increases and the daily maxima and mean monthly temperatures are suppressed. In the last half of the dry season, the potential for evapotranspiration is great, but there is very little moisture; however, once the rains begin the actual evapotranspiration must become quite high. Table 2.3 shows the daily maximum and minimum temperatures and their average differences for 4 selected months in 1971; there is a large daily variation in the dry season, and somewhat less in

TABLE 2.2

Mean Monthly and Annual Air Temperatures (°C)

Station [4]	Elevation m	Jan.	Feb.	Mar.	Apr.	May	June	July	Aug.	Sept.	Oct.	Nov.	Dec.	Average	Range
Cd. Valles	95	20.0	21.5	23.8	26.8	29.1	28.8	28.5	29.5	28.0	25.1	22.3	20.2	25.3	9.5
Antiguo Morelos	220	18.8	21.3	24.4	27.5	29.2	29.3	28.3	28.8	27.5	25.0	22.4	20.1	25.2	10.5
Ahualulco [4]	(80)	19.5	21.2	24.2	26.7	28.7	29.2	28.4	29.1	27.5	25.0	21.2	19.1	25.0	10.1
Joya de Salas [2,4]	1550	9.2	11.4	16.6	17.4	19.0	18.4	17.9	18.7	17.4	14.1	13.1	11.7	15.4	(9.8)
Tamapatz [3]	(750)	16.1	16.1	19.5	22.1	23.3	23.5	22.4	23.3	22.9	21.5	18.3	17.9	20.6	7.4
Agua Buena [4]	372	18.1	19.7	23.0	25.9	27.9	28.0	27.1	27.5	26.2	23.9	20.5	18.4	23.9	9.9
El Salto	(400)	16.8	19.0	21.7	24.5	26.4	26.2	25.0	25.7	24.7	23.0	19.1	18.0	22.5	9.6
Jaumave	750	15.3	17.3	19.9	22.4	24.8	25.3	24.6	24.8	23.8	21.5	17.8	16.1	21.1	10.0
Lagunillas [4]	950	17.6	19.4	22.4	24.2	26.1	25.9	24.7	25.5	23.8	2.17	19.9	17.4	22.4	8.7
Cd. del Maíz	1239	15.6	17.5	22.0	22.3	24.8	24.3	23.1	23.2	22.5	20.6	18.0	16.2	20.8	9.2
Río Verde	987	16.0	18.0	20.5	23.1	24.9	24.7	23.7	23.9	22.8	20.7	17.9	16.0	21.0	8.9
San Luis Potosí	1877	13.5	15.4	17.8	20.2	21.4	21.0	19.8	20.0	18.8	17.3	15.2	13.9	17.9	7.9

1. lowest and highest monthly average are underlined; data are from S.R.H. Boletín 19, except Tamapatz (unpublished).
2. only 1 year of data
3. 5 years of data
4. see Figure 1.1 for locations except for: Ahualulco, 11.5 km S of Gómez Farías; Joya de Salas, 20 km NW of Gomez Farias; Agua Buena, 3 km N of Tamasopo; Lagunillas, 30 km S of Rayon.

TABLE 2.3

Daily Maximum and Minimum Temperatures at Estación Santa Rosa (Cd. Valles)

	1971							
	January		May		June		October	
	Max	Min	Max	Min	Max	Min	Max	Min
Day								
1	28.0	19.0	30.5	21.5	38.0	27.0	33.0	21.5
2	30.0	16.0	35.0	18.5	38.0	27.0	32.5	22.5
3	34.5	14.5	36.0	17.5	38.0	25.0	32.5	23.5
4	23.5	15.0	37.0	22.5	37.5	25.5	32.0	23.0
5	15.0	11.5	40.0	24.0	37.0	22.5	32.5	23.0
6	13.0	11.5	46.0	22.0	37.0	25.0	29.0	23.0
7	17.0	9.0	43.5	22.5	37.0	24.0	31.0	23.0
8	18.0	8.0	38.5	24.5	38.0	26.0	33.5	22.0
9	25.0	8.0	36.5	26.0	39.5	25.5	34.0	22.0
10	29.0	9.5	37.0	23.0	38.0	26.5	27.5	22.0
11	30.0	14.0	39.0	20.0	39.0	26.0	29.0	20.5
12	29.0	16.0	32.0	23.5	30.5	23.0	29.0	18.5
13	30.0	18.0	29.0	22.5	35.0	24.0	29.0	20.5
14	28.0	19.5	31.0	17.0	36.0	24.0	30.0	21.5
15	30.0	20.0	37.5	19.0	35.5	23.0	32.5	22.5
16	23.0	20.0	38.5	19.0	34.5	23.0	32.5	22.0
17	32.0	15.0	37.5	18.5	30.0	24.0	33.5	24.0
18	34.0	15.0	37.0	19.0	32.0	22.5	33.0	23.5
19	23.0	19.0	37.0	23.0	31.0	23.5	33.5	24.0
20	22.5	14.0	37.5	25.0	31.0	23.0	32.5	22.5
21	29.5	12.5	37.0	22.0	23.0	22.0	30.5	20.0
22	29.5	12.5	38.0	23.0	30.0	22.0	32.0	19.5
23	30.0	12.0	36.5	26.5	31.0	20.0	31.5	18.0
24	30.5	13.5	39.5	25.0	30.5	22.0	30.5	21.5
25	29.5	13.5	31.0	22.0	28.0	23.0	32.0	20.5
26	28.5	17.0	34.0	23.5	31.5	22.5	32.5	20.0
27	26.0	18.0	36.0	23.0	32.0	22.5	32.5	20.0
28	30.0	20.0	36.0	23.0	34.0	23.5	33.0	21.5
29	30.0	18.5	36.0	24.0	32.5	22.0	32.0	19.0
30	32.5	16.5	38.0	24.5	32.0	21.5	33.0	20.0
31	35.0	14.0	37.5	26.5	–	–	32.5	19.5
Avg.	27.3	14.9	36.6	22.3	33.9	23.7	31.7	21.4
Difference	12.4		14.3		10.2		10.3	
Monthly Mean	21.1		29.3		28.8		26.6	

the wet season. The temperature data may be compared with daily rainfall for 1971 shown in Figure 4.7; very high daily temperature maxima continued until the rains came in mid-June.

Table 2.2 gives an indication of the regional and altitudinal variation in temperature as well as seasonal changes. The data are arranged from easternmost at the top to westernmost at the bottom. Nearly all the stations are located in valleys; hence, they do not accurately reflect the full range of temperatures to be expected in the region. The temperature difference between Ahualulco and Joya de Salas (at the eastern base and high on the western flank of the Sierra de Guatemala respectively) indicate the much cooler conditions that undoubtedly exist in the high sierras. Snow occurs only rarely in the Valles area, but light snows are likely more common in the high ranges. Winter frost at high altitudes and dew at all altitudes are common events.

The variety of vegetation in the region is of course very great in order to accommodate the extremes of climate and ground conditions. The Sierra de El Abra is covered with a dense thorn forest in which all the plants must be adapted to a long dry season with sparse water renewal, and very little soil. There are many types of cactus, stinging vines and nettles, epiphytes, and thorny bushes and trees. Except in relatively rare places where there is a significant soil accumulation, trees usually are not more than about 10 m high. On the coastal plain and in the low Valles valley, the natural vegetation is a scrubby bush with low trees, except where there are stream channels, especially those that are spring fed. In the much higher and wetter Sierra de Guatemala, P.S. Martin (1958)

has distinguished several vegetation zones; among them are tropical deciduous forest, tropical semi-evergreen forest, cloud forest, and pine and oak forest. Going further west into the semiarid region, there is chaparral and thorn desert.

2.5.2 Culture

Despite the ruggedness of the terrain, the region as a whole is moderately well populated. Probably the majority of the population lives in towns in valleys where there are water supplies, road construction is more tractable, and ranching and farming are more fruitful. Most of the larger towns and more productive ranches or farms are located along the eastern margin of the region and on the adjacent coastal plain. The principal products are cattle, oranges, sugar cane, and sisal, but a great variety of other fruits, vegetables, and grains are also grown; there is a small amount of irrigation. On the lower elevations in the front ranges of the Xilitla area, coffee, oranges, and corn are important crops. Much of the mountainous country is still poorly serviced by roads. Industrious natives have carved out small plots of land on slopes as great as 45° by slash-and-burn techniques; they grow corn, coffee, and beans, which are carried on their backs to market. The high parts of the ranges are sparsely inhabited, there often being only a few woodcutters and isolated farmers. Further west in the semiarid zones, the occurrence of water and arable land are the main factors in human occupation.

Access to the Sierra de El Abra is generally poor, and very little was known about the top of the range previous to this study and other

recent investigations by the Association for Mexican Cave Studies. Three roads cross the range transversely, two of them in wind gaps. There are no roads lengthwise along the crest -- only a highway parallel to the range several kilometers west of it, and a dirt track parallel to the east face that is impassable during much of the wet season. There are numerous trails on the crest that are used by woodcutters, a few farmers, and occasionally by jaguar, ocelot, or deer hunters. In general, the crest is almost totally uninhabited, and navigation often could only be made by air photo and machete.

CHAPTER III

GEOMORPHIC FEATURES OF THE SURFACE

The surface geomorphic features of the Sierra de El Abra and environs are described in this chapter. This is the area in which most of the field work was conducted, and which was studied by aerial photographs. Karst landforms in other parts of the region will be briefly considered at the end of the chapter.

The region is very large, access is poor, and the geomorphic studies only just begun.

3.1 The Sierra de El Abra

The Sierra de El Abra is an extremely elongate range at the eastern edge of the Valles-San Luis Potosí Platform. It begins in the south at the Río Tampaón and extends approximately 140 km northward to Puerto Chamalito (a wind gap), which is taken as the northern limit of the range (Figure 3.1). The Sierra de El Abra structure actually can be traced for 6-7 km north of Puerto Chamalito in a zone where it gradually merges with the much larger Sierra de Guatemala. The main range varies in width from a minimum of 2 km to a maximum of 5 or 6 km. The crest zone of the range (Plate 3.1) has very low relief. The crest rapidly descends southward from the Sierra de Guatemala to a low of 190-200 m just north of the

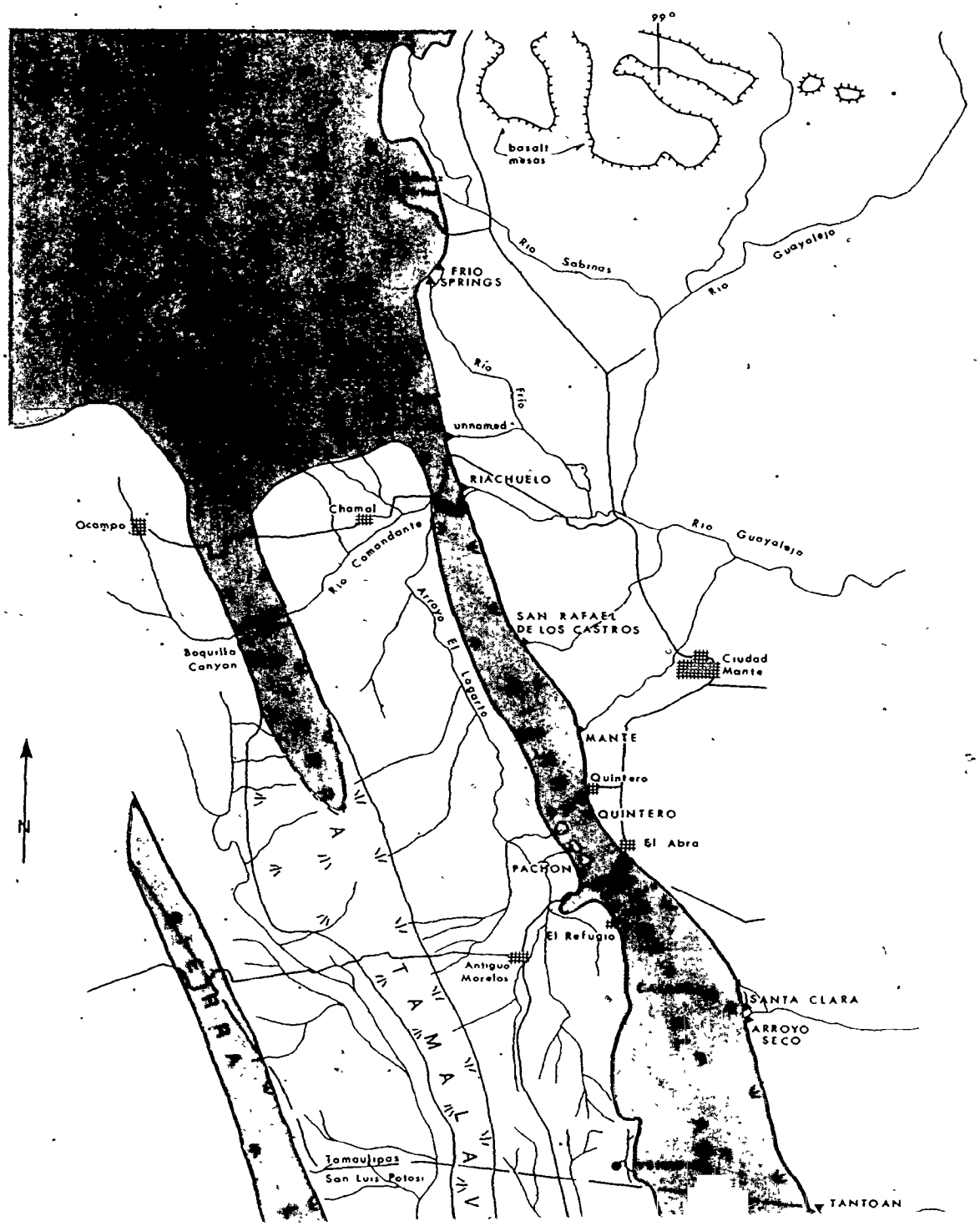
99°
basalt mesas
Rio Sabinas
Rio Guayalejo
FRIO SPRINGS
Rio Frio
unnamed
RIACHUELO
Chamal
Ocampo
Rio Comandante
Rio Guayalejo
Arroyo El Lagarto
SAN RAFAEL DE LOS CASTROS
Ciudad Mante
Boquilla Canyon
MANTE
Quintero
QUINTERO
El Abra
PACHON
El Refugio
Antiguo Morelos
SANTA CLARA
ARROYO SECO
TAMAULIPAS
Tamaulipas
San Luis Potosi
TANTOAN
N

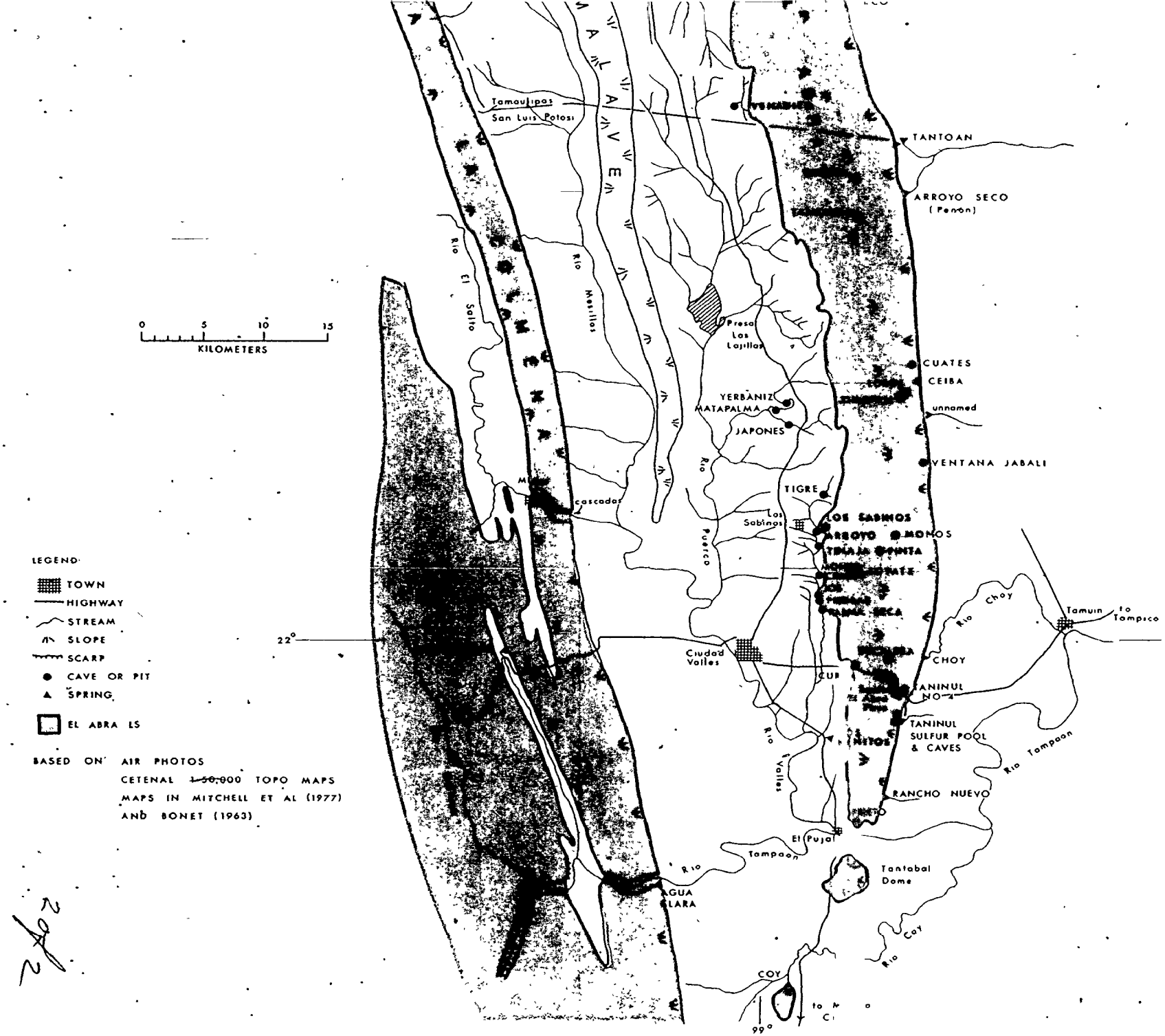

Figure 3.1 Sierra de El Abra and surrounding area.

Plate 3.1 Gulf coastal plain and Sierra de El Abra. This aerial view looks southward along the strike of the range from above the town Quintero. The coastal plain of shale rises gently to the eastern reef-front escarpment of the range. The crest typically has low relief, and the western margin dips westward to Valles-Antiguo Morelos valley. Note the residual hill of Méndez shale which is capped by a lacustrine limestone.

Río Comandante, then gradually rises to the high central portion of the range, and finally descends slowly to where the El Abra structure passes under the Río Tampaón at 28 m. The higher part of the range (that part 450 m and above) extends from about the latitude of Antiguo Morelos to a few kilometers north of Cd. Valles. Recent explorations in Cueva de Diamante (Peter Sprouse, personal communication), show that the crest probably reaches at least 700 m in the highest areas, much higher than the 450 m shown on the old 1:100,000 topographic maps.

The well defined eastern margin is a steep scarp that descends to the coastal plain varying from 33-120 (?) m elevation. The western flank of the range is much more complex. In many places, the El Abra limestone is structurally higher than the Méndez and San Felipe Formations in the Valles and Antiguo Morelos valleys. Thus, the western flank is quite variable in width, and the El Abra limestone is exposed both in anticlinal ridges and synclinal valleys at elevations intermediate between the crest of the main range and the lower portions of the Valles valley. The width of outcrop of the El Abra limestone reaches about 10 km in places. As pointed out by Mitchell, et al. (1977), the name "Sierra de El Abra" is often applied to the complete exposure of the El Abra Formation, though technically it should not be. Also, it should be noted that many other names are locally used for the El Abra range including Sierra Cucharas, Sierra de Tanchipa, and Sierra de las Palmas.

Based on air photos and some field observations, a geomorphic map of the southern part of the Sierra de El Abra is given as Figure 3.2. Most of the field work on the El Abra range was conducted in this area. It

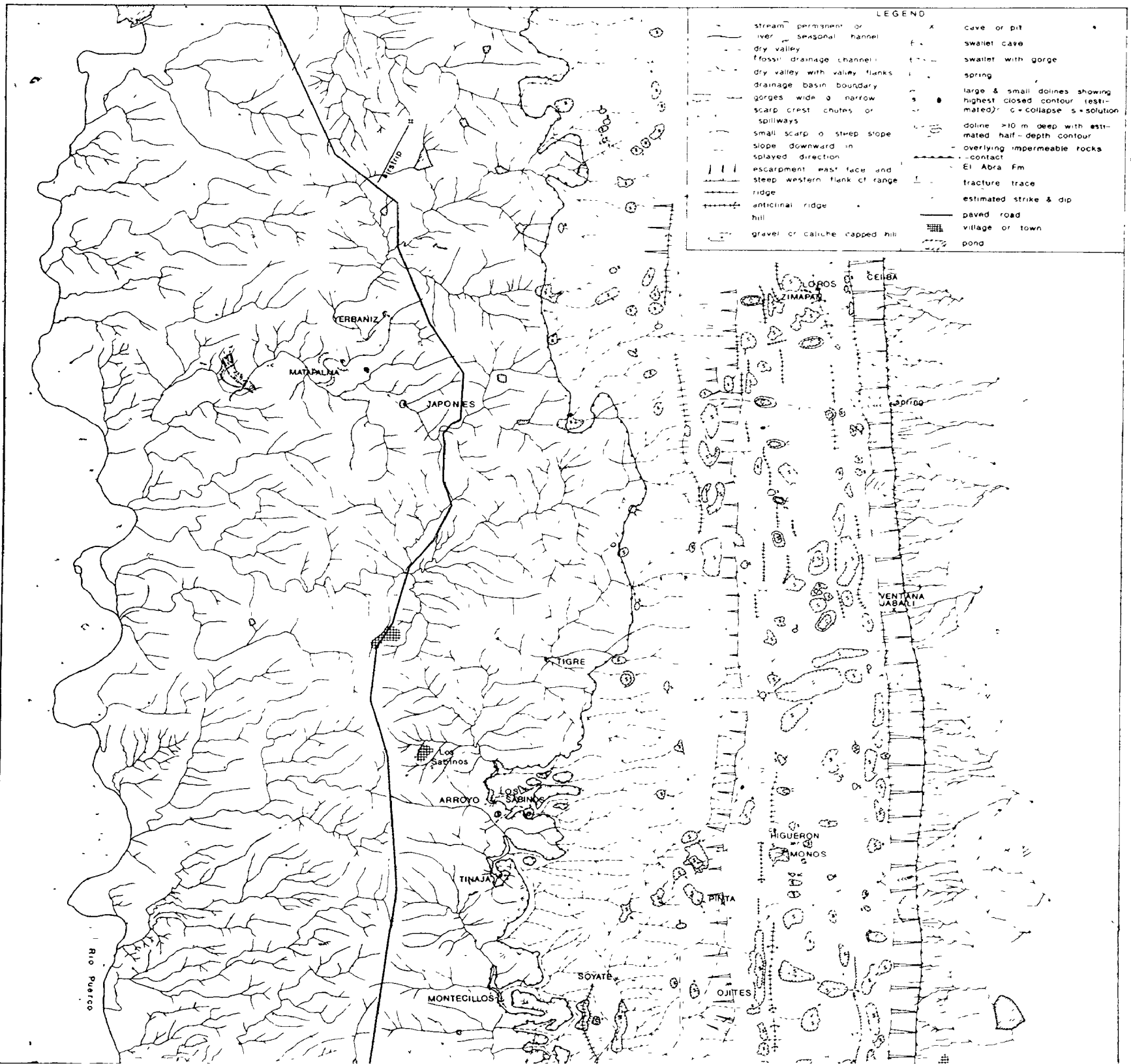
LEGEND
stream permanent or river seasonal channel
dry valley
fossil drainage channel
dry valley with valley flanks
drainage basin boundary
gorges wide & narrow
scarp crest chutes or spillways
small scarp & steep slope
slope downward in splayed direction
escarpment east face and steep western flank of range
ridge
anticlinal ridge
hill
gravel or caliche capped hill
cave or pit
swallet cave
swallet with gorge
spring
large & small dolines showing highest closed contour (estimated) c = collapse s = solution
doline >10 m deep with estimated half-depth contour
overlying impermeable rocks
contact
El Abra Fm
fracture trace
estimated strike & dip
paved road
village or town
pond
TERBANIZ
MATAPALMA
JAPONES
TIGRE
Los Sabinos
ARROYO
TINAJA
MONTECILLOS
SOYATE
Rio Puerco
LOROS
ZIMAPAN
CEIBA
spring
VENTANA
JABALI
HIGUERON
MONOS
PINTA
OJITES

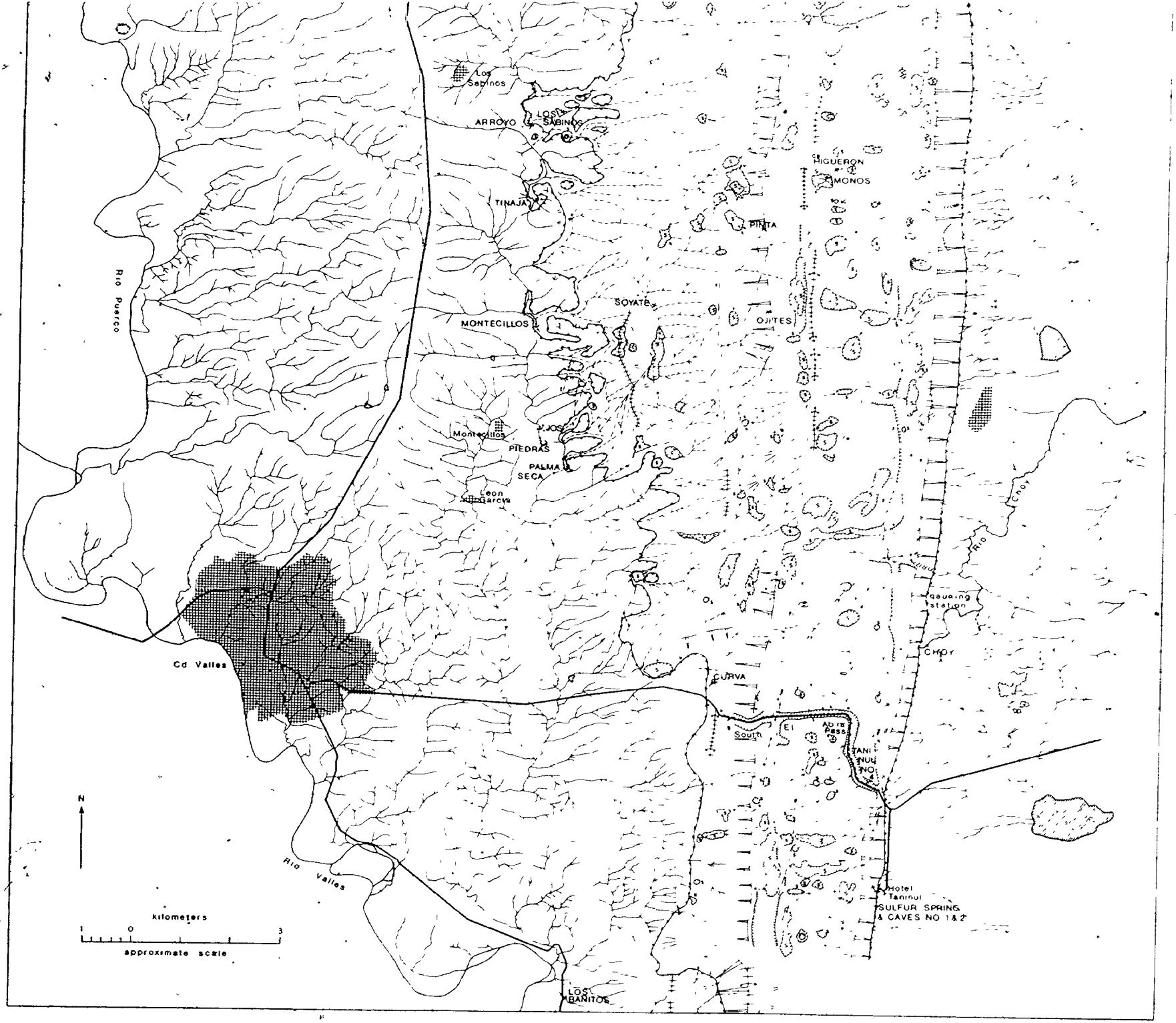

Figure 3 2 Geomorphic and hydrologic map of southern Sierra de El Abra

2 of 2

will be helpful to refer to it in the following sections and in the chapter on caves. Aside from the drainage pattern and other geomorphic features, the map includes one boundary of particular importance: it is the contact between the El Abra limestone and the overlying formations. On the west side of the range, the contact can usually be accurately determined, but along the east face it is drawn approximately at the base of the scarp. On the air photos, there is considerable scale distortion where there is local relief. The map was made simply from an air photo mosaic, using sightings along the highways as the control. The distortion has been corrected somewhat by the overlapping process, but there is undoubtedly still some error. The scale was determined by field measurements and by comparison with 1:50,000 topographic maps.

3.1.1 The East Face and the Coastal Plain

The 110 km wide coastal plain is a low relief erosion surface developed on weakly resistant Tertiary and Upper Cretaceous terrigenous rocks and sediments. In the western part of the plain, the surface becomes more irregular, and near the Sierra de El Abra, it is being rapidly eroded downward by streams that head on or at the base of the scarp. West of Tamuín near the Choy spring, there are several flat-topped hills that are remnants of an older erosion surface at an elevation of about 77 m (Plates 3.2 and 3.3). These hills have a cover of 2 m of caliche, containing abundant rounded gravel, that rests on Méndez shale. The gravel cap has been removed from most of the area, and the dissection by base level streams has reached down to elevations of 33 m at the origin

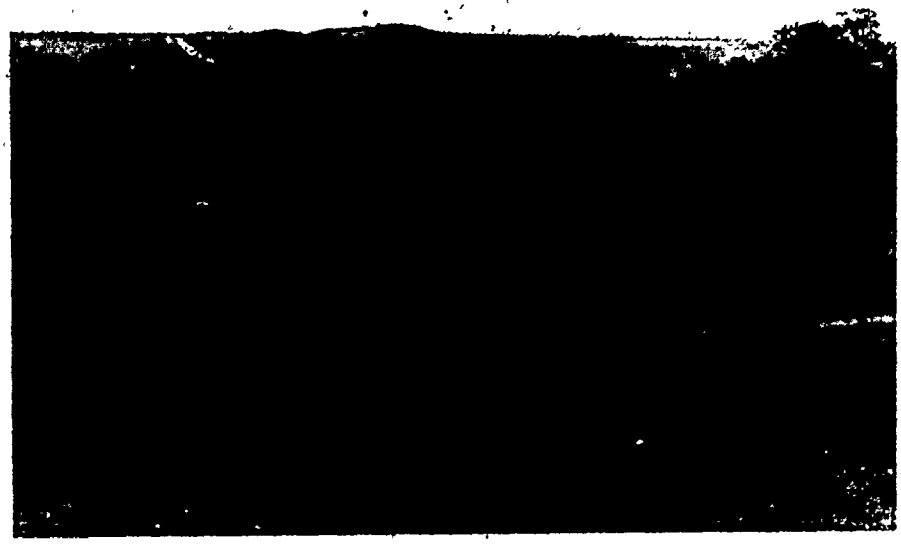

Plate 3.2 Flat-topped hills are remnants of an older coastal plain surface. At the right in the background is the present low relief erosion surface on Méndez shale.

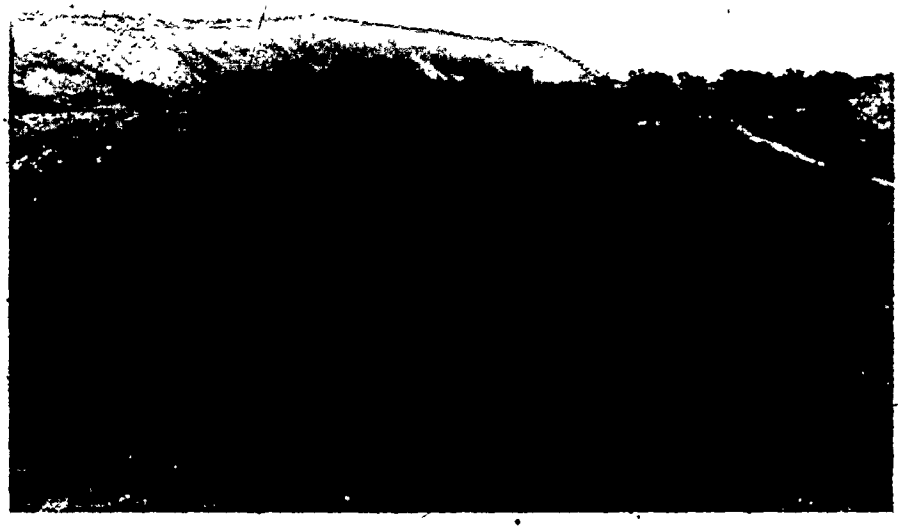

Plate 3.3 Typical relief on the coastal plain near the El Abra range. The gravel cap of the flat-topped hills has been removed and the hills are being dissected.

of the Río Choy, and 28 m where the Río Tampaón passes the southern end of the range. East of the high central portion of the range, the air photos show that the surface has considerable relief, perhaps more than 50 m in places. The area between the Santa Clara and Tantoán springs appears to be the most rugged. Some of the interfluves, e.g. on Rancho Tampacuala northwest of Tamuín, also suggest an older erosion surface, although not necessarily the one cited at El Choy. In the vicinity of Cd. Mante, the surface has low relief and rises to meet the scarp at 100-130 m elevation. There is only one residual hill at 220 m elevation to suggest older erosion levels in that area (Plate 3.1).

The topographic character of the east face may be seen in Plate 3.4. The upper half of the scarp is very steep, locally nearly vertical, and composed of the El Abra reef facies. The surface of the coastal plain, developed on the Méndez, becomes steeper and more dissected adjacent to the scarp. From a somewhat arbitrary "foot" of the scarp, the slope steepens and may be composed variously of the Méndez, San Felipe, or El Abra Formations, or of talus. In four places where limited investigations were made, the bedrock of the lower portion of the scarp was almost completely covered with boulders of El Abra limestone that had fallen from above, or by soil and thick vegetation. At the Nacimiento del Arroyo Seco on Rancho Peñon near the middle (north-south) of the range, the El Abra limestone is exposed by the spring at the base of the scarp; but Méndez shale crops out a few tens of meters downstream and in patches a hundred meters to the south on the lower slope of the scarp, where it is well above the spring level. The eastward dip of flaggy beds in the Méndez indicates that folding may be of considerable importance.

Plate 3.4 The eastern escarpment of the El Abra range in the high central zone. The steep upper part is developed on El Abra reef facies; talus, soil and occasional outcrops of San Felipe or Méndez are found on the lower slope.

Plate 3.5 Springs rise from the base of the east face and flow across the coastal plain. Here the Mante spring flows from a short cave into a small artificial reservoir.

Study of the air photographs reveals east dipping beds (either San Felipe or flaggy Méndez beds) and probable small anticlines in several localities along the east face. It appears that impermeable rocks normally extend some distance up the scarp, perhaps as much as 100 m or more in the central portion of the range. South of the Santa Clara spring, there are topographic features near the base of the scarp that appear (on air photos) to be small east-dipping hogbacks, formed where streams have cut across and behind resistant beds in the Mendez or San Felipe formations. The break in slope that often occurs about half way up the scarp might be caused by a facies change within the El Abra limestone or by the change from Méndez, San Felipe or talus to barren limestone. Based on observation and a few measurements, the scarp has an average slope of around 30°-35°, a minimum of about 25°, and slopes as great as 45° in the vicinity of springs.

Many springs discharge from the base of the range (Plate 3.5). Most of them are small. The two largest springs are the Choy and the Mante, at the opposite ends of the range. At most of the spring sites observed in this study, the discharged water rises vertically from some undetermined depth into a "rise pool". One exception is the Arroyo Seco spring (on Rancho Peñon), which has a horizontal "water table" passage for at least the first few tens of meters. The flow from the springs cuts more deeply and laterally into the coastal plain at the scarp than the nearby surface streams, stripping away the impermeable rocks back to the El Abra limestone. Thus, a sort of re-entrant is formed in the Méndez, but no significant steepheads or pocket valleys in the El Abra limestone are known. William H. Russell (personal communication,

unpublished manuscript) and Mitchell, Russell, and Elliot (1977) have suggested that the scarp has [sometime in the past] been etched backward in a number of places by swamps to form a "corrosion plain". They cite as an example the Nacimiento del Río Santa Clara, where the "[solutional] encroachment has progressed about one-half kilometer" (Mitchell et al., 1977, p. 13); and Russell (personal communication) states that the Santa Clara spring now lies about 500 m east of the base of the scarp. These statements must be incorrect because the erosional morphology and other characteristics shown on the air photos of the area near the spring indicate the bedrock is the Méndez shale (or San Felipe) rather than the El Abra limestone, and the spring occurs essentially <u>at the base</u> of the scarp (within 50 m). From the field observations and air photo analysis made during this study, it is concluded that solutional encroachment has not steepened the scarp, and probably has never had any significant effect on the El Abra range. This conclusion is supported by the lack of "swamp slots" or "solution notches" commonly found where swamp waters impinge laterally on a limestone surface (Wilford, 1964; Jennings, 1971). Lateral solution encroachment as suggested by Russell (personal communication) may be important near Micos in the valley west of the Sierra La Colmena.

Common features of the upper part of the scarp are fracture controlled recesses, as shown in Plate 3.6. Usually they are oriented vertically, but a few run diagonally down the slope. Some of the larger recesses are found where caves developed along fractures are collapsing. It is believed that most of the recesses are formed by enhanced solution and rockfall along fractures. Perhaps the majority of the talus

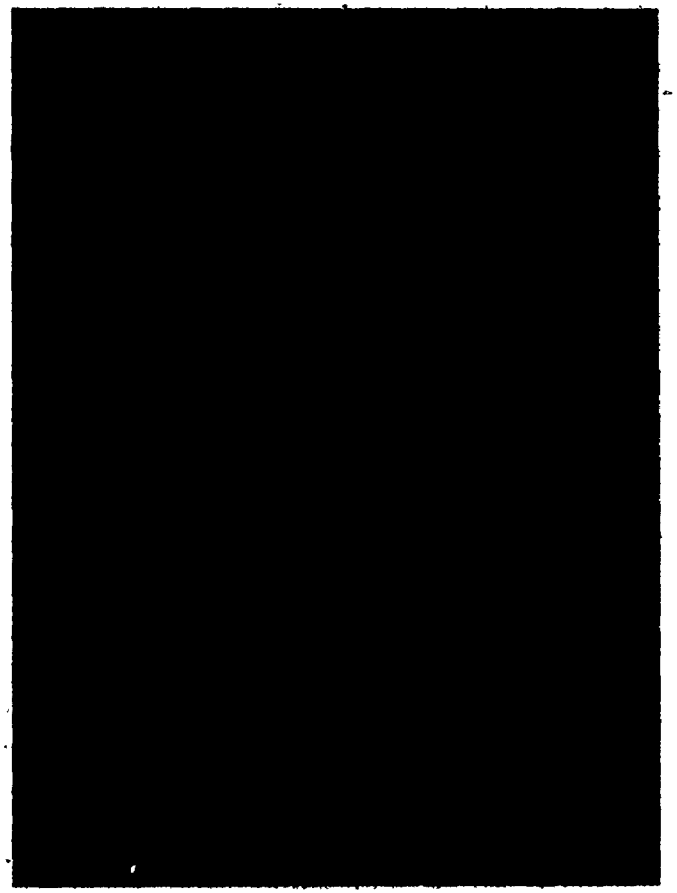

Plate 3.6 Fracture-controlled recesses in the east face. In some cases caves are developed along the fractures and have partially collapsed. This photo shows Cueva de las Cuates in the high central part of the range.

Plate 3.7 The surface of the crest of the El Abra range. There are many small vadose shafts (lapiez wells). Note the vegetal debris, loose blocks, and cactus.

on the lower slope is derived from retreat of the fractured rock. However, in some places gullies appear to reach high up the scarp, thus sometimes confusing the issue. Also, there are several clear examples of what are herein called "spillways" or "chutes" where streams have flowed off the top of the range, spilling down the face. Two prominent ones north of the Choy spring are indicated on the geomorphic map (Figure 3.2). A few of these chutes appear to be supplied with water from collapse dolines at the edge of the crest, and thus are still active.

3.1.2 The Crest of the Range

The top of the El Abra range has a relatively flat surface (Plates 3.1 and 3.4), rather than a rounded or sharply crested ridge. As indicated on the maps (Figures 3.1 and 3.2), it maintains a remarkably similar width of 2.5-3 km throughout most of its length of 140 km. The crest strata have low dips, and an anticline or west-dipping monocline marks the western boundary of the crest. The present surface is developed entirely on El Abra limestone, except for a few small patches of San Felipe just north of the North El Abra Pass (Figure 3.1). Observations in the southern part of the El Abra range show that the surface locally follows closely the structural attitude of the bedded limestone. For example, the anticline at Cueva Pinta and west of Monos (see Figure 3.2) has a moderately dipping (15°-20°) western limb and a gently dipping eastern limb: the ground surface quite accurately reflects the structure. In other places, one may walk for some distance on the same bed of limestone. Thus, the top of the El Abra range is a structural surface, to

a first approximation. However, over the whole length of the structure, much more limestone must have been removed from the high central zone than from the ends.

In the past, the Sierra de El Abra must have been covered by a small thickness of the San Felipe formation and at least hundreds of meters of the Méndez formation (and possibly by lowest Tertiary beds as well). The relevant facts are: 1) small patches of the San Felipe occur on the top of the range, near the North El Abra Pass; 2) at its southern end, the El Abra limestone passes into the subsurface, beneath a great thickness of Méndez; 3) J. Carrillo (1971) reports that the Méndez is over 1000 m thick southeast of Aquismón and several hundred meters have been penetrated in coastal plain wells near the El Abra range; 4) geomorphic evidence concerning the paleo-hydrology of El Abra range caves (to be developed in later sections) requires the coastal plain impermeable rocks to have formerly reached at least the highest present level of the Sierra de El Abra; 5) the Río Comandante (La Servilleta Canyon) and the stream which created the now dry North El Abra Pass (between Mante and Antiguo Morelos) are believed to have been superimposed on the El Abra structure; and 6) the structural and stratigraphic relations of the formations show that the folding (and faulting?) took place after, or possibly began very late in, the deposition of the Méndez; Muir (1936) says that the tectonism occurred during and after deposition of the lower Tertiary Chicontepec beds. Hence, at one time, the Sierra de El Abra had a thick impermeable cover.

As the less resistant impermeable cover was eroded from the top

of the range, the limestone was laid bare to form approximately a stripped structural surface. This process of course first exposed the limestone in the high central part of the range. As the regional base level has lowered (relative to the structure), the stripping progressed to the north and south along the axis of the structure and down its flanks as well, creating the present condition. Vestiges of the paleo-fluvial system that lowered onto the El Abra limestone are indicated by a network of dry valleys, "spillways" on the east face, and notches in anticlinal ridges along the western edge (Figure 3.2). The dry valleys are generally dendritic, but are structurally controlled in places. Some can be traced to "spillways" on the east face or to wind gaps on the western edge with associated dry valleys on the flanks. Evidently, the channels continued to function for some time after reaching the limestone, but gradually dried up as the impermeable interfluves were removed and secondary permeability developed in the El Abra formation. The valleys are most easily traced in the lower parts of the crest, such as near the South El Abra Pass. Only the largest paleo-fluvial features survive in the high part of the range. Karst solution has been active in the higher areas much longer than in the lower areas and has undoubtedly removed more of the El Abra limestone there; thus, most of the paleo-fluvial pattern has been obliterated. Figure 3.3 shows the morphology and drainage pattern of the North El Abra Pass area. Particularly important here are the patches of the San Felipe formation, which occur in synclinal depressions at 240-270 m elevation, and the erosional features caused by runoff from these impermeable beds. A much greater thickness of the San Felipe and Méndez will have covered the whole

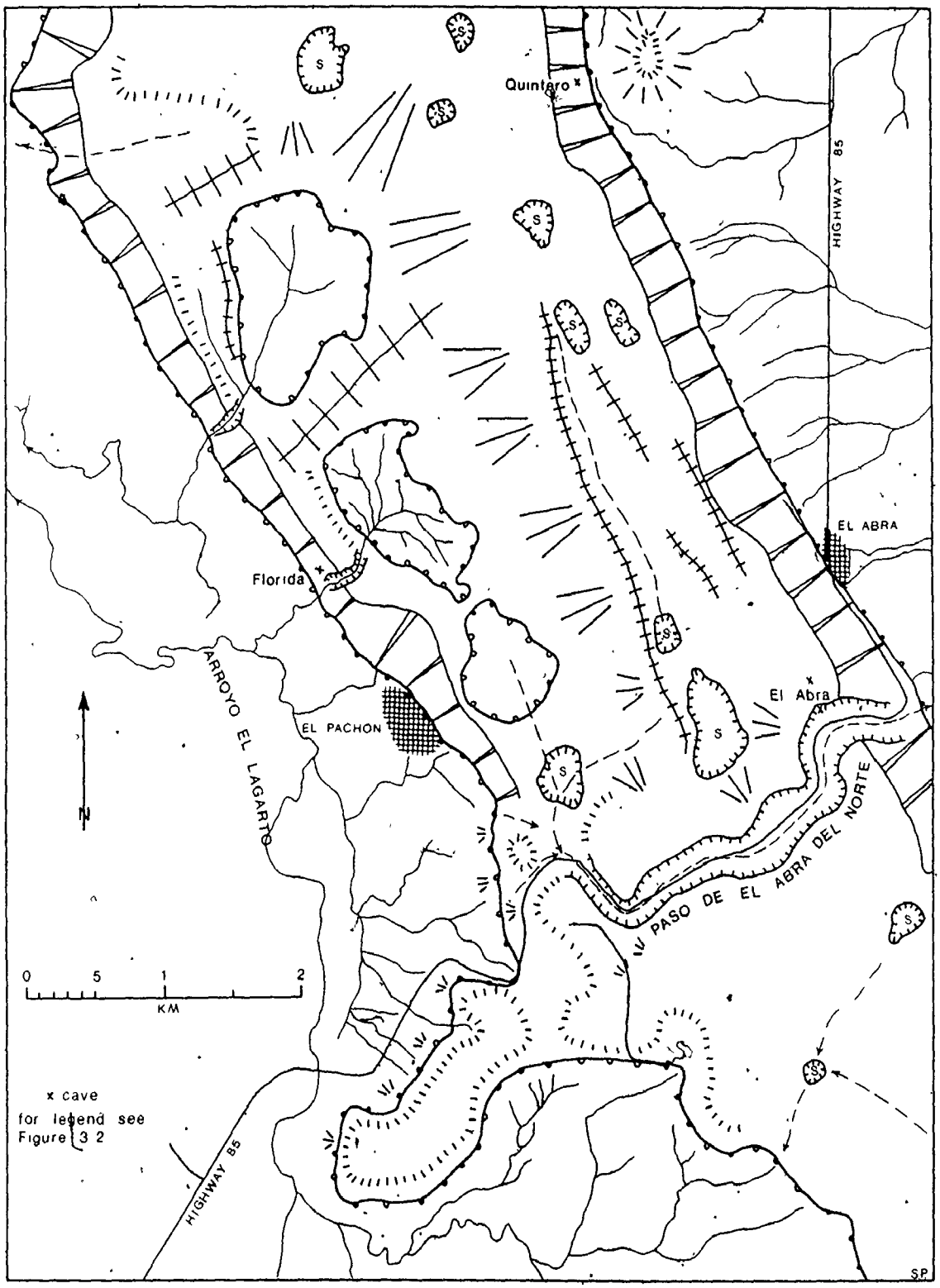

Figure 3 3 Geomorphology of North El Abra Pass area showing effect of San Felipe beds on the range.

area in the past, thus enabling streams to easily erode headward across the low anticlinal ridge along the western margin of the crest, and then to lower onto the El Abra limestone where they cut narrow gorges. This pattern -- an anticlinal ridge on the western margin of the crest, breached by a wind gap that joins an adjacent synclinal (and sometimes faulted) dry valley on the east with a dip-slope valley on the western flank of the range -- is common in the Sierra de El Abra; but in most instances, all the impermeable rocks have been removed.

The present surface of the crest has a variety of small scale solution features. In some places, the beds seem nearly unbroken, and only small solution hollows and channels have formed. In other places, joints have been dissolved downward 1-2 m to form lapies. Loose blocks of limestone are common. Much bare rock is exposed, and where there is soil, it commonly consists of no more than a few centimeters of vegetal matter (Plates 3.7 and 2.1). Some fine sediments and organic material are washed into open joints and broad depressions. A few of these depressions have sufficient soil to grow crops, but nearly all of the Sierra de El Abra is covered by vegetation (scrubby thorn forest) specifically adapted to life with little soil, very low moisture, and a strongly seasonal climate.

Large scale karst features on the crest are limited to two types of sinkholes. None of the "typical" tropical karst forms such as haystack hills, mogotes, or cockpits are present; nor are there poljes as found in many karst regions. Study of air photographs shows a considerable number of dolines that are believed to have been formed by surface

solution processes (indicated by an "S"). However, their density appears to be much less than the doline fields of Kentucky and Indiana, and their morphology is somewhat different because of the lack of soil. Their width varies greatly, ranging up to several hundred meters, but their depth below closure is usually not more than about 10 m. An attempt was made to trace the closure line of these dolines on the geomorphic map (Figure 3.2). Most of the larger solution dolines occur along the supposed paleo-drainage lines. In some places along these fossil drainage channels dolines deeper than 10 m have formed, apparently by surface solution. Large lineations several kilometers long appear on the photographs. They indicate major transverse or longitudinal fractures, probably faults, in the El Abra limestone. Some of these fractures have been especially favorable sites for surface solution processes, thus forming greatly elongated solution dolines and possibly bogaz, and solution depressions and trenches that are not closed. In many places, the east face of the El Abra gives the impression of having a "double crest". At these places a parallel valley, typically 30-50 m deep, lies a few hundred meters behind the first ridge; and another ridge sometimes higher than the first, lies along the west side of the valley. This morphologic feature (the valley) probably has been created by some combination of folding, faulting, paleo-fluvial erosion and enhanced solution along fractures. One or two fracture lineations commonly may be traced (on air photos) in the valley over distances of several kilometers.

The second type of sinkhole found in the El Abra is formed by stoping of ceiling rock in underground chambers until the ground surface is finally reached. These are collapse dolines (marked with "c"

on Figure 3.2). They range in size from 10 m across to spectacular ones more than 300 m across and 100 m deep (Plate 3.8 and Figure 3.4). That they are indisputably created by cave collapse will be shown in Chapter VI. Many of them are about three times as long as they are wide, and the elongated direction is usually parallel or perpendicular to the axis of the range. Others are roughly equi-dimensional in plan view. Many of them have some nearly vertical or overhanging walls as in the Caldera, while others have sloping walls that have apparently been partially degraded. Virtually all of the large collapse dolines occur between the North El Abra Pass and the latitude of Los Sabinos, i.e. the high central portion of the range (above 450 m).

3.1.3 The Western Flank and the Valles or Antiguo Morelos Valley

Just as on the crest, the impermeable cover has been removed from a large part of the western flank of the Sierra de El Abra to expose the El Abra limestone. Between the North and South passes, the belt of limestone on the flank usually has a width of several kilometers, reaching a maximum of about 6 km. At the ends of the range where the structure subsides, the flank is very narrow. Near the anticlinal western crest dips reach 20° or more to the west, while the lower part of the flank has lesser dips, circa 5°. Many small folds occur on the flank causing greater variation in dip, local relief, and geomorphology than occurs on the crest of the range.

The present and past drainage systems of the western flank and the Valles-Antiguo Morelos valley are easily traced on air photos (see

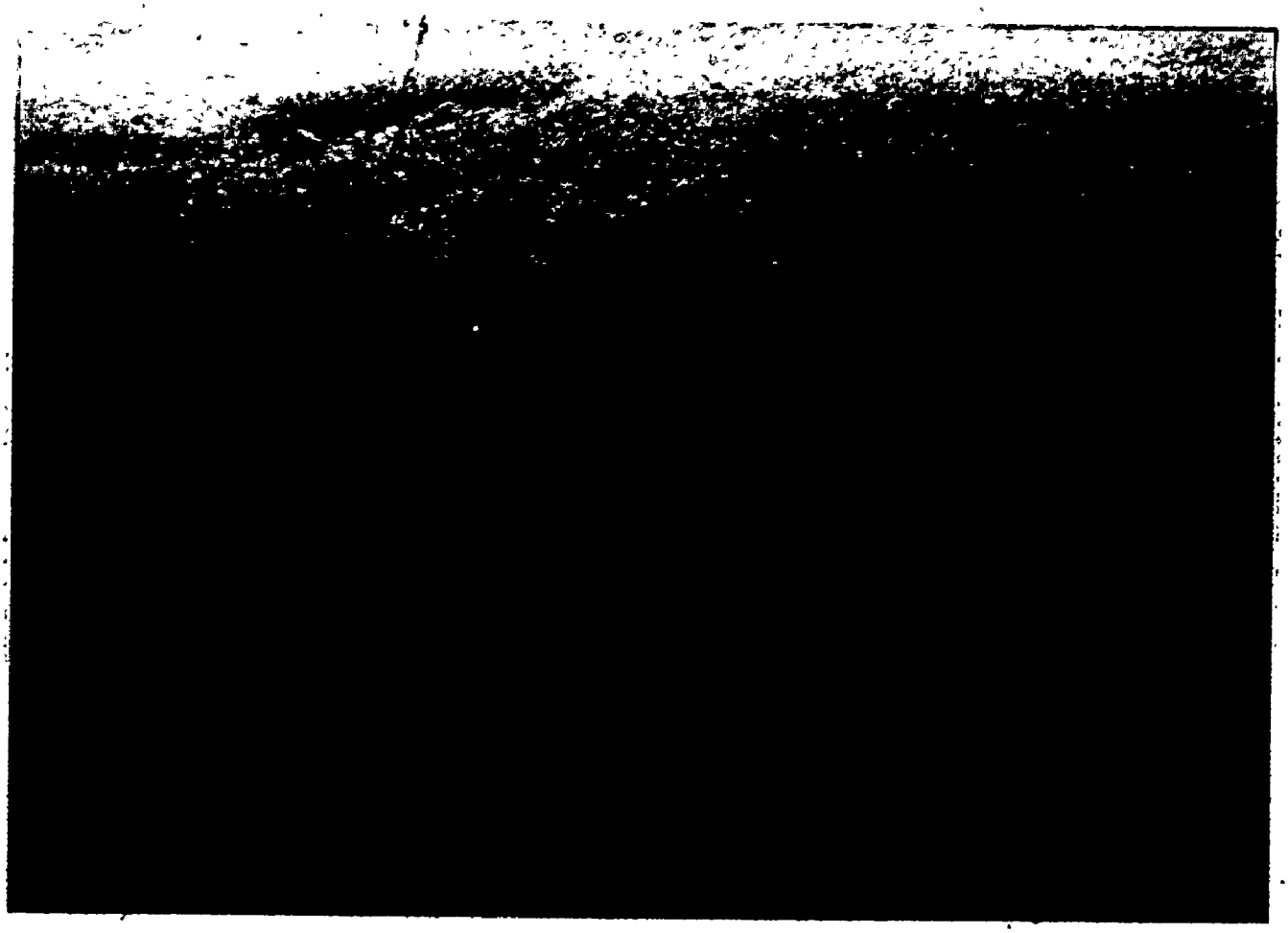

Plate 3.8 The Caldera, a giant collapse doline on the crest of the El Abra. It is 425 m long, 245 m wide, and 90 m deep. Another, having sloping sides may be seen in the background. Soil collects in these dolines, and supports a different vegetation than the surface.

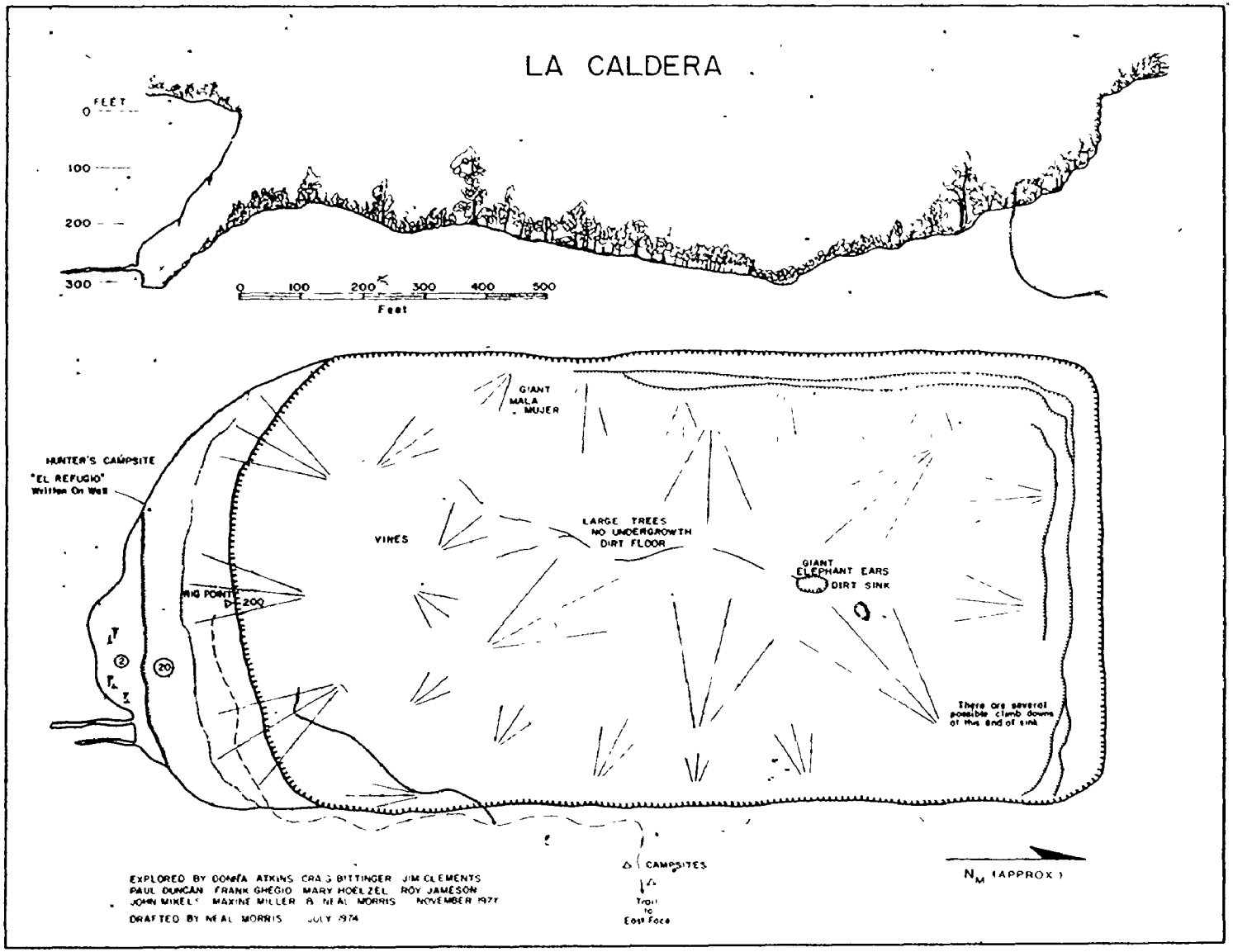

Figure 3.4 Map of Caldera, a large collapse sinkhole.

Figure 3.2). It is clear that the present condition is merely an "instant" of the continuing process of erosion of the impermeable cover from the El Abra limestone, followed by the development of a karst. The presently active fluvial systems are developed on the impermeable rocks. Their valleys usually continue headward onto the limestone surface, where they are equally well formed, but they are believed to be dry valleys. The fossil streams were generally oriented down the dip and they dissected the flank to form valleys often 50 m deep (estimate). The local erosional relief appears to be greater on the flanks than on the crest. It must have taken some time to remove the impermeable rocks from the interfluves, but presently the only cover remaining is found on knobs and ridges low on the flanks where the valleys leave the limestone. A few of the "dry" valleys have the appearance (on air photos) of being still active. For example, many of them do not seem to have a significant profile discontinuity between the parts developed on the El Abra limestone and on the impermeable cover. More field observations of the character of the "dry" valleys should be made, particularly during heavy storms, although access is difficult at those times. The whole limestone surface is presently being lowered by karst solution processes, and numerous closed valleys have formed. It is believed that the fossil surface drainage networks on the El Abra limestone have been almost totally destroyed, and that water now enters the subsurface via a great multitude of small infiltration points (mostly opened joints, but also bedding planes).

The small streams on the west flank of the Sierra de El Abra are tributary to larger, strike-oriented streams. A drainage divide

occurs 5.5 km north of the state line at an elevation of 290 m (the lowest point). The Arroyo El Lagarto (also called Arroyo Terroncillos) is the principal northern stream and it flows to the Río Comandante. The Río Puerco (or Arroyo Grande) is the principal southern stream and it flows southward along the western side of the valley to join the Río Valles. From about 3 km northeast of Cd. Valles, Highway 85 follows for about 13 km the crest of a north-south trending anticlinal ridge that has had an important effect on the local drainage pattern (see Figure 3.2). The ridge, here named the Sabinos Anticline, is a resistant structural high presently reaching just over 300 m elevation which allowed another strike-oriented stream to develop on the Méndez shale in the syncline between the Sabinos Anticline and the main range. This stream is here named the Río Sabinos (distinct from the Río Sabinas in the Gómez Farías area), after the village of Los Sabinos. The name is applied to the fossil river in this valley, and loosely to the present disrupted drainage as described below.

The Río Sabinos eroded downward until it impinged on the El Abra limestone in a number of places. Eight major and an unknown number of lesser stream piracies have occurred over a period of time, so that most of the drainage is now diverted underground. The piracies occur at large joints that often have a vertical range of more than 50 m. Once the diversion is effective, the stream begins to erode downward rapidly because the piracy causes a sudden lowering of local base level. An arroyo, initially developed on San Felipe beds, is shown in Plate 3.9 where it has passed against the dip onto the El Abra limestone, and has cut a deep canyon that leads to a degraded capture point. The amount of

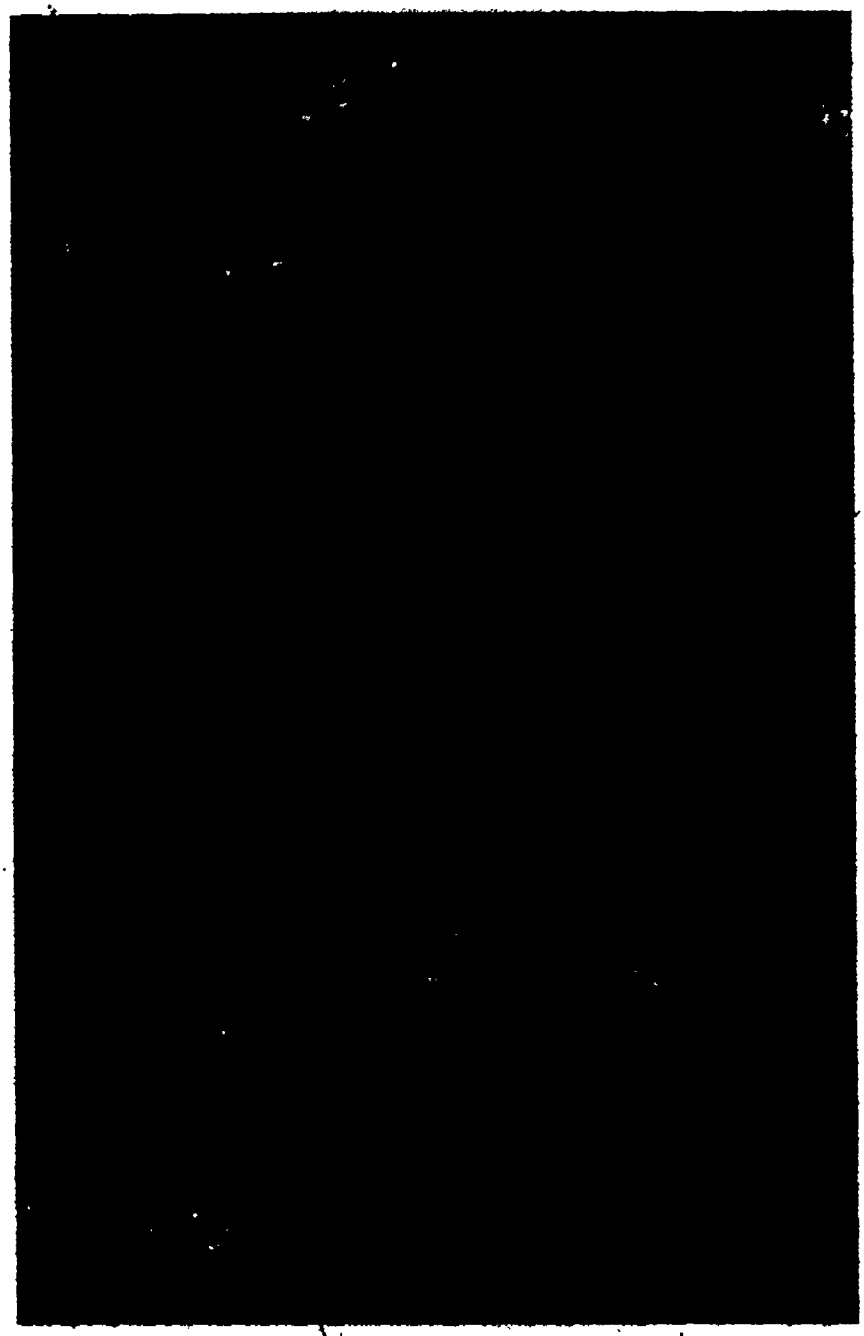

Plate 3.9 Stream capture along the western margin of the range. An arroyo developed on Méndez and San Felipe beds was captured when the stream exposed an 70 m deep joint in the El Abra limestone. The swallet is Sótano del Arroyo (lower right); the Cueva de los Sabinos entrance sink is visible in the upper center.

downcutting depends on the size of the stream and the antiquity of the capture. Mitchell et al. (1977) have illustrated the process of stream capture and degradation of the sink for this area. Most of the pirated waters are provided by runoff from San Felipe beds west of the Río Sabinos, on the east limb of the anticlinal ridge. Mitchell et al. (1977) and Russell (personal communication) have given estimates of the drainage area for each of the pirated streams. Improved estimates based on air photos are listed in Table 3.1. The areas should be accurate to ± 5%, except for the smallest ones. Only the drainage area on impermeable rocks is given (basin boundaries are shown in Figure 3.2). The drainage basin of some of the swallet streams may be significantly different (usually smaller) than in the past because upstream piracies may divert some of the flow underground or to another surface channel out of the basin. Also, the area of impermeable cover may have been slightly reduced during the time the swallet caves have existed. The air photos show that formerly there were many tributaries to the Río Sabinos from the east side of the channel, i.e., the west flank of the Sierra de El Abra. These sources have largely dried up as most of the impermeable cover has been removed and the channels have become karstified.

A morphologic pattern similar to that described above occurs higher up the west flank of the range. Two and one-half kilometers east of the Río Sabinos, there is a very large (300-1000 m wide) strike-oriented dry valley (Figure 3.2) that developed where the dip reduces or possibly reverses direction (anticlinal (?) ridge on the west side of the valley). It formerly received runoff from many dip slope tributaries on its eastern side. At the upper end of the valley in the

TABLE 3.1

Drainage Area of the Swallet Caves

CAVE	DRAINAGE AREA IN KM^2
Sótano de Venadito	7.7
Sótano de Yerbaniz	21.8
Sótano de Matapalma	1.9*
Sótano de Japonés	8.6
Sótano del Tigre	4.4
Sótano del Arroyo	12.4
Sótano de la Tinaja	5.1
Sótano de Montecillos	8.4
Sótano de Jos	4.3
Sótano de las Piedras	0.3*
Sótano de Palma Seca	0.7*
TOTAL AREA OF SWALLET CAVE BASINS	75.6 km^2

* was previously much larger, but is now reduced by upstream piracy (see Figure 3.2)

vicinity of Sótano de Soyate, the present valley floor has an elevation of about 290 m. The drainage was to the south, where it eventually turned southwest to join the Río Sabinos. Now the area is completely karstic, and includes development of closed solution valleys, but the largest geomorphic features are the paleo-fluvial valley and intervening ridges. Another 1.5 km up the west flank from this dry valley there appears to be yet another, although smaller, strike-oriented valley that likewise eventually joined the Río Sabinos.

North of the Los Sabinos area, the Sabinos anticline apparently plunges, which allows local streams to flow westward to join the Río Puerco. However, 20 km north of Cd. Valles, this or another anticline rises sufficiently high that two streams have eroded down to the El Abra limestone, and have been pirated. Three large swallet caves, sótanos Japonés, Matapalma, and Yerbaniz have developed about 3 km west of the El Abra-San Felipe contact along the west margin of the range. One other important swallet cave near the state line, Sótano de Venadito, is formed where a stream flowing from a synclincal valley having an impermeable cover, crossed an anticlinal ridge to the west and was captured underground when the El Abra limestone was reached.

3.1.4 Passes in the El Abra Range

There are three large wind gaps and only one water gap in the Sierra de El Abra (Figure 3.1). Two of the wind gaps are called Paso de El Abra or sometimes simply El Abra (the opening); hence, it is proposed here to refer to them more specifically as Paso de El Abra del Sur (South

Pass) and del Norte (North Pass). South Pass occurs in the southern El Abra east of Cd. Valles (see Figure 3.2). Its fossil river first impinged onto the El Abra limestone probably at about 300-350 m, and cut downward to about 160 m at the west end (high end) of the pass. Initially, the drainage may have included all of Río Valles and the Río Sabinos (Section 3.1.3). If so, it was probably altered relatively early by stream piracies to look nearly like the present drainage pattern(Figure 3.1), with only the ancient Río Sabinos continuing to flow through it. Finally, the pass was abandoned as the west flank of the El Abra became karstified, some streams were pirated underground, and still others captured by the Río Valles. For some time there was also a significant tributary network developed on the crest in the vicinity of the pass, particularly on the north side, that created the most dissected part of the crest.

North Pass crosses the range between Antiguo Morelos and Cd. Mante (Highway 85 uses the pass). The river that created it first reached the El Abra limestone probably around 450 m at the point where the range has a NW-SE kink and where it has subsided from the high central zone. The river cut downward exposing more limestone down the SW dip until it reached 250 m (see location map inset in Figure 6.4). Then the stream was captured by the modern Arroyo El Lagarto which is tributary to the Río Comandante.

The third wind gap is called Puerto Chamalito on the new 1:50,000 topographic maps (Loma Alta, no. F-14-A-59), and it is taken as an arbitrary northern boundary of the Sierra de El Abra. On air photos, it is

larger and more spectacular than all other gaps in the El Abra. It crosses the range where the crest is presently about 400 m. A river that formerly drained the southern flank of the Sierra de Guatemala passed through the canyon. Ultimately, the tributary streams were either pirated underground or captured by the Río Comandante; the area is now completely karstic.

The Río Comandante (also called Río Ocampo and Río Boquilla) forms the only contemporary water gap in the El Abra range at Cañon Servilleta. This river collects runoff from the northern Antiguo Morelos valley and the Ocampo valley west of the Sierra Tamalave. It has captured all the surface runoff in this area because it had the advantage of crossing the Sierra de El Abra where the El Abra limestone is structurally lower than at any other place in the north -- about 220 m elevation. The river is believed to be superposed on the El Abra. At present, it has cut downward to 120-130 m at the west side where there are rapids and waterfalls, and to 73 m on the east side. A much deeper canyon occurs where the Comandante crosses the Sierra Tamalave.

3.1.5 Origin of the Escarpment of the Sierra de El Abra

Although it was not an objective of the thesis research to determine the origin of the escaprment on the east face of the Sierra de El Abra, some pertinent facts concerning this problem have been observed. The origin of this most striking feature has been a controversial subject for many decades. A fault has been advocated by Bonet (1952), Muir (1936), [illegible] and [illegible] a is [illegible] by

(1940) and Mitchell, et al. (1977); and a steep platform edge is suggested by Griffith et al. (1969), Enos (1974), and to some extent by Rose (1963). A preliminary report on the results of this study (Fish and Ford, 1973) gave a cross section having a faulted scarp, in accordance with most Mexican geological reports but no direct evidence of a fault has been observed during this research. Most of the authors recognize that in the vicinity of the scarp, there is a transition zone from platform to basin facies limestones, and a few seem to suggest that there may be a combination of steep platform edge and faulting. The field observations and arguments of previous authors will not be reiterated here, although they are taken into some account, especially where confirmed in this study. Instead, what is offered are the observations made during the field work, and an analysis of new and old drilling information. The lack of deep borehole data very near the scarp has hindered resolution of the problem.

Two important wells have been drilled in recent years (Carrillo Bravo, 1971). The Pozo Tamlihuale No. 1, located 4 km west of the reef and near El Pujal, penetrated 1808 m of the El Abra formation, followed by 287 m of Lower Cretaceous and Jurassic beds before reaching metamorphic rocks (basement?) at 2011 m below sea level. Pozo Trangulo No. 1, located 3 km east of the Sierra de El Abra, cut 394 m of Upper Cretaceous beds, only 373 m of the El Abra, followed by 452 m of Lower Cretaceous and Jurassic beds, ending at a depth of 1128 m below sea level in the Jurassic (well invaded by water, probably fresh). In the latter well, the El Abra formation is the fore-reef facies and consists of 250 m of porous and permeable dolomite overlain by 115 m of dolomites that alternate with beds of calcarenites and oolites. Other wells 6 to 10 km

east of the Sierra de El Abra encounted either a "mixed facies" (Tamabra) which is composed of interfingering beds of reef debris and dense dark lime mudstones with chert (basin facies), or just the basin facies. Carrillo, 1971, calls the basin equivalent of the El Abra the Cuesta del Cura, rather than the Tamaulipas, which he correlates with the Lower Cretaceous platform facies. These wells clearly show that the middle Cretaceous beds thin by a factor of five times in a very short distance, and continue to thin until diminished by a factor of 10-20 times. Also, they show that the Jurassic beds are about 800 m structurally higher under the west edge of the coastal plain than under the east edge of the Platform. Thus, the reef zone cannot be more than perhaps 2 km wide. In fact, it may scarcely be wider than the outcrop, but may have migrated slightly with time. Exactly the same relationships as described here are reported for the Golden Lane Platform by Viniegra and Castillo-Tejero (1970), where the same problem has been argued.

Mitchell, et al. (1977) have argued that the El Abra reef is possibly 8 km wide, nearly all of which is buried below the coastal plain; that the east face of the range is the upturned west edge of the reef (and thus is essentially a dip slope); and that the folding occurred approximately at the junction of the weaker, bedded backreef limestones with the massive reef. As shown above, a "massive" reef does not exist in the area. The most likely locus of deformation would be the transition zone from the massive platform limestone to the thin basin facies limestone and weak overlying shales. The structural relief on the Lower Cretaceous and Jurassic beds described above suggests that a deep seated structure such as a fault block resisted the eastward tectonic movements

along the platform edge. The section of basin Cretaceous and Jurassic rocks presently known hardly seem capable of providing sufficient resistance to cause a major fold in the Platform limestones.

Other significant points concerning the scarp as noted in this study are:

1) The Méndez shale occurs directly at the base of the scarp and probably for a short distance up the face. Dips in these beds seem to be proof that some folding did occur.

2) There appears to be little structural relief on the crest of the range, although small folds and some longitudinal fault (?) traces may be seen on air photos. Strata exposed in the North and South El Abra passes and in caves remain horizontal to the reef zone. Thus, nearly all of the structural relief of any alleged deformation must be located between the top and the base of the escarpment.

3) The dips of facies (bedding) planes in the reef (which may not have been horizontal originally) as exposed in caves, and stratal dips in the Méndez or San Felipe at Nacimiento del Arroyo Seco on Rancho Peñon are much less than the steepness of the escarpment. An extreme case occurs at Grutas de Quintero (Chapter 6) where the dip of a major facies plane is about 5°, much less than the slope of the east face there.

4) None of the caves in the east face or on top of the range that have been investigated in this thesis bear any trace of the intense crumpling, shearing and faulting that would be expected in the interior of

a major fold. A cave that is presently being explored (Neal Morris, 1976) is partly developed in one of the supposed faults just west of the top of the east face; however, it does not seem likely that there is a large vertical displacement along the fault because it has no effect on the surface relief.

5) The slope of the scarp must be slightly reduced from times past by erosional processes, particularly solution and rock fall.

6) The width of the reef zone remains about the same throughout the length of the Sierra de El Abra. Just south of the North El Abra Pass, where the range turns to the northwest, N-S trending folds in the bedded facies on the crest are truncated at the northwest trending reef. The implication is that the present escarpment represents the upper part of the Platform edge, and that some deep-seated basement structure or topographic high controlled the locus of original reef development.

The data indicate that some folding has occurred but only part of the relief of the escarpment can be attributed to it. Much of the relief must be caused by exhumation of a steep platform edge, or by faulting, or both. Thus, some sort of combination model, possibly involving all three suggested origins, must be developed. It is suggested that the Platform edge was shoved eastward, up a steep basement slope or against a basement fault block to create the present Sierra de El Abra structure. The Platform edge (east face of the El Abra) would thus be uplifted relative to the basin rocks, causing some folding and possibly

faulting.

3.2 Karst Geomorphic Features in the Region

A brief description of some of the karst landforms in the rest of the Valles-San Luis Potosí Platform region will be given in this section. The discussion is unfortunately far from comprehensive, because so little is really known about the region. Reconnaissance trips have been made into some areas, but a large portion of the karst area has never been observed.

At its north end, the Sierra de El Abra merges into the Sierra de Guatemala, a much larger structure. It is a huge anticlinorium, having more than 2 km of structural relief, and reaching an elevation of 2320 m. The upper Cretaceous rocks were removed long ago, but the paleo-fluvial valleys can be traced up to at least the 1000 m level. A very rugged surface has developed that includes intense karren formation, karst pinnacles, hoyas (irregular closed karst valleys, commonly 200-1000 m wide and 25-100 m deep), areas of cone karst, fracture controlled solution corridors or valleys, collapse structures, caves and pits, and a polje at the village of Joya de Salas. On the east and south flanks of the range, the wettest areas, the precipitation probably exceeds 2000 mm, and there is a thick tropical jungle. Except the west side of the range where there may be some surface runoff, all rainfall sinks rapidly into the karst. Most of the ground water flows to the great springs at the head of the Río Frío; another important spring lies on the Río Sabinas.

The most spectacular karst landforms and scenery in the region occur in the Xilitla and Aquismón areas, south of Cd. Valles (Plate 3.10). There the elevations range from 100 m to 3000 m, and the rainfall may exceed 2500 mm per year. Intense karstification has produced landforms similar to the classic tropical karst found in Cuba, Jamaica, Puerto Rico, and the East Indies. Russell (1968) has briefly described the geology and geomorphology of the area west of Aquismón; Bonet (1953) and Russell and Raines (1967) have described some of the caves. Included in the Xilitla-Aquismón area are large karren forms and pinnacles throughout, abundant cone and cockpit karst up to about 1300 m, cones on steep slopes up to about 2000 m, hoyas and shallow dolines, uvalas, at least one polje located west of Tamapatz that is about 1 km wide and 10 km long, and caves and pits. The area west of Aquismón contains some of the world's most spectacular collapse structures, such as the 333 m deep Sótano de las Golondrinas (Fish, 1968). West of Xilitla, there is a massiff that has a large summit area between 2000-3000 m. Solution effects there are intense, but kegelkarst and cockpit karst are generally absent. The Huichihuayán and San Juanito (also called Mujer de Agua) are large permanent springs located along the east margin of the area at the base of an escarpment; other seasonal springs may be found in the interior, particularly along the Arroyo Seco, a major valley in the area.

West of Cd. Valles, the Sierra Madre Oriental comprises a series of N-S trending folded ranges (see Figure 1.1 and Figure 2.5). Most of the ranges reach much higher elevations than the Sierra de El Abra. Nearly all of the impermeable rocks have been removed except in some valleys, and karst solution processes have been active for a very

Plate 3.10 The spectacular Xilitla-Aquismón area karst. The Aquismón area at about 600-1000 m elevation is on the left, and the high plateau above Xilitla is on the right at 2000 m and more. Karst development here is the most intensive in the region.

long time. Karren, dolines, large closed karst valleys, and other karst landforms are abundant; but the classic forms often considered omnipresent in tropical karsts (namely cones and cockpits) have not been observed yet, or are not sufficiently developed to be recognizable. Most of the area has not been visited; but air photos of La Sierra la Colmena and the new 1:50,000 topographic maps show many vestiges of an older fluvial network, and there are some active channels. Part of the area may be considered holokarstic, while the remainder is fluviokarstic. Massive travertine dams, constructional karst forms, are found in Micos canyon, El Salto falls, in the lowest Río Tampaón canyon, and on the Río Gallinas just west of Tamasopo.

Very little is known about the extent of karstification of the El Abra limestone exposures in the western half of the Platform. From a few observations, it is clear that the limestone has undergone significant solutional modification, even though the precipitation is only 300-500 mm per year (rain shadow of the Sierra Madre Oriental). Very few closed valleys are shown on the topographic maps, which have a contour interval of either 10 or 20 m. One large spring, Manantiales de Media Luna, is known. It flows from a 75 m deep lake a few hundred meters across, at the southern end of the large, flat Río Verde valley. Three orifices at the bottom yield the discharged water. Two high mountain karsts have developed that are of particular interest and deserve more study. One is the area west of Jalpan, Querétaro where the mountains are high enough to cause increased precipitation. From Jalpan to Pinal de Amoles (about 3000 m elevation), karst forms are developed in in a variety of climatic zones, structural and lithologic settings and

topographic positions. Some very large caves and collapse pits have been found and a few springs are known. The other significant high mountain karst is located at Valle de los Fantasmos, approximately 30 km east of San Luis Potosí at about 3000 m elevation. The area is named "Valley of the Phantoms" because heavy ground fog often occurs, so that people, animals and objects sometimes seem like apparitions. The area is replete with karst pinnacles, sinkholes and pits.

A large portion of the western half of the Platform is covered by valley flats. Many of the valleys are or were bolsons, although the sediment thicknesses reported by Carrillo (1971) are surprisingly thin. Gypsum karst has been observed in some places and may be fairly common. A wide variety of other landforms occur, but will not be discussed.

3.3 Summary

The erosional history of the region has received very little attention in the literature, and in this study. The early history will be difficult to deduce because the known continental sediments are regarded as late Tertiary or Quaternary age. Segerstrom (1961, 1962) has briefly discussed the erosional history of two adjacent areas to the south and southwest. It appears that erosion on the Platform very likely started in the early Tertiary, or possibly very late Cretaceous. It is suggested that the major rivers were established approximately in their present positions relatively early (middle to early Tertiary), and were gradually lowered onto the El Abra limestone. The Río Tampaón is located in the structurally lowest part of the Sierra Madre Oriental fold

belt, and passes onto the coastal plain just at the point where the Sierra de El Abra structure dives beneath the Méndez shale. It could more quickly erode downward and capture a large drainage area than any of its competitors. Thus, the Río Tampaón is now the master drain for the southern half of the region, and the lowest point in the region occurs where it passes onto the coastal plain. In the north, the Río Comandante and the Río Guayalejo were also established long ago, but their development has been hampered by very high folds and smaller areas of structurally low impermeable rocks or sediments to form catchments. Hence, the Río Guayalejo has not provided as low a base level in the north as the Río Tampaón in the south because its discharge is less and because it has been "held up" by exposures of the El Abra limestone and by basalt flows on the coastal plain. All the major rivers cut across large folds forming spectacular water gaps. For example, the canyon of the Río Guayalejo at the north end of the Sierra de Guatemala is as much as 1000 m deep.

As erosion exposed the El Abra limestone on structural highs karstification began. The limestone in the high central portion of the Sierra de El Abra probably was first exposed during Pliocene time. Remnants of the paleo-fluvial system may be seen on the crest towards the ends of the range where it is lower (and more recently exposed), and all along the western flank. Solution features are most highly developed in the higher part of the range, but virtually all of the range has karstic drainage. The eastern flanks of the higher ranges nearby receive much more rainfall than the Sierra de El Abra, have been exposed much longer,

and have "tropical" karst landforms. The karst landforms found in the region show that a variety of karst landforms occur in tropical karst regions -- cone karst and cockpits do not predominate.

Flat-topped hills on the coastal plain in front of the El Abra range and waterfalls in the Micos and Servilleta canyons suggest intermittent uplifts of the area during later Pleistocene time. A deposit of continental (?) limestone (Heim, 1940) on the hill south of Quintero (Plate 3.1) may have been formed very near sea level during a stable period and then uplifted.

Among the many geomorphic problems that need further examination are: 1) the erosional history of the region; 2) the processes and rate of stripping of impermeable rocks from the crest and flanks of ranges, and of subsequent karstification; stripping of the Sierra Tamalave has lagged well behind that of the Sierra de El Abra; 3) the occurrence of large fossil swallet caves higher up the west flank of the El Abra range; fossil swallet caves with canyons similar to those in the Los Sabinos area should exist, particularly along the previously discussed dry valleys parallel to the Río Sabinos; however, none have yet been discovered and only a few potential sites are known from the air photos; and 4) karst landforms as a function of climate, structural attitude, carbonate rock type and impurities, slope, time and inherited paleogeomorphic forms.

CHAPTER IV

HYDROLOGY AND HYDROGEOLOGY

4.1 Introduction

In this chapter, the basic elements of the hydrology of the region are examined. This includes aspects of the hydrogeology, the hydrology information base, the temporal and spatial distribution of runoff, and the ground water. The treatment will be on two levels. Most of the chapter concerns the regional hydrology, but ground water is discussed at a local level with reference to field studies conducted in the Sierra de El Abra. The objective is to develop an understanding of the hydrology of this major karst area, and to lay the groundwork for the analysis and synthesis given in Chapter VII.

4.1.1 Hydrogeology

An important part of the study of the hydrology of a region is to identify the hydrogeologic units, and their hydrologic properties. In this section, the rock formations will be grouped into four broad categories of hydrogeologic behaviour, and described.

Using state geologic maps provided by the Instituto de Geología, geologic maps by J. Carrillo (1968) and Segerstrom (1961), and the new 1:50,000 Cetenal topographic sheets, a preliminary hydrogeologic map

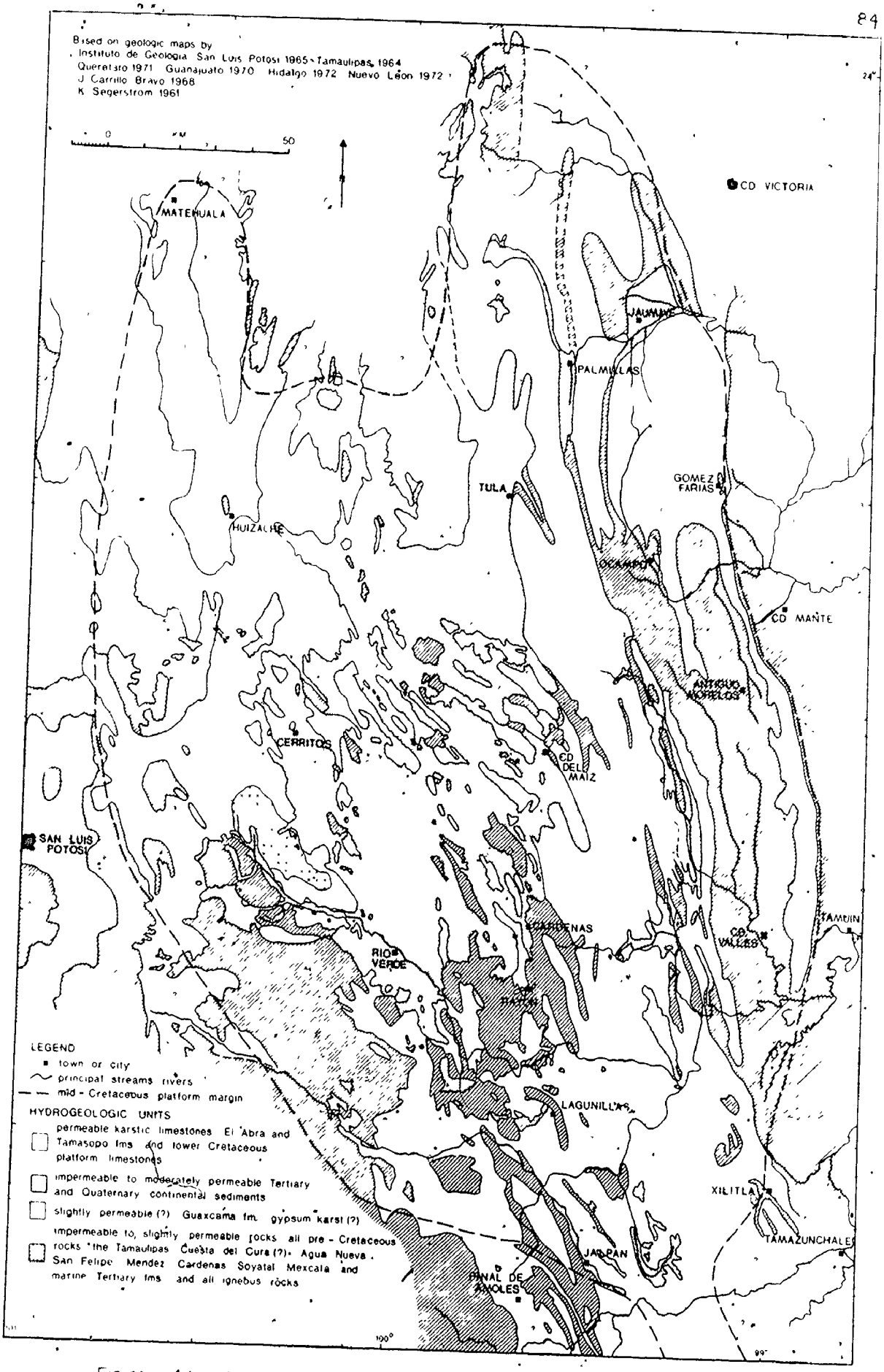

Figure 41 Hydrogeologic map of Valles-San Luis Potosí Platform

(Figure 4.1) has been prepared for the Valles-San Luis Potosí Platform and fringe. Unfortunately, the source maps differ considerably in age, detail of mapping, nomenclature, and type of stratigraphic unit mapped. Recent work of Pemex geologists synthesized by J. Carrillo (1971) has resolved some of the geologic problems in the area, and has provided a much better understanding of the regional geology. However, the scale and paucity of cultural features on his 1968 map make it difficult to use, e.g., to determine exactly the trace of the middle Cretaceous platform edge. It is desirable that more detailed geologic maps be made that employ a uniform nomenclature for rock stratigraphic units, so that among other things, a systematic study may be made of the hydrogeologic units and an improved map assembled.

The El Abra and Tamasopo Formations plus the suspected lower Cretaceous platform facies limestones form the principal aquifer of the region, and its permeability appears to be karstic, i.e., through solution conduits. The El Abra Formation occurs at the surface or in the subsurface over nearly the whole Platform. Around the margin of the Platform, exposures of the deeper water equivalents of these formations may exhibit some secondary permeability. Also, the lower Cretaceous shelf facies limestones may extend north of the middle Cretaceous platform (Enos, 1974). Where the deeper water or lower Cretaceous limestones are mapped adjacent to the platform facies, a question mark (?) indicates uncertain hydrologic conditions. It is thought that most of the total runoff from the region has passed for at least some distance through this karstic aquifer. Where there are steep slopes, thick soil, or insufficiently developed secondary permeability such as on "recent" exposures, surface runoff may

occur.

The second unit comprises all the impermeable rocks. It includes the upper Cretaceous and Tertiary formations of marine origin excluding the Tamasopo Formation (marine Tertiary formations only occur east of the Platform), all the igneous rocks, and a few small exposures of pre-Cretaceous rocks. The San Felipe, part of the Cárdenas, and some of the volcanic rocks may have minor permeability. This unit yields direct surface runoff.

The third unit comprises all the Tertiary and Quaternary continental deposits of sedimentary origin. These sediments have a variety of origins, and are poorly known. Most maps simply show Quaternary alluvium, but several Tertiary units are given on the San Luis Potosí map, and J. Carrillo (1971) briefly describes but does not map two Pliocene age (?) formations. Because erosion of the region commenced in early Tertiary time, there must be deposits dating back to that time in the bolsons of the northwestern part of the Platform, and perhaps beneath some of the volcanic rocks. The sediments include fragments of volcanic rocks and Cretaceous limestones, finer material derived from upper Cretaceous terrigenous rocks and volcanics, and chemical precipitates such as gypsum, tufa, and caliche. The thickness of these sediments is reported by J. Carrillo (1971) to be 20-30 m in the Río Verde valley, and more than 50 m in the large valley northwest of Cd. del Maiz. They are also generally thought to overlie the El Abra Formation, though in places the impermeable Cárdenas Formation might intervene. Thus, precipitation may be able to pass through the sediments into the El Abra limestone. Their permeability

is expected to be highly variable, from insignificant to moderate. J. Lesser (unpublished S.R.H. report, c. 1973) has shown that the potentiometric surface of the large Río Verde valley sediments indicates flow toward the Río Verde. From discharge measurements, he estimates the average annual seepage to be 16 x 10^6 m^3, or an average of 0.5 m^3/sec. Gypsum karst has been observed at a few localities in the long valley south of Matehuala (personal observations, and personal communication with William H. Russell).

The fourth unit is the lower Cretaceous Guaxcamá Formation, which has about 300 km^2 of outcrop in the interior of the Guaxcamá anticline, 40 km northwest of the town of Río Verde. It is dominantly gypsum and anhydrite (at depth), and would not be conducive to deep circulation of water were it not for interbeds of limestone and dolomite. At least some shallow flow seems possible, and a gypsum karst may have formed. It is distinguished from the other units because its hydrologic properties are unknown, and because it is thought to play an important role in the ground water chemistry. In the subsurface, it likely represents an impermeable barrier below the El Abra Formation.

In summary, the El Abra and the Tamasopo Formations plus the platform facies of the lower Cretaceous limestone are thought to form the only significant aquifer in the region, and its permeability is karstic. The areal extent of this unit defines a hydrogeologic province that is expected to have only a small flux of ground water across its boundary. Other rocks in the region are impermeable and yield surface runoff, or are slightly permeable. Most of the rest of this dissertation will be

concerned, either directly or indirectly, with the hydrologic character and function of the karst aquifer, particularly the El Abra Formation.

4.1.2 The Drainage Basins and Gauging Stations

The principal streams of the fluvial network that drain the region are shown in Figure 4.2. About 37% of the Platform area is not integrated into the surface drainage system. Part of the remaining portion yields direct surface runoff from impermeable rocks (refer to the hydrogeologic map, Figure 4.1), but much of the Platform is a fluvio-karst. The two principal rivers are the Río Tampaón in the southern part of the area and the Río Guayalejo in the northern part. Most other streams are tributaries to these two either on the Platform or on the coastal plain a few kilometers from the eastern margin of the Platform.

Mexican water resource planners have established a good system of gauging stations, controlled mainly by the Secretaría de Recursos Hidráulicos (hereinafter referred to as the S.R.H.). Figure 4.2 is taken from a map given in S.R.H. Boletín Hidrológico No. 32 (publication date not given, but after 1968). It shows the location of the gauging stations with reference to the rivers. When more detailed mapping is accomplished, it will be seen that the amount of karst between the channels is much greater than shown on the S.R.H. map.

Some information about the gauging stations, brief basin descriptions, and other comments are given in Table 4.1. Detailed information concerning the type of installation, method of measurement, and the

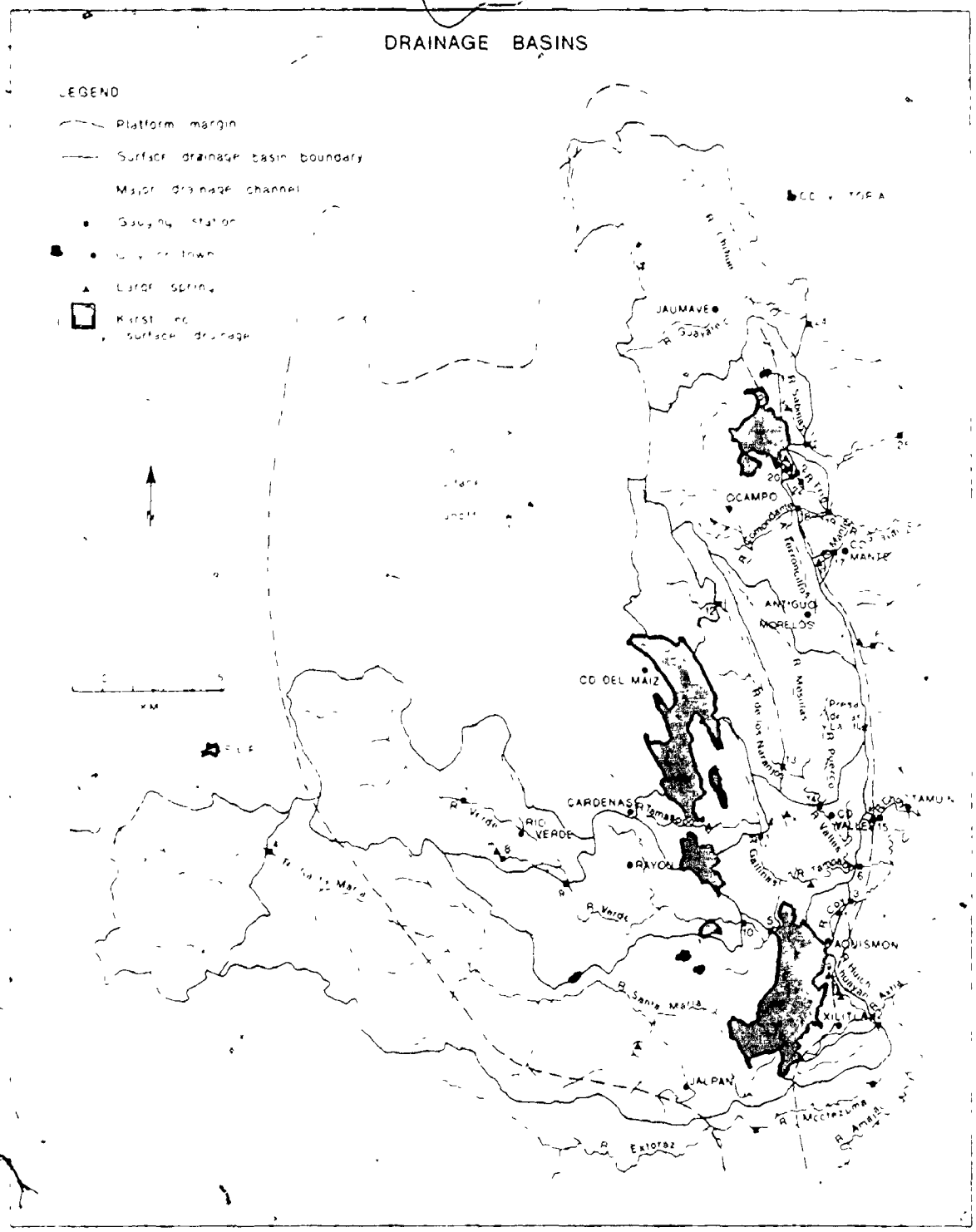

Figure 4.2 Drainage basins and gauging stations of the region. The numbers are keyed to Table 4.1. Springs: a) Choy, b) Santa Clara, c) Manié, d) Frío springs (includes Poza Azul plus others), e) Sabinas, f) Coy, g) Pimienta, h) San Juanito, i) Huichihuayán, j) Agua Clara, k) Tanchachín, l) Puente de Díos, m) Media Luna, n) name unknown

TABLE 4.1

Gauging Stations in the Valles - S.L.P. Region

Gauging Station	Number on Figure 4 2	River	Elevation (m)	Surface Drainage Basin (km^2)	Period of record
Tancuilín	1	Tancuilín	?	321	1961-68+
Pequetemú	2	Axtla	71 1	661	1954-68+
Ballesmí	3	Coy	29.1	194	1954-71+
Ojo Caliente	4	Santa María	1768	2574	1966-68+
Tansabaca	5	Tampaón	174	17532	1959-72+
El Pujal	6	Tampaón	28.2	23373	1954-71+
Nogal Obscuro	7	Verde	1027	2444	1965-68+
(Media Luna)	8	Media Luna	1000	–	sporadic measurements
Vigas	9	Verde	897	3571	1958, 1961-68+
Tanlacut	10	Verde	257	6039	1961-71+
Gallinas	11	Gallinas	280	789	1959-71+
El Salto	12	El Salto	399	900	1948-64 suspended
Micos	13	los Naranjos	210	1978	1961-71+
Santa Rosa	14	Valles	72.8	3521	1959-71+
El Choy	15	Choy	32.2	12(4.9)	1960-71+
Santa Clara	16	Santa Clara	70	16.5 ?	1972-73+
Mante	17	Mante	~ 80	42(69)	1927-30, 32-35,38-61, 63, 67-69, 71, 72+
Canal Oeste (West)	17	West Canal	–	–	1932-35, 38-61, 63, 67, 68+
Canal Este (East)	17	East Canal	–	–	1932-35, 38-61, 63, 67, 68+
La Servilleta	18	Comandante	75	2532	1928, 1960-72+
Río Frío	19	Frío	53.7	2785	1961-68+
Ahualulco	20	Poza Azul	78 (?)	17	1946, 1948-68+
Salida Conducto Cerrado	20	Canal Alto	87-88.5	–	1949-68+
Ahualulco	21	Nacimiento	78	25	1946-68+
Ahualulco	22	Frío	75.5	45	1927-35, suspended
Canal Bajo	22	Canal Bajo	77-77.5	–	1960-68+
Puente "T"	22	Canal Bajo	–	–	1951-54, 56-59, suspended
Sabinas	23	Sabinas	88.8	497	1961-68+
La Encantada	24	Guayalejo	≈310	3725	1950, 52-54, 56-68+
San Gabriel	25	Guayalejo	129	4937	1943-1968+

TABLE 4.1 CONTINUED

Station	Description of basins, Comments
Tancuilín	short, high gradient river in karst area, probably springs
Pequetemú	becomes R Axtla below junction of R. Huichihuayán and R. Tancuilín; drains high relief karst area, Huichihuayán, San Juanito, and Pimienta known large springs
Ballesmí	small, low relief surface basin on shale, contains the great Coy spring and other smaller ones in the Coy dome, possible small springs near Aquismón
Ojo Caliente	headwaters of R Santa María, off platform, very small flow, used for irrigation since 1968
Tansabaca	R Santa María becomes R Tampaón below confluence with R Verde; drains high relief region of varied rock types; many important tributaries, especially in eastern portion of basin, springs gauge R Tampaón
El Fuyal	the largest and base level river of the region, varied rock types, high relief, cuts across tectonic structures
Mojal Obscuro	measures flow from headwaters of R Verde to R Verde valley, high relief, varied rock type
Media Luna	actually, there are six stations on the 5 irrigation canals and the channel of this large spring
Vigas	situated near boundary of flat R Verde valley and Sierra Madre fold belt to the east, some flow from Media Luna
Tanlacut	located 10 km upstream of confluence with R. Santa María, varied geology and relief
Gallinas	high relief basin, karst and springs, some sediments and impermeable rocks
El Salto	high relief karst basin, high gradient stream, used for hydroelectric power just below station
Micos	below confluence of R El Salto and R Gallitos, the river becomes R de los Naranjos, high relief karst basin, but relatively low gradient in broad valley from El Salto to Micos
Santa Rosa	at Micos the R de los Naranjos crosses an anticline and descends to the broad, low relief Valles valley where tributaries are developed on impermeable rocks, below R Mesillas, the river becomes R Valles
El Choy	very small surface basin, nearly all the runoff comes from the large Choy spring, joins R Tampaón
Santa Clara	small surface basin, contains a spring group (3) that has third largest discharge from Sierra de El Abra
Mante	small surface basin of shale; Mante spring, largest in S de El Abra occurs along western margin, a small, control dam creates a small reservoir and divides the base flow into 2 irrigation canals, elevation of water surface in reservoir is about 80 m; before it was dammed, natural elevation was perhaps 1-3 m lower, excess low flow not taken by canals is measured by wading near dam, flood flow measured at bridge 4 km downstream
Canal Oeste	uses about one-half of the base flow of the Mante spring for irrigation
Canal Este	uses about one-half of the base flow of the Mante spring for irrigation
La Servilleta	about one-half of basin is high relief karst, other half is comprised of broad, low elevation valleys of impermeable rocks
Río Frío	gauges combined flow of R Comandante and R Frío, contains many springs closely spaced and designated the "Frío spring group", they drain the massive S de Guatemala karst area, some irrigation losses
Ahualulco	gauges flow from the large Poza Azul spring, very little surface runoff, irrigation losses
Salida Conducto Cerrado	takes base flow of Poza Azul under R. Nacimiento by tunnel for irrigation, undesired water goes to R Nacimiento
Ahualulco	gauges flow from several springs that form the R Nacimiento, no irrigation losses, occasional small gain
Ahualulco	station is 600 m below junction of R Nacimiento with R Poza Azul where it becomes R Frío, measured most if not all of discharge of "Frío spring group", this record is unaffected, i.e , there were no man-caused losses or gains
Canal Bajo	located 800 m downstream of old Ahualulco (on R Frío) station and 400 m below the control reservoir on R Frío
Puente "T"	old gauging station on Canal Bajo, located 7 4 km downstream of the control reservoir
Sabinas	high relief, mostly karstic basin, some non-karstic rocks along eastern margin, dry season flow comes from Nacimiento del R Sabinas, but there must be several (many?) seasonal springs and some surface runoff.
La Encantada	gauges flow of R Guayalejo as it leaves mountains, complex, high relief basin, but includes the broad Jaumave valley; various rock types; possibly springs
San Gabriel	gauges R Guayalejo downstream of La Encantada, one of oldest stations in region

complete discharge record of each station through 1968 in the whole Río Pánuco basin is contained in S.R.H. Boletín Hidrológico No. 32. Additional discharge records were obtained from the Tampico office of the S.R.H. for some stations through 1971, the latest year for which some data had been processed. The period of record shown in Table 4.1 is the period available for this study. The oldest stations were begun in 1927 for water availability studies for irrigation development of the Mante and Frío springs. Much later, El Salto (1948) and La Encantada (1950) were added, again for water use projects. In 1954, three stations began operations on major rivers in the southern part of the region, and in the period 1959-61, several more important stations were added that nearly completed the network of gauges as it now stands. For basin yield calculations given in Section 4.3, the base period selected is 1961-68.

4.1.3 Distribution of Precipitation

The geographic distribution of rainfall in the region is shown in Figure 4.3. Data sources used were the S.R.H. Boletín No. 19 (December, 1962) which has information through 1961, and unpublished data through 1973 provided by the S.R.H. for a large number of the stations in the eastern part of the region. Because a base period of 1961-68 is used in Section 4.3 for basin yield calculations, the average precipitation used for the stations in the principal area of interest (the eastern part of the region) is for the same period. For the rest of the region, the data points are drawn mainly from stations having long records listed in Boletín 19. Many of these stations have 25-40 years of data. A comparison

TABLE 4.2

Selected Climatology Stations in the Region

Climatology Station Name	Number in Figure 4.3	Average annual rainfall (mm)
El Choy	1	1124
Santa Rosa (Cd.Valles)	2	1172
Tamuín	3	888
El Pujal	4	1210
Ballesmí	5	1383
Penitas	6	1064
El Tigre	7	1048
Micos	8	1468
Antiguo Morelos	9	1223
El Refugio	10	—
San Felipe	11	939
Cd. Mante	12	921
Hacienda Santa Elena	13	949
Bellavista	14	943
La Servilleta	15	1099
La Boquilla	16	960
Ocampo	17	1383
Ahualulco	18	1585
Joya de Salas	19	801
Jaumave	20	519
El Salto del Agua	21	1503
Cd. del Maíz	22	608
Agua Buena	23	1846
Presa Palomas	24	504
Río Verde	25	488
Requetemú	26	2025
Aquismón	27	2057
Tamapatz	28	(2124)

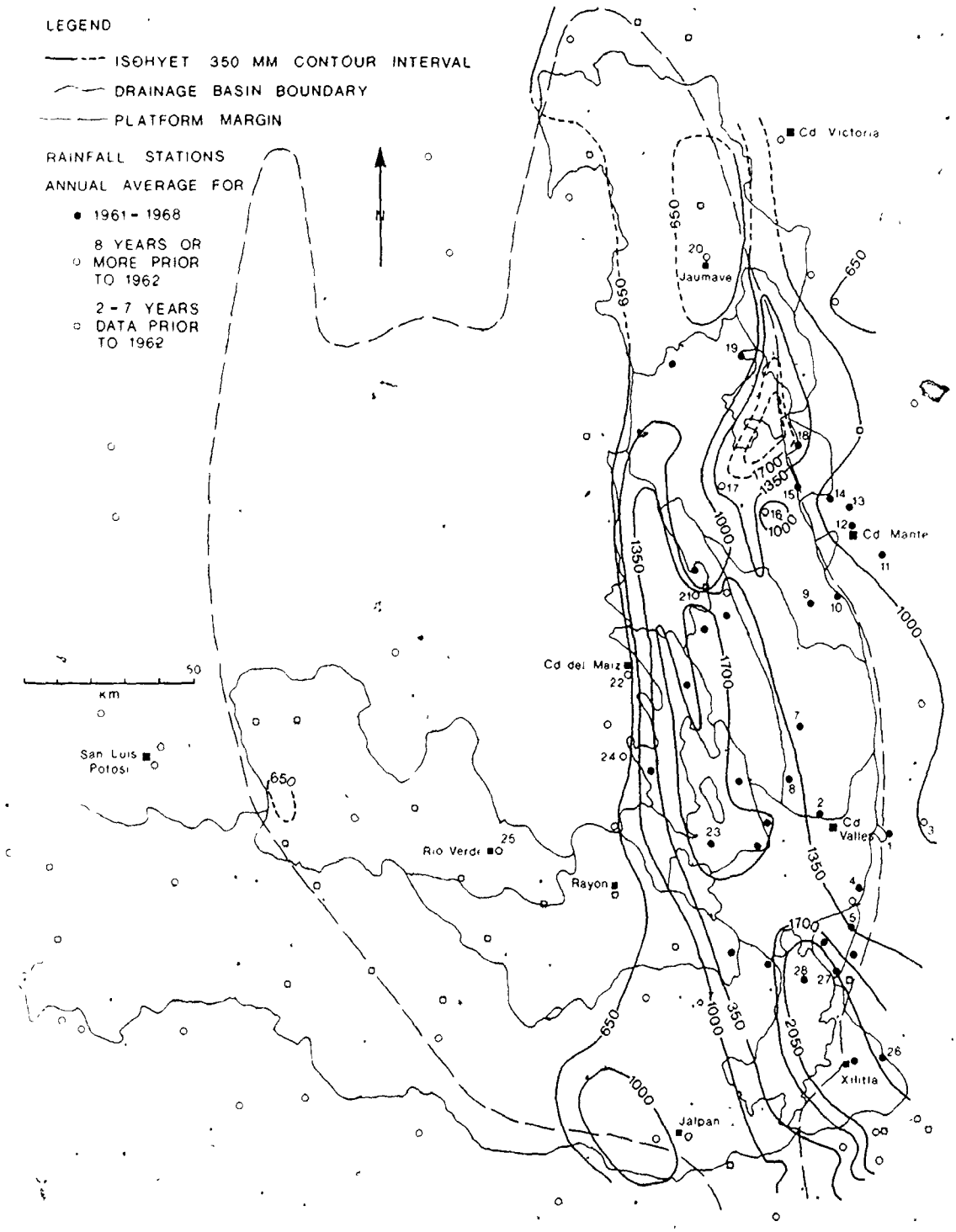

Figure 4.3 · Annual rainfall in the region. Numbered stations refer to Table 4 2.

of the average precipitation measured at 7 stations that have long records, against their averages for the 1961-68 interval is given in Table 4.3. The base period average annual precipitation appears to be not too different, possibly slightly drier, than the longer term average annual precipitation in the region.

There are two factors that influence the use of the data as a measure of the actual precipitation in the region. The first factor is that nearly all of the climatology stations are located in valleys in or near towns. As previously described, a large part of the region has a very large local relief. Somewhat greater precipitation must occur on the ridges or massifs adjacent to the valleys. In a few places where gauges are appropriately situated, this effect can be clearly seen. The second factor is the uncertain capability of the stations to measure the often heavy dew, the frost, and the light snowfalls that occur. These forms of precipitation in the area could not make an important direct contribution to the runoff, but may provide some moisture to vegetation.

The rainfall distribution is presented as an isohyetal map having a contour interval of 350 mm, beginning at 650 mm. Greater detail is not justified because of the first factor discussed above, and the mixed years of data. Considerable judgement has been used in drawing the isohyets, based on topography, exposure, and to a limited extent on field observations.

Warm, moisture-laden air moves from the Gulf of Mexico westward across the 110 km wide coastal plain (650-1100 mm precipitation) to

TABLE 4.3

Longer Term Rainfall Compared with Base Period Averages

Climatology Station	Period of record	Number of years	Average annual rainfall (in mm)	1961-68 average (in mm)	% greater or less than 1961-68
Ahualulco	1949-73	25	1581.9	1585.0	-0.2
Hacienda Santa Elena	1923-70	48	1023.0	949.1	+7.8
C.E.I. Mante	1952-73	22	1020.3	920.9	+10.8
Antiguo Morelos	1927-30 1942-68	31	1127.8	1222.5	-7.7
Requetemú	1954-73	20	2128.2	2024.8	+5.1
Ballesmí	1957-73	17	1483.6	1324.3	+12.0
Agua Buena	1942-73	32	1788.3	1846.5	-3.2

bring water to the region of interest here. The zones of greatest precipitation are coincident with the first group of high ranges (higher than 1000 m) of the Sierra Madre Oriental. There, the summer rains are torrential. The Xilitla area is known to have an average of more than 2000 mm, and it is likely that the eastern flank and crest of the Sierra de Guatemala and small similar areas of the fold belt ridges northwest of Micos exceed that value. In many years the total rainfall at Xilitla and at Tamapatz has exceeded 3000 mm. The Sierra de El Abra only reaches an elevation of about 750 m in the central part of the ridge. It was observed to have some effect on clouds, but unfortunately, there are no climatology stations on the range. The effect, however, is thought to be small compared with the effect of the much higher ranges. The central portion of the Sierra de El Abra might receive 1300-1400 mm, whereas the nearby valley stations receive between 1100-1200 annually.

On the westward (leeward) side of the first high ranges, a very strong rain shadow exists. Most of the western two-thirds of the region receives 350-550 mm of rainfall. Broad valleys between 1000 and 1300 m comprise a large portion of the area (Figure 1.1). A second series of high ranges is present along the western margin of the Platform. West of Jalpan, ridges up to 3000 m elevation occur. The sequence of greater rainfall on eastern slopes and crests followed by a leeside rain shadow is repeated, and a high mountain karst has formed. A similar pattern has been observed about 40 km east of San Luis Potosí, at the Valle de los Fantasmos.

4.1.4 Springs

The development of karst ground-water flow systems is the single most important aspect of the regional hydrology. There are a great many springs, principally in the eastern third of the Platform, and some of them are among the largest in the world. The physical and chemical characteristics of the springs and the ground-water systems will be extensively described and investigated in later sections of this and other chapters. The more important springs that this thesis will be concerned with are the Coy, Choy, Santa Clara, Mante, and Frío, all of which lie along the eastern edge of the Platform. Locations of the large springs known to the author are shown in Figure 4.2.

4.2 Temporal Aspects of the Hydrology

Some of the temporal aspects of the hydrology of the region will be discussed in this section. It is not the purpose of this thesis to quantitatively determine the long term periodicities of annual rainfall and discharge in the region, or to make statistical or predictive models of their relationships. Rather, the objectives are to analyze short term events and the seasonal pattern to establish a general understanding of the rainfall-runoff relationship and the dynamics of the karst aquifers.

4.2.1 Long Term Trends at El Choy Spring

The relatively short record (1960-1971) at El Choy is given in

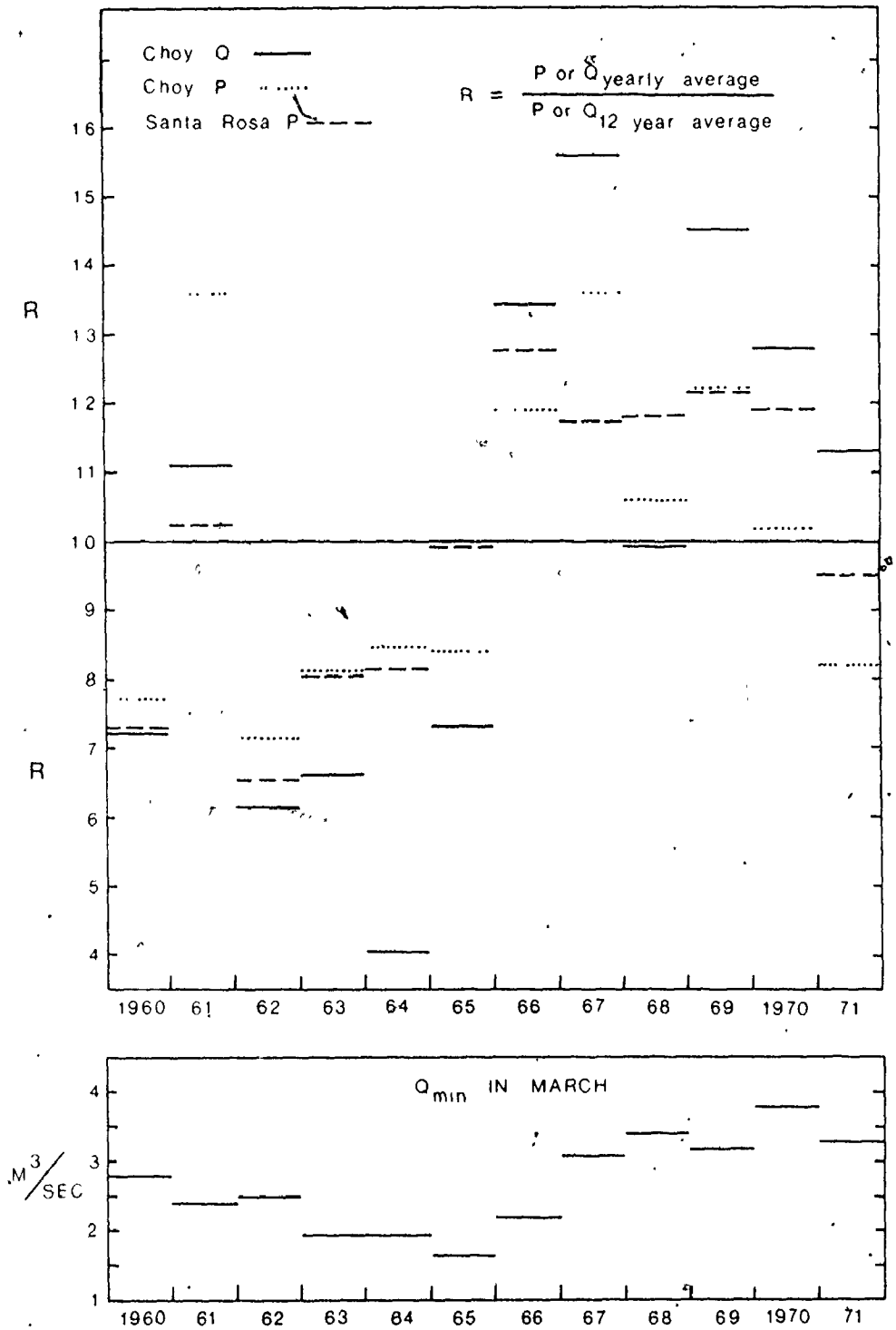

Figure 4.4 Annual flow of Choy spring compared with rainfall for 1960-1971. Also shown is the minimum instantaneous flow in March of each year.

Figure 4.4 to show what had happened in the years leading up to this study (1971-1973), and to suggest the controls on the annual runoff. The ratio of the yearly runoff to the average annual runoff for the 12 years of El Choy data is compared with similar ratios for the same time base of the rainfall at the El Choy and the Santa Rosa (Cd. Valles) stations. Considerable variation does exist, controlled by the very large scale phenomena which create tropical storms and hurricanes in the Atlantic and Gulf of Mexico region and guide them onto the mainland. The period 1960-1965, excepting 1961, was a sequence of dry years and below normal discharge, followed by wet or about average years from 1966 up to the thesis field study period.

For most of the years the runoff ratio has the same sign as, and is more extreme than the rainfall ratios. Thus, as might be expected, the annual precipitation is usually the most important factor in determining the annual runoff at El Choy. Three other factors are: 1) number, intensity, and duration of precipitation events during each year; 2) ground water stored during antecedent years; and 3) the degree to which the precipitation measured at the climatology stations around the periphery of the Sierra de El Abra reflect the true rainfall on the range.

Despite only slightly deficient rainfall, the year 1964 had the lowest runoff and by far the smallest annual flood (only 12 m^3/sec) on record at El Choy, because no large sustained storms occurred and the ground-water reservoir was very low from the preceding years of below average rainfall. The highest annual runoff and the greatest flood, 143 m^3/sec, occurred in 1967 when, after a wet 1966 season, about 800 mm

of rain fell in three storms during a five week period in August and September. Though 1968 precipitation was above normal, it was dispersed in many small storms, and flow was partially maintained by water stored during 1967. The importance of stored water may be seen by comparing the 1965 and 1971 years, which had nearly equal precipitation and reasonably similar numbers of concentrated rainfall events.

At the bottom of Figure 4.4, the minimum discharge that occurred in March of each year is plotted. This is an excellent indicator of the quantity of stored ground water available, and it follows perfectly in step with the previous season's rainfall-runoff trend.

4.2.2 Seasonal Pattern

One of the two dominant features of the temporal distribution of rainfall and runoff in the region is its strongly seasonal pattern. The year is normally discussed in terms of wet and dry seasons instead of our four temperature-oriented divisions. The second dominant feature is the rapid and distinct response of the karst ground-water flow systems to large precipitation events.

Figure 4.5 compares the average monthly rainfall and discharge for the years 1960-1971 at the Choy station. The rainfall pattern at Cd. Valles on the other side of the range is similar to that at El Choy. Nominal showers may occur during the months December to April, but often one or more months pass with no precipitation -- hence the high coefficient of variation. May brings an increase in shower activity.

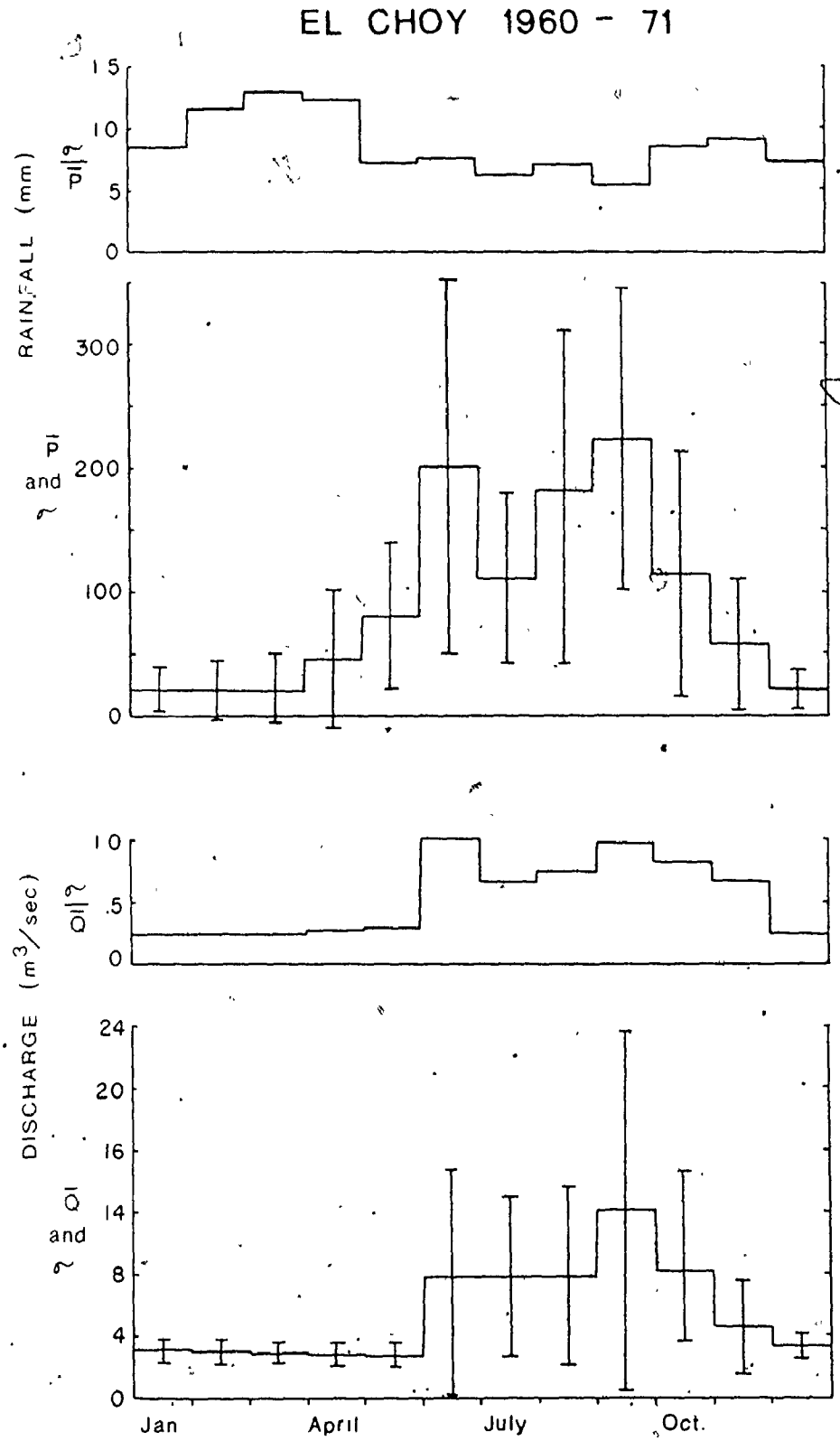

Figure 4.5 Monthly average, standard deviation, and coefficient of variation of discharge and precipitation at El Choy station for 1960-1971.

The first intense storms of the rainy season usually come in June (average 200 mm or 8 inches), but are sometimes delayed until July or August. September nearly always receives heavy storms, and occasionally early October does also. On the average, the wet season begins in early June and the dry season begins about mid-October to early November.

The discharge pattern resembles the gross shape of the rainfall curve. The Choy maintains a strong, steady base flow as water is supplied from karst storage at a gradually diminishing rate until June. June through October are the high discharge months. These months also have the highest coefficient of variation of discharge because the occurrence of heavy storms and the arrival of the wet season varies considerably from one season to the next. Though July and October are relatively deficient in rainfall, discharge is maintained by ground water stored during the previous wet month, and probably by increased infiltration efficiency and responsiveness of the aquifer.

The mean monthly discharge and coefficient of variation are shown for the Río Coy and Río Tampaón (El Pujal station) for the same 12 year period in Figure 4.6. The Coy exhibits an almost identical pattern to that of the Choy spring, the only difference being lower coefficients of variation of the Río Coy because of the very strong base flow from the spring, and a tendency for rainfall-runoff events to begin earlier in the Coy basin. The graphs of the Río Tampaón represent the average runoff pattern for a very large portion of the region. Floods are clearly a much more important part of the annual runoff of the Río Tampaón than than the Choy or the Coy.

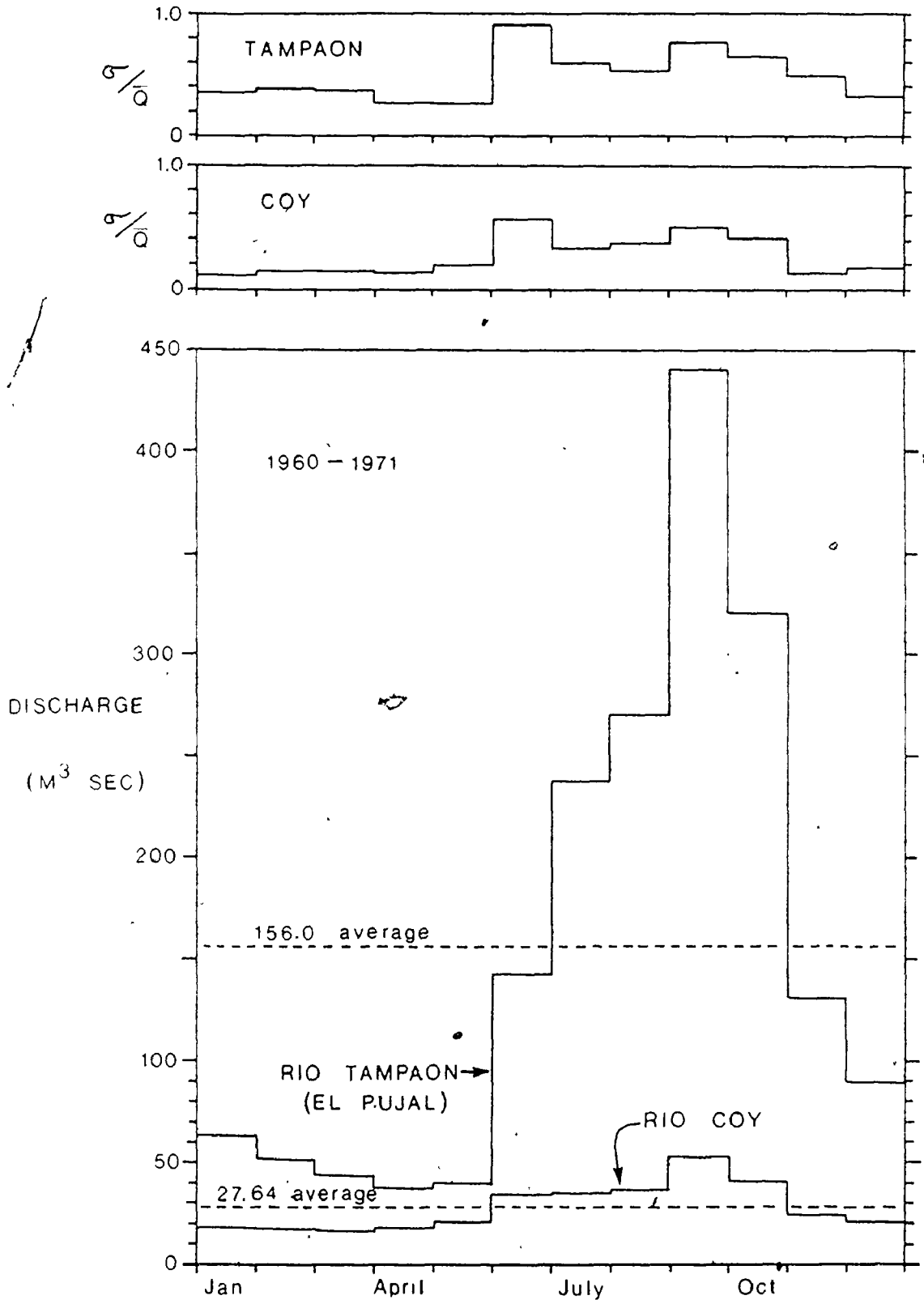

Figure 4.6 Monthly average and coefficient of variation of discharge of Río Coy (Estación Ballesmí) and Río Tampaón (Estación El Pujal) for 1960-1971.

4.2.3 Short Duration Events

The second time varying phenomena of interest in this thesis is the effect of major storms and hurricanes on the hydrology. These storms may occur as a single large daily rainfall, but normally precipitation is distributed over several days to two weeks, with several large downpours during that period. More than 300 mm of rain may fall on the El Abra range in a few days, and over 600 mm on the adjacent higher ranges. The monthly distribution of hurricanes that have affected some part of the Gulf coastal zone of Mexico in the period 1921-1961 is given in Table 4.4 (data from S.R.H. Boletín 19). It bears a strong resemblance to the regional runoff pattern as shown by the Río Tampaón (Figure 4.6).

Table 4.4

Monthly Distribution of Gulf Coastal Zone Hurricanes, 1921-61

Jan.-April	May	June	July	August	Sept.	Oct.	Nov.	Dec.
0	7	16	16	27	53	16	4	3

Examples of the response of various basins to storms are shown in the next several figures. The Choy and Coy hydrographs along with rainfall data are given for January, 1971 - June, 1973 (S.R.H. unpublished data), the period of field work in this study, though the largest floods in their records did not occur during that time interval. Daily averages have been calculated by the S.R.H. for the Río Coy for

1972 and 1973, but the data have not yet reached the yearly summary stage. The instantaneous flow hydrograph for El Choy has been derived from S.R.H. stage and discharge measurements and rating curves. As a whole the year 1971 had slightly below average precipitation in the southern Sierra de El Abra, and slightly above average in the Coy area, the northern Sierre de El Abra, and the Sierra de Guatemala. In 1972, the rainfall was 15-30% greater than average at most stations, but was about normal for El Choy. The daily precipitation at the climatology stations is collected at 8:00 A.M., so the measurements shown in the graphs are plotted at 8:00 P.M. of the 24 hour period they represent.

As may be seen in Figure 4.7, there are only a few large precipitation-runoff events each year. At the springs, a response occurs within 24 hours (thought to be much less) and the flood peaks within 48 hours after heavy precipitation. Because the time interval of rainfall measurement is about the same as or larger than the aquifer response time, it is difficult to tell what the time lag really is. Furthermore, when the Choy hydrograph and accompanying rainfall data are examined closely, it is evident that the daily precipitation values of the stations are often a poor indication of the amount that must have fallen on the Sierra de El Abra. This demonstrates the considerable spatial variation in rainfall that is also apparent in the climatology station data. It is also noted that quite often, early wet season showers or heavy rains (near the climatology stations anyway) do not produce floods comparable to similar rainfalls later in the year. Probably, a large percentage of the early rains is captured by vegetation or dissipated as replenishment of ground-

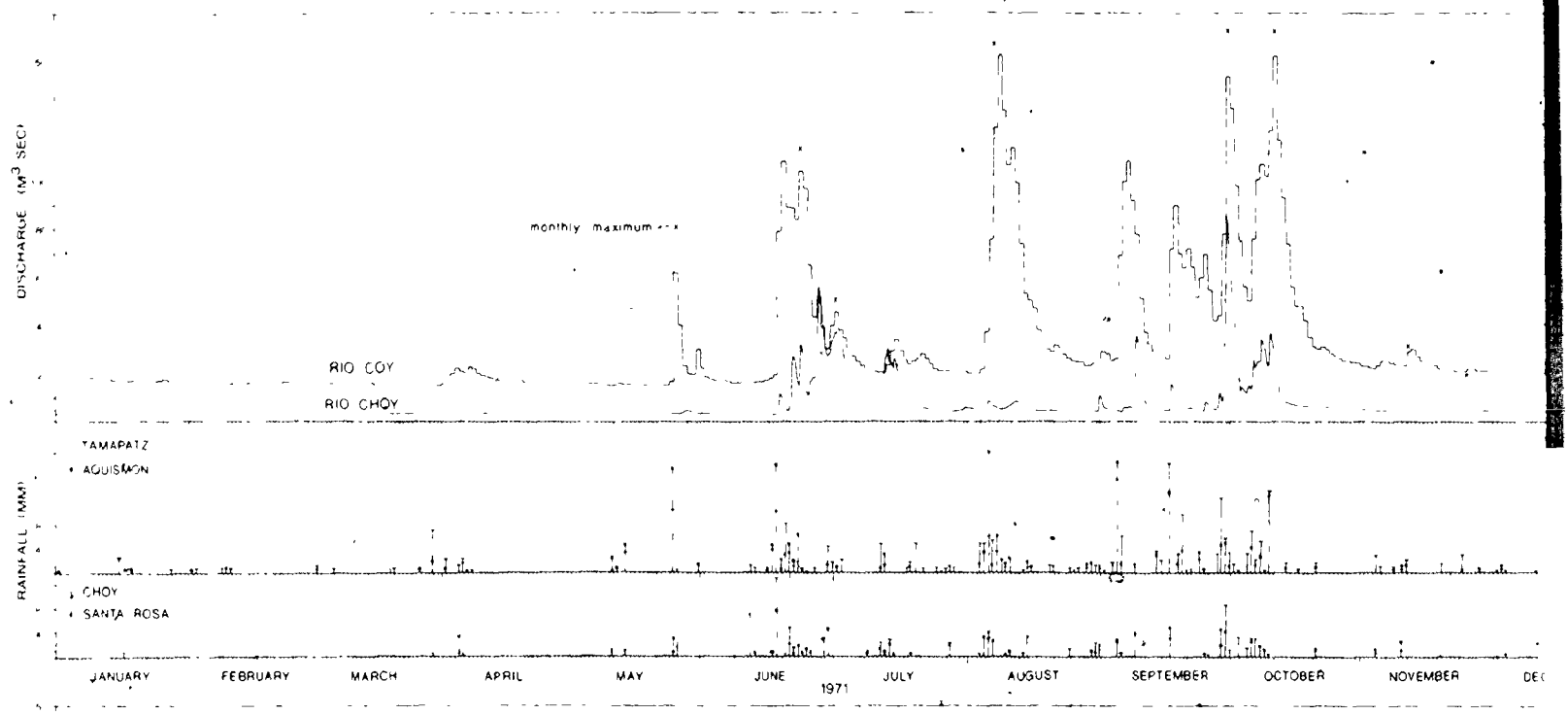

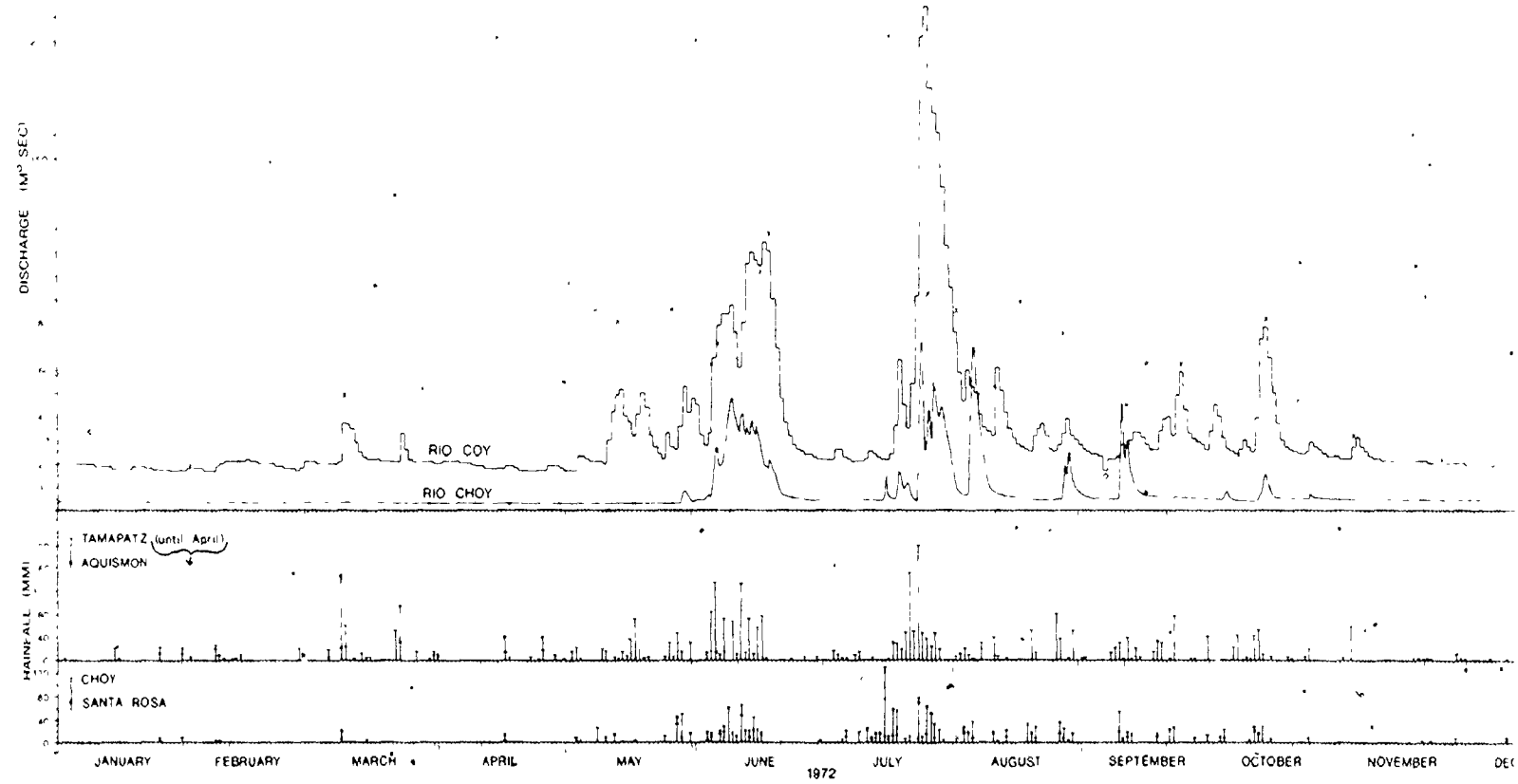

Figure 4.7 Choy and Coy hydrographs and rainfall for Jan 1, 1971-

2 of 2

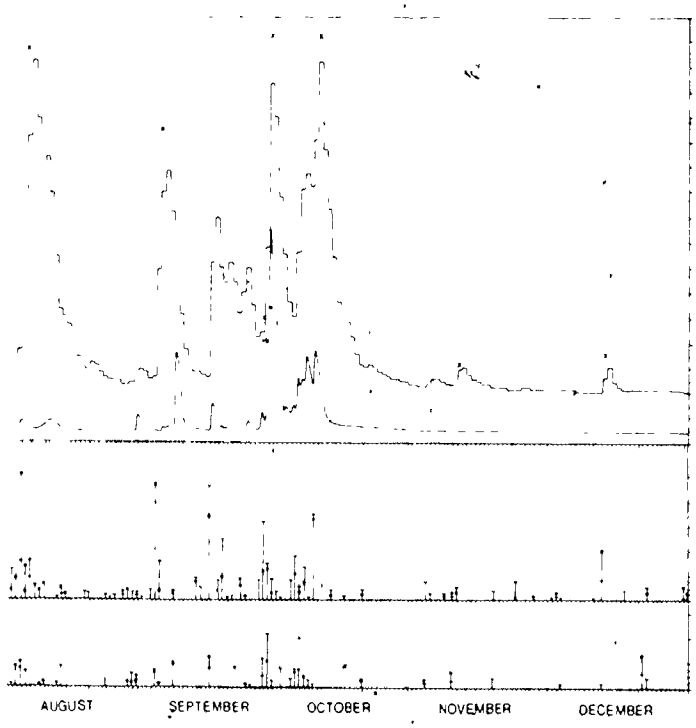

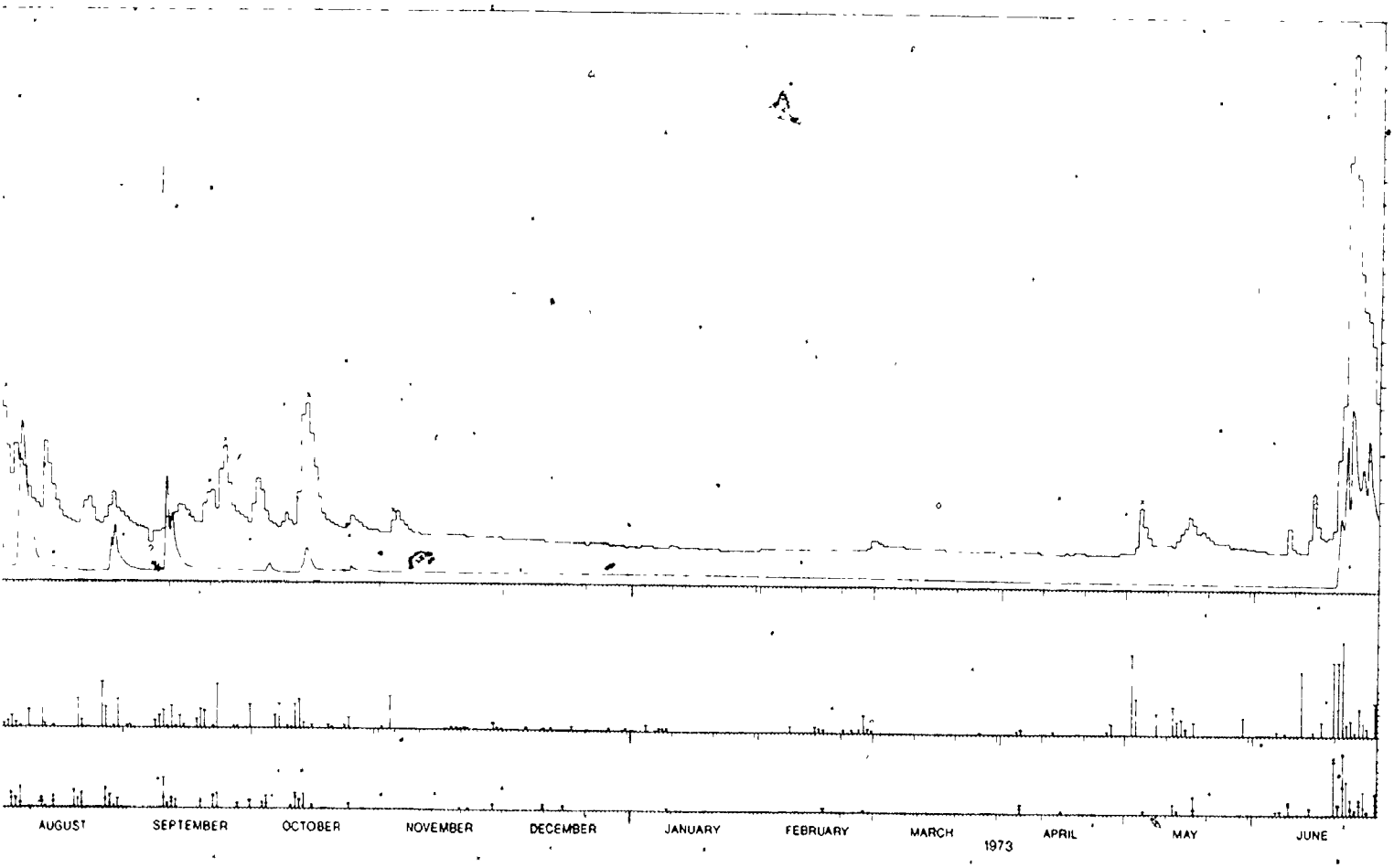

d Coy hydrographs and rainfall for Jan 1, 1971- June 30, 1973

water storage. Nevertheless, it is clear that large precipitation events cause floods at the karst springs, and that the aquifer response time is very rapid. For storms that are reasonably widespread over the recharge area, it seems doubtless that a one-to-one correspondence of rainfall-discharge events could be established. This is in marked contrast with big springs of Florida (G. Ferguson, et al., 1947), which have a broader response and have ratios of maximum to minimum flow of less than 2.

There are many flood events which deserve attention, but only a few will be considered here to illustrate the nature of the hydrographs of the other basins and springs. The effect of Hurricane Inez in October, 1966 on several basins is shown by the hydrographs published in Boletín Hidrológico No. 32 of the S.R.H. and reproduced in Figure 4.8. The Río Guayalejo above La Encantada, the Río Comandante and the Río Valles receive large portions of their runoff from shale valley catchments, whereas the Río El Salto and Río Frío are predominantly spring fed. The flow at Micos has been drawn with the flow at Santa Rosa (Río Valles) and the flow at La Servilleta with that at the Río Frío station (where the Río Comandante and the flow from the Frío springs join) so that the components may be compared. Relatively little precipitation had occurred in the previous month: nearly all of the base flow of the Río Frío and at least 2/3 of the Río Valles was supplied from springs. On October 10, rainfall began in the late morning and became very intense in the afternoon and evening over the northern and the central portion of the region (from S.R.H. detailed observations in Boletín 32). Nearly 200 mm fell in about 15 hours at many stations. Micos recorded 300 mm, the largest amount. Runoff from the shale catchments began to reach the gauging stations within hours

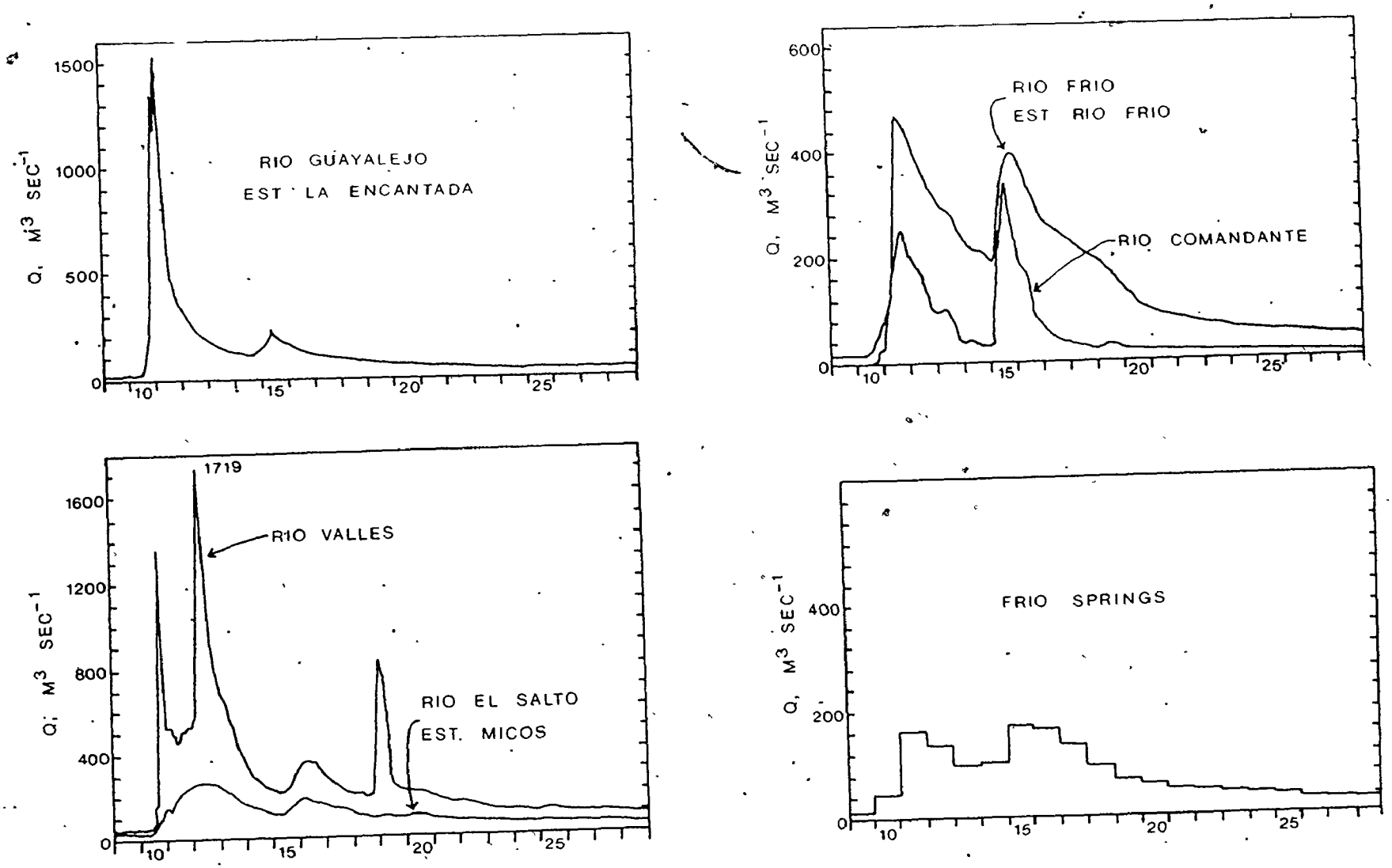

Figure 4.8 October 1966 flood events -- Hurricane Inez.

of the storm's initiation. The very sharp pulses of the Río Guayalejo and from the Valles valley on top of the flow from the Río El Salto are especially notable. Additional smaller rains fell in the mornings of the 11th and 12th on the Valles valley and the Sierra de El Abra and around midnight on the 14th over most of the eastern part of the region. These later storms exceeded 100 mm in some places and their effects may be seen either as distinct peaks or as bumps on the hydrographs. The daily average flow hydrograph of the Frío springs (sum of Río Nacimiento + Río Poza Azul + Canal Alto) shows that it too has a very rapid response, and it peaks 18-24 hours after intense rainfalls; however, it recedes from the peak much more slowly than the hydrographs of the shale catchments. Comparison of the Río Valles and Río Guayalejo with the Frío springs and El Choy springs show that the flood pulses from the surface basins have a narrower "width" and the peak is reached more quickly than at the springs. The Santa Rosa and La Encantada gauging stations measured the highest floods in their years of record during this October, 1966 event. Most other basins yielded a moderate response, but produced greater floods in June of that year, and in many other years.

Another event of particular interest occurred in August, 1951 (flow data from Boletín 32). Daily precipitation data are not available, but the discharge and monthly rainfall values (Table 4.5) indicate an ordinary year until near the end of August: A relatively large flood of 178 m^3/sec occurred in late June at the Frío springs and both the Frío and Mante springs had a modest flood in mid-July (see Figure 4.9 a). Judging from the daily average flow, showers began in the third week of August -- then a large part of the monthly precipitation (by no means are

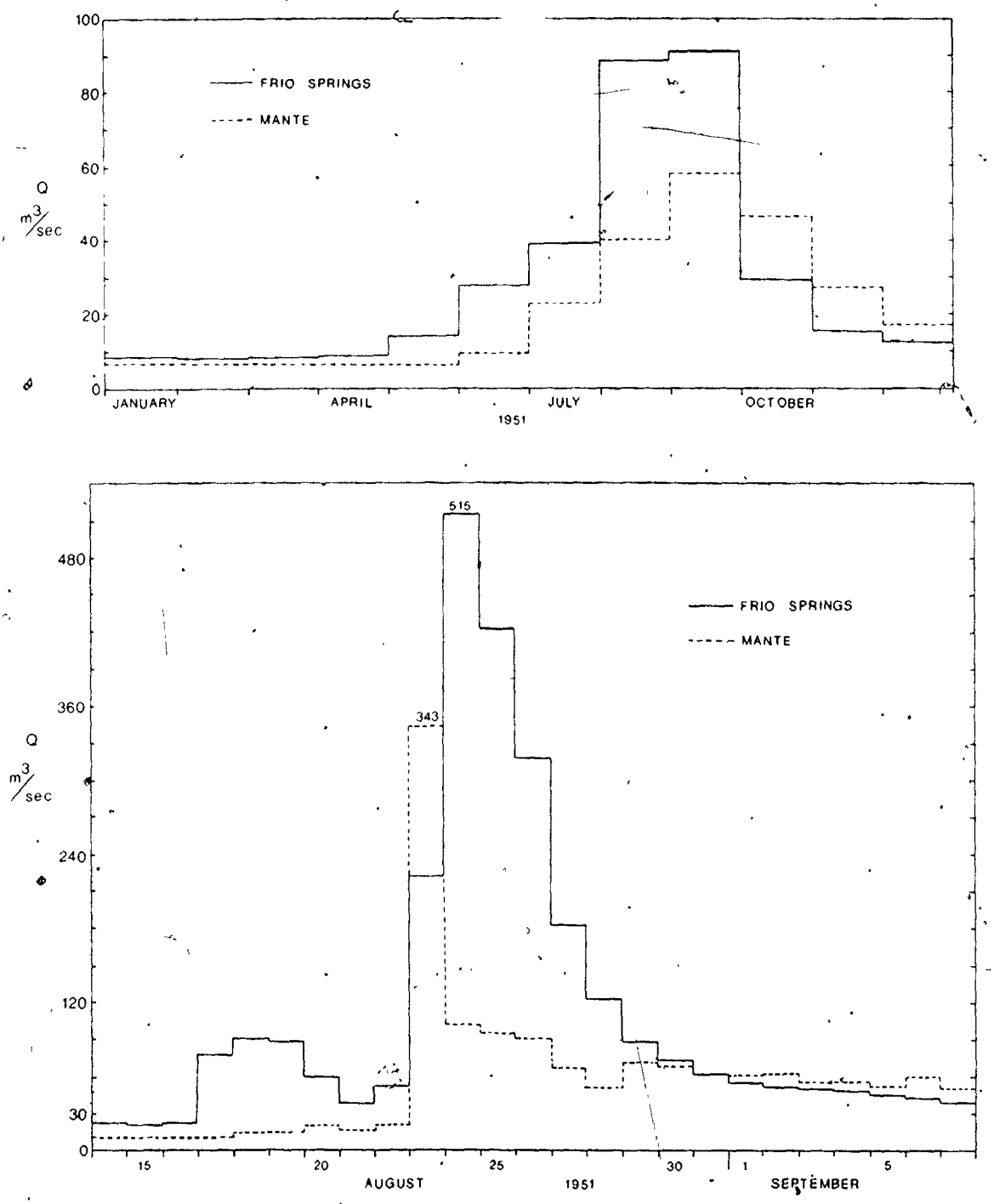

Figure 4 9 Hydrographs of Río Monte and Frío springs in 1951 a) monthly, and b) daily in August - September.

they extraordinary monthly totals) fell on August 22 and 23. The phenomenal response of the springs is the greatest in their records (Figure 4.9 b). Some surface catchment is included in the measurements of the Río Mante gauging station. Based on old topographic maps, the S.R.H. gave 42 km^2 as the area; but using the new 1:50,000 maps and air photos, a new estimate of 69 km^2 is given, assuming the canals do not interfere with the runoff. Thus for the Mante, as with the Coy, runoff from a surface basin must provide a significant part of the flood hydrograph. Most of the surface runoff would have occurred rapidly, as discussed for the Río Valles. Thus, the average flow of the Mante spring on August 23, is suggested to be in the range 120-200 m^3/sec, and the spring peak flow between 150-250 m^3/sec. Most of the discharge on the succeeding days is interpreted as spring flow recession.

TABLE 4.5

1951 Rainfall (mm)

Station	May	June	July	Aug.	Sept.	Oct.	Nov.	Total Year
Ahualulco Tamps.	181	171	60	514	266	37	15	1311
Hacienda Santa Elena Tamps.	63	140	127	402	280	66	5	1103
Antiguo Morelos Tamps.	148	139	270	530	270	67	4	1448
Peñitas S.L.P.	87	245	124	261	180	173	11	1126
Presa Palomas S.L.P.	19	90	141	360	172	30	0·1	853

The combined flow of the Río Frío springs was even more remarkable, probably the greatest known in the world. The peak discharge at the stations was 554 m^3/sec on August 24 -- 304 m^3/sec for the Río Nacimiento and 250 m^3/sec for the Poza Azul. However, because there appears to be considerable additional input from springs just downstream of the gauging stations, the maximum may have been nearer 700 m^3/sec. Since there were no hydrologic stations in operation in the southern part of the Platform in 1951, the effect of the event in this area is not known. However, the Río El Salto, flowing from a 900 square kilometer karstic basin above the El Salto station, produced a 1260 m^3/sec crest on August 23, its largest during 16 years of measurements.

One of the biggest surprises of the regional hydrology is the large floods that come from springs that have a small base flow or are seasonal. Access to the small springs along the east face of the Sierra de El Abra is almost impossible during the wet season so that little is known of their flow behaviour at this time of year. However, the S.R.H. established a hydrologic station on the Río Santa Clara in February, 1972. When the data were obtained, they had not yet processed their measurements into daily flows. Hence a simple rating curve with more than 150 points was constructed from S.R.H. measurements. A computer program was then used to convert the stage readings at two-hourly intervals into discharge for 1972-1973 (Figure 4.10). The dry season flow of the spring is about 0.3 m^3/sec, one-tenth that of the Nacimiento del Río Choy, but the flood flows appear to be nearly the equal of El Choy. Remembering the sharp pulses that may come from surface basins in the area, some of the extreme peaked-

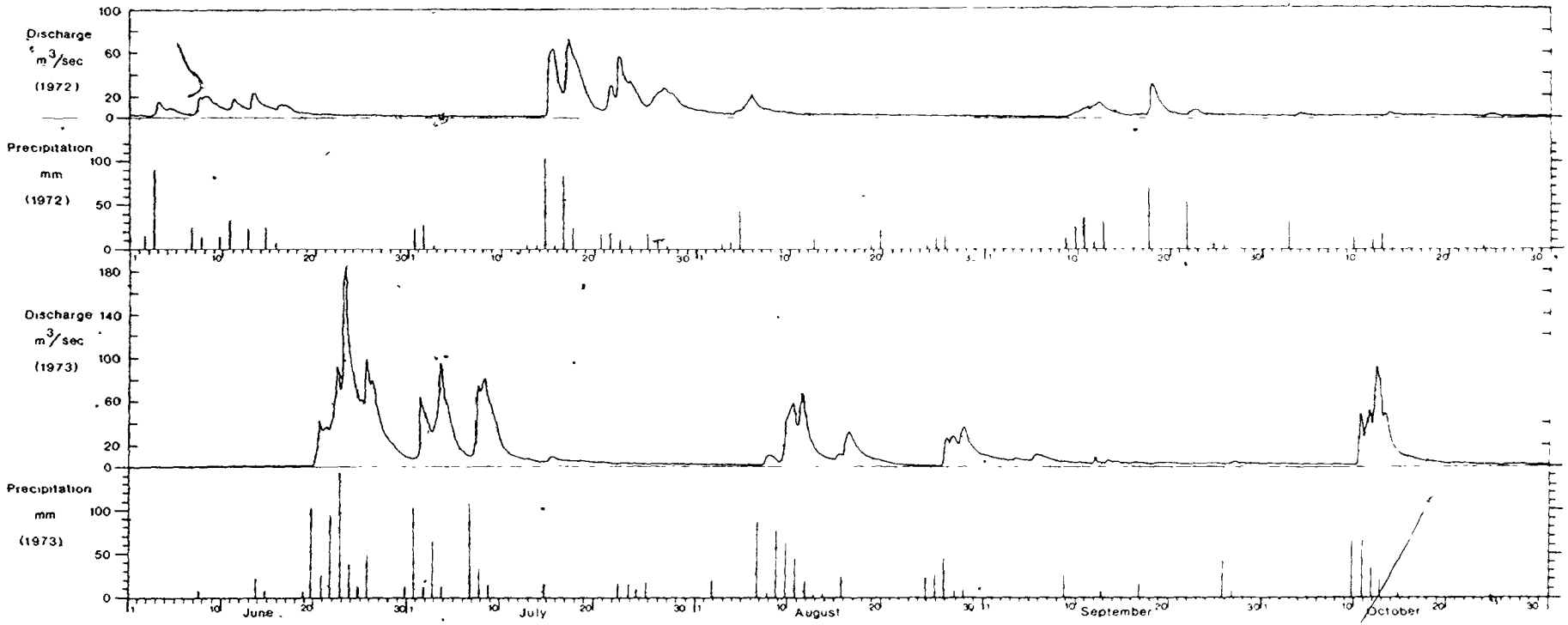

Figure 4.10 Río Santa Clara hydrograph, June - October for 1972-1973.

ness may be due to surface runoff included at the gauging station. However, most of the discharge must come from the spring (actually 3 springs); i.e., spring flow is the primary factor in the hydrograph shape.

Another example observed during this study is the Nacimiento del Río Pimienta, which rises from holes in a limestone stream bed about 10 km south of Aquismón. In the summers of 1971 and 1972, the low flow of a few observations was established to be several m^3/sec. The high flow may have been on the order of 100 m^3/sec, including many additional inputs from sources at the base of the adjacent scarp. Yet when the spring was observed in January of 1972, it had dried up completely!

Thus, the karst springs exhibit extreme responses to storms. The flood events are superimposed on a strong base flow from storage at some springs, and at others, on a small or intermittent flow. As would be expected, the response on the surface basins is even more peaked. During the recession period, many of the springs maintain a significantly elevated flow for some time, whereas the flow from the shale basins and some springs recedes very rapidly. The Río Tampaón, the principal river in the region, carries the integrated output of a large number of karst springs and surface basins, and this is reflected in its hydrograph (Figure 4.6).

4.2.4 Flood Exceedance; Major Events

To lend some perspective to the climatic-runoff events in the region and to summarize the magnitudes of floods that various springs or

basins experience, a flood-frequency analysis was made according to procedures described by Dalrymple (1960). For the purposes given above, it was not necessary to extend the records for the stations having the shorter records -- only the real data are used. Flood data for a few stations were made available by the S.R.H. for 1972-1973 in addition to the period of record listed in Table 4.1. The highest annual peak discharges are plotted with their calculated recurrence interval in Figure 4.11 (note the ten times difference in the discharge scale for the two groups). In this method, the recurrence interval is defined as the average time interval in which a flood of a given magnitude will be equalled or exceeded as an annual maximum. Unfortunately, the Mante data cannot be used because for most years, only the maximum annual <u>average daily</u> flow is reported, rather than the instantaneous maximum. The Frío springs are represented here by the Río Nacimiento. Inspection of their records shows that the Río Nacimiento and the Río Poza Azul peak almost simultaneously, but in six of twenty-three years, the <u>calculated</u> maximum annual discharge of each occurred during different flood events. The peak for the Frío springs (the combined flow) may be approximated as 1.75 times the value shown for the Río Nacimiento.

The pertinent points may be summarized as follows:

1) Spectacular floods from the many springs in the region are commonplace, and compare with the largest reported in the literature. This is particularly remarkable because the outflows are mostly derived from a myriad of small infiltration points rather than from the sinks of major rivers.

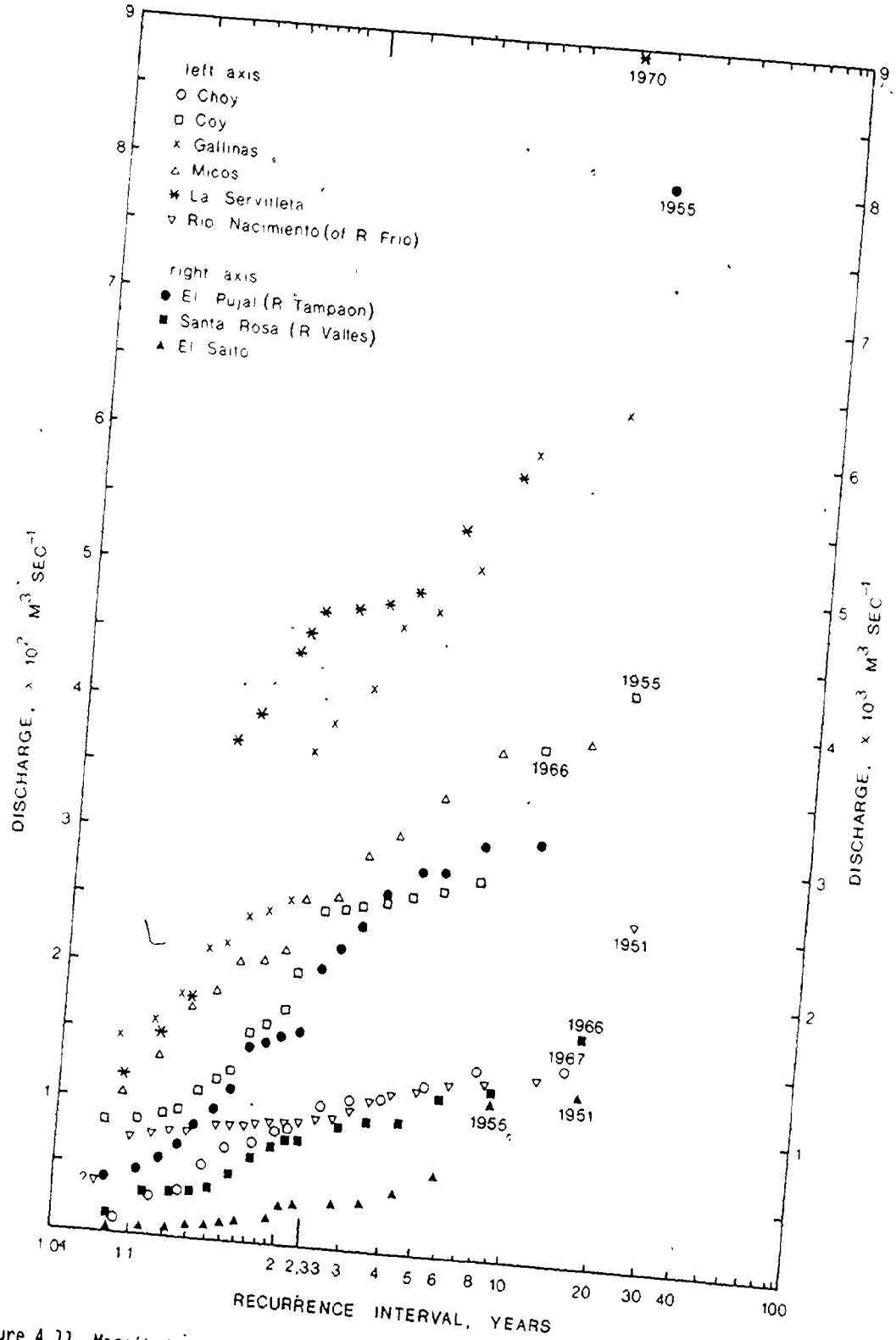

Figure 4.11 Magnitude of flooding of springs and rivers as shown by flood exceedance. The basins and possibly the causal precipitation events are inhomogenous.

2) Many of the stations display erratic patterns. In particular, there are great discontinuities in the exceedance flow that occur in the interval 1.1-2.3 years. This appears to be caused by long term cycles of wet and dry years that may be partially self-dependent, by inhomogenous drainage basins comprising both surface and complex underground watersheds, and by possible inhomogeneity of the causative climatic events.

3) According to Dalrymple (1960), streams in large regions which are homogenous with respect to flood-producing properties will have frequency curves of about equal slope independent of the size of drainage area. The slopes of the "curves" in Figure 4.11 are clearly widely disparate. The Frío and Choy springs have the lowest slopes, while the basins with mixed karst and surface drainage have higher slopes. This suggests that the apparent inhomogeneity may be caused by differences between surface channel and cave conduit hydraulics.

4) The 1955 flood was an exceptional regional event in the relatively short history of gauging in the area. It appears to have produced record floods over most of the region, except at the Mante and Frío stations. The Río Tampaón yielded a "1 in 300 year" flood at El Pujal, and part of the La Encantada installation was destroyed. The 1951 event also may have been a major regional event, but the documentation is insufficient. It may have been more similar to other events, such as the October, 1966, floods that were (are) felt at many places in the region, but that produced a very strong response at

only a few localities.

5) No abnormally large flood occurred at the Choy spring during the period 1960-1973; however, the rainfall measured at Cd. Valles suggests that the 1955 event may have been substantially larger than any in its record.

4.2.5 Flow Duration

The data presented so far have indicated the stability of spring discharge during the dry season and the variability during the wet season. To quantify the time distribution of discharge, a flow duration graph of the daily average flow of the Choy spring for the years 1960-1971 was prepared (Figure 4.12). The curve is composed of two segments -- the gently sloping base flow regime and the steeply sloping flood regime. Curiously, the 12 year average of 5.47 m^3/sec falls at the junction of the two segments. It is equalled or exceeded only 13.5% of the time.

The graph confirms that the base flow regime is strongly dominant, that flood flow is short lived, and that about 50% of the total volume of water is discharged in floods. The median value (50th percentile) was 3.3 m^3/sec, and the flow either equalled or exceeded 56 m^3/sec or fell less than 1.63 m^3/sec only 1% of the time. Also shown are the curves for 1967, the year with the highest annual discharge, and 1964, with the lowest annual average. All of the flows less than 1.65 m^3/sec occurred in 1965 following several years of drought.

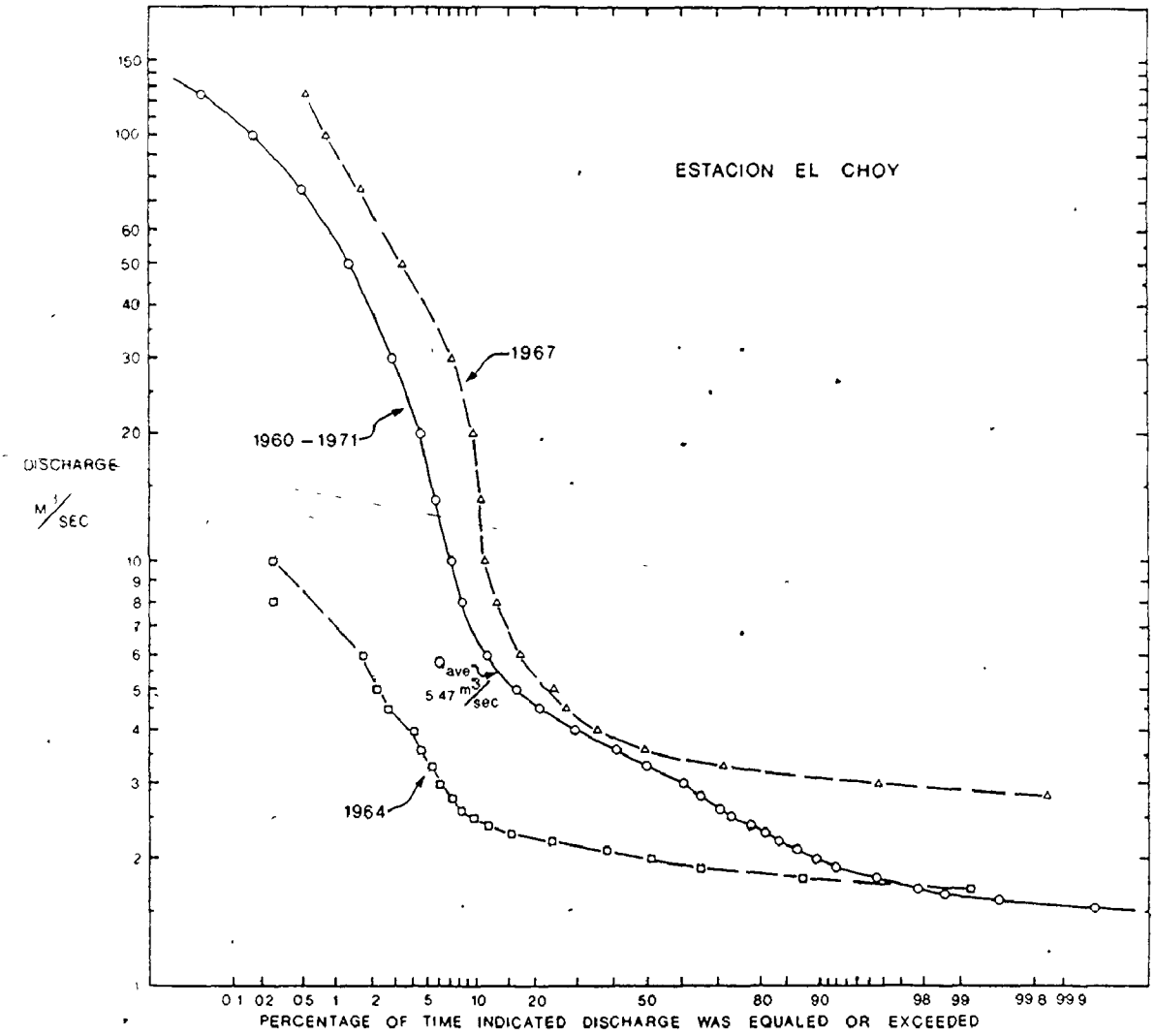

Figure 4.12 Flow duration graph of Choy spring for 1960 - 1971. Despite the occurrence of severe floods, base flow predominates.

4.3 Spatial Distribution of Runoff; Basin Yield

In order to gain a quantitative knowledge of the magnitude of the springs and their contribution to the regional runoff, an analysis will be made here of the low and average flow, and the unitary yield of the drainage basins. The analysis will also establish some areas that have excess or deficient runoff. This will be used in Chapter VII, where the regional surface and ground-water systems are discussed.

4.3.1 Low Flows

The dry season runoff from the region is provided almost entirely by springs. Table 4.6 gives the lowest recorded discharge at various gauging stations, and compares the average daily discharge from the basins on several days during seasons of unusually low flow. Inspection of the S.R.H. daily discharge data indicates that the May 1, 1963 runoff budget is about the lowest total runoff thus far measured. Thus, the aggregate discharge from the springs very rarely falls below 60 m^3/sec. The lowest flows for the Frío springs and the Mante springs are not given because the water is split between 3 channels in each case and the Mante has a small control reservoir as well. Virtually all the base flow of the Río Valles comes from above Micos. It may be subject to control -- the value given by the S.R.H. as the minimum recorded certainly appears affected in some way.

Some springs maintain a strong base flow while others are strictly seasonal or intermittent. This seems to be controlled partly by the

TABLE 4.6

Low Flows and Low Flow Budget

Station or Basin	elevation in m	lowest recorded flow m^3/sec	date	Mar. 25 1963 m^3/sec	May 1 1963 m^3/sec	Mar.25 1965 m^3/sec	Jan.6 1972 m^3/sec
E. Requetemú	71.1	1.28	March 25/64	2.317	1.591	1.928	–
E. Tancuilin	–	0.290	July 03/60	0.900	0.674	0.850	–
Huichihuayán valley=Requetemú-Tancuilin	71.1	–	–	1.417	0.917	1.078	–
E. Ballesmí (Coy)	29.1	13.00	Apr. 15/63	15.07	14.08	14.33	19.92
E. El Pujal (Río Tampaón)	28.2	19.60	May 09/64 June 14/65	26.300	21.20	24.100	87.5
E. Tansabaca	174	4.51	May 25/66	7.820	7.020	6.092	30.21
E. Tanlacut	257	0.00	many days in 1963/64	0.741	0.00	0.814	–
E. Vigas	897	1.03	June 9/64	3.004	2.075	1.804	–
E. Gallinas	280	0.458(?)	June 24/60	2.077	1.553	2.720	7.2
E. Santa Rosa	72.8	0.34(?)	Apr. 24/65	4.672	3.276	4.431	21.6
E. Micos	210	0 ?	Apr. 23/65	4.442	3.495	3.190	13.7
E. El Salto	399.3	5.51	July 1961	6.68	6.000	8.10	–
E. El Choy	32.2	1.53	June 11/65	2.023	1.906	1.690	(3.75)
Micos-El Salto	210	–	–	-2.24	-2.50	-4.91	–
Santa Rosa-Micos	72.8	–	–	0.230	-0.219	1.241	7.90
Tansabaca-Tanlacut	174	–	–	7.079	7.020	5.278	–
Tampaón Upper	–	–	–	14.569	11.849	13.243	59.0
Tampaón Lower	28.2	–	–	11.731	9.351	10.857	28.5
Tanlacut-Vigas	257	–	–	-2.263	-2.075	-0.990	–
E. La Servilleta	75	0.00	many months	0.002	0.002	0.002	0.067
Mante Spring (3 stations)	(80)	?	?	6.685	6.296	?	–
E. Río Frío	53.7	0.605	June 17/65	1.779	1.058	1.586	–
Poza Azul (Canal Alto)	(90-95)	?	–	3.559	2.939	3.735	–
Río Nacimiento	(90-95)	?	–	1.792	1.330	1.960	–
Canal Bajo	–	–	–	2.588	2.307	2.491	–
Frío Springs	(76)	–	–	5.351	4.269	5.695	–
E. Sabinas	88.8	0.120	May 14/65	0.391	0.272	0.242	–
La Encantada	(310)	0.537	May 03/54	3.548	3.145	3.012	–
Ungauged Springs	–	–	–	(2.00)	(2.00)	(2.00)	–
Laguna Media Luna	(1000)	?	–	(4.00)	(4.0)	(4.00)	–
REGIONAL TOTAL				67.687	58.761	(63 -64)	

elevation of the spring. The Coy spring, 32 m elevation, is probably at the lowest point in the whole region where ground-water discharge from the limestone could occur (the only possible exception is where the Río Tampaón passes the southern end of the Sierra de El Abra). Its lowest instantaneous flow in 20 years, 13.0 m^3/sec, is equal to 2/3 the low flow of the entire Río Tampaón at El Pujal, 1/4 of the low flow of the entire Platform, and at least twice the low flow of any other spring in the region! The big springs between Huichihuayán and La Pimienta are at about 100-120 m elevation and do not yield such a large base flow (measured at Estación Requetemú). In the northern part of the region, the Manfe and Frío springs are the principal points of base flow discharge. They are at nearly the lowest elevation of the El Abra limestone available for discharge in that area, approximately 80 and 90-95 meters respectively. The flow from each probably does not fall below 6 m^3/sec. The surprisingly large base flow of the Río Guayalejo at La Encantada may be derived from springs in the canyon upstream. The relatively small dry season flow of the Río Sabinas comes from one spring, the Nacimiento del Río Sabinas, at 160 m elevation. The channel characteristics above and below the Sabinas spring, and the topographic maps indicate that there is extensive wet season runoff produced further upstream.

The selected daily budgets given in Table 4.6 allow the location of zones of water loss or excess discharge (springs). Reference to the basin map (Figure 4.2) will assist the reader. The basin of the Río Tampaón above El Pujal may be divided into contributions from the Tampaón upper basin (Tansabaca + Gallinas + Santa Rosa) and the Tampaón lower

basin (El Pujal - Tampaón upper). For the three days of very low flow given, 45% of the base flow of the Río Tampaón was derived from the Tampaón lower basin, which contains only 1,531 (6.6%) of the 23,373 square kms of the Tampaón basin. The eastern half of the Tampaón lower basin is formed in shale, and is an extension of the Valles valley. Thus, karst springs in the canyons of the Río Tampaón below Tansabaca, along the Río Gallinas below its gauging station, and the Nacimiento del Río Tanchachín form a major zone of ground-water discharge in the region. On January 6, 1972, a day of higher base flow early in the dry season, the Tampaón lower basin contributed 28.5 m^3/sec (33%) of the total flow of 87.5 m^3/sec at El Pujal. On the same day, the discharge of the Nacimiento del Río Tanchachín was measured to be 2.207 m^3/sec (special gaugings, Table 4.7), and the Nacimiento de Agua Clara was estimated to be 1-2 m^3/sec. Hence, most of the water comes from springs still unknown.

Just downstream of the Ahualulco Río Nacimiento station lies the Nacimiento La Florida, and other small springs occur in the Sierra de El Abra north of the Río Comandante. Their discharge can only be estimated by a complicated budget, shown in Table 4.8. The sources of the Río Frío are the Nacimiento Poza Azul (where the base flow is abstracted into the Canal Alto for irrigation), the Río Nacimiento and the Río Comandante. The difference between their total and the sum of Estación Frío and Canal Bajo (which is derived from the Río Nacimiento below the gauging station) gives the discharge of the ungauged springs. The low flows are calculated for two dry season months in 1963, that follow a period of regional drought. There would be no contribution from soil moisture or surface runoff at these times. Because it is not known how much water

TABLE 4.7

Special Gaugings

Spring	Location	Date	Discharge m^3/sec
Santa Clara	Sierra de El Abra	Jan. 7/72	0.379
Tantoán thermal	Sierra de El Abra	Jan. 7/72	0.0142
Arroyo Seco	Sierra de El Abra, Rancho Peñon	Jan. 7/72	0.0071
Huichihuayán	near Huichihuayán	Jan. 6/72	3.70
Tanchachín	Sierra de la Colmena	Jan. 6/72	2.21
San Juanito (Mujer de Agua)	near Huichihuayán	Jan. 6/72	2.53
Río Pimienta (San Juanito & Pimienta springs	bridge to Rancho Huiche	June 2/72	22.1

TABLE 4.8

Indirect Calculation of Flow of Smaller Frío Springs

Discharges*

STATION	MAR./63	APR./63	1966 YEAR	1961-1968
Río Frío	1.905	1.430	48.863	27.68
Canal Bajo	2.645	2.365	2.70	2.54
	4.550	3.795	51.563	30.22
La Servilleta	0.002	0.002	11.49	4.95
Río Nacimiento	1.844	1.256	18.62	12.25
Poza Azul	0.0	0.0	9.31	6.10
	1.846	1.258	39.42	23.30
Q of other springs	4.550	3.795	51.563	30.22
	-1.846	-1.258	-39.42	-23.30
	2.704	2.537	12.14**	6.92**

* All discharges in m^3/sec

** Includes flow of other springs and surface basin

is returned by the Canal Bajo to the Río Frío, the 2.5-2.7 m^3/sec figures are the maximum possible during those months. The dry season minimum value is 1.1 m^3/sec, estimated by subtracting the Río Nacimiento flow from the Canal Bajo flow and assuming that the Río Frío is supplied entirely by return flow from the Canal Bajo. The true value probably is closer to the maximum possible.

Two areas of considerable water losses are easily determined from Table 4.6. These are herein termed the Rayón basin (Tanlacut - Vigas) and the El Naranjo basin (Micos - El Salto). The El Naranjo basin and the eastern portion of the Rayón basin are intensively karstified. Water losses occur throughout most of the dry season. However, it is not known whether all the losses are due to piracy underground, or in part to anthropogenic causes such as irrigation or the El Salto hydroelectric plant. The Rayón deficit is most likely due to karst piracies along the Río Verde.

If there are losses along the Río Santa María, they must occur above the Estación Tansabaca (above the Tampaón lower basin). Unfortunately, there are no helpful gauging stations. The strong base flow suggests that there is no loss. In fact, most of the flow is probably derived from karst springs in the thirty kilometer section of the river immediately above Estación Tansabaca, and in the karst area west of Jalpan. Other areas where losses or gains might occur are the canyons at Micos, El Puente near Ocampo, La Servilleta, and La Encantada. Field observations of the canyons need to be made during the full range of discharge.

4.3.2 Average Flows

To assess the spatial distribution of total runoff from the Platform, the 8 year period 1961-1968 was selected for analysis. The average flow for each year and the drainage area are given in Table 4.9 for all the major gauging stations on the Platform. Unfortunately, the Mante record is incomplete. The record was "completed" by plotting the mean annual discharge for 9 years against the average of 4 nearby rainfall stations, estimating the best fit line, and then reading the discharge for the missing years. A small subjective adjustment was made if the previous seasons' rainfall was abnormally high or low. Also listed are various subbasins obtained by subtraction or addition of appropriate station values. For example, the runoff from the Valles valley is obtained by subtracting the Micos values from the Santa Rosa values. Except for the Río Santa María above Tansabaca, which needs more stations, a reasonably detailed analysis is possible. It is immediately evident (as would be obvious from the rainfall map, Figure 4.3, or a casual perusal of the area) that the wet, eastern basins provide much more runoff than the dry, western basins.

As was done in the section on low flows, Table 4.9 may be checked for unusual flows. Amazingly, the Rayón basin showed a net loss, or negative average discharge, during the years 1962 and 1963, and only a marginally positive flow in 1964. The eastern half of this basin and the bed of the Río Verde are thus important zones of karst infiltration. The El Naranjo basin, which has a steady loss during base flow, shows a small plus in the average flow figures (only 4 years overlap of data).

TABLE 4 9

Runoff from Basins, 1961-1968

Gauge or Drainage Basin (E = Estación)	elevation in m	A area sq km	AVERAGE DISCHARGE (Q) FOR EACH YEAR, M³/SEC 1961	1962	1963	1964	1965	1966	1967	1968	Q_{avg} m³/sec	σ	$\frac{\sigma}{Q_{avg}}$	unit runoff $U = \frac{Q_{avg}}{A}$	$\frac{U_{basin}}{U_{region}}$	% = $\frac{Q_{avg}}{Q_{reg}} \times 100$
E Requetemu	71 1	661	42 03	28 96	24 45	20 29	31 89	43 57	44 01	47 71	35 36	10 27	0 29	0 0535	6 32	12 50
E Tancuilin	?	321	12 13	7 12	6 92	5 58	10 04	14 05	19 66	17 39	11 61	5 15	0 44	0 0362	4 28	4 10
Huichihuayan-Requetemu-Tancuilin	71 1	340	29 9	21 84	17 53	14 71	21 85	29 52	24 35	30 32	23 75	5 88	0 25	0 0699	8 26	8 39
E Ballesmi Fos	29 1	194	27 76	22 05	21 18	21 44	25 36	32 16	32 41	30 24	26 575	4 74	0 18	0 1370	16 19	9 39
E Choy	42 2	4 9	6 07	3 36	3 62	2 21	3 98	7 36	8 53	5 43	5 07	2 16	0 43	1 035	122 30	1 79
E Micos	210	1978	24 64	14 45	18 34	16 64	19 62	33 16	34 40	27 29	23 57	7 54	0 32	0 01192	1 41	8 33
E Santa Rosa	72 8	3521	36 12	15 81	23 73	18 89	25 71	59 37	46 72	36 72	32 88	14 84	0.45	0 00934	1 10	11 62
Valles valley-Santa Rosa-Micos	72 8	1543	11 48	1 36	5 39	2 25	6 09	26.21	12 32	9 43	9 32	7 91	0 85	0 00604	0 714	3 29
E Gallinas	280	789	38 08	13 87	14 74	22 63	30 82	45 49	42 02	32 50	30 02	11 98	0 40	0 0380	4 49	10 61
E Tansabaca	174	17532	34 98	19 64	19 21	13 34	16 71	31 07	66 33	46 80	31 01	18 12	0 58	0 00177	0 209	10 96
E. Tanlacut	257	6039	7 21	3 06	2 23	2 51	3 36	9 31	22 11	10 80	7 57	6 73	0 89	0 00125	0 148	2 68
Santa Maria = Tansabaca-Tanlacut	174	11493	27 77	16 58	16 98	10 83	13 35	21 76	44 22	36.00	23 44	11 72	0 50	0 00204	0 241	8 28
E Vigas	897	3571	4 72	3 36	3 08	2 34	2 18	5 68	12 56	6 73	5 08	3 42	0 67	0 00142	0.168	1 80
Rayon basin = Tanlacut-Vigas	257	2468	2 49	0 (-0 30)	0 (-0 85)	0 17	1 18	3 63	9 55	4 07	2 64 (2 49)	3 23 –	1 22 –	0 00107 (0 00101)	0 126 (0 119)	0 95 (0 88)
E El Pujal	28 2	23373	162 04	69 54	79 19	76 02	105 39	186 97	227 64	169 34	134 52	59 70	0 44	0 0058	0 685	47 54
Tampaon Upper = E Tansabaca + E Santa Rosa + E Gallinas	–	21842	109 18	49 32	57 68	54 86	73 24	135 93	155 07	116 02	93 91	40 50	0 43	0 00430	0 508	33 19
Tampaón Lower = E El Pujal - Tampaón Upper	28 2	1531	52 86	20 22	21 51	21 16	32 15	51 04	72 57	53 32	40 60	19 54	0 48	0 0265	3 13	14 35
E La Servilleta	75	2532	4 85	2 77	1 85	1 36	5 17	11.49	7 30	4 81	4 95	3 29	0 66	0.00195	0 230	1 75
Mante	?	69	12 39	(8 4)	10 57	(10 1)	(12 0)	(14 0)	13 23	13 47	(11 77)	(1 93)	(0 16)	(0 171)	20 21	4 16
Frío springs		42	19 77	17 00	19 45	21 57	22 99	32 08	21 84	21 76	22 06	4 46	0 20	0 5252	62 06	7 80
E Sabinas	89 8	497	16 27	11 33	8 27	10 38	12 35	25 69	15 96	11 31	13 945	5 46	0 39	0 0281	3 32	4 93
E La Encantada est	310	3725	9 90	9 90	6 20	6 13	5 79	12.80	20 95	10 36	10 88	5.63	0 52	0 00292	0 345	3 85
E Río Frío	53 7	2785	25 66	18 10	19 87	21 59	29 24	48 86	30 87	27 22	27 68	9 676	0 35	0 00994	1 17	9 78
E Canal Bajo	–	–	1 76	2 38	2.81	2 71	2 66	2 70	2 63	2 69	2 54	0.34	0 13	–	–	0 90
E Canal Alto		–	3 02	3 31	3 72	4 19	3 67	4 15	3 79	3 82	3 71	0 39	0 11	–	–	1 31
E El Salto	399 3	900	20 77	14 22	16 81	14 53	–	–	–	–	–	–	–	–	–	
El Naranjo Basin = E Micos-E El Salto	210	1078	3 87	0 23	1 53	2 11	–	–	–	–	–	–	–	–	–	

This basin of 1078 square km has a high average precipitation and should have a runoff comparable to that above El Salto. The deficit is believed to be greater than can be accounted for by domestic, irrigation, and hydroelectric plant use. Much of the deficit is thought to occur by seepage in the river bed into alluvium where it is lost by evapotranspiration or by continued seepage down into the limestone aquifer, and by karst subsurface drainage out of the basin (to the Río Tampaón ?) from recharge into high relief karst over a large part of the basin.

The lower Frío basin, shown previously to have a spring or springs providing a significant base flow, has an 8 year average of 6.92 m^3/sec. Most of this must be assigned to flow from springs because the surface catchment (208 km^2) is too small to account for the excess. Furthermore, referring back to Figure 4.8, the daily budget on October 14 and October 15,1966, yields an average runoff of 69 and 89 m^3/sec respectively, coming from the area below the Ahualulco and La Servilleta gauging stations and above the Río Frío station. No correction for lag time has been allowed, but it will not seriously affect the result on those dates. Also, on each of those days, surface runoff will have diminished to a small fraction of the water discharged from the springs in the lower Frío basin. Thus, these springs and the Santa Clara spring (Figure 4.10), despite their comparatively modest base flow, produce an important part of the karst discharge from the Sierras de Guatemala and El Abra. The average flow at Santa Clara station in 1972 was 2.53 m^3/sec and in 1973 was 5.09 m^3/sec. Several ungauged El Abra springs that have either a very small or nil dry season flow will probably be found to have a significant mean discharge.

The lower Tampaón basin is again identified as a major zone of ground-water discharge. It provided an average of 40.6 m^3/sec.

The determination of the total regional runoff is shown in Table 4.10. There is no surface runoff from the semiarid northern quadrant of the Platform. What happens to the meager quantity of ground-water recharge is not known. Also, the S.R.H. discharge data (Boletín No. 32) and elevation considerations indicate that the loss along the southern edge of the Platform into the Río Moctezuma could not be more than a few percent of the total regional runoff, and is probably negligible. Significant losses are not likely along the northern margin either. Runoff from the arid western half of the Río Santa María basin could not be more than a few cubic meters per second, and much of it is used for irrigation. Thus, the runoff from the Platform is closely approximated by adding the flow of the Axtla, the Coy, the Tampaón, and the Choy rivers, and the subbasin of the Río Guayalejo within the Platform. The flow from the ungauged springs along the east face of the Sierra de El Abra, the Santa Clara springs, and the springs in the lower Frío basin has been set equal to the flow from the Mante spring. Due to the extremely flashy or even intermittent flow from these springs, their total discharge is likely to be considerably less than the Mante spring during dry years and somewhat more than the Mante during very wet years. The average flow might be slightly less than the Mante.

One other factor in the budget is losses due to irrigation. The water taken from the Mante and Frío rivers has been accounted for at the source. So far, other irrigation usage is estimated to total

TABLE 4.10

Annual Regional Runoff

Station	drainage area sq.km.	YEAR 1961	1962	1963	1964	1965	1966	1967	1968	$Q_{avg.}$	% of total $\frac{Q_{s.a.*}}{Q_{r.a.**}} \times 100$
E. Requetemú	661	42.03	28.96	24.45	20.29	31.89	43.57	44.01	47.71	35.36	12.50
E. Ballesmí	194	27.76	22.05	21.18	21.44	25.36	32.16	32.41	30.24	26.575	9.39
El Pujal	23373	162.04	69.54	79.19	76.02	105.39	186.97	227.64	169.34	134.52	47.54
El Choy	4.9	6.07	3.36	3.62	2.21	3.98	7.36	8.53	5.43	5.07	1.79
Mante	69	12.39	(8.4)	10.57	(10.1)	(12.0)	(14.0)	13.23	13.47	11.77	4.16
La Servilleta	2532	4.85	2.77	1.85	1.36	5.17	11.49	7.30	4.81	4.95	1.75
Frío springs	42	19.77	17.00	19.85	21.57	22.99	32.08	21.84	21.76	22.06	7.80
Sabinas	497	16.27	11.33	8.27	10.38	12.35	25.69	15.96	11.31	13.945	4.93
La Encantada	3725	9.90	9.90	6.20	6.13	5.79	17.80	20.95	10.36	10.88	3.85
Ungauged El Ábra & S. de Guatemala springs	—	(12.39)	(8.4)	(10.57)	(10.10)	(12.0)	(14.0)	(13.23)	(13.47)	(11.77)	4.16
Irrigation losses	—	(6.)	(6.)	(6.)	(6.)	(6.)	(6.)	(6.)	(6.)	(6.)	2.12
Subterranean drainage area not included above	2335	—	—	—	—	—	—	—	—	—	—
Region Totals	33433	319.47	187.71	191.75	185.60	242.92	391.12	411.10	333.90	282.93	99.99%

* = station average ** = regional average

5-10 m^3/sec or only 1½ - 3% of the runoff. Areas of irrigation on the Platform include: 1) numerous small sites along many streams and valleys; 2) the Río Verde valley, supplied by the nearly constant flow of the Manantiales (springs) de Media Luna; and 3) the Upper Río Puerco basin in the Valles valley. The Presa (dam) de Las Lajillas on the Río Puerco was built sometime during the period 1961-1968, and is capable of storing about one-half of the runoff from its catchment of approximately 275 square km. Hence, the flow of the Río Valles will have become affected sometime during this period. The regional average discharge during 1961-1968 is thus about 283 m^3/sec.

Table 4.11 lists the average discharge of various basins during their complete record. The averages range from 2.0% to 40.0% greater than for the 8 year study period. The eastern, karst-spring dominated basins show only a small increase, whereas basins that have a significant percent of impermeable cover, such as Tanlacut and Valles valley, have a much greater increase. Also, the variations are due in part to differences in the period of record. The large increase at El Pujal reflects the enhanced runoff of the impermeable basins during wetter years, and the very large 1955 event (Section 4.2). A few years of the very long record at El Mante could not be used because of uncertain data reporting by one of the many agencies that have controlled the spring. As with the rainfall data, these data suggest that the 8 year base period may have been slightly drier than the long term mean.

TABLE 4.11

Runoff of Full Record Compared with 1961-68 Average

Spring or Station	$Q_{avg.}$ m^3/sec	years	σ	$\frac{\sigma}{Q_{avg.}}$	% > 1961-68 average
El Pujal	175.66	18	83.99	0.48	30.6
Ballesmí (Coy)	29.28	18	5.70	0.19	10.2
Choy	5.45	12	2.00	0.37	7.5
Mante	12.41	31	3.62	0.29	(5.4)
Frío springs	22.5	20	5.02	0.223	2.0
Est. Ahualulco (Frío springs)	30.89	10	6.06	0.196	—
Valles valley	11.86	11	7.95	0.67	27.3
Micos	27.26	11	9.53	0.35	15.7
El Salto	20.38	16	8.75	0.43	—
Tansabaça	41.52	14	23.17	0.56	33.9
Gallinas	33.17	13	13.36	0.40	10.5
Tanlacut	10.62	11	7.79	0.73	40.2
La Servilleta	6.48	13	4.11	0.64	30.9

4.3.3 Basin Yield

The average flows given in the previous section are, in reality, the basin yields. However, the data are not directly comparable. Table 4.9 includes columns of figures which make comparison more tractable.

One column gives the yield of each basin expressed as a percentage of the total regional runoff. About one half of the area, but only 11% of the discharge comes from the basin above Estación Tansabaca. Most of the region of low annual precipitation that is included within the surface drainage network is included within this basin. The Coy, the Frío and the Mante springs (actually includes some surface drainage) produced a remarkable 9.4, 7.8, and 4.2 percent respectively of the total average discharge. The Choy, with an average discharge of 5.07 m^3/sec, is a first magnitude spring, but this was only 1.8% of the regional total. Nearly all of the flow from the Huichihuayán and Lower Tampaón basins comes from springs, and this appears to be true also for the Gallinas and Micos basins. Thus, probably between 70-80 percent of the total regional runoff passes through the subsurface karstic systems and is discharged at springs.

Further comparison may be made by calculating the unitary discharge (i.e., the average discharge divided by the area) of each basin (Table 4.9). During the 8 year period, the calculated values ranged from a low of 0.0010. $m^3/sec/km^2$ for the Rayón basin to a high of 1.035 $m^3/sec/km^2$ for the Choy spring. The Rayón basin has previously been identified as an area of substantial karst losses. The very low yield from the La

Servilleta basin was caused by two factors: 1) about 50% of the area is high relief karst which yields little runoff to this basin, and 2) in the shale valleys, insufficient rainfall in the drier years to produce an excess of water (available for runoff) above the requirements of soil infiltration, surface detention, and evapotranspiration. The other basins with low unitary discharges are affected by a dry climate. The northwestern portion of the Platform produces no surface runoff because no integrated surface drainage has developed, though there is likely a small amount of infiltration into the subsurface. The basins with very high values are influenced by springs which bring in water from outside the topographic basin. Except for the Choy and the Mante basins, which were measured in this study from aerial photographs, the areas listed are those given by the S.R.H. in Boletín No. 32.

From Table 4.10 the regional unitary discharge, $U_{regional}$, is calculated to be:

$$U_{regional} = \frac{282 \cdot 93}{33433} = 0 \cdot 00846 \ \frac{m^3/sec}{km^2} .$$

The area used in this calculation includes the areas on the S.R.H. map which are marked as having total internal drainage plus a crudely estimated 100 km^2 of the crest of the Sierra de El Abra, which does not appear to be included within the region. Another column in Table 4.9 shows the ratio of the unitary discharge of each basin to the unitary discharge of the region. This ratio makes comparisons of basin yield easy. Values greater than about 3 stand out clearly as influenced by karst ground water captured from outside the surface basin. For areas having only moderate

rainfall, a lower ratio might still indicate captured ground water.

Because of the wide range of climatic and geologic conditions which have been included in the regional mean unitary discharge, attempts were made to determine the actual yield of some basins having a narrower range of conditions. This is impossible for most of the basins in the area, because the "underground drainage divides" or source areas for the springs are not known. The best candidate is the Valles valley, which is underlain by shale. The runoff from the Valles valley may be derived by subtracting the flow at Micos from the flow at Santa Rosa, provided that there are no gains or losses in the Micos canyon. The 1543 km^2 area of the Valles valley given by the S.R.H. includes some of the Los Sabinos and Japonés area drainages which are pirated underground, the area which supplies the Presa de las Lajillas, and probably too much of the Sierra de la Colmena. Thus, 0.00604 $m^3/sec/km^2$ is the minimum value for this valley. From the new 1 : 50,000 topographic map series of México, the minimum effective area was measured to be 975 km^2, assuming that the Presa de las Lajillas retained <u>all</u> the runoff from its drainage basin throughout the 8 year period. This gives a maximum value of 0.00955 $m^3/sec/km^2$ for the Valles valley. As previously stated, it is not known exactly when the Las Lajillas reservoir became effective. Its storage capacity is 41.5×10^6 m^3 (S.R.H., Bol. No. 32), which is one-half to two-thirds of the expected average annual runoff from its catchment of 275 km^2. Also, there are a few small ranch ponds which impound runoff. The value of the unitary discharge is taken to be about 0.008 $m^3/sec/km^2$ in this valley. For a mean annual precipitation of approximately 1150 mm during the 8 year period, and using the estimated

unitary discharge, the runoff was approximately 22% of the precipitation.

From the data presented, it is obvious that most of the runoff from the region is produced in the high rainfall belt in the eastern half of the Platform. A "reduced region" unitary discharge may be calculated by subtracting the runoff and area of the La Encantada and Tansabaca basins and the irrigation losses from the total regional values:

$$U_{\text{reduced region}} = \frac{282{\cdot}93 - 10{\cdot}88 - 31{\cdot}01 - 6{\cdot}0}{33433 - 3725 - 17532}$$

$$= \frac{235{\cdot}04}{12176} = 0{\cdot}0193 \text{ m}^3/\text{sec/km}^2 .$$

The resulting area, the "reduced region", is 70-75% karst terrain with predominantly subsurface drainage, versus 25-30% shale or sediment filled valleys which produce surface runoff. It contains nearly all of the moderate to high rainfall area -- the range of measurements was 801 mm to 2125 mm. Thus, the average yield of the "effective" runoff producing region was 0.0193 $m^3/sec/km^2$. An upper limit of 0.03 $m^3/sec/km^2$ is suggested for the average yield of the wettest areas, such as the Xilitla-Tamapatz area. If ground water originating from the western portion of the Platform resurges in the "reduced region", the effect would be to decrease the value given above, though the correction could only be a small percentage of the total. The fact that the long term average discharges may be greater than the 8 year period selected for analysis would demand somewhat greater values for the long term unitary discharges than those given above. The mean annual precipitation of the "reduced region" during the 8 year study period was calculated to be

about 1500 mm. The runoff was 41% and the evapotranspiration was 59% of the estimated rainfall, assuming that the change in storage was negligible.

Some support for the analysis above may be obtained from S.R.H. data for the Río Tempoal basin which drains predominantly clastic sedimentary rocks along the eastern Sierra Madres about 100 kilometers southeast of Cd. Valles. It has an area of 5275 km^2 and lies outside the study area. The long term average precipitation for the basin was calculated to be roughly 1650 mm/year (data from S.R.H. Boletín No. 19) and the unitary discharge for the years 1955-1968 was 0·017 m^3/sec/km^2 (S.R.H. Boletín No. 32). The yields are compared in Table 4.12.

TABLE 4.12

Unitary Discharges of Various Basins

Basin	U (m^3/sec/km^2)
Total region	0·00844
Valles valley, minimum	0·00604
Valles valley, maximum	0·00955
"reduced region"	0·0193
Tempoal region	0·017 (14 year average)

The calculated unitary discharges for the four areas are reasonably consistent with one another, but their numbers are few. Quantitative comparisons of the efficiency of the surface and subsurface routes have not been accomplished yet. A much greater percentage of the rainfall on

shale valleys is converted into runoff during wet years than during dry years. This may also be true in the karst areas, but changes in ground-water storage must be taken into account. From the tables of unitary discharge, it is clear that in this region, as has been found in many other karst areas, there is little or no relationship between the topographic surface basins, and the subsurface karst drainage basins. One of the principal objectives of future work in the region should be the determination of the source areas of the springs, and the detailed study of the karst flow systems.

4.4 Ground Water in the Sierra de El Abra

In previous sections of this chapter, some of the gross characteristics of the regional hydrology were discussed, i.e., the water budget, and aspects of the temporal variations of precipitation and of discharge. In this section, some field observations of the karst ground water, principally in the Sierra de El Abra, will be presented. Further discussion of the hydrology of the El Abra will be given in Chapter VII.

4.4.1 Distribution of Ground Water; Storage

For 6 to 8 months of every year, recharge of the El Abra aquifer in the Sierra de El Abra is negligible. Thus, the flow of the springs must be maintained by ground-water storage.

Observations in the caves yield important information concerning the distribution of karst ground water. Approximately 45 kilometers of

cave passage have been explored (most of them have been surveyed) in the Sierra de El Abra. More than one-half of this total has been seen by the writer. Eighty percent of the known passage length lies within the western margin caves, which are predominantly swallet caves (see Chapter VI).

In the wet season, particularly during and shortly after a storm, points of vadose seepage or flow into the caves are very active. Within a few days following a storm, most of these vadose inlets are reduced to a moderate or slow rate of drip from cracks or stalactites. During the dry season, nearly all the vadose inlets are inactive. The active sites are drips, except for a very few continuous flows. There may be some bias in the above observations because so much of the known cave passage length is along the western margin, and because the relatively impermeable Méndez Formation covers the majority of the passages of the swallet caves. However, the vadose inlets in the caves in the El Abra range do not seem to be more active than those in the swallet caves. Unless the preponderance of the vadose percolation water bypasses the larger conduits (passages) and reaches the phreatic zone unobserved, then judging from the cave drips the total seepage rate is perhaps two orders of magnitude less than the estimated 10-15 liters/sec/km^2 needed to supply the base flow of El Choy.

One of the notable features of the swallet caves is the numerous lakes and pools. Data collected during this study (to be presented later) indicate that all of the cave lakes thus far encountered in the Sierra de El Abra, with the exception of the lake in Sótano de Soyate and possibly

the terminal sump in Cueva Chica, are perched water bodies. To the explorer the lakes seem large, and they often pose exploration problems. For example, a lake in Sótano del Tigre is 270 m long, 15 m wide, and (fortunately for the explorer) only 1.4 m deep for the most part. Excluding the lakes in spring caves such as El Choy, all of the known large lakes occur in the western margin caves, again with the exception of the lake in Soyate. From maps, estimates were made of the volume of water in the lakes in the Arroyo, Tinaja, Los Sabinos, Tigre, and Jos caves, which contain 40% of the known passage length and most of the large lakes. The total calculated volume is 48,000 m^3. The lakes in most of the remaining swallet caves are generally smaller, and the known pools within the El Abra range do not amount to more than a few tens of cubic meters. Thus, the total volume of the known vadose cave lakes is roughly 80,000 m^3. This is enough to supply the Choy spring for only <u>one-third</u> of <u>one</u> typical dry season day -- if all the water from the lakes were drained. Certainly most of the interior of the El Abra range has not been explored. Yet, because most of the lakes do not lose much water during the dry season, and because their total volume is believed to be relatively small, it does not seem possible for the El Abra springs to be supplied by the change in storage of the vadose lakes.

Only four dry season cave "streams" have been found in the El Abra. They are located in La Cueva de El Pachon, El Sistema de Montecillos, El Sótano de la Tinaja, and El Sótano del Arroyo. There is a good chance that the "stream" in Arroyo is the same as the one in Tinaja (see descriptions and maps, Chapter VI). Because of the limited number

of observations, it is not known whether the streams are really permanent; though in May, 1973, near the end of a severe dry season, a tiny trickle still flowed in Arroyo. In reality, all of these "streams" are merely trickles of a few liters or less per minute, depending on the date during the dry season. Thus, they do not constitute a significant discharge of water.

From the above data, it is believed that the total dry season vadose flow that passes through cave passages of explorable size does little to support the discharge of the El Abra springs. If it is true that a significant portion of the vadose seepage waters are integrated into the major conduits while still in the vadose zone, then most of the base flow of El Choy and El Mante is drawn from the phreatic ground water body.

An estimate of the storage supporting the flow of a spring may be made from an analysis of the base flow recession. Burdon and Papakis (1963) give the equations:

$$Q_t = Q_0 e^{-kt} \qquad (4.1)$$

and

$$S_t = \frac{Q_t}{K} \qquad (4.2)$$

which represent the exponential decay of the discharge Q and the storage S_t of the aquifer at time "t"; K is the recession constant. If Q and t are plotted on semilog paper, the data will form a straight line where the equations are applicable. Inspection of the Choy daily discharge data from 1960-1971 indicated that the most stable long period of flow occurred during the unusally severe dry season of 1970-1971 (see Figure 4.7).

A semilog plot (not shown) of the data yielded an excellent straight line fit for the period January 1, 1971 to May 1, 1971. Deviations from the fitted line were less than the expected errors of the discharge measurements. From this graph, the recession equation was determined to be:

$$Q_t = Q_0 e^{-(0.001643 \text{ days}^{-1})t} \qquad (4.3)$$

The storage was calculated to be 200,000,000 m^3 on January 1, and 164,000,000 m^3 on May 1. Thus, the volume of phreatic storage behind El Choy in the dry season is about the same as its average annual discharge of 172,000,000 m^3 (5.45 m^3/sec). The storage value given above is the volume of water that theoretically could drain to El Choy due to the force of gravity, and does not include the phreatic storage below the spring point.

Similar calculations were not attempted for El Mante because of the complications of the reservoir and distributary canal system, but were made for the Coy spring. As previously noted, the hydrograph of the Río Coy at Ballesmí gauging station is more variable than El Choy during the winter and spring months because of greater and more frequent rainfall on the surface basin and on the recharge area. Reasonably long recession periods are not available for analysis. A straight line can be fitted to the base flow recession from December 20, 1962 to February 6, 1963. This gives a gravity storage of 327,000,000 m^3 on January 1, 1963. The Coy has a greater storage than El Choy, but it also has a larger base flow. Calculations for a short period in April, 1963 and for a 30 day stable period in April - May, 1970 give slightly over 400,000,000 m^3 of storage. According to these calculations, early in the dry season, the gravity storage for the Coy spring is pro-

bably about one-half of the average annual discharge (18 year record) of 923,000,000 m^3 measured at the Ballesmí station, which also includes 194 km^2 of surface drainage. However, the storage given here should be considered a minimum, because a long recession limb could not be examined, and because the dry season base flow has so little variation from year to year that a larger storage may exist.

4.4.2 Ground Water Level Fluctuations

Cave lakes exist over a wide range of elevations within the Sierra de El Abra. Previous workers (Bonet, 1953a, and William H. Russell, personal discussions) have believed that most of these lakes, particularly those which "terminate" passages (i.e., where the passage becomes filled with water), lie at the water table. An important part of the hydrological field studies of this thesis was aimed at testing this hypothesis, mapping the water table, and collecting quantitative data about water level fluctuations. This section will discuss field measurements of water level fluctuations. Other data and interpretations concerning water levels are contained in Chapter VII.

Two cave lakes representing contrasting situations were selected. One was the terminal sump in Sótano de Jos (map and description, Chapter VI), deemed the swallet cave in which a stage recorder could most feasibly be placed in a satisfactory position, although many of the other swallet caves are larger and have greater catchment areas. The known part of the cave is about 350 meters long, and has a surface basin of 4.3 square kilometers. A continuous recording Ott recorder was bolted to a

board spanning the gap between two ledges 6 m above the static level of the lake. A quasi-flexible plastic pipe, secured at the bottom by a board bolted to the wall and along its length by wires to bolts in the cave walls, was emplaced to protect the float and counterweight during floods. The deep lake in Sótano de Soyate (Chapter VI) was the other lake selected. It is a deep shaft on the western flank of the Sierra de El Abra. The cave has a negligible surface catchment though a small vadose inlet is active during storms. It descends via a deep shaft and two shorter drops to a large lake room, 150 m long and 20 m wide. The water depth was measured in many places, the maximum being 54 m and the minimum 34 m; thus, the bottom of the lake is near sea level and well below the base level of the El Abra range. An Ott water level recorder was placed over a hole about 12 m above the general dry season level of the lake, which gave a free drop to the lake. The results of these projects are shown in Figures 4.13-4.15. Also shown in these figures for comparative purposes, are the Choy discharge hydrograph and appropriate precipitation data.

The important features of the Jos hydrograph may be seen in Figure 4.13, although these particular floods are very small. The hydrograph was perfectly flat for two days until a storm occurred between 8:00 A.M. on July 11 and 8:00 A.M. on July 12 -- probably very early in the morning of July 12. A flood pulse entered the cave causing a response at the Lake Room beginning at 9:25 A.M. and 50 minutes later the crest stage of 7 cm was reached. Another shower on July 12 caused a second pulse to build on the first, reaching a crest of 15 cm. A third rainfall-flood event occurred on July 14, after which the water level rapidly

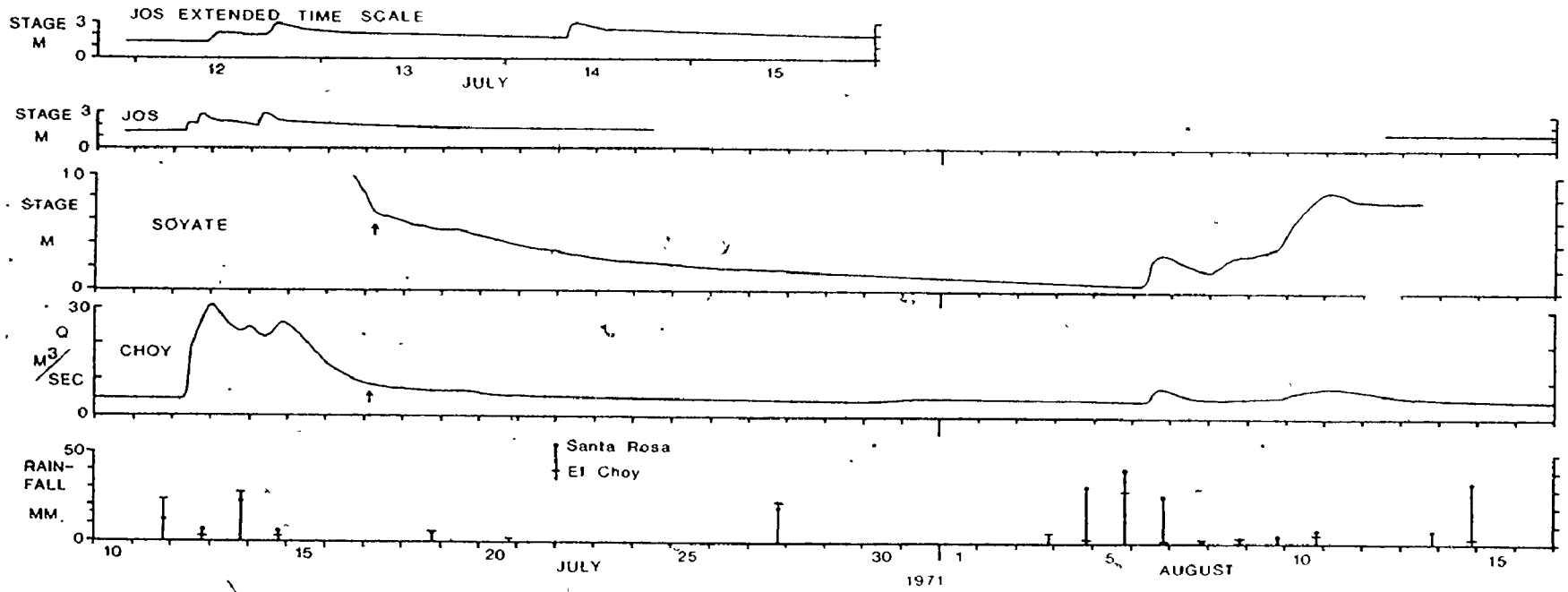

Figure 4.13 Soyate and Jos cave-lake hydrographs compared with rainfall and Choy discharge, July and August, 1971.

returned towards its normal level. There seems to be a close relationship between the events recorded on the Jos and Choy spring hydrographs, although the amount of water which passed through Jos could not have had much effect on the Choy's discharge. The Jos basin apparently received less rainfall than some other parts of the Choy's source area. Also, the flood hydrograph is substantially broader at the Choy than in Sótano de Jos. An additional 4½ days of record in August was completely featureless, and at static level.

The hydrographs obtained in Sótano de Soyate are very different from those obtained in Jos. Unfortunately, the Soyate record began on July 16, 1971, missing the floods of the preceding four days. A gradual recession, totaling 92 cm, occurred over the next 21 days, in harmony with the Choy discharge recession. The water level fluctuations during the July 12-16 floods must have been much larger at Soyate than at Jos. Three small flood events were recorded in early August. Because the distance from the stage recorder to the water surface was not measured for this particular record, only the change in elevation of the water surface is known. However, measurements at other times suggest that the reference line shown in Figure 4.13 was about 11 ± 0.5 m below the support (datum) of the stage recorder.

Figure 4.14 shows a shorter, but more active hydrograph of Soyate in June, 1972. The first showers of the wet season in late May and early June were already causing the water surface to rise when the recorder was started on June 5. An afternoon rainfall on the western flank of the El Abra, including the Soyate area, probably caused the steepening

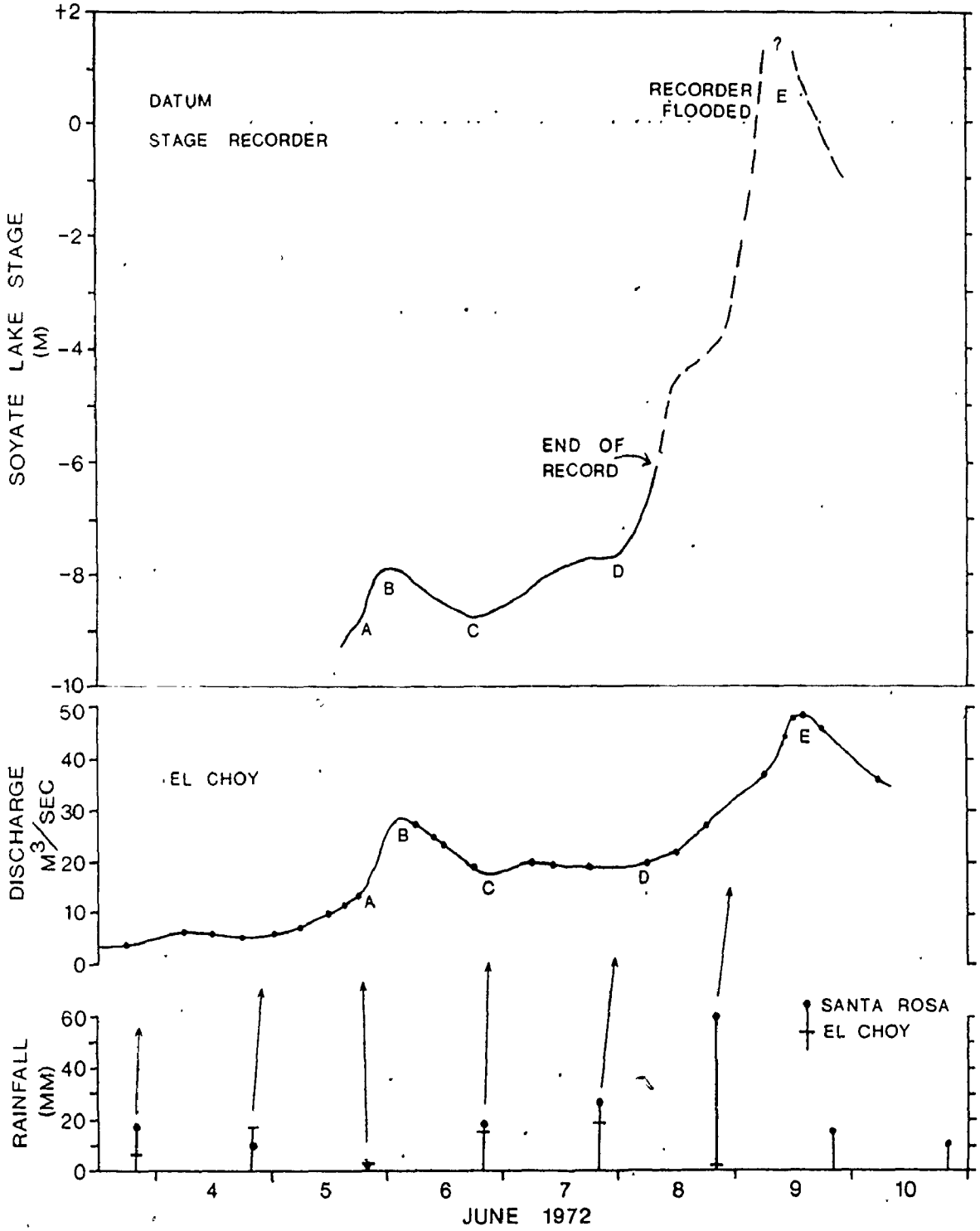

Figure 4.14 Soyate cave lake hydrograph and correlation with rainfall and Choy discharge, June 1972.

of slope at point A on the Choy and Soyate hydrographs (note that this observed shower was scarcely felt at Cd. Valles or El Choy). Two to three days later, heavy rainfall again caused the water level to rise rapidly. Although no record of the crest of the flood was obtained, the stage recorder was inundated (leakage around the pulley axle bearings). Thus, the water level rose more than 9 m after the record began on June 5, and probably more than 12 m from mid-May.

Attempted stage recording operations in September, 1971, provided information concerning the most spectacular flood events for which some data were obtained. Figure 4.15 shows an interpretative sketch of the events based on the limited data and on the character of the previously discussed hydrographs. Personal communications from Steven Bittinger and Don Broussard, who along with Frank Binney and Diana Porter went to service the stage recorders on September 11, have provided important information concerning the events. From July 16 through September 8, only a few very minor floods occurred at El Choy; none exceeded 10 m^3/sec (see Figure 4.7). From the data obtained during the first half of this long stable period, it is reasonable to assume that the terminal lake in Jos was at its static level and that the Soyate lake surface was about 11 m below the datum board. The ground surface and vegetation were undoubtedly dampened by several moderate rainfalls during early September. On September 8, about 40 mm of precipitation fell which produced a sharp 34.7 m^3/sec flood crest early on September 9 at El Choy. On September 11, both recorders were found full of water, presumably having been flooded out by the pulse on September 9. In Jos, the flood wave crested less than 2.5 m above the recorder, but its

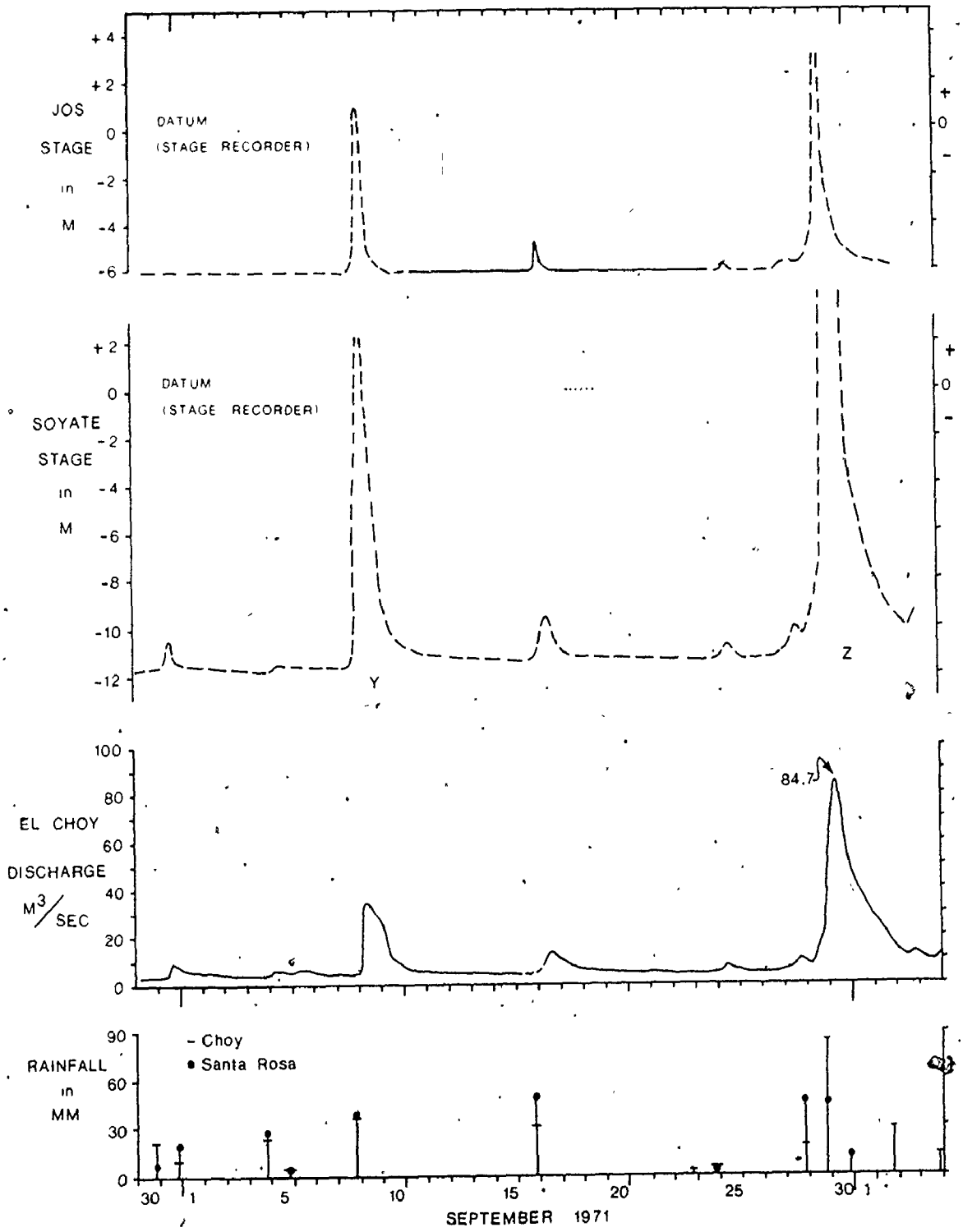

Figure 4.15 Flood events at Jos, Soyate, and Choy, September, 1971.

force had torn loose one end of the board at the bottom of the pipe. The lake surface had returned to its static level, and the flow through the cave was estimated to be equivalent to that of few "garden hoses". In Soyate, the water level appeared to be back down to approximately its normal range (when the Choy is at base flow). Fortunately, the Jos recorder worked for the next thirteen days. A single storm caused a sharply peaked flood pulse in Jos and a much broader pulse at the Choy on the 17th. The crest of the flood of slightly more than 1 m was reached 2 hours after the stage began to rise and approximately seven hours before the crest at El Choy. Then it subsided almost as rapidly. At the end of the month, a major storm hit the southern El Abra region. When the recorders were removed in January, 1972, both were found to have been disastrously inundated. This must have occurred on September 29-30, and possibly again during the second week of October (see Figure 4.7 for the complete Choy hydrograph). More damage had been done to the still pipe in Jos, and water in a can placed 2.5 m above the recorder demonstrated that the crest had reached at least that level. In Soyate, the water rose so high and so quickly above the recorder that the water pressure popped the glass window out of its stiff rubber frame and into the case. In early January, 1972, the water level was 11.5 m below the Soyate recorder board, and the Jos lake was at its normal static level.

Inspection of all the above Figures shows a close temporal relationship of events recorded at Jos, Soyate and El Choy. Furthermore, each event is in response to a particular precipitation event.

A one-to-one correlation is attempted in Figure 4.14, but such correlations are more easily seen when the storms are isolated events. It is also clear that the amount of precipitation received at El Choy or at Cd. Valles (Santa Rosa station), both of which lie off the El Abra range and peripheral to the source area of the Choy spring, is often not a good predictor of the magnitude of response that is observed at Jos, Soyate or El Choy.

Although year-round observations in Jos are not available, it appears that the water surface at the Lake Room siphon stays at a constant static level, except when wet season flood pulses of very short duration enter the cave. Possibly, a few centimeters are lost because of evaporation or leakage during the dry season. The hydrograph is similar to a desert arroyo which occasionally has flash floods, but maintains only a trickle or no base flow at all. The character of the hydrograph combined with elevation and geomorphic data to be discussed later lead to the conclusion that the lake is a perched water body. It is predicted that more air filled passage exists on the other side of a water trap (inverted siphon).

In contrast with the Jos lake hydrograph, the water surface in Soyate is always moving -- up when it rains, and down when it does not. These movements occur in almost perfect temporal correlation with the Choy hydrograph. Note in particular the similar time span (breadth) of the flood hydrographs of Soyate and El Choy, the correlations of Figure 4.14 and during more subtle fluctuations in August, 1971, and the correlated break in slope on July 17, 1971, followed by an

increasingly gradual decline. Figure 4.16 is an attempted comparison of the stage at Soyate with the discharge at El Choy. Although based on sparse and sometimes shakey correlations, a broad relationship is evident. The letters are keyed to the hydrographs. Vertical lines represent the three times the level of the recorder was surpassed. Event Y probably only slightly exceeded the height of the board; floods such as Z likely cause the water surface to rise 20 m or more.

Based on the hydrographs, the lake's elevation of approximately 59 m (or 24 m above the spring at base flow), and the lack of known air filled passages below that elevation (except at inappropriate places such as near the Río Tampaón) the Soyate lake is interpreted to be a "water table" lake. The cave in reality is a rather large piezometer; the elevation of the water surface reflects the local piezometric surface of the pressure conduits (water filled caves) which carry water to the Choy spring.

To date, the Soyate lake is believed to be the only "water table" lake known in the Sierra de El Abra. This is unfortunate, because Soyate may connect with the large conduit(s) coming from the swallet caves to the west to El Choy. This is suggested by the thick mud deposits at and above the recorder, by the large population of blind fish, and by their need for organic debris for food. The smaller fluctuations in Soyate are probably the result of local infiltration, but the larger fluctuations may be influenced by sharp pulses from swallet caves. Discovery of more lakes such as that in Soyate will be very important in achieving a better understanding of the aquifer.

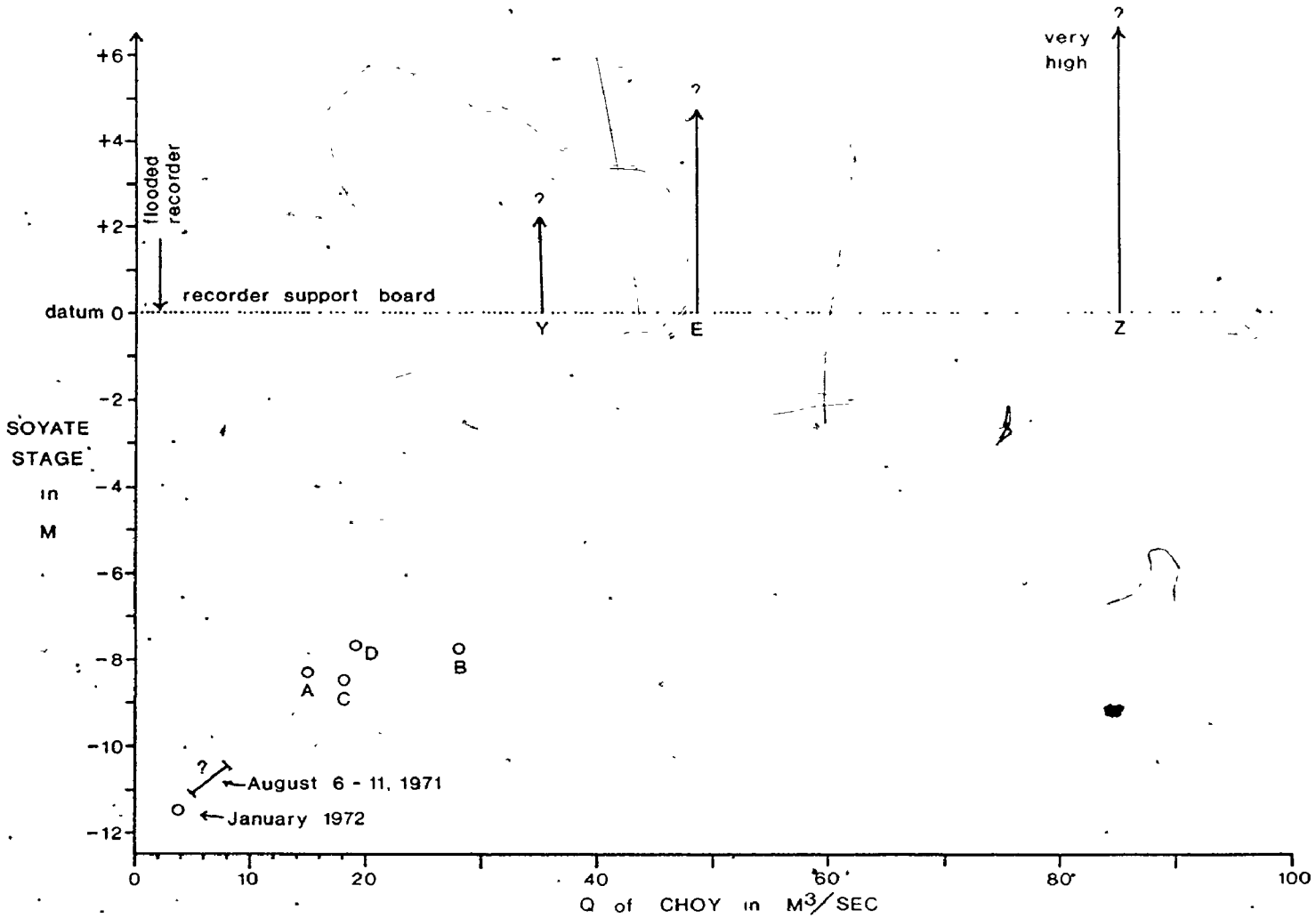

Figure 4.16 Relationship between Soyate cave lake stage and Choy discharge.

4.4.3 Water Tracing

A large number of water tracing experiments are needed in the El Abra range to determine sink to rising connections, drainage divides, ground water velocities, and possible dispersion of the tracer into several flow paths and to more than one spring. In practice, such experimentation in this region is difficult because very few of the sinking arroyos can be observed from the highway to know when they are running. Furthermore, when large rains come, access to the sink points involves walking several kilometers on muddy tracks and access to most of the smaller springs is generally impractical.

It was decided to conduct a lycopodium spore tracing test of Sótano de Japonés (see Chapter VI) to its most likely discharge point -- the Choy spring. Nets of 25 micron mesh nylon were made approximately in the manner described by Drew and Smith (1969) though somewhat smaller, and five were placed in the Choy stream about 100 m downstream from the spring on July 15, 1971. They were attached to a wire and floated in mid-stream with about 90% of their catchment area below the water surface. Twenty-four pounds of dyed spores were injected at 6:15 P.M. on July 18 into the arroyo leading to Japonés where it crosses the highway 1.6 km upstream of the sink. Local showers during the day had caused a small flood. The discharge was estimated to be about 0.3 m^3/sec at the time of injection.

The nets were sampled on July 22, 28, August 5 and 14. A very few spores were found in the first sample and none in the others. Such

a low catch might be explained by the fact that only 2-3% of the stream's cross section was sampled, and by the large amount of sediment caught which tends to block flow through the nets. Unfortunately, the possibility of contamination cannot be completely ruled out; hence, the test is only tentatively positive. The straight-line distance from sink to spring is 22.9 km and the sample time was 92 hours after injection. If the test is positive, an average ground water velocity of at least 250 m/hr is calculated. This value appears reasonable when compared with a list of velocities determined for karst flow systems having a wide range of relief and distance (Prof. D.C. Ford, personal communication of unpublished list derived from the literature and his own data).

4.5 Summary

The El Abra and Tamasopo Formations plus suspected Lower Cretaceous platform facies limestones form a karstic aquifer that is continuous over most of the Valles-San Luis Potosí Platform. Other rocks have low permeability or are impermeable and yield surface runoff. The El Abra limestone (geologic mapping has generally not distinguished between the El Abra and the Tamasopo Formations) crops out over a large portion of the Platform, and karst caves and major springs have developed in this high relief region. The S.R.H. (Secretaría de Recursos Hidráulicos) has established many hydrologic gauging and climatologic stations in the region to collect data for water resources control and development. A surface drainage network reaches about two-thirds of the Platform, but no surface runoff leaves the north-

western area. Rainfall is strongly temporally distributed into wet and dry season (June-October and November-May respectively), and spatially distributed into a wet eastern zone (800-2500 mm/year) and a semiarid western zone (250-600 mm/year). Very large precipitation events are common during the wet season.

Runoff from Platform basins closely correlates with annual precipitation, with the season (wet or dry), and with individual precipitation events. This statement is true for springs as well as surface catchments on impermeable rocks such as the Valles Valley. There are several very large, karst springs in the region -- two are among the largest reported in the literature. Springs provide essentially all the dry season base flow from the Platform; and 70-80% of the total runoff is estimated to have passed for at least a short distance through subsurface karst channels. Most of the large springs occur at or near the eastern edge of the Platform or along the lower part of the Río Tampaon, the largest river in the region. The Coy spring has a minimum recorded flow of 13.0 m^3/sec (459 c.f.s.; 18 year period) and discharges about 20% of the entire base flow of the Platform; its long term average flow is estimated to be about 24 m^3/sec (847 c.f.s.) including the nearby small intermittent springs at the Coy dome (29.28 m^3/sec was the average at the Ballesmí gauging station which includes a surface basin of 194 km^2, and there may be other small springs near Aquismón). The Frío springs, a cluster of springs in a small area that form the headwaters of the Río Frío, have an estimated long term average discharge of about 28 m^3/sec (988 c.f.s.), including some "ungauged" springs below the principal spring guages. The Choy and the Mante are the largest springs in the Sierra de El Abra and have average flows of

5.4 and 11.9 m^3/sec respectively. The karst ground-water flow systems and the flows of springs are extremely dynamic, in response to large wet season precipitation events. Most springs exhibit discharge variations (Q_{max}/Q_{min}) of 25-100 times or more. In 1951, the Frío springs produced a flood crest of 554-700 (?) m^3/sec, the greatest from a karst spring known to this author. This is particularly remarkable because recharge, as for most of the springs in the region, occurs at myriad localities rather than a very few discrete points. The Choy, which was the most intensively studied spring in this work, usually yields several pulses of 30 m^3/sec or more each year, and occasionally surpasses 100 m^3/sec. The Choy (and probably all the other springs except Media Luna) shows a response within a few hours of heavy rainfall and usually crests roughly 24 hours after a major precipitation event; some larger springs may take slightly longer. The S.R.H. discharge data for the Santa Clara, and observations in this study show that the many springs having small base flows are also extremely dynamic, and yield a large part of the runoff from the region. Studies of the spatial variation of discharge, as measured at the gauging stations, have located areas of deficient and excess runoff, and showed some differences between the distribution of base flow and flood flow. The areas having deficient runoff have zones of karstic losses and the areas having excess runoff have karst springs that receive ground water from areas not related to the "surface basins".

Some observations and field work concerning the hydrology of the Sierra de El Abra were reported in this chapter, but a broader discussion is given in Section 7.3. The water in dry season gravity storage behind

the Choy spring was calculated to be equivalent to about one average year of its discharge. Based on observations in caves all across the range, it was concluded that the water must be stored in the phreatic zone, although some of it might exist as vadose seepage if it by-passes the larger conduits. Stage recorders placed over the terminal siphons in Sótano de Soyate and Sótano de Jos (a swallet cave) produced records that indicate the former is a genuine water-table lake, whereas the latter is a perched lake. It is believed that all of the siphons yet discovered in the western margin caves are perched siphons. Both recorders were inundated, showing that large water level fluctuations often occur.

CHAPTER V

HYDROGEOCHEMISTRY

5.1 Introduction

The objectives of the water chemistry studies in this thesis are: 1) to determine the chemical character of the karst waters in the region, especially the springs, and make comparisons with the karst water chemistry of other regions; and 2) to use the water chemistry as a tool for hydrologic analysis, particularly hydrograph separation. This chapter will examine the chemical composition of karst waters in various environments and some variations that occur during the wet season. Further analysis and modeling will be given in Chapter VII.

Four classes of karst water have been sampled. They are: 1) large streams on shale catchments which are pirated underground (swallet water), 2) cave drips, 3) cave lakes, and 4) springs. Figure 5.1 shows the schematic relationship of these karst waters in the Sierra de El Abra. The first two classes are represented by just a few samples; hence, they serve only as an indication of their character. Many more samples from cave lakes were obtained. Most of these lakes are perched water bodies in the western margin swallet caves. However, the sampling plan was principally aimed at differentiating the types of springs and studying their response to flood pulses. Sampling of the first three water classes was confined to the Sierra de El Abra, whereas sampling of the

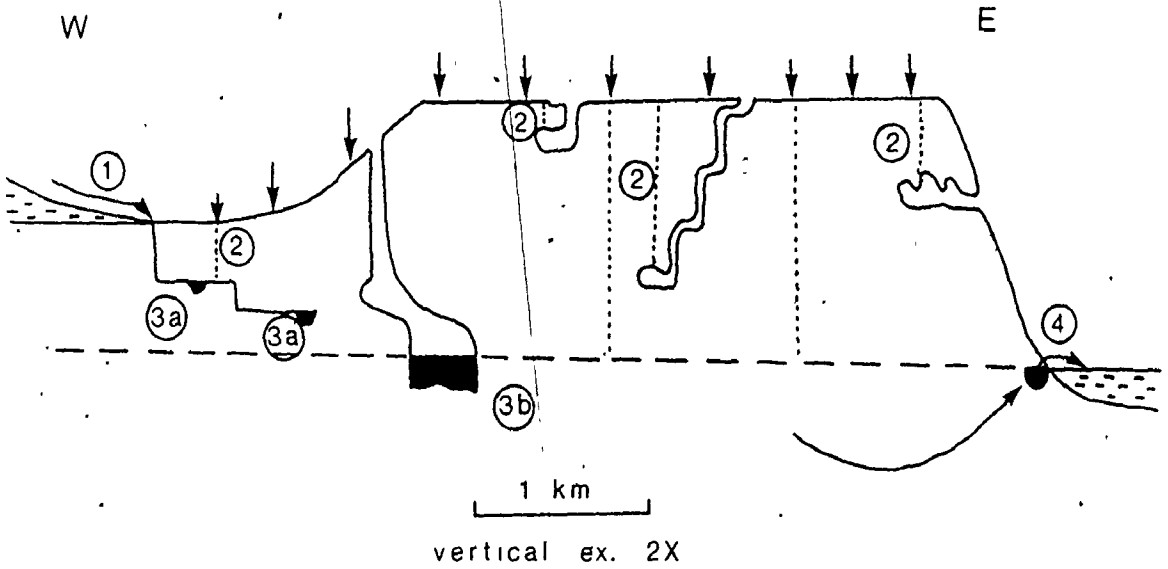

Figure 5.1 Hydrochemical environments in the Sierra de El Abra:
1) swallet waters from shale or flaggy limestone;
2) cave drips;
3) cave lakes, "a" are perched and "b" is water table;
4) springs.

fourth type included most of the major and several of the smaller springs in the region. Three classes of water which were not sampled are the main surface drainage systems such as the Río Tampaón, and the diffuse or unconcentrated surface and vadose trickle input water on top of the El Abra range.

A statement of the sampling procedures, the analytical methods, and the errors is given in Appendix I. Here, it is sufficient to say that the analyses of samples collected during the summers of 1973 and 1972 are regarded as high quality data (the Ca, Mg, and SO_4 listings are the average of at least two determinations and the temperature, pH, and alkalinity were carefully measured); the analyses of the summer 1971 and December-January of 1971-1972 are less reliable principally because the pH determination was less precise and the Ca, Mg and alkalinity analyses were generally performed only once. A few samples simply have unexplained errors; however, most of the analyses are believed reasonably good. The data have been processed on a CDC 6400 computer using Watchem II, a program written by John Drake and modified by T.M.L. Wigley (1972). The program calculates the saturation conditions of a sample with respect to calcite, dolomite, and gypsum; the theoretical P_{CO_2} ; and several other results such as the percent error, the Ca/Mg and Ca/SO_4 ratios, and the ionic strength. Saturation conditions are calculated using temperature dependent equilibrium expressions, and take into account the ion pairs $CaSO_4^\circ$, $MgSO_4^\circ$, $MgHCO_3^+$, $CaCO_3^\circ$, and $MgCO_3^\circ$. Only the first three ion pairs are significant in the area and $CaHCO_3^+$ is ignored completely (after Langmuir,

1971). The results agreed within ± 0.04 log units of the calculated calcite and dolomite saturation indices given by both references, and within ± 0.02 for the pP_{CO_2} on three samples by Langmuir. The slight differences are probably the result of variations between authors as to what ion pairs are important, and what values of the equilibrium constants are used, especially for dolomite.

In this study, only the saturation state of the water with respect to calcite, dolomite, and gypsum is of interest. The degree of saturation may be evaluated by the "saturation index" or "SI" which is calculated as follows:

$$\text{calcite:} \quad SI_c = \log(a_{Ca^{++}} \cdot a_{CO_3^{=}}) - \log K_c$$

$$\text{dolomite:} \quad SI_d = \tfrac{1}{2}[\log(a_{Ca^{++}} \cdot a_{Mg^{++}} \cdot a^2_{CO_3^{=}}) - \log K_d]$$

$$\text{gypsum:} \quad SI_g = \log(a_{Ca^{++}} \cdot a_{SO_4^{=}}) - \log K_g$$

where the "a's" are activities and the "k's" are the appropriate equilibrium constants. Note that the saturation index for dolomite (SI_d) is calculated for the stoichiometric form so that it may be compared directly with the values for calcite and gypsum. A positive (+) number is supersaturated, and a negative (-) number is undersaturated. Samples having a value within ± 0.10 of zero are approximately saturated with respect to that particular mineral. More information about thermodynamic calculations is available in Garrels and Christ (1965), Stumm and Morgan (1970), Langmuir (1971), and Back and Hanshaw (1970). Because of the importance of ion pairs in the waters studied here, the total concentration (analytical value) of a species in solution will be indicated by a symbol without charge (e.g. Ca, or Ca_{tot} for emphasis), and that part that is ionized will be indicated as such (e.g. Ca^{++}).

5.2 Chemistry and Environment of the Karst Waters

In this section, the chemistry of the karst waters will be examined and compared. For the springs, the discussion will be oriented toward their dry season chemistry in order to show their character during that long period of stable aquifer conditions and spring discharge. For other classes of water, all available data will be examined.

Nearly all the analyses performed and some calculated parameters are listed in Table 5.1. The variables generally measured were Ca, Mg, alkalinity, SO_4, temperature, pH, turbidity (qualitative), and discharge (where applicable). These data have been divided into two groups according to the quality of the determinations: Table 5.1a, high quality and Table 5.1b, less reliable (but in most instances believed reasonably good). A few good analyses were placed in the second category for reasons other than the quality of the analytical measurements (e.g., the Covadonga thermal spring "Los Bañitos", because the actual source could not be sampled). In addition, many springs were checked for Na, K, and Cl. Except for the Taninul Sulfur Pool, a thermal spring, the concentrations of the last three constituents were found to be unimportant (see Table 5.2). Many of the characteristics of the karst waters in the area are shown in Figures 5.2-5.5, which will be referred to in the following pages. Figure 5.2 shows the chemical composition of representative samples from each class of karst water so that they may be easily compared.

Swallet Streams

The [illegible]inal valley [illegible] the [illegible] side of the Sierra de El Abra

TABLE 5.1

CHEMICAL ANALYSES AND DERIVED GEOCHEMICAL MEASURES

5.1a BEST ANALYSES

LOCATION	NO.	DATE	TEMP. °C	pH	Ca [1]	Mg [1]	ALKA-LINITY [1]	SO_4 [1]	% ERROR	Ca/Mg MOLAR	pP_{CO_2}	SI_c	SI_d	SI_g	$Q\ m^3/sec$ [2]
SPRINGS															
CHOY	1	5/21/73	26.4	6 91	204 / 10.16	44 3 / 3 64	300 / 4.91	422 / 8 79	+ 0 36	2 79	1.45	+ 0.02	- 0 11	- 0.73	2 85
	2	6/7/73	26 4	6 92	203 / 10 14	44.5 / 3 66	303 / 4.97	422 / 8.79	+ 0 15	2.77	1 46	+ 0 03	- 0 09	- 0.73	2.84
	3	6/13/72	25.1	6 74	98.1 / 4.90	5.6 / 46	276 / 4.53	37 / 77	+ 0 56	10.6	1 30	- 0 35	- 0.78	- 1.84	FLOOD
	4	6/15/72	25.0	6.69	97.3 / 4 86	5.6 / .46	271 / 4.44	35 / 73	+ 1.43	10.6	1.26	- 0.42	- 0.84	- 1 86	FLOOD
	5	6/17/72	24 9	6.70	97.3 / 4 86	5.6 / .46	273 / 4 47	41 / 85	0 00	10.6	1.27	- 0 41	- 0 83	- 1.80	FLOOD
	6	6/19/72	24 9	6.80	98.5 / 4.92	6.1 / .50	267 / 4.38	44 / 92	+ 1 12	9.83	1 38	- 0 31	- 0 72	- 1 76	FLOOD
	7	6/23/72	24.9	6.83	95.3 / 4 76	5.8 / .48	270 / 4.43	40 / 83	- 0.19	9.90	1 40	- 0.29	- 0 70	- 1 81	6 5
	8	6/28/72	25.1	6 87	98 1 / 4 90	6.6 / .54	265 / 4.34	53 / 1 10	0 00	9 06	1.45	- 0 25	- 0 64	- 1 69	4 4
	9	7/7/72	25.2	6.93	112 / 5.60	10.7 / .88	267 / 4.37	90 / 1 87	1 89	6.37	1 51	- 0 15	- 0.46	- 1 44	4 2
MANTE	10	5/25/73	26.5	6.88	228 / 11.38	44.8 / 3.68	309 / 5.06	487 / 10.15	- 0.50	3 09	1.41	- 0 04	- 0 11	- 0 65	11.32
	11	7/11/72	25.8	6 92	152 / 7 58	25.5 / 2 10	291 / 4.77	240 / 5 00	- 0.46	3.61	1.47	- 0.06	- 0 24	- 1.00	23
COY	12	5/17/73	24.6	7 06	291 / 14.52	46.7 / 3.84	253 / 4.15	693 / 14.42	- 0.57	3.78	1.70	+ 0 17	- 0.04	- 0.45	29 1
	13	6/04/73	23.9	7.02	262 / 13.06	40.6 / 3 34	235 / 3 85	614 / 12 78	- 0 67	3.91	1 69	+ 0 06	- 0.16	- 0.52	17.2
	14	6/17/72	21 6	7.10	58 1 / 2.90	9.2 / 76	187 / 3.06	26 / 54	+ 0.83	3 81	1.86	- 0 40	- 0.63	- 2.15	115
	15	6/20/72	21.5	7 11	56.9 / 2.84	9 0 / .74	184 / 3.02	25 / 52	+ 0 56	3.83	1.87	- 0 41	- 0.63	- 2 17	68.8
	16	6/27/72	21 6	7 08	76.1 / 3.80	10.5 / . 86	206 / 3.38	61 / 1.27	+ 0 11	4 42	1 80	- 0.30	- 0 55	- 1 71	24 4
	17	7/07/72	22.4	7.08	182 / 9 08	29.2 / 2.40	232 / 3.80	366 / 7.62	+ 0 26	3.78	1.76	0.00	- 0.22	- 0 79	21 9
POZO AZUL (FRIO)	18	5/25/73	22 6	7.10	125 / 6.26	17.7 / 1 46	262 / 4.30	169 / 3 52	- 0.64	4.29	1.72	- 0.01	- 0.25	- 1.17	TOTAL 5.40+
NACIMIENTO (FRIO)	19	5/25/73	22 5	7.09	122 / 6.08	16.8 / 1.38	264 / 4.33	158 / 3.29	- 1.06	4.40	1.70	- 0 03	- 0 28	- 1.21	
SABINAS	20	5/25/73	21.0	7.35	65.3 / 3 26	11.2 / .92	241 / 3 95	12 / .25	- 0.24	3.55	2.00	- 0.01	- 0.22	- 2 46	0 3[e]
TANCHACHIN	21	6/20/72	24 6	6 79	118 / 5.88	8.8 / .72	251 / 4.12	111 / 2.31	+ 1 30	8 18	1 40	- 0.31	- 0 68	- 1 34	FLOOD
CANOAS	22	6/18/72	21 8	6.92	84.9 / 4.24	5.1 / 42	269 / 4.41	13 / 27	- 0.21	10.1	1.52	- 0.27	- 0.70	- 2 32	0 4[e]
MEDIA LUNA	23	6/18/72	29.6	6 74	340 / 16.95	61 8 / 5.08	304 / 4.98	839 / 17.46	- 0 92	3 33	1.26	+ 0 02	- 0.12	- 0 37	4
TANIMUL SULFUR POOL	24	5/17/73	39 0	6.82	137 / 6.86	21.2 / 1.74	437 / 7.17	47 / .98	+ 2.69	3.94	1 06	+ 0.16	+ 0.06	- 1.74	0.04[e]
	25	6/13/72	40.5	6.32	138 / 6.88	20.2 / 1.66	417 / 6.83	50 / 1.04	+ 4.08	4 14	(0.55)	(-0·32)	(-0 40)	(-1.67)	0.05[e]
	26	6/15/72	32.0	6.60	124 / 6.18	8.3 / .68	360 / 5.90	32 / .67	+ 2.16	9.09	1.01	- 0 20	- 0.53	- 1.86	0.34[e]
	27	6/17/72	31.6	6.62	128 / 6.38	10.7 / .88	389 / 6.38	36 / .75	+ 0.90	7.25	(0.98)	(-0.16)	(-0.45)	(-1.80)	0 57[e]
	28	6/28/72	36.0	6.76	133 / 6.62	12.6 / 1.04	386 / 6.32	36 / .75	+ 4.01	6.37	(1.08)	(+0.04)	(-0.18)	(-1.80)	–
TANTOAN THERMAL	29	5/18/73	31.0	6.88	97.3 / 4.86	6.1 / .50	297 / 4.87	15 / .31	+ 1 71	9.71	1.36	- 0.11	- 0.46	- 2.23	.006[e]
WELL															
ON RANCHO PENON; IN SHALE	30	5/18/73	25.5	7.22	125 / 6.24	12.6 / 1.04	410 / 6.71	17 / .35	+ 1.46	6.00	1.62	+ 0.38	+ 0.09	- 2.13	–

1 top value in milligrams per liter, lower in milliequivalents per liter; alkalinity in mg/l assumes all is HCO_3^-

2 discharge. the Coy, Choy, Mante, Frío and Media Luna values are by the Secretaría de Recursos Hidráulicos, all others are from this study
m - measured by current meter
e - estimated, usually by measurement of surface velocities and rough channel area

1971). The results agreed within ± 0.04 log units of the calculated calcite and dolomite saturation indices given by both references, and within ± 0.02 for the pCO_2 on three samples by Langmuir. The slight differences are probably the result of variations between authors as to what ion pairs are important, and what values of the equilibrium constants are used, especially for dolomite.

In this study, only the saturation state of the water with respect to calcite, dolomite, and gypsum is of interest. The degree of saturation may be evaluated by the "saturation index" or "SI" which is calculated as follows:

$$\text{calcite:}\quad SI_c = \log(a_{Ca^{++}} \cdot a_{CO_3^{=}}) - \log K_c$$

$$\text{dolomite:}\quad SI_d = \tfrac{1}{2}[\log(a_{Ca^{++}} \cdot a_{Mg^{++}} \cdot a^2_{CO_3^{=}}) - \log K_d]$$

$$\text{gypsum:}\quad SI_g = \log(a_{Ca^{++}} \cdot a_{SO_4^{=}}) - \log K_g$$

where the "a's" are activities and the "K's" are the appropriate equilibrium constants. Note that the saturation index for dolomite (SI_d) is calculated for the stoichiometric form so that it may be compared directly with the values for calcite and gypsum. A positive (+) number is supersaturated, and a negative (-) number is undersaturated. Samples having a value within ± 0.10 of zero are approximately saturated with respect to that particular mineral. More information about thermodynamic calculations is available in Garrels and Christ (1965), Stumm and Morgan (1970), Langmuir (1971), and Back and Hanshaw (1970). Because of the importance of ion pairs in the waters studied here, the total concentration (analytical value) of a species in solution will be indicated by a symbol without charge (e.g. Ca, or Ca_{tot} for emphasis), and that part that is ionized will be indicated as such (e.g. Ca^{++}).

fourth type included most of the major and several of the smaller springs in the region. Three classes of water which were not sampled are the main surface drainage systems such as the Río Tampaón, and the diffuse or unconcentrated surface and vadose trickle input water on top of the El Abra range.

A statement of the sampling procedures, the analytical methods, and the errors is given in Appendix I. Here, it is sufficient to say that the analyses of samples collected during the summers of 1973 and 1972 are regarded as high quality data (the Ca, Mg, and SO_4 listings are the average of at least two determinations and the temperature, pH, and alkalinity were carefully measured); the analyses of the summer 1971 and December-January of 1971-1972 are less reliable principally because the pH determination was less precise and the Ca, Mg and alkalinity analyses were generally performed only once. A few samples simply have unexplained errors; however, most of the analyses are believed reasonably good. The data have been processed on a CDC 6400 computer using Watchem II, a program written by John Drake and modified by T.M.L. Wigley (1972). The program calculates the saturation conditions of a sample with respect to calcite, dolomite, and gypsum; the theoretical P_{CO_2} ; and several other results such as the percent error, the Ca/Mg and Ca/SO_4 ratios, and the ionic strength. Saturation conditions are calculated using temperature dependent equilibrium expressions, and take into account the ion pairs $CaSO_4^o$, $MgSO_4^o$, $MgHCO_3^+$, $CaCO_3^o$, and $MgCO_3^o$. Only the first three ion pairs are significant in the area and $CaHCO_3^+$ is ignored completely (after Langmuir,

TABLE 5 1b CONTINUED

LOCATION	NO	DATE	TEMP °C	pH	Ca[1]	Mg[1]	ALKALINITY[1]	SO_4[1]	% ERROR	Ca/Mg	pP_{CO_2}	SI_c	SI_d	SI_g	Q m^3/sec[2]
CAVE LAKES															
SOTANO DE JOS	100	1/14/72	24 5	7.3	84 9 / 4 24	3.4 / 28	256 / 4.19	15 / .31	+ 0 18	15 14	1 90	+ 0.12	- 0.38	- 2 25	–
SOTANO DE SOYATE	101	7/16/71	–	–	84 1 / 4 20	2 4 / 20	247 / 4 05	–	–	21 0	–	–	–	–	–
	102	1/03/72	–	7 0	73 7 / 3.68	3 9 / 32	220 / 3 60	6 / 12	+ 3 5	11 5	1 66	- 0 28	- 0 72	- 2 69	–
SOTANO DEL TIGRE	103	12/21/71	–	7 2	83 3 / 4.16	5 8 / 48	272 / 4 47	23 / 48	- 3.2	8 62	1 77	+ 0 04	- 0 33	- 2.09	–
CUEVA DE LOS SABINOS	104	7/15/72	24 1	7 40	87.0 / 4 34	1 9 / 16	236 / 3 87	14 / 29	+ 5.7	27 1	2 04	+ 0 19	- 0.28	- 2 27	–
	105	7/15/72	23 5	7 40	92 6 / 4 62	1 7 / 14	239 / 3 91	11 / 23	+ 6 2	33 0	2.04	+ 0.21	- 0.46	- 2 25	–
SOTANO DE LA TINAJA	106	1/04/72	–	7 2	82.5 / 4 12	4 6 / 38	256 / 4.19	4 / 08	+ 2 5	10 8	1 80	+ 0 02	- 0 40	- 2 83	–
	107	1/04/72	–	7 15	94.5 / 4.72	4.9 / 40	304 / 4 99	6 / 12	+ 0 04	11 8	1 67	+ 0 09	- 0 36	- 2 63	–
	108	1/04/72	–	7 05	88 1 / 4 40	7 3 / 60	289 / 4 73	4 / 08	+ 1 9	7 33	1 60	- 0 06	- 0 39	- 2 83	–
	109	7/26/71	–		92 2 / 4 60	3.6 / .30	–	–	–	15 3	–	–	–	–	–
	110	7/26/71	–	–	94 2 / 4 70	3 6 / 30	–	–	–	15 7	–	–	–	–	–
SOTANO DEL ARROYO	111	12/31/71	–	7 2	67 3 / 3 36	3 6 / 30	210 / 3 44	3 / 06	+ 2 1	11 2	1 88	- 0 14	- 0 57	- 3 01	–
	112	12/31/71	–	7 3	66 5 / 3 32	3.4 / .28	204 / 3 34	3 / 06	+ 2 8	11 9	1.99	- 0 06	- 0.49	- 3 01	–
	113	12/31/71	–	7 3	85 7 / 4.28	4 9 / 40	264 / 4 33	10 / 21	+ 1.5	10 7	1.88	+ 0.14	- 0.27	- 2 43	–
	114	01/12/72	–	7 0	121 / 6.04	10.2 / 84	396 / 6.49	12 / 25	+ 1 0	7 19	1.42	+ 0 14	- 0.20	- 2 28	–
CAVE STREAM (BETWEEN LAKES)															
SOTANO DEL ARROYO	115	01/12/72	–	7.55	80 1 / 4 00	4 9 / 40	263 / 4.31	6 / 12	- 0.30	10 0	2 14	+ 0.36	- 0.04	- 2 67	TRICKLE
CAVE DRIPS															
GRUTAS DE QUINTERO	116	06/14/72	–	7 32	99.4 / 4.96	1 7 / .14	287 / 4.70	–	–	35 4	–	–	–	–	–
	117	06/14/72	–	7 4	83 3 / 4.16	1 7 / 14	247 / 4 05	–	–	29 7	–	–	–	–	–
	118	06/14/72	23.9	7 4	101 / 5.06	1 9 / .16	–	–	–	31 6	–	–	–	–	–
SOTANO DEL ARROYO	119	01/12/72	–	7 05	133 / 6 64	6.8 / 56	434 / 7 12	4 / 08	- 0 11	11 9	1 43	+ 0 27	- 0.17	- 2.72	–
SOTANO DE JOS	120	08/12/71	–	–	80 / 4 00	4.9 / 40	–	–	–	10 0	–	–	–	–	–
SOTANO DE LA TINAJA	121	07/26/71	–	–	100 / 5 00	4 9 / 40	–	–	–	12.5	–	–	–	–	–
	122	07/19/71	–	–	136 / 6 80	7.3 / 60	423 / 6 94	–	–	11 3	–	–	–	–	–
	123	07/19/71	–	–	TOTAL HARDNESS 6 20 meq/l		–	–	–	–	–	–	–	–	–
	124	07/20/71	–	–	88 2 / 4 40	1.2 / 10	–	–	–	44 0	–	–	–	–	–
	125	07/20/71	–	–	102 / 5 10	1.2 / 10	–	–	–	51.0	–	–	–	–	–
SURFACE STREAMS															
YERBANIZ ARROYO NORTH BRANCH	126	07/25/72	25.1	7 28	32 0 / 1.60	1.2 / .10	96.5 / 1.58	–	–	16.0	2.28	–		–	0.15[e]
ARROYO LIMONCITO	127	07/25/72	26.3	7.48	61.7 / 3.08	1.0 / .08	271 / 4.44	–	–	38 5	2.04	–	–	–	0 04[e]
ARROYO ARROYO (S.DEL ARROYO)	128	07/25/72	26.4	7.95	72.1 / 3.60	0.5 / .04	236 / 3.86	–	–	90.0	2.59	–	–	–	0.06[e]
JAPONES ARROYO	129	07/18/71	–	7.4	46.5 / 2.32	1.5 / .12	130 / 2.13	–	–	19.3	–	–	–	–	0.03[e]
	130	07/18/71	–	7.2	TOTAL HARDNESS 2.64 meq/l		148 / 2.42	–	–	–	–	–	–	–	0.03[e]

1 top value in milligrams per liter, lower in milliequivalents per liter; Alkalinity in mg/l assumes all is HCO_3^-

2 discharge: the Coy, Choy, Mante, Frio and Media Luna values are by the Secretaria de Recursos Hidraulicos; all others are from this study

m - measured by current meter

e-- estimated, usually by measurement of surface velocities and rough channel area

* pH or alkalinity measured by Russell S. Harmon and of uncertain accuracy; any error will affect pP_{CO_2}, SI_c, and SI_d

TABLE 5.2

Analyses for Na, K, and Cl

Spring	Sample No. in Table 5.1	Na^+ mg/l	K^+ mg/l	Cl^- mg/l
Choy	1	3.6	0.7	4.8
	35	3.3	0.8	4.2
	3[1]	—	—	6.9
Mante	10	6.1	1.5	4.2
Coy	12	4.2	1.2	3.3
Taninul Sulfur Pool[2]	24	88.4	10.2	225
	87	55.0	6.2	—
	26[1]	11.0	1.5	30.0
Los Bañitos (Covadonga)	82	9.1	1.3	3.8
Tantoán thermal	29	9.0	0.7	—
Arroyo Seco	59	2.3	0.7	< 7.5[3]
Poza Azul (Frío)	18	4.8	1.0	—
Sabinas	20	1.3	0.2	1.5
Media Luna	23	13.9	5.7	—
San Juanito	73	0.7	0.3	—
Agua Clara	77	3.3	0.9	—
Canóas	22	—	1.2	—
Santa Clara	57	—	—	7.5-15[3]
Taninul Limestone Pool	95	—	—	144-152[3]
	96	—	—	136-144[3]
	97	—	—	23-30[3]

1. In flood
2. See Figure 5.11 for other chloride measurements
3. Measured by Hach kit; all other samples listed measured by Cl^- specific ion electrode

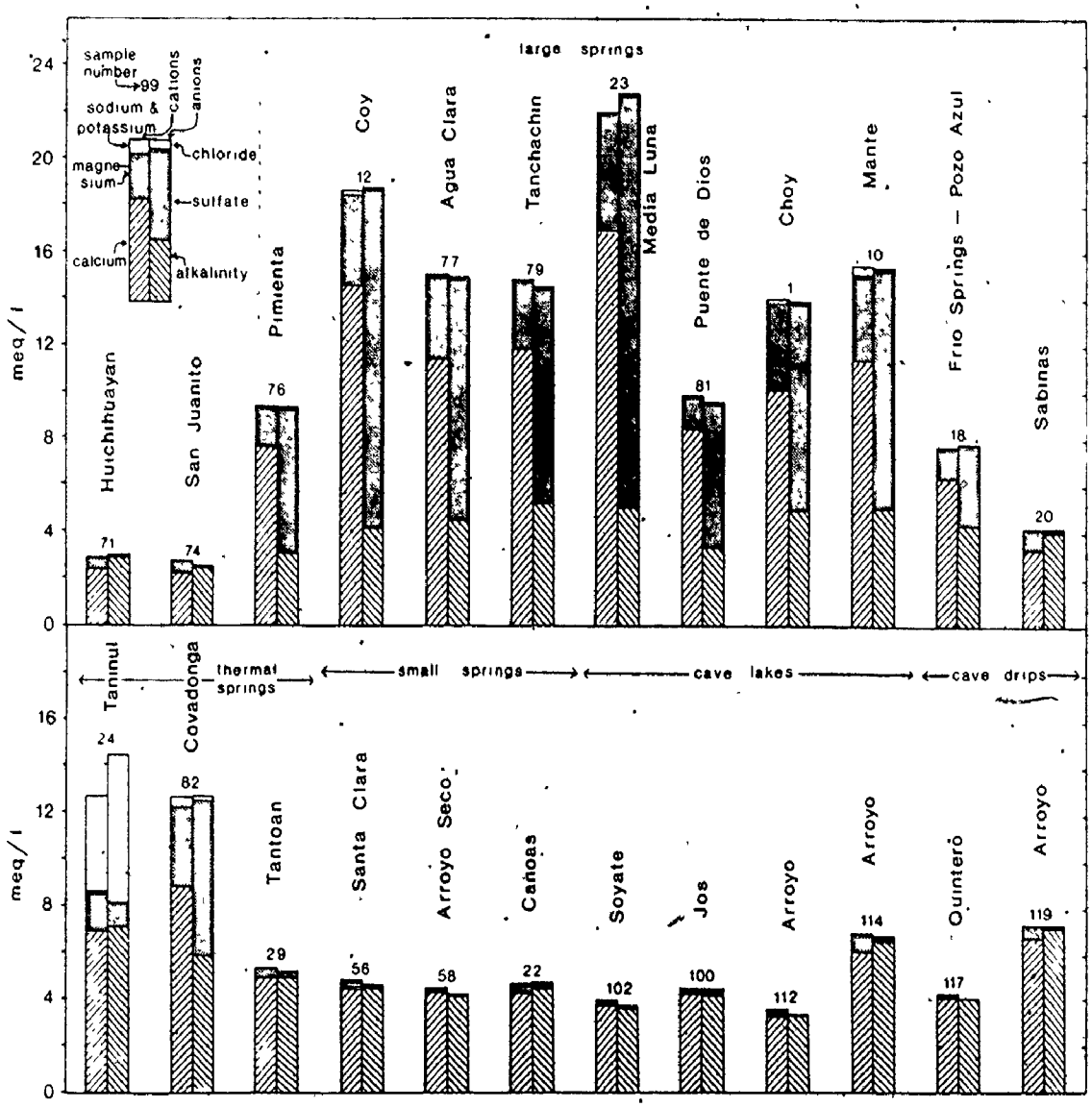

Figure 5 2 Comparison of chemistry of water samples from various environments in the Sierra de El Abra.

contains a fluvial system developed on shale and flaggy limestone, with a thin veneer of soil. As previously described, many of the arroyos have cut down to the El Abra limestone and subsequently have been pirated underground. The streams are seasonal: they are completely dry except for small pools during the dry season, but carry large floods during major wet season storms. A great deal of sediment and organic material, including logs, is swept into the caves during floods. The five samples listed were collected at very low discharges and have a range of 85 mg/l to about 200 mg/l total hardness (as $CaCO_3$). The total hardness was mostly calcium carbonate. For these samples, there was considerable difficulty in obtaining precise determinations of Ca and Mg, possibly because of organic compounds in the water. However, the alkalinity roughly balances the measured cations. Thus, these samples serve as an indication of the dissolved load entering the swallet caves. The concentrations seem surprisingly high, but the Méndez shale evidently contains a large amount of $CaCO_3$ (confirmed by J. Carrillo Bravo, personal communication). It seems likely that the dissolved load will be considerably diminished during flood stage, which is volumetrically much more important.

Cave Drips

Cave drips (vadose seeps) and vadose flows (verical shaft or open crack waters) are the predominant recharge water types in the Sierra de El Abra. Ten drip samples were collected, seven of them in swallet caves. The total hardness ranged from 215 mg/l to 360 mg/l as $CaCO_3$. In all the samples, the Ca/Mg molar ratio was 10 or greater. Because this

contains a fluvial system developed on shale and flaggy limestone, with a thin veneer of soil. As previously described, many of the arroyos have cut down to the El Abra limestone and subsequently have been pirated underground. The streams are seasonal: they are completely dry except for small pools during the dry season, but carry large floods during major wet season storms. A great deal of sediment and organic material, including logs, is swept into the caves during floods. The five samples listed were collected at very low discharges and have a range of 85 mg/l to about 200 mg/l total hardness (as $CaCO_3$). The total hardness was mostly calcium carbonate. For these samples, there was considerable difficulty in obtaining precise determinations of Ca and Mg, possibly because of organic compounds in the water. However, the alkalinity roughly balances the measured cations. Thus, these samples serve as an indication of the dissolved load entering the swallet caves. The concentrations seem surprisingly high, but the Méndez shale evidently contains a large amount of $CaCO_3$ (confirmed by J. Carrillo Bravo, personal communication). It seems likely that the dissolved load will be considerably diminished during flood stage, which is volumetrically much more important.

Cave Drips

Cave drips (vadose seeps) and vadose flows (verical shaft or open crack waters) are the predominant recharge water types in the Sierra de El Abra. Ten drip samples were collected, seven of them in swallet caves. The total hardness ranged from 215 mg/l to 360 mg/l as $CaCO_3$. In all the samples, the Ca/Mg molar ratio was 10 or greater. Because this

is such an important class of water in the El Abra range, it would be desirable to greatly expand the sampling program. The few samples collected have an average total hardness of 274 mg/l, somewhat higher than the small springs along the east face of the El Abra. This is not surprising in as much as the area appears to be in a minor phase of calcite deposition. All except one of the samples were collected during the wet season, since many sources are inactive, or nearly so, during the dry season. At present no relationship between the dissolved solids and the drip or flow rate can be given.

Cave Lakes

The cave lakes in the Sierra de El Abra may be distinguished in two ways. One consideration is the source of the water, i.e., whether it comes from vadose seeps and flows, or from swallet flood waters. Nearly all the samples are from swallet cave lakes in which the stored water is flushed out probably 4-8 times each year by floods, counting successive days of rainfall and flooding as one event. In many lakes, water is slowly exchanged between flood events by trickles. The second consideration is the hydrologic position of the cave lake. All of the lakes sampled except one are perched above the zone of permanent saturation. The lake in Sotano de Soyate is the only known water-table lake in the Sierra de El Abra.

Fourteen different lakes were sampled. The analyses are placed in Table 5.1b because, with the exception of the Cueva de Los Sabinos lakes, the pH of the samples was measured at the field laboratory (as

soon as possible) rather than in the cave, and because most of the lake samples were collected during the earlier part of the sampling program. The pH of samples from the two lakes in Cueva de los Sabinos was measured a) in the cave, b) 1 day later in the field house, and c) 10 days later in the field house. The pH increased +0.02 units after one day for both samples and +0.08 for one sample and +0.10 for the other samples after after 10 days. Thus, the true pH of the other samples may be within 0.05 units of the value listed, including the reading error. A pH error affects the calculated P_{CO_2} and SI_C values. If the pH error is 0.05 units, the error in the pP_{CO_2} and SI_C values would be about 0.05.

The cave lakes are calcium bicarbonate type water, as would be expected from a limestone region. The average concentrations of calcium and magnesium were 4.34 meq/l and 0.36 meq/l respectively for a total hardness of 235 mg/l. These cations are balanced by the alkalinity, which would effectively be bicarbonate, and by an average of about 0.2 meq/l of sulfate. The Ca/Mg ratio ranged from 7.19 to 33.0 (Figure 5.3). The data indicate that the water has not come in contact with a significant amount of sulfate bearing rock, and has dissolved little dolomite or magnesium from magnesian calcite. Figure 5.2 shows 4 selected analyses for comparison with other water types.

The environment of the cave lakes has considerable spatial and temporal variation. Few data are available yet, but some observations have been made. In the preceding paragraph it was noted that the principal source rock is a relatively pure limestone (also see Carrillo Bravo, 1971). The CO_2 reservoir that the water is in contact with will

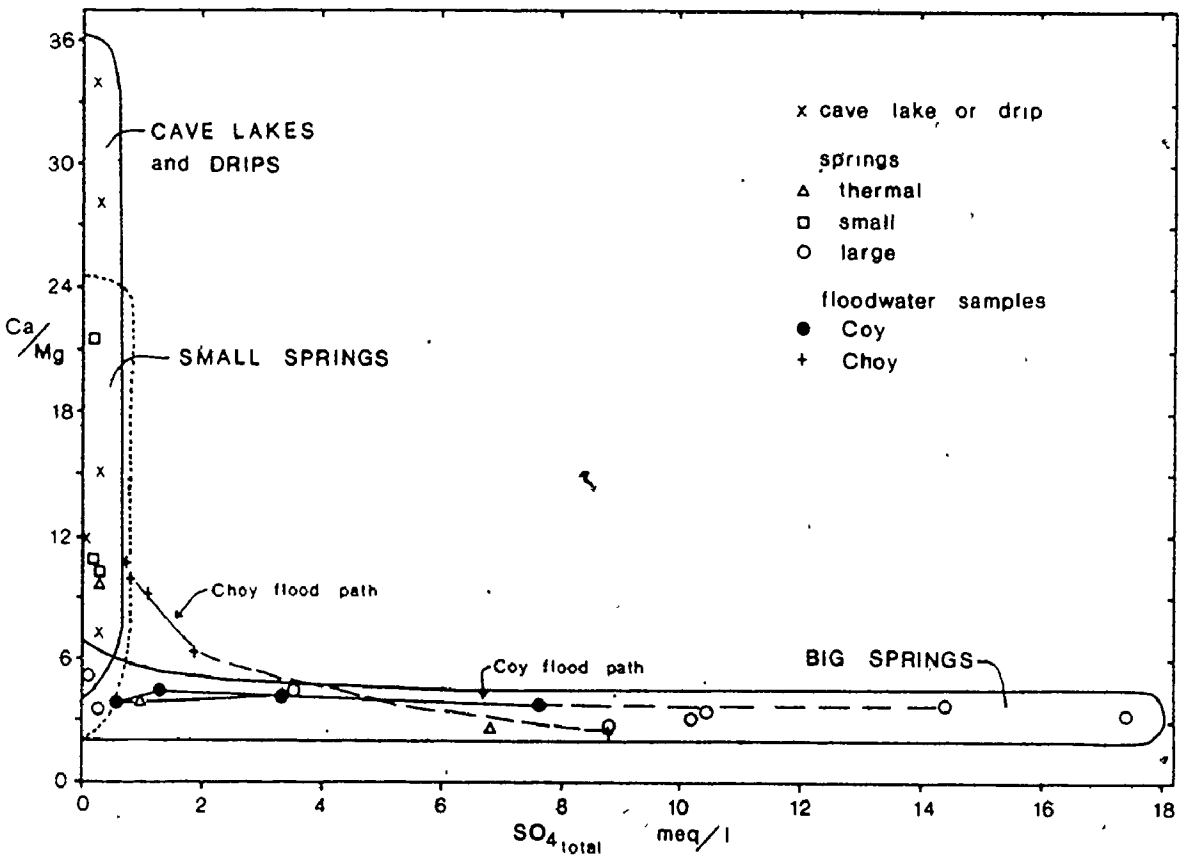

Figure 5.3 Ca/Mg against SO_4 for El Abra region karst waters. The graph distinguishes the calcium-bicarbonate type waters from the calcium-magnesium sulfate type waters. Also shown are the effects of flooding at the Choy and Coy springs (discussed in Section 5.3).

ultimately exert a control on the amount of dissolved calcite. Some sites are relatively open and an exchange between the cave air and the atmosphere occurs, whereas other sites are relatively closed. For example, the two lowest hardness concentrations measured were collected in the Main Passage of Sótano del Arroyo (see cave description, Chapter VI) when there was a noticeable air current blowing into the cave through this passage. Using a Draeger kit, the CO_2 in the cave air was measured to be 0.03 to 0.035%, the same as the average atmospheric CO_2 content. By far the highest hardness measured occurred in a lake at the bottom of a 30 meter drop in Stricklands Bad Air Passage, also in Sótano del Arroyo. This is a downstream passage, the lowest explored point in the cave, and very near the water table. The air was stagnant because of restricted circulation; the CO_2 was measured to be 3.8%, identical to the calculated P_{CO_2} (and dangerous as well!). The average calculated pP_{CO_2} for 12 sample sites is 1.80 (1.6%), which is considerably greater than the CO_2 content of the cave air at the sample time (see Table 5.3). Also, it should be noted that the samples were approximately saturated with respect to calcite (assuming the pH drift was not large). At the end of the dry season in early June 1973, many of the lakes in the lower part of Arroyo had a layer of calcite completely covering their surfaces.

The chemical processes that occur in the perched lakes and the phreatic zone of the Sierra de El Abra are probably very significant. Floods wash huge quantities of organic material into the swallet caves. Significant quantities must also be entrained in the smaller vadose flows of the El Abra range, and bats introduce waste in both environments.

TABLE 5.3

CO_2 of Soil and Cave Air

LOCATION	% CO_2
Sótano del Arroyo: (December, 1971-January, 1972)	
1. top of first drop inside cave	0.03
2. lake at bottom of Big Triangular Room	0.035
3. junction of The Wallows and Neals' Passage	0.035-0.04
4. The Wallows near First Right Hand Lead	0.045
5. The Wallows at Second Right Hand Lead	0.045
6. 60 m before fissure on other side of flowstone block in Stricklands Bad Air Passage	0.50
7. top of fissure (30 m drop) at end of Stricklands Bad Air Passage	2.7
8. 16 m down the fissure in No. 7 above	3.5
9. bottom of fissure in No. 7 above	3.8
Sótano de Soyate: (January 3, 1972)	
1. jungle atmosphere 0.6 m above ground at Soyate, 11:00 A.M.	0.025
2. soil air near Soyate at 10 cm depth; reasonably loose humus and earth	0.080
3. bottom of 195 m entrance pitch	0.060
4. at 220 m depth; 14 m above the lake	0.065
Sótano de la Tinaja: (December, 1971)	
1. cave air above vegetal debris and guano pool just before Traverse Lake	0.08
2. 10 cm down in debris at (1) above; sticks and leaves	0.31
3. air at Second Lake, Sandy Floored Passage	0.10
Trail to Cueva de Tanchipa: (January, 1971)	
1. in loose vegetal debris on main range	0.055

In the swallet caves, Cueva de los Sabinos, Sótano de Soyate and many other caves, large populations of blind fish and other aquatic animals survive on this influx of material. Mitchell et al. (1977) discuss the occurrence of the cave fishes. Reducing conditions evidently exist in the bottom sediments of many of these lakes, for as one wades across them, gas bubbles rise to the surface, and may then be lighted with a carbide lamp. The gas is almost certainly methane, created by the decomposition of vegetal debris. From these data and hydrologic and geomorphic observarions, two important hypotheses are made: 1) that during intense storms, swallet flood waters on the western margin and vadose flows on the El Abra range introduce into the phreatic zone and the perched lakes large quantities of water with considerable capacity for calcite solution; and 2) that the oxidation of organic matter in these subsurface environments may provide a significant increase in the CO_2 available for solution, especially in sites where air circulation is restricted. Vadose trickles might become saturated with respect to calcite before they reach the phreatic zone, but flood waters almost certainly would not.

Cave Streams

Dry season vadose streams in the El Abra are almost non-existent in the approximately 45 km of explored passage. Only 4 trickles are known, and each has an estimated flow on the order of 1 l/min or less. One sample of a trickle in the Wallows in Sótano del Arroyo is listed. The composition of this class of waters should not be very different from the cave lakes, because the "streams" are usually flows between lakes.

Springs

Karst springs are the integrated output of karst hydrologic systems. The physical and chemical character of the output depends on the type of recharge, aquifer hydraulics, soil cover, climate, relief, rock structure, mineralogy, reaction kinetics, and other geologic factors such as intrusive bodies and heat flow.

For this study, the original plan was to sample only the Sierra de El Abra springs. However, the chemistry of the Choy and Mante springs indicated that the hydrogeology was more complicated than initially envisioned. Hence, the sampling program was expanded in an effort to determine the origin of the high sulfate - magnesium waters. Two types of studies have been conducted: 1) the determination of the major chemical constituents of a large number of springs in the region during the dry season base flow period, and 2) the examination of the chemical and physical changes which occur during wet season flood pulses at selected springs. This section will consider the first type of study.

Twenty springs were sampled at least once, including all of the large springs that occur near the eastern margin of the Platform. Only a few springs in the interior of the Platform were sampled. The data given for the small San Rafael de los Castros and the Riachuelo nacimientos may not represent the ground water that supplies them, because there was no visible flow when the former was sampled (the sample was taken from the pool directly at the spring), and the latter rises into a small artificial reservoir, thus making it difficult to obtain a direct sample.

As described in Section 4.2, many of the small springs cease flowing sometime during the dry season. Though the Media Luna spring rises from the bottom of a 75 meter deep lake, its flow is so great that the chemistry could not change significantly. Each of the remaining 18 springs (including Media Luna) are represented in Figure 5.2 by a dry season chemical analysis, except for the Pimienta, the Puente de Díos, and the Canóas nacimientos which were at an intermediate flood stage. The 12 large springs are grouped in the upper row, and arranged approximately from the southernmost on the left to the northernmost on the right. Two other groups are also shown: 3 thermal springs and 3 other relatively small springs. The variety of chemical types of spring water in the region as compared to the internal waters of the Sierra de El Abra is apparent.

Figure 5.4 presents the observed temperature regimes for the springs. The top mark is the highest or nearly the highest temperature likely to be measured at each spring during the year. Where other temperatures have been measured, the observed range is given by a vertical line. For the Coy, the Choy, and the Taninul Sulfur Pool, this must represent nearly the full range of variation that occurs at these springs, since they were studied in detail over a wide range of discharge. The three thermal springs stand out clearly, especially the Taninul Sulfur Pool. The Media Luna temperature would appear to be anamolous (measured 10 cm below the surface). A warm surface layer might be partly responsbile, but this seems unlikely because the discharge is so large (about 4 m^3/sec.) The fourteen other springs exhibit a range from 19.6-26.5°C, for a difference of 6.9°C. More information will have to be

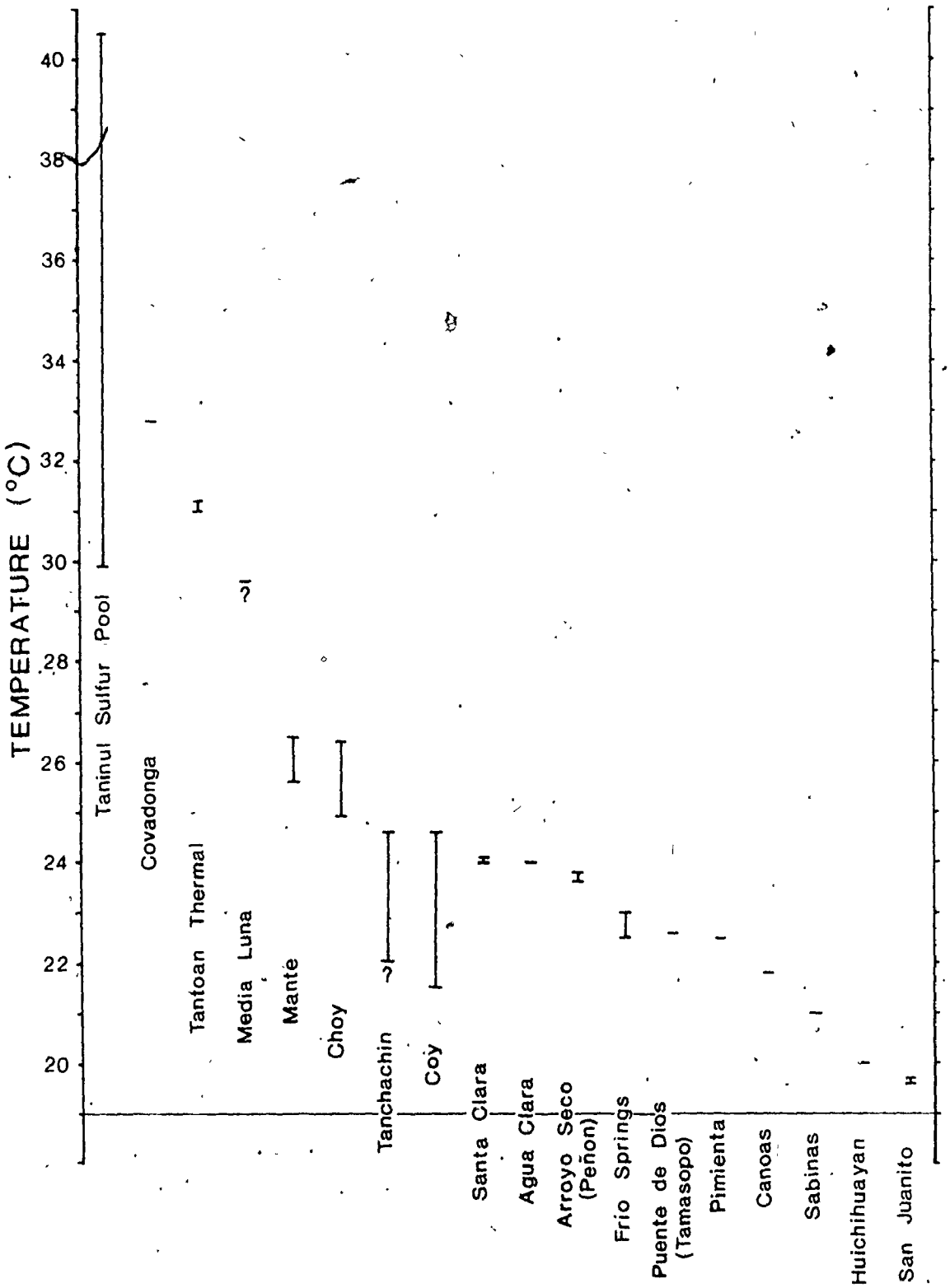

Figure 5.4 Temperature regime of springs in the region.

developed before the spring water temperatures can be properly understood; hence, an explanation will be given in Chapter VII.

Some of the springs have relatively pure calcium bicarbonate type water, with a Ca/Mg molar ratio greater than 10. Others have somewhat greater amounts of Mg, but contain very little SO_4. Many of the large springs have Mg concentrations between 40 to 60 mg/l, with Ca/Mg ratio between 2.5 to 4.5, and have very high Ca and SO_4 concentrations reaching as much as 340 and 840 mg/l respectively. These relationships are best seen in Figure 5.3. Many springs were tested for Na , K , and Cl . Only the Taninul Sulfur Pool has significant concentrations of these constituents, which are not normally important in karst regions. Analyses from 6 springs were plotted on a trilinear diagram, Figure 5.5. All of the points except the Taninul Sulfur Pool lie near the line which would be produced if calcite, dolomite, and gypsum were the only dissolved minerals.

The thermal springs do not seem to have a well defined chemical pattern. Three have been sampled and two others are known. The Tantoán thermal spring has nearly the same composition as other small El Abra springs, but has an elevated temperature and a slight odor of H_2S. The Los Bañitos (Covadonga) source has a very small flow, and a chemical content somewhat similar to the Choy. To the contrary, the Sulfur Pool at the Hotel Taninul is the hottest, has by far the largest discharge, and Na plus Cl comprises nearly one half of the dissolved load. Visibility in it is normally only a few feet. A spongy precipitate of complex sulfur compounds collects on the pool surface, and there is a strong smell of H_2S.

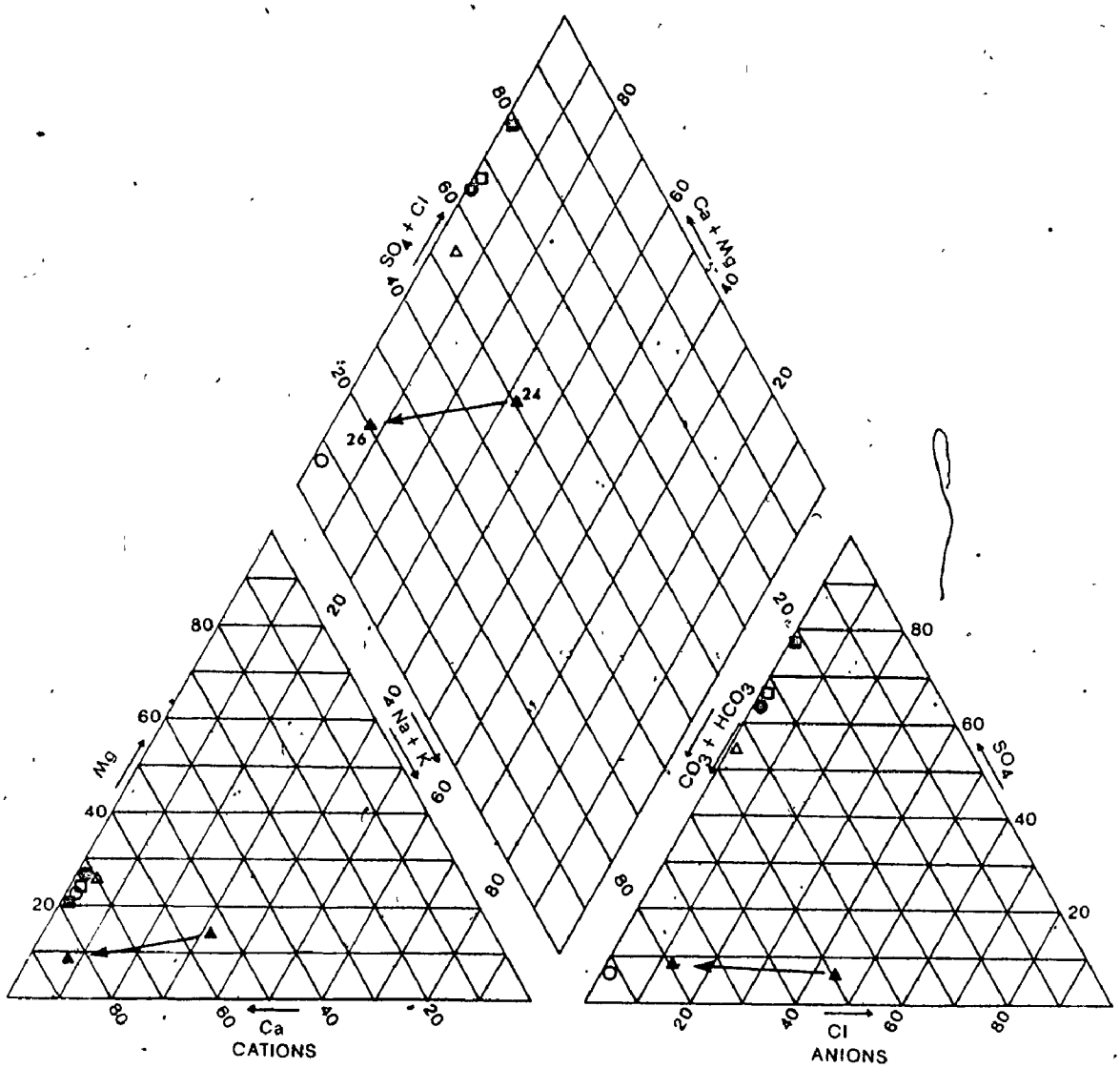

spring	sample	symbol
Choy	1	●
Mante	10	□
Coy	12	■
Sabinas	20	○
Los Bañitos	82	△
Taninul Sulfur Pool	24	▲
" "	26	▲

Figure 5.5 Trilinear plot of samples from 6 springs. The effect of flooding on the Taninul Sulfur Pool is shown.

The factors that control the concentrations of dissolved species are the minerals exposed along the flow paths, solution kinetics (and time), saturation with respect to various minerals, partial pressure of carbon dioxide and other gases, and temperature. Where the data are of sufficient quality, the saturation state with respect to calcite, dolomite, and gypsum is given in Table 5.1.

All of the springs are undersaturated with respect to gypsum. The Coy and the Media Luna were the most nearly saturated, reaching an SI_g of about - 0.35. With the possible exception of the Taninul Sulfur Pool, all of the springs were also undersaturated in dolomite. Springs such as the Mante, the Coy, and the Choy, which contain a large amount of dissolved gypsum also have the highest Mg concentrations. Late in the dry season, they have an SI_d of about - 0.10, only slightly undersaturated. Springs such as the Sabinas and the Frío group, in which carbonate minerals provide most of the dissolved load, have an SI_d between - 0.20 and - 1.0. The springs for which good quality data were obtained at the end of the 1973 dry season are approximately saturated with respect to calcite. Unfortunately, not enough samples were collected from springs containing principally dissolved carbonate minerals to determine if, as a general pattern, they tend to become saturated with respect to calcite without the assistance of "excess" Ca from dissolved gypsum (many of the springs cease flowing late in the dry season). Because the Santa Clara and Arroyo Seco de Peñon were found to be only mildly undersaturated early in the dry season, and the Sabinas and Frío springs were saturated in May, 1973, it seems likely that by the end of the dry season, these "normal" karst spring waters approach equilibrium with respect to calcite

(the Frio springs are actually transitional in composition; see Figure 5.2). Calculated carbon dioxide partial pressures ranged from $10^{-2.00}$ (1%) to $10^{-1.26}$(5.5%) and averaged about $10^{-1.5}$(3%) for the springs. The El Abra springs have a higher P_{CO_2} than those discharging water from nearby higher mountains. Also, the P_{CO_2} of the El Abra springs is much higher than the cave air CO_2 measurements at all but one cave locality (Table 5.3; another bad air passage that is small, with restricted air circulation is known in Sótano del Tigre, but was not measured). This suggests that most of the cave sample sites are relatively open, and that fissures and passages near the phreatic zone must generally have restricted air circulation and higher CO_2 concentrations. Comparison of the chemistry of these springs with other regions will be given in Chapter VII.

Normally, the karst spring waters have a bluish cast and are clear. The best example is the Media Luna where, with the aid of a diving mask, one can easily see the bottom 75 meters below. On occasion, a very slight milkiness has been observed at the Coy, the Mante, and the Choy -- all high sulfate springs. This may be due to precipitation of calcite in the highly turbulent flow below the exit point as the water begins to equilibrate to surface conditions. However, no tufa deposits exist in these channels, although some are found at waterfalls around the region. The thermal waters have a pronounced milkiness.

5.3 Flood Pulse Behavior of the Springs

Ashton (1966) was one of the first workers to apply the "black

box" model to karst hydrologic networks. The basic concept is that a flood wave which enters the subsurface, undergoes a transformation in its physical and chemical character dependent on the nature of the karst underground system and the properties of water, before it is discharged back to the surface. The trick is to interpret what is in the "box" by measuring the characteristics of the output. Brown (Ph.D. thesis, 1970), Brown and Ford (1971) and Atkinson et al. (1973), have subsequently made contributions to this field. Also, there have recently been a great number of studies on the related problem of the relationships of various chemical and isotopic parameters to discharge and separation of the hydrograph of surface streams. In this thesis the water chemistry is used as a hydrological tool to study the dynamics of the El Abra region karst systems. The Choy, the Coy and the Taninul Sulfur Pool were selected for detailed studies during flood pulses. A few other springs were also sampled during floods to see if they might behave in a similar manner.

Figure 5.6 shows the data for El Choy spring for the period June 1 to August 14, 1971. The first samples are typical of the dry season character of El Choy: clear bluish water at 26.4°C, with very high Mg, Ca, and SO_4 concentrations (see the May, 1973 samples for the most accurate values). The Ca and SO_4 values may be read directly in milliequivalents per liter (meq/l), and Mg is obtained by subtraction of Ca from the total hardness curve. An estimate of the depth to visible rocks in the water was made as a crude measure of its turbidity (labelled visibility in Figure 5.6). Though it may be possible to see more than 30 m in the water in the dry season, all values greater than 6 m are plotted

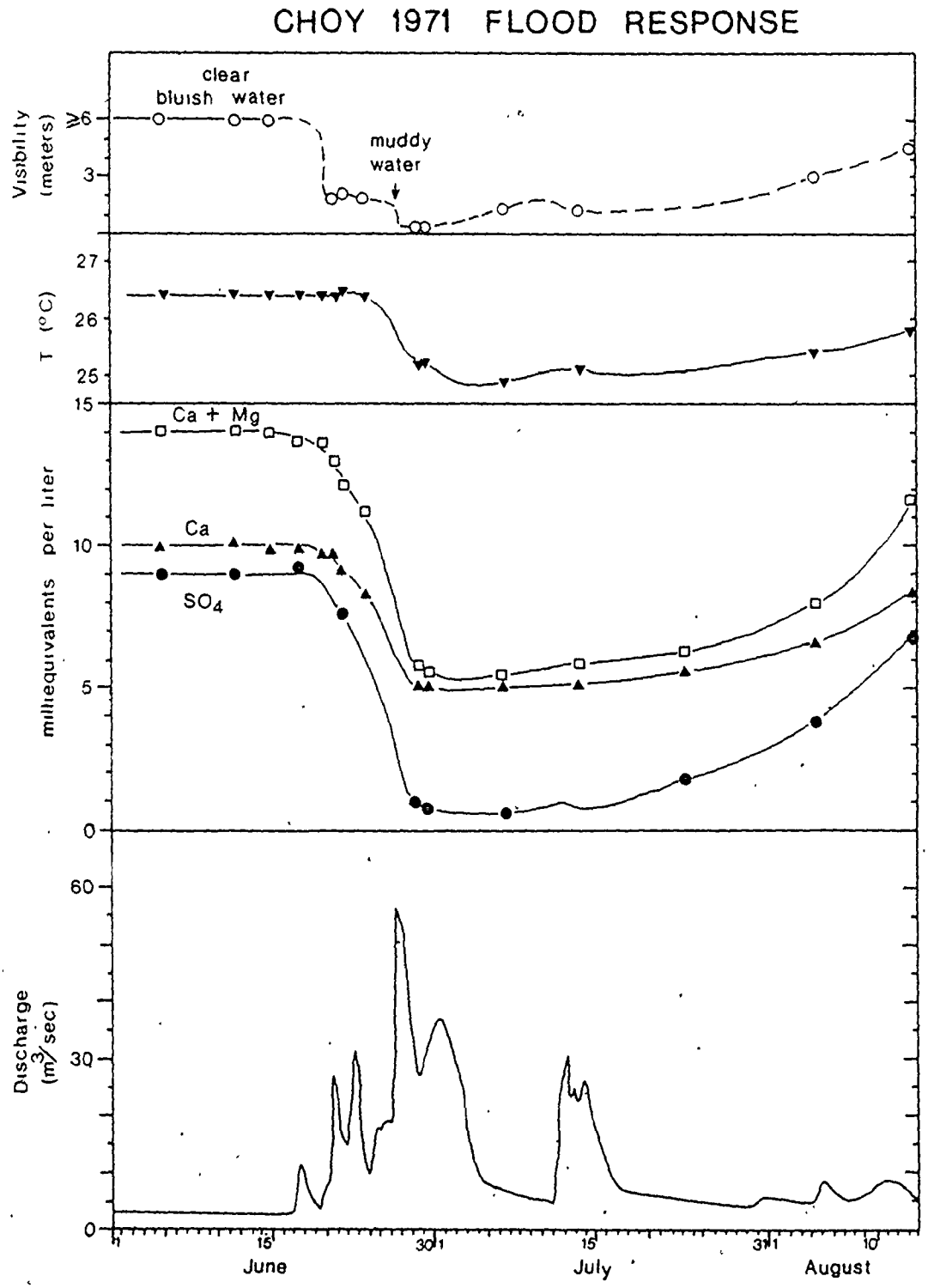

Figure 5.6 Effect of flooding on chemistry of Choy spring, June-August, 1971.

as 6. The first major stormy periods of the rainy season began in mid-June (see Figure 4.7) and lasted about 2 weeks. Each peak of the discharge curve represents a distinct rainfall event, rather than the successive arrival of flood waves via different channels for the same rainfall, as was common in the works by Ashton (1966, 1967). Though water analyses were not made more than once daily at best, they appear to adequately define the concentration curves, losing only the fine detail. The first pulses were relatively small causing a gradual decrease in dissolved solids and an increase in very fine suspended sediment, which may have been remobilized from within the aquifer rather than indicating swallet water. Brown muddy water, probably from the swallet caves such as Sótano del Arroyo, first appeared during the large pulse on June 27 (oral communication, foreman of Rancho Florida near El Choy). The dissolved load decreased until the water had nearly the same composition as the Santa Clara and Arroyo Seco de Peñon springs: principally calcium bicarbonate. The unequal flood-water dilution of chemical species shown in Figure 5.6 is different from that reported by Shuster and White (1971) in their study of spring water chemical variations. The chemical response seems to lag slightly behind the onset of flooding, reaching its lowest values late in the storm period or after it, and then gradually returning to its previous state. A smaller flood, July 12-16, had little effect on the chemistry or temperature because nearly the maximum effect had already been produced. It is important to note that the physical response (discharge) of the aquifer is sharp and strongly peaked, quickly returning almost to its pre-flood state; whereas the chemistry, temperature, and turbidity responses are not as sharp and take about 2 months to return to their pre-flood state. This means that a substantial

volume, probably several million cubic meters, of phreatic water was flushed out by the ground-water recharge, and it took 2 months for the chemistry of the newly stored water to become "normal" again.

In the summer of 1972, both the Coy and the Choy springs were studied during flood pulses (Figure 5.7). Though lacking the detail during the early stages of the flood compared with the previous years' study, the same phenomena seem to have been repeated at El Choy. Here the turbidity data are of special interest. Dark, muddy water was flowing on June 13 (during a period of high flow, about 35 m^3/sec, maintained by smaller pulses following the largest on June 9). This indicates that the arroyos of some swallet caves had run (probably on June 8, and on following days as well) and some of the water was being discharged on June 13. By June 15, the turbidity had decreased somewhat though the discharge was similar, and the water was a murky olive green color. Probably most of the water from the swallet caves had already passed, and a large part of the discharge was being drawn from the main range. The turbidity continued to improve over the next two weeks, but quite a lot of sediment must have been placed in suspension in the aquifer. As before, the chemical wave was much broader than the physical wave. Unfortunately, three moderate floods occurred at the Coy during May, 1972, before sampling began in June (refer to Figure 4.7). These floods probably reduced the dissolved solids in the discharged water a little below the values recorded at the end of the dry season in May-June, 1973 and June 8, 1971, so that these data may not reflect only the effects of the June flood. However, the June flood was much larger than the others; hence, most of the chemical changes are ascribed to it.

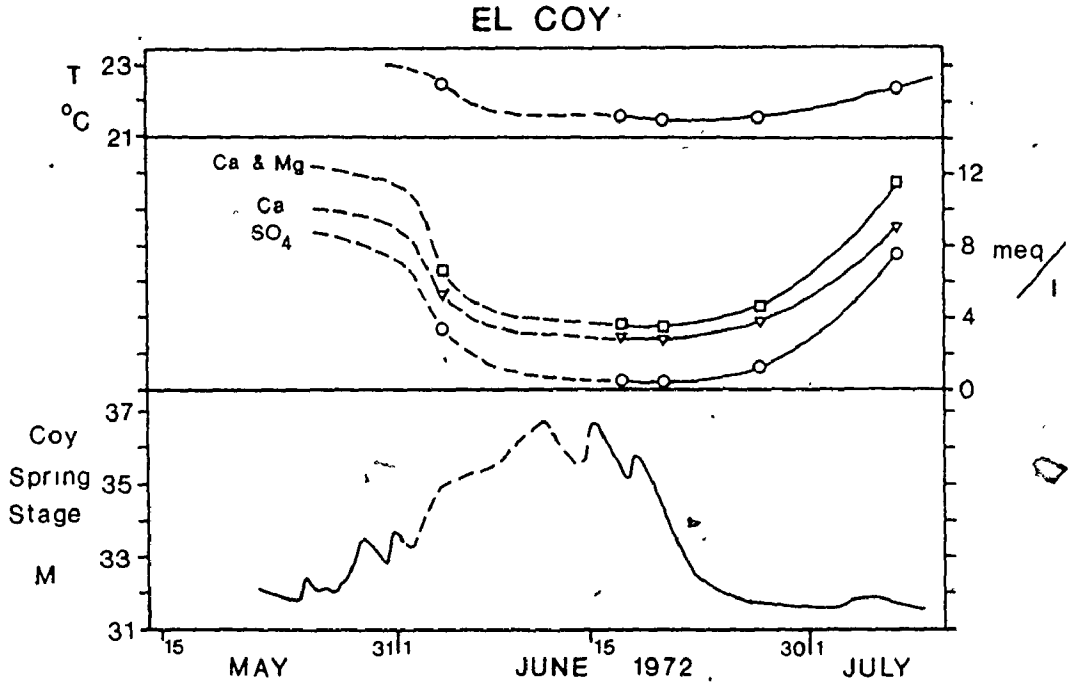

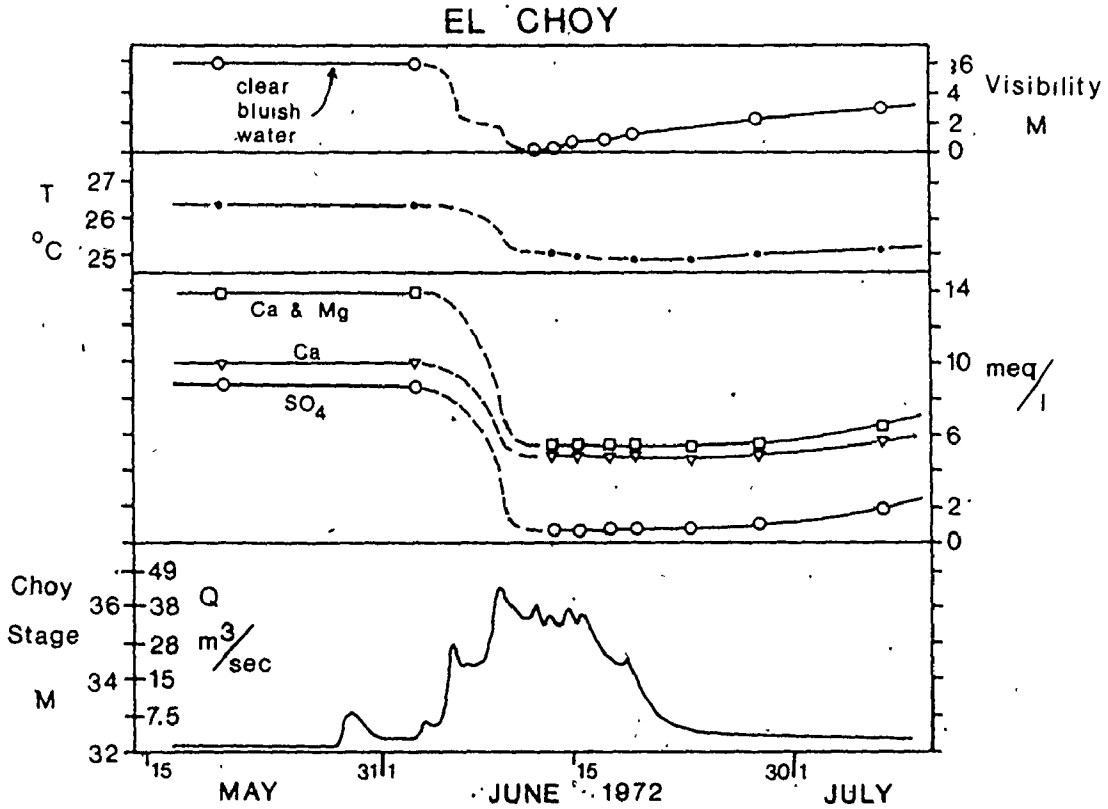

Figure 5.7 Effect of flooding on chemistry of Choy and Coy springs, May-July, 1972.

The Coy chemistry and temperature behave in a manner similar to El Choy, decreasing during flooding to a calcium bicarbonate type water with a total hardness of only 180 mg/l, but returning toward dry season concentrations and temperature regime more rapidly than El Choy. This may be due to the fact that the Coy has a very strong base flow, the largest of any spring in the region. One point of difference is that the Coy spring was never observed to carry muddy water.

Three chemical analyses of Coy waters were made during the summer of 1971 (Table 5.1). They are sufficient to show that the Coy can change from its dry season chemical character to its flood-diminished content in less than two weeks. On June 8, 1971, Coy water contained the highest dissolved solids of 12 samples collected -- 341 mg/l Ca, 51.1 mg/l Mg, and 836 mg/l SO_4. Undoubtedly there was little change until flooding began on the 18th. On June 29, the water had only 88.1, 12.2, and 120 mg/l of Ca, Mg, and SO_4 respectively. By August 5, at the beginning of the next major flood, the concentrations were up to 204, 31.6, and 430 mg/l respectively.

Obviously, there would be a good correlation between the Ca and SO_4 content over the range of discharges for the Coy or Choy, because the Ca excess over that derived from carbonate rock solution and the SO_4 are derived from gypsum or anhydrite. Figure 5.8 shows a very strong correlation between the Mg and SO_4 content of the springs for all the flood pulses studied. The chemistries rapidly pass diagonally downward during floods from the dry season values at the upper right to the minimum values at the lower left, and then slowly return toward the upper right after the

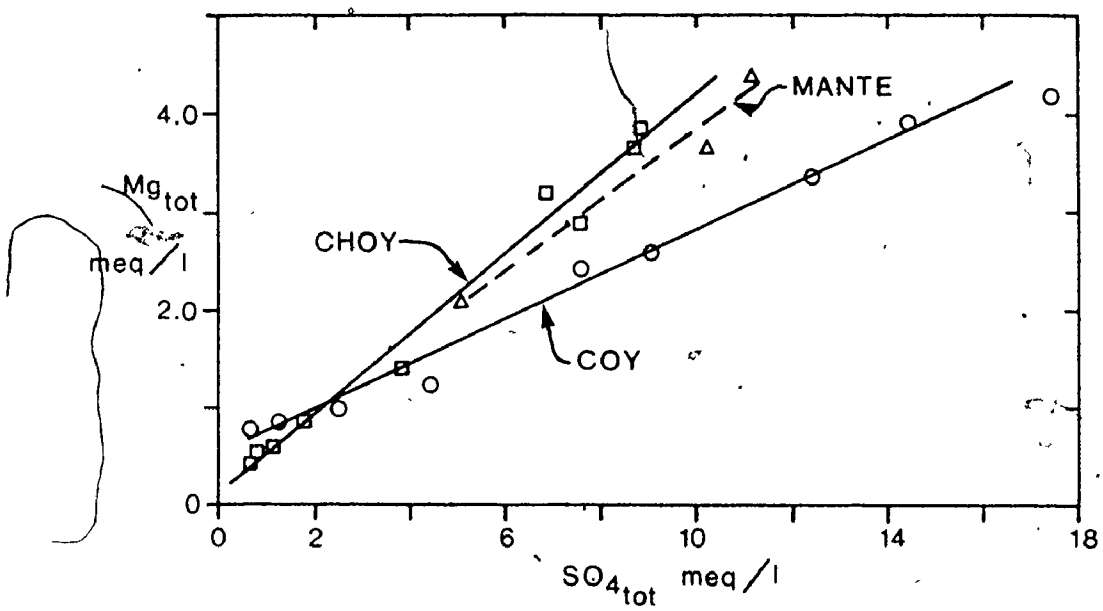

Figure 5.8 Relationship between Mg and SO_4 for Choy, Coy, and Mante during flooding.

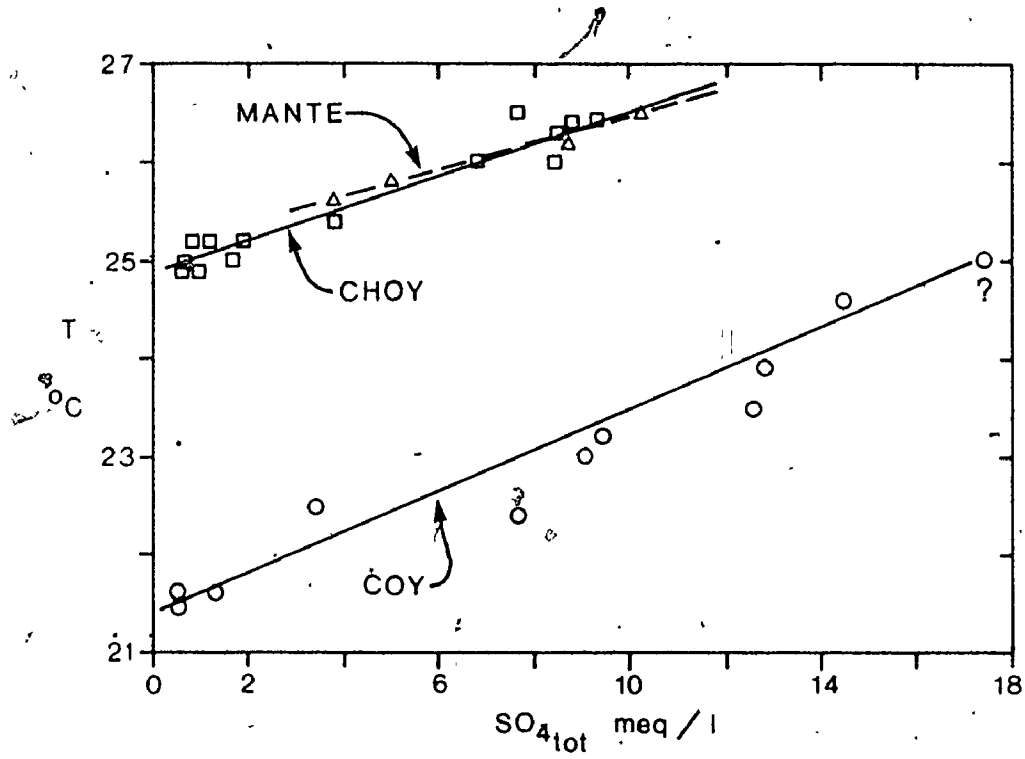

Figure 5.9 Relationship between T (°C) and SO_4 for Choy, Coy, and Mante during flooding.

flood. There may be some slight looping, but the data are not sufficient to detect it or seasonal variations. Note that the paths of the Choy and Coy cross. This may be explained by the lower dolomite content of the El Abra limestone in and near the reef than in the limestone further from the reef (Carillo Bravo, 1971) that is the source of the Coy floodwater. This may also be seen in Figure 5.3, where the chemical "paths" are likewise shown. The three summer analyses of El Mante do not show the full range of variation to be expected, but plot near the Choy line in Figure 5.8. A similar plot, Figure 5.9, of temperature against SO_4 content also shows a very strong correlation for all three springs. El Choy and El Mante give nearly identical results. The Coy line is approximately parallel to the others, but 3½°C lower. This must be due, at least in part, to the cooler temperature of its recharge water.

From the data and correlations discussed above, it is inferred that there are <u>two sources</u> of water for the springs (it would be helpful for the following explanation to refer to Figure 2.2 and the lithologic descriptions in Chapter II). The first source, referred to as the "local" source, is water which circulates entirely within the limestone of the El Abra or Tamasopo Formations. This source is a nearly pure calcium bicarbonate type water near the reef; but passes to calcium - magnesium bicarbonate water (Ca/Mg~4) further west of the reef, where the Mg content in the rock increases. It is believed that the local source supplies all the discharge of the smaller springs such as the Santa Clara (Figure 5.2), as well as some of the base flow and nearly all of the flood flow of the large springs. The second source provides a water that contains much more dissolved Ca, Mg, and SO_4 than the local source, but about the same

amount of HCO_3. It is also warmer than the local source, as shown by the temperature decrease during flooding. If the geology of the area as described by Pemex geologists is correct, particularly with respect to the distribution of gypsum in the subsurface (Carrillo Bravo, 1971), then the second source is a regional deep flow system originating in the mountain ranges far west of Cd. Valles. The regional system must pick up its Ca, SO_4 load from the Guaxcamá Formation. Most of the Mg probably is dissolved from the dolomite at the base of the El Abra Formation in the interior of the Platform, or from the Lower (?) Cretaceous dolomite encountered in the Tamalihuale well. The two sources mix to produce the output of the Choy, the Coy, the Mante, and several other large springs. Further analysis of this model will be given in Chapter VII.

The changes that occurred in the degree of saturation with respect to calcite, dolomite, and gypsum of the Coy and the Choy waters during the 1972 flood pulse studies may be seen in Figure 5.10. The leftmost point for both springs is a representative dry season value from May, 1973, because no completely pre-flood samples were collected in 1972. Unfortunately, the SI_c and SI_d of the second point for both springs are considered unreliable (pH and alkalinity were measured by R.S. Harmon). Though the interpretation is also complicated by some small floods at the Coy spring during May of 1972, it is apparent that the saturation indices decrease not more than a few weeks from the beginning of flooding. In fact, the saturation states seem to vary in a manner similar to the chemical constituents shown in Figure 5.7, i.e., they respond rapidly to each major flood and gradually return to normal. This is clearly so for El Choy.

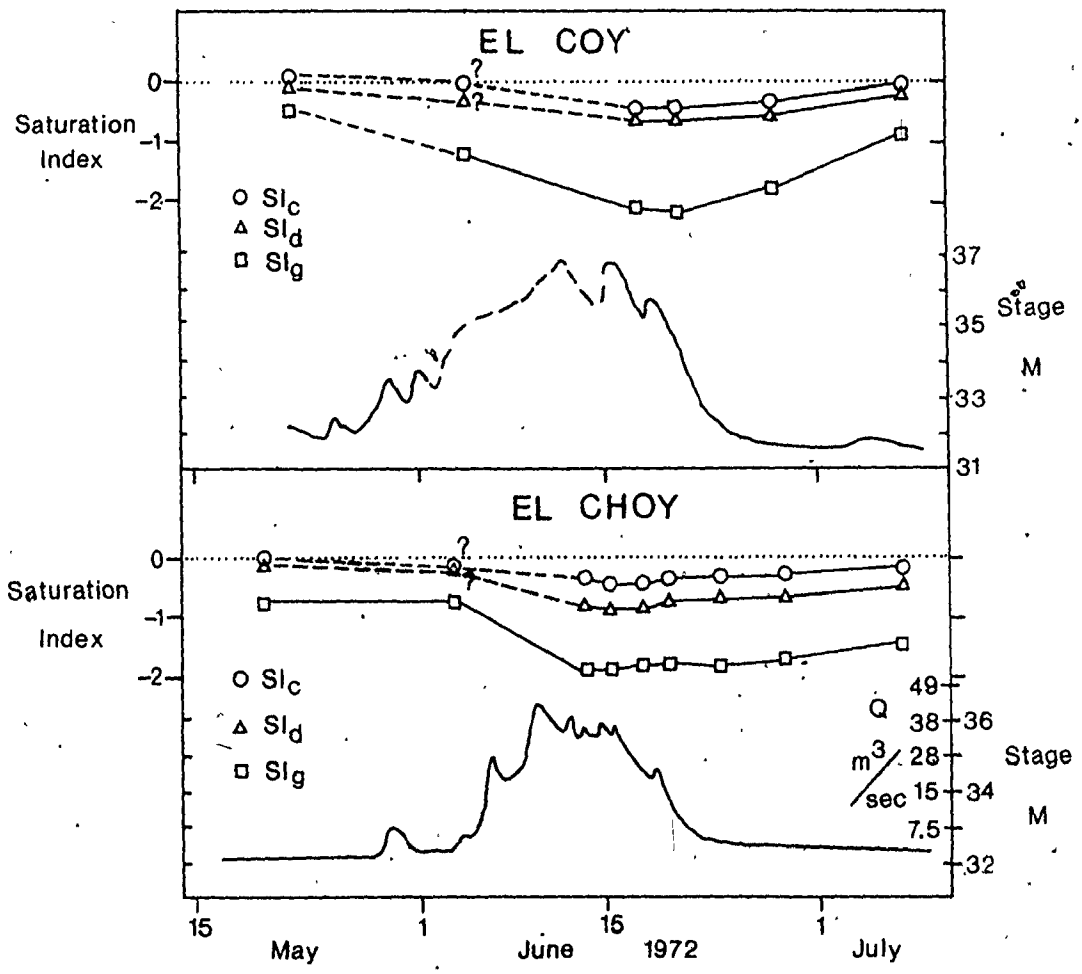

Figure 5.10 Effect of flooding on degree of saturation with respect to calcite, dolomite, and gypsum at Choy and Coy, May-July, 1972.

Several data in this chapter may be drawn together here to make an important conclusion: that a significant portion of the water circulating within the El Abra limestone has a hydrologically short residence time, ranging from perhaps 1 day to several months. In fact, a large portion of the discharge during a flood event probably comes from the rainfall which stimulated the flood. The large conduits developed in the El Abra are capable of passing water from sink to spring very rapidly. The above conclusion is supported by the following data and interpretations:

1) The fact that the Coy and Choy became considerably undersaturated with respect to calcite, SI_c about - 0.4, during these relatively modest floods suggests that some ground-water recharge from the June storms passed completely through the system in a few days. The discharge was a mixture of extant phreatic water and the new recharge. This result is particularly surprising for the Coy spring because of its great distance from any possible recharge area (at least 10 km). It should also be noted that the dry season SI_c values of the carbonate springs -- Sabinas, Santa Clara, Arroyo Seco de Peñon, and Canóas -- are higher than the SI_c values of the flood flow of the Choy and the Ooy.

2) The muddy water discharged from El Choy is believed to come directly from the swallet caves such as Arroyo and Tinaja on the west side of the El Abra range. Based on the Choy 1971 turbidity observations (Figure 5.6), the swallet waters may travel to the Choy at a velocity on the order of 1 km/hr. The flood water at these sinks is a highly turbid mass of water, mud, and organic debris. During the early stage of flooding the changes in color and turbidity of El Choy might be due

to remobilized sediment from within the aquifer, rather than swallet water or soil washed in from the top of the range. Neither muddy water nor suspended fine matter was ever observed at El Coy, though the water seemed to lose a little of its clarity during floods. This may be explained by the fact that the karst west of Aquismón, which is believed to be the local source for El Coy, does not have extensive pirated streams from shale catchments as the southern El Abra does.

3) If the lycopodium test from Sótano de Japonés to El Choy is correct, then the conclusion is proven, at least for the swallet caves of the southern Sierra de El Abra (Section 4.4.3).

Undoubtedly, some of the water has a longer residence time than the flood waters described above. The springs obviously continue to flow throughout the long dry season. Some of the recharge water may pass into deep or restricted flow paths that might take as much as a few tens of years or more to traverse. The high SI_C values of the carbonate springs during the dry season also suggest a longer residence time.

One other sequence of observations, concerning the Taninul Sulfur Pool spring, is of interest. The data and interpretative curves are shown in Figure 5.11 for June, 1971. The physical situation is that the thermal spring has been developed into an artificial pool as a health spa, and about 80 m to the north (parallel to the east face) lies a stagnant pool, approximately 15 m across and at least 5 m deep (Figure 6.2). The water surface of the Sulfur Pool (thermal spring) is ½ meters <u>above</u> that of the

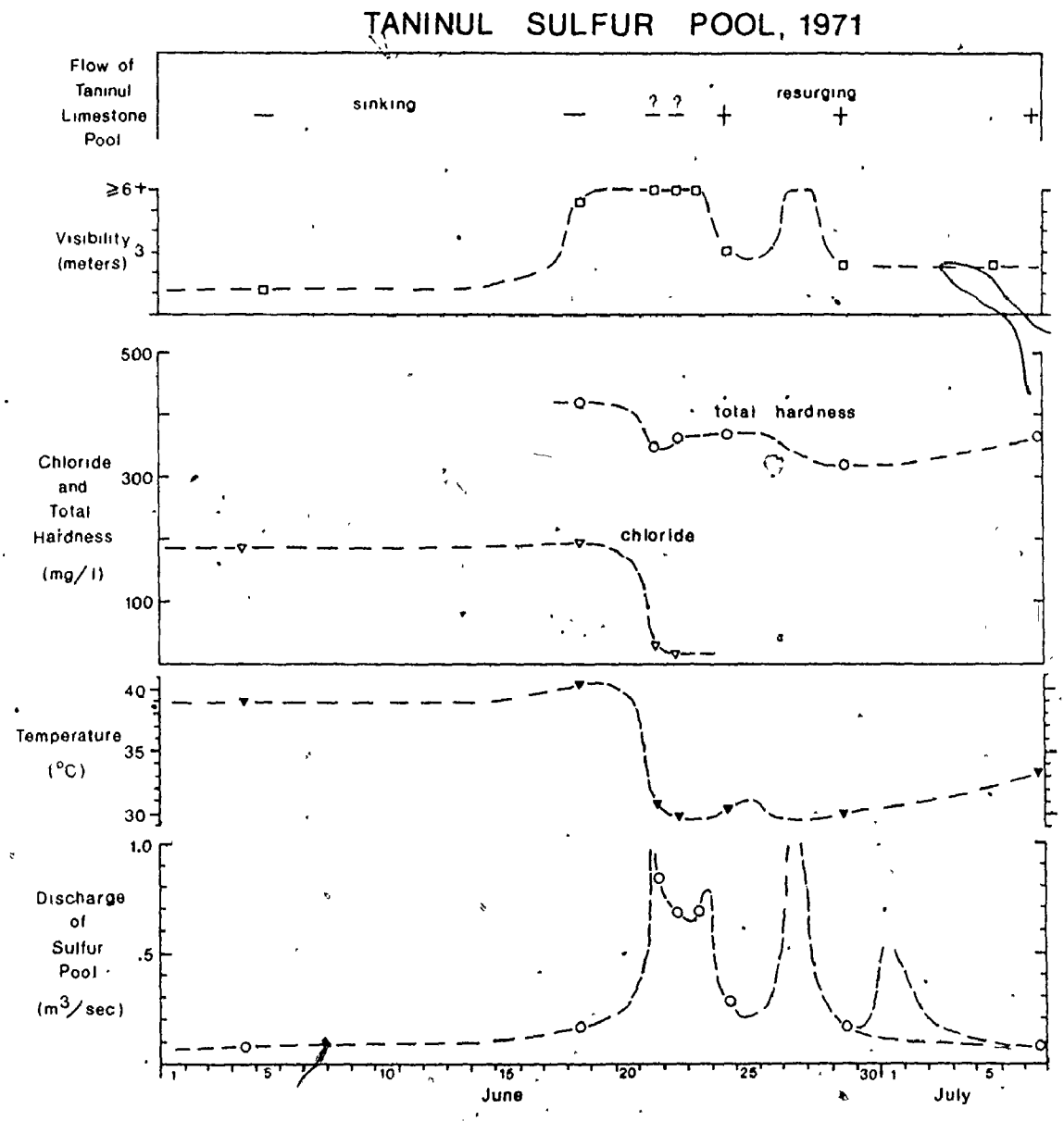

Figure 5.11 Effect of flooding on chemistry of Taninul Sulfur Pool, June - July, 1971.

"limestone" (stagnant) pool. Normally, the base flow of the Sulfur Pool, 0.05-0.1 m^3/sec, flows in a channel past the "limestone" pool; but often a tiny trickle is lost from the channel to the stagnant pool, as on June 4, 1971 (see top line of Figure 5.11) when roughly 0.5 l/min entered the pool. As previously described, during the dry season the Sulfur Pool has a milky opaqueness, is hot, has a strong smell of H_2S, has an abundance of sulfurous coagulate, and has a high NaCl content. Chloride contamination shows up in the limestone pool samples (Table 5.2).

By June 18, the discharge had increased to about 0.17 m^3/sec in response to the first rains of the wet season (compare the discharge curve with that of El Choy, Figure 5.6). Curiously, the temperature increased slightly and the visibility increased greatly. More importantly, a lot of Sulfur Pool water had entered the "limestone" pool; the flow was about 0.05 m^3/sec into the pool at the time of observation. Many fish were gulping air at the pool surface. Other were dead. The entire water body was moving in a giant clockwise vortex -- it was sinking back into the El Abra in the center of the pool !

During the next 11 days, several flood pulses passed through the sulfur spring system. The high discharges shown are estimates based on surface water velocity and approximate channel size. On June 21, the Sulfur Pool was at flood stage. The artificial chute to the normal channel could not handle all the water. Up to 0.1 meter depth of water was spilling over the northwestern edge of the pool and flowing overland directly into the "limestone" ppol. About 0.1 - 0.2 m^3/sec was flowing into the "limestone" ppol from one channel and out the other, and the overland flow

appeared to have been higher before the time of observation. It is not known if there was a small loss back into the El Abra, as on the 18th. The effect on the chemistry is readily apparent from the graphs. The flow from the sulfur pool had become almost totally dominated by El Abra calcium bicarbonate type water. The Cl content decreased an order of magnitude, the total hardness and sulfate content decreased somewhat, the temperature decreased by more than 10°C though it was still 5°C above normal El Abra water, the water became clear, and it had lost most of the H_2S odor. During the next two days, the discharge decreased somewhat. There was only a small overland flow into the "limestone" pool. Other conditions remained about the same.

By the late afternoon of June 24, the discharge from the Sulfur Pool had deceased substantially. There were slight changes in the hardness and temperature toward "normal" conditions, and the visibility was much less. There was no flow into the "limestone" pool, but it was discharging about 0.1 m^3/sec of relatively clear water at 27.7°C. Thus, the "limestone" pool is really an estavelle. Sometime during the previous few days, the water level inside the Sierra de El Abra, or more particularly inside the cave system behind the "limestone" pool, must have risen sufficiently to reverse the flow.

Residents at the Hotel Taninul reported that a very large flood had occurred on the 27th, but the flow had waned on the 28th. By the 29th, the discharge and visibility were approaching base flow conditions. Thus, the Sulfur Pool yields a rapid, sharp response to rainfall events. The chemical and temperature curves had a broader response pattern, like the

Coy and Choy springs! During the period from June 18, to June 29, the crude hydrograph of the Taninul Sulfur Pool appears to be very similar to the Choy hydrograph (Figure 5.6). In June 1972, flooding at the Sulfur Pool lagged behind the Choy (see Table 5.1 and Figure 5.7). On June 13 (also June 4), the Sulfur Pool was at base flow, hot and sulfurous, and there was no sign of previous flooding; whereas the Choy had been at flood stage for several days. However, on June 15 and 17, the Sulfur Pool was in flood, and its chemistry and temperature were again severely affected by the El Abra water.

5.4 Summary

An extensive program of water chemical analysis had the following objectives: 1) to determine the chemical character of karst waters in the region, especially the springs, and 2) to use the water chemistry as a tool for hydrologic analysis, particularly hydrograph separation. Samples of swallet waters, cave drips, and cave lakes were confined to the Sierra de El Abra, whereas springs were studied wherever they could be located, but especially along the eastern edge of the Platform. The El Abra cave waters were found to be of calcium bicarbonate type, with only small amounts of Mg and SO_4. However, three types of springs were found: 1) small to large springs of calcium-bicarbonate type, generally having only small amounts of Mg and SO_4; 2) large springs of calcium-magnesium sulfate type waters (with bicarbonate also) that are somewhat warmer than the "1" above; and 3) thermal springs, each having a different chemistry. The Ca, Mg, and SO_4 concentrations at the Coy springs were 341 (as Ca not $CaCO_3$), 51.1, and 836 mg/l for a sample late in the dry

season. Several spring samples were tested for Na, K, and Cl, but these were found to be important constituents only for the Taninul Sulfur Pool (thermal spring). Hence, several of the springs discharge a large quantity of water that has had prolonged contact with calcite, dolomite, and gypsum (or anhydrite), but apparently there is little or no salt in contact with the ground-water flow systems. The chemical analyses obtained in this study (Table 5.1) indicate that all of the spring water analyses (and perhaps the other types) published by Harmon (1971) are suspect: many of the bicarbonate and sulfate values he reported are erroneous, some by as much as 300%; the very high bicarbonate concentrations caused the calculated carbon dioxide partial pressures and the saturation with respect to calcite to be excessively high; hence, most of the conclusions are incorrect.

Wet season floods cause large changes in the physical and chemical characterisitcs of the high sulfate springs. The response of the chemical "waves" lags somewhat behind the discharge hydrograph or flood wave because some water in the phreatic zone must first be expelled. The concentrations of dissolved species become greatly reduced and approach those of the calcium-bicarbonate type springs. It takes several weeks to a few months, following a large flood, for the water chemistry to approach its preflood state, whereas the discharge returns to base flow much more rapidly. The correlated behavior of magnesium, sulfate, and temperature suggest that there are two sources of water for the high sulfate springs. Several lines of evidence indicate that some of the discharged flood water was derived from the causal precipitation event.

CHAPTER VI

THE CAVES

6.1 Introduction

Caves in the middle latitudes have been extensively explored, surveyed, and studied scientifically. There are many thousands of caves known in the United States, and the karst and caves of Europe are famous. In the tropics, however, although caves are known to exist in many areas, there are relatively few data available on their numbers and general character, and even less knowledge of their geomorphology and genesis.

The objectives of the cave studies are two-fold. The first is to provide maps, fairly detailed descriptions, and geomorphic analyses of tropical caves in a high relief area. The second is to study the hydrology of the presently active caves, and to develop a model for all the caves of their different forms as a function of their hydrology or paleohydrology and geomorphic setting. With only two exceptions, the caves studied were in the Sierra de El Abra. However, the author is familiar with a number of caves in the remainder of the region, and brief mention of their character will be given. Each cave will be treated as a separate entity: a map, a general physical description, and substantial geologic and genetic information will be given. The caves will be grouped into the same physiographic assemblages as the surface geomorphic features in Chapter III, i.e., the east face, the crest, and the west flank and west margin. In

Chapter VII, a summary and analysis of the caves in each physiographic zone is given, and they are placed in the context of a broader hydrologic-geomorphic model.

Scientific study of the caves of México has been very sparse. Previous work in the region of interest is limited, but greater than any other region in México, with the possible exception of Yucatan. A few early observations were made in connection with biological studies, especially of blind fish caves. Bonet has published two reports, one on the Xilitla area (1953b), and the other on the Sierra de El Abra (1953a) that contain relatively simple maps, temperature data, descriptions, and geomorphic interpretations of some horizontal caves (as well as the surface). These papers provided the beginning of cave and karst research in the area, and Bonet correctly interpreted many morphologic features and controls. However, his studies were hampered by lack of equipment and techniques for descent of pits so that the caves beyond could be observed, by too great an emphasis on Davisian concepts of deep phreatic solution and the karst cycle of erosion (Davis, 1930), and by a relatively small sample of caves. In the Sierra de El Abra, he observed caves along the east face, along the western margin, and in the passes; thus, most of the range remained unknown. In the early 1960's, members of the Association for Mexican Cave Studies began exploring and mapping caves in México. By the time their first Bulletin was published (edited by Russell and Raines, 1967), most of Bonet's caves had been visited; some of the swallet pits had been descended and extensive passages were found, but there was not much new surveying or new caves located. The Bulletin contained 8 maps, brief descriptions of 24 caves

in the El Abra range (caves in other areas were also described), and a simple geomorphic model of the caves.

Since 1967, exploration has greatly increased the total length of known caves in the El Abra to its present value of about 45 km, most of which have been surveyed. About 19 km were mapped as part of this study, and a few existing maps were improved by resurveying or additional sketching of detail. In addition, Neal Morris (personal communication) is preparing a book that will give an account of exploration activities in recent years, and many maps and descriptions not included here; he has made available maps of some caves which were studied in this research. Two caves that were not visited are included because of their importance, and some others that were visited are excluded because they were similar to others described here. The cave surveys were conducted by measuring the the bearing, inclination and distance between successive stations, while sketches were made of the passage plan and cross section, and sometimes the profile. A legend of map symbols is given in Appendix II. The survey data were normally processed and plotted by a CDC 6400 computer. Elevations were obtained for many of the caves with a Pauling altimeter that was graduated in 5 foot (1.52 m) increments. Some of the elevations were measured in a reconnaissance manner in conjunction with other work where very long traverses were necessary, and are considered only approximate; others were measured more accurately. Mitchell et al. (1977) have recently obtained elevations for most of the blind fish caves and claim great accuracy. The data collected here agrees in some instances within a few meters, but others have larger differences. Where available, their elevations will generally be used. Some caves that are particularly

important for water-level information should be located by a transit survey.

The cave studies have emphasized plan and profile characteristics, hydrology if the cave is active, geomorphic features, passage shape, the more important structural and stratigraphic features, chemical and clastic sediments, and relation of the cave to surface. Because it was necessary to survey so many kilometers of passages, very detailed studies generally have not been possible. The general geomorphic and hydrologic aspects of the caves are documented, but insufficient structural, lithologic, and geomorphic information have been gathered to propose detailed speleogenetic models for individual caves. Aside from the observations and maps, the results will be a characterization of cave features and development in each geomorphic setting in the El Abra, and a hydrologic model. Some previous studies which have been useful for interpretation of cave geomorphology are Davis (1930), Bretz (1942), Ford (1965, 1968, 1971), Palmer (1969, 1972, 1975), Pohl (1955), Lange (1960), Ewers (Ph.D. thesis in preparation), Jennings (1971), Davies (1960), and G. Deike (1960). The general locations of caves and springs are shown in Figure 3.1.

6.2 Caves of the East Face of the Sierra de El Abra

6.2.1 Cueva del Nacimiento del Río Choy

The Cueva del Nacimiento del Río Choy is a short, but grand cave 3½ km north of the south El Abra Pass. Though often thought of as two caves, it is in reality one, having an upper and a lower chamber (or

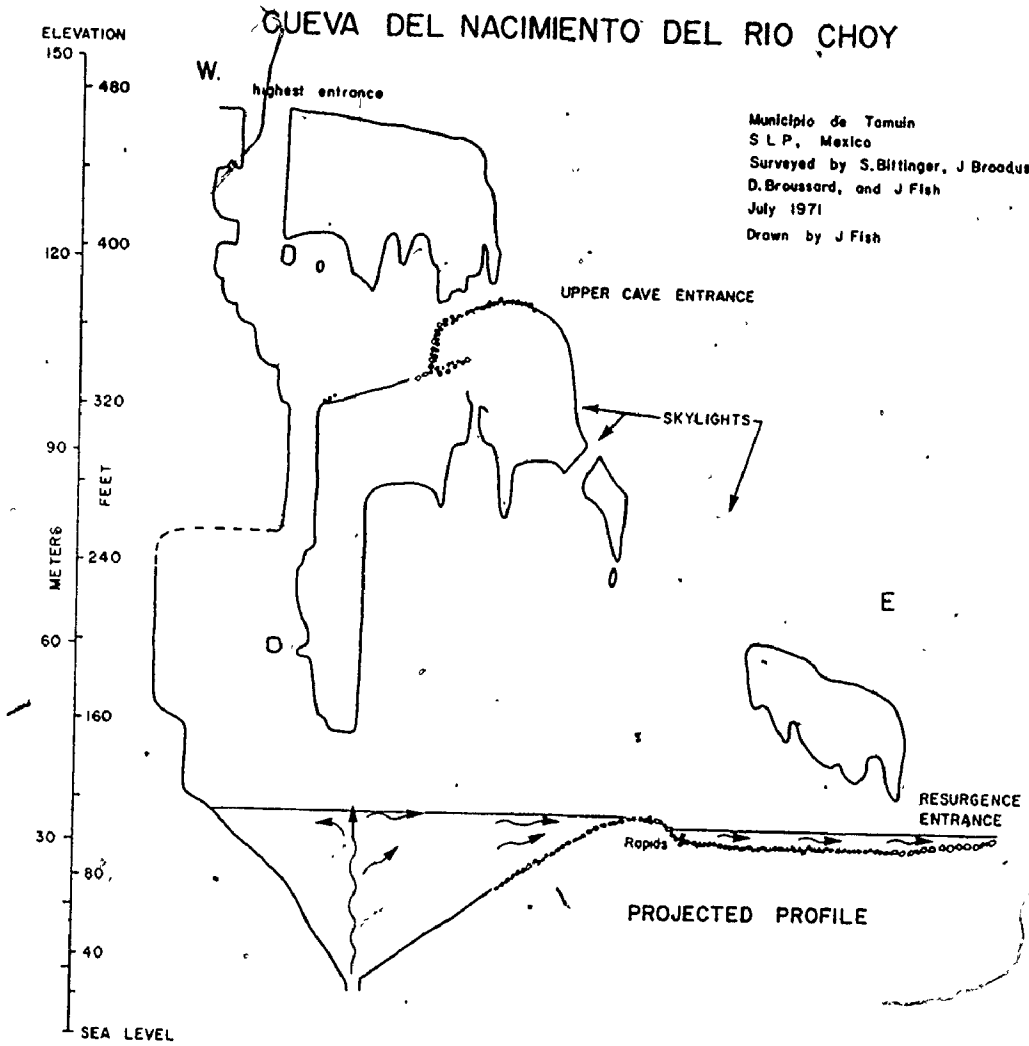

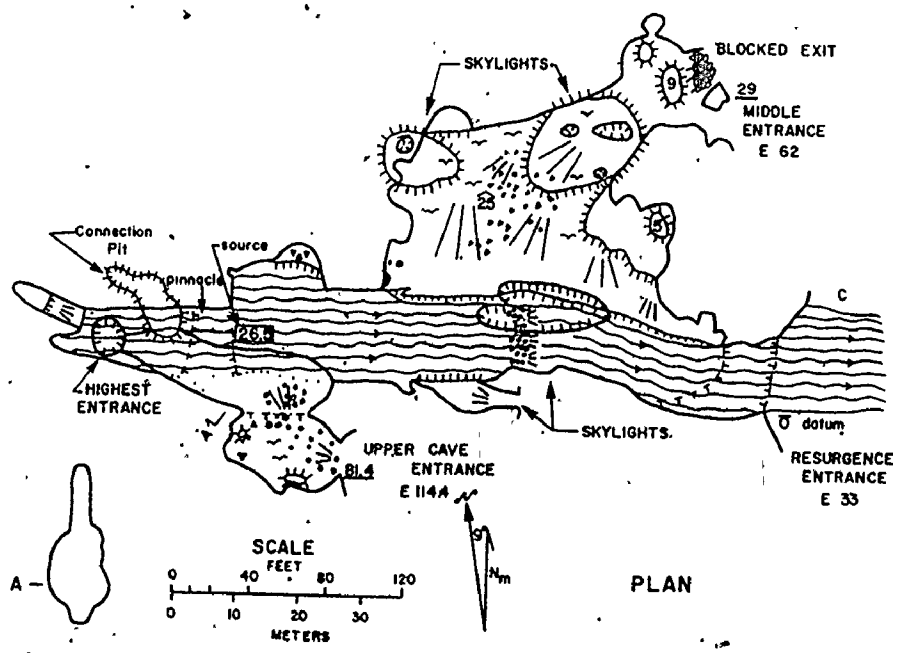

Figure 6.1 Map of Cueva del Nacimiento del Río Choy.

passage) connected by a 62 m shaft (Figure 6.1). The upper cave, especially the top of the shaft where the river may be heard below, is used as a religious site by some local people.

This cave is particularly important because it is the site of a first magnitude spring, and because its geomorphic features provide considerable information about karst flow systems in the range. Normally, the flow is 2-4 m^3/sec (Plate 6.1). Occasionally, floods crest at more than 100 m^3/sec, completely filling the lower entrance (river exit) (Plate 6.2). During flooding, the lake surface often rises more than 2 m. Organic debris is often trapped against the back wall by the circulation pattern. Collapse of part of the ceiling over the lake has created a large skylight, and the boulders have formed a dam which raises the lake level (also the base level) about 1.5 m. Boulders may also have partially blocked the source conduit, which would impede the flow and access for scuba divers.

The smooth, blind domes, the wall pocketing, the uniform walls of the large shaft, and the irregular solutional ceiling and bedrock floor are proof of solution under water-filled conditions (Plates 6.3 and 6.4). Joints were the prinicpal loci of ground-water flow and solutional enlargement in the unbedded reef limestone, but some surfaces separating subfacies of the reef may also have been used (Plate 6.4). Modifications of the original solution cave are slight and include partial collapse of some of the phreatic domes to form skylights and breakdown, thin accumulation of entrance talus in the upper cave, and deposition of very minor amounts of chemical sediments and guano. Phreatic

Plate 6.1 The Choy spring at base flow (3-4 m^3/sec). The reef facies is unbedded, but has many fractures, other separation surfaces, and occasional "facies" planes.

Plate 6.2 The Choy in moderate flood, around 35 m^3/sec. The water has risen about 3 m (compare with above photo). Large floods completely fill the entrance.

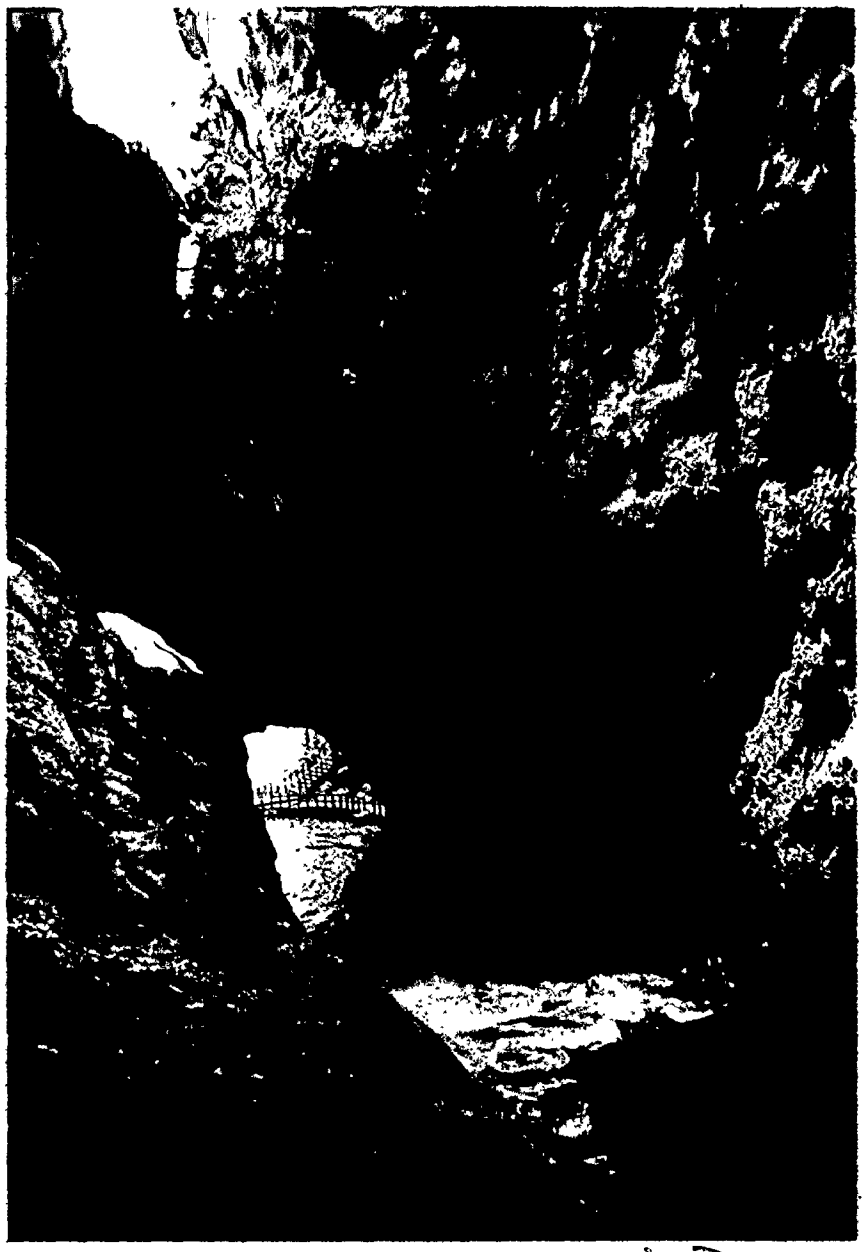

Plate 6.3 View from inside Choy cave looking out the lower or Resurgence Entrance (note people for scale). Water from the rise pool flows over a boulder dam created by ceiling collapse to form a skylight. The walls display broad phreatic pockets and much smaller reef cavities (?). Note the steeply inclined joint.

Plate 6.4 Phreatic ceiling pocketing and high phreatic domes at El Choy create a highly irregular ceiling. This view from Middle Entrance also shows the rise pool which is at least 26.5 m deep, and a major "facies" plane which probably provided the route for water to reach Middle Entrance when it functioned as a spring.

features extend up to about 10 m below the Pit Entrance (elevation approximately 132 m) where any higher evidence has been removed by collapse. Depth measurements of the lake show that the deepest point coincides with a water boil seen during floods (Figure 6.1). The floor of the lake slopes rather uniformly down to the deepest point. Thus, water presently rises at least 26.5 m to resurge. Geomorphic observations suggest that in the past when the coastal plain stood at higher levels, water climbed to the Middle Entrance and the Upper Cave Entrance to resurge. If this interpretation is correct, then a phreatic rise of lift of at least 120 m occurred. A group of flat-topped gravel capped hills of Méndez shale lie a few kilometers east of the Choy spring. The tops of the undisturbed hills are about 77 m elevation and are remnants of a paleo coastal plain which probably correlates with the middle resurgence level.

6.2.2 Las Cuevas de Taninul Numeros 1 and 2

Figures 6.2 and 6.3 show the plans and profiles of springs and caves near Hotel Taninul, two kilometers south of the south El Abra Pass. Two springs occur at the base of the scarp. The Taninul Sulfur Pool is a thermal, sulfurous spring with a permanent flow. It is an artificial pool except for the source area where water appears to rise through boulders partly blocking a natural conduit in the limestone. Nearby, and about 1.5 m below the Sulfur Pool level, lies a normally stagnant pool, referred to in this thesis as the "limestone pool". This pool is really an estavelle. During the wet season, flood water from the Sulfur Pool often enters it and sinks in the center, back into the El Abra.

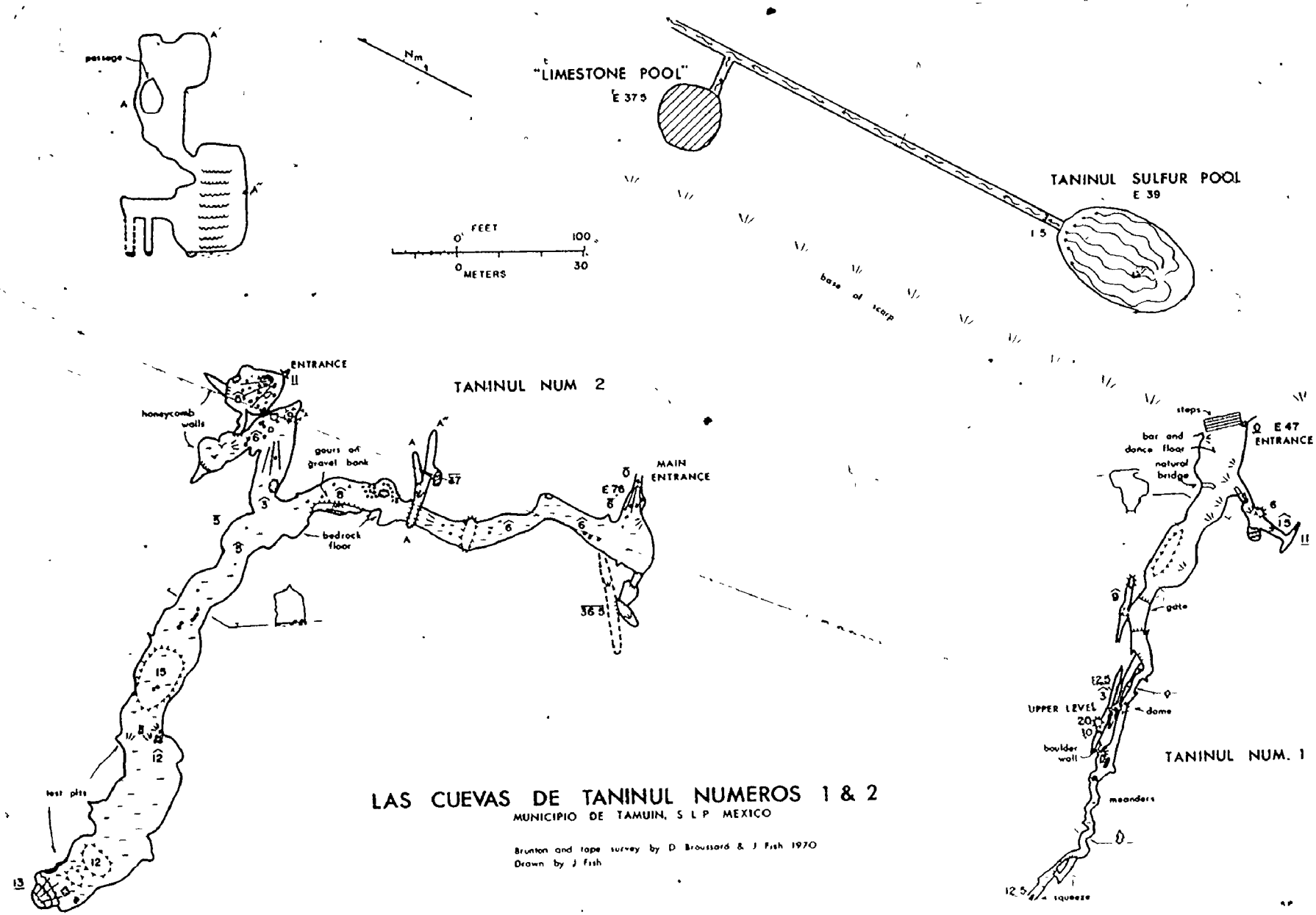

Figure 6 2 Maps of Cuevas de Taninul No 1 and 2, and the Taninul springs

LAS CUEVAS DE TANINUL NUMEROS 1 & 2

EXTENDED PROFILE

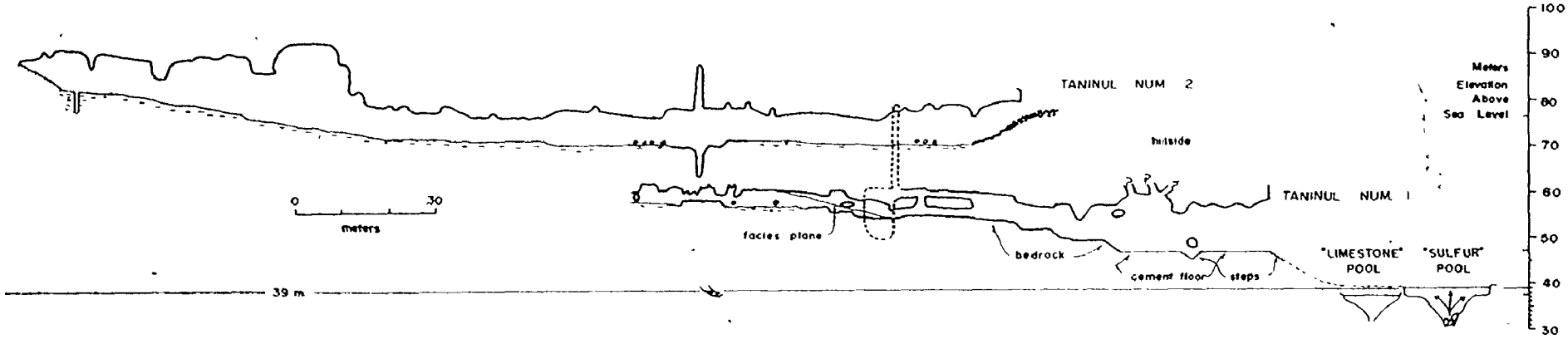

Figure 6.3 Profile of Cuevas de Taninul No 1 and 2.

Sometime later, it reverses the direction of flow to become a spring. It is likely that some El Abra water is then discharged as well as the Sulfur Pool water. No bedrock was observed in the limestone pool. More hydrological information is given in Section 5.3.

Cueva de Taninul Numero 1

Taninul Number 1 is an inactive cave oriented perpendicular to the scarp; it is a favored place for geologists to see a cross section of the Cretaceous reef trend. The large entrance area has been developed into a bar and dance floor. Natural bridges, wall and ceiling pocketing, and domes indicate solution under phreatic conditions. The cave gradually rises on a bedrock floor and diminishes in size, becoming typically 1 m wide and 2-3 m high, until a narrow bedrock squeeze is encountered 135 m from and 12.5 m above the entrance. The solution features and passage pattern of the back portion of the cave are dominantly phreatic, but some 8 cm scallops and passage meanders (?) may be evidence of moderate flow velocity under pressure or of a vadose phase. This is the only cave visited which has a reddish earth fill in some wall and ceiling cavities. Small joints have controlled the passage location and cross section in the back half of the cave. Note that the passage descends at a lesser angle than the boundary plane between two subfacies of the reef trend.

Near the middle of the cave, there is a joint-controlled Upper Level complex which connects with the main passage in at least two places. One of the passages has a high dome, and a 10 m drop in a fissure, which

has one wall composed of boulders held in place by dirt and flowstone. The dip-oriented side passage near the entrance, the joint domes, the Upper Level, and the end of the main passage probably were sources of water integrating to form a small fossil spring approximately at the present cave entrance.

Cueva de Taninul Numero 2

Taninul Number 2 lies 120 m north and farther up the scarp than Number 1, and is a considerably larger cave. Part of the roof of an east-trending passage has collapsed to give access via the Main Entrance. Perhaps there was an exit a few meters to the east for water that used to flow through the cave. A breakdown slope descends 6 m to one end of a moderately large passage at 70 m elevation. This 6 m wide, 7 m high passage trends northward parallel to the scarp for 85 m, then turns westward for 110 m, becoming still larger. The north-trending portion contains only a thin sediment veneer and in some places none at all, whereas the fill in the west-trending portion thickens until a flowstone bank blocks the passage. The test pit (for phosphate) shown on the profile penetrated 4.5 m of fine-grained sediment with a few boulders. The other test pit penetrated perhaps 2 m of sediment then 3 m more down a narrow slot which may have been an enlarged joint in the original bedrock floor.

At the bend, an east-trending passage slopes upward over sediment and breakdown to a small chamber to the north, which connects by a narrow passage to another chamber. A thick breakdown pile in this second chamber

blocks what may have been a larger connection with the main passage, and probably blocks another fossil ground-water exit. Both chambers have honeycomb or spongework walls as described by Bretz (1942).

There are two other unusual side passages. Fifty meters north of the entrance a cross-joint(s) has been dissolved out forming an embayment into the entire periphery of the walls of the passage (section A-A'-A''). The bottom slopes down to an 18 m fissure drop to a static pool of water at approximately the same elevation as the Taninul Sulfur Pool. The nature of the embayment and the uniform solution exhibited by the walls could only have been created by water-filled conditions. The other passage is a series of short drops from the west end of the entrance chamber to a mud-floored fissure at the same elevation as the bottom of the other fissure.

The tubular passage cross-section, solution sculpture including spongework and the fissures show that the cave was in the phreatic or epiphreatic zone during virtually all its formative phase. The lower-level fissures could have been sources or distributaries in this 3-dimensional system. Near the bend of the main passage, there is a 1 m high bank of rounded gravel that demonstrates a minor vadose phase of deposition and then retrenchment. The relationship of the vadose phase to the fissures is not understood.

6.2.3 Grutas de Quintero

Grutas de Quintero is a locally well known cave in the northern part

of the Sierra de El Abra. The entrance is a stoopway near the base of the range at an elevation of 179 ±5 m (Figure 6.4). Inside, the passage enlarges to 9 m wide by 4 m high, and contains some sediment fill. Plate 6.5, taken at point A on the map, shows phreatic wall and ceiling solutional forms and a prominent bedding plane that probably was the locus of passage initiation. The small passages lead into The Loop, which is comparable in size with the larger part of Main Passage. Main Passage is a large, tubular, paleophreatic conduit typically 10-12 m wide and 8-12 m high (Plate 6.6). In several places large travertine dams have formed, which occasionally create deep wet season pools. At 180 m and 240 m from the entrance, there are low alcoves sloping downward from the north side of Main Passage. They eventually become blocked with sediment, travertine, or water. Beyond the second alcove, the floor of Main Passage rises rapidly over what is probably a massive fill of flowstone and sediment that causes a decrease in ceiling height to 5 m. Three hundred meters from the entrance Stalactite Chamber is encountered. The left-hand portion of this chamber slopes upward to a blind alcove and is barren except for one large stalagmite. The ceiling of the right-hand portion is covered with stalactites, and the next 60 m of Main Passage is well decorated. From Stalactite Chamber to The Pit, 200 m beyond, the passage is horizontal and has a slightly lower average ceiling height because of a deep fill of fine-grained sediments. The fill is 15 m thick in a test hole dug by miners. The Pit is 12-15 m deep and marks the end of Main Passage. It is not known how much of it is formed in bedrock versus how much is in the sediment fill; the back wall is definitely bedrock.

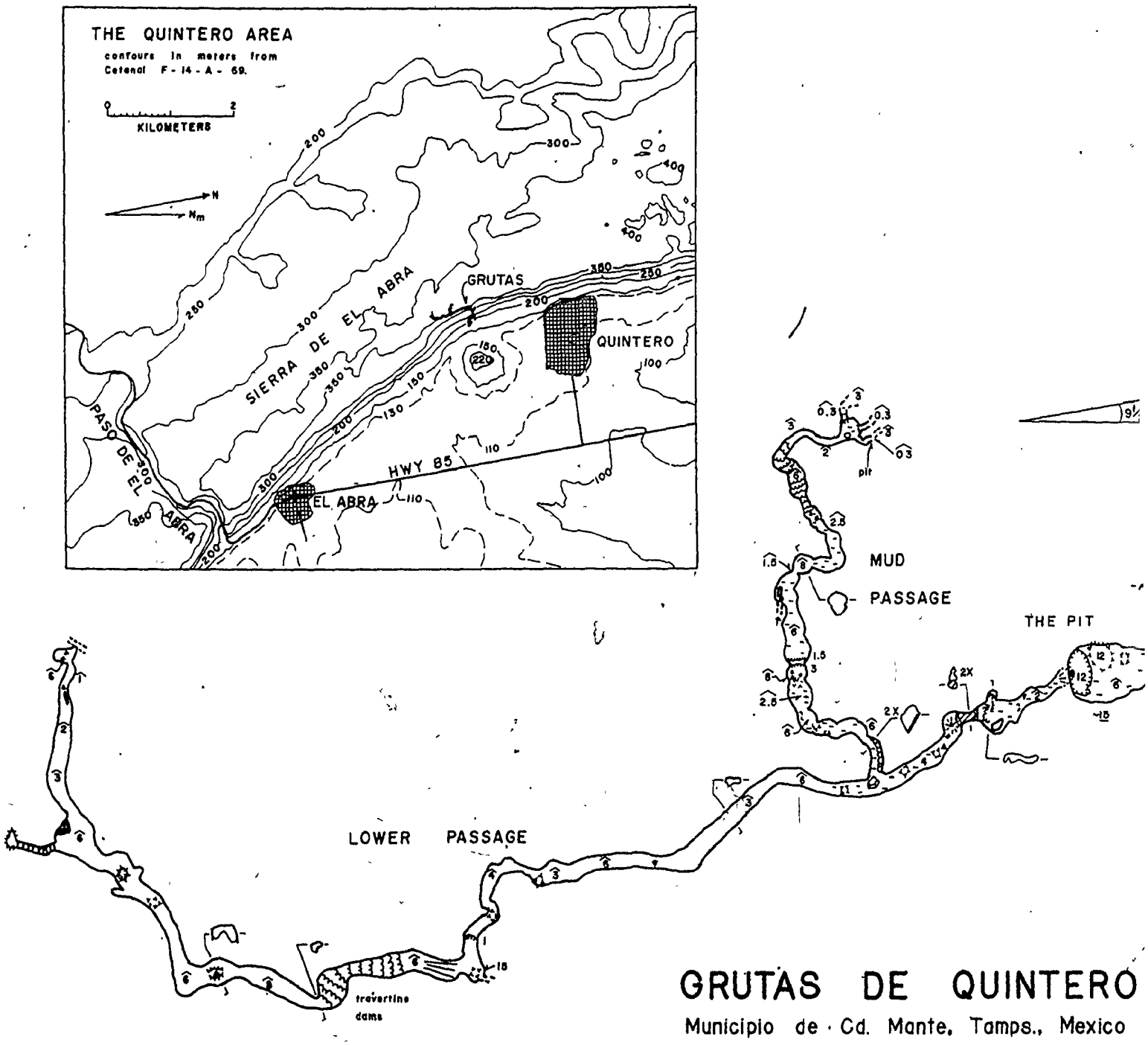

GRUTAS DE QUINTERO

Municipio de Cd. Mante, Tamps., Mexico

Brunton or suunto B tape survey by B Bell, D. McKenzie, J. Reddell, A. R. Smith, Nov. 1965; E. Alexander, J. Fish, T. Raines, Jan. 1966; J. Broadus, D. Broussard, D Honea, Nov. 1968; D. Atkins, S. Bittinger, D. Broussard, J. Greer, June 1972.
Additional sketchs by J Fish, June 1972.
Inked by S. Patrick.

Figure 6.4 Map of Grutas de Quinter

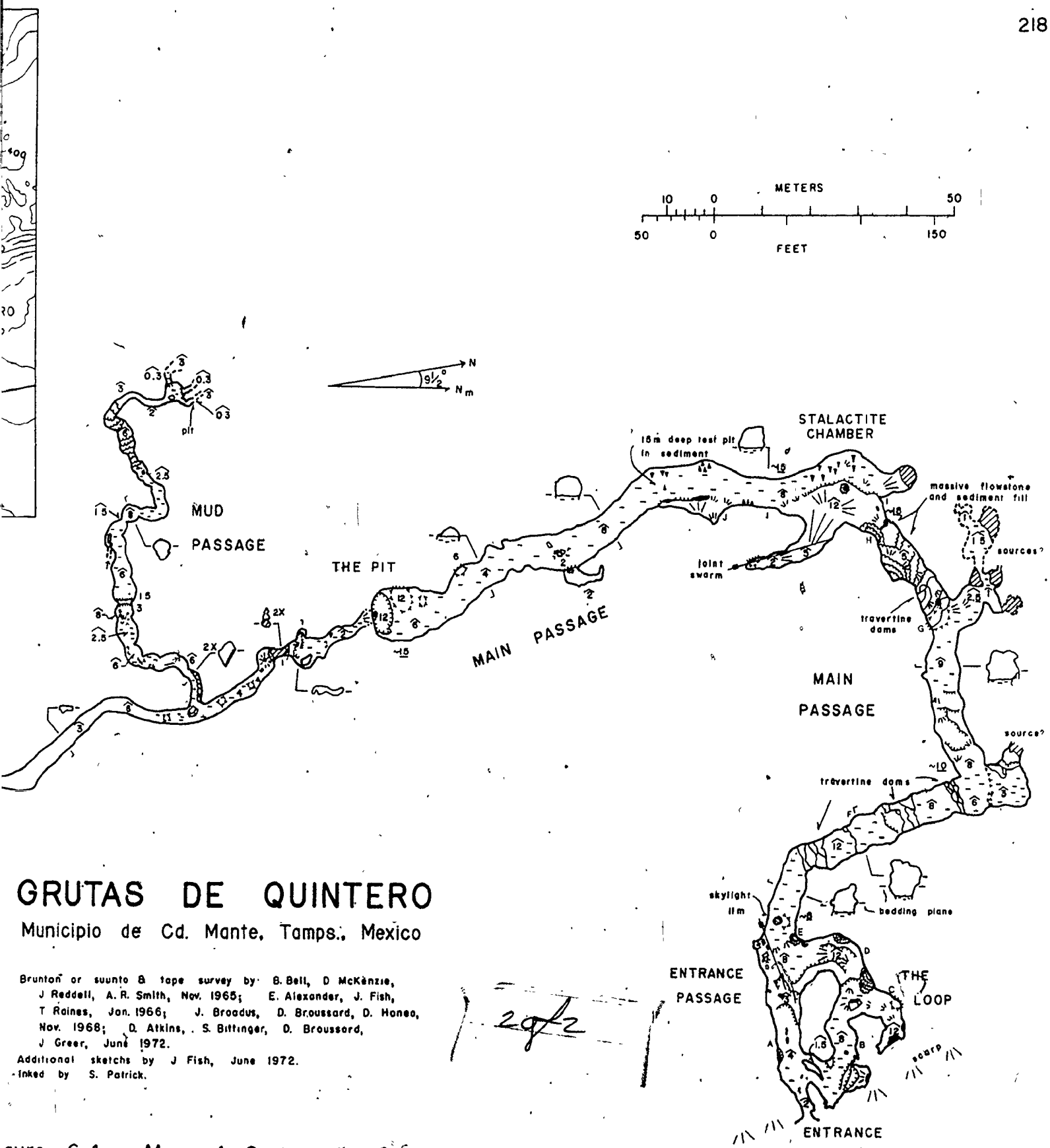

GRUTAS DE QUINTERO

Municipio de Cd. Mante, Tamps., Mexico

Brunton or suunto & tape survey by B. Bell, D McKenzie, J Reddell, A. R. Smith, Nov. 1965; E. Alexander, J. Fish, T Raines, Jan. 1966; J. Broadus, D. Broussard, D. Honea, Nov. 1968; D. Atkins, S. Bittinger, D. Broussard, J Greer, June 1972.
Additional sketchs by J Fish, June 1972.
Inked by S. Patrick.

gure 6.4 Map of Grutas de Quintero.

Plate 6.5 The Entrance Passage of Grutas de Quintero. View from point A on the map toward small passages leading to The Loop. The passage exhibits phreatic solution features and cross section. Note the prominent facies plane.

Plate 6.6 The Main Passage of Quintero, looking into the cave from point F. It is an excellent display of phreatic features including tubular passage shape, pocketing, and blind domes. The bedding plane probably controlled the locus of passage development.

A hole at the bottom of The Pit passes through a muddy pool to the back half of the cave. Lower Passage is generally muddy, and averages 3 m wide and 4 m high. It extends 530 m, rising slightly along the way, to a small room blocked by flowstone where the gurgle of flowing water beyond a crack can often be heard. Mud Passage is of similar size and character, and is 210 m long. The floor rises initially about 3 m, declines 4 m in the central area, then climbs steeply over a flowstone slope to a room 10 m above the Mud Passage entrance. Three small passages leave the room, one of which has a 9 m drop ending in a crack and dirt floor.

Unfortunately, Grutas de Quintero was surveyed by several different groups and most of the original notes were lost before the elevations were added to the map. Also, the geomorphological studies extend only to The Pit, and may be impossible to continue because the cave is being mined in a serious way. Nevertheless, many important aspects of the cave are known and others may be hypothesized.

All of the cave back to The Pit is developed in the massive El Abra reef limestone. Probably all of Main Passage formed initially along the gently dipping undulating bedding plane shown in the photographs and cross sections, and grew to its present size in the permanently water-filled zone. Phreatic features include wall and ceiling pocketing, smooth blind solutional domes that are developed along small fractures, and a tubular passage cross section. An altimeter traverse of Main Passage was made to obtain approximate elevation data. From the entrance, the passage rises 8 m up the dip in 100 m, then turns north along the

strike for 80 m, and then turns up dip again to Stalactite Chamber 18 m above the entrance. The remaining passage to The Pit is approximately along the strike at about +15 m. Thus, the bottom of The Pit is about the same elevation as the entrance. The passages beyond are thought to be within the elevation range of the first half of the cave. The dip is 5-6° E in the Entrance Passage, and becomes less in Main Passage.

With the exception of a drip basin below a dome at point C, any vadose solution features that may be present are buried. As the water table gradually lowered below the cave, the cave's hydrologic function changed from a phreatic trunk conduit to an intermittently active vadose channel of small discharge. The principal vadose activity has been the deposition of travertine dams, flowstone, and fine-grained sediments. At points B, H, and J, "phreatic" pocketing of stalagmite and flowstone show that the details of the cave's later history are complicated. In the area of point J, the following phases or "events" are believed to have occurred: 1) deposition of massive stalagmites, 2) severe phreatic (or paraphreatic) re-solution of the stalagmites, 3) another period of growth of large stalagmites and stalactites, and finally 4) a later (present?) phase of deposition of small stalactites. From D to E, the bedding plane has supplied the water for the flowstone deposits.

The relationship of Grutas de Quintero to the topography of the El Abra range is shown in Figure 6.4. From near the base of the scarp, the cave penetrates 240 m perpendicular to the face to a point directly underneath the top of the scarp, then follows the strike of the range

southward for 600 m. It was almost certainly a spring-cave system, whose exit was approximately at the present entrance. Phreatic features in Stalactite Chamber reach an estimated 30 m above the entrance, or an elevation of about 210 m. This suggests that water may have flowed upward 40+ m from the present entrance along joints or along the reef front to an old coastal plain level at 220+ m elevation (indicated by the capped hill of Méndez shale directly in front of the cave which is capped by a freshwater limestone; see Figure 6.4 and Plate 3.1). The pattern of the cave is interpreted to be that of an integrating system. Water must have come to Mud Passage and Lower Passage from sinks and crevices on top of the range 150 m above, flowed up The Pit, down Main Passage and up to the fossil spring. The three alcoves on the north side of Main Passage may also have been sources of water. Alternatively, the alcove off Stalactite Chamber may be just part of a loop to the middle alcove. The contrast of passage size between the front and back halves of the cave is puzzling and demands further study. Among the possible explanations are a change of limestone facies, or other sources that may be buried below The Pit or the deep sediments in Main Passage. The back half of the cave is generally wet and muddy, indicating it is still somewhat active hydrologically; but the water now evidently seeps down to unknown passages. Drips and possibly the alcove sources (?) create very small intermittent flows in the first half of the cave.

6.2.4 Cueva de las Cuates

This cave is located in the high central portion of the El Abra

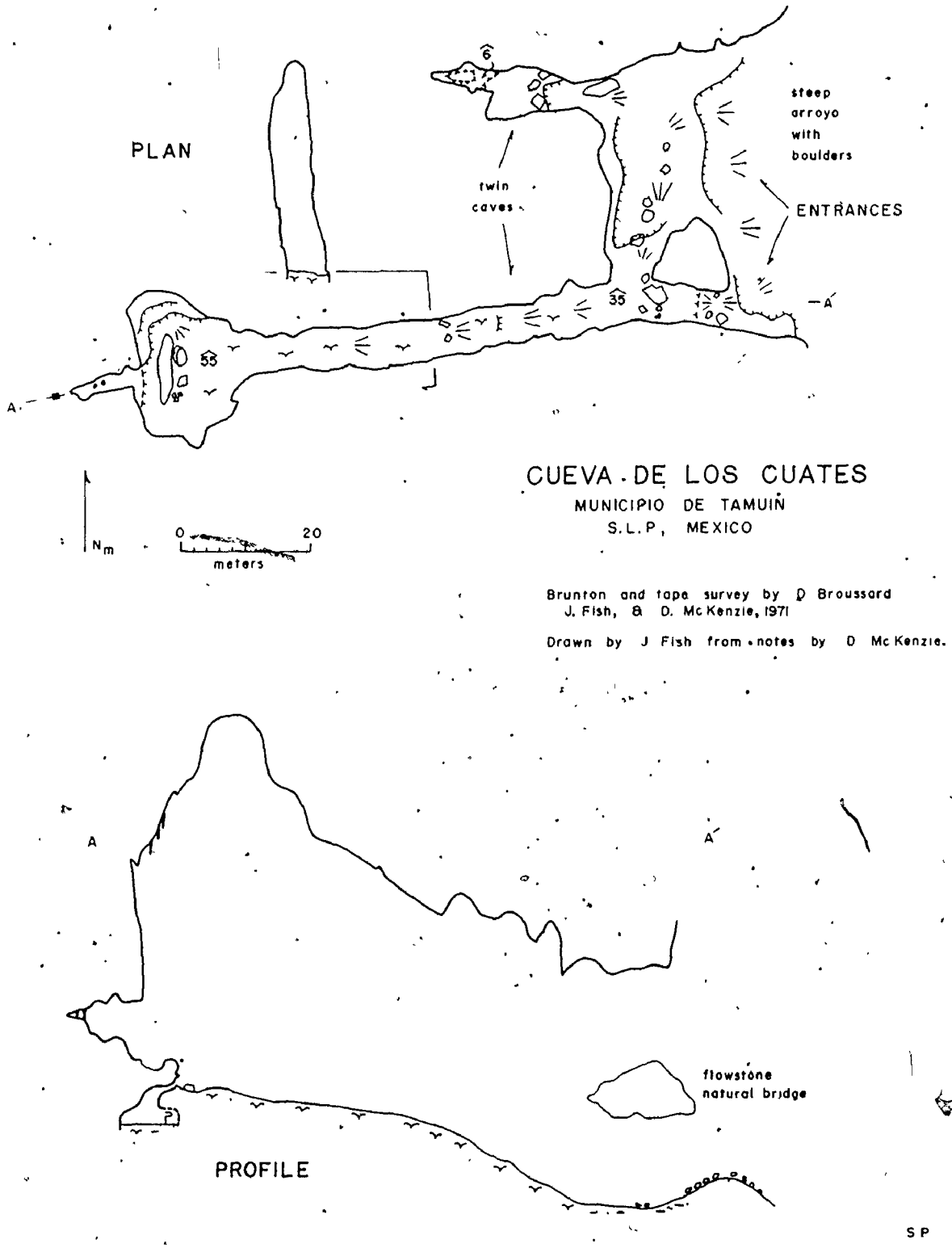

Figure 6.5 Map of Cueva de las Cuates.

range. It is named for its twin entrances which are near the top of the east face at an estimated 500-600 m elevation. A steep climb over boulders leads to the entrances which are in a recess formed by collapse of the cave (Plate 3.6).

The main cave is short (only 102 m), but high. It appears to be formed along a single, large, nearly vertical joint. As indicated by the pocketing and smooth solutional forms, smooth blind domes, and irregular ceiling profile (Figure 6.5), the cave was formed under water-filled conditions. The floor is covered with dry guano. At the back of the cave, a small hole leads to a drop (unclimbable?) to a small room which was not explored. A flowstone natural bridge at the entrance indicates that a higher sediment floor existed in the past, and that material is somehow being removed, possibly by vadose trickles.

6.2.5 Cueva de la Ceiba

This description is adopted from a description plus map by John Bassett (1971), and from personal discussions with him. The cave was not visited for this study, but is included because it has an important hydrologic implication.

The cave is located about half way up the eastern scarp in the central portion of the range at an estimated 300 m elevation. The high arched entrance is typical of the east face caves. A 30 m long passage leads to the main part of the cave which consists of a large chamber 160 m long, varying from 6 to 23 m wide and having an irregular

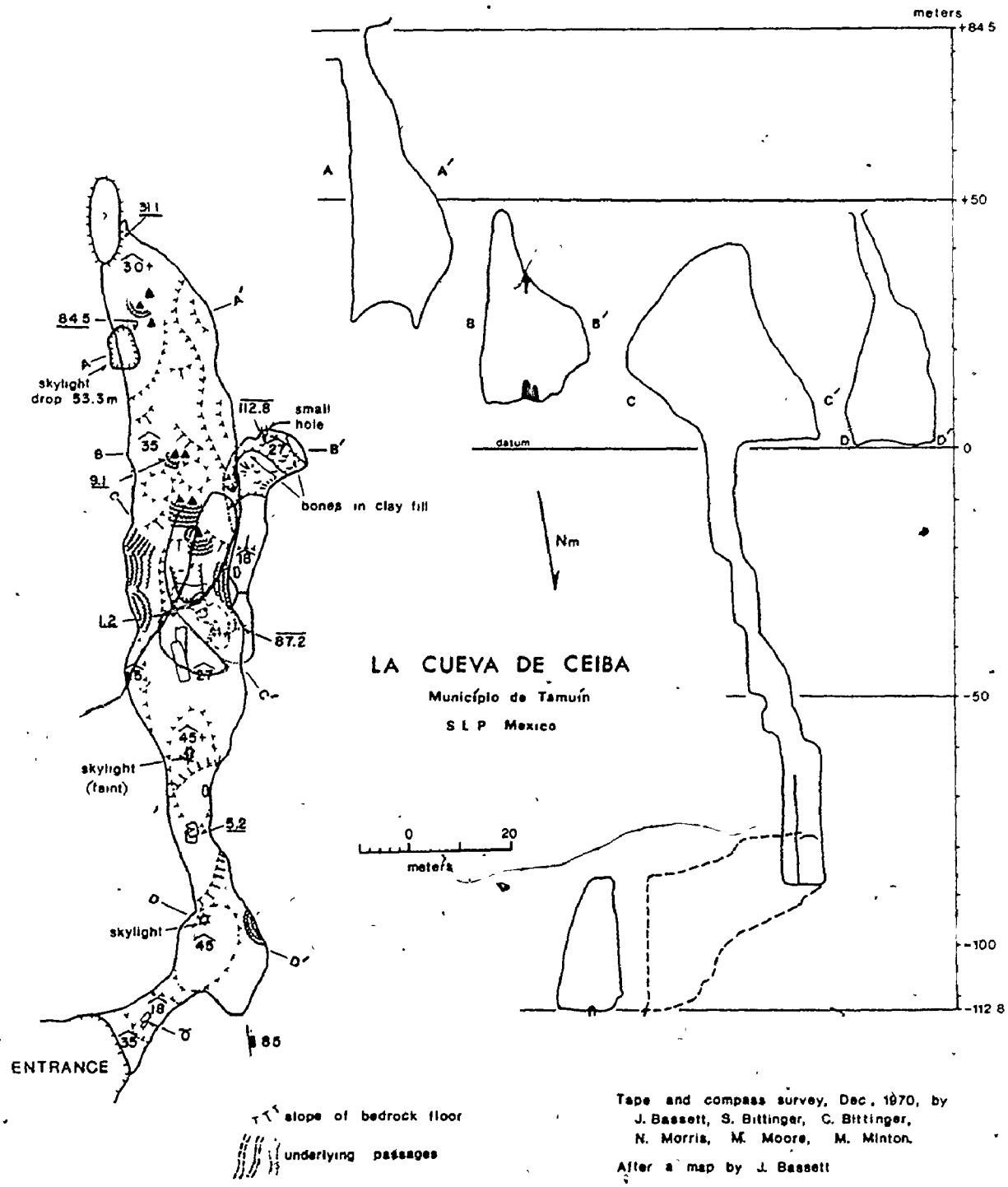

Figure 6.6 Map of Cueva de la Ceiba.

ceiling with many high domes (Figure 6.6). This chamber is developed along a single large fracture parallel to the east face, which may be seen extending at least 30 m vertically at the north end of the chamber. The floor in the first half of the chamber is relatively level except for a broad bedrock mound. The floor of the back half rises along a bedrock incline to 31 m above the entrance (see the cross sections on the map which are arranged to serve as a crude profile). The cave appears to end abruptly in a crack a few centimeters wide, but a 40 m dome may be a continuation.

In the middle of the chamber, a pit series descends 88 m to a steeply sloping room which is blocked at the bottom by sediments. An eroded mudbank contains several layers of large mineralized bones. The pit series is developed along a swarm of microfractures rather than large joints, and displays smooth forms characteristic of uniform solution under phreatic conditions.

Vadose solution features are completely absent and current-deposited sedimentary structures are minor. The only changes that have occurred since the cave was drained are the formation of some flowstone and stalagmites beyond the pit, a minor amount of collapse, and deposition of a small amount of sediments, mostly washed down the pit.

6.2.6 Ventana Jabalí

Ventana Jabalí is located 18 km NW of Tamuín. The large entrance is the most conspicuous of the east-face caves (Plate 6.7), and lies about

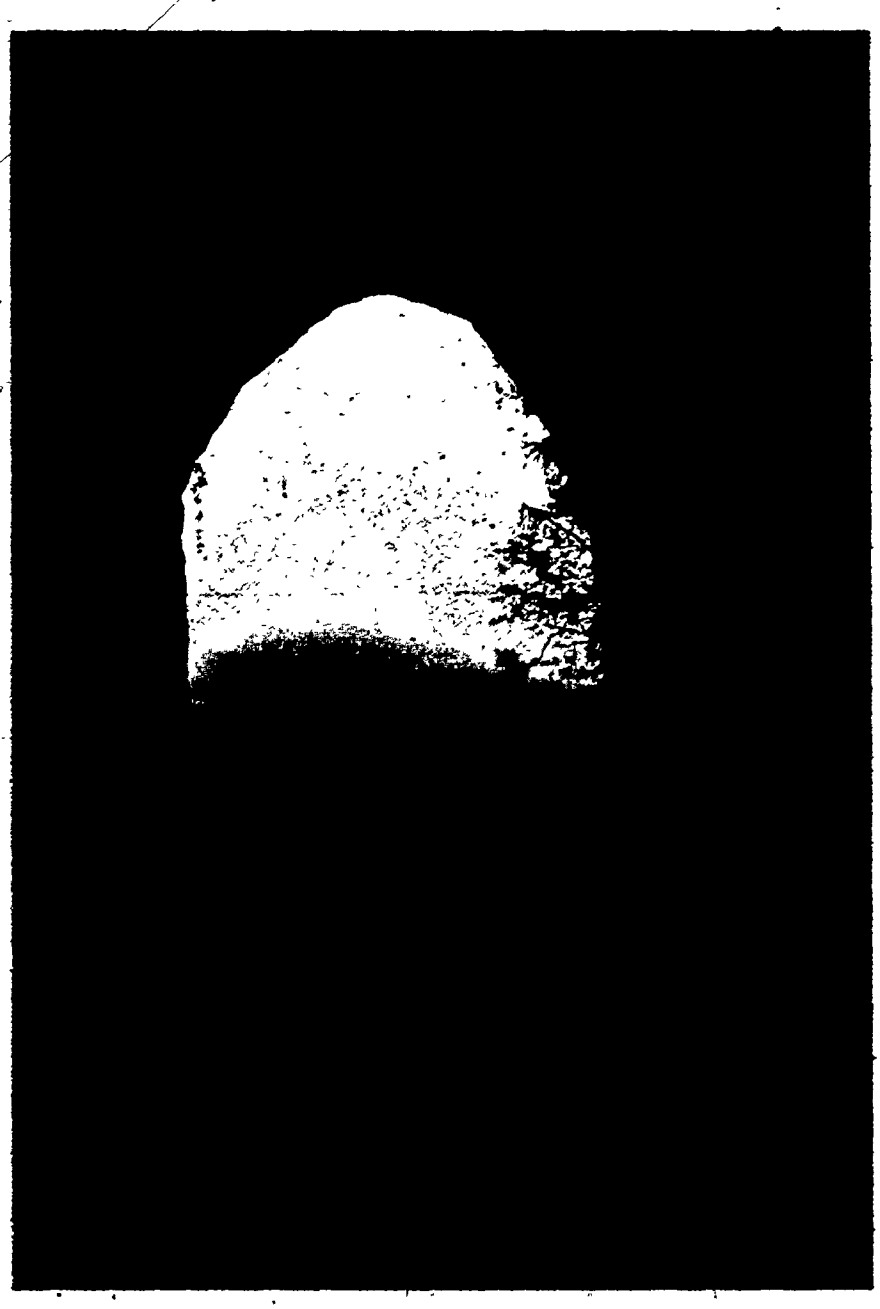

Plate 6.7 View out the high arched entrance of Ventana Jabalí to the coastal plain 200+ m below. The equipment is left from mining operations. The ceiling and walls are of phreatic origin.

two-thirds of the way up the scarp at about 350 m elevation. The cave has been mined extensively for phosphate and guano, and is well known among cave explorers for its spectacular size and skylights. It deserves to be equally well known among karst geomorphologists for its deep phreatic solution features. Figure 6.7 is a map of Ventana Jabalí, modified slightly from one published in Russell and Raines (1967, p. 77); Figure 6.8 is a profile drawn in this study; and Plates 6.7-6.10 show various views of the cave.

The cave is a single immense passage 380 m long and 15-20 m wide, oriented generally perpendicular to the scarp. It lies entirely within the unbedded reef facies of the El Abra limestone. An extraordinary ceiling profile was created by solution upward along joints under completely water-filled conditions (see profile). Near the middle of the cave a phreatic dome extends upward about 140 m and is spanned by a bedrock natural bridge about 70 m above the floor (Plates 6.8 and 6.9). The few meters of overburden above the dome has collapsed in several places to form small skylights 153.4 m high. The phreatic ceiling profile of the cave is mostly extant because there has not been much collapse.

In the front half of the cave, sediments have accumulated so that the floor varies only a few meters in elevation. Mining operations have removed a large volume of the fill, up to 7-8 m in places and have not reached the bedrock floor. If detailed sediment studies were carried out, there would probably be much information of geomorphic and climatic significance (Plate 6.11). Underneath the skylights, rocks and washed-in soil accumulates in mounds. Away from the skylights the sediments are almost

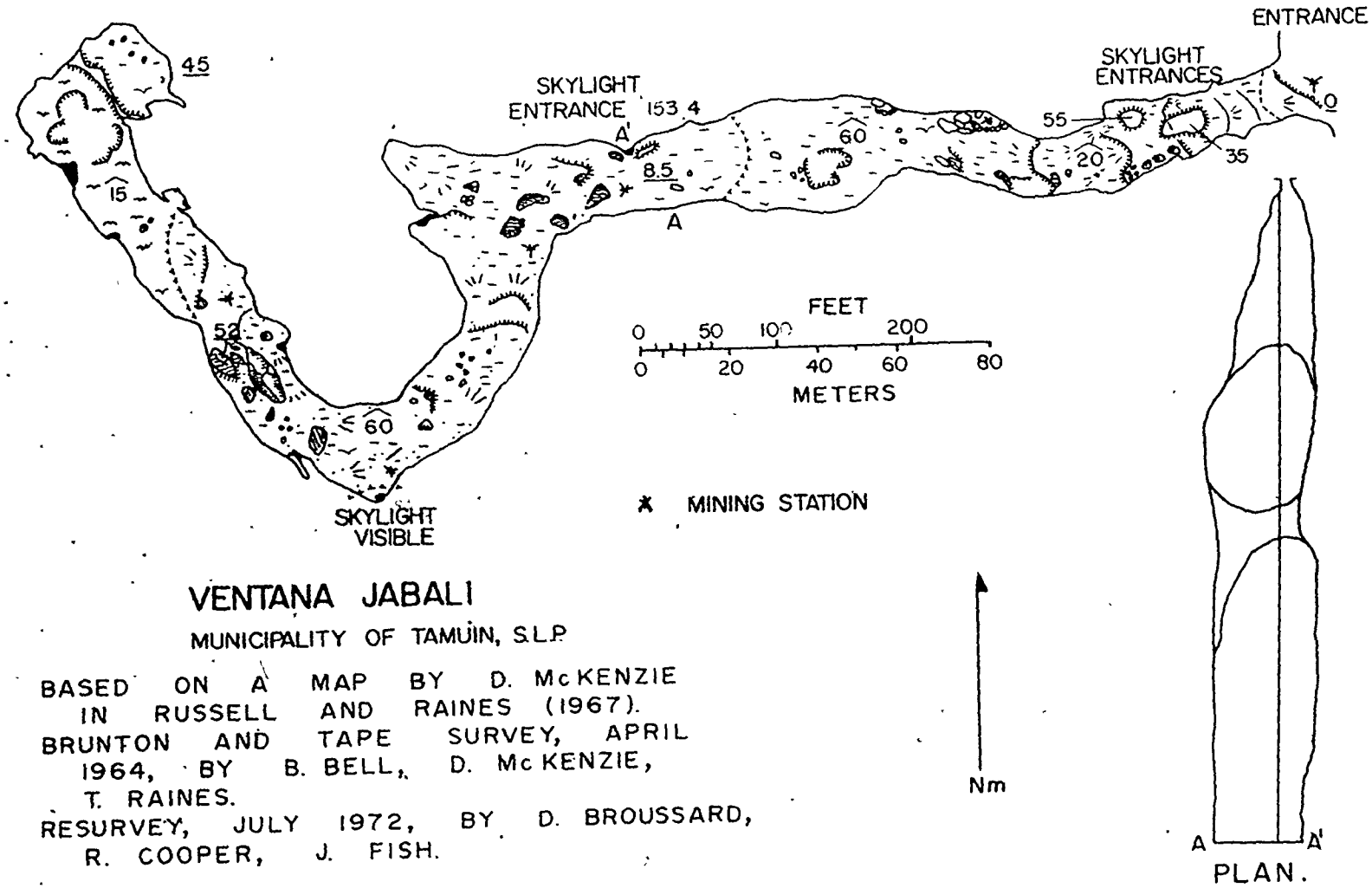

Figure 6.7 Map of Ventana Jabalí.

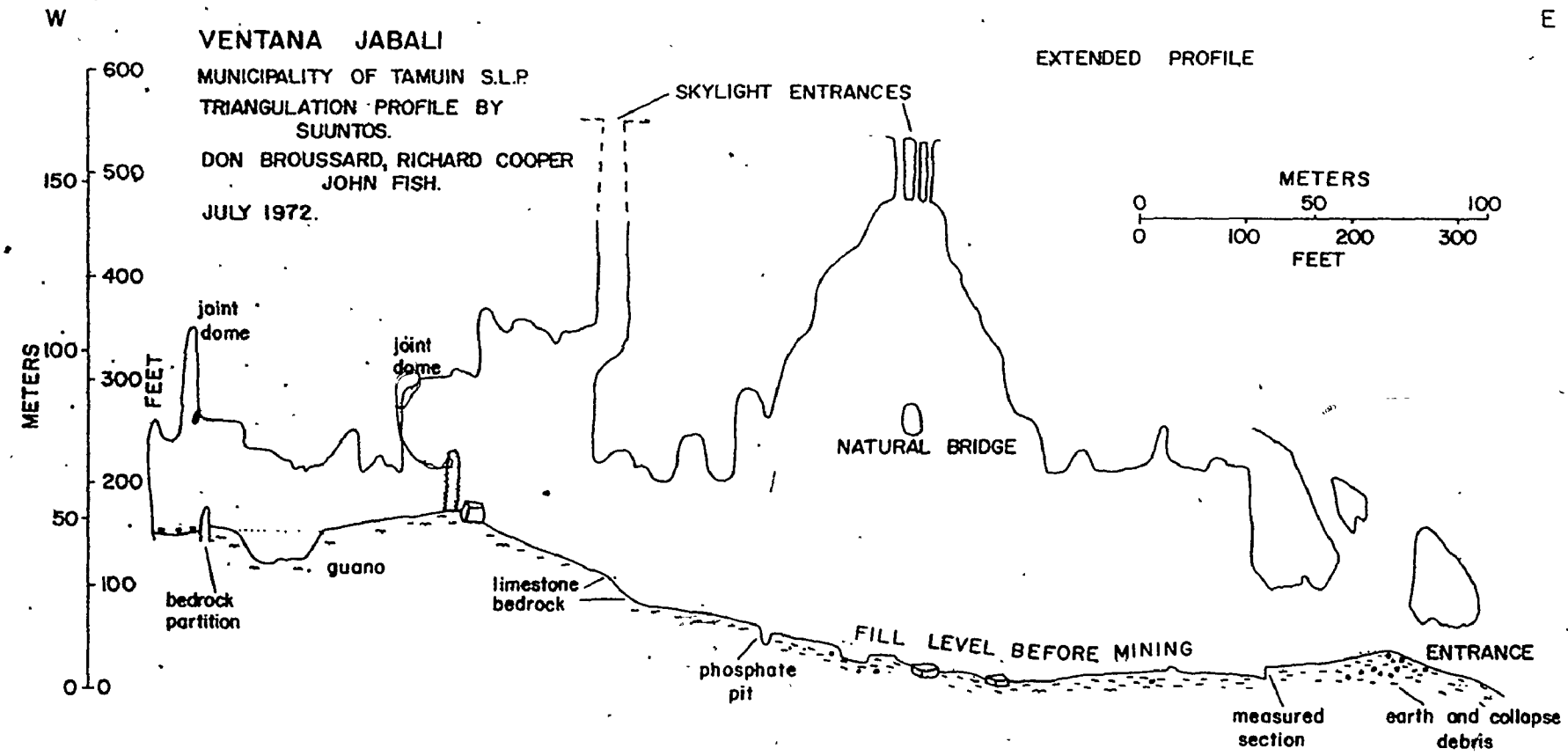

Figure 6.8 Profile of Ventana Jabalí.

Plate 6.8 The immense chamber of Ventana Jabalí. A very high phreatic dome has collapsed to allow summer sunbeams to enter from 153 m above (there is a person to the left of the lighted floor). One beam strikes a natural bridge 70 m above the floor. Sharp exterior phreatic solution edges may be seen 35 m above the floor, and there is a high fracture to the right of the bridge.

Plate 6.9 The high dome and bedrock natural bridge in Ventana Jabalí. Phreatic features extend upward about 140 m.

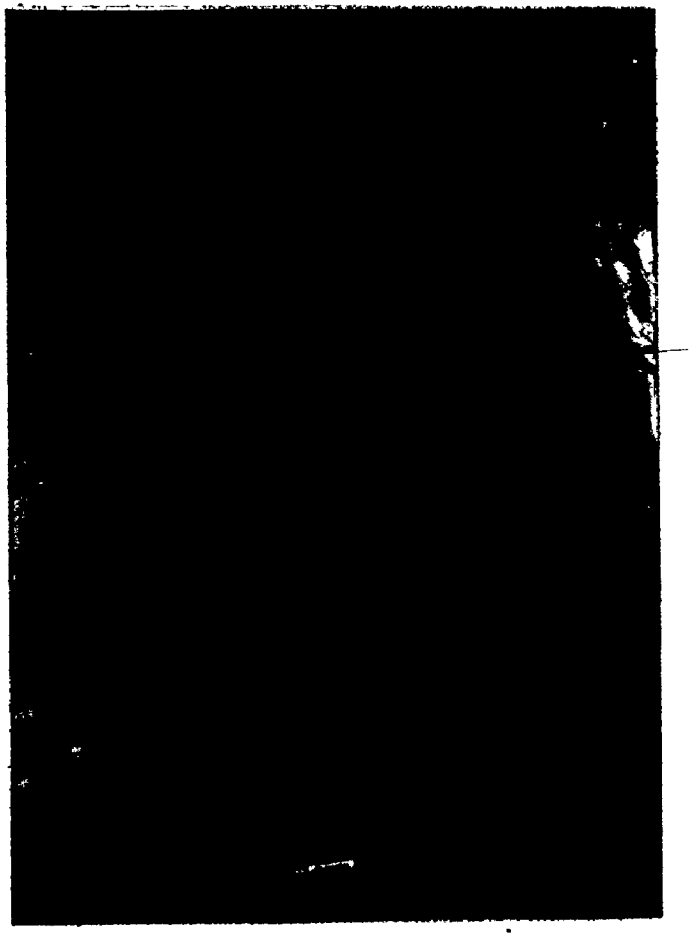

Plate 6.10 The rear portion of Ventana Jabalí showing irregular ceiling profile, sharp exterior angles and other water-filled solution forms. There is at least 10 m of guano fill.

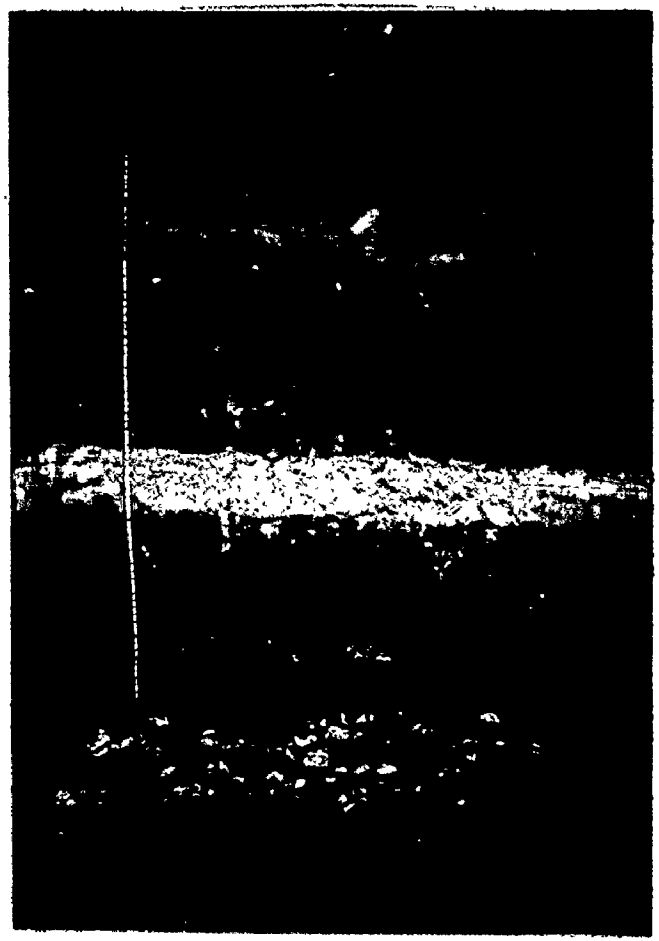

Plate 6.11 A 5 m sediment section exposed in a test pit near the entrance of Ventana Jabalí. There probably is a very interesting history recorded in the sediments here and in other caves in the range.

as thick, and may include remobilized entrance or skylight-facies sediments (moved by animals or vadose trickles), breakdown, guano, wind-blown dust, and possibly chemical precipitates in the sediment matrix. Beyond the big dome, the floor climbs steeply over what appears to be partly a bedrock slope to 52 m above the entrance, and then descends slightly. Beyond the rise, guano deposits have accumulated to a depth of at least 10 m. Near the end, there is an unusual bedrock partition that rises 6 m above the floor, and completely crosses the passage. The cave terminates abruptly at a high bedrock wall.

The source(s) of the water that made this immense cave are unknown, but it is likely that the conduits are buried. The solution pocketing, the sharp exterior corners or edges (Plate 6.10), the bedrock bridge and partition, and the highly irregular solution ceiling are conclusive evidence of formation under water-filled conditions. Phreatic waters circulated through a vertical range of at least 140 m.

6.2.7 Other East Face Caves

There are many other cave openings at all elevations along the east face that have not yet been examined. The caves better known locally are included here, but it is certainly possible that important discoveries and scientific information will be found in the unexplored caves. Also, there are several active springs not described here; some of these will be referred to where appropriate in the discussion in Section 7.4.

6.3 Caves on the Crest of the Sierra de El Abra

6.3.1 Sótano de la Escalera

Sótano de la Escalera lies about 1½ km north of the south El Abra Pass, on the relatively flat top of the range at an estimated 300 m elevation. The entrance is a 28 m deep pit created by ceiling collapse into a large void (Figure 6.9). A rubble slope descends into the center of the cave which comprises a single chamber 75 m in diameter and 35 m high. The upper portion of the walls and the ceiling appear to have been formed by upward stoping. They show slight solutional modification of the stairstep shape up to about the level indicated on the profile. The lowest part of the floor is flat and composed of washed-in soil, guano, and some very large stalagmites, several at least 12 m tall. They show that the floor of the chamber has been stable for a long time. No signs of stalagmite re-solution were observed.

6.3.2 Cueva Pinta

Cueva Pinta (Figure 6.10) is located east of Sótano de Soyate, very near the top of the monoclinal western flank of the range. The entrance lies at an elevation of roughly 465 m, and as in so many of the caves on the top of the range, it has been altered or was initially formed by collapse into an old phreatic chamber (Plate 6.12). A breakdown ramp slopes down to a large "L" shaped room that has more than a hundred Indian paintings, mostly handprints. The floor is flat, aggraded by sedimentary processes thought to be principally the washing-in of soil from the entrance

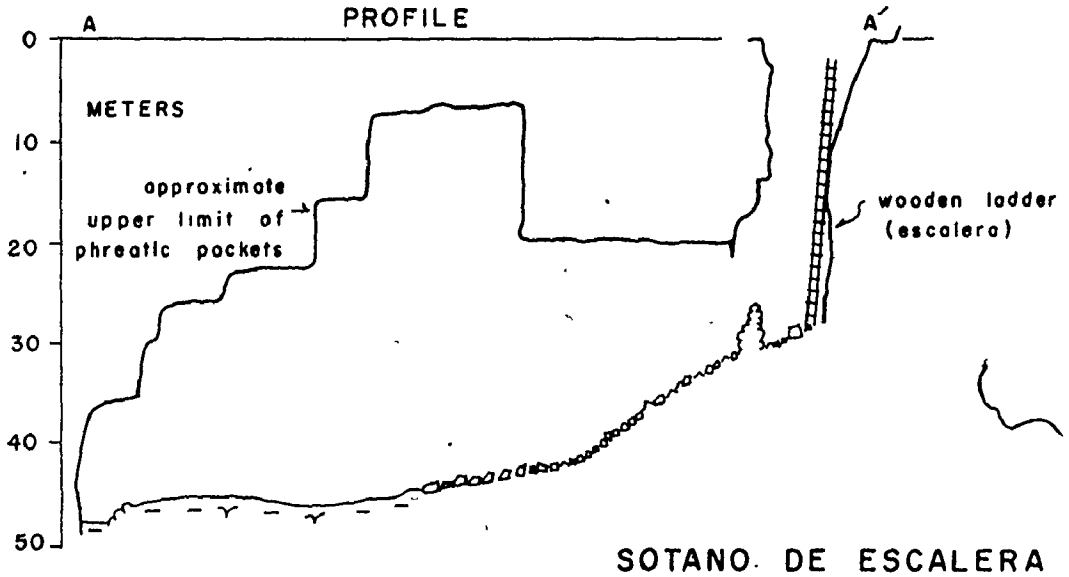

SOTANO DE ESCALERA
MUNICIPIO DE CD. VALLES
S. L. P., MEXICO

BRUNTON AND TAPE SURVEY JULY 1971
BY D. BROUSSARD, J. FISH, S BITTINGER.

DRAWN BY J. FISH.

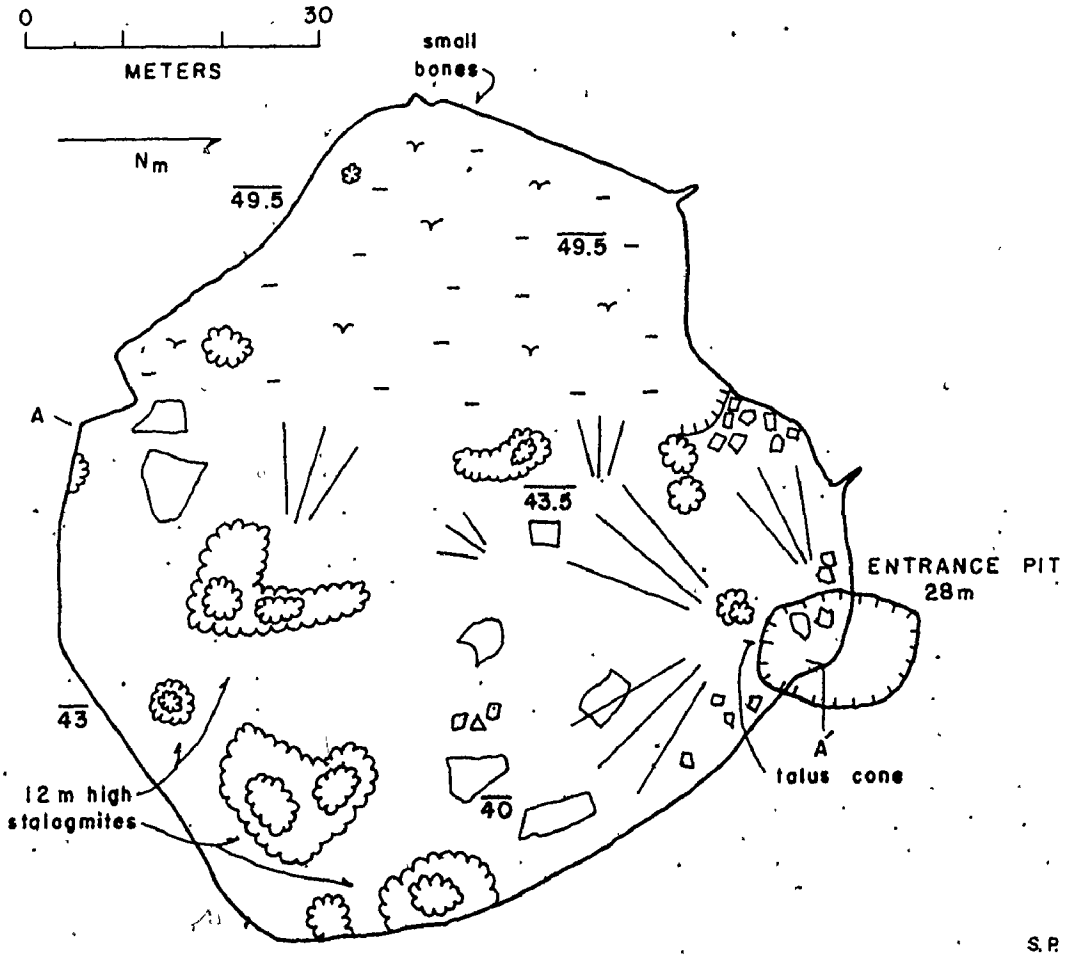

Figure 6.9 Map of Sótano de Escalera.

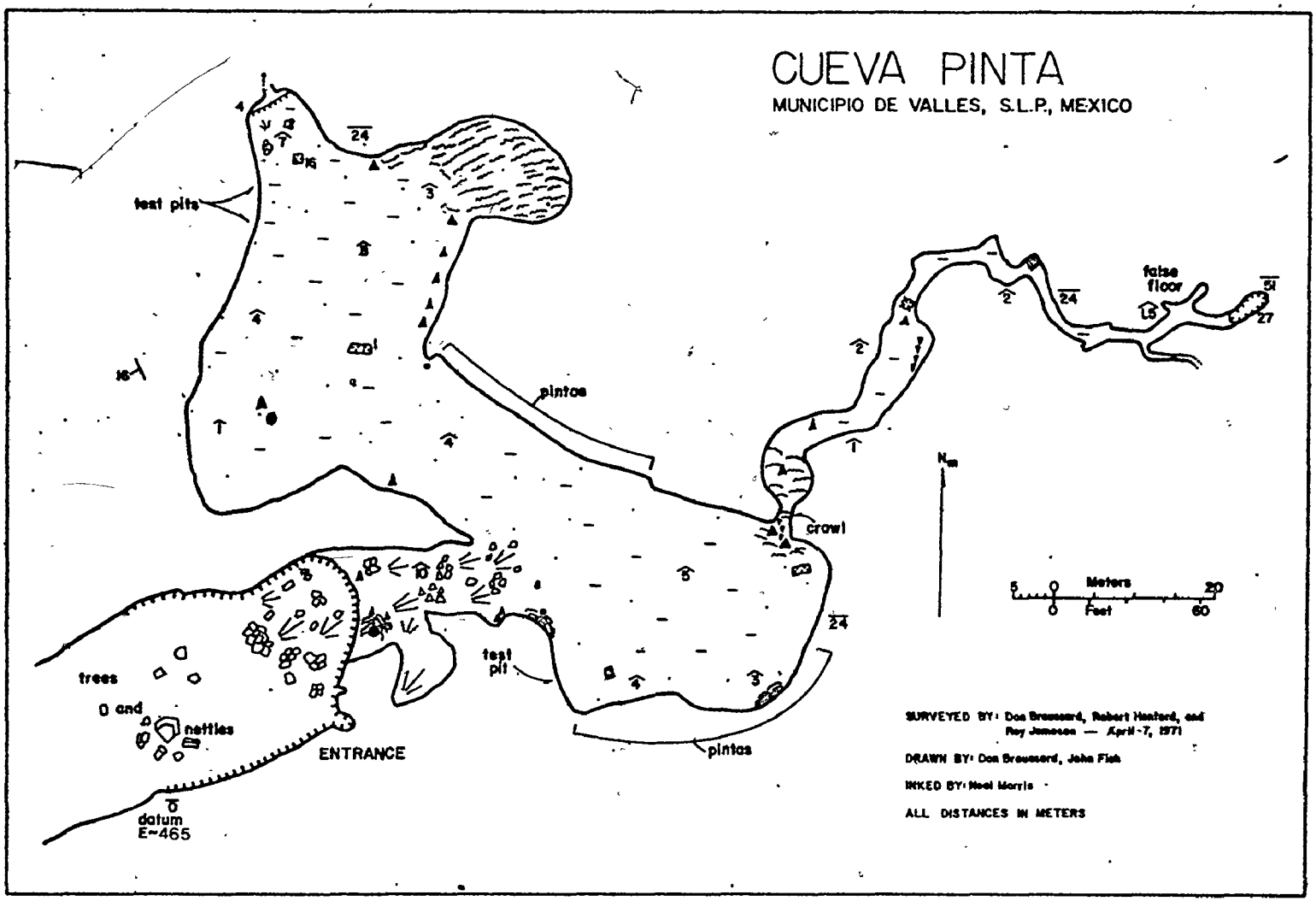

Figure 6.10 Map of Cueva Pinta.

Plate 6.12 (left) The entrance to Cueva Pinta, showing the original solution morphology, and the thin roof which has collapsed.

Plate 6.13 (below) View toward the entrance from near the 15 m deep test pit in sediments. The photo shows smooth phreatic sculpturing, sharp exterior ceiling angle, flat sediment floor and the entrance debris ramp.

area. Guano and possibly wind blown dust may be important components of the fill. At the north end of the chamber, miners have dug a test pit downwards through at least 15 m of sediment; hence, the room is actually much larger than it appears. Plate 6.13 shows solution features in the room that were created by water-filled conditions, and also shows part of the entrance debris cone in the background. The cave contains abundant stalagmite and stalactite deposits, many of which have been partly to almost totally redissolved. From the east end of the room a crawlway over fill leads to 90 m of small passage that ends at a 27 m blind pit. Other than size, the passage has the same features as the room.

6.3.3 Sótano de la Cuesta

Sótano de la Cuesta is located at the western edge of the crest in the high central portion of the range. This cave has not been personally investigated so only a brief description can be given. In the bottom of a small doline, two small holes and a larger one 18 m across drop 174.3 m into an enormous chamber (Figure 6.11; map provided by Neal Morris of Austin, Texas; note all map data are in feet). The chamber measures 327 m long, about 95 m wide in the central area, and for the most part 165-200 m high. In map view, it is approximately trapezoidal. The total depth is 217 m. The floor is covered with flowstone, breakdown, and finer-grained sediments that probably include guano. From photographs (by Peter Strickland, Austin, Texas), it appears that the upper walls and the ceiling exhibit only angular forms caused by breakdown processes, but it was not possible to tell whether the lower walls were formed by solution or break-

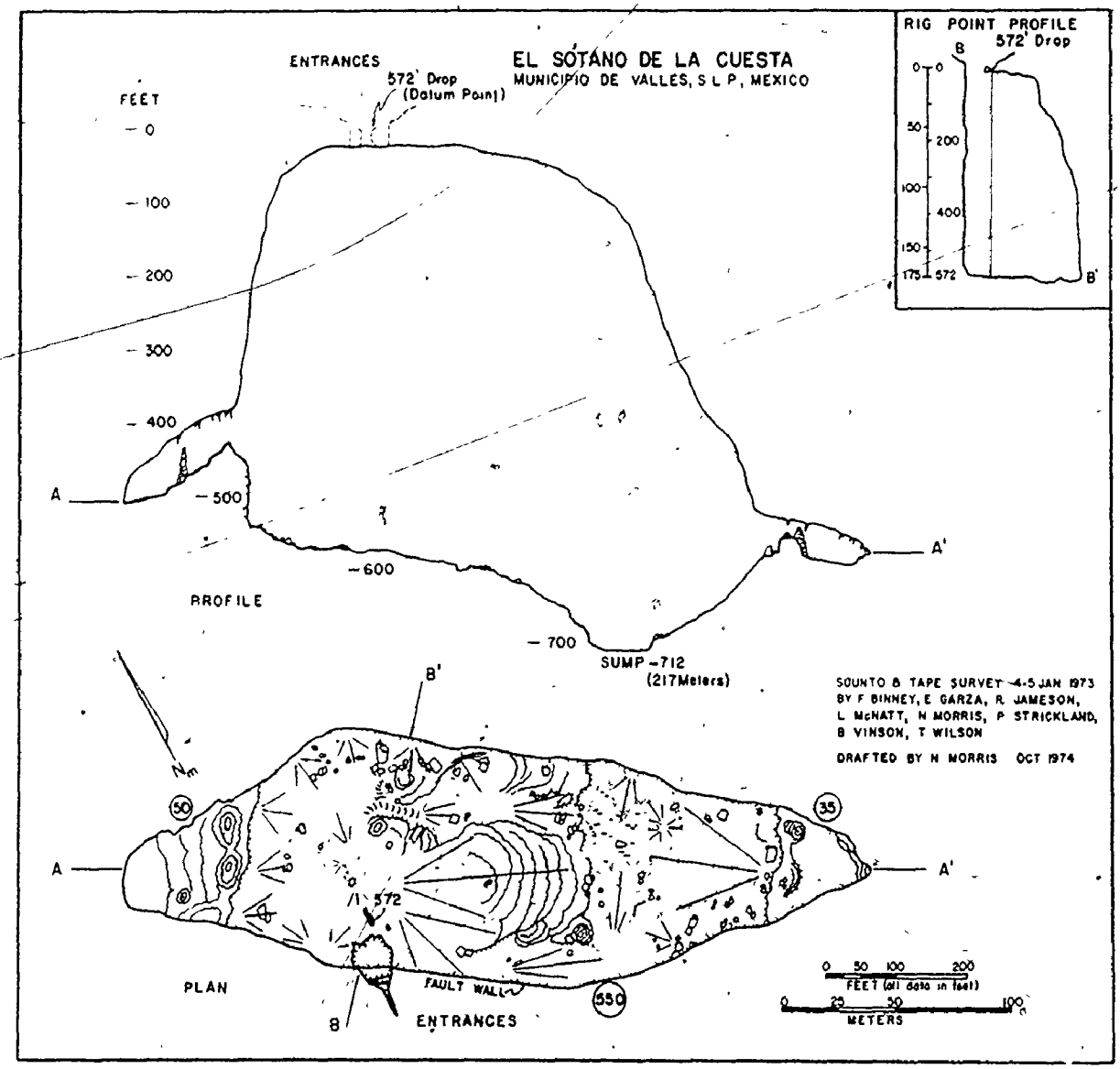

Figure 6.11 Map of Sótano de la Cuesta (provided by Neal Morris; all data are in feet).

down. Note that the southwest wall is fault-controlled. It is suggested that a major active or formerly active cave channel lies somewhat below the present floor level. The fault and probably associated fractures formed a localized weakness in the cave roof, which has undergone gradual upward stoping for a very long time. Presently, the roof is within about 15 m of the land surface. In a short time, geologically, this chamber will become a collapse doline, similar to the Caldera (Figure 3.4) and many others in the El Abra range. Knowledge of this cave now leaves no doubt about the origin of most of the large El Abra sinkholes. The room has a volume estimated to be between 1.5-2.5 x 10^6 m^3, by far the largest yet discovered in the El Abra range. The entire central floor area beneath the main chamber may still be actively subsiding.

6.3.4 Sótano de los Loros

Sótano de los Loros lies about 750 m west of the crest of the east face, near La Cueva de Ceiba. The 15 x 30 m entrance is located on the top of a low hill, and was formed by collapse of the thin roof over a large phreatic dome or chamber. At the bottom of the 50 m entrance pit, a passage, typically 6 m high and 10 m wide, extends 200 m in a north-northwesterly direction (Figure 6.12). Wall and ceiling solution pocketing and rounded passage cross section indicate phreatic development. The cave is profusely decorated with formations, particularly the floor which is mostly covered by flowstone and some fine-grained sediments. The original passage may have been much larger, but the bedrock floor is hidden entirely by sedimentary fill that may be quite thick. Possibly, this cave

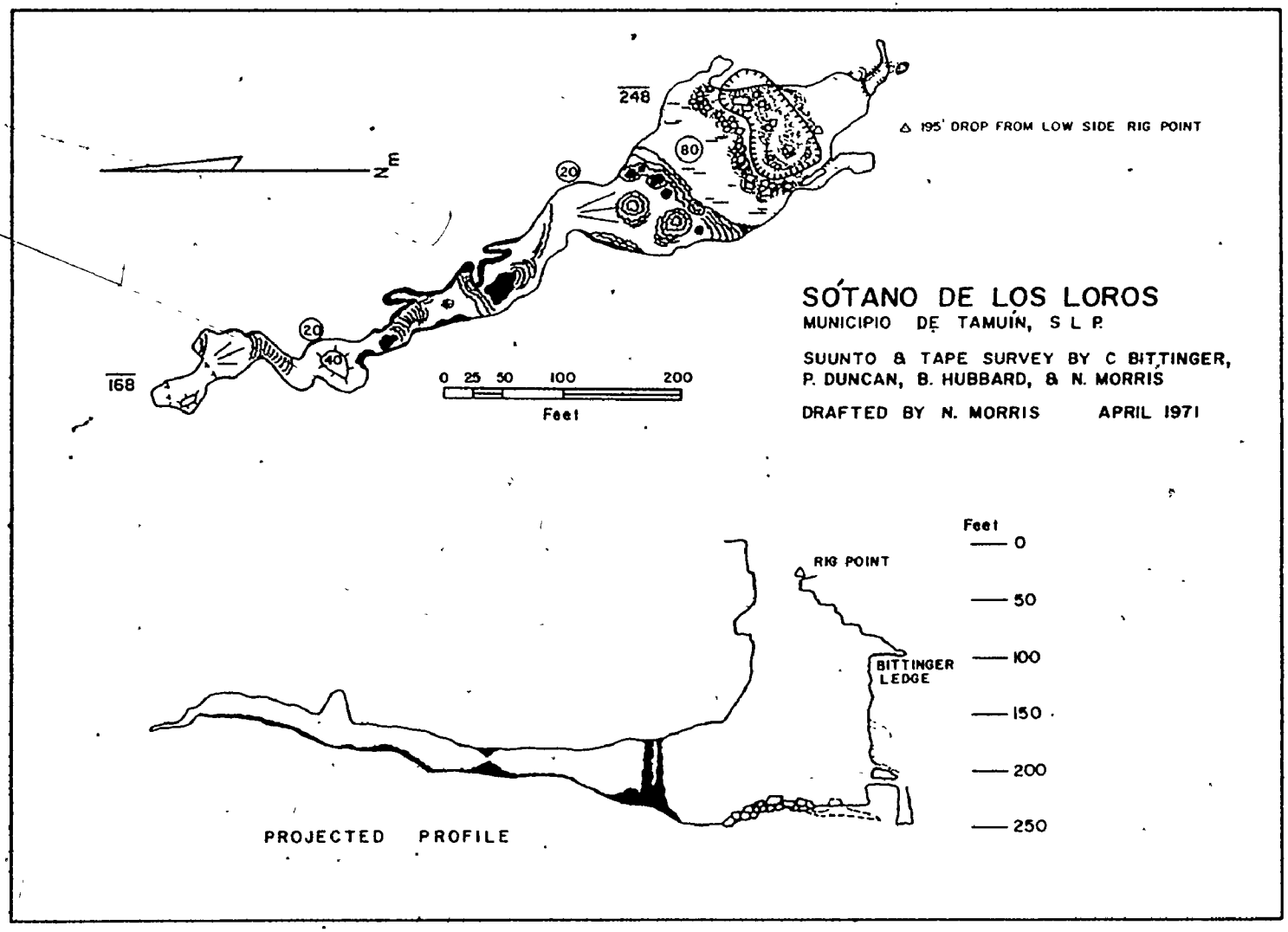

Figure 6.12 Map of Sótano de los Loros (provided by Neal Morris; all data are in feet).

is related to Hoya de Zimapan, which lies about 300 m to the west. The passage is "terminated" at a point where the ceiling lowers and the clastic sediment-flowstone fill appears to thicken.

6.3.5 Cueva de Taninul Number 4

Taninul Number 4 is located on the north side of the south El Abra Pass and 200-300 m from the east face. It is composed of one large horizontal passage about 140 m long plus many smaller passages and fissures, and the cave is well known for its numerous entrances and skylights (Figure 6.13). This cave is believed to be representative of the conduits that carry or have carried slowly moving phreatic waters in the El Abra range. Phreatic solution forms are ubiquitous. The cave is developed at the western margin of the reef facies where some faint horizontal bedding begins to appear. Water sought every available joint, fracture and minor sedimentary parting creating a highly irregular conduit cross-sectional area and blind fissurelike alcoves. Structural control by NNE-SSW and E-W joint sets may be seen on the map. Most of the cave is developed in one massive bed at least 6 m thick. Along the main conduit, solution has proceeded upward to the top of this bed, and many low arches have been carved into a 1 m thick and less soluble overlying bed. Where joints have permitted (which is quite often) the latter bed has been breached and domes have been formed in another massive bed that extends to the surface. The ceilings of several of the larger domes have collapsed, creating many skylights with piles of breakdown below them. Sediments cover all the floor except in the small bypass loop, hence, the character of the

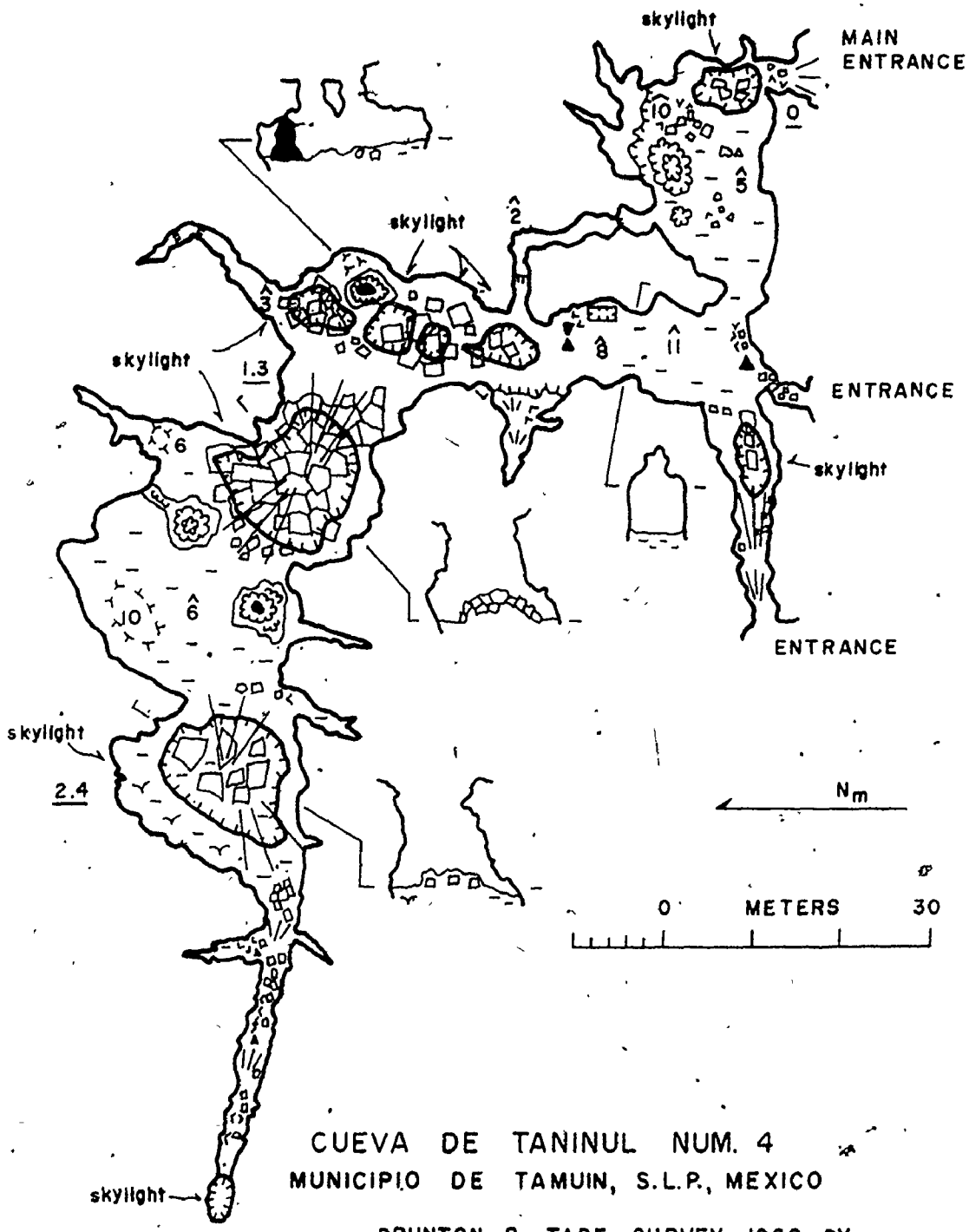

CUEVA DE TANINUL NUM. 4
MUNICIPIO DE TAMUIN, S.L.P., MEXICO

BRUNTON & TAPE SURVEY, 1966, BY
J. DAVIS, B. JOHNSTON, C. LOVING,
M. MEREDITH.

ADAPTED FROM A MAP BY C. LOVING
IN RUSSEL AND RAINES, 1967.

Figure 6.13 Map of Cueva de Taninul No. 4.

original floor is unknown. A careful study of the sediments and pollen here and in many other east face or crest caves could be very informative. Included are the collapse skylight facies, fines with some stones near the entrances, and thick guano deposits with rodent or bat bones in the rear. The cave may be older than and generally unrelated to the adjacent valley. The continuations of the conduit are probably buried.

6.3.6 La Cueva de Tanchipa

Tanchipa is located marginally below the west crest in the central part of the range, a few kilometers south of Sótano de la Cuesta. The ceilings of two rooms of the cave have collapsed to form sinkholes (Figure 6.14; map provided by Neal Morris; note all data are in feet). North from one sink, there is an old phreatic room that slopes downward over a thin veneer of talus to a complex series of fissures. These fissures (Plate 6.14) form a vertical maze and have well developed phreatic pocketing. They are controlled by longitudinal joints related to the N-S fold at the western edge of the crest. It is not known whether water formerly went down or up the passages, but is was clearly part of a deep phreatic flow system of at least 157 m vertical extent. For some reason, the fissures are smaller near the bottom of the cave. Perhaps the system diffuses into many small passages. The cave is well decorated with formations, but has very little clastic sediments.

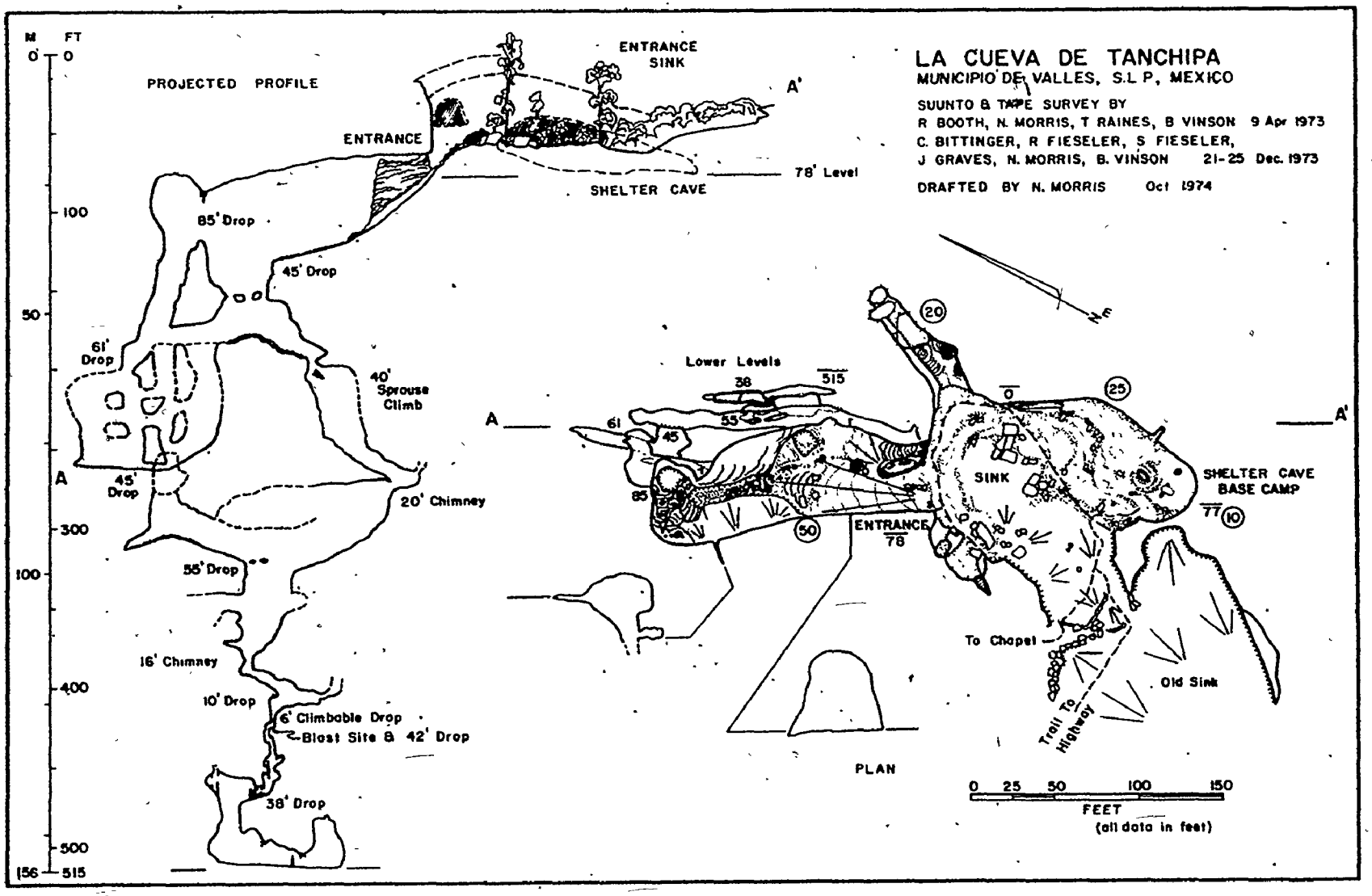

Figure 6.14 Map of Cueva de Tanchipa (provided by Neal Morris; all data are in feet).

Plate 6.14 (left) Phreatic fissure in Tanchipa. It is now well decorated.

Plate 6.15 (below) The entrance to La Hoya de Zimapán. Collapse of the passage produced a doline and the breakdown ramp (person at top for scale). Note the broad phreatic pockets on the wall and ceiling.

6.3.7 La Hoya de Zimapán

Description

La Hoya de Zimapán is located 1 km west of the top of the east face of the El Abra, in the high central portion of the range. Here, as in many other places along the range, the eastern portion of the crest has two strike oriented ridges and an intervening valley estimated to be 75 m deep in this area. The entrance to the cave lies in the northwestern side of a doline, about 50 x 70 m across, near the western base of the westerly ridge. The doline is believed to have formed by ceiling collapse of a large phreatic passage (Plate 6.15).

The view into the entrance passage that greets the explorer is breathtaking (Plate 6.16). A steep breakdown slope leads down to an almost perfectly round tunnel fully 30 m in diameter (Figure 6.15). Two massive formations partially block the passage. The second infills the lower 20-25 m of passage (Plate 6.17); water ponded by it has opened a narrow drain at the base.

Immediately beyond the second stalagmite, the passage turns on end and descends via 3 large shafts to a depth of 300 m. The shafts maintain the smooth, tubular phreatic shape and sculpturing of the entrance passage except where thick flowstone deposits have formed. The lower shafts may be a little smaller in diameter than the entrance tunnel. Between the first and second drops, there is a long slope where the flowstone accumulation is so thick that it nearly blocks the passage at one point. Other thick deposits drape over the top of all three drops and cover the floor

Plate 6.16 The nearly circular entrance passage of Zimapán. It is 30 m in diameter. A large column partially blocks the passage.

Plate 6.17 A 20 m high stalagmite barrier across the end of the entrance passage in Zimapán. Ponded water has dissolved a hole through the base.

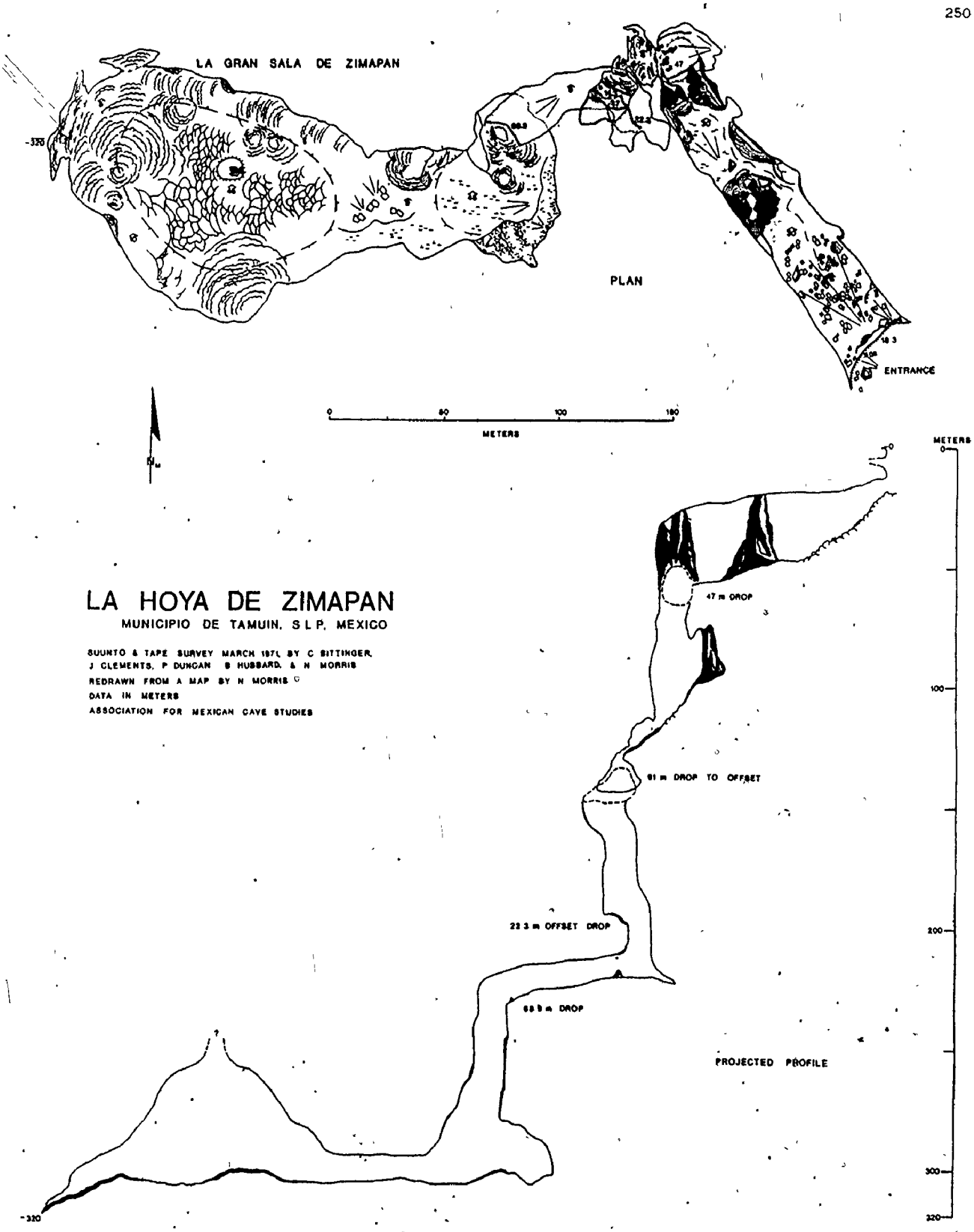

Figure 6.15 Map of La Hoya de Zimapan.

between the second and third drops. The walls of the shafts and connecting passages show no sign of past vadose activity, but the flowstone slopes have been extensively redissolved by vadose flows.

The third pit drops into the end of a huge room, here named the Zimapán Room (Plate 6.18). Initially, there is a mud-floored "passage" or alcove 10 m high and 40 m wide before the main chamber is reached. The total room is 225 m long, up to 95 m wide, and an estimated 40 m high. As may be seen in the photograph, the lower walls have smooth solution surfaces, whereas the higher walls or roof exhibits both solution pocketing and the steplike form caused by the breakdown process. There may be a small dome or inlet shaft in the center of the ceiling, but to date no one has had sufficient light to determine if this is correct. The floor is covered with gour pools created by a drip source near the middle of the room. The pools contain some mud washed in from the entrance. There are also several large stalagmites, some of which have been extensively redissolved (Plates 6.19 and 6.20). These chemical deposits and the mud have aggraded the floor, concealing all information there may have been concerning the original floor and the amount of breakdown. Also, the continuation of the cave has unfortunately been buried.

The volume of the Zimapán Room is estimated to be between 175,000 and 250,000 m^3. Thus, it may be comparable in size to the famous Big Room in Carlsbad Caverns. The total depth of the cave is 320 m and the horizontal length is about 480 m. A detailed discussion of the history of the cave is given in Section 7.4.2.

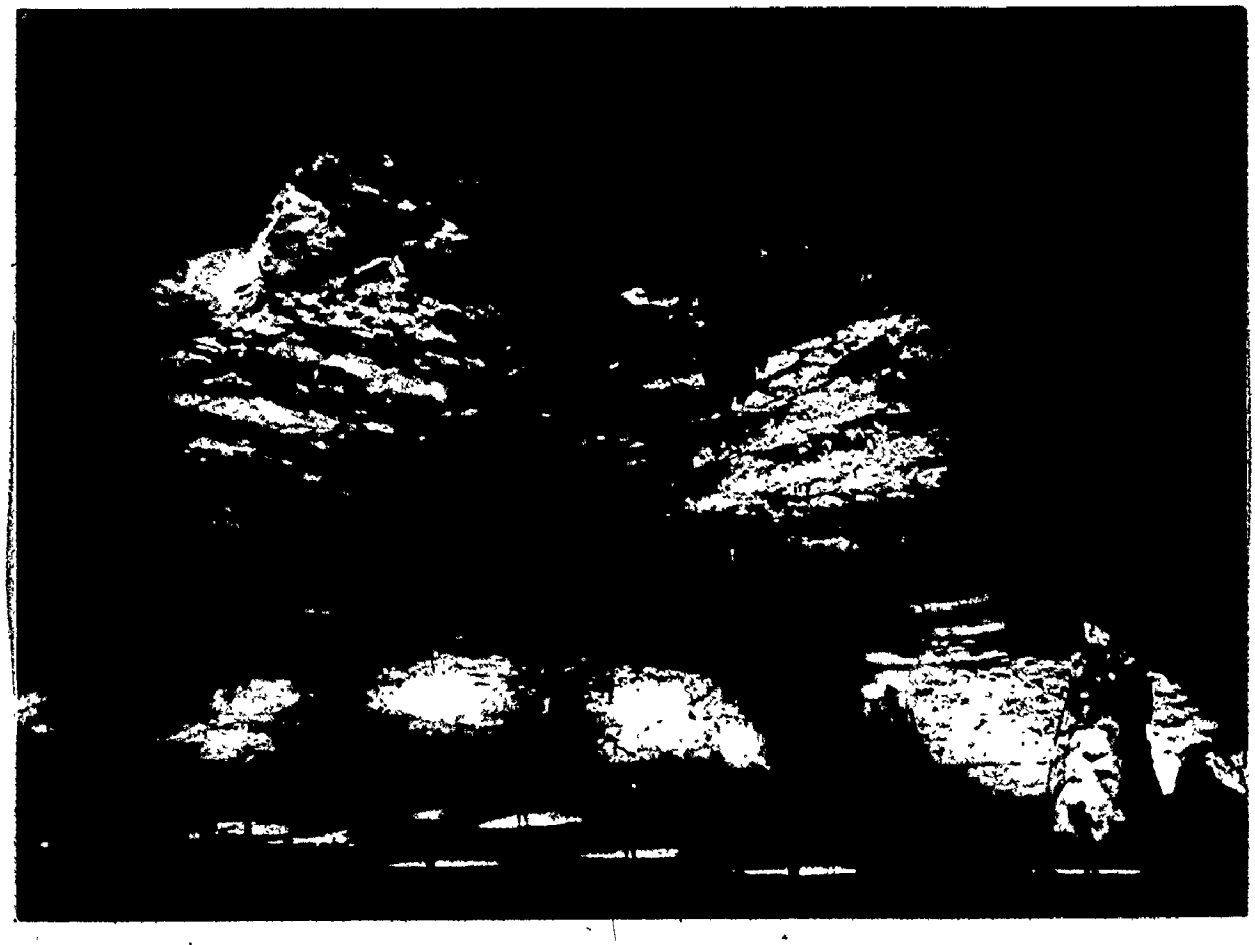

Plate 6.18 The Zimapán Room, looking west across 140 m of the room from the northeast corner. The lower walls show solution pocketing, but the high ceiling exhibits both solution pocketing and steplike forms caused by collapse.

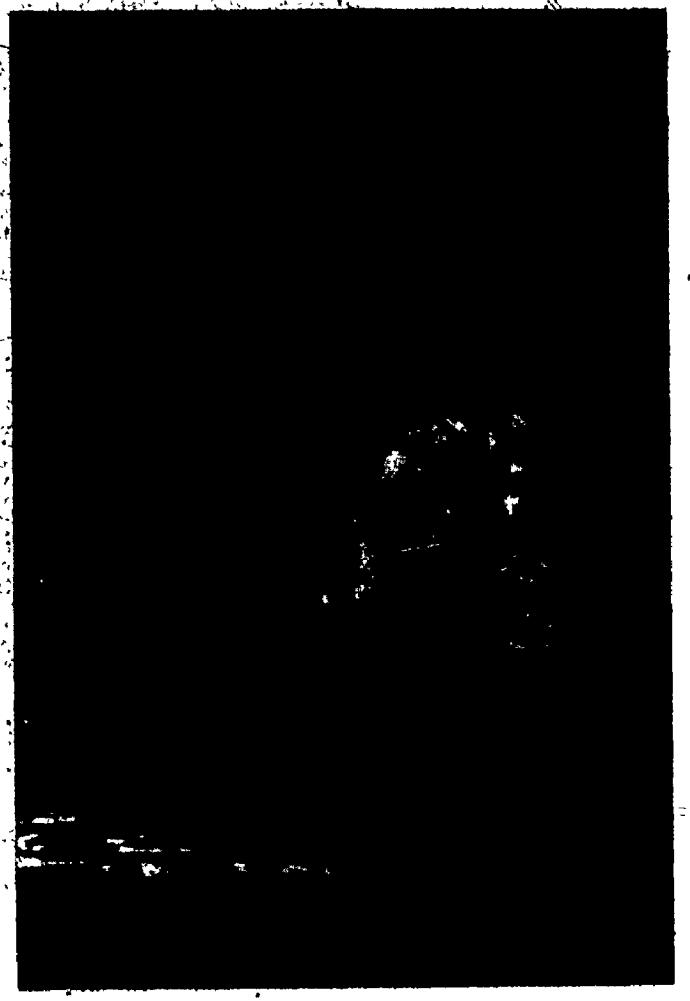

Plate 6.19 Large stalagmites that have undergone substantial "phreatic" re-solution. There is a prominent solution notch around the base. Most of the floor of the Zimapán Room is covered with gour pools (dry at this time) as shown here.

Plate 6.20 Another stalagmite that has been partially redissolved in the Zimapán Room, and solution features on the wall.

6.3.8 Sótano and Cueva de los Monos

La Cueva and Sótano de los Monos are located east of Sótano de la Tinaja (Los Sabinos area) near the middle of the crest. They lie in the northeastern corner of a closed basin of about one-fourth square kilometer area. The datum for the survey (Figure 6,16) has an elevation of about 465 m.

La Cueva de los Monos is an old phreatic cave at the top of a big pit. It is explorable for about 60 m and consists of two rooms. The lower one, Crystal Chamber, has several pockets of large calcite crystals (6 cm across) for which the room is named. It appears that the cave was formed under water filled conditions, then calcite deposited on the walls and in pockets (possibly under water because of the size and clarity of the crystals), only to be later partially redissolved forming "phreatic" pockets in the crystals. Some time later, large masses of flowstone and stalagmite were deposited. Some of these have petroglyphs of monkeys, coatis, deer, and people. The name "mono" means "monkey", but it also means "mimic" -- the glyphs "mimic" animals and people. Holes in the floor below the glyphs connect to the bottom of the main pit. Upper Chamber is reached by climbing up a steep slope at the back of Crystal Chamber. It is well decorated by large old stalactites that have superb examples of re-solution (Plate 6.21), and by a younger generation of small stalactites. The room is 2-3 m high and may continue beyond the sediment block at the far end. There are several domes (inlets?) that may have supplied the material for at least 1.5 m of clastic fill which has thin interbedded flowstone layers and perhaps some guano.

EL SÓTANO Y LA CUEVA DE LOS MONOS

MUNICIPIO DE TAMUÍN,

S. L. P., MEXICO

1974

NOTES:

1. Surveyed by: S. Brittinger, D. Broussard, E. Dumas, J. Fish, D. Hess, D. McKenzie, and C. Pickstone

   Drawn by S. Brittinger, J. Fish, and D. Broussard

   Inked by H. Harris

2. Suunto and tape survey July, December 1971

3. Datum elevation ~465 M.
   Passage length 840
   Horizontal length 571
   Vertical range 290.6

   Data processed by CDC 6400 computer

4. Special symbols:

   All distances are in meters (M)
   C ceiling height
   E ..... elevation above ℄
   DC climbable 5M drop
   DR 10M rope required
   - - - drip line

© 1977, John Fish

EXTENDED

PROFILE

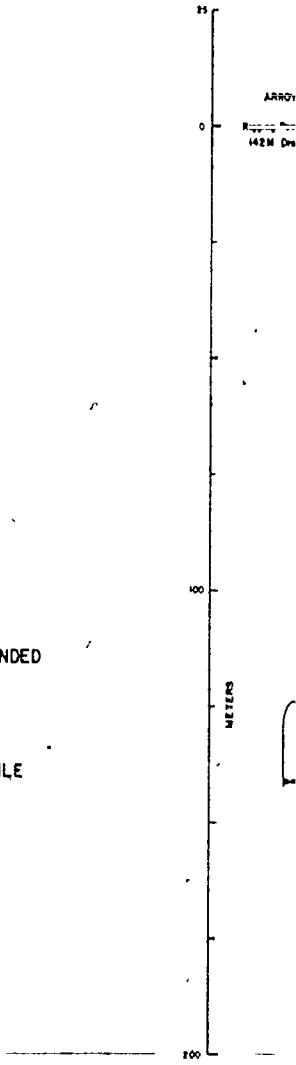

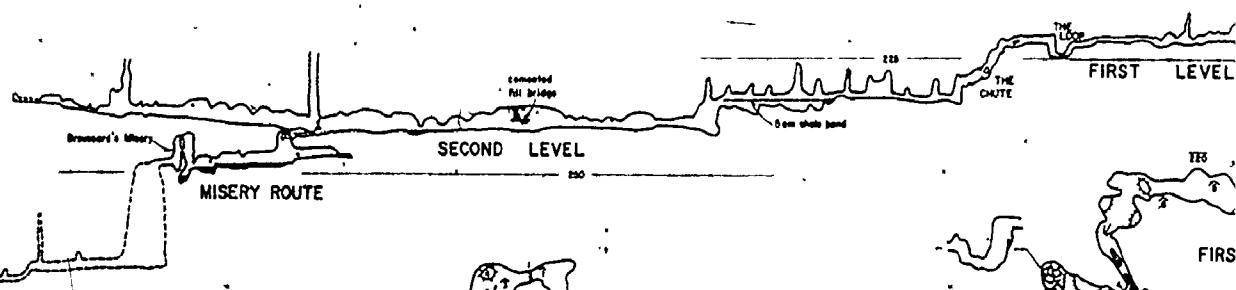

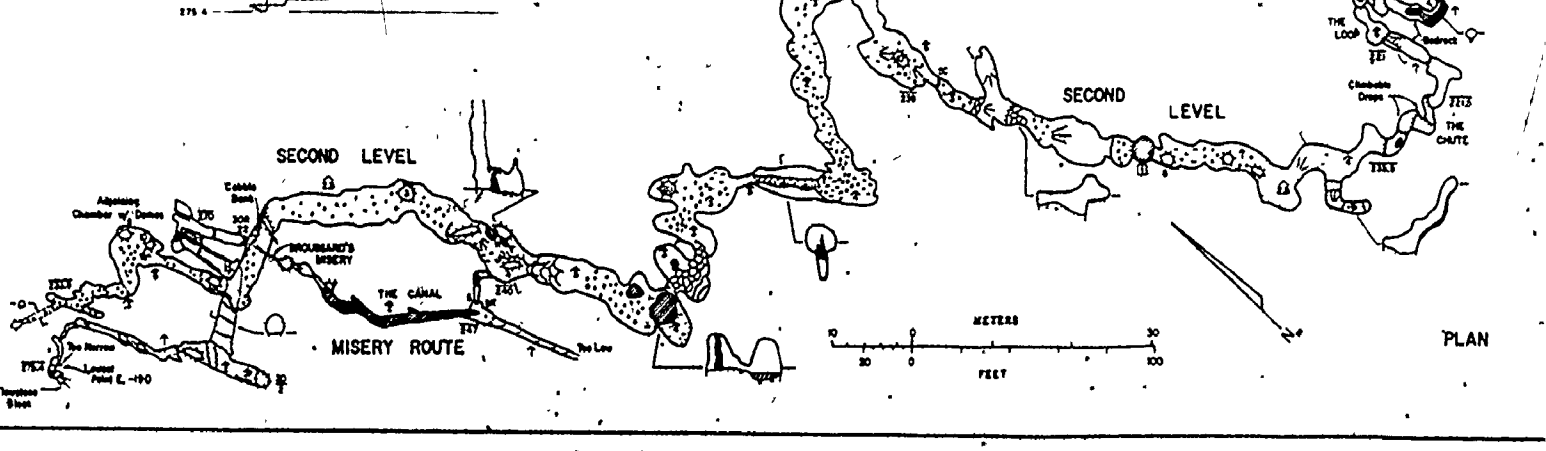

EVA DE LOS MONOS

DE TAMUÍN,

MEXICO

'4

2 of 2

EXTENDED

PROFILE

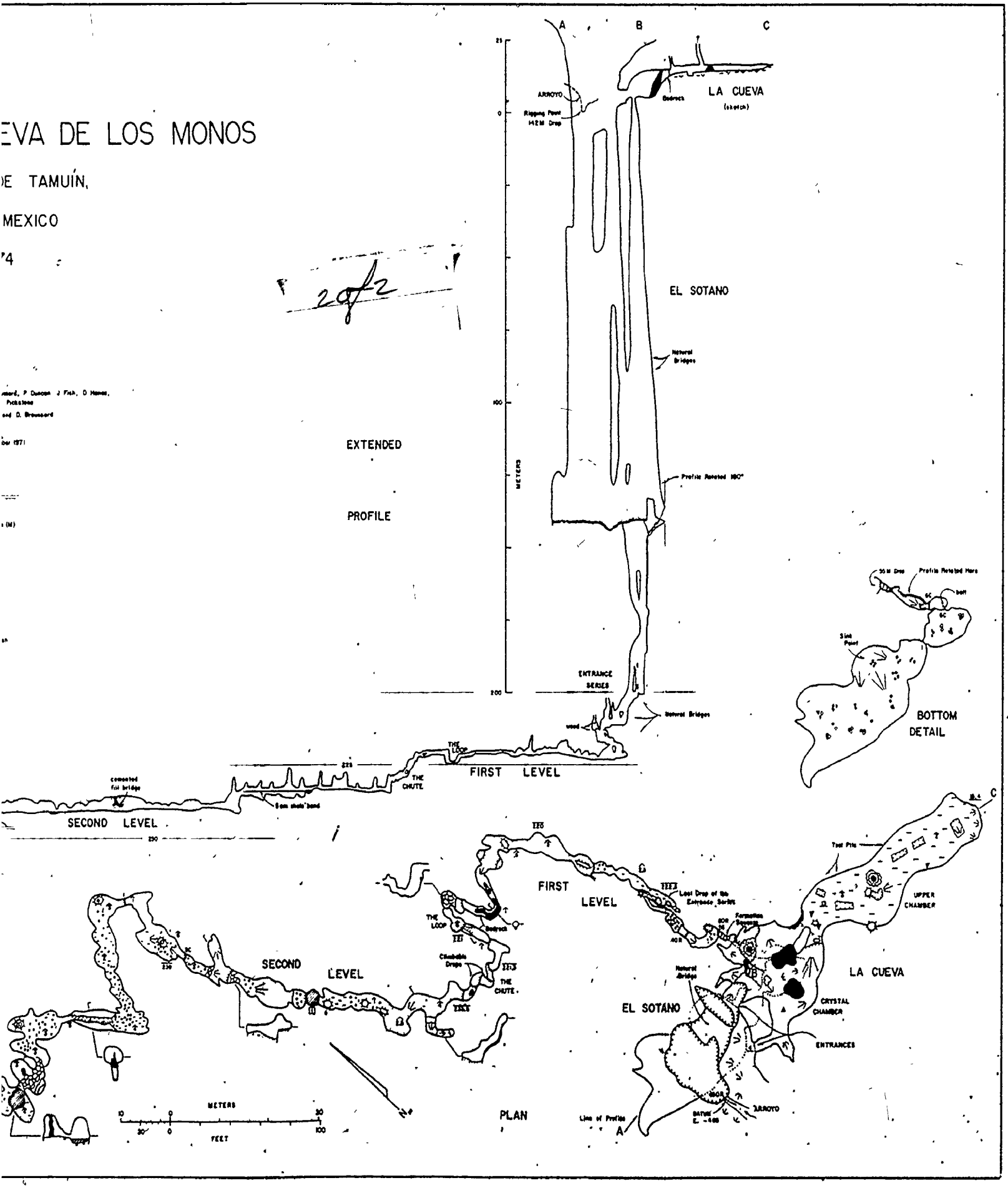

Plate 6.21 A very broad and deep pocket dissolved without discontinuity into bedrock and flowstone by a "phreatic" re-solution phase.

El Sótano de los Monos is thought to be a much younger cave than La Cueva de los Monos. Water collected on a surface catchment of soil and was pirated down a group of N-S joints, possibly before a closed basin had developed. The surface of the basin has gradually lowered and the arroyo is now entrenched an estimated 30 m below the back wall of the pit (see the profile). The spectacular entrance pit, 15 m across at the level of entry and 141.5 m deep (464 feet; about 171 m or 560 feet from the high side) is by far the largest feature of the cave. The bottom is larger than the top and natural bridges partition the pit. It is believed that the entrance pit is a group of coalescing vertical shafts formed under vadose conditions. The intersection with La Cueva may have been fortuitous, or perhaps the same joints also supplied water to La Cueva when it was active. Small breakdown covers the floor of the pit. In an alcove at the east end of the bottom; a climb over a 6 m high bedrock partition leads via a crawlway to a succession of smaller vadose shafts (the Entrance Series) which have many natural bridges. Some wood jammed in domes indicates past floods. This route may not be used presently because most of the water probably sinks in a depression of boulders on the floor of the entrance pit. Where the water goes is unknown.

At the bottom of the Entrance Series, -222 m, the "horizontal" part of the cave begins. This portion of the cave is very interesting because the passage forms and profile are not what one expects in a vadose cave. Rather than a relatively uniform tunnel or pot-holed canyon passage with a continuously descending profile, First Level and Second Level often are more like a series of water-filled solution formed rooms connected

by short crawlways. In many places, solution upward has created blind chimneys. Another anomaly of the profile is The Loop where water first must rise up a 3 m high bedrock wall to a small tube with a canal (Figure 6.16), next flow down into The Loop and back up about 4 m, and then continue as a free-surface stream down The Chute. The strata are nearly flat lying. A combination of structural and stratigraphic features such as the 5 cm shale band marked on the profile apparently controlled passage initiation in these levels. Second Level is much larger on the average than First Level, and is slightly concave up in profile. It probably continues beyond the present "end", where sediments rise to fill the passage. It is suggested that these levels derived their features from water ponded in the irregular or concave up profile. Floods which were larger than the passage could handle may also have had some effect.

In the past, there was a major fill of cobbles and sand (see cross section of cemented fill bridge). Much of the fill has now been removed. There also is a poorly developed lower passage, Misery Route, which begins as a hole low on the wall at the lowest point in Second Level. At Broussard's Misery, the passage dissipates to a few holes along a vertical joint so that it is necessary to raise the explorer and push him through with his arms outstretched. The passage ends in narrow cracks and a small flowstone bank. This passage probably was created by a piracy of Second Level water. Subsequently, the piracy caused the entrenchment of the Second Level fill up to the entrance to Misery Route, and slightly beyond. There continue to be small flows that enter via the known cave and from several inlet domes. Under present conditions, the First and Second Levels must not flood violently because delicate soda straws that

are greater than 1 m long and found near the entrance to Misery Route would not survive. If major floods enter the cave, they must be taken to new lower levels. The Second Level is abundantly decorated with gour pools, flowstone, stalagmites, stalactites, and soda straws-- especially where there are active inlet domes.

At the present time, El Sótano de los Monos is the only known vadose cave on top of the El Abra range that has extensive passages. As a simplified model, it is similar to the shaft-drains of the Mammoth Cave area (Pohl, 1955; R. Brucker et al., 1972) where the vertical shaft is many times larger than its horizontal drainage conduit because of differences in the rate of solution. The total surveyed passage length of the Monos cave system is 571 m, and its vertical range is 291 m. It is still a long way from El Choy where its waters probably reappear.

6.3.9 Other Caves on the Crest

From the results of this study and other recent explorations, it is certain that the crest of the range contains a very large number of caves. Analysis of the caves has provided information concerning the nature of ground-water circulation in the El Abra range, and important findings for theories of cavern genesis and karst hydrology (discussed in Section 7.4). There are several caves known that are similar to ones described here, hence their inclusion would have only been repetitious. Other than Monos, one type not mentioned is the vadose shaft or lapiez well. Perhaps, the majority of caves known on the range are merely blind shafts

ranging from 10-200 m deep. They are "blind" in the sense that no continuation that is humanly explorable was found, but water surely flowed onward through cracks or through passages that may be blocked. These shafts have not been studied closely. Some of them may be old phreatic fissures or pits, but most probably are vadose shafts. In reality, joints and bedding planes opened by vadose zone solution which are too small to permit human entry are much more common than the pits that can be explored.

6.4 Caves on the Western Flank and the Western Margin of the Sierra de El Abra

As described in Chapter III (surface geomorphology), the western flank of the range dips relatively gently compared with the eastern escarpment. The removal of the overlying rocks has exposed the El Abra limestone to solutional processes over a belt as much as 6 km wide. However, the caves, the structure, and the geomorphology of this zone are poorly known. A few caves are included here.

At some places along the western margin of the El Abra limestone outcrop, the structural geology and the geomorphology are such that arroyos having catchments on Méndez or San Felipe beds are pirated underground a short distance after they pass onto the limestone (Section 3.1.3). The largest number occur in the Los Sabinos area, and several of these caves were mapped and studied. An isolated cluster of three swallet caves is located about 8 km north-northwest of the village of Los Sabinos -- one cave from that area is also described. The location and relationship of the caves to surface geology, drainage and geomorphology can be seen in

Figure 3.2.

6.4.1 Sótano de Soyate

Sótano de Soyate lies about half way up the western flank of the El Abra range, 2 km east of the Los Sabinos area swallet caves. Figure 6.17 is a map and a profile modified from ones by Elliott (1970) by a new cave depth survey including use of a wire and the inclination for the entrance, by water depth measurements, and by minor alterations of detail. The entrance is a very deep shaft along a major joint or joints inclined at 83°. It descends 103 m typically 6 m x 12 m in cross section to a ledge or restriction of the pit, then another 92 m as a long fissure to the floor 195 m (639 feet) below the surface. There are a number of places where the fissure and other recesses extend beyond the reach of the light from a carbide lamp. Vadose films have left a 1 m thick deposit of flowstone for the lower 150 m of the pit on the "footwall" or wall descended by explorers. The floor is covered by small angular breakdown that has come mostly from the top 20 m of the pit, and by some mud. At the south end of the floor of the entrance pit, a series of travertine dams and slopes drop 20 m into the end of a large chamber. At this level, the walls and the floor are covered by a thick deposit of mud, and there are some cobbles washed down from above. A small hole in the floor drops another 11-12 m (under normal water conditions) to a deep lake that fills the lower part of the chamber. The lake is 147 m long and 20-25 m wide for the most part. It was plumbed in a number of places approximately along a lengthwise center line, at a time when the lake was 11 m below the top of the

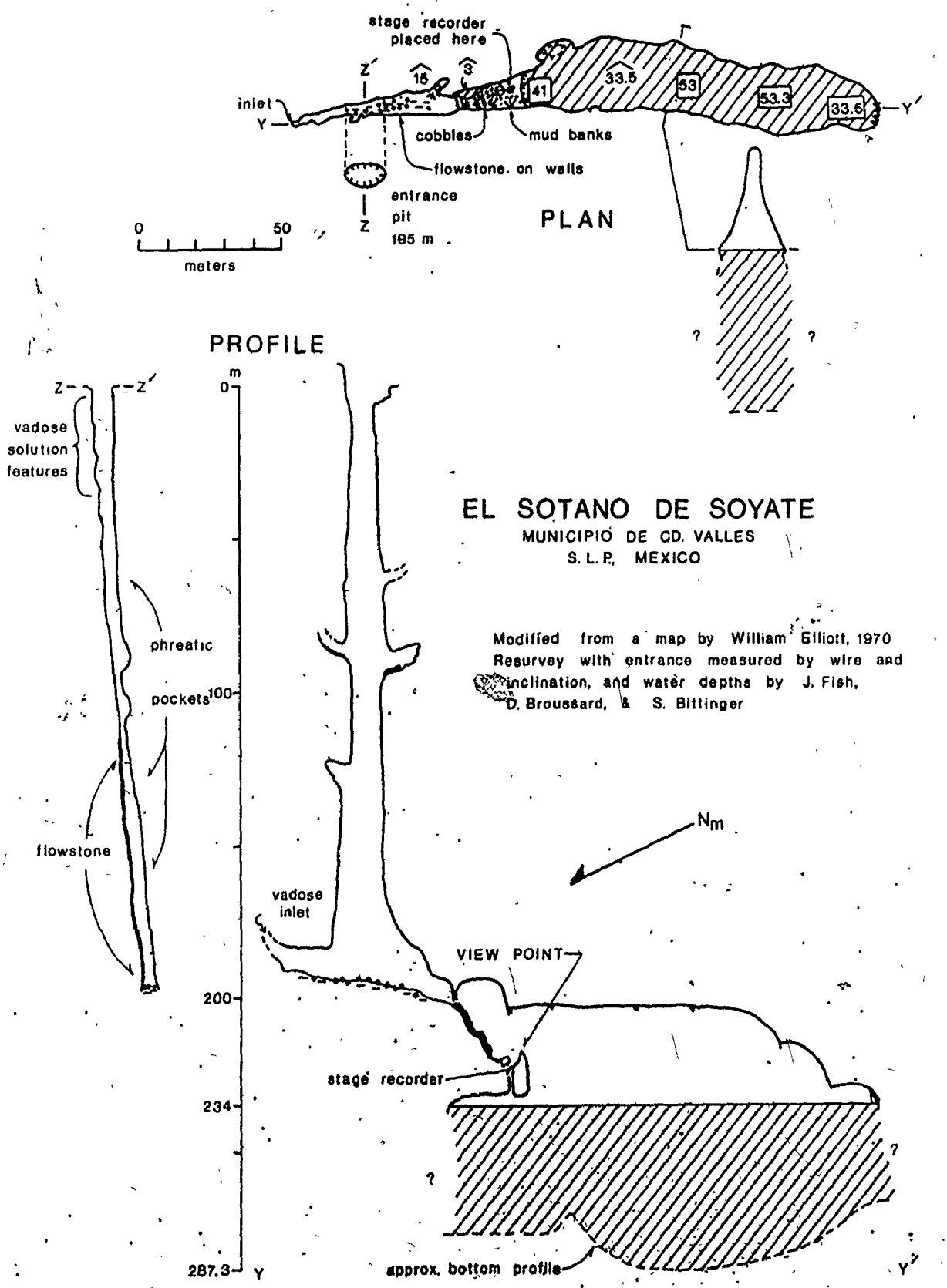
stage recorder placed here
Z'
15
3
41
33.5
53
53.3
33.5
Y'
inlet
Y
cobbles
mud banks
flowstone. on walls
entrance pit 195 m
Z
0
50
meters
PLAN
PROFILE
m
0
Z
Z'
vadose solution features
phreatic
pockets
100
flowstone
vadose inlet
VIEW POINT
200
stage recorder
234
287.3
Y
approx. bottom profile
Y'
EL SOTANO DE SOYATE
MUNICIPIO DE CD. VALLES
S. L. P. MEXICO
Modified from a map by William Elliott, 1970
Resurvey with entrance measured by wire and inclination, and water depths by J. Fish, D. Broussard, & S. Bittinger
Nm

Fi of de

hole. The deepest point measured was 53.4 m (175 feet) and no depth less than 33.5 m was found. Thus, the bottom of the lake is nearly at sea level and well below the El Abra base level. From the View Point, the chamber appears immense -- possibly higher than the 34 m (110 feet) given by Elliott (1970). The total depth to the lake surface was surveyed to be 233.9 m (767.3 feet).

Soyate is an important cave because of its morphology, and because of its present hydrologic activity. The entrance is situated at the base of a hill on the east side of a major valley, now a closed karst basin, which formerly drained southward in a manner similar to the Río Sabinos (see Section 3.1.3) before the latter was pirated by the swallet caves (Figure 3.2). Near the surface in the entrance pit, vadose waters have cut many small drip pockets and sharp pinnacles and edges common to vertical shafts, and have formed a vadose chute that reaches about one-half way down the "footwall" of the shaft. Rock fall has removed the original solution features of the upper approximately 80 m of the overhanging wall, but for the rest of its depth, the wall exhibits smooth, usually equidimensional solution pockets up to a meter or more in diameter and 0.1-0.3 m deep. Where they were studied, the pockets show some bedding control. They also are often asymmetric, like scallops, having a greater deviation from the vertical on the higher side; and on the lowest few meters of the shaft, they are strongly elongated, resembling flutes. After considerable debate, it is believed that these pockets were made by phreatic solution rather than by vadose films. Furthermore, the overhanging wall lacks vadose features such as pothole remnants, pebbles or clay in niches, and in contrast with

the "footwall", virtually no flowstone. The walls above the lake are smoothly sculptured; there are partitions with solution holes; and the ceilings above the south end of the lake and above the travertine slopes contain phreatic domes.

Studies of the cave during the thesis research have shown that it is very active hydrologically even though it has no direct surface catchment (see Section 4.4.2). A stage recorder was placed over the hole that drops to the lake to record water-level fluctuations. It was found that dramatic water-level oscillations occur several times a year, and that the hydrograph correlated very well with the Choy hydrograph. Mitchell et al. (1977) give 293 m for the elevation of the entrance. Hence, the dry season lake surface must have an elevation of about 59 m. The elevation of the lake surface, the depth of the lake, and the character of its hydrograph are strong evidence that it is a water table lake, i.e., part of the potentiometric surface of the aquifer.

At the north end of the bottom of the entrance shaft, there is a small intermittent source of water, that can occasionally be heard gurgling down to a lower level between rainy spells. Flood water from this source has cut a very small channel in the floor, but it is believed that it would have neither the correct hydrograph shape nor a sufficient discharge of water to cause the observed lake level variations. Instead, flood pulses passing through cave passages below the lake surface cause its level to rise. The lake surface undoubtedly reflects the local hydraulic head of the aquifer. However, the mud deposits and the large

of

by bats in this cave) suggest that one or more of the Los Sabinos area swallet caves is (are) also connected with Soyate. Thus, the lake hydrograph may be the complex result of both local and distant events.

There is a lack of evidence to demonstrate that Soyate has undergone significant vadose enlargement. There is: neither an active nor a dry valley leading to the cave; no degradation of the entrance pit by stream entrenchment as found in the Los Sabinos swallet caves; no major assemblage of vadose solution forms within the cave such as stream potholes or features of vertical shafts as in Kentucky (Pohl, 1955). Rather, the cave seems to have reached nearly its full size under water-filled conditions. Thus, Soyate is believed to have been part of a deep phreatic flow system. The asymmetric pockets on the overhanging wall suggest that water leaked in from the surface or from side passages (?) along the joint, and then flowed downward to depths more than 200 m below an ancient water table. This source diminished as karstification of the surface increased. The hypothesized connection with the swallet caves would have occurred later in the caves' history. However, Soyate must always have been connected directly with the water table, and may owe a part of its enlargement to solution upward from below or, more likely, a mixing of water from above and below.

6.4.2 Cueva del Prieto

Cueva del Prieto is located in the extreme southern part of the El Abra range, about 1 km northeast of El Pujal and perhaps 1 km north of Río [illegible] is [illegible]

blind fish literature as "Los Cuates" by Mitchell et al. (1977), but it was called as given here by the ranch owner. The entrance lies in a collapse sinkhole (Figure 6.18) on top of a broad hill or knoll, and does not capture a surface stream. El Abra limestone is exposed over the surrounding area. The cave is very strongly structurally controlled by N-S joints, and the traces of these joints can be easily followed on the surface by the presence of solution and collapse features. There are actually two pits in the sink. The easternmost is merely a fissure-like pit that descends to water. The other "pit" is actually an entry to the top of a fissure cave (see plan and profile, Figure 6.18). At the bottom, 22.2 m below, the floor slopes downward underneath the entrance sink to a deep pool, where the passage is blocked by breakdown. In the opposite direction the cave extends at least 100 m. Initially, there is a climb over breakdown boulders, followed by a short drop to a mud floor. The passage continues relatively horizontally and contains abundant formations. Near the "end" the ceiling lowers, and several pools are encountered. This passage was not explored beyond a 3 m drop into a deep pool, but it may continue under a massive formation. As shown by solution domes, natural bridges and other features, the cave is of phreatic or epiphreatic origin, and was initiated when water levels were higher in the past. Elevation data given by Mitchell et al. (1977) show that the lowest pools are very near the elevation of the Río Tampaón, and thus may be at the top of the phreatic zone. Their surfaces may fluctuate during the wet season. Resolution features in stalagmites were observed up to nearly the level of the entrance.

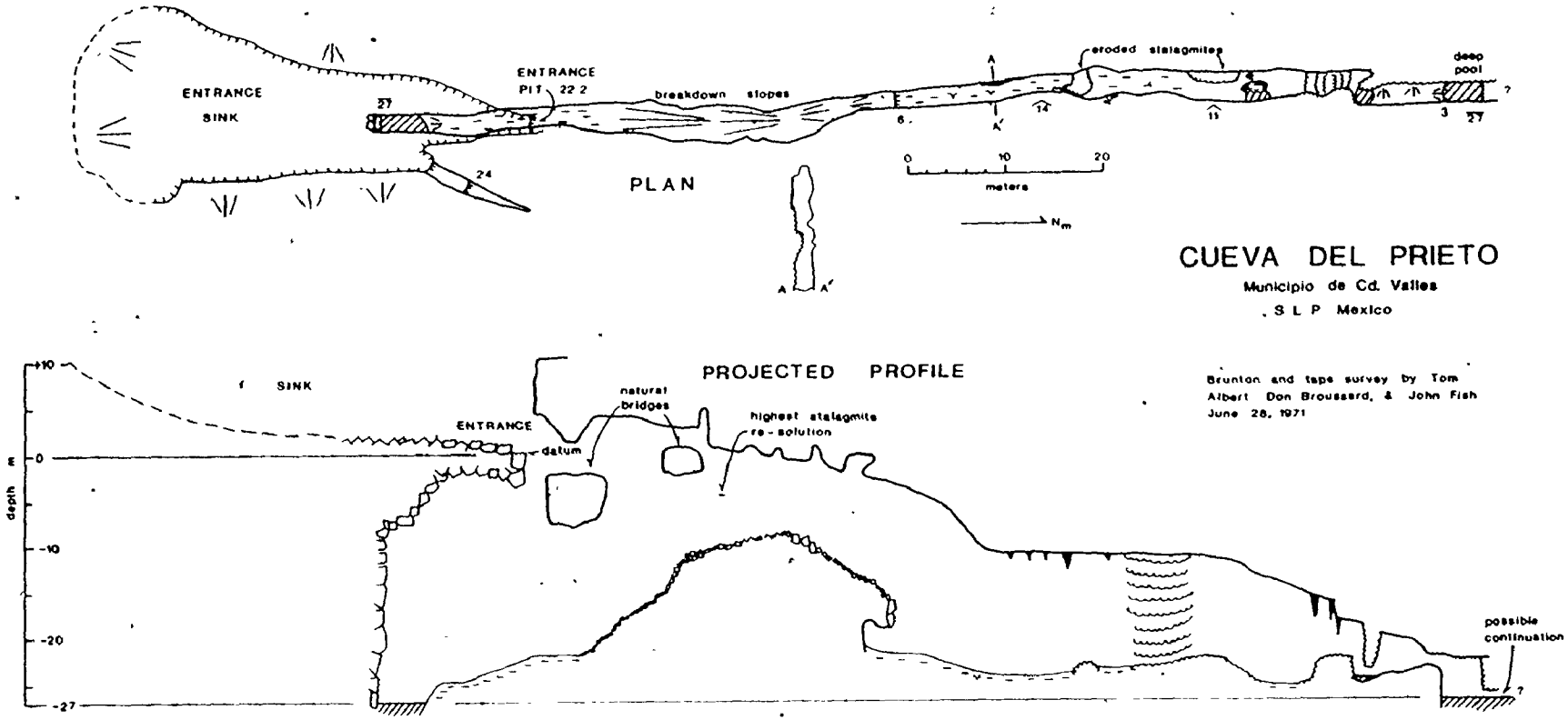

Figure 618 Map of Cueva del Prieto.

6.4.3 Sótano de Japonés

Sótano de Japonés is the southernmost of a group of three large swallet caves that lie 8 km north-northeast of the village of Los Sabinos and 18 km north of Cd. Valles. Japonés captures a west-flowing arroyo that has breached a structural high of the El Abra limestone. The drainage area is about 8.6 km^2, including a small tributary northeast of the entrance. The initial capture was down a large N-S joint in the Main Sink (Figure 6.19; "S-I" is for shaft number 1, "Level I" for the highest passage level, etc.). Since the piracy, the upper part of the west and north walls have retreated by collapse and slope processes so that the sink is now rather large. However, the El Abra has been exposed for only a few hundred meters in the streambed, and the arroyo has entrenched no more than about 10 m below the top of the formation at the cave entrance. These facts and the passage dimensions indicate that this cave is much younger than the larger of the Los Sabinos area swallet caves. Presently, another entrance (S-II) developed on a N-S joint completely crossing the arroyo about 25 m upstream from the Main Sink captures the majority of flood waters except for perhaps the largest pulses. Primitive captures occur still further upstream.

As can be seen from the map, Japonés is very complex, and there may be quite a lot more passage yet unexplored and unsurveyed. Offsets of overlapping passages and a projected line profile are shown as aides. Nearly all the cave is developed on four "levels" (see profile in Figure 6.19). Level I is the highest and least extensive, but includes the present main flood channel (about 3 m in diameter), a smaller up-dip tributary

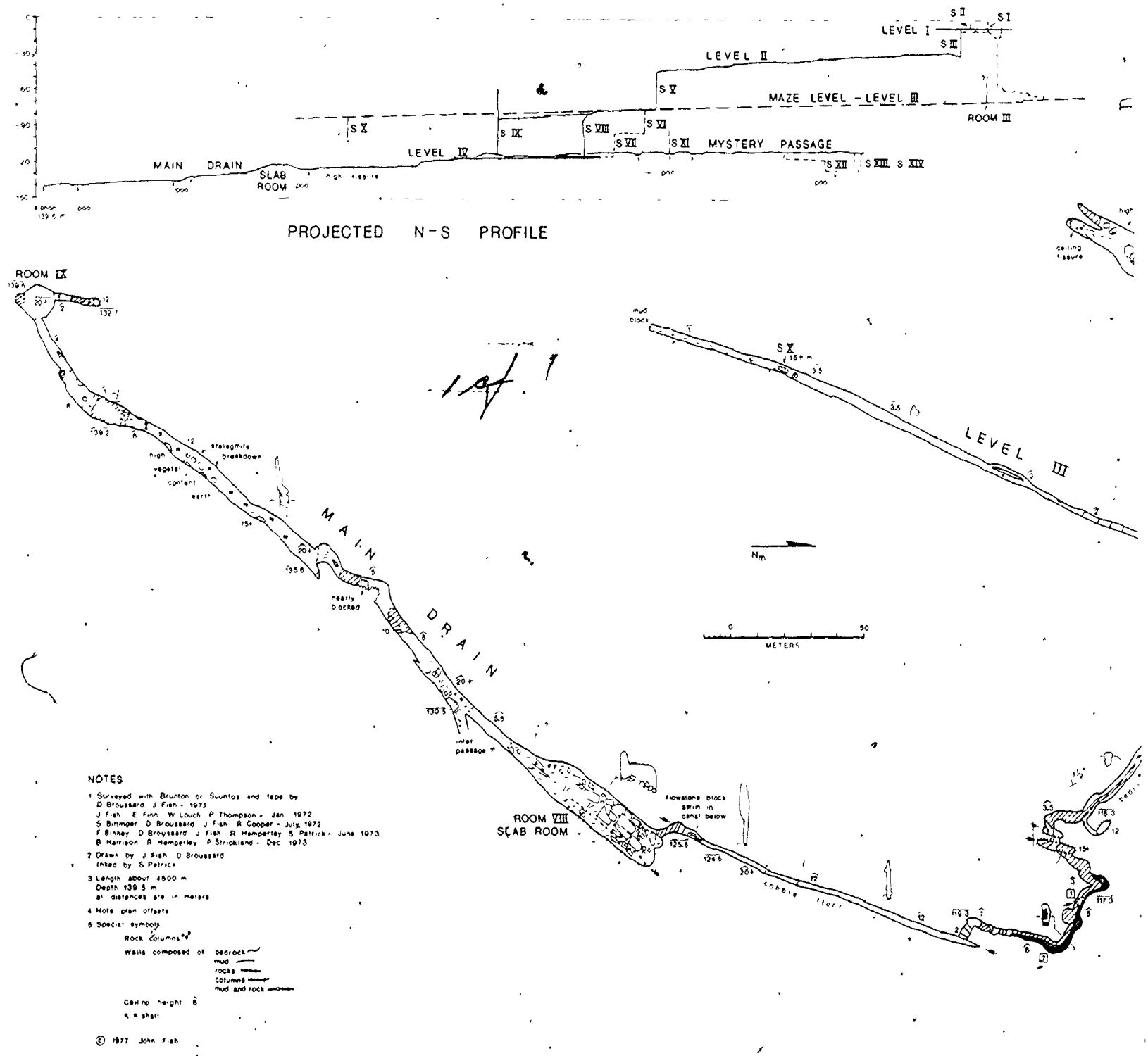

Figure 6.19 Map of Sótano

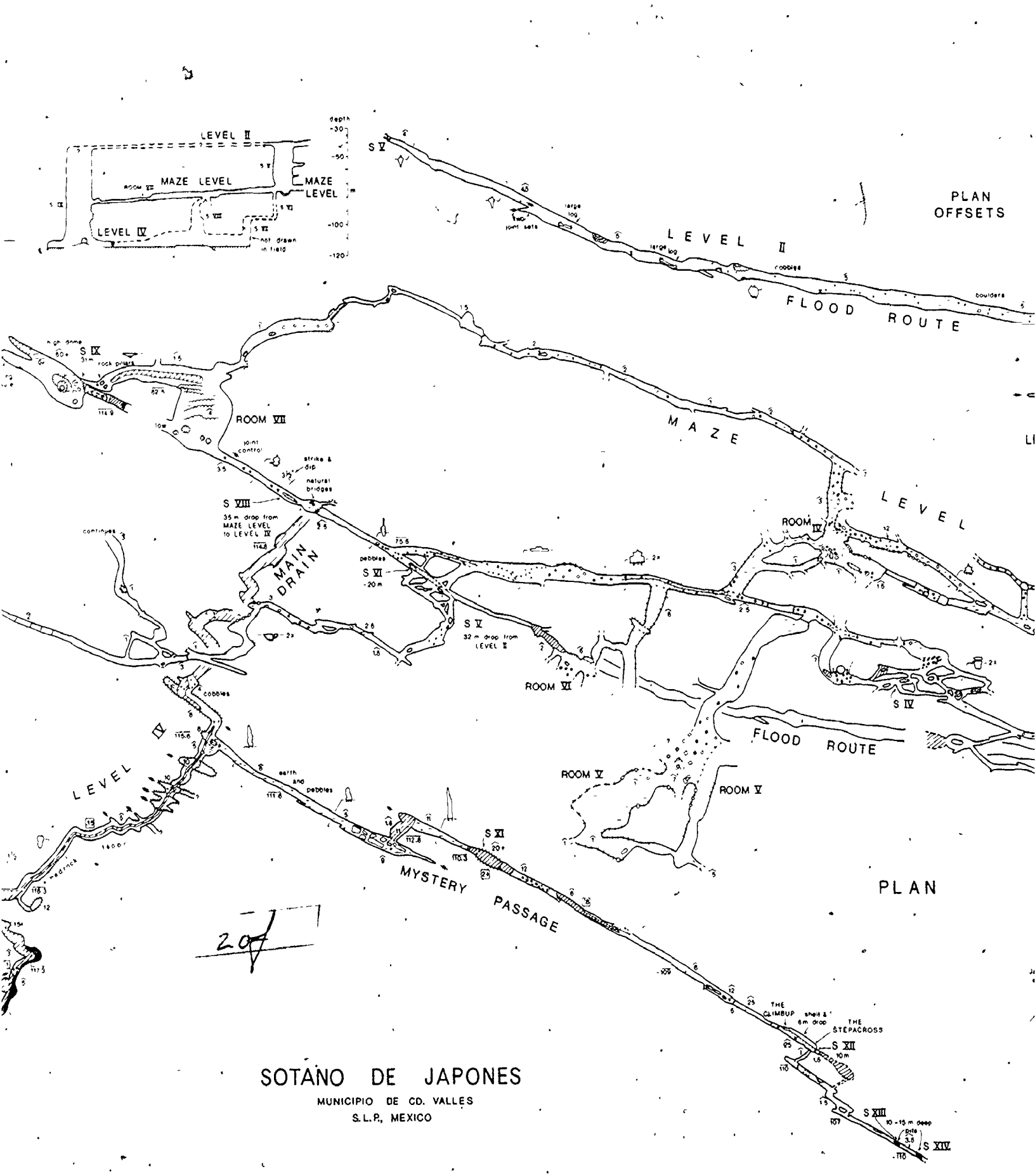

SOTANO DE JAPONES

MUNICIPIO DE CD. VALLES

S.L.P., MEXICO

f Sótano de Japonés

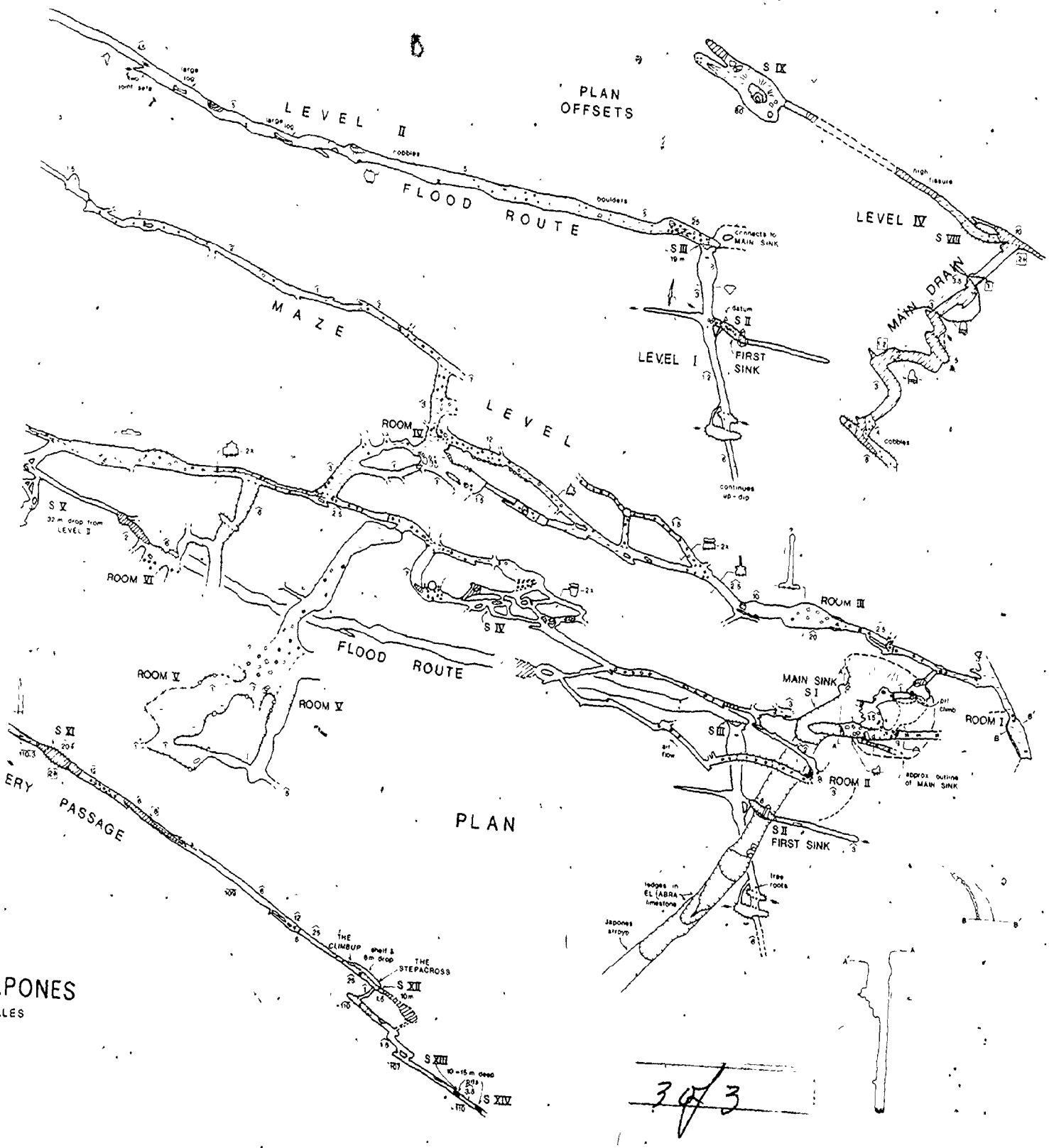
PLAN
OFFSETS
LEVEL II
FLOOD ROUTE
MAZE LEVEL
LEVEL I
FIRST SINK
LEVEL IV
MAIN DRAIN
S IX
S VIII
S III
S II
ROOM IV
S V
ROOM VI
ROOM III
S IV
FLOOD ROUTE
ROOM V
ROOM V
MAIN SINK
S I
ROOM I
S III
ROOM II
S XI
PASSAGE
PLAN
S II
FIRST SINK
THE CLIMBUP
THE STEPACROSS
S XII
S XIII
S XIV
APONES

3 of 3

from upstream piracies, and a maze-like alcove off the Main Sink. Level I quickly plunges down a 19 m drop (S-III) to Flood Route (Level II). This 4-5 m high flood water passage has a somewhat ovate form caused by joints and minor vadose trenching. Sediments include boulders to mud and logs. After a gradual descent along 300 m, a 32 m deep fissure (S-V) descends to Level III -- the Maze Level. This level is reached more directly by S-I in the Main Sink. It comprises a labyrinth that is only partly explored. Passages are commonly only 0.5-1.0 m high, but some of the principal routes reach 3 m diameter. Although the idea has not been carefully checked, it appears that most of this level is developed at one stratigraphic horizon. The initial flow control may have been a bedding plane, but a bed or beds having small, closely spaced joints have had a pronounced effect. Special symbols are used on the map to indicate that in many places, the "walls" of the passages are poorly defined. Flood waters have sought every penetrable joint and enlarged it. Often, (more often than shown), the "walls" are merely a collection of bedrock columns remaining between the joint openings. In other places, loose rocks and mud form the "wall". Several extraordinary low rooms have developed, such as Room V which is more than 100 m in diameter, but only 1 m or less high. The net flow direction is southwest, and the larger passages are oriented in that direction. They generally slope downward in the direction of flow, but elevation data are not available for most of this level; hence, a dashed line is shown on the profile as an approximation. There are at least five shafts that descend from the Maze Level to still lower passages. Three of them (S-VI, S-VIII and S-IX) are aligned beyond S-V, the shaft that connects Level II to Level III. They descend

about 35 m to an underlying passage that also connects them together (see detailed profile). This is the beginning of Level IV, the lowest known level in the cave. At present, Level IV is composed of only two passages. Main Drain is the largest known passage in the cave, and is so named because it is thought to re-collect much of the distributary waters from the Maze Level. Initially, it trends horizontally 230 m southeast along the strike before it turns southwestward like the principal passages in higher levels. Bedrock floor is exposed for about 100 m of the strike-oriented passage, but there are also large lakes having much clastic sediments. From the turning point, the Main Drain gradually descends 22 m over a distance of 450 m to a dome-like room with a small siphon lake 139.5 m below the datum. This part of Main Drain is large, but varies considerably in cross-sectional shape, area, and height. The effect of large NE-SW joints can be clearly seen in both parts of the passage. Water, mud, coarser sediments, breakdown, vegetal debris, and formations are much more abundant in Level IV than in higher levels. About the middle of the strike passage, there is a large joint-controlled passage named Mystery Passage that is entered by climbing up a sediment bank. It trends horizontally northeastward for 330 m, reaching all the way back to the overlying surface channel. Near the middle, there is a high vadose dome (S-XI) that probably brings water in from an undiscovered pit in the Maze Level. At its end, there are several unexplored pits, where water apparently excapes to another drainage route.

The morphology and genesis of Sótano de Japonés are complex and warrant further study, particularly after the cave is more fully known. A preliminary interpretation is given here. Water was first pirated at

Main Sink, and was divided, part going down S-III to Flood Route (Level II) and the remainder going down a large joint (in S-I) to the Maze Level (Level III). The very great amounts of water provided by floods from the large surface basin produced extreme local hydraulic gradients, which in combination with the jointing and other hydrogeologic characteristics of the beds at Level III caused a distributary maze of passages to develop from the base of S-I. The larger channels may be dip tubes, but intermediate size joints were significant in controlling passage orientation and enlargement. Several large joints provided targets where water was taken down to Level IV. The Main Drain is believed to have re-integrated some of the distributed flood waters. Abundant active formations and high domes or fissures, as well as the several known connecting shafts substantiate this point; however, other lower level downstream passages might be found as in Sótano de Yerbaniz (Mitchell et al., 1977). The basic skeleton of the cave was established at an early stage. Level II flow may originally have extended over to the top of the large dome pit, S-IX, which is known to reach much higher than Level III (see detailed profile), and subsequently was pirated down S-V. All of Flood Route (Level II) may have been temporarily abandoned as S-I became large enough to capture all the flow. Later, the development of S-II and other upstream holes has captured the majority of flow for Flood Route.

In summary, it is believed that the pattern or skeleton of the cave was established very early in the cave's development. All of the levels were formed in a single phase -- none are related to a water table. The two basic processes are: 1) development of a complex set of distributary channels in the initially (presumably) unaltered bedrock in an attempt to

transmit the water supplied, and 2) regressive piracy down joints between levels and in the surface arroyo. The first process can be especially important for floodwater caves. Palmer (1972) has described many characteristics of floodwater caves, including maze development around passage restrictions or blockages (e.g., breakdown) where high local hydraulic gradients are generated, that make them a distinct class. An analogous situation occurred in the primary development of Japonés when far more water was provided by floods than could be passed. Water was forced into a great many structurally controlled routes simultaneously and conduits formed. As the conduits enlarged to a small fraction of their present size, the dry season or between-flood water level was lowered probably below the "terminal" siphon in Main Drain. During floods, water would back up in the system inversely with its capacity to quickly transmit the flood. Presently, moderate floods may not cause water to fill the larger passages, except where water may have backed up in the lowest parts of the cave. Although it is difficult to assign a length to a complex cave such as Japonés, about 4-4.5 km are shown on the map, and its depth to the water trap is 139.5 m. There is likely to be more air filled passage on the other side of the water trap (siphon).

6.4.4 Sótano de Jos

Sótano de Jos is a very active swallet cave near the southern end of the Los Sabinos group of caves. It has a catchment of 4.3 km^2, which is pirated down the joint-controlled entrance slot. The cave must be very young relative to the large swallet caves nearby because its

passages are comparatively small, and because the arroyo has entrenched only about 3 m below the top of the El Abra limestone, which is exposed for only a few tens of meters upstream of the capture point. The cave lies in a valley perhaps a few hundred meters wide, and is a recent capture of most of the drainage that formerly flowed to Sótano de las Piedras and Sótano de Palma Seca.

Jos is a very simple cave (Figure 6.20) compared with the larger swallet caves. The entrance is 27 m deep, and displays potholes and vertical shafts common to vadose water flow. A dome that intersects the side of the entrance pitch descends another 34 m to a high vadose canyon containing large rounded boulders. After 40 m, a small tributary passage joins. The main passage turns northward, gradually descends, and generally follows NNE joints away from El Choy spring for 275 m to a deep permanent siphon 84.5 m below the entrance. In Tiptoe Lake, vein calcite occurs along a fracture.

Bedrock is exposed on the floor in many places, and where it is covered, the sediments are believed to be very thin. The cave contains abundant flowstone deposits. These deposits and numerous inlet domes are undoubtedly caused by leakage down joints and in the bed of the arroyo, and down the stratal dip. On September 11, 1971, two days after a moderate storm, some water was observed flowing in the arroyo, but not down the entrance drop (D. Broussard, personal communication). In the cave, the water entered via the domes and the inlet passages. A particularly large flowstone mass is located almost directly underneath the arroyo (see map).

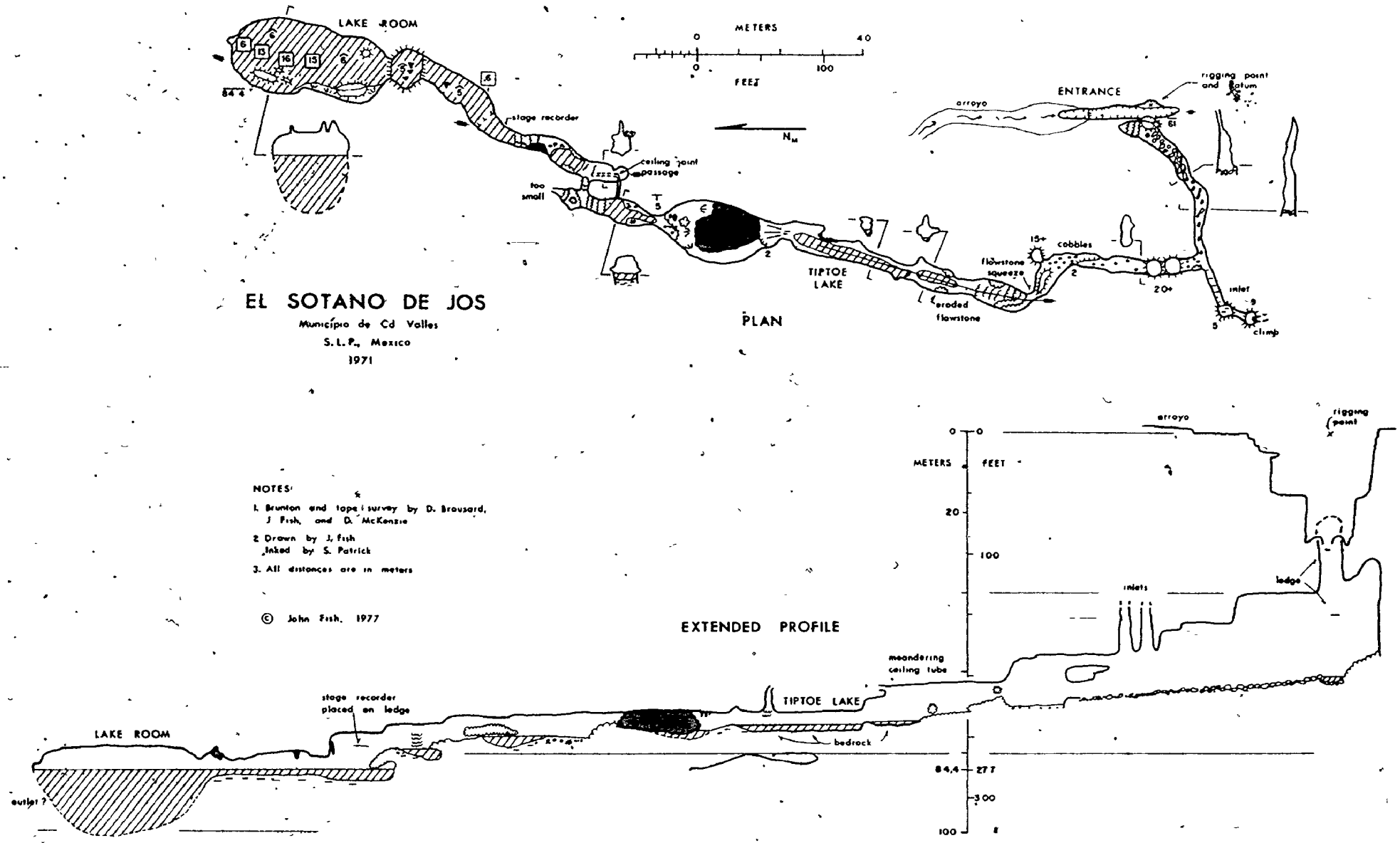

Figure 6.20 Map of Sótano de Jos

A stage recorder was placed over the shallow end of the siphon lake to monitor the hydrologic activity of the cave (Section 4.4.2). The location of the outlet from this lake is unknown, but it is believed that the ceiling of the siphon will rise sufficiently to form an air-filled passage again. The crests of large floods that pass through the cave must be damped at several places where the passage cross section is reduced by flowstone or resistant bedrock. For example, Tiptoe Lake has a tubular cross section including a smoothly-arched solution ceiling created by frequent flooding to the roof. The cave is not yet large enough to immediately transmit all of the water provided by major floods; thus, water backs up, causing large rises of the siphon lake surface, and possibly flooding the cave back to the canyon at the base of the entrance pitches. Fast flow is indicated by small scallops, and by the lack of sediment in many places, although much sediment is washed into the cave. Sediment is transported through the known cave; some of it may be deposited within the aquifer, but probably most of it is discharged at El Choy spring.

Some indication of the complicated history of flowstone deposition and erosion in the El Abra region, even in this very young cave, is given by one flowstone mass (marked "eroded flowstone" on the map) which formerly blocked the bottom 1.5 m of the passage. It has been sliced in half by flood waters. A round boulder one-half meter in diameter previously included within the flowstone, now bridges the top of the slot; the exposed flowstone cross section reveals several distinct periods of deposition which were interrupted by periods (or events) of erosion. It is not known whether the erosion phases were the result of a few unusual rainfall-

flood events or longer climatic changes.

In summary, Jos is a young floodwater cave.

6.4.5 El Sistema de los Sabinos

El Sistema de los Sabinos is the name given to a complex of three large caves that are believed to be connected, but as yet have short distances remaining between them (Fish, 1974). The system is named after the village of Los Sabinos. The three caves are La Cueva de los Sabinos, El Sótano del Arroyo, and El Sótano (Cueva) de la Tinaja. A line map of the system is shown in Figure 6.21.

6.4.5.1 Cueva de los Sabinos

Cueva de los Sabinos is a large cave about 2 km southeast of the village of Los Sabinos, and about 700 m east-northeast of the sink of Sótano del Arroyo (Plate 3.9). The entrance is in the north wall of a large sink (Figure 6.22) that was at least partly created by collapse into the cave. The portal (Plate 6.22) is 13 m wide by about 8 m high and is prominently marked with "phreatic" domes and pockets. A ramp of collapse debris from the sinkhole descends 21 m to a room dubbed the "Temple of Karnak" for the magnificent bedrock pillars on the east side. The pillars are remnants of solution along a number of joints. Straight ahead, First Level (passage) is split into an upper and lower route for about 70 m to a large shaft that reconnects it. The lower route initially is a wide crawlway with a dirt floor, followed by a room with formations; the upper route is

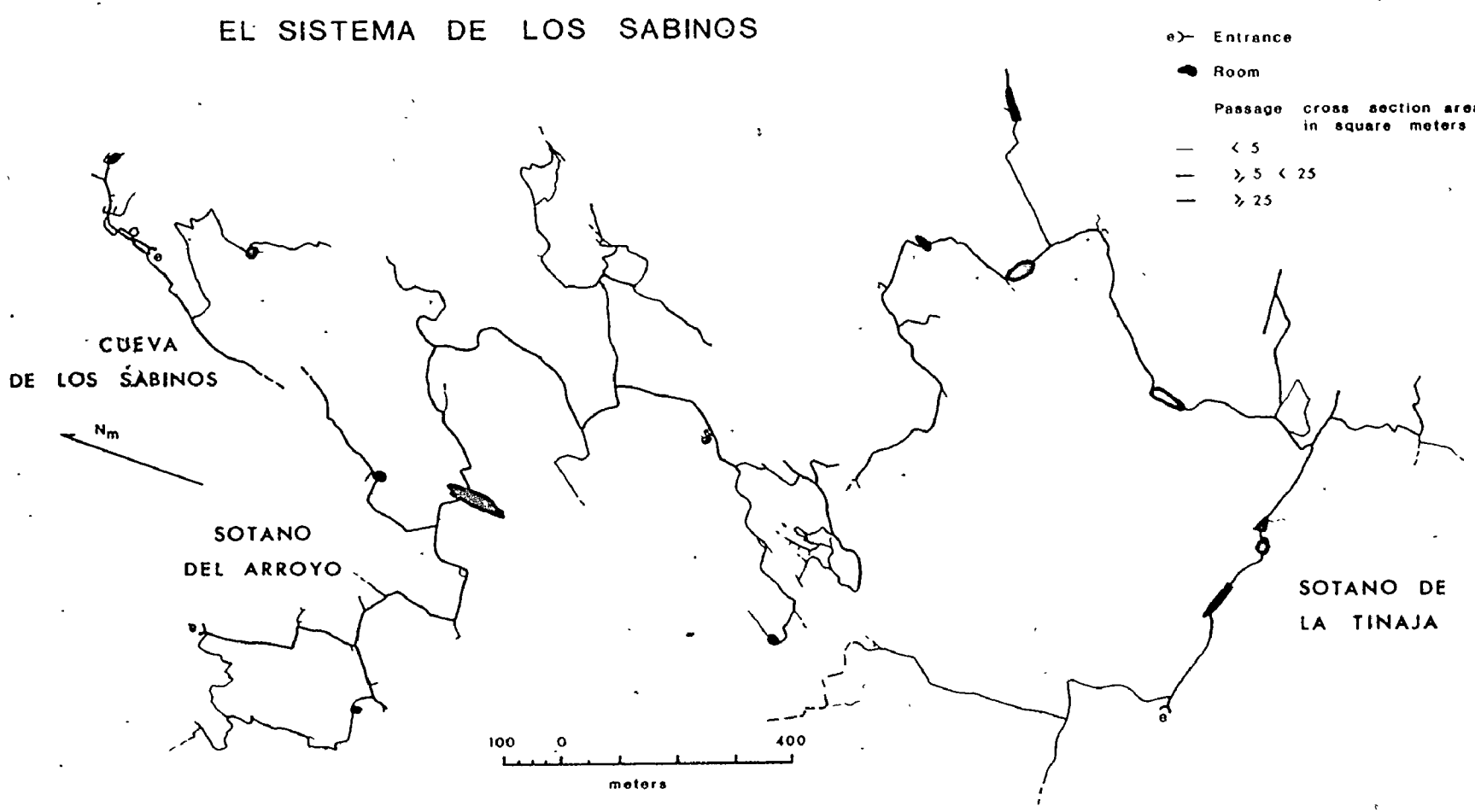

Figure 6.21 Map of El Sistema de los Sabinos

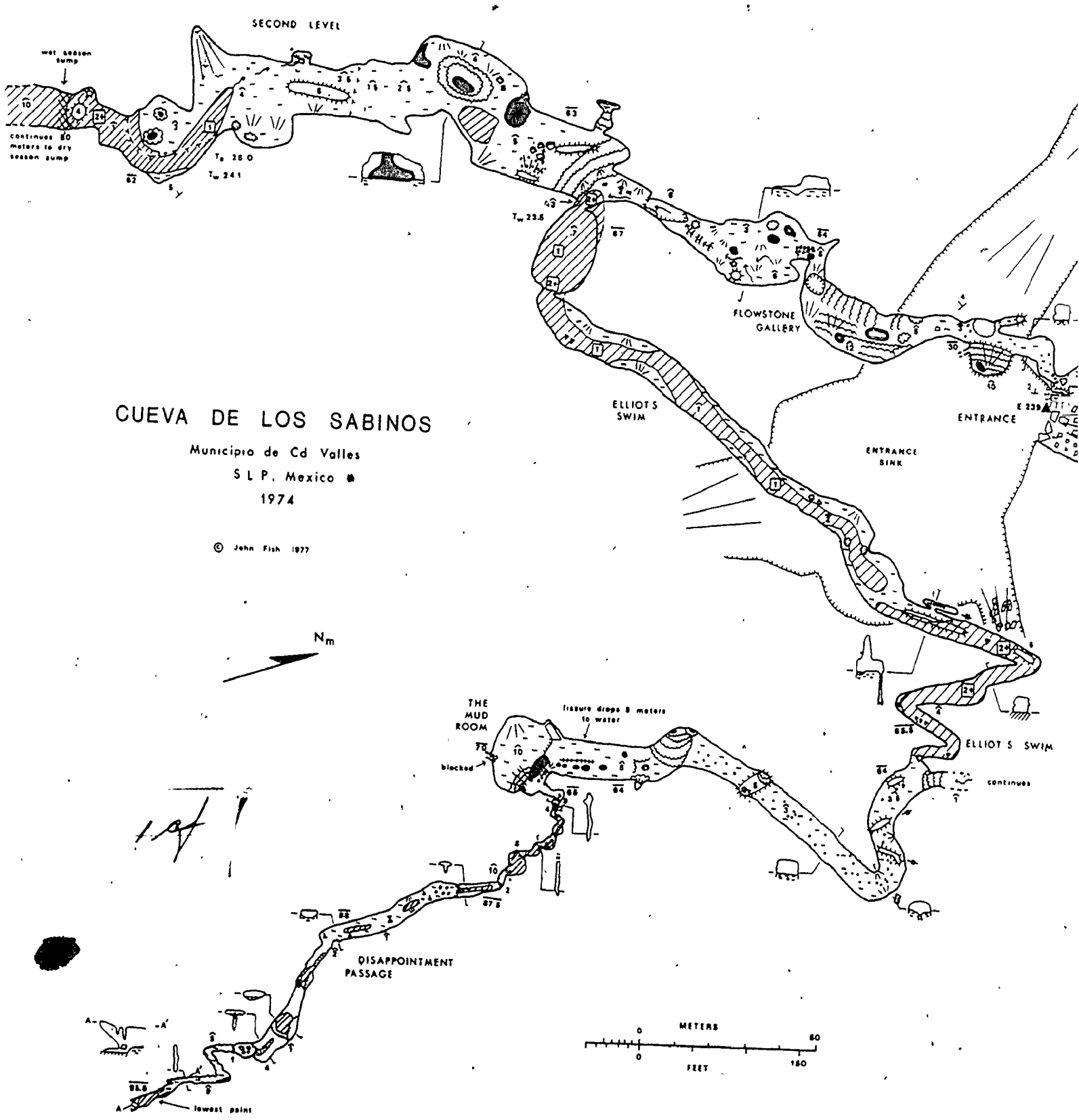

Figure 6.22 Map of Cueva de los Sabinos

2 of 2

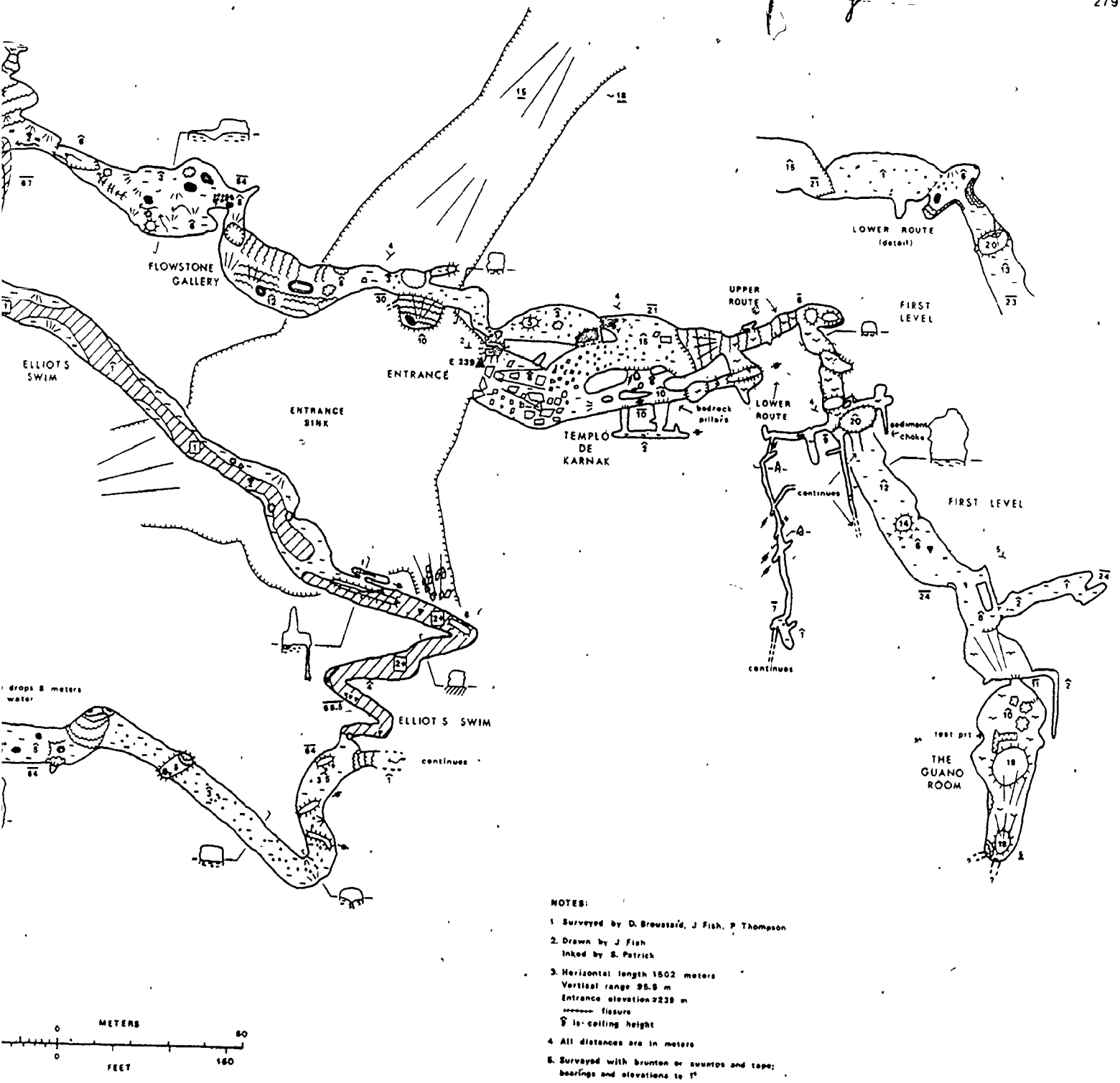

NOTES:

1. Surveyed by D. Broussard, J. Fish, P. Thompson
2. Drawn by J. Fish
   Inked by S. Patrick
3. Horizontal length 1502 meters
   Vertical range 95.5 m
   Entrance elevation ≈239 m
   ⟶⟶ fissure
   ⟨ 1s ⟩ ceiling height
4. All distances are in meters
5. Surveyed with brunton or suuntos and tape; bearings and elevations to 1°
6. Data processed by CDC 6400
7. Temperatures 7/15/1972

Map of Cueva de los Sabinos.

Plate 6.22 Entrance to Cueva de los Sabinos in the north wall of a broad sinkhole (partially collapse). The ceiling has phreatic domes. A slope over breakdown leads down to the main cave level.

roughly equidimensional in cross section, and contains abundant flowstone, guano, and several domes. Several small passages displaying phreatic forms and strong joint control meet at the top of the connecting pit. On the lower route, First Level continues horizontally beyond the pit as a large dirt-floored passage 24 m below the entrance. It abruptly ends at a small side passage and a steep climb up a bedrock slope to the Guano Room. This room appears to be of phreatic origin. The ceiling of the eastern end of the room has the highest elevation in the cave, approximately 15 m above the ceiling of the entrance.

From the "Temple of Karnak", the First Level also continues in the opposite direction as a smaller passage underneath the entrance sink to Flowstone Gallery. Along the way, it slowly descends; and there are three domes on the left that contain abundant formations and flowstone, and in at least one case breakdown from the entrance sink that is cemented by flowstone. In Flowstone Gallery, a slope and a pit descend about 25 m to Second Level. A wide mud-floored room with formations and a vadose channel leads down to a pool 67 m below the entrance, the lowest point in Second Level. The passage that continues is quite large and probably has several meters of flowstone, guano, and clastic fill. It "terminates" at a permanent sump only about 30 m from the sump at the end of Left Hand Passage in Sótano del Arroyo (see Figure 6.21). These two passages are very similar in size, elevation, and morphology; therefore, they very likely connect. During the wet season, water emerges from the siphon lake and either trickles down a nearby hole, or at higher stage flows to the pool at the low point in the passage. Vegetal matter accumulates on the

mud banks around this pool.

Beyond a low constriction over the above mentioned pool is a wet, muddy passage named "Elliott's Swim" that trends northeast underneath the entrance sink and then turns back southward. Eventually dry land is reached 1.5 m above the normal lake level. Beyond a low inlet, the passage continues horizontally for 150 m as a 4 m high, 8 m wide tunnel with cobbles and mud on the floor. It ends at the Mud Room where mud banks may have buried a continuation of the passage. Just before the Mud Room is the entrance to a smaller passage that descends 30 m in its 200 m length. It ends in another siphon (hence Disappointment Passage) 95.5 m below the entrance, the deepest point in the cave. The total surveyed length is 1502 m.

6.4.5.2 El Sótano del Arroyo

The entrance to El Sótano del Arroyo lies 1.7 km southeast of the Los Sabinos village. It is a swallet type sink that has a drainage basin of 12.4 km^2 (Figure 3.2 and Plate 3.9). The surface stream was first pirated down large north-south joints about 70 m above the bottom of the sink (Plates 6.23 and 6.24). Since then, the arroyo has entrenched rapidly, exposing the El Abra limestone in a gorge for more than 1 km upstream, and forming several waterfalls in the stream bed. Presently, the large entrance pit is degraded so that drops of 8 m and 15 m in the arroyo bed reach the bottom of the sink, whereas all other walls are 60 m or more high (see the profile of the entrance sink on Figure 6.23). The datum for the cave survey is taken as the top of the 15 m entrance drop.

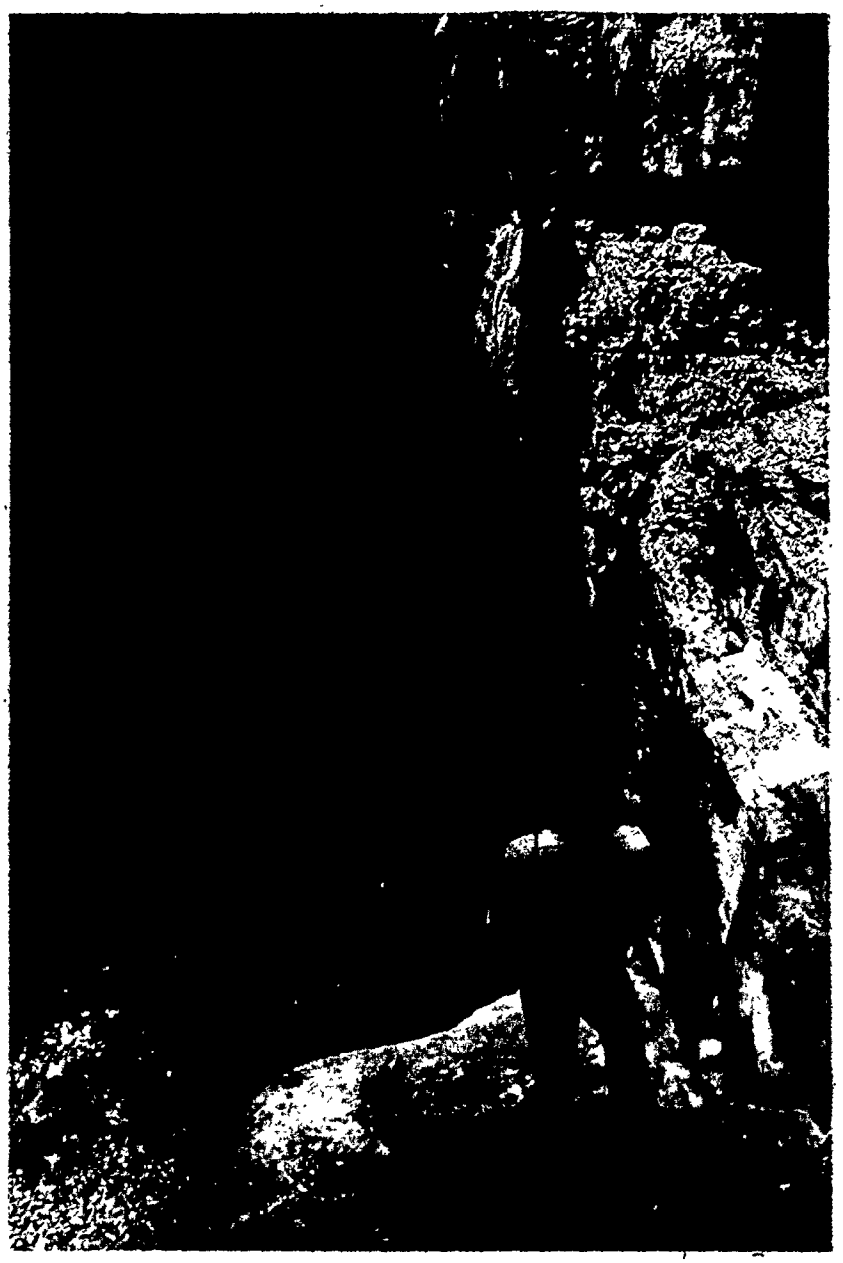

Plate 6.23 The entrance pit of Sótano del Arroyo. The walls are 60 m high except where the arroyo has cut a canyon down to the view point 15 m above the floor. The joints extend from the top of the El Abra limestone to the floor. Main Passage leads from the bottom of the sink.

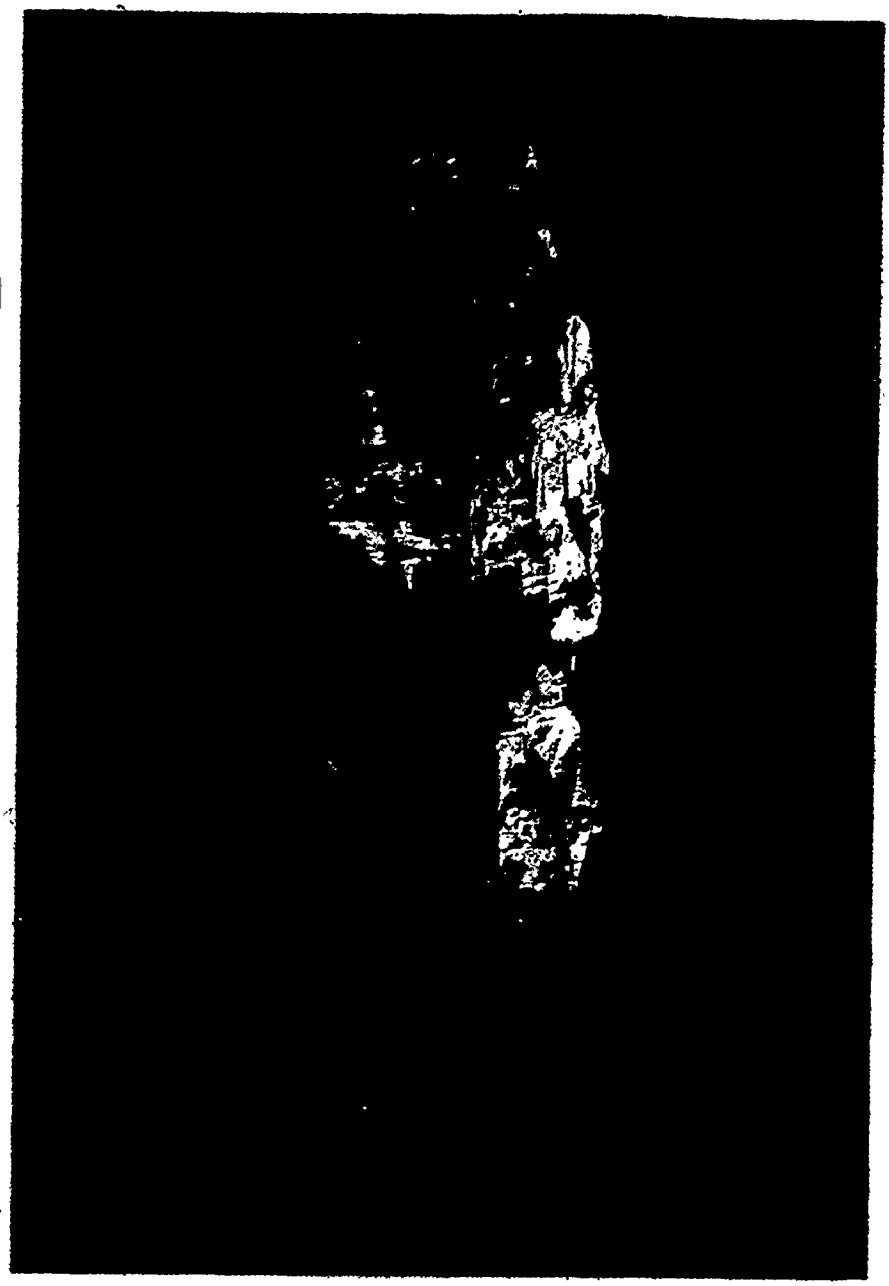

Plate 6.24 View out Main Passage of Sótano del Arroyo into the entrance sink. Wet season floods enter via the arroyo 15 m above the floor (there is a person standing at the edge of the drop). Particularly important is the large joint which initially captured the stream. The leftmost hole on the wall leads to the Thirty Foot Level.

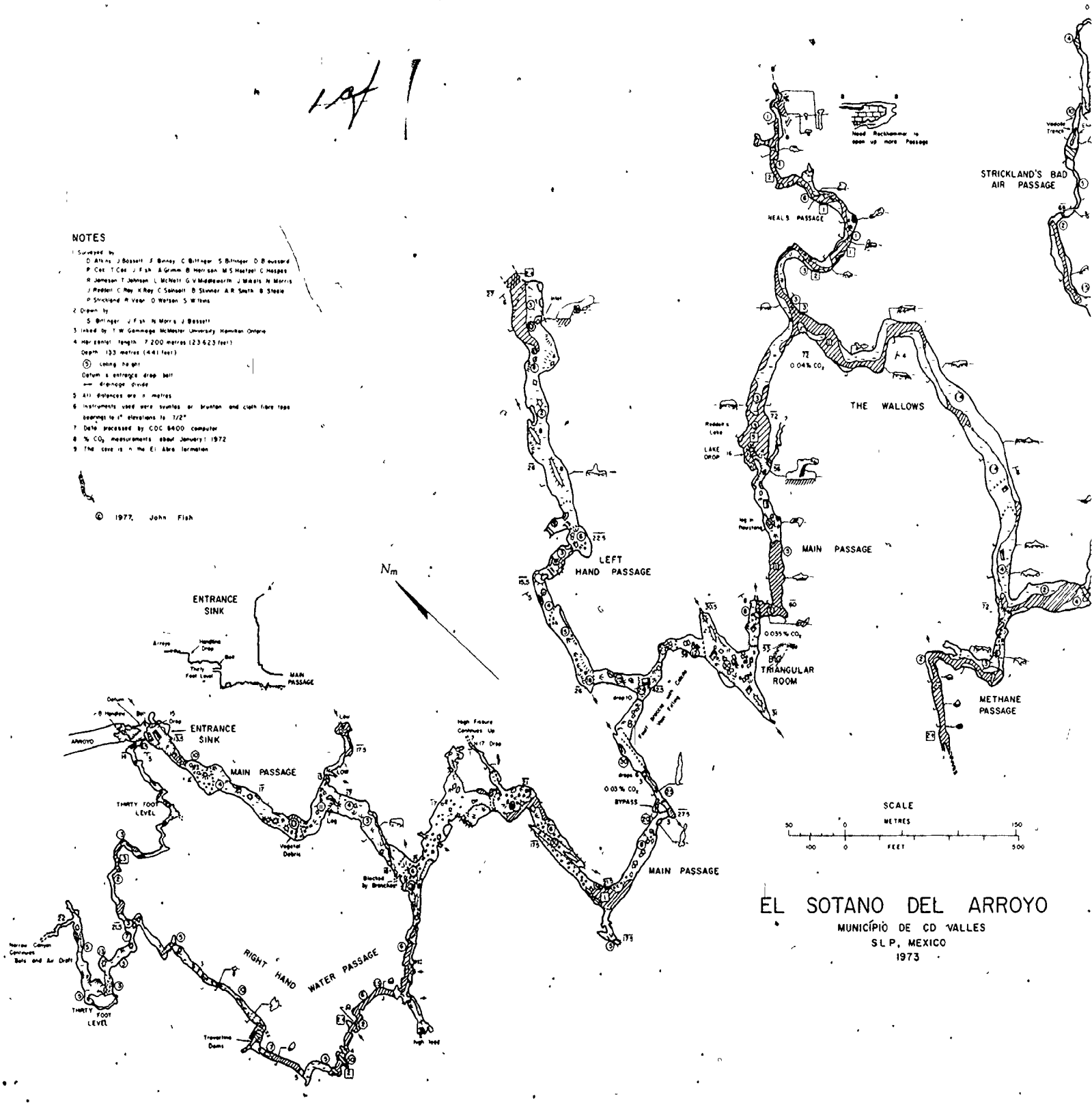

Figure 6.23 Map of Sótano del Arroyo

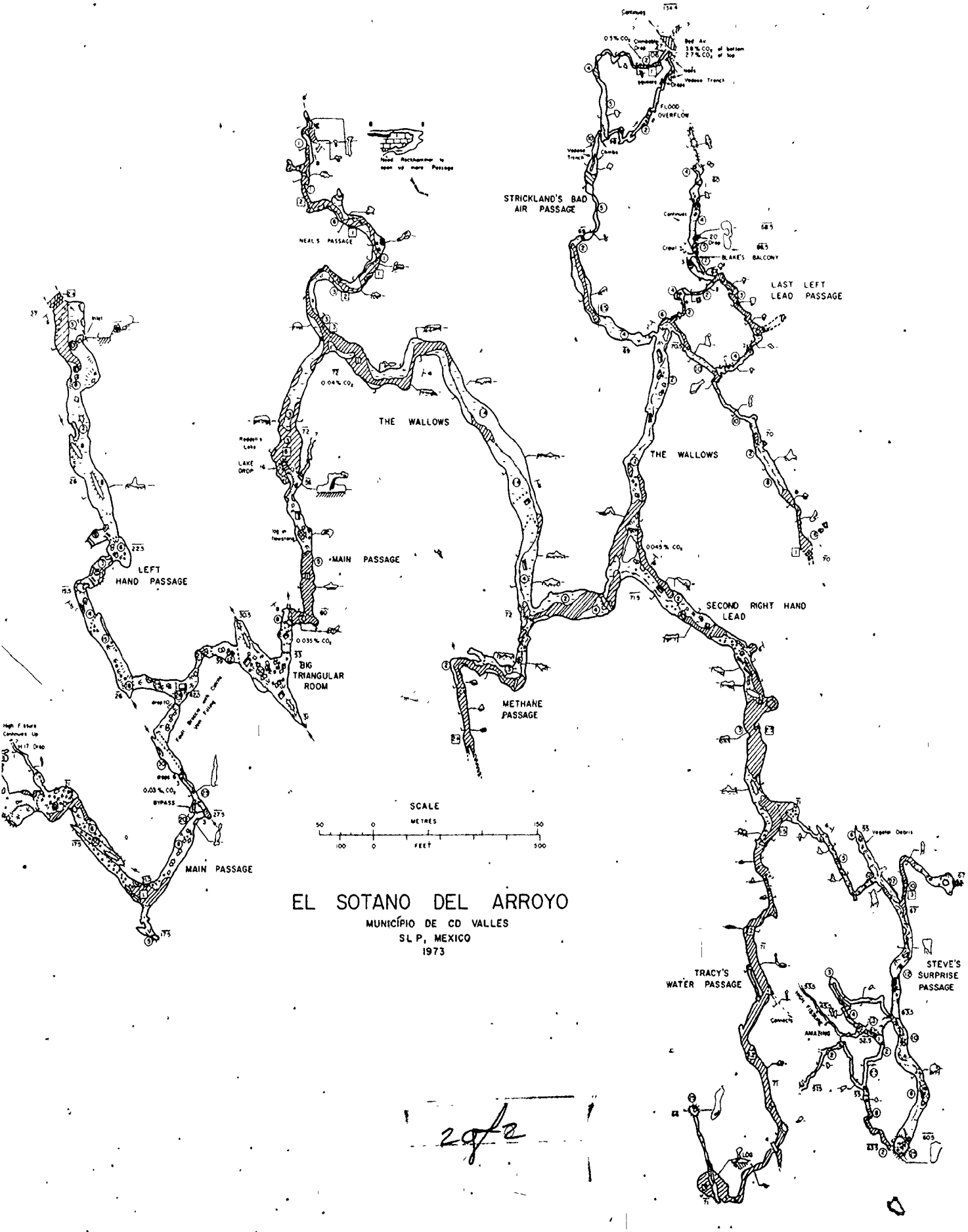

e 6.23 Map of Sótano del Arroyo

Two passages lead from the entrance. A small passage, the Thirty Foot Level, trends southwest down the 5° dip from a point 10 m above the sink floor and directly under the arroyo. It is nearly blocked by flowstone, but this can be passed to reach a junction 260 m from the entrance. The Thirty Foot Level becomes larger and dirt-floored for the next 160 m, and then continues as a high narrow fissure for at least 150 m beyond the end of the survey. The south branch from the junction is also relatively large and passes obliquely across the dip to join the Right Hand Water Passage, which is a 4 m by 5 m passage with deep lakes, interrupted by a 4 m high flowstone dam. This passage has a very irregular floor profile with the lowest points being on either side of the travertine dams in the middle, 26.5 m below the datum. The passage appears to be a down-dip loop.

The other passage, leading southward from the bottom of the entrance sink, is the large Main Passage (Plate 6.25). This is the trunk channel for the wet season floods that enter the cave. It contains abundant deposits of washed-in mud, sand, fine gravel, and vegetal debris (Plate 6.26). There are several small associated passages, some of which appear to be active distributaries, and others (higher) which may be fossil distributaries or may be small vadose inlets. The Main Passage is nearly horizontal except for several piles of breakdown, until at about 700 m, two 10 m drops are encountered in a 30 m high canyon. Strong fracture control of the passages is clearly evident in a number of places in this part of the cave (see map). The floor profile is very irregular: the stream has cut downward along fractures forming waterfalls, but beyond each drop the water must rise several meters over breakdown and mud. Immediately, to the

Plate 6.25 (above) Main Passage in Sótano del Arroyo, looking downstream from 20 m inside the entrance. There are collapse boulders and formations on the left, and cobbles and coarse sand on the right.

Plate 6.26 (left) A log in Main Passage in Arroyo. Violent floods carry in huge quantities of mud and coarser sediment (see floor), and vegetal matter including logs. A person stands at the left edge.

left from the base of the second drop is the Left Hand Passage. A steep climb over breakdown and vegetal debris ascends in a 25 m high canyon almost to the level of the bottom of the entrance sink. The highest part of the floor of this passage is in the middle where large stalagmite and flowstone masses have been deposited. The last 200 m descends slightly in a wide, mud-floored passage to a large siphon lake room. Probing the siphon has shown that it continues at least a short distance underwater. It likely connects with the Second Level sump in Cueva de Los Sabinos. The trickles of water that enter Los Sabinos via its sump lake probably come from the small inlet at the end of the Left Hand Passage. Modern flood water from the Main Passage probably rarely uses this passage.

Straight ahead from the second drop, the Main Passage continues to the so-called "Big Triangular Room", which is over 100 m long and 30 m high, and contains room-size breakdown swept clean of mud by flood waters. Again fracture control is evident. Diagonally, across the room, a passage descends to a deep lake 60 m below the datum, having as little as 0.3 m of air space. This is the main flood route, and the majority of the cave lies beyond this point. The passage rises up the stratal dip to Lake Drop, which is a 16 m descent on a flowstone chute to the middle of a deep lake (Reddell's Lake). This marks the beginning of the lower "level" of the cave.

The Wallows is the main trunk channel of the lower level. Typically, it is 2 m high by 15 m wide, and filled with lakes and sticky mud. It begins at 72 m below the datum, but surprisingly, beyond Neal's Passage it rises very gradually over its 1.1 km length to a terminal sump at about -70 m. The roof is solutional and generally flat except for a few domes or

crevices dissolved along joints. It is believed that the right-hand passages off The Wallows are inlets (i.e., sources), whereas all the left-hand passages and probably the sump of The Wallows are downstream passages. During the dry season, water trickles out of the right-hand passages and drains into Neal's Passage. Large floods, however, rise up the entire length of The Wallows, entering all passages.

Neal's Passage, the first encountered downstream passage in the lower level, is horizontal for 300 m before it descends a short fissure. It becomes blocked by flowstone at least 50 m above the local water table. Water escapes through crevices and through a small hole in the flowstone. Strickland's Bad Air Passage is a very active flood-water route. It has an irregular bedrock profile, rising slightly up the dip before descending several short drops and tight vadose trenches. Beyond a flowstone squeeze near the present limit of exploration the CO_2 content of the air reaches dangerous concentrations (see CO_2 measurements at several points in the cave). A fissure drops 30 m to a large passage at -134 m (441 feet), the lowest point known in the cave (unfortunately, one questionable survey leg in the Bad Air Passage could change the depth by ± 10 m). Here, the CO_2 reaches 3.8%, which has inhibited further exploration. This passage must be near the local water table; hence, it may soon siphon. The CO_2 is likely formed by the decay of organic matter swept into the cave, and is maintained at high concentrations because air circulation is restricted. A small passage, Flood Overflow, is used only by large floods. Water must rise high enough to flow <u>up</u> some short pitches and over two bedrock drainage divides (shown as ↔ on the map) before it also connects with the top of the

fissure. Last Left Lead Passage initially is divided into two passages, smaller than the previous downstream ones, that join and continue as one. This passage is probably not used as a discharge route as often as the others because of its profile. It rises 6 m up dip, before it descends almost back to its initial elevation via short drops, and finally ascends to 10 m above its starting level, where it becomes very low or may be completely blocked. At the low point of the passage, a 20 m unexplored pit drops into a large canyon that must be the route for flood water that enters this passage. It may connect with the bottom (or even the top) of the fissure in Strickland's Bad Air Passage.

There are about 2 km of known passages off the right side of The Wallows. The first is the 190 m long Methane Passage, named for the flammable gas bubbles that rise from the lake bottom when it is disturbed. This passage is oriented in the same direction as the dip of the strata; therefore, it quickly siphons in a deep lake. A trickle of water has been observed to flow from this passage even late in the dry season. The Second Right Hand Lead is a very large tributary (?) passage developed along the strike of the beds. Like most of the other passages in the lower level, it is very wet, muddy, and contains some breakdown. A small trickle often flows from it in the dry season. After 300 m, it branches. Tracy's Water Passage, the right fork, extends 400 m to a deep lake room, where a ceiling slot leads to a high inlet dome. Access to the left fork is under a low ledge in an alcove. A passage of modest size ascends slightly up-dip over cobbles and sand to connect with Steve's Surprise Passage, a big canyon 300 m long, 8-10 m wide, and 10+ m high. This canyon has some massive

stalagmites, and a thick mud fill that is dissected by an intermittent stream. There are several large domes (inlets ?) and the passage ends at a high dome with a possible continuation at the top. A large side passage on the east quickly ends in a siphon. Along the west side of the canyon near the middle, a small hole leads into the "Amazing" complex of passages. Only the larger ones have been surveyed and shown on the map. The passages seem to have a totally erratic profile and destination. A high fissure which has undergone considerable collapse along a fracture, reaches at least 30 m above The Wallows. It seems likely that either flood backwater enters the area and escapes to lower levels, or vadose dome inlets supply water that continues on to Tracy's Water Passage and Steve's Surprise Passage or to lower levels.

Sótano del Arroyo is a very complex and active cave. Its surveyed length is 7200 m which makes it the longest known cave in México.

6.4.5.3 Sótano (Cueva) de la Tinaja

Tinaja is the southernmost cave of the hypothetical Los Sabinos System. The entrance sink is about 50 m deep, but entrenchment of the arroyo and by rockfall have degraded the sink so that the cave at the bottom is easily accessible. The rock of the entrance sink is (was) heavily fractured, and as at Sótano del Arroyo, the large fracture that originally captured the stream passes from the surface all the way down to the cave (Plate 6.27). A map of part of Tinaja drawn by David McKenzie (published by Russell and Raines, 1967) was considerably improved during the field work, several passages were added (Figure 6.24), and a profile of part of the cave was

Plate 6.27 Entrance to Sótano de la Tinaja. The entrance sink has been sufficiently degraded so that the cave is easily accessible. Large joints captured the stream about 50 m above, and have promoted rockfall.

Plate 6.28 Entrance Passage in Tinaja just above Cable Ladder Drop. The photo shows common solution features in the massive bedded limestone of the swallet caves. Here water initially rose updip before descending a joint at the drop.

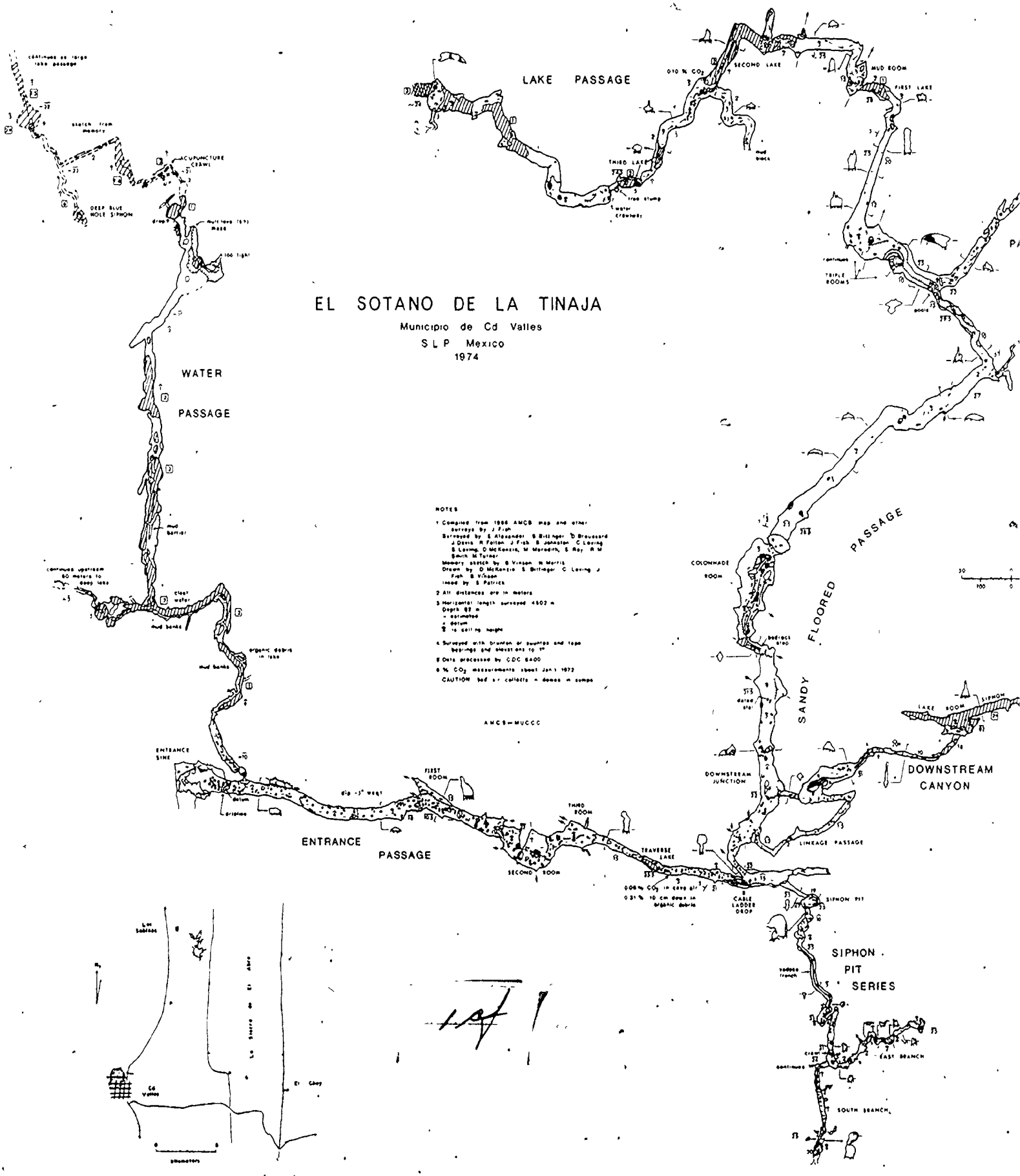

Figure 6.24 Map of Sótano de la Tinaja

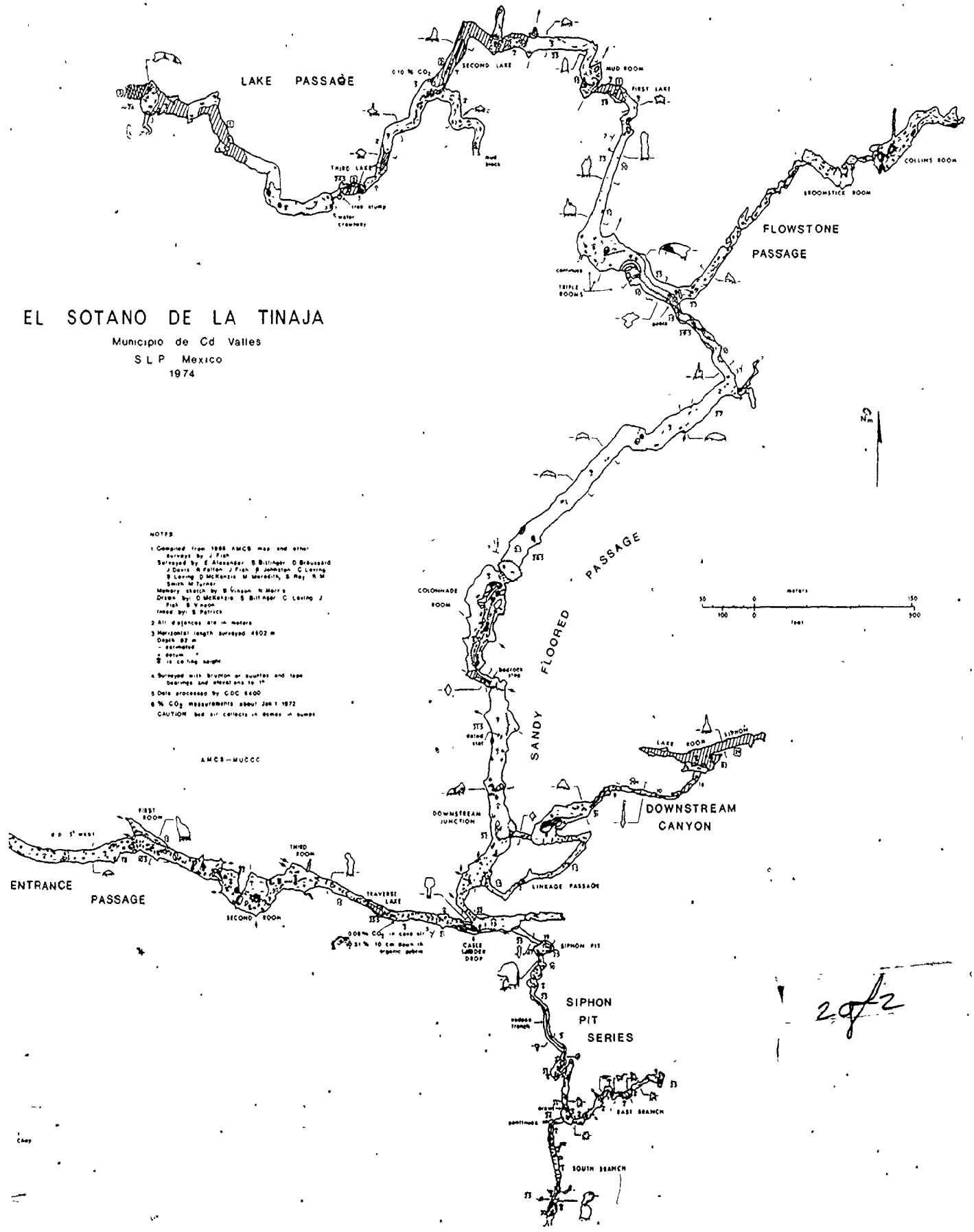

Figure 6.24 Map of Sótano de la Tinaja

SOTANO DE LA I

EXTENDED PROF

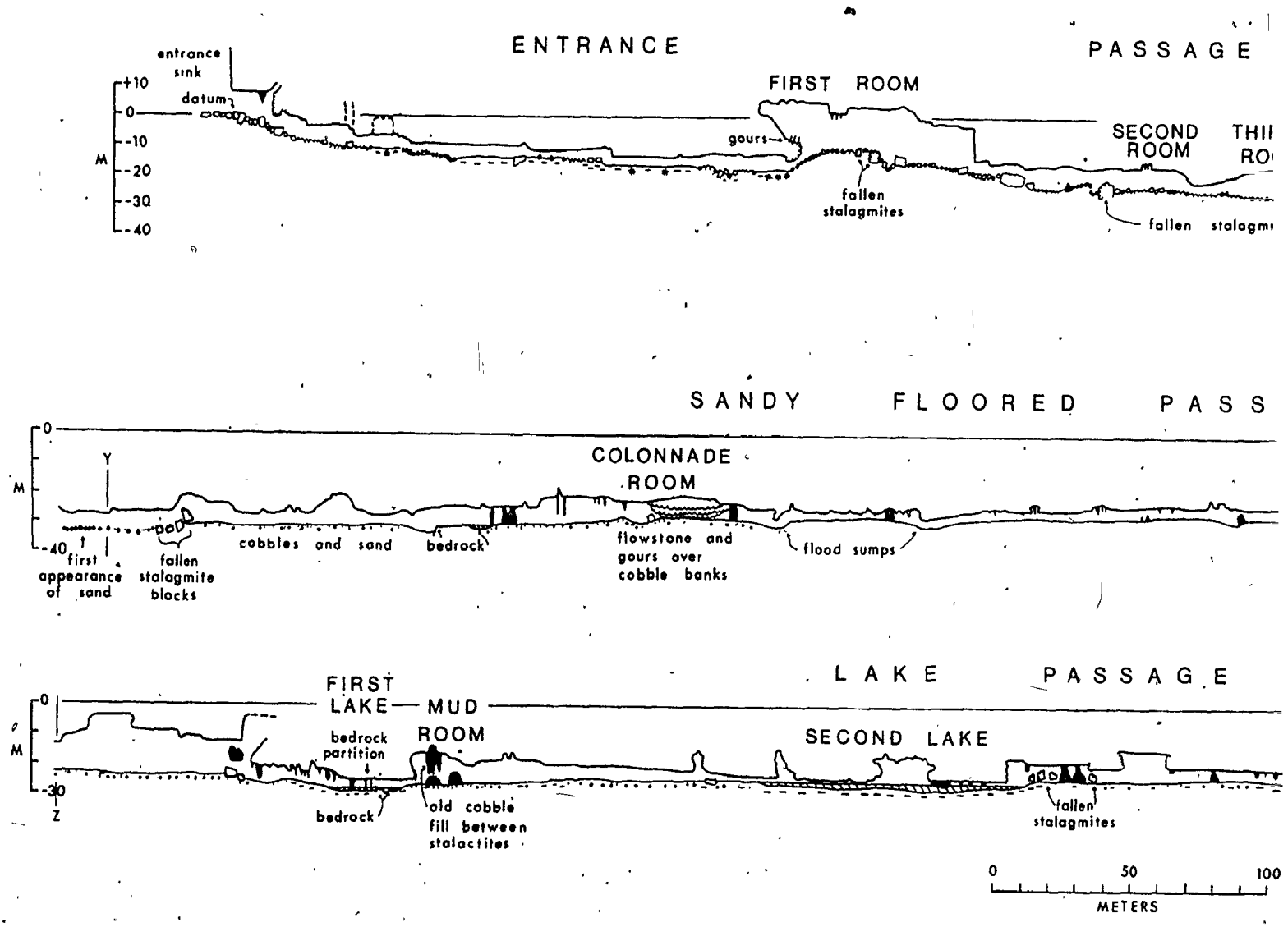

Figure 6.25 Profile of part of Sótano

ANO DE LA TINAJA

EXTENDED PROFILE

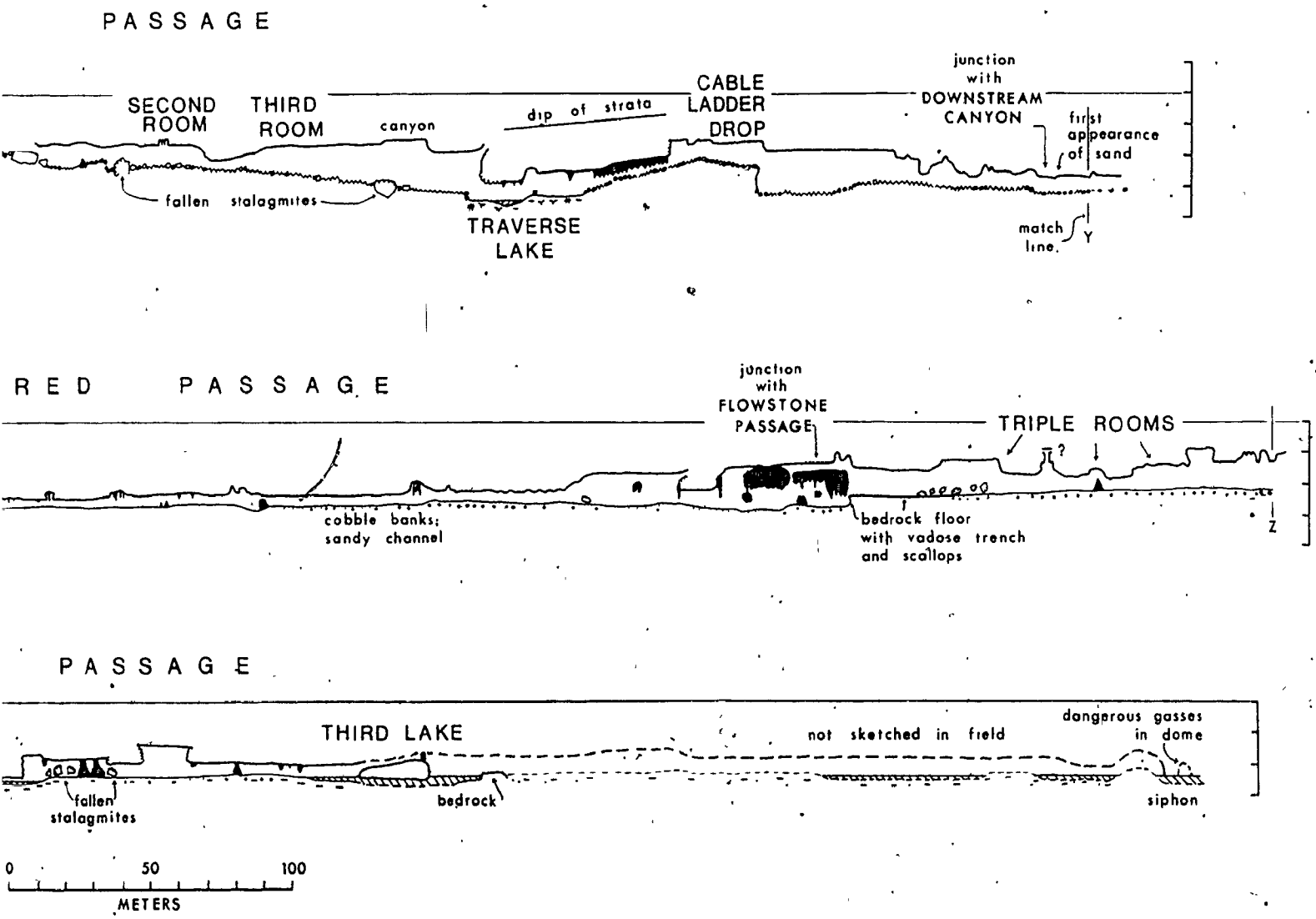

2 of 2

e . of part of Sótano de la Tinaja.

prepared (Figure 6.25). The boulder strewn floor of the sink continues as a ramp down into the first part of the Entrance Passage. This passage trends eastward for 550 m against the 5° WNW stratal dip. It usually varies from 25-50 m in cross-sectional area; and 3 rooms are encountered. The floor is covered by rounded collapse boulders except where mud, vegetal debris, and guano have collected in ponded areas against breakdown piles. Traverse Lake at -35.5 m is the lowest point; from it, flood waters must rise 14 m to reach the 8 m Cable Ladder Drop, the end of the Entrance Passage (Plate 6.28). Entrance Passage is a floodwater passage.

Directly east of Cable Ladder Drop, a large canyon becomes blocked by stalagmites after only 95 m. A side passage on the south wall of the canyon leads to Siphon Pit, a large 19 m deep pit. A climb up flowstone banks on the south wall of the pit leads to the Siphon Pit Series, a group of moderate to small passages and rooms at about the same elevation as the top of the Cable Ladder Drop. These passages are well decorated, and are not an important flood route. They probably developed as tributaries to the main cave. Exploration of South Branch has stopped at a 20 m pit containing bad air; there is a high level passage on the other side of the pit.

North of Cable Ladder Drop is the Sandy Floored Passage, one of the largest and most interesting in the Sierra de El Abra. The first 100 m is covered with rounded boulders, similar to Entrance Passage. At this point, a smaller passage trends to the east, meeting Linkage Passage in a muddy room. At the east end of the room at a depth of -31 m (4.5 m above Traverse Lake), the Downstream Canyon begins. It descends 51 m via short

drops and mud-coated slopes to a large lake that siphons at -82 m, the deepest known point in Tinaja. This passage is the major course for flood water in the cave, but the siphon must be above the local water table.

North of the downstream junction, the Sandy Floored Passage continues as a large horizontal gallery (Plate 6.29). Solution along cross joints has formed many domes and rooms. Large columns, flowstone banks, and a profusion of stalactites make this one of the best decorated passages in the El Abra. The terrigenous sediments are predominantly sand and gravel up to cobble size, with some mud deposited in areas of slower water velocity such as alcoves. Sand does not appear in the cave until just beyond the downstream junction. The 200 m of passage beyond the Colonnade Room has the best display (best sorting) of the sandy floor. At 575 m beyond the downstream passage, the Sandy Floored Passage makes a sharp left turn and bears generally northwest. After another 75 m, a bedrock vadose trench is encountered where the passage shifts up-section about 5 m. High up on the east wall at this point is Flowstone Passage. Although a large passage, it is smaller in comparison, and is often nearly blocked by flowstone. It bears northeast for 370 m and ends in a wide mud-floored room having several massive columns.

Beyond the junction with Flowstone Passage, the Sandy Floored Passage continues through some of its most spacious galleries to the Lake Passage. The passage is renamed here because it changes character. Morphologically, Lake Passage is generally similar to the Sandy Floored Passage, but it contrasts in having a series of six lakes and more mud. Second Lake is nearly a siphon, and Third Lake is a permanent sump that may be bypassed by

Plate 6.29 Part of the 1½ km long Sandy Floored Passage in Tinaja. There is a thick accumulation of sediment ranging from cobbles to silt or clay size. The sand and mud are derived from the Méndez or San Felipe formations. Here a recent coat of mud covers the floor.

Plate 6.30 An old fill in the Sandy Floored Passage. It contains cobbles in a matrix of clay (?) and sand. The old fill is being eroded and redistributed or removed.

a crawlway over it. Just beyond Second Lake is a large side passage that appears to be an active source of water, but it is blocked with mud. In the flowstone mass at the far end of Third Lake, a large re-solution hole, with a 0.5 m diameter tree stump in it, leads to a wide bedding-plane water crawlway that may be either a tributary or distributary of the main passage. Another 250 m of large horizontal passage with lakes and sandy floor reaches a permanent sump. The passage continues quite large, but its roof is just below the water surface. The siphon of this passage is perhaps only 30 m from Steve's Surprise Passage in Sotano del Arroyo.

At some time in the past, the sediment fill in the Sandy Floored Passage reached higher than it now does. There are some cobble banks (Plate 6.30), and there are several places beyond Triple Rooms where narrow remnants of the fill rise up to 2+ m above the floor. Also, there are good examples of stalagmites left hanging by the removal of the fill. The old fill is composed of sediment sizes ranging from clay to cobbles. The highest occurrence of the fill is between stalactites in Mud Room, 5.5 m above the present floor (see Figure 6.25). If the passage were uniformly filled to this level, First Lake (and possibly other low points) would have been blocked.

Presently, the Sandy Floored Passage-Lake Passage is an inlet. The water is derived from a large number of sources ranging from stalactite drips and flows, to spouting cracks, to tributary passages. These sources were observed to provide moderate flows soon after summer storms (no observations were made during storms when the flux must have been much greater). They decreased to seeps or drips over a few days, and most cease flowing

during the dry season. The flow direction is toward the Downstream Canyon, as shown by sand ripples up to 8 cm high, 1.5-2 cm scallops, cobble imbrications, and other flow markings in the channel. Large flows occurred at least twice in the period 1971-1972, wiping out the footprints of previous visits; and judging from the fresh mud veneers, the water reached a depth of 1 m in the Sandy Floored Passage. Thus, the two sites marked "flood sump" on the profile plus First and Second Lake must form temporary siphons during modest floods. Standing water was observed in the "flood sumps" after moderate summer storms.

The modern sediment distribution may be explained in terms of the sediment source, the flow direction, and the passage profile. Small floods are gradually eroding the old fill, causing many of the giant stalagmites that were resting on it to fall over. Material up to pebble size is being removed, leaving cobbles that armor the floor in many places. The highest point on the floor profile occurs just beyond Triple Rooms, and from there to Downstream Canyon, the floor descends gradually. There, the mud is winnowed out by the fast flows, except in alcoves and behind obstructions, leaving sand which is transported in the bedload, often as ripples. Beyond Triple Rooms, the percentage of mud increases because of ponding behind the high point of the passage. New sediment introduced via surface sinks into the Sandy Floored Passage is probably nearly all mud (and occasionally pieces of trees). The best information concerning the sequence of events occurs at the site marked "dated stal" on the map. At that locality, broken and abraded stalagmites are included in a sandy-gravel fill, on which rests a 2 m in diameter column. The fill probably does not extend downward more than a few meters because the bedrock floor

is exposed at several places along the passage.

Near the cave entrance, a small hole in the north wall drops down through breakdown to the Water Passage. It is a low, wide, wet and muddy passage that takes flood water through the breakdown. Curiously, this passage drains northward, in the opposite direction to the Sandy Floored Passage. After 300 m, there is a junction with an inlet passage that continues westward above a dome; it is not fully explored. It probably comes from an upstream piracy in the bed of the arroyo. It evidently provides a permanent trickle of water that flows down the north branch of the junction. The Water Passage continues horizontally northward true to character to a multilevel maze. Beyond a 9 m drop, a passage continues (unsurveyed) through a tight crawlway (Acupuncture Crawl) to more water passage and another drop. The Deep Blue Hole Siphon may be another water inlet. This passage may connect with Sótano del Arroyo, providing the permanent (?) trickle found in The Wallows, but there will probably be a sump in between.

The horizontal surveyed length of Tinaja is 4502 m and its depth is 82 m.

6.4.5.4 <u>The System</u>

Individually, the caves described above are among the larger caves known in México. El Sótano de Arroyo is México's longest, at 7200 m. The three are believed to be part of a much greater system named El Sistema de Los Sabinos (Fish, 1974). The aggregate length of known passages is over 13,200 m, but there unquestionably is much more passage to be found (see the inset in

Figure 6.24 which shows the caves in relation to the range and the Choy spring; also, see the geomorphic map, Figure 3.2). As yet no connections have been made, either by explorers or by dye tracing, although the intervening distances are probably no more than several tens of meters. The passage sizes and relationships are shown in a line plot (Figure 6.21) which was made from the cave surveys and air photo measurements of the distances between their entrances. It is believed that the Left Hand Passage in Arroyo connects via a siphon with the Second Level siphon in Cueva de Los Sabinos, and that the Water Passage in Tinaja connects (probably via a siphon) with Methane Passage or Second Right Hand Lead in Arroyo; however, although a connection between the end of the Sandy Floored Passage (or Lake Passage) in Tinaja and some part of Arroyo seems likely, any genetic relationship between these parts of the caves is unclear. It is also entirely possible that Disappointment Passage in Los Sabinos connects with one of the downstream passages of the Wallows in Arroyo. It is predicted that large quantities of water infiltrate the limestone outcrops (some of it in explorable caves) east of the presently known system and on the western flank of the range, and integrate with lower levels of the system. One particularly likely prospect for connection (as well as serving as a "target" during cave development) is a large sinkhole near the end of Stricklands Bad Air Passage in Arroyo; a dry valley leads to the sinkhole.

The origin and subsequent history of the system is most complex. More field data are needed before a detailed model can be proposed, but some generalities will be considered here. Not all parts of the caves are the same age. The First Level in Cueva de los Sabinos has different morphologic features than those found in Arroyo and Tinaja, and it is thought

to be of phreatic origin, and thus older than the others. Furthermore, there is no deeply entrenched arroyo leading to the cave, but it appears that the main channel or a tributary of the Río Sabinos passed over or near the entrance some time in the past. Perhaps water leaked down fractures at the entrance, which is located on some sort of anticlinal flexure (see strikes and dips on Figure 6.22). A group of small joint-controlled passages may also have been inlets, but they may have been distributaries. The lower parts of the Los Sabinos cave contrast with the character of First Level, are more like Arroyo, and in fact, are probably related to it. Sótano del Arroyo was created principally by its swallet stream. All of the passages on the left side of Main Passage and the Wallows (viewed into the cave) are downstream drains; the uppermost, the Left Hand Passage is now largely abandoned in favor of passages of the Wallows. The Thirty Foot Level is an old down-dip loop which was left behind as the entrance sink deepened and Main Passage became dominant. In Tinaja, at least the Entrance Passage, the Downstream Canyon, and (a large part of) the Water Passage have been created by flood waters sinking at the entrance. However, water presently enters the Sandy Floored Passage at many points and flows southward to the Downstream Canyon, and faint imbrication of cobbles in the old fill suggests that this has been the flow direction for a long time. The Sandy Floored Passage lies underneath the major channel of the ancient Río Sabinos (see Figure 3.2), which cut deeply below the top of the El Abra limestone, and there are additional dry valleys (tributaries), and up-dip El Abra exposures to the east. It is suggested that this passage was generated by many inlets from the overlying valley, forming an integrating system that flowed southward. The northern end of the Sandy Floored

Passage (actually the name is changed to Lake Passage there) and the complex of passages at the end of Second Right Hand Lead in Arroyo are particularly favorably situated to receive infiltration because they lie below the bed of an arroyo having 2-3 km^2 catchment at or near the point where it passes from the impermeable cover onto the El Abra limestone. No sinkholes could be detected on the air photos -- it appears that the valley floor contains alluvium. Perhaps a proto-major piracy is developing, but it seems possible that the Sandy Floored Passage is older than the Entrance Passage of Tinaja.

6.4.6 Other Caves

There are several other swallet caves along the western margin besides the ones described above. They will be mentioned only briefly here; locations for most are shown on Figure 3.1. La Cueva Chica, famous in the blind-fish literature, is a short cave having a relatively small catchment, and probably drains to the Río Tampaón. Sótano de Palma Seca and Sótano de las Piedras are two small, simple swallet caves that lie downstream on the drainage that has been captured by Jos (Mitchell et al., 1977). Between Tinaja and Jos lies the Sistema de Montecillos, a 3070 m long, 114 m deep system having two entrances (map and personal communication from Neal Morris). A deeply entrenched arroyo leads to a major swallet of an 8.4 km^2 basin; the cave below is well developed, but quickly siphons. An upstream piracy in the bed of the arroyo has generated a newer cave of smaller dimensions which has one passage that connects with the older cave, and another that leads to a large isolated passage, probably created by water pirated from an eastern tributary to the main arroyo.

This isolated passage apparently contains a permanent dry season stream (trickle). Part of the cave shows very strong joint control.

Approximately 3300 m north of Sótano del Arroyo lies another large swallet cave called Sótano del Tigre. It has a catchment of about 4.4 km^2, and is the highest of the Los Sabinos area swallets. The cave was surveyed, but the map is not given here because 600 m of the passage needs to be resketched. The arroyo has entrenched about 20 m into the El Abra limestone and the stream is captured down a joint-controlled shaft about 80 m deep. The passages in the vicinity of the entrance form a complex multilevel maze, formed in the early stage of the cave's development when flood waters forced open many bedding plane and joint distributaries; some of the routes rejoin at a lower level. One route predominated, and after passing horizontally 210 m and descending two drops, it intersects a major N-S passage. The northern part, the Ricinuleid Passage appears to have a thick sediment fill. The southern part is the main drain of the cave. It is a large conduit, 20 m wide and 10 m high in places, that gradually descends to a room 120 m long, 45 m wide, and 15-20 m high. A siphon occurs in an adjacent, smaller room. This conduit passes southward about 1400 m towards the Los Sabinos system. Altogether, more than 3000 m of passages have been surveyed and the total depth is 160 m.

Near Japonés, two other large swallet caves have developed. Walsh (1972) published a map of Sótano de Matapalma which shows that it consists mainly of one large conduit that generally traverses southeast from the entrance, and has a length of 1722 m and a depth of 86.3 m. Sótano de Yerbaniz (Plate 6.31) has recently captured most of the Matapalma drainage.

Plate 6.31 The slot-like entrance to Sótano de Yerbaniz. This is a young stream capture compared with Arroyo and Tinaja. The arroyo has entrenched only a few meters below the top of the El Abra limestone.

It has a catchment of approximately 21.8 km^2, the greatest of the El Abra swallets. No map of the cave has yet been published, but a description by Mitchell et al. (1977) indicates that it is a complex multi-level maze like Japonés. Russell (1972) reports a length of 1615 m and a depth of 95 m for the cave.

Sótano de Venadito, the only major swallet outside the southern El Abra area, is a large, incompletely explored system fed by a surface catchment of 7.7 km^2. One large western-flank cave, Cueva de Florida, is located in the northern El Abra range; it was not observed in this study.

6.5 Caves in Other Parts of the Region

6.5.1 The Coy Caves and Spring

The Nacimiento del Río Coy and associated caves are located at the north end of the Coy dome, 30 km south of Cd. Valles. The dome is an outcrop of backreef facies El Abra limestone in a broad valley of Mendez shale. It is about 3 km in diameter, and at the sharply folded northern end, it rises 140 m above the surrounding country to an elevation of 170+ m above sea level (see topographic map on Figure 6.26).

The Coy spring is one of the larger springs in the world, having a minimum instantaneous discharge of 13.0 m^3/sec and an average of about 24 m^3/sec in the period 1954-1971. It emerges horizontally through collapse boulders and cracks along a 50 m front. At base flow, the water surface is normally around 31.4 m a.m.s.l. (S.R.H. data), the lowest major spring site in the region. During floods, the stage often rises several meters

and water flows from cracks above the road as well as smaller ephemeral springs on the western side of the dome.

Above the spring, two caves have been found, and there undoubtedly are more. Figure 6.26 shows maps of the caves and their relationship to the spring. Directly up the hillside from the spring, the entrance to La Cueva leads down over a boulder slope to a short spacious cave, totally of phreatic origin and development. All the walls and ceiling are smoothly sculptured and pocketed. The first half of the cave passes directly through the 55° dipping beds. Then the cave turns along the strike and passes over a bedrock rise on the floor to a swiftly flowing stream. It is possible to swim and wade upstream 15 m to a siphon. Although it has not been tested, this stream undoubtedly connects to the spring. However, its flow is much less than the spring, so there is at least one, and probably several other sources (conduits). The S.R.H. has placed stage poles at the spring and in the cave stream. The correlation of the stage data shows good hydraulic connection, with a head loss of about 0.6 m at base flow and up to 1.2 m for large floods. The cave contains some stalagmite and flowstone deposits, and a minor amount of guano and earth.

Fifty meters east of the entrance to La Cueva and a little higher on the hillside is the steeply sloping entrance to another cave -- El Sótano de El Coy. The pit is an inclined tunnel that descends 26 m to a large room, 40 m long, 20 m wide, and 15 m high. The room has predominantly phreatic forms, but several large pieces of rock have fallen in the north part. A climb up through a small hole leads to what was an alcove of the room, now littered with talus from a collapse that formed another en-

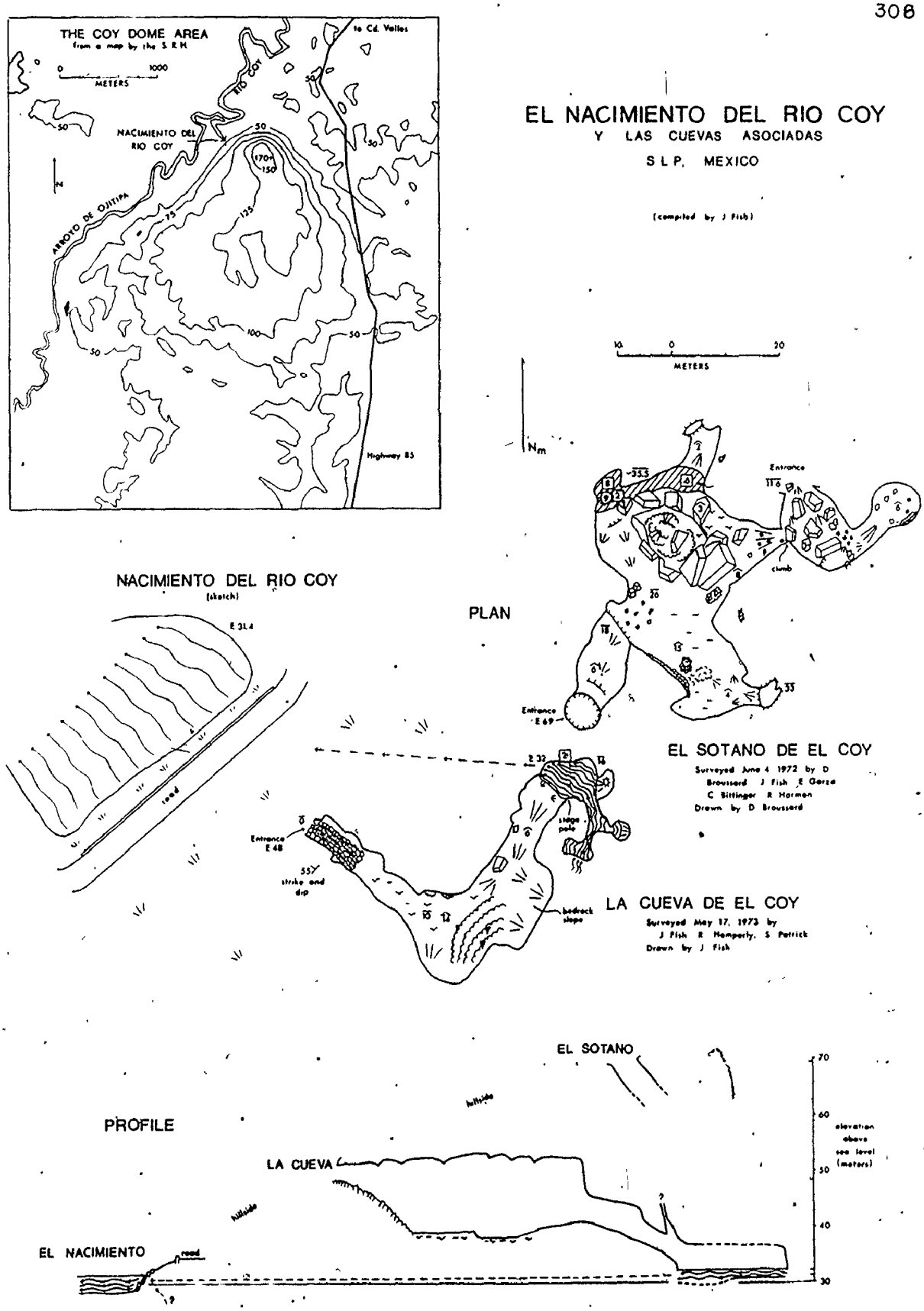

Figure 6.26 Maps of Las Cuevas y El Nacimiento del Río Coy.

trance. Along the north wall of the room, there is a lake up to 8 m deep. There appeared to be only slight movement of the water when the cave was visited. The cave and overland survey put the lake 3.6 m above the spring, which is probably too much.

6.5.2 Other Caves in the Region

Caves have been observed and explored by the author and by others in many parts of the region. However, because access is usually difficult, the nature of cavern development in most of the region is poorly known. Many areas have not been reconnoitered. Presently, the local relief is very high, up to 2000+ m, and very deep vadose cave systems can be expected. Access to the systems will often be hindered because so much of the infiltration occurs through a myriad of small sinks rather than at major swallets such as the Los Sabinos swallet caves. The Xilitla area has been subjected to karst solution processes for millions of years, and caves and pits have been found throughout most of the elevation range. Blind shafts are very common. There are some small stream sinks which lead to deep vadose caves. Sótano de Tlamaya is 454 m deep and over 1 km long, and Sótano de Huitzmolotitla is 245 m deep and about 3 km long. Some short, fossil phreatic caves have been found and there are also collapse rooms. The nearby Aquismón area has caves and some very large collapse pits and sinkholes. Sótano de las Golondrinas has approximately the shape of an upright elliptic cone 333 m deep, with a base measuring 134 x 305 m. The Sierra de Guatemala is also intensely karstified and caves have likewise been found at all elevations across the range. On the western side, there is a small polje at

1500 m where a lake often overflows in the wet season into a deep and complex cave called Sótano de la Joya de Salas.

It is suggested that significant cave development in the El Abra limestone will be found wherever the rainfall exceeds about 600-800 mm in the region. Some caves and solutional enlargement of fractures and bedding planes should be found in the drier areas. The importance of caves to the hydrology of the region is indicated by the above examples. Although more are known, they will not be described here, except to mention one other area. The area north and west of Jalpan lies near the southwestern margin of the Platform in a moderate rainfall zone (Figure 4.3). Caves and pits are very well developed there, including one collapse pit called El Sótano del Rancho Barro that is larger than the Golondrinas shaft. Some additional information on caves in the region can be found in Bonet (1953b), Russell and Raines (1967), Raines, ed. (1968), and Mitchell et al. (1977).

CHAPTER VII

ANALYSIS AND SYNTHESIS

Previous chapters have each considered an individual subject, presenting data, calculations, and some interpretations for each topic. This chapter summarizes that information, analyzes it further, synthesizes it into models and interpretive discussions, and occasionally compares the results with others reported in the literature. This task is complicated by the fact that the subjects are intimately interrelated; a full understanding of the regional ground-water hydrology cannot be attained without knowledge of the local hydrology (here represented mainly by the Sierra de El Abra studies), and vice versa. It was deemed best to begin with the hydrochemical modeling and its hydrologic implications, followed successively by analyses and discussions of the regional ground-water system, the Sierra de El Abra hydrology, and the caves. This sequence, therefore, proceeds from regional to local considerations.

7.1 Hydrochemical Analysis

In this section the hydrochemistry of the springs will be analyzed to develop a hydrochemical model of the karst flow systems in the region.

7.1.1 Review of Hydrochemical Data and Interpretations

Excluding the thermal springs, the chemical analyses presented in Chapter V reveal that there are two basic types of effluent karst ground waters in the region. The first is a "normal" karst water, i.e., a calcium-bicarbonate type, with a calcium carbonate hardness of 120-220 mg/l (2.4-4.4 meq/l of Ca). The Mg content is small and variable, probably depending upon how much dolomite or magnesian calcite the water has been in contact with, and the residence time in the aquifer. The second type has much higher concentrations of Ca, Mg, and SO_4 than the first and about the same or slightly higher alkalinity. It is really a calcium-sulfate water, but with a lower Ca/Mg ratio than the first type.

These springs represent the integrated output of complex karst ground-water flow systems. Although the precise source areas of the springs are not known, it is often assumed that the water comes from the mountain range in which each spring occurs. However, in this region, the possible source rocks for the dissolved constituents indicate a more complicated hydrogeologic system. The source of the aqueous SO_4 and high Ca concentrations is believed to be the gypsum and anhydrite of the Guaxcamá Formation, which is thought by Pemex geologists (Carrillo Bravo, 1971) to underlie the El Abra Formation over a large portion of the Platform, west of a Lower Cretaceous reef. This reef is thought to be approximately coincident with the Sierra la Colmena in the southern part of the Platform, but shift somewhat eastward farther north (see Figures 2.2 and 2.4). Some of the SO_4 might be derived from the La Borreguita Formation which occurs in the broad Río Verde valley in the western portion of the

Platform; this possiblity will be discussed later. In Figure 7.1, the Mg_{tot} and SO_{4tot} contents of 13 springs are plotted, using the best base flow analysis of each. It clearly distinguishes the two water types discussed above, and shows that the Mg_{tot} and SO_{4tot} concentrations are broadly correlated. Some of the Mg may be derived from a solution of dolomite-bearing limestone and leaching of magnesian calcite; however, a more likely source rock is the basal dolomite of the El Abra Formation.

The distribution of minerals in the region requires that a mixing model of two or more sources be developed to explain the chemistry of the calcium-sulfate type springs. The correlation between Mg and SO_4 suggests that a simple two-source model may be adequate. Such a model for the Coy and Choy springs is shown in Figure 7.2 where a "local" source supplies a calcium-bicarbonate type water derived from circulation strictly within the El Abra or Tamasopo limestones, and a deep regional source from recharge areas farther west brings a concentrated solution of Ca, Mg and SO_4 plus carbonate species to the springs. For the Choy, the local source is of course the Sierra de El Abra. For the Coy, the nearest possible local source is the area west of Aquismón; thus, both its local and regional flow are artesian in the valley surrounding the Coy dome and water from both sources must flow a long way to reach the spring. The "flood" paths of the Coy and Choy springs from Figure 5.8 are reproduced in Figure 7.1. The approximately linear paths strongly support a two-source model meaning the mixing of two gross chemical types of water (of course, in reality there are a multitude of physical sources for the water that is discharged from each spring, but only two chemical types). Whatever the composition (somewhat variable) of the regional source, the local source

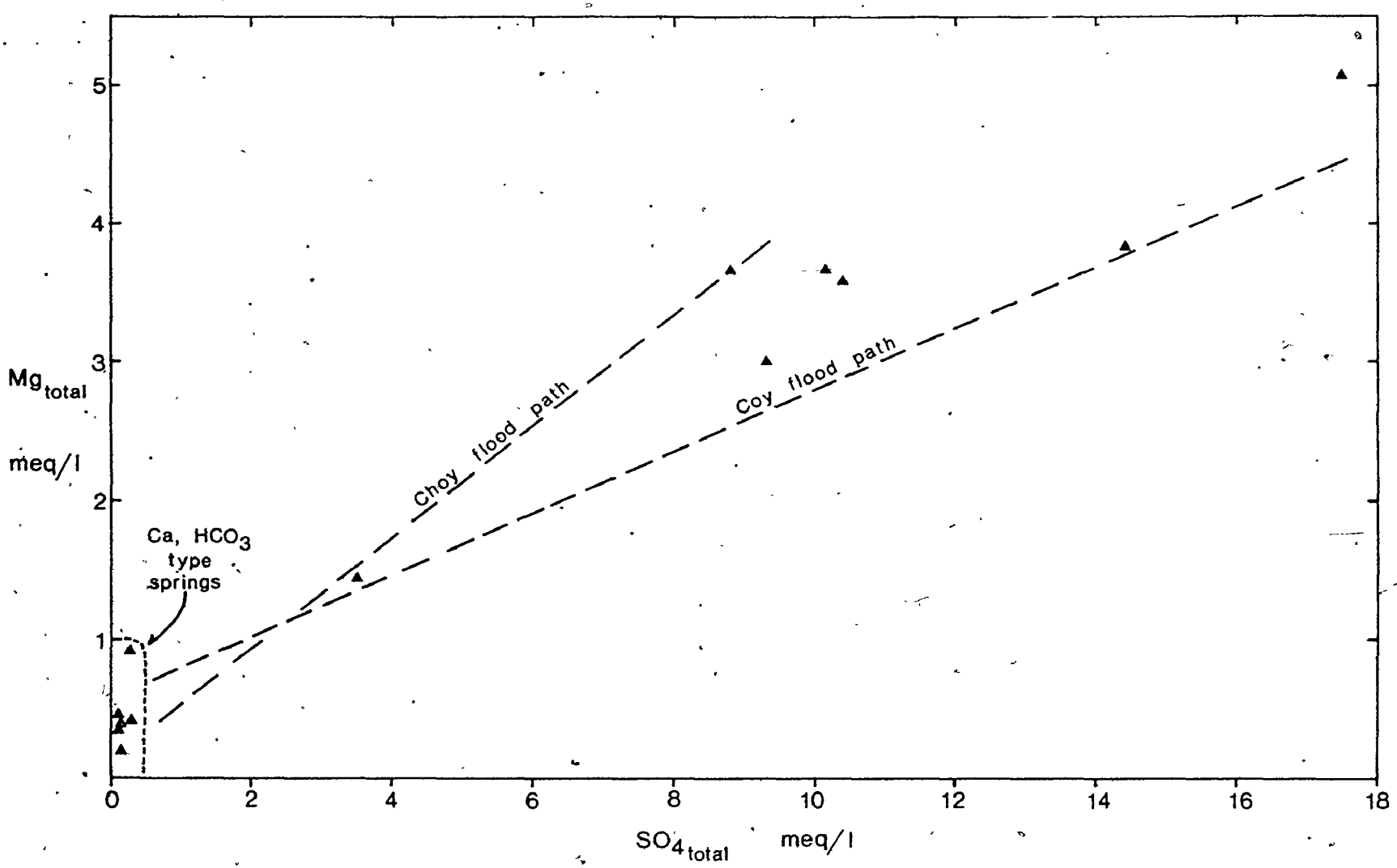

Figure 7.1 Plot of Mg against SO_4 for best base flow analysis of 13 springs. A high Ca, Mg, SO_4 water mixes in varying amounts with a Ca, HCO_3 water.

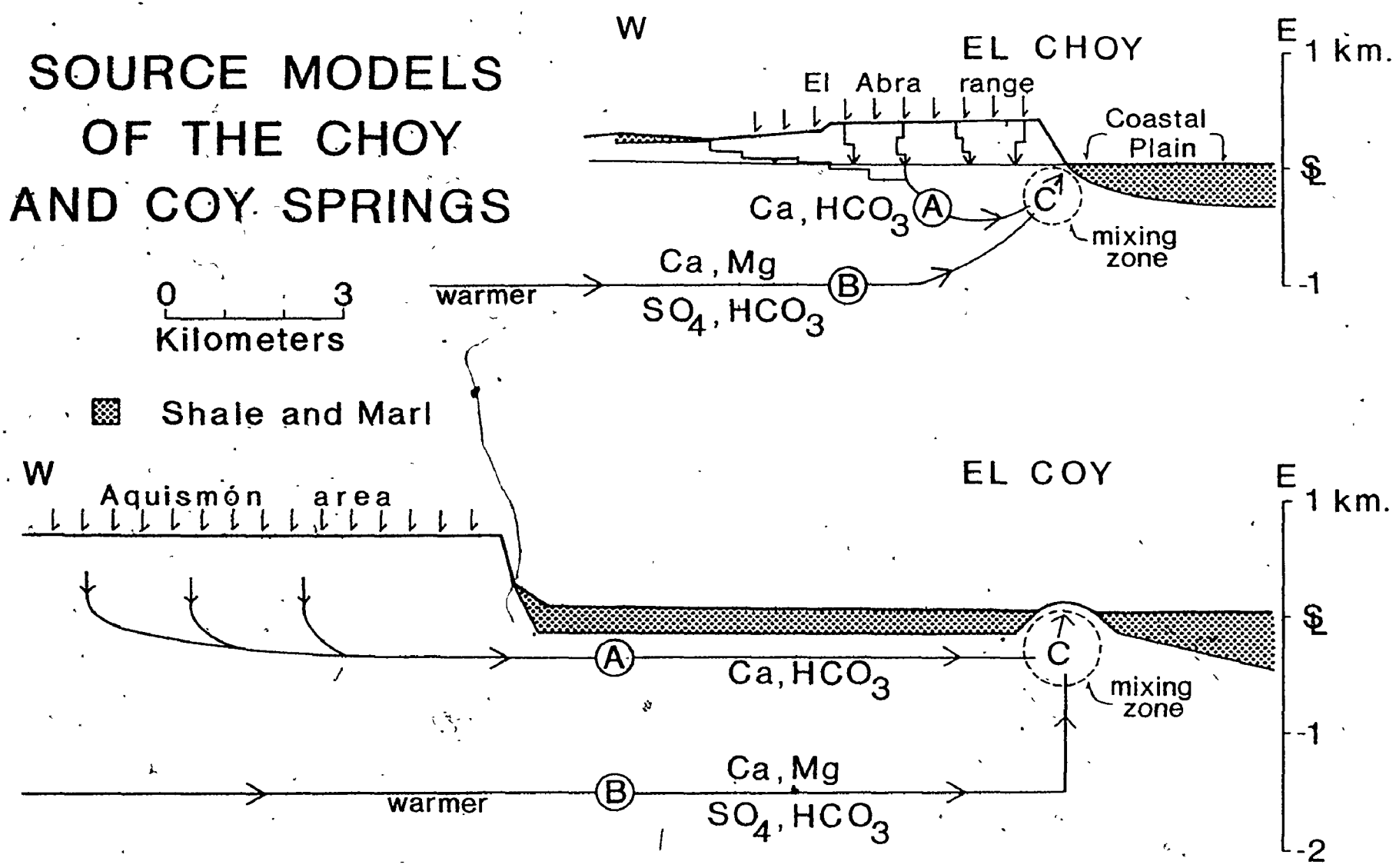

Figure 7.2 Two - source mixing model for the Choy and Coy springs.

is a nearly perfect "dilutant", because it has very little dissolved SO_4 and Mg. For each spring, the dry season discharge would be a mixture of differing amounts of the two sources of water. During flooding, the output concentrations would greatly decrease as the flux from the local source dominates the mixing volumes (Figure 7.2). The Coy and Choy lines appear to represent the extreme values of the Mg/SO_4 ratio of the regional water; the other springs sampled lie somewhere between them.

It was shown in Section 5.3 that there is also a correlation between temperature and SO_4 concentration for individual springs during flooding. The interpretation is that the local sources for each spring will have a temperature dependent largely on the climatic conditions of its recharge area; some of the local water mixes with the warmer regional water to produce the family of parallel flood mixing curves shown in Figure 5.9. Thus, the Choy and the Mante are very similar, while the Coy "dilution" curve is nearly parallel, but offset because its local source water comes from a higher, cooler area. The temperature of the regional water also undoubtedly differs (slightly?) from spring to spring, but it is likely constant for a given flow system.

7.1.2 The Geochemical Model

In this section, a geochemical model of the hydrogeology will be developed. Such models are helpful in understanding the flow system, in placing limits on the concentrations of dissolved species, and may be useful for quantitative hydrology. Wigley (1973) has given a theoretical discussion of the calcite-gypsum-water system, which shows various

"evolutionary chemical paths" of water as it comes in contact alternately with each of the minerals. Here, some aspects of the more complicated calcite-gypsum-dolomite-water-carbon dioxide system will be examined.

The chemical model is shown in Figure 7.3. Initially, water infiltrates the massive El Abra limestone, becoming highly charged with CO_2 from the soil and fissure (or cave) air. Ground-water type "A" is the general chemical composition of the vadose and phreatic waters circulating within the limestone where calcite solution (and a little dolomite) in a relatively open system is the principal process. The residence time for most of the type A water in the aquifer is probably short, and most of it is discharged back to the surface as type "1" spring water. This couplet is represented by the cave drip and cave lake samples taken in the El Abra range (type A), and by the small springs (Canoas, Santa Clara, Arroyo Seco) and some of the large springs such as the Huichihuayán, the San Juanito, and the Sabinas (type 1).

Some fraction of the total of the type A ground water circulates more deeply. It passes through the limestone to reach the basal dolomite of the El Abra Formation and the gypsum below that. By then, the water is well below the water table, thus effectively closed to additional CO_2, and will probably have reached equilibrium with respect to calcite. Upon contact with the new minerals, the water begins to <u>evolve</u> toward type "B" ground water. As gypsum (or anhydrite) and dolomite dissolve, the Ca_{tot} content greatly increases causing precipitation of calcite. Note that the dolomite solution reaction (Figure 7.3) is written in the incongruent form to show that to a large extent, what occurs is the exchange of Ca for Mg

CROSS SECTION

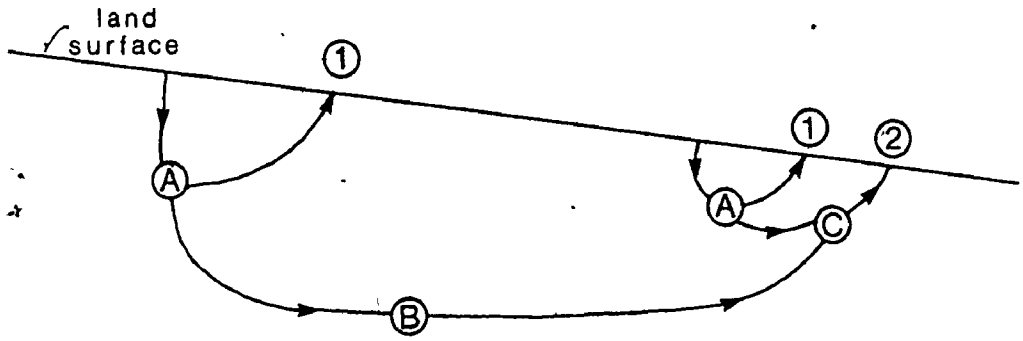

REACTIONS:

Ⓐ

$CaCO_3 \rightleftharpoons Ca^{++} + CO_3^{=}$
$H_2O + CO_2 \rightleftharpoons H_2CO_3$
$H_2CO_3 \rightleftharpoons H^+ + HCO_3^-$
$HCO_3^- \rightleftharpoons H^+ + CO_3^{=}$
$H_2O \rightleftharpoons H^+ + OH^-$

Solution of calcite in a partially open system with pP_{CO_2} between 1.4-2.0; nearly saturated with respect to calcite

Ⓑ

$Ca^{++} + CO_3^{=} \rightleftharpoons CaCO_3$
$CaSO_4 \cdot 2H_2O \rightleftharpoons Ca^{++} + SO_4^{=} + 2H_2O$
$CaMg(CO_3)_2 + Ca^{++} \rightleftharpoons 2CaCO_3 + Mg^{++}$
$Ca^{++} + SO_4^{=} \rightleftharpoons CaSO_4^{\circ}$
$Mg^{++} + SO_4^{=} \rightleftharpoons MgSO_4^{\circ}$
$Mg^{++} + HCO_3^- \rightleftharpoons MgHCO_3^+$
plus carbonate equilibria

Solution of gypsum or anhydrite and incongruent solution of dolomite; precipitation of calcite; formation of important ion pairs; increase of temperature

Ⓒ

$CaCO_3 \rightleftharpoons Ca^{++} + CO_3^{=}$

Mixing of types A and B above; possible precipitation or solution of calcite; Mg_{tot} and SO_{4tot} conserved

FIGURE 7.3 The geochemical model

in the solution. The result would be calcitization of the dolomite beds, with the added possibilities of the formation of dedolomite, and calcite after gypsum (or anhydrite). A similar scheme has been recently proposed by Abbott (1974) for the Edwards limestone (equivalent to the El Abra Formation) of central Texas where there is much more petrographic, geochemical, hydrologic, and geological information available. An instance and a petrographic description of a dedolomite has been given by Lucia (1961).

Type B ground water eventually loses contact with the gypsum and the dolomite. It passes laterally and upwards through limestone beds, but theoretically, the chemical composition should not change because the solution is saturated with respect to calcite, and it has left the gypsum-dolomite region. Ultimately, it mixes with some local Ca, HCO_3 (type A) ground water to form type C ground water. This water is then discharged from the aquifer, providing the second type of spring water chemistry found in the region -- the high Ca, Mg, and SO_4 waters of springs such as the Coy and the Choy (type 2). The undersaturation with respect to dolomite and gypsum in all of the type 2 springs, and the nearly monomineralic solid phase of calcite in the mixing zone of type C water means that SO_4 and Mg are conserved after the mixing occurs. As shown in section 5.3, the base flow of these springs is saturated to slightly supersaturated with respect to calcite except for periods of a few weeks (for the Coy) to a few months (for the Choy) after moderately large floods. This means that Ca and the CO_3 (species) may not be conserved -- calcite could be precipitated or dissolved after mixing. If the volume of the mixing zone

is approximately the same as the volume that was flushed out by the local source flood water, then type C ground water would have a relatively short (up to a few months) residence time. This suggests that not much additional calcite could be dissolved by type C ground water. Hence, in this chemical model, there are three kinds of ground water, and two kinds of spring water.

The ionic concentrations and the degree of calcite saturation varies spatially within the limestone aquifer (they are distributed parameters of the system), depending on each hydrochemical environment (see section 5.2) and on the residence time. Some theoretical evolutionary models for the solution of pure calcite in water with CO_2 have been given by Langmuir (1971). These have been recalculated for 25°C and are shown in Figure 7.4. Ground water open to a reservoir of constant P_{CO_2} and dissolving calcite would pass diagonally upwards along a line parallel to the lines of constant P_{CO_2} shown. If the water at some time loses contact with the CO_2 reservoir, then the CO_2 is gradually used up and the chemistry will move along a curved path such as the one marked "no more CO_2 added". A water that has become saturated, but that is exposed to varying P_{CO_2} along its flow paths, will adjust to each new condition by moving along the calcite saturation line. Based on these models and the field data (Table 5.1), the deep type A ground water will probably be saturated with respect to calcite, and have 3.5 to 5.25 meq/l of Ca^{++} and HCO_3^- at pP_{CO_2} ranging from 2.0 to 1.5.

Unfortunately, there are no samples of type B ground water for analysis. Because it would be useful to know what its composition might be, a theoretical investigation was made. The pertinent chemical reactions are: the solution (or precipitation) of calcite, dolomite and gypsum;

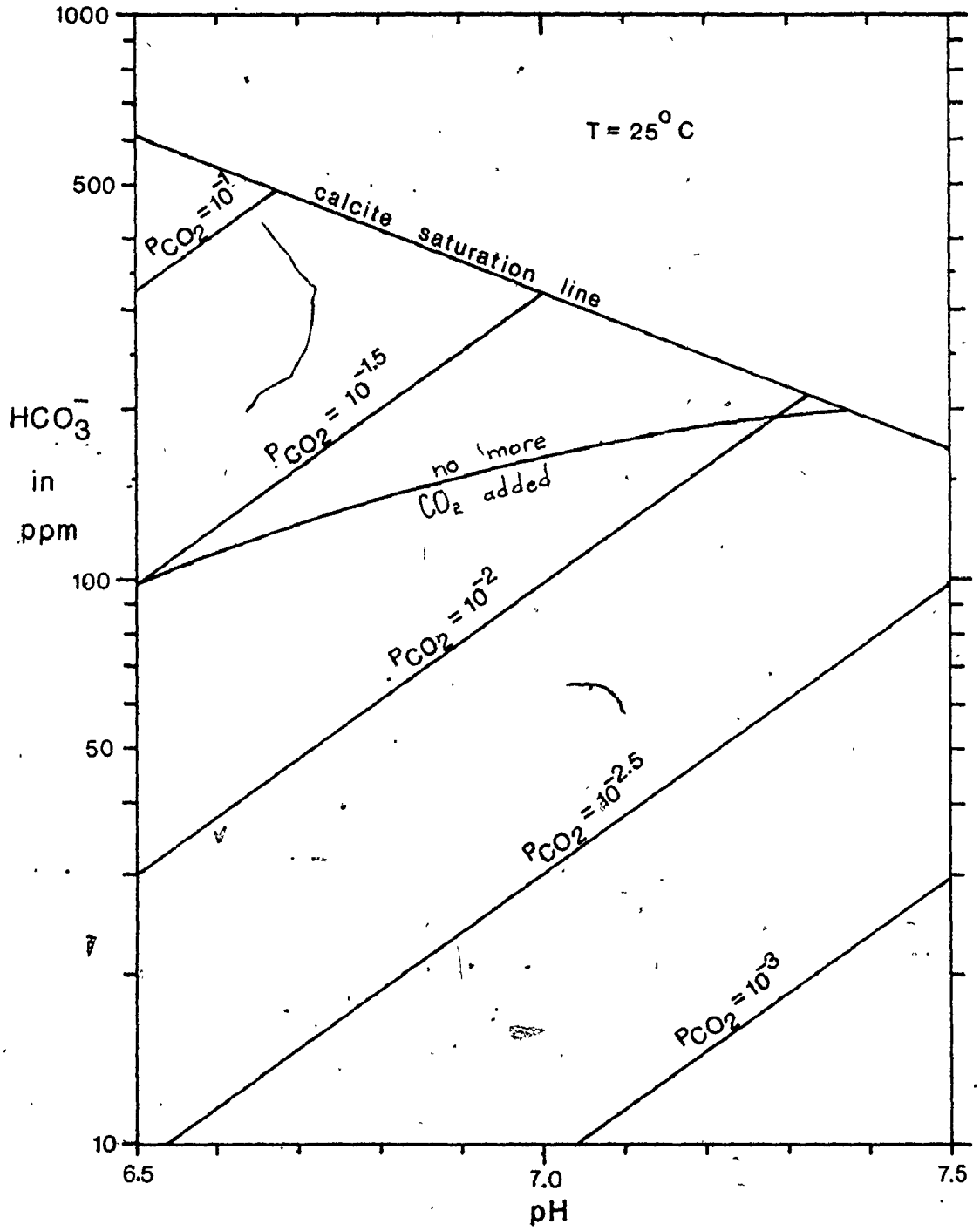

Figure 7.4 Evolutionary calcite solution diagram, HCO_3 against pH.

TABLE 7.1

Equilibrium Constant Functions

Equilibrium constant (temperature "t" dependent)	source
$\log(K_{calcite}) = -8.3389 - 0.001236t - 0.00005t^2$	1
$\log(K_{dolomite}) = -16.5614 - 0.012486t - 0.0001999t^2$	1
$\log(K_{gypsum}) = -4.6407 + 0.002488t - 0.0000592t^2$	1
$\log(K_{CaSO_4^\circ}) = -2.2000 - 0.002517t - 0.0000433t^2$	1
$\log(K_{MgSO_4^\circ}) = -2.03 - 0.0132t$	2
$\log(K_{MgHCO_3^+}) = -0.95$ (at 25°C; assumed for all temperatures)	3
$\log(K_{H_2CO_3}) = -6.577 + 0.01264t - 0.000144t^2$	1
$\log(K_{HCO_3^-}) = -10.25$ (at 35°C); -10.29 (at 30°C)	4
$\log(K_{CO_2}) = -1.585$ (at 35°C); -1.53 (at 30°C)	4

1) Wigley (1972)

2) Langmuir (1971)

3) Hostetler (1963)

4) Garrels and Christ (1965) - interpolated from their values

Individual activity coefficients were calculated with the Debye-Huckel equation:

$$-\log \gamma_i = \frac{A\, z_i^2 \sqrt{I}}{1 + \mathring{a}_i\, B \sqrt{I}}$$

The constants were taken from Garrels and Christ (1965).

solution of CO_2 and the various carbonate species dissociation equilibria; and the ion pair reactions to form $CaSO_4^o$, $MgSO_4^o$, and $MgHCO_3^+$. The equilibrium constant functions used are given in Table 7.1. A computer program was written which calculated the concentrations of the dissolved species and the pP_{CO_2} for a specified temperature, pH, and degree of saturation with respect to calcite (SI_c), dolomite (SI_d), and gypsum (SI_g). Selected results are given in Table 7.2.

An equilibrium model ($SI_c = SI_d = SI_g = 0$) was tested over the pH range 6.0-8.5 at 30° and 35°C (Table 7.2a). The following observations are made:

1) the CO_{3tot} and the P_{CO_2} decrease greatly with an increase in pH; the extreme values of pH give unreasonable values of CO_{3tot} and P_{CO_2};

2) for the pH range of 6.5-8.5, there is very little change in Ca_{tot}, Mg_{tot}, and SO_{4tot}; for increasing pH, the Ca_{tot} and Mg_{tot} decrease slightly while the SO_{4tot} increases slightly; thus, within the range of its possible values, the P_{CO_2} is not an important control of the concentrations of the three principal constituents;

3) the $CaSO_4^o$ and $MgSO_4^o$ ion pairs are important components of the solution; about 45% of the Mg_{tot} and 40% of the SO_{4tot} are tied up in these ion pairs;

4) the equilibrium calcite-dolomite-gypsum-water system has one-third more SO_{4tot} than the simple gypsum-water system at 35°C

(Column 1) because the ionic strength is larger and because the $MgSO_4^{\circ}$ ion pair is quantitatively important; these factors overwhelm the suppressing effect of the common ion Ca^{++}; note that the equilibrium models do not contain more Ca_{tot} than the pure gypsum water;

5) the ionic strength decreases slightly with both increasing pH and increasing temperature; the greatest change is in Mg_{tot} with temperature;

6) in the evolution of type A water to a saturated type B water, the $a_{Ca^{++}}$ will increase about 2.5 times causing a reciprocal change in the $a_{CO_3^{=}}$; then, from the dissolved carbonate species equilibria, the expected change in the pH would be a decrease of a few tenths (less than log 2.5) and the CO_{3tot} would remain about the same; thus, the favored composition would have a pH in the range 6.5-6.9 for temperatures between 30-35°C; at 35°C, a pH of 6.84 is neutral.

Some authors (e.g. Langmuir, 1971) believe that the theoretical solubilities of calcite and dolomite may effectively control the chemistry of ground water in carbonate rocks. Others (e.g. Back and Hanshaw, 1970 and 1974) have found that the concentrations of dissolved species commonly increase with the length of the flow path. Frequently, the water becomes supersaturated with respect to calcite and dolomite, but often the specific concentrations of sulfate and the saturation condition with respect to sulfate minerals in particular is not given. It appears that the waters are generally undersaturated with respect to gypsum. Possible explanations

TABLE 7.2

Possible Theoretical Compositions of Type B Ground Water

7.2a Equilibrium Models — concentrations in millimoles per liter

Column No.	1	2	3	4	5	6	7	8	9	10	11	12	13	14
T (°C)	35	30			35									
SI_c	$-\infty$	$SI_c = SI_d = SI_g = 0$			$SI_c = SI_d = SI_g = 0$									
SI_d	$-\infty$													
SI_g	0													
pH	—	6.5	6.8	7.0	6.0	6.5	6.6	6.7	6.8	6.9	7.0	7.5	8.0	8.5
Ca_{tot}	15.07	15.12	14.48	14.23	17.66	15.36	15.13	14.93	14.78	14.65	14.55	14.29	14.20	14.18
Mg_{tot}	—	8.57	8.19	8.05	8.61	7.49	7.38	7.29	7.21	7.15	7.10	6.98	6.94	6.92
SO_{4tot}	15.07	20.47	20.97	21.19	18.80	20.11	20.29	20.44	20.55	20.65	20.74	20.97	21.05	21.07
CO_{3tot}	—	9.65	4.21	2.50	38.03	8.15	6.13	4.65	3.55	2.73	2.11	0.619	0.192	0.061
pP_{CO_2}	—	.946	1.522	1.91	0.046	0.974	1.17	1.36	1.55	1.75	1.94	2.93	3.93	4.93
Ca^{++}	9.88	10.16	9.52	9.27	12.47	10.17	9.94	9.75	9.59	9.46	9.37	9.10	9.02	8.99
Mg^{++}	—	5.02	4.71	4.59	5.07	4.16	4.07	3.99	3.93	3.88	3.84	3.74	3.70	3.69
$SO_4^{=}$	9.88	12.10	12.61	12.82	10.38	11.69	11.87	12.02	12.13	12.23	12.32	12.55	12.63	12.65
HCO_3^-	—	6.17	3.25	2.10	14.32	5.28	4.28	3.45	2.77	2.23	1.78	0.577	0.184	0.058
$CaSO_4^o$	5.19	4.96	4.96	4.96	5.19	5.19	5.19	5.19	5.19	5.19	5.19	5.19	5.19	5.19
$MgSO_4^o$	—	3.41	3.41	3.41	3.23	3.23	3.23	3.23	3.23	3.23	3.23	3.23	3.23	3.23
$MgHCO_3^+$	—	0.138	0.069	0.043	0.315	0.098	0.078	0.062	0.049	0.039	0.031	0.010	0.003	0.001
$CO_3^{=}$	—	.0019	.0019	.0020	.0015	.0017	.0018	.0018	.0018	.0018	.0018	.0019	.0019	.0019
H_2CO_3	—	3.34	0.886	0.361	23.40	2.76	1.78	1.14	0.729	0.465	0.296	0.030	0.003	.0003
% CO_2	—	11.32	3.00	1.22	89.98	10.63	6.84	4.38	2.80	1.79	1.14	0.117	0.012	.0012
Ca_{tot}/Mg_{tot}	—	1.764	1.768	1.768	2.051	2.051	2.050	2.048	2.050	2.049	2.049	2.047	2.046	2.049
Ca_{tot}/SO_{4tot}	1.00	0.739	0.691	0.672	0.939	0.764	0.746	0.730	0.719	0.709	0.702	0.681	0.675	0.673
Mg_{tot}/SO_{4tot}	—	0.419	0.391	0.380	0.458	0.372	0.364	0.357	0.351	0.346	0.342	0.333	0.330	0.328

TABLE 7.2

Possible Theoretical Compositions of Type B Ground Water

7.2b — Non-equilibrium models — concentrations in millimoles per liter

Column No.	15	16	17	18	19	20	21	22	23	24	25	26	27	28	29	30	31	32
T (°C)				35°C													35°C	
SI_c	0	0	0	0.18	0.30	0.18	0.30	0	0	0	0.10	0.12	0.12	0.12	0.30	0.30	0	0.18
SI_d	0	0	0	0.18	0.30	0.18	0.30	-0.12	-0.12	-0.15	0	0	0	0	0.18	0	0.18	-0.18
SI_g	0	-0.18	-0.30	0	0	-0.30	-0.30	0	-0.30	0	0	0	-0.10	-0.30	0	0	0	-0.18
pH	6.8	6.8	6.8	6.8	6.8	6.8	6.8	6.8	6.8	6.8	6.8	6.8	6.8	6.8	6.8	6.8	6.8	6.8
Ca_{tot}	14.78	10.95	8.98	15.08	15.36	9.35	9.71	15.17	9.28	15.25	15.28	15.37	13.00	9.53	15.80	16.18	13.93	12.02
Mg_{tot}	7.21	5.31	4.33	7.36	7.49	4.50	4.67	4.25	2.57	3.72	4.70	4.31	3.63	2.64	4.33	1.97	15.37	1.15
SO_{4tot}	20.55	14.58	11.44	20.33	20.11	11.18	10.96	18.10	10.13	17.67	18.31	17.96	14.77	9.97	17.62	15.81	27.55	11.11
CO_{3tot}	3.55	4.19	4.67	5.21	6.79	6.69	8.57	3.30	4.33	3.25	4.14	4.28	4.68	5.54	6.27	5.89	4.23	5.20
pP_{CO_2}	1.55	1.47	1.42	1.39	1.27	1.27	1.16	1.58	1.45	1.59	1.48	1.47	1.42	1.34	1.30	1.33	1.49	1.37
Ca^{++}	9.59	7.49	6.38	9.89	10.18	6.75	7.11	9.98	6.67	10.06	10.09	10.18	8.89	6.93	10.61	10.99	8.75	8.56
Mg^{++}	3.93	3.10	2.66	4.05	4.16	2.81	2.96	2.36	1.61	2.08	2.62	2.41	2.12	1.67	2.45	1.13	7.98	.706
$SO_4^{=}$	12.13	8.96	7.22	11.91	11.69	6.96	6.73	11.06	6.59	10.86	11.08	10.92	9.17	6.43	10.61	9.81	15.09	7.23
HCO_3^-	2.77	3.26	3.63	4.06	5.30	5.21	6.66	2.58	3.38	2.55	3.24	3.35	3.66	4.32	4.92	4.63	3.27	4.08
$CaSO_4^o$	5.19	3.46	2.60	5.19	5.19	2.60	2.60	5.19	2.60	5.19	5.19	5.19	4.12	2.60	5.19	5.19	5.19	3.46
$MgSO_4^o$	3.23	2.15	1.62	3.23	3.23	1.62	1.62	1.86	.932	1.62	2.04	1.86	1.48	.932	1.82	.808	7.27	.426
$MgHCO_3^+$	.049	.048	.048	.074	.099	.072	.096	.028	.027	.024	.039	.037	.037	.036	.055	.024	.113	.014
$CO_3^=$	.0018	.0020	.0022	.0027	.0035	.0031	.0040	.0017	.0020	.0016	.0021	.0021	.0023	.0025	.0032	.0029	.0022	.0024
H_2CO_3	.729	.875	.986	1.066	1.388	1.410	1.800	.684	.923	.676	.857	.887	.980	1.179	1.298	1.230	.845	1.107
% CO_2	2.80	3.36	3.79	4.10	5.34	5.42	6.92	2.63	3.55	2.60	3.30	3.411	3.77	4.53	4.99	4.73	3.25	4.26
Ca_{tot}/Mg_{tot}	2.050	2.062	2.074	2.049	2.051	2.078	2.079	3.569	3.611	4.099	3.251	3.566	3.581	3.610	3.649	8.213	.906	10.452
Ca_{tot}/SO_{4tot}	.719	.751	.785	.742	.764	.836	.886	.838	.916	.863	.835	.856	.880	.956	.897	1.023	.506	1.082
Mg_{tot}/SO_{4tot}	.351	.364	.372	.362	.372	.403	.426	.235	.254	.211	.257	.240	.246	.265	.246	.125	.558	.104

of these discrepancies include: 1) uncertain value of $K_{dolomite}$; 2) precipitation kinetics, and degree of supersaturation necessary to overcome the nucleation potential (Plummer, 1972, suggests that an SI_c of about +0.3 is necessary to precipitate calcite); and 3) greater solubility of impure calcite. Supersaturation with respect to calcite or dolomite may especially occur where gypsum is being dissolved faster than calcite (or dolomite) can be precipitated to maintain equilibrium (Back and Hanshaw, 1970; Mercado and Billings, 1975). Considering the sequential exposure of source minerals along the flow path in this model and the increase of ionic strength in type B water, it is also possible that the regional flux may be undersaturated with respect to either or both dolomite and gypsum. Therefore, using the computer program, the chemical composition for a variety of saturation states has been determined at pH 6.8 and 7.0. Selected results are listed in Table 7.2b.

The only checks available on the possible composition of type B ground water are the analytical data for the springs, aqueous chemistry theory, and field results of other studies. Figure 7.5 is a plot of Ca_{tot} and $Ca_{tot} + Mg_{tot}$ against SO_{4tot} for selected analyses from this study; most of the samples are from the dry season base flow, but a few intermediate to high flood flow samples are included for comparison. Presumably, the higher the concentrations of these constituents, the greater the percentage of type B water in the mixed output. The $Ca_{tot} + Mg_{tot}$ line is approximately parallel to the $Ca_{tot} = SO_{4tot}$ line (gypsum solution), but the Ca_{tot} line has a lesser slope. The relatively linear fit of the data shows that a mixing model of two waters having greatly different and constant composition is a good first approximation of the system. The di-

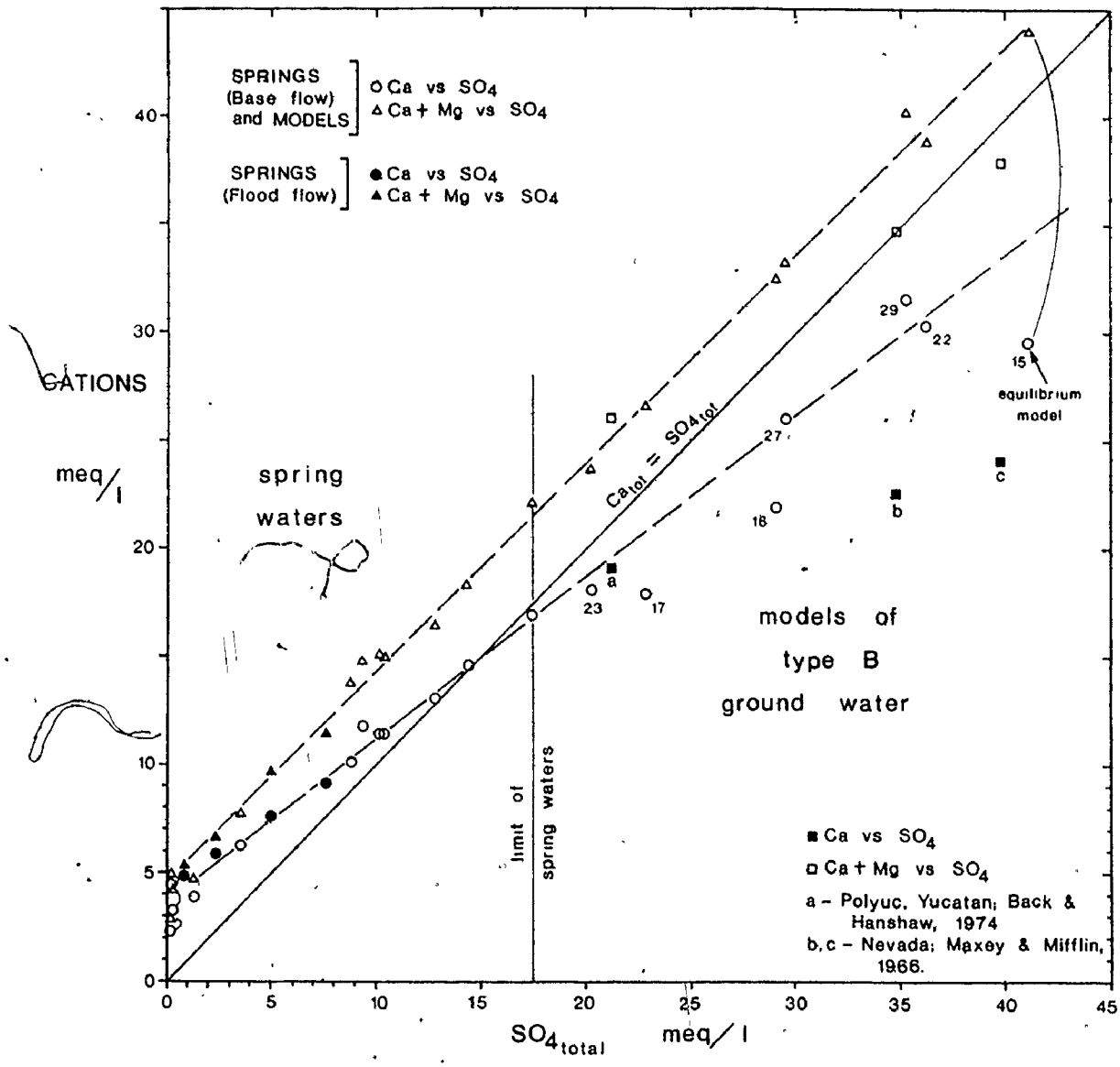

Figure 7.5 Ca against SO_4, and Ca + Mg against SO_4 for springs and theoretical models of type B ground water.

vergence of the two lines supports the chemical model of type B water in which as gypsum is dissolved, the common ion Ca^{++} is "suppressed" by calcite precipitation and the "exchange" of Mg for Ca by incongruent solution of dolomite. Note that the Ca_{tot}/SO_{4tot} of the Media Luna and of the Coy (sample no. 65, Table 5.1; not plotted) have just crossed into the realm where the Ca_{tot}/SO_{4tot} is less than 1. Also, the Coy values of Ca_{tot} + Mg_{tot} fall slightly below the line indicated by the others.

The Ca_{tot} and Ca_{tot} + Mg_{tot} lines of Figure 7.5 have been extrapolated so that the various hypothetical chemical compositions in Table 7.2 may be tested for agreement, within the reasonably expected deviations from the lines. First note that the extrapolated total hardness line shows that the type B water would have an alkalinity of about 4 meq/l if, as previously discussed, there is no great change in SI_c of the type C water. The following general observations are made for 35°C:

1) it is assumed that $0 \leq SI_c \leq +0.3$, and that $SI_g \leq 0$;

2) $SI_c - 0.15 \leq SI_d \leq SI_c$ defines approximately the relationship of SI_d to SI_c in the potentially acceptable compositions; therefore $-0.15 \leq SI_d \leq +0.3$; $SI_d < SI_c - 0.15$ suppresses the Mg_{tot} too much, and $SI_d > SI_c$ gives too high a Mg_{tot};

3) statement (2) above holds for the entire tested range of $-0.3 \leq SI_g \leq 0$; as SI_c-SI_d increases the Mg_{tot}/SO_{4tot} decreases;

4) slight adjustments of the pH (and hence P_{CO_2}) will cause very small changes in CO_{3tot}; this adjustment may be used to bring a solution of particular Ca/SO_4, Mg/SO_4, and Ca/Mg ratios

into a "better fit";

5) solutions which have $SI_c = SI_d$ = variable and SI_g = constant are almost identical in Ca_{tot}, Mg_{tot}, and SO_{4tot} concentrations; allowing SI_c and SI_d to vary (while remaining equal) simply changes the CO_{3tot} and the P_{CO_2};

6) the equilibrium model $SI_c = SI_d = SI_g = 0$ for a specified pH has the <u>highest</u> SO_{4tot} of any model composition permitted by the assumptions above in (1); $SI_c = SI_d > 0$ with $SI_g = 0$ give nearly equivalent results; for SI_c and SI_d constant, the Mg_{tot} varies directly with the SO_{4tot} (and SI_g).

The analysis so far has placed an upper limit on the concentrations of Ca_{tot}, Mg_{tot}, and SO_{4tot} in type B water, and indicated that there is a range of acceptable compositions if a nonequilibrium model is allowed; certainly, it is possible that equilibrium with respect to dolomite and more particularly gypsum may not be reached in the type B waters. The Mg_{tot}/SO_{tot}, and to a lesser extent the Ca_{tot}/SO_{4tot} and the Ca_{tot}/Mg_{tot}, serve to limit the possible compositions of type B ground water, and thus the range of possible saturation conditions as well. This will be examined more closely in the next section.

7.1.3 Mixing Model Calculations

The two-source model hypothesized in previous sections may be analyzed quantitatively by the dissolved load equation:

$$C_A Q_A + C_B Q_B = C_2 Q_2 \qquad (7.1)$$

and $$Q_A + Q_B = Q_2 \qquad (7.2)$$

where Q_A = discharge of the local source

C_A = concentration of some ion in the local source

Q_B = discharge of the regional source

C_B = concentration of the same ion in the regional source

Q_2 = discharge of the spring

C_2 = concentration of the same ion in the spring water

Hem (1970), Hall (1970), and Pinder and Jones (1969) have used mixing model equations in other works. The relationships assume that there is no change in the volume of the mixing reservoirs (i.e. no change in storage), and that the parameters or dissolved species used are conserved after mixing. Based on the geology of the region and the undersaturation of the springs with respect to dolomite and gypsum, it is believed that both SO_{4tot} and Mg_{tot} qualify as conservative parameters. Equation 7.1 is often modified by dividing through by Q_2, so that Q_A and Q_B become fractional discharges:

$$C_A Q'_A + C_B Q'_B = C_2 \qquad (7.3)$$

where $$Q'_A + Q'_B = 1 \qquad (7.4)$$

During the dry season, the chemistry and the discharge of the flow systems are approximately stable; this is the optimum time for model calculations. There are 4 independent variables, 2 dependent variables, and 2 equations relating the variables. C_2 and Q_2 can be measured, C_A may be estimated from nearby samples of type A water, and a value of C_B may be chosen from Table 7.2; this leaves only 2 unknowns and 2 equations.

Using the SO_{4tot} concentration in the Choy spring in May 1973, and selecting the equilibrium model at pH = 6.8 and 35°C (column 15):

for C_2 = 4.40 mmol/l

$C_A \cong$ 0.1 mmol/l based on cave lakes; Santa Clara and Arroyo Seco springs

C_B = 20.55 mmol/l

we have $(0.1)(1-Q_B) + (20.55)Q_B = 4.40$

$$Q_B' = \frac{4.30}{20.45} = 0.2103 \text{ or } 21.0\%$$

and $Q_A' = 0.7897$ or 79.0%

Thus, remembering that the equilibrium model had the highest theoretically possible SO_{4tot} concentration, <u>at least</u> 21% of the discharge of the Choy was supplied by the regional flow system on that date. This represents a Q_B of 0.60 m^3/sec.

Because the Mg_{tot} and the SO_{4tot} are correlated and are conserved, the Mg_{tot} of the equilibrium model type B solution may be tested to see if it predicts a reasonable value of Mg_{tot} in the type A water. Thus:

$$(0.7897)C_A + (0.2103)(7.211) = 1.82$$

and C_A = 0.385 mmol/l = 9.4 mg/l of Mg_{tot}.

The calculated C_A is about twice the value that would be expected from the average of the cave lake and type 1 spring water samples; however, the local discharge to the Choy may have sufficient average residence time to dissolve more dolomite or leach magnesian calcites than the small local springs. Also, because the expected value is small, any deviation appears to be a large error, but the predicted value is actually quite close. A slightly greater Mg_{tot} in the type B water would give a better fit.

Although the Ca_{tot} is not necessarily conserved, no large change is anticipated. Then:

$$(0.7897)C_A + (0.2103)(14.775) = 5.08$$

and $C_A = 2.498$ mmol/l = 100 mg/l of Ca_{tot}.

This result is only 12-14 mg/l (15%) larger than that of the Santa Clara and Arroyo Seco springs, which were measured early in the dry season when they were slightly undersaturated with respect to calcite.

The calculated composition of the equilibrium model at 35°C (Table 7.2b, column 15) fits very closely the requirements of type B water for the two-source model of the Choy spring. Similar or even improved results are obtained for $SI_c = SI_d > 0$ and $SI_g = 0$ (columns 18 and 19), and for the equilibrium model at 30°C (column 3); the calculated results are shown in Table 7.3a. Solutions with $SI_c = SI_d \geqslant 0$ and $SI_g = -0.3$ also meet the compositional requirements of the model (see Table 7.3a). Hence, the type B ground water that mixes with type A El Abra water in the Choy spring may have an upper limit of the SO_4 concentration of 20.55 mmol/l (1974 mg/l; varies slightly with pH and temperature choices), and have proportions specified by $Ca_{tot}/Mg_{tot} \cong 2.07$ and $Mg_{tot}/SO_{4tot} \cong 0.40$. There is little change in the results if say 0.05 or 0.2 mmol/l is used as the SO_{4tot} of the Sierra de El Abra type A water; in fact, 0.1 mmol/l appears to be a reasonable figure for at least the eastern part of the region.

Unfortunately none of the Coy analyses may be taken as completely untainted samples of the stable system conditions at the end of the dry season because small floods occurred before the 1971 and the 1973 samples

TABLE 7.3

Mixing Model Calculations for the Choy and Coy Springs

7.3a Results for Choy Spring; May 21, 1973 Base Flow Sample

Composition of Type B water; column no. in Table 7.2	15	18	19	3	17	20
SI_c	0	+0.18	+0.30	0	0	+0.18
SI_d	0	+0.18	+0.30	0	0	+0.18
SI_g	0	0	0	0	-0.30	-0.30
% of type A	79.0	78.7	78.5	79.4	62.1	61.2
% of type B	21.0	21.3	21.5	20.6	37.9	38.8
Calculated Mg_{tot} for type A in mg/l	9.4	8.2	6.5	4.05	7.0	2.9
Calculated Ca_{tot} for type A in mg/l	100	95.2	90.8	106	108	95.1

7.3b Results for Coy Spring; May 17, 1973 Base Flow Sample

Composition of type B water; column no. in Table 7.2	15	22	23	25	26	28	29
SI_c	0	0	0	+0.10	+0.12	+0.12	+0.30
SI_d	0	-0.12	-0.12	0	0	0	+0.18
SI_g	0	0	-0.30	0	0	-0.30	0
% of type A	65.2	60.5	29.0	60.9	60.2	27.9	59.4
% of type B	34.8	39.5	71.0	39.1	39.8	72.1	40.6
Calculated Mg_{tot} for type A in mg/l	-21.9	9.6	8.2	3.4	8.3	1.7	6.7
Calculated Ca_{tot} for type A in mg/l	130	83.8	93.7	85.0	75.9	56.1	56.8

were taken (Figure 4.7). Nevertheless, 3 samples probably closely approach the desired condition. Calculations similar to those above have been made for the Coy spring using the May 17, 1973 sample and a large number of possible type B compositions; selected results are given in Table 7.3b. The Huichihuayán, San Juanito, Sabinas, and Canoas spring water samples, and the minimum concentrations observed during flooding at the Coy spring (see Table 5.1) are taken to be representative of type A ground water farther away from the reef than the local source area for El Choy. The equilibrium model does not make close predictions of the Mg_{tot} and Ca_{tot} of this type A water. The best results at 35°C were obtained for SI_c-SI_d of +0.10 to +0.12; a slightly larger difference would be necessary at 30°C. Thus, the regional flux to the Coy spring has a maximum SO_{4tot} content of about 18.5 mmol/l (1780 mg/l), and has chemical proportions specified by $Mg_{tot}/SO_{4tot} \cong 0.25$ and $Ca_{tot}/Mg_{tot} \cong 3.4$. A few of the "best fit" type B solutions were also tested with the June 4, 1973 and June 8, 1971 Coy samples; the results were about the same. At least 40% of the Coy base flow discharge is derived from regional sources.

The studies discussed above have shown the character and possible range of ion concentrations that the regional water must have to satisfy the hypothesized two-source models of the Choy and Coy springs. As shown in Figure 7.1, these two springs appear to form the "boundaries" of the chemical character of the high sulfate springs. All the other springs sampled have an intermediate Mg_{tot}/SO_{4tot}; hence, they must have regional sources whose chemistries fall within the rather narrow difference between the chemistry of the regional sources of the Coy and the Choy. This may

also be seen in Figure 7.5, where the Choy and Mante samples plot above the trend line while the Coy samples consistently are below the line.

Now that the upper limits of the type B water have been established, a graphical technique may be used to determine the mixing proportions for any spring. Mixing equation 7.3 is used, with C_A equal to 10 mg/l of $SO_{4\,tot}$. In Figure 7.6, Q_A and Q_B may be determined in percent (%) from the $SO_{4\,tot}$ of the mixed output (type 2 spring) and the chosen curve. Curves numbered "1" and "2" represent the dilution curves for the Choy and Coy respectively, using their maximum permitted type B $SO_{4\,tot}$. Thus these curves give the minimum possible flux of the regional system. Because the lines are close together for $SO_{4\,tot}$ less than 1000 mg/l, the mixing proportions of other springs may reasonably be determined by choosing either line, or by estimating their correct position. For type B water supersaturated with respect to calcite and dolomite according to the specifications previously given, and at equilibrium with respect to gypsum, the respective curves would be little different. The exact $SO_{4\,tot}$ content of the type B ground water is not known, and so far no minimum SI_g or $SO_{4\,tot}$ has been established. It is assumed that the type B water flowing to each of these type 2 springs will have reached about the same SI_g. On this basis, a lower limit may be taken as the 836 mg/l of the June 8, 1971, Coy sample. This would of course mean that all of the Coy discharge on that date was from the regional source. The lower limit of 836 mg/l was used to compute curve "3", which yields what is assumed to be the maximum possible proportion of type B water in the mixed output of the springs.

An estimate of the regional base flow has been determined using Figure 7.6 and the discharge of the principal eastern sulfate (type 2)

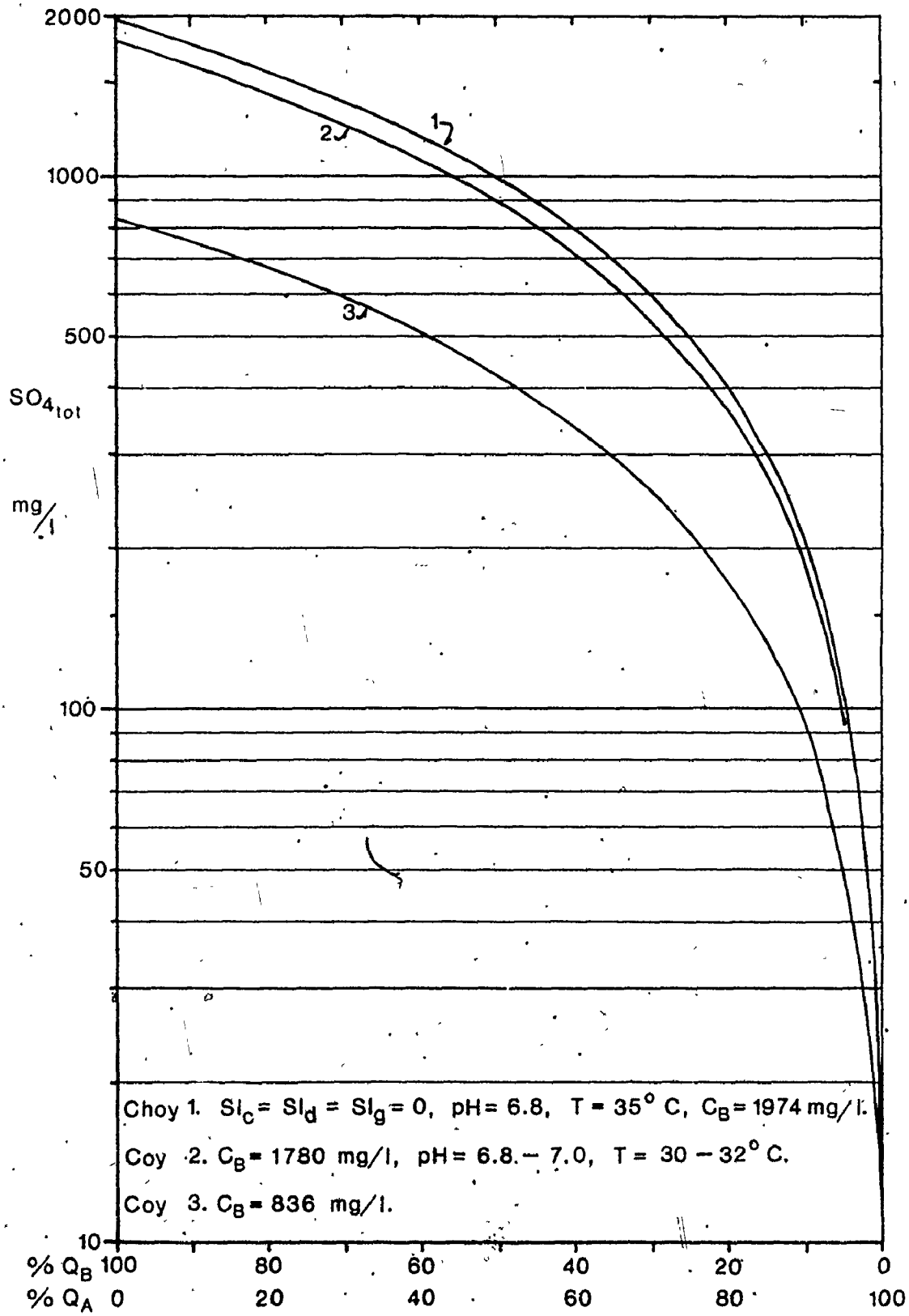

Figure 7.6 Mixing curves of type A with type B ground water.

springs. For these calculations, it is very important that the flow system be stable. In terms of the model as shown in Figures 7.3 and 7.2 and the mixing equation 7.3, it is necessary for Q_A, C_A, Q_B, and C_B to be constant for a sufficiently long time so that C_C, the concentration of the ion in the mixing reservoir, becomes constant. This will be most closely achieved late in the dry season. The effects of flooding are shown in Figure 5.6, where a flood pulse from the local source area flushed out the mixing reservoir; the chemical concentrations could not be strictly correlated with discharge because of the aquifer hydraulics and the volume of the mixing reservoir. Even slight flooding will give an aberrant discharge for the SO_{4tot} during the flood, and vice versa when the discharge is back to normal but the SO_{4tot} is somewhat diluted.

From the results (Table 7.4), the regional flux of type B water is predicted to be at least 12 m^3/sec to the springs at or near the eastern margin of the region. The calculated maximum possible flux to these springs is 27 m^3/sec. It is focused primarily on two very large springs -- the Mante in the northern and the Coy in the southern part of the area. Coincidentally (?) these two springs also have the largest base flows of all the springs in the region. The calculated regional flux may be increased from 0-10 m^3/sec when the springs above the Agua Clara in the Lower Tampaón basin (see section 4.3) are located and sampled. The amount of increase will depend on their SO_{4tot} and the dilution curve selected. The value given for the regional flux is only for the high sulfate water: any regional flow of type A water would not be detected by the model.

For the springs with more than one calculated Q_B, there is some

TABLE 7.4

Dry Season Regional Flow (Q_B)

SPRING	DATE	Q_{total} m^3/sec	MINIMUM Q_B m^3/sec		MAXIMUM Q_B (curve 3) m^3/sec		COMMENTS
CHOY	05/21/73	2.85	0.60		1.42		Stable conditions at end of long dry season; showers 1 week earlier
	06/07/73	2.85	0.60		1.42		Stable conditions at end of long dry season
	12/23/71	4.04	0.80	0.65	1.93	1.6	Early in dry season after September and October floods; 40 mm rain on Dec. 21, caused slight increase in flow
	01/15/72	3.64	0.73		1.76		More stable than on 12/23/71
	05/20/72	3.07	0.67		1.60		At end of long dry season; preceded only by showers
	06/05/71	3.00	0.65		1.53		End of dry season; minor flood of 3.6 m^3/sec in last week of May
MANTE[1]	06/06/71	11.85	3.26		7.56		End of severe dry season; preceded by some May showers and wet year
	05/25/73	11.32	2.75	3.0	6.54	7.0	End of dry season; discharge seems stable; 50-100 mm rainfall during April-May
	01/17/72	14.514	3.09		7.16		Middle of dry season; discharge slowly declining
COY[2]	06/08/71	(15)	(7.0)	(7.0)	(15)	(15)	Follows one large storm of 140 mm on May 24, 1971, but should be about stable;
	12/23/71	22.2	7.41-		16.1-		Early dry season; small flood on Dec. 13
TANCHACHIN	01/01/72	2.21	0.52	0.5	1.17	1.2	Early dry season
AGUA CLARA	01/01/72	est. 2	(0.53)	(0.5)	(1.2)	(1.2)	Early dry season
FRIO SPRINGS[3]	05/25/73	5.40+ to 5.90+	0.46+ to 0.50+	0.55+	1.03+	1.2+	Discharge from Poza Azul unknown but probably < 0.5 m^3/sec; end of dry season
	06/15/71	8+	0.72+		1.64+		Follows wet year and severe dry season; May and early June showers
TOTAL[4]			MIN.	12.2	MAX.	27.2	

1. P and Q data indicate stability; the available Q data was once weekly measurements for the canals; for the stream channel average daily flows through 1972, and once weekly measurements in 1973.
2. Gauging station Q includes surface drainage and temporary springs; on June 8, 1971, total Q was 16.2 m^3/sec and an estimated 1.2 m^3/sec was subtracted to obtain Coy spring Q; on Dec. 23, 1971, a Coy Q of 20 m^3/sec gives Q_B = 6.7 m^3/sec.
3. Q of Frío springs used here is Canal Alto + Poza Azul + Río Nacimiento; the (+) indicates probable ungauged springs.
4. Excluded springs are: Pimienta, a seasonal or overflow spring; Puente de Díos and Media Luna are western springs.

variation in the result. This may be caused by the factors discussed previously, i.e., those that may cause slight instability of mixing conditions. Alternatively, some of the variation might be real. This would be of significance in understanding the hydraulics of the regional aquifer. From the results shown in Table 7.4, it is suggested that there might be a small gradual decrease in Q_B during the dry season, and that Q_B might be greater following a wet year(s) than after a dry year(s). These possibilities should be checked by carefully selected sample times in the future. The samples for the Choy and especially for the Mante are from years having relatively high base flows. It would be desirable to learn what their SO_{4tot} and calculated Q_B values are during seasons of lower base flow.

Additional knowledge of the aquifer might be gained by studying the dilution effects of floods. During major floods at the springs, it has previously been shown (section 5.3) that the local source is strongly dominant. If it can be assumed that each instantaneous great slug of local water causes a dilution in the mixing reservoir proportional to its flow, and that each mixed slug will eventually appear at the spring, then the maximum spring discharge can be correlated with the SO_{4tot} minimum in the chemical curves. Using the Q_B given in Table 7.4 and the peak spring discharge of the series of floods (Figure 4.7) the mixing proportions are calculated, and then an expected value is read from Figure 7.6. The predictions are very close to the analytical determinations (Table 7.5) for the two major flood events monitored at El Choy. This indicates that the dilution model of the Choy works over a wide range of discharge: specifically, Q_B remains constant while Q_A varies due to local precipitation and dry

TABLE 7.5

Flood Dilution Mixing Model Calculations

SPRING	Sample Date	Q_B from Table 7.4 m^3/sec	Q_{max} of spring m^3/sec	$\frac{Q_B}{Q_{max}} \times 100\%$	Predicted* SO_4tot mg/l	Measured SO_4tot mg/l	COMMENTS
CHOY	7/07/71	0.65	56	1.16	32	30	1
	6/15/72	0.65	48	1.35	37	35	2
MANTE	8/17/71	3.0	≈28	10.7	220	180	3
	7/11/72	3.0	≈23	13.0	255	240	4
FRIO	12/27/71	0.55	13.2+	4.17	90	92	5
COY	6/20/72	7.0	<118	>5.93	>112	25	6

* using curves 1 or 2 in Figure 7.6

1,2. First major flood of year

3. Flood of 80 m^3/sec (plus Q of canals, unknown) on June 25, declining to 19.5 m^3/sec on July 29; small, broad flood with approximately constant Q of 28 m^3/sec (including canals) from August 5-12, falling to 24.0 m^3/sec on August 19.

4. Flood of 27.6 m^3/sec (plus canal flow if any) in mid-June; constant Q for week preceding sample

5. Strong wet season flooding ending in mid-October; Q fluctuates slightly in December

6. First major flood of year; follows 2 smaller ones; the peak Q at the gauging station was 118 m^3/sec; thus when the Q supplied by surface runoff from 194 km^2 basin and small wet weather springs is subtracted, the Coy spring Q is less, which affects the calculations as shown

season drawdown. However, the two floods are of comparable magnitude. Similar data and calculations need to be obtained during floods of say 15 and 100 m^3/sec; dilution measurements for 10-30 m^3/sec floods will be especially critical.

Some of the Mante and the Frío spring data may also be used to check the model. For these springs, there is not enough information to compare the flood peak with the SO_{4tot} minimum as was done for the Choy. The data for which the calculations are made are believed to represent approximately stable mixing reservoir conditions, in which Q_B is constant, but Q_A is changing slowly and is about 2-5 times larger than during the "average" late dry season. This is a test of the dilution model over a range where the predicted value is very sensitive to small changes in discharge. The calculated values are in error by not more than 22%, which is a good result considering the limited knowledge of Q_B, and the quasi-stability of the mixing reservoir. These calculations test the proposed two-source mixing model for the Choy, Mante, and Frío over a range of discharge conditions; they have shown that Q_B may be considered approximately constant and Q_A variable. These results are <u>independent</u> of which mixing curve in Figure 7.6 is selected; i.e., the calculations are a test of the two-source model, and not of the specific composition of the type B water.

The same assumptions and computations as above do not work when applied to the Coy spring (Table 7.5). It would take a spring discharge of 1000 m^3/sec to dilute a constant Q_B of 7 m^3/sec to the measured SO_{4tot} concentration. This implies that Q_B is not a constant for the Coy spring

during flooding; and for the example, it must have been reduced to something less than 0.83 m^3/sec. The contrast in the mixing behavior of the springs is believed to result from the fact that the Choy, Mante, and Frío springs drain directly from large unconfined local aquifers, whereas all of the Coy discharge is artesian water (except for the very small amount that is derived from infiltration into the small dome itself; see Figure 7.2). A large increase in Q_A seems to have little or no effect on Q_B at the Choy, Mante, and Frío springs, but it hydraulically damps the regional flux to the Coy spring.

The above result may explain a puzzle regarding the Pimienta, a spring very near the base of the limestone scarp south of Aquismón at about 100 m elevation. The two water samples collected show that it is a high sulfate spring, yet it is also a seasonal spring (Section 4.2). Its aquifer is unconfined. Hence, when ground-water levels in the area west of Aquismón are high, part of the regional flux as well as some of the local flux is apparently diverted from the Coy to the Pimienta, and perhaps to other springs.

7.1.4 Summary and Comparison of the Hydrochemistry with Other Regions

The studies reported in this thesis have shown that there are two major types of karst ground water in the region. One is a "normal" karst calcium-bicarbonate type having a calcium carbonate hardness of 120-220 mg/l (type "A" water); this type results from flow within the El Abra limestone. The second (type "B") is believed to be a deeply circulating regional flow

system water that has much higher Ca, Mg, and SO_4 concentrations. Wherever the deep regional water resurges, these two combine, forming a mixed effluent. Hydrochemical techniques used in conjunction with hydrogeologic information often provide powerful methods of studying ground-water flow systems. In this study the chemical and physical changes that occur in spring waters during flooding have been particularly important because flooding changes the mixing ratio. Many of the large eastern springs have been found to discharge mixed-source water (type 2). Based on limited data, they appear to behave as El Choy, where during floods the local source greatly predominates, and the chemistry is reduced to nearly that of the local source springs (type 1).

Because no samples of type B water were available for analysis, it was necessary to investigate its possible composition by other means. A geochemical model was developed based on sequential exposure to minerals (calcite, dolomite, and gypsum), aquatic chemistry theory, and field results of other works. The model took into account the very important ion pairs $CaSO_4^{\circ}$ and $MgSO_4^{\circ}$, as well as the much less significant $MgHCO_3^{+}$. Using the spring water samples as controls, it was found that the type B water had to have specific proportions of Ca, Mg, and SO_4. This in turn restricted the appropriate saturation conditions with respect to calcite, dolomite, and gypsum; the difference between SI_c and SI_d could range from 0.0 to about +0.12, depending on the spring, and SI_g could vary freely except that it was not allowed to supersaturate. The equilibrium model (at 35°C) proved satisfactory for the type B source to the Choy spring, and had a composition of about 29.5 meq/l of Ca_{tot}, 14.5 meq/l of Mg_{tot}, and 41 meq/l of SO_{4tot}. The equilibrium model allowed the highest SO

for the regional source. Models suitable for other springs had up to 10% less SO_{4tot} than the equilibrium model.

Using a two-source dissolved load equation, which has four independent variables and two dependent variables, the amount of local and regional flow to the eastern margin type 2 springs was determined for stable base flow conditions. The total regional flow of type B ground water was calculated to be between 12 and 27 m^3/sec; the amount as determined by the model depends on the degree of saturation with respect to gypsum in the type B water. It was also shown that the regional flux is approximately oonstant, possibly exhibiting small variations in response to seasonal or longer term changes in hydraulic head. For most of the springs, it appears the regional flux is constant even during floods.

There have been numerous studies of surface streams that have related dissolved load to discharge, some studies that have shown annual trends or cycles in water quality (e.g. Hendrickson and Krieger, 1964; Gunnerson, 1967), and recently, a few that have used a two or three source dissolved load equation to separate the hydrograph of surface streams into surface runoff and ground-water components (Hem, 1970; Pinder and Jones, 1969; Drake, 1974). Bassett (1976) presented extensive correlations between chemical species, calculated parameters, and discharge for the Orangeville Rise, a large karst spring in southern Indiana; and some researchers (initiated by Ashton, 1966) have discussed some of the chemical and physical variations that occur during floods of karst springs in limestone and dolomite terrain. This thesis is believed to present the first development of a quantitative mixing model for ground-water systems. The data given by

Bassett (1976) and the local geology of southern Indiana suggest that such a model could be applied there, and that it may be useful elsewhere.

Curiously, the thermal, sulfurous Taninul Sulfur Pool also responds to local ground-water conditions as shown in Figure 5.11. Thus, it too can be modeled as having two (or possibly more) sources, one of which is a local recharge area in the Sierra de El Abra, and the other is some unknown source(s) of hot, sulfurous, and sodium chloride bearing water. Each of the three thermal springs examined has a different chemical character and thermal regime; it is not known if the other two undergo such large changes in discharge, chemistry and temperature as the Sulfur Pool. The thermal springs discharge a rather ill-defined third type of ground water that probably does not exceed a total flow of 0.1 m^3/sec in the region.

The flood behavior of small springs was not studied because it is very difficult to reach them during the rainy season. Not very many of them have been sampled, but it is believed they will usually be local source springs. During large floods, probably most of the water discharged at the small springs and perhaps the major part of that discharged at El Choy are believed to have been derived from the causal precipitation event. The short-resident local source waters undoubtedly have lower calcium bicarbonate concentrations and lower SI_c values than the longer resident local source waters that are discharged sometime after the flood or during the dry season: the decrease might be about 20-40% and 0.2-0.5 log units respectively depending on the spring, magnitude of the flood, and antecedent conditions. This and certain lag effects associated with the mixing reservoir are of secondary importance in the mixing model of the type 2

springs. More data are required to make a detailed analysis of the more subtle aspects of the mixing model. The more obvious effects of volume of the mixing reservoir and of the phreatic hydraulic conditions are the lag of the chemical response behind the discharge increase at the onset of flooding, and the much greater period of time required for the chemistry to return to its normal base flow character than for the discharge. This effect rules out the straight-forward comparison of chemical concentration with discharge.

Besides the need for more data from the region of interest, there are some questions or problems with the geochemical model. They are really a group of problems concerning some disparities between aqueous chemistry theory and results reported in the literature, and the need for more laboratory measurements such as the temperature dependence of $K_{MgHCO_3^+}$ and reaction rate data. The only problems that might be thought of serious consequence to the model are the still uncertain value of $K_{dolomite}$, and the precipitation kinetics and nucleation potential of dolomite, calcite, magnesian calcites, and possibly aragonite. In Florida, the high Mg concentrations relative to Ca and the dolomite supersaturations reported by Back and Hanshaw (1970) clearly pose a geochemical problem, but it does not seem to be a concern for the Valles-S.L.P. Platform area. The compositional requirements of type B water for the mixing model as specified by Mg/SO_4 and Ca/Mg ratios and tested by extrapolation of chemical data in Figure 7.5 are such that the dolomite saturation state relative to the calcite saturation state is controlled, and the Florida problem does not occur. This study used a temperature dependent K_d that has a value of $10^{-17.0}$ at 25°C

(after Langmuir, 1971). Another commonly used value for this temperature is $10^{-16.7}$. On the assumption that the difference in the K_d's is also 0.3 log units at 35°C, the geochemical model was tested to determine what effect the increased solubility of dolomite would have; the new equilibrium model is given in Table 7.6. This model contains 27% greater SO_{4tot}, 91% greater Mg_{tot}, and 5% less Ca_{tot} than the other equilibrium model (column 15, Table 7.2). From the Mg_{tot}/SO_{4tot} and Ca_{tot}/Mg_{tot} ratios and comparison with Figure 7.5, it is clear that this new equilibrium model is not a satisfactory choice for type B water. If $10^{-16.7}$ (at 25°C) is truly the equilibrium constant for dolomite, nonequilibrium models similar to those in Table 7.2b must be generated. It was found that SI_c-SI_d must be increased by about +0.15 (which is 1/2 log ($10^{-16.7}/10^{-17}$)) compared with the differences given earlier in this chapter to obtain suitable compositions for type B water. In fact, this reduces the chemical concentrations to almost exactly those given earlier (Section 7.1.2) and no changes are necessary in the mixing model calculations. Changes in SI_g alone cannot compensate for the increased K_d. Thus, solutions having the required Mg_{tot}/SO_{4tot} and Ca_{tot}/Mg_{tot} ratios have saturation conditions limited to specific relationships: SI_c-SI_d is constant and SI_g is variable, but less than or equal to zero. The important aspects of a greater K_d, if correct, are the implications: 1) the solution may be undersaturated with respect to dolomite, thus suggesting a younger age than the Florida ground waters where radiocarbon dates indicate that dolomite saturation is reached in about 10,000 years (based on Figures 1 and 11 in Back and Hanshaw, 1970); and 2) although acceptable type B waters for the area have a maximum SO_4 of about 41 meq/l and reach equilibrium with respect to gypsum, if

the waters were exposed to dolomite and gypsum for a longer period of time, the SO_{4tot} would increase with the Mg_{tot} as dolomite continues to dissolve, and the molar ratios of the constituents would be changed.

TABLE 7.6

Equilibrium Model with Greater K_d

pH	Ca_{tot}	Mg_{tot}	SO_{4tot}	CO_{3tot}	pP_{CO_2}	$CaSO_4^\circ$	$MgSO_4^\circ$	Mg/SO_4	Ca/Mg
6.8	14.08	13.76	26.15	4.10	1.50	5.19	6.45	0.53	1.02

One of the objectives of the water chemistry studies was to compare the concentrations of dissolved species, the calculated equilibrium P_{CO_2}, and the estimated denudation rate with published results, particularly for other climatic regions. However, the chemistry of the Valles-San Luis Potosí region karst waters has been shown to be more complex than "normal" calcium-bicarbonate or calcium-magnesium bicarbonate type waters most commonly reported in karst areas. This is partly because many workers have only measured the calcium and total hardness (especially for comparing the hardnesses of different regions), and partly because the hydrochemistry of the area is indeed more complex. The chemistry of the ground water in the region of interest here is considered to be a property of the hydrogeologic flow systems, which will be discussed in Section 7.2. Some support for the geochemical model is obtained from studies in eastern Nevada and in Yucatan. Maxey and Mifflin (1966) list detailed analyses of 40

limestone spring waters in Nevada. Here there also seem to be two chemical types; the waters have a nearly constant total hardness, except two that have a very high sulfate content (see Table 7.7; also plotted in Figure 7.5). The concentrations of some species appeared to increase with length of flow path. The two samples plotted contained considerable Na + K and Cl. It is suggested that they have an excess of Na over Cl caused by cation exchange, and that this is the reason they fall somewhat below the extrapolated lines in Figure 7.5. These samples are from a still more complicated hydrochemical system. In Yucatan, Back and Hanshaw (1974) have shown that two principal types of chemical trends occur. One is the mixing of normal calcium-bicarbonate type water with varying amounts of sea water; and the other is a gypsum or anhydrite solution trend coupled with solution of carbonate minerals (as in the geochemical model developed here) and possibly with minor mixing with sea water. The Polyuc sample (from the south-central Yucatan peninsula) had by far the highest SO_4 concentration, and is also plotted in Figure 7.5. It too has some Na and Cl (Table 7.7), but fits the model extremely well. The Florida data reported by Back and Hanshaw (1970) do not fit the model because the Ca/Mg is much lower (their sample having the highest SO_4 is given in Table 7.7). This indicates that dolomite solution is more important there, that water might be exposed to the minerals in a different sequence than in this model (possibly greater dolomite solution before encountering gypsum), and that the solution may evolve along Ca versus SO_4 and Ca+Mg versus SO_4 lines with different slopes, especially if a greater K_d is allowed.

TABLE 7.7

Some Published Data for Comparison with the Geochemical Model

Sample	°C	pH	Ca	Mg	Na	K	HCO_3	SO_4	Cl
Blue Point[1] Spring	—	—	482	169	428*		122	1910	368
Rogers Spring[1]	—	—	451	149	395*		185	1670	343
Polyuc[2]	26.7	6.71	384	85	98	6.5	354	1020	106
Ellenton[3]	26.2	7.58	140	68	19	2.7	178	458	25

* value quoted is ppm of Na+K

1. Nevada, concentrations in ppm - Maxey and Mifflin (1966)
2. Yucatan, concentrations in mg/l - Back and Hanshaw (1974)
3. Florida, concentrations in mg/l - Back and Hanshaw (1970)

One of the major controversies in the karst literature concerns the intensity of karst development as a function of climate. The debate has significance for permeability development as well as surface karst forms. Many authors believed that the maximum intensity (or rate) occurred in the tropics, putting forward the spectacular corrosional landforms as evidence; the opposition camp maintained that the intensity would be higher in northern latitudes because carbon dioxide is more soluble in cold water than in warm water. Quantitative support eventually was sought from the chemistry of karst waters. Because so many of the El Abra region spring waters have proven to be more complex than "normal" karst waters, not enough appropriate data have been gathered to offer either a statistically based or scarcely even a rationally based measure of the limestone denuda-

tion rate in the region. Hence, an extensive survey of the literature and comparison with published results will not be given here. Instead, a general discussion of some of the requirements for such chemical comparisons will be given (especially with reference to some recently published papers), and the possible implication of the El Abra waters to the debate will be suggested.

The chemistry of ground water, even karst ground water is most complex. Some important factors are mineral solubilities and degrees of saturation, solution and precipitation kinetics, ion exchange, ionic strength and common ion effects, aquifer mineralogy, effects of trace metals, gaseous phases, diffusion of gases and ions, hydrodynamic effects including type of flow (granular, diffuse, or conduit), seasonal variations, and whether the system is open or closed. Thus, it is very important that only karst waters that are from appropriate or similar situations be used if it is desired to critically and objectively compare their chemistry and their calculated denudation rates. William B. White and students (William B. White, personal communication) conceived the idea of using water temperature as a measure of latitude (and hence at least a partial indicator of climate), and testing spring waters for correlations between temperature and various chemical species concentrations or calculated parameters. Russell S. Harmon took up the concept, collected data from a number of co-workers (including this author) and the literature, attempted to prove the idea, and published a series of papers comparing averaged values from geographic areas (Harmon et al., 1972, 1973, 1975). Unfortunately, the data, particularly the Mexican data, have not been properly handled; there-

fore, although the published results "proved" the theory, it is here considered to be an untested theory.

Some of the principal points of contention are:

1) The data sets used for all the papers contain analytical data by Harmon from a preliminary report on the Sierra de El Abra karst waters (Harmon, 1971) which have some very large analytical errors for all constituents, sometimes as much as several hundred percent. The alkalinity and sulfate values are especially in error.

2) Figure 7.7, reproduced from the 1973 paper, shows the "correlation" between Ca^{++} and water temperature. The México point is simply the average of the Ca^{++} values of all samples of all the El Abra region springs that were sampled, including the very high calcium-sulfate type springs. Clearly, the latter waters are not appropriate! Of the springs sampled in this thesis study, only 6 (Table 5.1) may be suitable for such a plot (flow conditions prior to sampling are uncertain for 3 of them). They have an average Ca^{++} of 69.5 ppm (the range was 45.5 ppm to 88.1 ppm), which would greatly change the correlation line. Note that the original line has a negative intercept on the Ca^{++} axis. A value of 1.99 was given as the ratio of the slope of the line in their HCO_3^- versus T plot divided by the slope of their Ca^{++} versus T plot; this was taken to show that the waters were of calcium-bicarbonate type, when in reality, it was a statistical accident which misrepresents the true water chemistries. Aside from the calcium-sulfate waters in México, many of the waters contain significant amounts of Mg, and a

har and more appro-

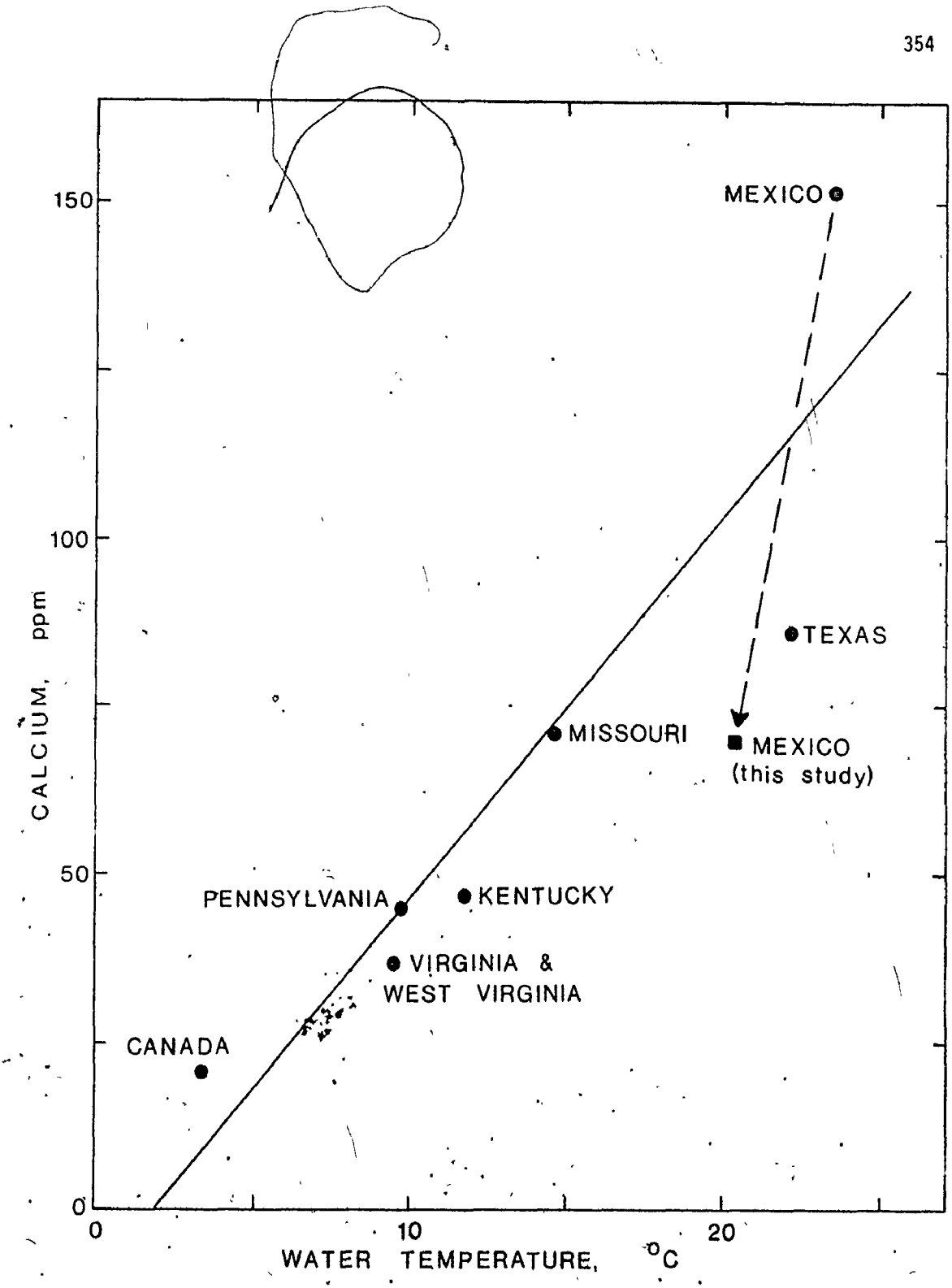

Figure 7.7 Plot of Ca^{++} against T (°C) for various geographical regions from Harmon et al. (1973), with a new México point from this study.

priate, or better still, use only of waters from nearly pure limestone terrains.

3) The 1975 paper gives regression relationships between a number of chemical variables and temperatures, but the use of some inappropriate and some unreliable data negates the effort. Greater emphasis is placed on P_{CO_2} versus T, using $|SI_c| \leq 0.1$ as the criterion for selecting "only" diffuse flow springs. Although conduit and diffuse flow springs could be distinguished in Pennsylvania by the coefficient of variation of SI_c or other chemical variables (Shuster and White, 1971), it is clear from this study that the chemistries and saturation values of many of the Mexican springs are strongly influenced by gypsum solution, and that the local flow systems are of the <u>conduit</u> rather than the diffuse type! It seems very likely that many of the other chemical analyses taken from the literature are actually from conduit springs. The 29 Mexican samples (all from the Cd. Valles region) are from only 11 springs, some having been sampled many more times than others. Twelve analyses were assumed to be from diffuse flow springs based on their $SI_c = 0 \pm 0.1$. If all those that have been significantly influenced by gypsum solution are deleted, their Mexican data collapses to just <u>one</u> sample (from the Harmon (1971) paper). Some of the Texas data may also be influenced by gypsum solution. There is also the problem that probably many of the pH's reported in the literature were measured in the laboratory rather than on location, which makes the calculated SI_c's and P_{CO_2}'s unreliable. Furthermore, despite the statement that the computer program used makes "full allowance for ionic strength and ion pairing", because

the sulfate concentrations were never included with the input data, the important ion pairs $CaSO_4^o$ and $MgSO_4^o$ could not have been taken into account, nor the effect of high sulfate concentrations on the ionic strength.

There are additional problems with the data treatment and analysis presented in the series of papers, but they will not be discussed here. Using the corrected México point in Figure 7.7 and presuming the other averages are valid (?), it appears that there might be a trend, although the slope of a regression line would be much less than before; the México and Canada points are based on very few samples. Brook (1976) and Cowell (1976) have added a few samples to the Canadian data from their studies; and they have reanalyzed the data. They found that there may be a slow increase in Ca^{++} with increasing temperature, but that the HCO_3^- versus temperature correlation was inconclusive. A recent study having data from many more areas in eastern North America showed that there was no relationship between bicarbonate content and latitude in the region (Trainer and Heath, 1976). They attribute the variations of HCO_3^- concentration primarily to factors which control CO_2 production and storage in soil, to the type and timing of aquifer recharge (i.e. how much CO_2 is carried down with the recharge), and to the type of aquifer flow system on residence times of the water (after Shuster and White, 1971). They did not give a regional comparison of data restricted to one type of flow system or aquifer mineralogy.

Figure 7.8 shows a plot of SI_c against pP_{CO_2} for springs in the El Abra region, using samples from dry season conditions where possible. The large calcium-sulfate type springs are approximately at equilibrium

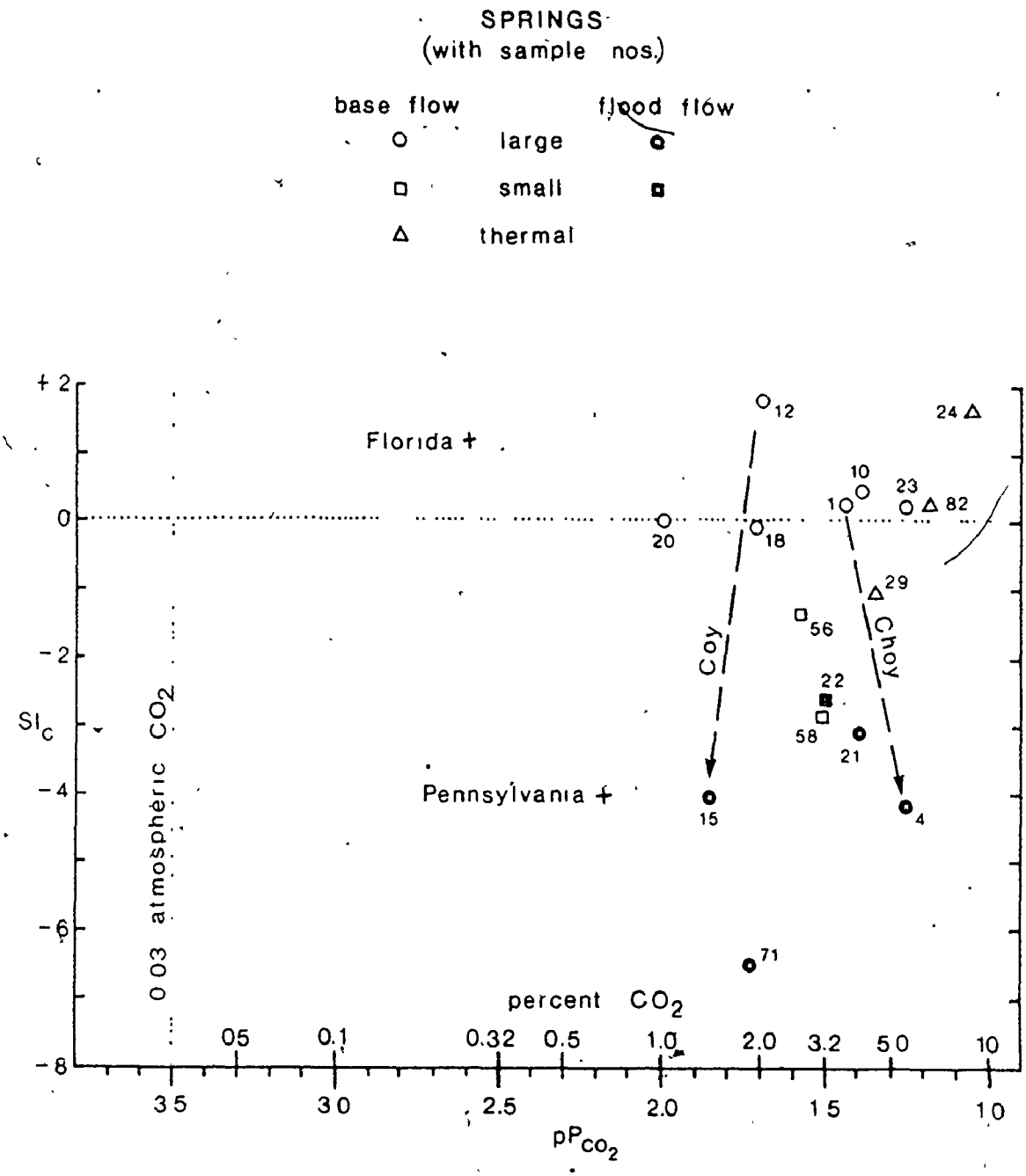

Figure 7.8 Calcite saturation index (SI_c) versus negative logarithm of partial pressure of carbon dioxide (pP_{CO_2}) for region springs.

with respect to calcite and have P_{CO_2} ranging from 1.72 (1.9%) to 1.26 (5.5%). The Sabinas is the only large non-sulfate spring for which a sample at or near equilibrium with respect to calcite was obtained, and it had the lowest pP_{CO_2}, 2.0 (equivalent to 1%) of all the springs sampled. Not enough samples were obtained from the smaller El Abra springs to determine what variations occur in their saturation conditions or chemical concentrations. Based on early dry season samples from the Santa Clara and Arroyo Seco springs, it appears that their effluents may approach near equilibrium with respect to calcite later in the dry season. The effect of flooding is shown for the Coy and the Choy springs where moderate floods reduce their SI_c's to about -0.4. The interesting aspect of the data for the Sierra de El Abra springs is that they have equilibrated with a high P_{CO_2} reservoir, from 2.5-5%, whereas the surface of the range has only a thin, spotty cover of soil. It is suggested that a significant part of the CO_2 is generated by decay of organic material washed down into fissures and caves both above and below the water table. From the calculated P_{CO_2}'s for spring waters in the region, it is concluded that the karst ground waters have a large potential for limestone solution. Based on the calculated SI_c's, (remembering that only 6 "normal" springs have been sampled), most of this potential is used at base flow, but flood waters flow too quickly through the caves to use all the potential, as shown by the Choy and Coy where flood waters are considerably undersaturated. The average values for 29 Pennsylvania springs (includes both diffuse and conduit types; from Langmuir, 1971), and 8 Florida well waters (those unaffected by gypsum solution or ocean water mixing; from Back and Hanshaw, (1970) are shown in Figure 7.8 for comparison. Because the Florida waters

are old, often several thousands of years, and evidently are from relatively diffuse flow systems, they perhaps are not comparable. Four "normal" karst waters from Yucatan (Back and Hanshaw, 1974), which has a conduit-type aquifer, have averages of +0.015 and 1.61 for SI_c and pP_{CO_2} respectively. Hence, the Yucatan karst waters, before they mix with sea water, appear to have about the same potential for solution as El Abra region waters, but utilize that potential more fully as shown by their SI_c values and their average of 92.5 mg/l of calcium. The Yucatan waters must have a longer residence time than the El Abra waters, and the Yucatan aquifer is likely less dynamic than the El Abra aquifer, although both areas receive similar amounts of precipitation and are affected by large storms and hurricanes. It is concluded that the potential for karst solution, as indicated by P_{CO_2}, may be generally higher in the tropics than in more northerly climates, but the extent to which the potential is utilized depends on the type of aquifer and other environmental factors. More high quality data from selected environments are needed before this conclusion can be considered proven.

7.2 The Ground-Water Hydrology of the Region

"A ground-water flow system is a region within saturated earth materials where there is dynamic movement of ground water from a source [recharge zone] to a sink [discharge zone]" (Mifflin, 1968, p. 3). Water at each point within a flow system possesses a specific velocity, fluid potential, chemistry, temperature, viscosity, turbidity, and density. A system is perfectly defined or "known" when the value of all the parameters are known

at all points, i.e. as a function of their spatial distribution (they are referred to as distributed parameters). The measurement of these parameters at even a modest number of points is exceedingly expensive and time consuming. Hence, it is usually only possible to hypothesize the general characteristics of the ground-water body based on geologic and geomorphic relationships, output characteristics of the flow systems, inference of likely recharge zones and recharge capacity, measured or estimated permeabilities, and limited well data. Karst springs represent the integrated output of karst ground-water flow systems, and the same parameters as above, but also including the discharge may be studied. The values of the parameters measured at a spring are the average for all of the flow paths that reach the spring; their magnitudes and temporal variations, as shown in this study, provide a great deal of information about the gross characteristics of an aquifer.

One of the principal contentions of this study is that the physical and chemical characteristics of the spring waters in the Valles-S.L.P. region, and the elevation and discharge of the springs together have a consistent and reasonable pattern. They are functions of ground-water flow systems, and the variables of interest are geologic setting, aquifer hydraulics, fluid potential, climatic events, chemical reactions, heat flow, heats of reactions, and time. In the preceding section, a schematic hydrochemical model of the flow systems was developed that was based on spring water chemistry (plus a few chemical measurements within the aquifer), chemical theory, and the schematic distribution of minerals. It successfully modeled the mixing phenomena of the high sulfate springs, estimated the amounts and locations of regional ground-water discharge, and showed that the extremely

variable output of the springs could be separated in most instances into dynamic local sources and approximately constant flux (of water and chemistry) regional sources. In this section, the information and interpretations of previous chapters and the hydrochemical model are drawn together to provide a summary and speculative discussion of the real ground-water hydrology. Although there are no data on ground-water as a distributed parameter except for a few in the Sierra de El Abra, it is possible to gain some knowledge of various portions of the Platform by analyzing the discharge characteristics of each of the basins given in Chapter IV.

7.2.1 Geology and Hydrogeology

Figure 7.9 is a regional cross section based on the topography along 22°N latitude (through Cd. Valles) of the new 1:50,000 maps by CETENAL, the geology and well records as given by Carrillo Bravo (1971), Heim (1940), and Muir (1936), and a geologic map of the state of San Luis Potosí provided by the Instituto de Geología (1965, compiled by Ing. Lopez Ramos). Names enclosed in parentheses give the relative location of features that have been projected into the section from some distance away. No structural cross section of the region has been previously published probably because subsurface information is still scanty. This simplified section emphasizes hydrogeologic aspects. Shown are the broad coastal plain of impermeable rocks, the Sierra de El Abra at the eastern edge of the folded Platform, the high Sierra Madre Oriental fold belt, and the broad Río Verde valley. This section extends about 60% of the way across the Platform, just north of the structurally lowest part of the Sierra Madre. Nearly all of the ridges

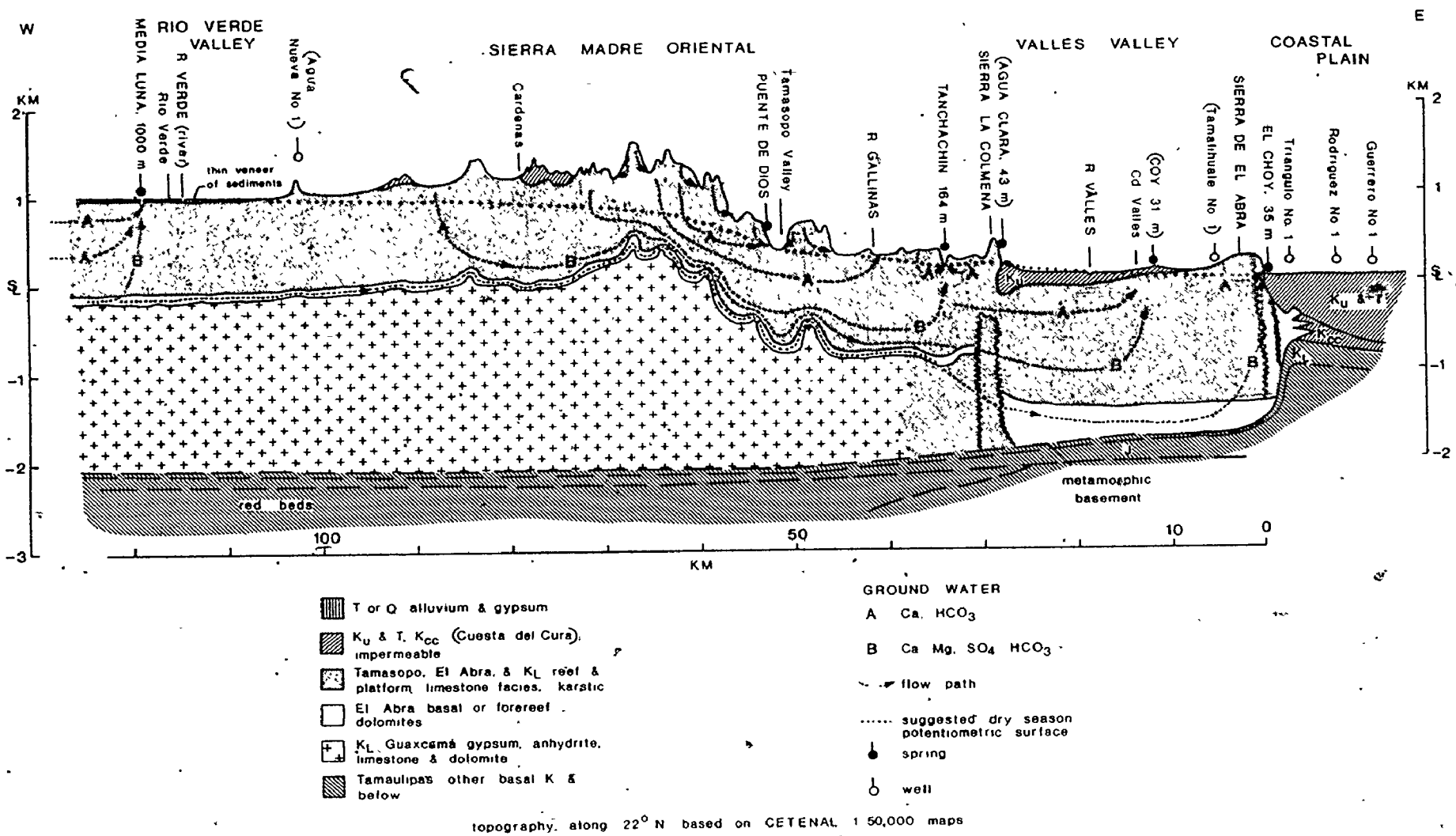

Figure 7.9 Regional E - W hydrogeologic cross section showing hypothesized local and regional ground - water flow systems.

are anticlines. The thick section of Upper Cretaceous rocks has been removed from most of the region, and the El Abra Formation is either exposed or covered by only a thin veneer of sediments over most of the Platform. The Guaxcamá Formation is shown here to have a thickness of about 2000 m except where thickened by folding, because according to Carrillo Bravo (1971), it extends downward to -2110 m below sea level in Pozo Agua Nueva (penetrated 120 m of basal Cretaceous and Upper Jurassic before reaching redbeds), and to -1834 m in Poza Guaxcamá (west of the section) where 3009 m of the formation was cut (underlain by 800+ m of redbeds). Thus, the base occurred at roughly the same elevation. The eastern limit of the Guaxcamá Formation is unknown.

The principal aquifer of the region is the reef and platform limestone facies of the El Abra Formation, where the flow is through large conduits (caves) and solutionally widened bedding planes and joints. Because the large tectonic structures are folds rather than faults, the aquifer is continuous over most of the region. One known discontinuity in the aquifer is the Guaxcamá anticline where erosion has removed the El Abra, exposing gypsum in its interior. Possible discontinuities in the ground-water body may occur in the Xilitla area where faulting is important, the Miquihuana arch where Precambrian (?) metamorphic and other pre-Cretaceous rocks are exposed in the interior of the fold, and in the interior of the Sierra de Guatemala which has great structural relief (Figure 2.5). The Tamasopo Formation is part of the same karstic aquifer, but it is volumetrically much smaller. The Tamasopo and El Abra Formations plus similar Lower Cretaceous platform facies limestones constitute a hydrostratigraphic unit (Maxey, 1964). The basal and forereef dolomite of the El Abra For-

mation has been found in wells to be porous and permeable. In Pozo Tamalihuale No. 1, Carrillo Bravo (1971) reported that the dolomite had "frequent and small caverns, irregularly distributed"; hence, the flow may be more restricted than in the limestone caves, i.e., it is probably a fractured dolomite aquifer. The Guaxcamá Formation has some limestone and dolomite beds within the gypsum and anhydrite; it does not seem likely that there would be a significant flow in this unit, but Carrillo Bravo (1971) reported a loss of circulation during drilling. The only other aquifers are the late Tertiary or Quaternary alluvial fan, fluvial, and lake deposits. These sediments, which are relatively thin, occur mainly in the broad flat valleys and bolsons west of the Sierra Madre Oriental folded ranges (Figure 7.9 and 4.1). They are quite variable in type and size of sediments, and hence in permeability. Based on a report by J. Lesser (unpublished, circa 1973), they are of limited importance as aquifers in the total regional picture developed here.

7.2.2 Spatial Variation of Runoff

In Chapter IV, some aspects of the runoff from the region were discussed. Table 4.9 lists the yearly discharge for the study period 1961-68 of the S.R.H. gauging stations in the area. The average unit runoff was calculated for the supposed surface basin of each station, and this result was compared with the average value for the whole region. A specific relationship between annual precipitation and annual runoff has not been possible because the true boundaries of the basins, surface and subsurface, are not known. Therefore, based on the discussion of Section 4.3, Figure 7.10

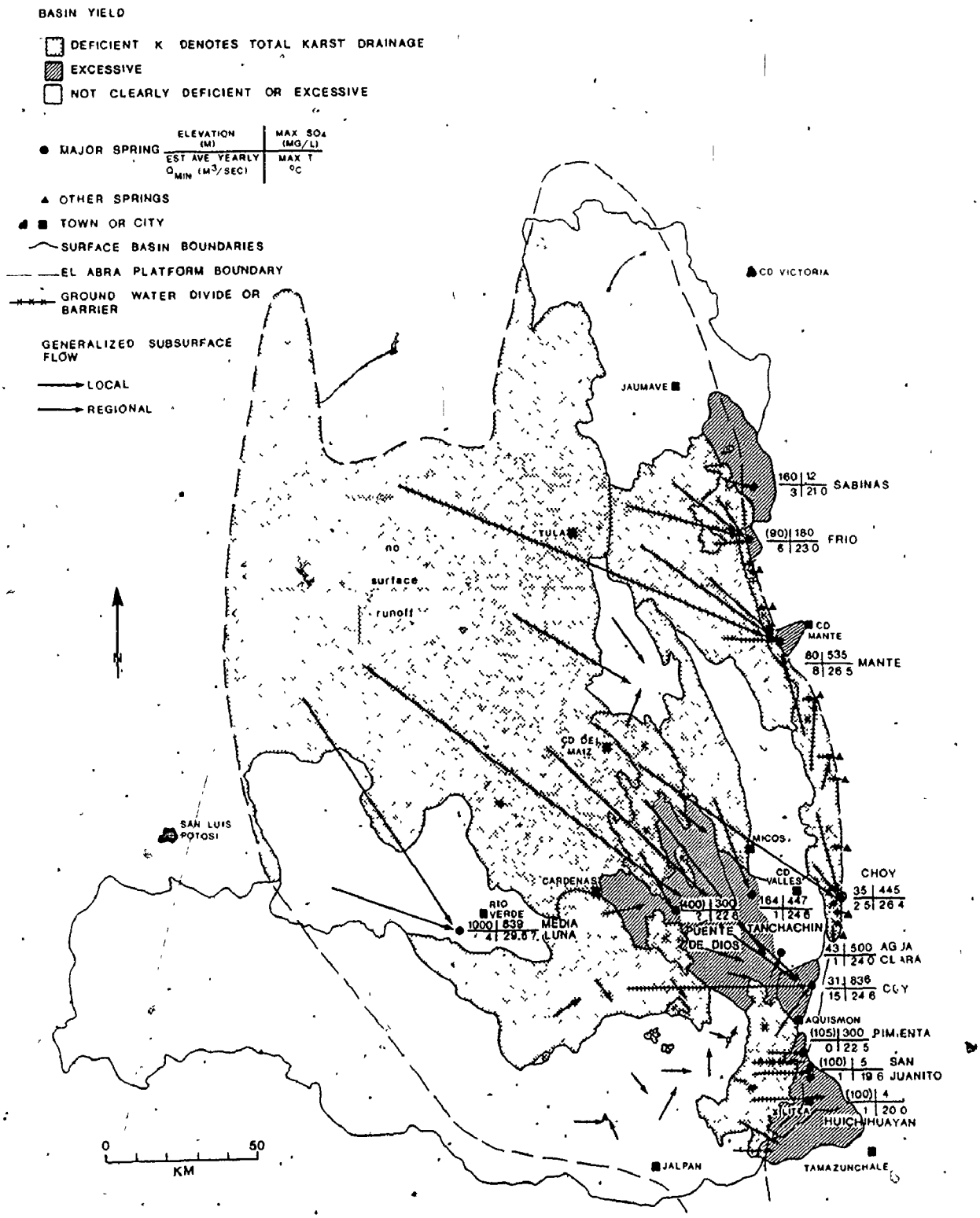

Figure 7.10 Map summarizing spatial distribution of runoff in the region, possible directions of ground-water flow, and base flow chemistry, discharge, and elevations of the major springs.

distinguishes the areas that are believed to have clearly excessive or deficient average unit runoff from those that have values deemed "reasonable" for the given rainfall (see Figure 4.3).

The basins are the same as those given by the S.R.H. in Bulletin 32 (and in Figure 4.2) except that the Sierra de El Abra, including the drainages in the adjacent western valley that are pirated underground, is delineated as a karst area. More detailed mapping of the region will reveal other areas that have totally or partially internal drainage. The hydrogeologic map (Figure 4.1) may be used to infer areas of infiltration or surface runoff within the basins of Figure 7.10.

It is striking what a large proportion of the Platform has a deficient yield compared with the proportion that has excessive yield. Excluding that part of the Río Santa María basin west of the Platform, but including the small areas of surface basins beyond the eastern reef trend, 58% of the Platform has below the expected runoff, only 7.3% has considerably more runoff than expected, and 34% can not be clearly assigned to either category. This distribution is due mostly to karstic effects even in those areas not marked "K" ("K" indicates areas of complete internal drainage). For example, the Río Comandante (Estación La Servilleta), which has roughly one-half of its area as high relief El Abra limestone and the other half as low elevation impermeable cover, produces sharp flood pulses, deficient average flow, and virtually nil base flow. During the study period 1961-68, the Comandante basin of 2532 km^2 had less runoff (4.95 m^3/sec) than the Choy spring (5.07 m^3/sec). The lower Micos basin appears to be a zone of karst losses. The northwestern portion, about one-third of the total Plat-

form area, is not yet integrated into the surface drainage network of the region. However, despite its low annual rainfall, there must be a significant amount of infiltration to the ground-water zone. The El Abra limestone, which forms the mountain ranges and underlies the sediments in the valleys, has undergone sufficient solution to allow some infiltration. Carrillo Bravo (1971) reported: 1) frequent loss of circulation in the El Abra and Guaxcamá formations in the Agua Nueva No. 1 well west of Cd. del Maiz; 2) a "dolina" (in this case a cavity) in the middle of the El Abra limestone in the same well that has a vertical dimension of 251 m) and is filled with an upper Tertiary deposit of clastic material; and 3) general lack of success (repeatedly emphasized) with their seismic work in the entire northwestern area, which he attributed to the "cavernous" limestones (and in some instances to gypsum). Personal observations of gypsum caves near Matehuala and in the same valley farther south, one of which had a small flowing stream 25 m below the surface, show that the valley sediments permit some water to escape the zone of evapotranspiration. J. Lesser (unpublished report, c. 1973) has estimated the average ground-water discharge into the Río Verde of the sedimentary aquifer of the large Río Verde valley to be 0.5 m^3/sec for the period 1962-70. It is believed that most of the northwestern region acts as a recharge zone to deeply circulating ground-water flow systems, although the rainfall is not large and there is no surface runoff. This ground water is believed to flow to springs along the surface drainage network; therefore, the surface basins shown in Figure 4.2 have a larger catchment than shown, and the actual runoff derived from them is slightly smaller than shown in Section 4.3.

The basins having a "normal" amount of runoff are principally of two types: 1) the low to moderate rainfall western areas that have been dissected by a major river; the rivers receive both surface runoff and ground-water discharge; water budget calculations are subject to great errors in such areas; and 2) the eastern basins which have a large percentage of impermeable rocks in their valleys. The one exception is the upper Micos basin (above Estación El Salto) which is dominantly karstic, and has neighboring karstic ranges to the north and south. This high rainfall basin is tapped by the Río de los Naranjos, and has a yield that verges on the excessive (0.022 $m^3/sec/km^2$ for 1949-1964, S.R.H. Boletín 32).

The basins having excessive average yield occur along the eastern margin of the Platform or in the lower reaches of the Río Tampaón. All of the known major springs in the region except the Media Luna lie within these basins; however, it is likely that some additional second or possibly some first magnitude springs will be found along the Río Santa María above Estación Tansabaca up to and including the Ayutla area, in the upper Micos basin, and in the Gallinas basin. From the basin relationships shown in Figure 7.10, the areas having surplus flow undoubtedly derive most of their extra water from adjacent, higher karst areas. The lower Tampaón basin, which overall has excessive yield, was divided on the map into two parts: excessive (karstic) and normal (impermeable Valles valley). It is estimated that the total regional runoff may be divided as follows: 33% from the major springs shown in Figure 7.10 (excluding the Puente de Díos) 15% from the impermeable valleys and 52% from the combination of smaller springs, wet season springs, and direct surface runoff from karst areas.

7.2.3 Base Flow and Flood Flow

Insights into the hydraulics and storage of the aquifer and into the types of flow systems that may be present may be gained by studying the low and high discharges of the basins. Section 4.3 discussed the low and average flows. The eleven great springs shown in Figure 4.10 account for 53% of the estimated average annual minimum regional discharge (taken to be about 75 m^3/sec). The Puente de Dios, west of Tampasopo is not included because it is not known whether it is a piracy across a river bend, or a genuine point of ground-water discharge; it is probably the latter. Including the lower Tampaón basin and the unguaged springs of the front ranges (Table 4.6), about 70% of the annual minimum flow is discharged at less than 100 m elevation. In the southern zone, the Coy is by far the largest spring, (about 15 m^3/sec), but many others are also important (Figure 4.10). In the northern zone, only the Mante (8 m^3/sec) and the Frío springs (6 m^3/sec) maintain large base flows; the sources of the base flow (2-5 m^3/sec) of the Río Guayalejo above Estación La Encantada are not known, but are very likely springs. Excepting the upper Micos basin, the karst basins at intermediate to high elevations such as Gallinas and Sabinas have relatively small base flows.

For each basin, the relative importance of base flow versus wet season flooding in the total surface runoff (that which leaves the basin on the surface as measured at the gauging station) may be determined by the ratio $Q_{minimum}/Q_{8\ year\ average}$ (Table 7.8). Values from Table 4.6 are used as representative minima because the lowest recorded discharge for each station given by the S.R.H. (Boletín 32) is often affected. The smaller the

TABLE 7.8

Ratio of Minimum to Average Flows for Basins

Station	Elevation (m)	$\frac{Q_{base\ on\ date}}{Q_{8\ yr.\ avg.}} \times 100$	
		May 1/63	Mar. 28/65
Media Luna	1000	(80-95)	
Coy	31 (at spring)	53.0	53.9
Mante	80 (at spring)	53.5	--
Vigas	897	40.8	35.5
Choy	35 (at spring)	37.6	33.3
El Salto* (Upper Micos basin)	399	(29.3)	(39.6)
La Encantada	(310)**	28.9	27.7
Santa María (Tansabaca-Tanlacut)	174	29.9	22.5
Tampaón Lower	28.2	23.0	26.7
Frío Springs	(90)(at springs)	19.4	25.8
Tansabaca	174	22.6	19.6
El Pujal (R. Tampaón)	28.2	15.8	17.9
Micos	210	14.8	13.5
Tampaón Upper	--	12.6	14.1
Santa Rosa	72.8	9.96	13.5
Gallinas	280	5.17	9.06
Tancuilín	(100?)	5.81	7.32
Valles Valley	72.8	negative	13.3
Tanlacut	257	0	10.8
Requetemú	71.1	4.50	5.45
R. Huichihuayán	--(~100 at springs)	3.86	4.54
Sabinas	89 (160 at spring)	1.95	1.74
La Servilleta	75	0.04	0.04
Rayón Basin (Tanlacut-Vigas)	257	negative	negative

* uses 16 yr. average of 20.499 m^3/sec for 1949-64 (S.R.H. Boletín 32)
** ( ) = estimated or approximate

percentage, the greater the dependence on flooding, or conversely the larger the percentage, the greater its dependence on karstic base flow.

No single factor is apparent that will explain the variable ratios calculated in Table 7.8. Rather, it is believed that the ratio is dependent on the combination of elevation, geographic location, geomorphology, type of rock exposed, and aquifer hydraulics. The first two of the above factors relate the ground surface to local ground-water levels. Generally, among a group of springs in an area, the one having the lowest elevation has the greatest base flow.

7.2.4 The Ground Water-System

In this thesis, it is advocated that a regional ground-water system exists comprising the whole of the Valles-San Luis Potosí Platform. The mathematical framework of such flow systems has been given by Hubbert (1940), Toth (1963), and Freeze and Witherspoon (1966, 1967). Several field studies of regional systems have been reported, and Toth (1972) has summarized their characteristics. The most interesting with respect to variety of supportive data and similarity to the El Abra region are the ground-water systems in the carbonate rocks of eastern Nevada as described by Mifflin (1968), Maxey (1968), Eakin (1966), and Maxey and Mifflin (1966). In such ground-water bodies, the flow is divided into shallow local flow systems, and deep regional flow systems; sometimes, an intermediate flow system is added. The evidence developed here that support the existence of such a system in the El Abra region are: 1) chemical character of the water; 2) spring water

temperature; 3) aquifer hydraulics as deduced from the hydrochemical modeling (section 7.1.3); 4) spatial variations of average yield, particularly the existence of areas that have no surface runoff and that are capable of ground-water recharge; 5) the concentration of most of the flow to a few springs at or near the regional base level; 6) the Coy spring, which unequivocally must obtain its discharge from some distant area(s); 7) exploration oil-well records that demonstrate deep solution effects, permeability, and sometimes actual flow; 8) continuity of the rock body of the supposed aquifer over nearly all of the region.

Fundamental elements of most studies of flow systems in theory and in the field are Darcy flow through granular media, and the concept of fluid potential. The ground-water body will have a smooth, continuous potentiometric surface. Where the potentiometric surface lies below the ground surface recharge may occur, and where at or above water should appear on the ground surface provided there are no confining beds. Because the flow of karst systems is so strongly integrated into discrete conduits (particularly in the Valles-San Luis Potosí Platform) and the flow is commonly turbulent, the application and interpretation in karst regions of the concepts of "phreatic zone", "water table", and "piezometric" or "potentiometric surface" have been questioned and debated (Drew, 1966; White and Longyear, 1962; LeGrand and Stringfield, 1971; and Thrailkill, 1968, to name but a few). It is clear that spatial and temporal variations of aquifer hydraulics and extreme concentration of flow, limit the utility of the above concepts in many karst aquifers. It is believed that the El Abra aquifer has a phreatic zone within which: 1) all openings that have undergone significant

solutional enlargement are conduits, filled with water, that may range in size from caves to fissures and opened bedding planes; 2) all conduits are integrated with karst flow systems; and 3) those openings at shallow depth within the phreas have a distribution of fluid potential that forms a smooth, continuous surface when viewed at the regional scale. The supporting evidence, although meager, includes: the observations in the Sierra de El Abra (discussed in Section 7.3), the existence of regional flow which has an approximately constant discharge as calculated in Table 7.4, the hydrogeologic setting and stability of discharge of the Media Luna spring, the very large number of phreatic conduits that must occur in this large region, and the flooding of deep wells (Carrillo Bravo, 1971). At the micro scale, there will likely be a discontinuity of hydraulic gradient between slightly opened fissures or bedding planes and large conduits, and the potentiometric surface would be quite "bumpy" or even discontinuous.

Based on the criteria listed in Table 7.9, a hypothesized configuration of the dry season potentiometric surface is shown in Figure 7.11. Cross sections are shown in Figures 7.9 and 7.12. The map is of course very crude and highly interpretive, the large springs and to some extent the rivers, being the only positive fluid potential data. There must be a relationship between the discharge of a spring and the size of its recharge area (also the infiltration rate). Hence, regardless of variations in the aquifer hydraulic regime, Figure 7.11 estimates the fluid potential available at each point for driving the flow system, the level to which water would rise in a well if a water-bearing conduit were tapped, and the net directions of regional water movement. Local flow systems may completely disregard the gross regional gradients shown. Some local anomalies occur, such as the 100 m

TABLE 7.9

Data Used to Construct the Potentiometric Map

1. Elevation profile of: Río Tampaón (Santa María)
   Río Verde
   Río Guayalejo
   Río Micos
   Río Gallinas
   Río Comandante
   Río Moctezuma

2. Elevation and base flow of gauging stations

3. Elevation and base flow of major springs

4. Elevation of land surface in the west and in the karst valleys or valley margins that have no surface water -- gives the maximum potential

5. Caves in the El Abra range

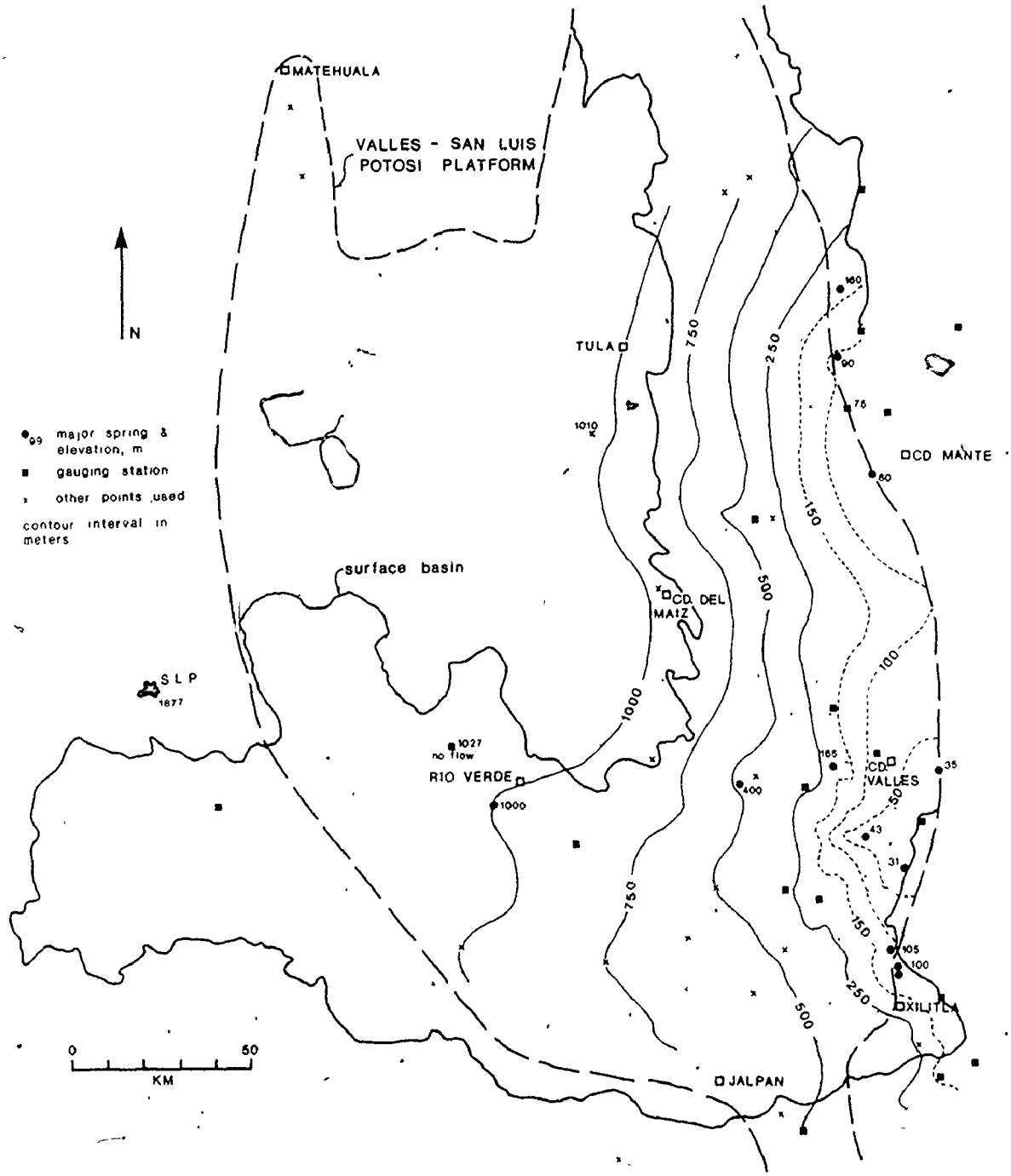

Figure 7.11 Hypothesized regional dry season potentiometric surface.

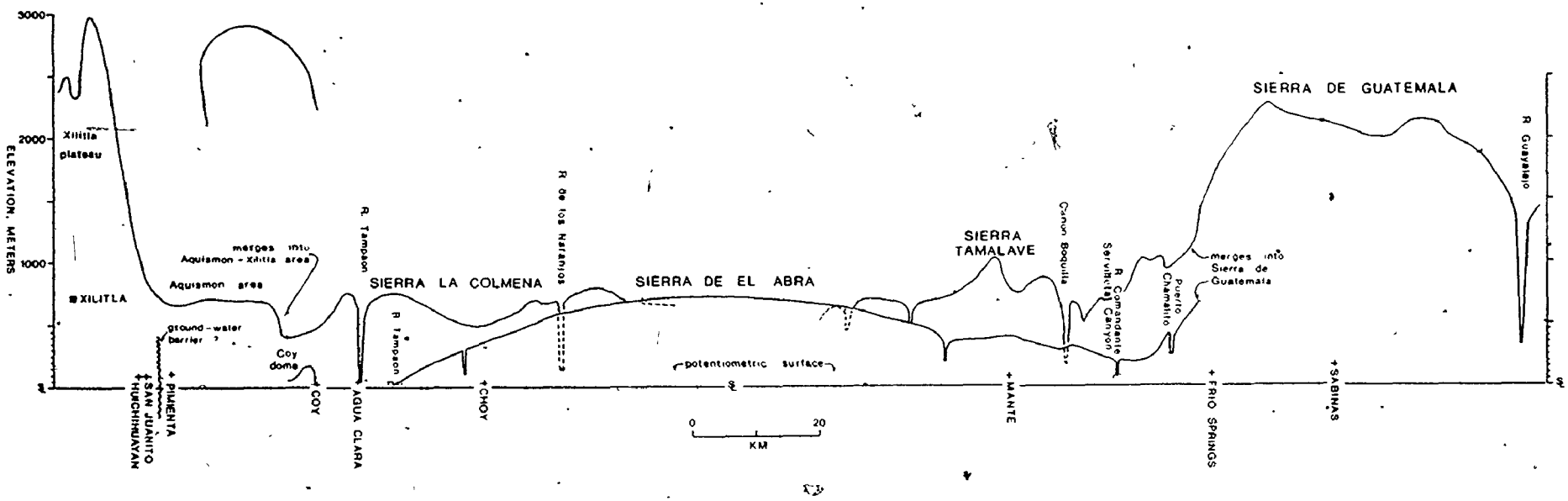

Figure 7.12 N-S cross section of front ranges of Sierra Madre Oriental with regional base levels, major springs, and potentiometric surface

elevation changes at the Micos canyon cascades and at the Salto del Agua cascades, where a major stream may be perched for a short distance. Unless the major rivers are perched and receive their water from vadose storage, the general pattern of the potentiometric surface must be something like that shown in Figure 7.11. Much more information such as influent and effluent reaches of the major streams, possible geologic barriers to ground-water flow, water tracing, cave surveys, and direct measurements of fluid potential is needed.

The ground-water body of the Platform is divided into a large number of flow systems that feed the springs. These systems are classified into three types (see Figure 7.9); 1) local flow where recharge water into a range is discharged to an adjacent valley; 2) intermediate flow where recharge into a range is discharged to a non-adjacent, but nearby valley or at great distance along the strike, or where water from a large karst plateau or massif is discharged at peripheral springs; e.g., the large area of karst ranges and valleys east of Cd. del Maíz has no surface runoff and likely discharges most of its recharge to the Gallinas and upper Micos basins; and 3) regional flow where recharge water circulates deeply and passes through the tectonic structures for great distances before reappearing at the large springs. Presently, the distribution of systems between the first two types is more a conceptual matter of scale than a proven separation of flow systems having distinct boundaries; thus, "local" is often used in this thesis to include "local and intermediate". For the large eastern margin springs, high sulfate and magnesium contents in conjunction with an anomalously high temperature are believed to indicate the presence of a

regional component in the spring discharge.

The potentiometric map plus knowledge of discharge and likely recharge areas, particularly those with deficient runoff, were used to infer the general source areas and directions of flow of the local and regional ground-water systems (Figure 7.10). The arrows indicate probable or possible general directions of water movement, not specific source to spring flow paths, because no such relationships are yet known. For example, the recharge water that eventually leaves the karst area east of Cd. del Maiz via the subsurface might flow to the Coy, to springs along the Río Tampaón, Río Gallinas, or Río de los Naranjos (upper or lower Micos basins), or possibly even to the Choy or Mante springs. The general directions of regional ground-water flow must be to the east or southeast. Local flow systems may be oriented in any direction. Intermediate systems will normally have an eastward component of movement, but may also have a large north or south component.

To summarize, many lines of evidence support the existence of regional, as well as local components of flow to the large eastern margin springs of the Platform. Such systems are usually quite difficult to "prove" by water budget calculations alone, but here the combined evidence seems conclusive. It is hypothesized that the limestone aquifer has a phreatic zone, which at the regional scale is smooth and continuous, and indicates the general amount of hydraulic head available to drive regional flow systems. At the local scale, flow system theory may break down if ground water is concentrated into too few conduits.

The magnitude and amazing stability of the Media Luna discharge (Table 7.8) must result from the fact that its likely source areas lie far to the northwest and that large precipitation events are rare compared with the Valles area. The well water-level data of J. Lesser (unpublished S.R.H. report) show that the Media Luna discharge is unrelated to the flow system of the Río Verde valley sediments, and thus could only be derived from the El Abra and Guaxcamá Formations. The morphology of the spring and the concentrated discharge point (rather than a long zone of discharge) also support this conclusion. The Sierra Madre fold belt creates a partial barrier, which helps to maintain a high zone of saturation west of a N-S line from Tula to Rayón. The Media Luna spring probably discharges a considerable part of the water that infiltrates in the limestone mountains west of the Río Verde valley. The surprisingly high ratio (Q_{min}/Q_{avg}) at Estación Vigas (Table 7.8) is caused by ground-water seepage from the Río Verde valley sediments (0.5 m^3/sec) and return irrigation water from the Media Luna (1.8 m^3/sec; data from J. Lesser, unpublished report). The Nogal Obscuro station (elevation 1027 m, only 27 m above the Media Luna) which gauges the upper half of the basin above Vigas and is situated at the eastern edge of the limestone mountains west of the Río Verde valley, has zero discharge during most dry seasons. It is not known if there is hydraulic continuity between the valley sediments and the adjacent El Abra water bodies.

The large fraction of the total discharge of the Mante, the Coy, and the Choy that is provided by their base flow is not surprising, considering their elevation and location: they receive water from both local and regional sources. The Sabinas spring (160 m) has only a modest dry season flow (0.3 m^3/sec) because the Frío springs (about 90 m) have the elevation

advantage to capture nearly all (95%) of the base flow from the massive Sierra de Guatemala and ranges farther west (Figure 7.12). The Frío springs also capture about two-thirds of the total discharge from that area. This is an example of the control of elevation on local and intermediate to regional flow systems.

During the wet season, the dynamics of the aquifer become most complex. Large storms apply a "stress" to the aquifer causing rapidly changing water levels and hydraulic conditions. Individual flow channels behave according to the amount of input and their capacity to transmit the water supplied. When this transient state exists, the potentiometric surface is undoubtedly discontinuous, extremely variable, and generally unmappable. Note that in Figure 7.9, the trace of the potentiometric surface has not been shown as a subdued version of the topography, although it might have such a profile, because in the high karst area of the Sierra Madre Oriental, both the ridges and the valleys act as recharge sites. The wet season conditions are unknown, will be very complicated, and need a great deal more field work. The flood-pulse chemical dilution analysis of some eastern margin springs presented in Section 7.1.3 suggests that the local and intermediate flow systems are the dynamic systems, while the regional flow systems are discrete and relatively unaffected by wet season events. The very low ratio of Q_{min}/Q_{avg} (Table 7.8) for such basins as Río Gallinas and Río Sabinas means that in those basins, there is relatively little water in gravity storage above the springs and most of the flood recharge is quickly discharged. More discussion of local flow systems is given in Sections 7.3 and 7.4.

The presence of high sulfate concentrations in such eastern margin springs as the Choy and the Coy is a clear demonstration of a regional component in their discharge. This may not be true for springs in high ranges 50 km to the west. As may be seen in the cross section (Figure 7.9), tectonic deformation is expected to have raised gypsum (or anhydrite) to a few hundred meters elevation above sea level in the high sierras, causing a considerable thinning of the phreatic zone. Some of the folds are of sufficient breadth to contain a gypsum core ridge (Carrillo Bravo, personal discussion, suggests that many of the folds are of the injection type). Further north, in a large area east of Cd. del Maiz, some of the folds are higher yet and have a structural and topographic relief of about one kilometer. There, gypsum may be brought up to an elevation of 500 m or more, and would therefore nearly reach the level of the valley bottoms. Under these conditions, it seems quite likely that many of the intermediate and local systems may obtain moderately high sulfate concentrations. The Puente de Díos spring above Tamasopo may represent this kind of situation, and some of the springs along the Río El Salto probably will contain sulfate. Another effect of the gypsum ridges or of longitudinal fracturing might be to channel water along the strike to the southeast.

The boundaries of the regional ground-water body are not known, and thus will be hypothesized. In general, the extent of the system is probably delimited by the aerial extent of the El Abra Formation, including the forereef, reef, and backreef to lagoonal facies; in other words, a paleogeologic unit, the Valles-S.L.P. Platform, effectively defines the zone of significant ground-water movement. The deep water sediments of the Mesozoic Basin of Central México (Carrillo Bravo, 1971) are not expected to transmit large

quantities of water eastward into the El Abra Formation; some of the volcanic rocks and the valley-fill sediments west of the Platform might transmit a small quantity into the region. However, it is known that there is some ground-water flow in that area; Waring (1965) lists a radioactive thermal spring 40 km south of San Luis Potosí having a very large flow of 5.27 m^3/sec, and two smaller thermal springs in the Querétaro area. The northern and southern margins of the Platform must be considered partially open because the reef trend continues as a narrow belt to the south and the Cuesta del Cura, the deeper water equivalent of the El Abra to the east and the north, probably can develop some secondary permeability. However, the principal flow direction is thought to be eastward; hence, ground-water gains or losses across the northern or southern margins should not exceed a few percent of the total regional budget. Finally, as may be seen in the cross section (Figure 7.9), the juncture of the Platform and the ancient Gulf of México deep water sediments clearly forms the eastern boundary of the flow systems. Some permeability has been reported in the transition zone from forereef dolomite and reef debris to the Cuesta del Cura Formation, where some wells have been invaded by water (Carrillo Bravo, 1971); and in some oil fields near Tampico, the Tamaulipas Formation possesses some fracture permeability. The coastal plain is the spill point of the aquifer: all ground-water flow must return to the surface at this juncture because that is the easternmost point at which it can escape.

7.2.5 Ground-Water Temperature

The analysis of ground-water temperature is placed here rather than

in the chemical modeling section because it can be best understood in the context of the local and regional flow system analysis given in this section, particularly with reference to Figures 7.9 and 7.12.

The observed distribution of spring water temperatures is given in Figure 5.4. Excluding the thermal springs and the Media Luna, the range was from 19.6 to 26.5°C. Springs such as the Choy and the Coy exhibit larger temperature changes during flooding than they do seasonally. The temperature difference between early and late dry season measurements of the Santa Clara and San Juanito springs was only 0.1°C, and at Arroyo Seco was 0.2°C (Table 5.1).

There are very few measurements of temperature as a distributed parameter of the aquifer. A few are reported by Mitchell et al. (1977) and Bonet (1953a, 1953b); all are from the Sierra de El Abra except those from the Xilitla area given in the latter paper by Bonet. Furthermore, all except two or three are from perched cave lakes, many of which are sufficiently close to a cave entrance to be controlled or strongly influenced by the average seasonal temperature. The range seems to be about 19-26.5°C for the Sierra de El Abra.

As previously indicated, there is a relationship between the temperature of a spring (during dry season base flow), the elevation of the supposed recharge area, and the chemistry of the spring. Those springs which yield nearly "pure" calcium-bicarbonate type water have the expected inverse relationship between temperature and elevation of the recharge area. Arroyo Seco (Rancho El Peñon) and the Santa Clara springs (in the

Sierra de El Abra) were very similar at 23.6-24.1°C, whereas the Sabinas, Huichihuyán, and San Juanito springs were cooler at 19.7-21.0°C (see Figure 7.12). The discharge of all these springs is interpreted as coming from local flow systems with relatively shallow circulation and short residence time. The high sulfate springs, with their regional component of flow, have higher temperatures derived from deeper circulation that has a longer residence time. The flood pulse studies described in Section 5.3 were particularly valuable in interpreting the thermal characterisitcs of the ground-water system. The correlation between the sulfate content and the temperature of a spring support the model in which the regional flow is warmed above the temperature of the local flow. No overall direct relationship exists between the chemical and physical properties of the springs as a group. On the contrary, each has its own physico-chemical characteristics dependent on the characteristics of its local source(s) and of its regional source(s). The Choy and the Mante have nearly identical geochemical "paths"; thus, the source areas of the Choy and the Mante springs are believed to be similar in character. The springs differ principally in magnitude of flow and mixing ratio. The Coy spring has an offset "path" because its local source area(s) has different climatic conditions, and as previously shown, its regional source has slightly different chemical properties than those of the Choy and Mante, and thus may have a different temperature as well.

To summarize, the principal water-temperature controls are believed to be: 1) local climatic conditions and geothermal heat flux in the local flow systems, and 2) only the geothermal heat flux in the regional flow system. The temperature would vary with position in each flow system,

gradually becoming warmer from the recharge point to the discharge points. Other influences that are believed to be less important are: 1) geochemical reactions such as solution processes or mineralogic changes of anhydrite to gypsum or vice versa; in some zones of nearly stagnant flow, the oxidation of hydrocarbons and the reduction of sulfate ions; 2) possible anomalies around intrusive bodies; and 3) lag effects induced by the reservoir rock as cooler flood pulse waters alternate with warmer local or mixed flow waters.

In the proposed hydrologic model of the region, the temperature of the low sulfate springs is presumed to be the integrated result of the above effects on type A water. The temperature of the type B water will be estimated by a mixing equation, with notation as in Section 7.1.3:

assume $T_2 = T_C$, i.e. there is no change in the temperature of the mixed water before it is discharged.

$$Q'_A \Delta T_A = -Q'_B \, T_B, \text{ where } \Delta T_A = T_2 - T_A$$

$$\Delta T_B = T_2 - T_B$$

$$\text{and } Q'_A + Q'_B = 1$$

$$\Delta T_B = -\frac{Q'_A}{Q'_B} \{\Delta T_A\}$$

T_2 is measured, Q'_A and Q'_B are calculated as in Section 7.1.3, and T_A must be estimated by some means. For the Choy on May 21, 1973:

$T_2 = 26.4°C$

$T_A = 24.8°C$ by extrapolation of Figure 5.9

TABLE 7.10

Calculated Temperatures for Type B (Regional) Water

Spring	T_2	T_A	Model No. used for Q_A&Q_B	Calculated T_B	Criteria used for T_A
Choy	26.4°C	24.9°C	15	32.0°C	extrapolation of Choy line in Figure 5.9
		24.0°C	15	35.4°C	temperature of Arroyo Seco & Santa Clara springs, and cave lakes
		24.9°C	20	28.8°C	extrapolation of Choy line in Figure 5.9
		24.0°C	20	30.2°C	Santa Clara & Arroyo Seco springs, plus cave lakes
Coy	24.6°C	21.4°C	22	29.5°C	extrapolation of Coy line in Figure 5.9
		20.5°C	22	30.9°C	suggested to be slightly warmer than Huichihuayán and San Juanito springs
Mante	26.5°C	24.0°C	15	34.3°C	Santa Clara & Arroyo Seco springs plus cave lakes
Frío	22.6°C	21.0°C	15	36.7°C	Sabinas spring

Q'_A and Q'_B as calculated from model number 15 (equilibrium model) in Table 7.2

then $\Delta T_B = -(0.79/0.21)(26.4-24.9) = -5.64°C$

and $T_B = 26.4°C + 5.6°C = 32.0°C$

If 24.0°C is used for T_A, based on measurements of two small springs and selected cave lakes, a value of 35.4°C is obtained. These and other results are given in Table 7.10. Chemical models of type B water that are at equilibrium with respect to gypsum yield temperatures ranging from 30-37°C. The Coy has distinctly the lowest calculated T_B, as it had with the dissolved species (Section 7.1.3). If the deep regional flow has not reached chemical equilibrium with respect to dolomite or gypsum, then Q'_B must increase and Q'_A must decrease (Section 7.1.3), causing the calculated T_B to decrease as shown for the Choy in Table 7.10. The differences between the early and late dry season temperatures of the high sulfate springs appears to be greater than the local flow springs; perhaps this is because the mixing ratio of the type 2 (high sulfate) springs gradually changes during the dry season.

7.2.6 Discussion

Figures 7.9, 7.10 and 7.12 summarize many of the important regional geologic, geomorphic, hydrologic, and hydrochemical relationships. Erosion first exposed the structurally highest parts of the El Abra and Tamasopo Formations probably sometime in the early to middle Tertiary. The El Abra

Formation is believed to have a karstic permeability over the whole Platform, and it forms a nearly continuous aquifer.

As previously stated, one of the principal contentions of this thesis is that the chemistry and temperature characteristics of the springs together with their elevation and discharge form a consistent and reasonable pattern. The properties listed above have been studied for many large and several smaller springs generally in the eastern part of the Platform. For each of the large springs, Figure 7.10 lists the elevation, the estimated average dry-season minimum flow, the highest measured sulfate concentration (mg/l), and the highest measured temperature so that their geographic distribution and properites can be seen. According to the interpretations given here, the local flow systems along the eastern part of the Platform have Ca and HCO_3 as their major constituents and a temperature that reflects the elevation (and climate) of their recharge area; examples of springs believed to have only local sources are Santa Clara, Arroyo Seco, Huichihuayán, San Juanito, Sabinas, and Canoas. Some large springs combine local sources with a regional source of water that is of calcium-magnesium sulfate type, and that is much warmer. These mixed flow springs (type 2) exhibit temperatures a few degrees higher than nearby local flow springs (type 1). Furthermore, the greater the sulfate content, the greater the temperature difference; hence, the greater the <u>percentage</u> of regional water in the mixed output. There is also the very important relationship whereby the springs that have the highest sulfate contents also have the greatest base flows and are the lowest elevation springs in their areas. The Coy is the principal outlet for regional flow in the southern part of the region and has the lowest

elevation and the greatest base flow of all the springs; the Mante is its northern counterpart. Based on elevation and the water budget calculations (Section 4.3), Figure 7.10 shows some of the possible general directions of local and regional ground-water flow. Springs supported only by local flow systems rapidly discharge flood recharge and retain relatively small quantities of water in gravity storage -- they are principally conduit flow systems. The mixed source springs have greater stability of flow and have much larger quantities of water in gravity storage; it is concluded they have conduit type local flow systems, but probably have a large quantity of water stored in more slowly moving regional flow systems that have smaller in diameter conduits.

The general concept of the two water types, the local and regional ground-water systems, and the geologic basis are shown in Figure 7.9. The sulfate content of the water is believed to be derived mostly from the massive Guaxcamá Formation, although some of it might be derived from the thin sediment veneer (including gypsum) in the Río Verde valley; however, sulfate water derived from the sediment probably would be deficient in Mg. It is hypothesized that water circulates deeply through a fractured dolomite aquifer at the base of the El Abra Formation where it also contacts and dissolves gypsum (or anhydrite). The intensely deformed fold belt is an especially likely place of gypsum solution, and the broad "basin" west of the high sierras should also be favorable.

The real system is undoubtedly more complicated than the simple model proposed in Figure 7.3. One possible deviation is the alternate source of sulfate mentioned above. Another deviation would occur if some

type B water leaves the dolomite-gypsum area, but remains in contact with the basal dolomite near the reef trend (Figure 7.9); this could explain the greater Mg/SO_4 ratio in Choy water compared with the Coy. As previously mentioned, in the high sierras, gypsum in the interior of folds may be raised to nearly the level of the valley bottoms; hence, some of the local and intermediate flow systems there may contain significant amounts of sulfate. The Puente de Dios spring at Tamasopo did have high sulfate content, but the Canoas (farther west) did not. Another complication is loss during base flow of some high sulfate water from the Río Verde (and possibly the Río de los Naranjos) back into the subsurface. Probably the most important factor not covered in the model is regional movement of type A water. Such movement is clearly possible (in fact probable), and it would remain an undetected third source in the two-source hydrochemical model developed here.

It has been previously shown that the Coy discharge is strongly dominated by its local source during flooding. Because the Coy is the lowest major spring in the region (31 m) and because it does carry local source water during floods, it is therefore likely that part of the Coy's base flow is derived from local sources also. This suggests that the chemistry of type B water is probably nearer the model with the maximum sulfate content than the model with the minimum (taken to be identical to the largest value measured at the Coy spring), and that the regional flux of type B water is nearer the calculated minimum than the calculated maximum. Temperature considerations also support this conclusion. The regional sources of each type 2 spring have slightly different concentrations of the major chemical species as demonstrated by their chemical ratios and chemical dilution paths.

This might be explained by some of the complicating factors discussed in the preceding paragraph, particularly variations of flow path, or by differences in residence time.

Another important point to note in Figure 7.10 is the geographic distribution of the high sulfate springs: they encompass all of the major eastern margin springs except those at the extreme north and south ends. There is a sharp break in the hydrochemistry between the Pimienta and the San Juanito-Huichihuayán springs; the separation of flow systems is probably caused by a structural discontinuity between the Xilitla and Aquismón areas (Figures 7.10 and 7.12). This constitutes the only boundary between flow systems known with any degree of geographic precision. The latter two springs are the most important in the intensely karstic Xilitla area, but have surprisingly low minimum flows compared with the Coy, Choy, and Mante for example. At the northern end, the change is more gradational. The Frío springs have a very large base and total flow, but only about 10% of the base flow is supplied by type B sources. This great spring group is the principal outlet for Sierra de Guatemala ground water and probably for nearby ranges to the west (the Frío springs may receive intermediate or regional flow from western ranges). This suggests that there is little or no gypsum in the subsurface of those ranges.

A few final points are:

1) Despite the potentiometric map given in Figure 7.11, the permeability development (i.e., conduits) may be anisotropic; geologic structure and fractures may often favor strike-line flow; in the high, folded karst area east of Cd. del Maiz, it appears that water is transmitted along

the strike to the north and the south rather than eastward to the lower Micos basin;

2) The interpretation given in Section 7.1.3 that the regional source (type B) water to the Coy is diverted during flooding to the Pimienta and perhaps to other springs implies a well-integrated system of conduits within the limestone aquifer. This would have serious consequences to the success of a proposed artificial surface reservoir that would flood a large area of the Valles valley west of El Pujal, including the Coy spring.

3) A minimum value for the average gradient of the regional potentiometric surface may be determined between the Media Luna and the Coy springs. The value is:

$$\text{gradient} = \frac{(1000-31)\text{m}}{115\ \text{km}} = 8.43\ \text{m/km or } 0.0084 \text{ dimensionless}$$

This is a very high gradient for large karst-conduit systems, and indicates that the conduits are often constricted or generally poorly developed.

4) Some support for the regional ground-water flow system described is obtained from a report by Lesser Jones (1967) on deep water wells in the Monterrey area which obtain large quantities of fresh water from massive confined Cretaceous limestones hundreds of meters <u>below</u> sea level. The probable recharge areas are located 50-100 km to the west. Water levels in the wells recover very rapidly after pumping ceases, respond quickly to rainfall on the recharge areas, and exhibit seasonal fluctuations of 20-80 m.

7.3 Hydrology of the Sierra de El Abra

One of the principal goals of the thesis was to collect data to develop a qualitative and quantitative understanding of the hydrology of the Sierra de El Abra. Some of the information and analysis has been given in Chapter IV, particularly Sections 4.2 and 4.4. This section will utilize previously developed and other data and interpretations to summarize the presently known hydrology of the range.

7.3.1 Water Budget and Distribution of Discharge of the Sierra de El Abra

Recharge into the Sierra de El Abra occurs wherever the El Abra limestone is exposed including numerous places along the western margin where streams flowing from shale catchments are pirated underground; the piracies usually occur a short distance beyond the point where the streams pass onto the limestone. Surface runoff from the El Abra limestone does not occur except along the steep eastern escarpment and possibly at a few other minor localities. Thus, precipitation on the range may effectively be divided into evapotranspiration losses and ground-water recharge.

Discharge from the El Abra aquifer is from springs. The two most important are the Mante and the Choy -- they are first magnitude springs. Both maintain a large base flow, estimated to average about 8 and 2.5 m^3/sec respectively late in the dry season (from inspection of S.R.H. data). Subtracting the surface runoff included in the gauging station measurements, the long-term average discharges of these springs are calculated to be about 11.9 and 5.41 m^3/sec. However, there are also a number

of smaller springs that are significant to the hydrology. These latter springs have a very small base flow; many dry up completely during the dry season. The third most important spring in the range is probably the Nacimiento del Río Santa Clara (actually, there are two temporary and one perennial springs). Although its dry season base flow is only about 0.3 m^3/sec, wet season floods are sufficient to produce a significant yearly total discharge (Figure 4.10). The average discharge at the gauging station for 1972 was 2.53 m^3/sec and for 1973 was 5.09 m^3/sec (calculated from S.R.H. stage and discharge measurements, Section 4.2). Using rainfall data at El Refugio (an S.R.H. Climatologic station 12 km northwest of the gauging station), a minimum contributing basin area was calculated for the major floods of 1972 and 1973, assuming that storm runoff equalled the volume of precipitation. The pre-flood base flow component was subtracted from the total flow, but changes in aquifer storage were only partially taken into account. The values of the minimum contributing total area ranged from 82-123 km^2. From air photos, the maximum surface basin included within the catchment was measured to be 16.5 km^2; it may be less because there may be artificial diversions of one of the principal streams out of the basin. Thus, the infiltration water into at least 85 km^2 of the El Abra limestone is required to provide the measured flow of the Santa Clara springs. These calculations demonstrate the extremely dynamic discharge pattern of the springs in the Sierra de El Abra and other places in the region that have small base flows, and also their capacity to yield important yearly total volumes of water. Based on the size of their drainage channels, it is suggested that many of the other small El Abra springs

such as the Tantoán, San Rafael de los Castros, and Arroyo Seco on Rancho Peñon carry moderately large floods and have significant total discharges, although less than the Santa Clara springs.

It is desirable to determine the water budget for the Sierra de El Abra. Unfortunately, there are several problems including: 1) complete lack of raingauge stations on the range (Figure 4.3); 2) not all the springs are monitored for runoff; 3) the basin or catchment area is not clearly defined because the El Abra limestone of the Sierra de El Abra connects directly at its north end with the Sierra de Guatemala, and via the subsurface with other exposures in ranges to the west; and 4) no drainage divides for the springs have been established. Enjalbert (1964), on the basis of a brief field trip in the region and apparently having no quantitative data on the regional hydrology, hypothesized that the principal source area of the Mante and Frío springs is a calcareous plateau or mountain ranges 30-40 km to the west. He even gave a cross section showing ground-water flow through caves under the Antiguo Morelos valley to the Mante spring. Mitchell et al. (1977) have argued that all of the discharge from the Sierra de El Abra is derived locally, based on a crude water budget and the response of the Choy and Mante springs to storms.

An improved water budget calculation is given here. The approximate local source area involved is determined in Table 7.11. For the period 1961-68, the discharge of the Mante was 11.77 m^3/sec and of the Choy 5.07 m^3/sec. Of the two years for which data are avilable for the Santa Clara springs, 1973 was exceptionally wet, but 1972 was about average or slightly above for the nearby area. Hence, the long term average discharge of the

Santa Clara springs should be about 2.5 m /sec, and this value is taken for 1961-1968.

TABLE 7.11

Drainage Area of the Sierra de El Abra "Basin"

			km^2
Outcrop area of El Abra limestone in El Abra range*			740
Surface catchments included at gauging stations			
	Mante	69	
	Choy	4.9	
	Santa Clara	16.5	
		90.4	90.4
Basins of western margin swallet caves (Table 3.1)			75.6
		Total Area	906 km^2

*Mitchell et al. (1977) give 718 km^2 for the El Abra range up to the Río Comandante; an additional 22 km^2 is allowed for the extension of the range to Puerto Chamilito.

The total discharge of all the other small El Abra springs including losses from the southern end of the range into the Río Tampaón and from the northern end into the Río Comandante is assigned a value equal to that of the Santa Clara springs; this is likely within a factor of 2 of the real value. Any direct runoff from the east face is not allowed for. Hence, the average discharge from the Sierra de El Abra was about 21.84 m^3/sec. Rainfall in the area is about 1000 mm per year near Mante, 1100-1250 at the ends of the range and along the western side, and might be on the order of 1300-1400 mm on the high central portion of the range. Using a "basin" average of 1250 mm per year, the potential runoff is 35.89 m^3/sec. If all of the observed

(or estimated) runoff came from the basin given in Table 7.11, runoff would be equal to 61% and evapotranspiration would be only 39% of the precipitation. A high amount of infiltration into the El Abra aquifer would be expected because it has spotty soil cover over a highly permeable karst surface; but the 166 km^2 that yield surface runoff (swallet cave catchments plus surface areas included at gauging stations) should be less efficient at producing runoff, like the Valles valley (Section 4.3.3), because of soil infiltration and other losses. It was observed in the field on some occasions that several days of showers did not cause the arroyos of the swallet caves to run. Furthermore, dry season showers of as much as 30 mm seldom cause a noticeable response at the springs. The percentage of runoff calculated above is a very high value, and is thought to be too high.

Using figures from above, the unitary discharge of the El Abra range is calculated to be:

$$U_{\text{El Abra Range}} = \frac{21.84\ m^3/sec}{906\ km^2} = 0.0241\ \frac{m^3/sec}{km^2}$$

This is <u>three times</u> the value calculated for the Valles valley (taken to be about 0.008 in a possible range of 0.00604-0.00955 $\frac{m^3/sec}{km^2}$; see Table 4.12), and 25% greater than the 0.0193 $\frac{m^3/sec}{km^2}$ value determined for the high rainfall karstic belt in the eastern part of the Valles-San Luis Potosí region. This latter area was termed the "reduced region" in Section 4.3.3, and its estimated average yearly rainfall was 1500 mm. Ergo, the calculated hydrology of the Sierra de El Abra, the analysis of the regional hydrology (Section 7.2, particularly 7.2.4), and the hydrochemical model (Section 7.1) all support the existence of a regional com-

ponent of flow in the discharge from the range. It is thought that the smaller springs are local flow systems, whereas the Choy and Mante springs have both local and regional sources. If the minimum and maximum components of regional flow to the Mante and Choy as determined in Table 7.4 are subtracted from the El Abra discharge, the new unitary discharges are 0.0201 and 0.0146 $m^3/sec/km^2$ respectively. Runoff from the local source areas would then be equal to 51% or 37% of the precipitation. These new figures delimit the range of possible values for the El Abra range hydrology as determined by the modeling in this thesis. Based on the hydrochemical model, the regional component of flow to the Choy and Mante represents 17% to 39% of the total discharge from the El Abra range while the local component represents 83% to 61%. Most of the regional flow is focused on the Mante spring, where it comprises 25-60% of the total flow. If there is regional ground-water flow of type A water (as discussed in Section 7.2.6) to the Mante and Choy springs, then the amount of local discharge would be less still, and the calculated values above would have to be further amended. Thus, Enjalbert (1964) was correct when he guessed that there is regional flow to the Mante and Frío springs, but according to the hydrochemical model developed here, he may have overestimated the amount. Reasonable changes in the quantity of runoff and of precipitation used in the calculations above will cause only about a 10% and a 15% change in the calculated unit runoff and percentage of runoff respectively.

7.3.2 Analysis and Discussion of the Ground-Water Systems

This section will examine the data concerning El Abra ground water,

present models in an attempt to explain the observed hydrology, and indicate some of the problems and uncertainties that remain.

A significant part of the field work was devoted to mapping caves, observation of the relationship of caves to the hydrology, and mapping water levels to determine hydraulic gradients, the potentiometric surface if possible, and whether the swallet cave siphons were perched or at the water table. The El Abra limestone itself has essentially no capacity to transmit water. All flow occurs along fractures and bedding planes that have been enlarged by karst solution processes. The amount of solutional enlargment is highly variable. Field observations of the aquifer and the extremely dynamic response of the springs to rainfall demonstrate that recharge rapidly infiltrates the aquifer and is integrated into large caves (conduit flow systems) that are commonly 5-10 m (or more) in diameter. Flood waters should be rapidly discharged from the cavern systems. Evidence that supports the idea of high flow velocities includes: 1) emergence of muddy water at El Choy within a few days after heavy rains cause runoff to the swallet caves; 2) undersaturation with respect to calcite of flood waters at all springs sampled and at local flow springs such as Santa Clara during the dry season; and 3) the tentatively positive spore tracing test from Sótano de Japonés to El Choy. Furthermore, the Santa Clara spring does not have a large quantity of water in gravity storage compared with the volume of its flood discharge; this implies a short residence time. The discharge from the Choy and Mante springs is estimated to be 82% of the annual flow and 97% of the dry season base flow from the El Abra range (including surface catchments as discussed in Section 7.3.1).

Hence, the aquifer would appear to be strongly integrated into two ground-water systems that have a very large amount of water in gravity storage. Water discharged during the dry season obviously has been in the aquifer a minimum of several months — much longer than at least part of the flood waters, but still a very short time for ground water.

Discharge from the Sierra de El Abra usually has some component of lift or rise to it, i.e., the springs are openings at the top of flooded portions of caves. None of the springs are thought to be perched. It is believed that the El Abra has a phreatic zone in which all secondary openings are filled with water. Circulation within the phreatic zone likely reaches several hundred meters below regional base level and might extend downward to the base of the aquifer. Large fractures provide the routes for vertical movement of water in the aquifer, and may play an important role in horizontal movement to the two major springs in this greatly elongated range (e.g. along longitudinal fractures in the reef zone). The depth of circulation is discussed further in Section 7.4.

The problems of the phreatic zone in a karst aquifer such as the El Abra are the hydraulics and dynamics of the aquifer, the nature of the potentiometric surface, and the distribution of storage. It is anticipated that the potentiometric surface will be highly irregular because the range of cross-sectional area of the conduits is extreme. Water in narrow fissures requires a much greater hydraulic gradient for a significant flow rate than water in large caves. If only large conduits are considered, the potentiometric surface might be reasonably smooth; perhaps more significant is the hydraulic gradient of each of the large conduits. Figure 7.13

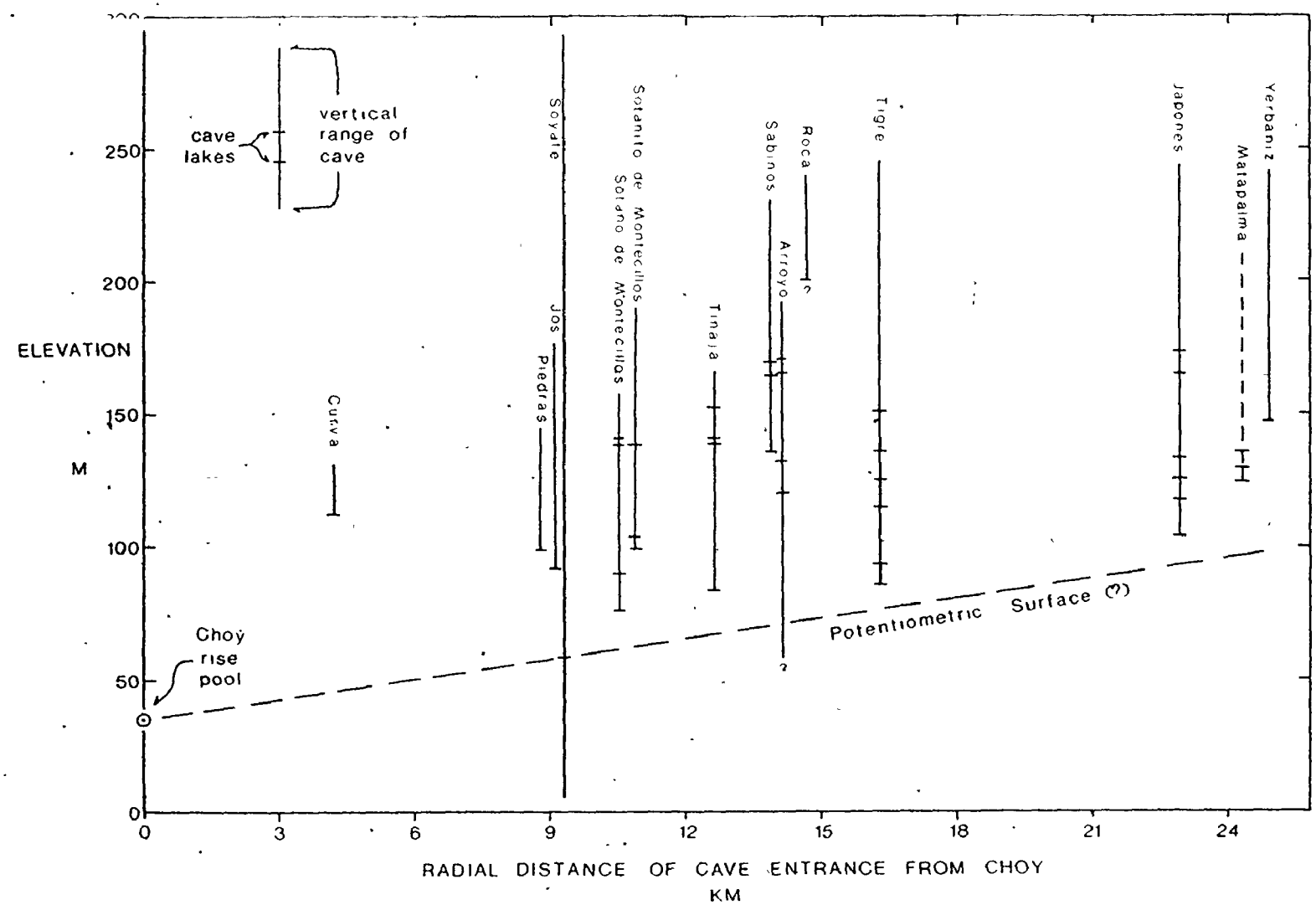

Figure 7.13 Comparison of elevation of cave lakes and deepest point known in caves with radial distance to and elevation of El Choy rise pool.

is a plot of the elevation of most of the more important cave lakes in the southern El Abra range against their radial distance from the Choy spring (Table 7.12 lists cave depths and terminal siphons). The caves are drawn vertically instead of in true profile, but this will not introduce a large error. Obviously, most of the lakes are perched, usually on mud. As discussed in Section 4.4.2, the elevation, the water depth, and most importantly, the hydrograph of the lake in Sótano de Soyate are indicative of a genuine "water table" lake. However, data through the dry season have not been obtained, so it is possible that after some drawdown the lake will become isolated by a rock barrier in the conduit, causing stabilization of the surface. A straight line has been drawn from El Choy through the early January, 1972, elevation of the Soyate lake as an approximation of the potentiometric profile for large El Abra flow systems. The gradient of this profile, is 2.6 m/km, which is greater than a preliminary estimate of 1.0 m/km given by Fish and Ford (1973). The geomorphology of the swallet caves suggests that <u>all</u> of their "terminal" siphons are perched lakes, still above the level of permanent water saturation in each conduit. Open air passage is predicted to be beyond their siphons, even though several of the large swallets have been explored to depths that approach the projected fluid potential line. Exploration in Sótano del Arroyo was halted by 4% CO_2 in the air rather than by a sump. According to the profile drawn, it should have reached the phreatic zone, but the cave survey, the altimeter reading, or the potentiometric profile may be in error. The hydrographs from Sótano de Jos reveal the character of these perched lakes. Their surface levels remain approximately static except when they are in flood.

TABLE 7.12

Cave Survey Data and Elevations for Water-Level Profile

CAVE	surveyed cave depth m	entrance[4] elevation m	deepest known free air point m
Choy resurgence pool	—	—	35
Curva (Ferrocarril)	19[1]	131.5	112.5
Palma Seca	52.5[1]?	151.5	99?
Piedras	46.5[1]	145	98.5
Jos	84.5	176	91.5
Soyate	234	293	59
Sótano de Montecillos (Pichojumo)	81.5[2]	157.5	76
Sotanito de Montecillos	91.5[2]	190	98.5
Tinaja	82	165.5	83.5
Sabinos	95.5	231	135.5
Arroyo	134.5	192	57.5
Roca	(42)[1]	240.5	(198)
Tigre	160.0	245.5	85.5
Japonés	139.5	243	103.5
Matapalma	86.5[3]	(210*)	(123.5)
Yerbaniz	95[1]	241.5	146.5
Prieto (Los Cuates)	32.5[1]	61.5	29
Chica	18[1]	49	31
Venadito	> 183 [1]	312	< 129
Pachón	8[1]	210.5	202.5

1. Mitchell et al., 1977.
2. Morris, Neal, personal communication.
3. Walsh, M., 1972
4. The elevations used here, except for El Choy, are those given by Mitchell et al. (1977).

* estimate

It was previously stated that the dry season flow from the El Abra range is concentrated almost exclusively at the Choy and the Mante springs, and that this implies a very strong integration into 2 flow systems. However, in previous sections of this chapter, it has been shown that at least part of the base flow is derived from regional sources. Furthermore, all of the springs yield moderate to very large flood pulses. These facts lead to three possible models to account for the observed flow behavior:

1) there are two distinct types of flow system (cave) development and storage in the Sierra de El Abra aquifer -- one for the two high base and total flow springs, the other for the smaller springs; the smaller springs have drainage systems that are not integrated with the two main systems; a large part of the base flow comes from El Abra range storage;

2) the aquifer is almost completely integrated into two systems and the smaller springs function as spillovers for high water levels that occur during the wet season; a considerable part of the base flow comes from El Abra range storage;

3) the dry season flow of the Mante and Choy springs is derived almost completely from regional sources to the west, and the local flow system behind each spring is essentially isolated and supplies the flood waters.

The first model seems unlikely because no adequate causal factors have been observed which could account for two distinct types of flow-system development. Basically, the model requires one type to be capable of vast

storage and the other type to be relatively incapable of storage. Infiltration into the range should be greatest in the high central portion of the range, yet the two largest springs occur near the ends. Water stored in narrow bedding plane or fissure openings and in larger conduits should be relatively uniformly distributed throughout the range, yet the smaller springs except the Santa Clara (and the thermal springs) dry up completely sometime during the dry season. The capacity for three-dimensional circulation within the aquifer is believed sufficient that flow should continue even if some horizontal conduits contain bedrock barriers to movement during low water stages; shale barriers can not be called upon as an explanation. If the systems were truly isolated from one another some base flow would be expected from all the springs in rough proportion to their catchment areas. Ergo, the first model is rejected.

The third model implies that there is very little water in gravitational storage within the Sierra de El Abra. It suggests that each local ground-water flow system is isolated (not connected with other systems) and they all behave in a similar manner, i.e., as dynamic wet-season flood-water systems. The smaller springs would then be the true indicator of the character of the Sierra de El Abra aquifer. The available data do not adquately test this model -- for example, water tracing tests for dispersion and residence time, and pump tests. According to the hydrochemical calculations (section 7.1.3), regional sources provide at least 24% of the combined dry season flow of the Mante and Choy (using Q_B's for May, 1973 from Table 7.4), and perhaps as much as 56%. Because it is possible that there may also be a

regional source of shallow circulating type "A" ground water, the latter figure might not be the true maximum contribution from regional sources. If a dry season average of about 8.0 and 2.6 m^3/sec for the Mante and Choy respectively is subtracted from the total runoff as determined in the previous section, the new unitary discharge would be 0.0124 $m^3/sec/km^2$ and the local runoff would be 31% of the local rainfall. These figures cannot be dismissed as totally unreasonable and if correct about one-half of the El Abra range discharge would be derived from outside sources. However, data given by Faulkner (1976) show that the great Silver Springs ground-water basin of Florida has an average recharge of about 31% of the total rainfall of 1350 mm (53.2 inches), including 2% lost to pumpage. Because the soil cover on the El Abra range is spotty, a slightly higher percentage may be expected. Furthermore, it seems likely that there is a significant amount of water in storage within the El Abra range that is gradually discharged. Evidence for storage include water levels in a number of observation wells drilled by the S.R.H. in the southern part of the range (S.R.H., unpublished data), some vadose zone water discussed in Section 4.4.1, and most importantly, the large water-table lake in Soyate (there are probably a great many in the El Abra). The well data suggest that considerable water may be stored in small solution channels, and that variable hydraulic gradients exist. Finally, the stability of dry season discharge of the Coy spring has previously been attributed to its large component of regional flow. For the period 1960-1971, the coefficient of variation of the yearly minimum discharge of the Choy is three times greater than for the Coy (0.220 versus 0.068 respectively). The lesser stability of annual minimum discharge of the Choy suggests greater dependence on its local source.

In model number "2", most of the aquifer is integrated into the two main ground-water flow systems. Extremely dynamic ground-water conditions occur during the wet season, when storms cause large temporary increases in water levels and replenish ground-water storage. All of the springs respond quickly to the increased hydraulic gradients and more than half of the recharge water is rapidly discharged. In this model, the smaller El Abra springs act as overflow systems for high aquifer water levels, and develop specifically because of temporary high local hydraulic gradients. They are left high and dry during the dry season as water levels decline in the large conduits that drain the aquifer, and as water that has been retarded by flow in small solution openings seeks larger conduits at lower elevations. The basic premise is that there is some degree of physical connection between the large and small springs. Figure 7.14 shows a hypothesized N-S profile of dry season ground-water conditions and surface base levels along the east face of the Sierra de El Abra, based on nine base-level points (Table 7.13), including the Soyate lake, and on model "2". Springs are shown as open circles, and where their elevation is unknown, a "?" is given. A number of caves are projected eastward into the section to assist placement of upper limits on the profile (remember however, that they provide only apparent gradients in the section, but the error is small except for caves directly west of El Choy). Both Arroyo and Venadito continue in the vadose zone and a "?" indicates they will attain some unknown greater depth before reaching a siphon. Using their altimeter survey of cave entrances, and using cave surveys conducted by other cavers and many from this thesis work, Mitchell et al. (1977) have given a somewhat similar diagram to Figure 7.14 for that part of the El Abra range

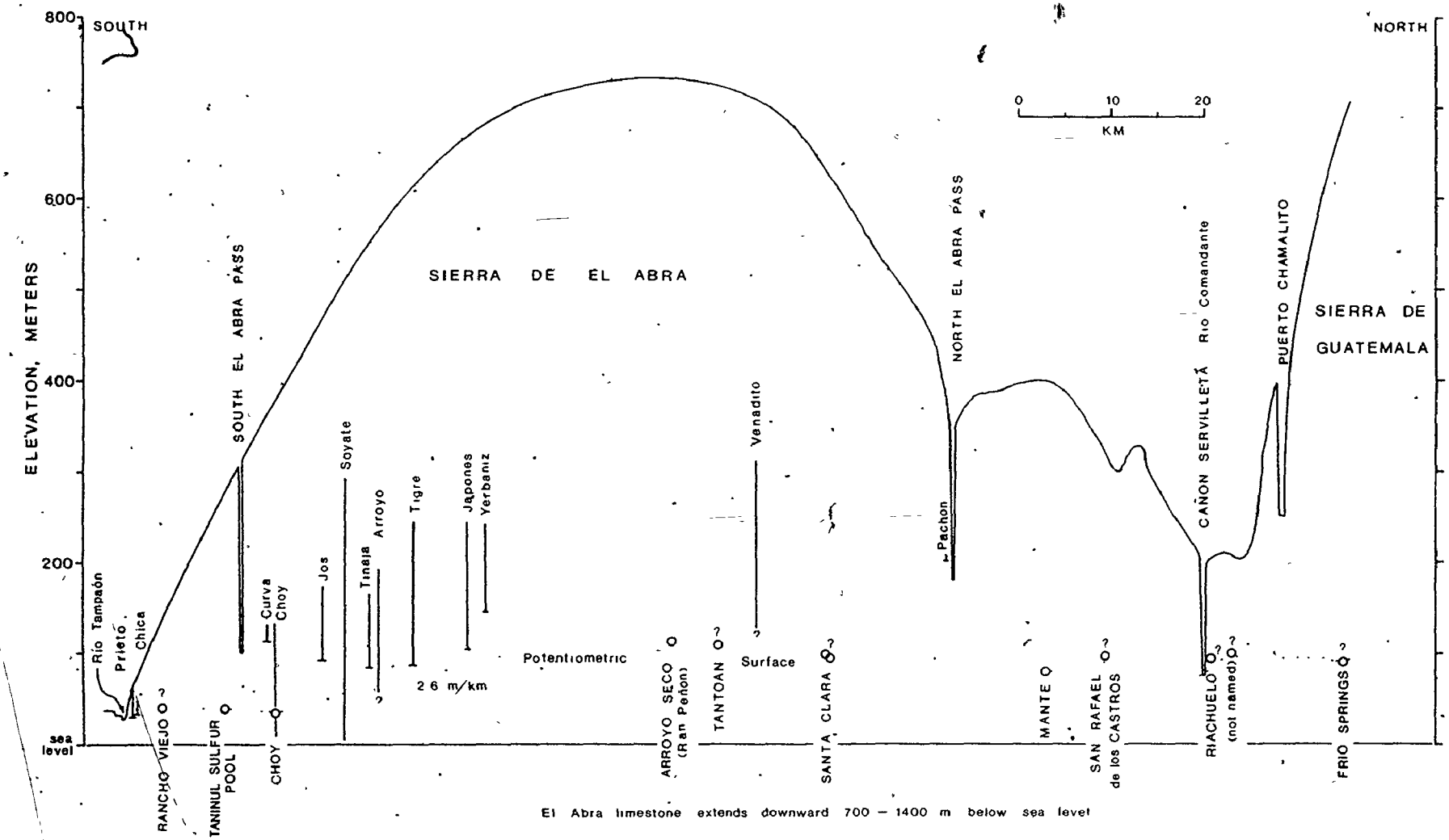

Figure 7.14 Hypothesized N-S dry season ground-water profile in the Sierra de El Abra. Base level points are listed in Table 7.13.

TABLE 7.13

Base-Level Points of the Sierra de El Abra

Base Level Points	elevation m	source
Choy resurgence pool	35	altimeter, rise pool rather than outlet elevation is used
Taninul Sulfur Pool	39	artificially raised 1-2 m; altimeter and S.R.H. topographic data
Río Tampaón	28	S.R.H. gauging station data
Santa Clara Spring	(75-100)	dry season water level at gauging station is 70.0-70.2 m
Mante	80	topo map indicates just under 80 m; Mitchell et al. (1977) give 80.5 m; was 1-3 m lower before construction of reservoir
Río Comandante	75	S.R.H. gauging station data
Poza Azul (Frío Springs)	(90)	estimated from S.R.H. data
Taninul "Limestone Pool"	37.5	altimeter
Soyate lake	59	altimeter and cave survey

between the Choy and the Mante springs, and have given a discussion of the hydrology, particularly as it relates to the distribution of blind fish in the area.

Many aspects and problems of the El Abra range hydrology may be seen in Figure 7.14, keeping in mind the breadth of limestone outcrop and location of swallet caves shown in Figure 3.1. Among the problems are directions of local flow, location of drainage divides, variable hydraulic gradients, the potentiometric surface, and flow system separation or interconnection. In model "2", the regional component of flow is taken to be within the range calculated in Table 7.4. After the regional component and an estimate for the surface runoff included at the gauging stations are subtracted, the Mante (between 8 and 4 m^3/sec) still has the largest discharge from the local aquifer, the Choy (4.4-3.5 m^3/sec) the second largest, and the Santa Clara (2.25 m^3/sec) is thought to have the third largest discharge. As pointed out by Mitchell et al. (1977), the fact that the Mante is the largest poses some interesting problems (however, they assumed or believed that all of the discharge measured at the Mante gauging station was derived solely from the El Abra range). It lies in the narrow northern part of the range at an elevation of about 80 m, whereas the Choy lies at the southern end of the broad central portion of the range at an elevation of 35 m. The Mante spring obviously taps a considerable ground-water body above 80 m elevation. Thus, a ground-water divide must occur that is closer to the Choy than to the Mante spring (Figure 7.14). Based on their simple water-budget calculations and on the assumption that siphon lakes at about the same elevation in three separate passages in Sótano de

Yerbaniz indicate the "water table" of the Mante drainage, Mitchell et al. (1977) predicted that the divide occurs between Tigre and Japonés. However, the depth attained in Japonés (by this study, where exploration was terminated by what is believed to be a perched siphon) proves that their water-level profile must be lowered substantially, and strongly indicates that the conformity of siphon elevations in Yerbaniz is a coincidence or the result of strong structural control. It is likely that the Yerbaniz-Matapalma-Japonés group of caves drain to the same spring, probably the Choy, but perhaps to one of the smaller springs along the east face. The location of the divide as determined by water-budget techniques will depend on the magnitude of regional flow and the flows assigned to the smaller springs.

Other drainage divides must also exist. Probably a significant part of the recharge south of El Choy (35 m elevation) flows to the bed of the Río Tampaón (28 m elevation) and to wet season springs along the east face (Figure 7.14). Two caves near the Río Tampaón have free-air lakes several meters below the level of the Choy and thus could not drain to it (Table 7.13). Another major divide evidently is located somewhere between the Frío and the Mante springs. An unusual dry season flood occurred in February, 1957, at the Frío springs. Monthly rainfall data at a number of stations in the area (see location map in Figure 7.15) show that five to ten times the average February precipitation fell during this month in the Sierra de Guatemala area, whereas the northern Sierra de El Abra area received only a little more than the average and the upper Río Guayalejo basin (Jaumave area) received very little precipitation. Apparently, most

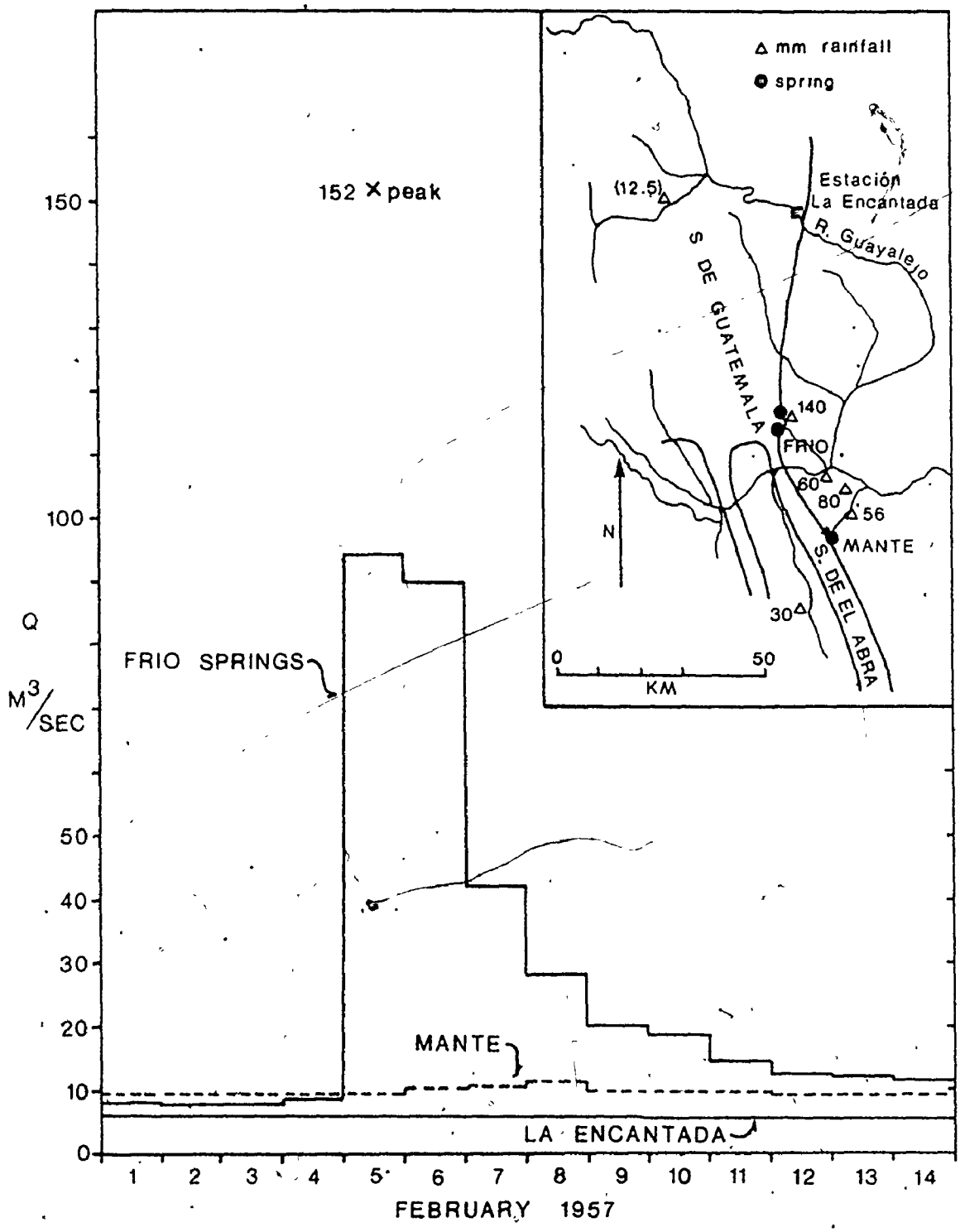

Figure 7.15 Hydrographs in February, 1957, of Frío springs, Mante, and Río Guayalejo showing an unusual, isolated dry season flood.

of the precipitation occurred during a very localized storm on February fourth and fifth, causing the strong response at the Frío springs (Figure 7.15). The fact that there was no response at La Encantada and virtually none at Mante means that for all practical purposes, the local components of their ground-water flow systems are hydrologically separated, although it is possible that small connections exist. The very small increase in flow at the Mante gauging station on subsequent days was most likely caused by local showers, but might have come from the Sierra Tamalave or Sierra de Guatemala.

Unfortunately, gauging stations on Río Comandante and Río Sabinas (Figure 4.2) were not operative in 1957. It would also be interesting to observe the response of the smaller springs between the Mante and the Frío springs during isolated events such as the one above.

Studies of the Mante spring have been limited in this thesis, and more are required. Figure 4.9 shows a common discharge pattern recorded at the gauging station, although other floods have lesser flows than the 1951 event. After a few small pulses on days having showers, a large rainfall-runoff event occurs. In such circumstances, runoff from the 69 km^2 surface catchment included with the gauging station measurements would provide an important part, perhaps as much as 50% of the large pulse on the first day. However, it is clear that the spring also responds rapidly. Following the initial peak, there commonly is a lengthy period of high, gradually declining discharge that is derived predominantly from the spring. With the support of additional showers and storms, the period of sustained high to moderate flow may last for several months (compare the August-Sept-

ember-October rainfall in Table 4.5 with the Mante hydrographs in Figure 4.9).

Another Mante hydrograph pattern is shown in Figure 7.16, where it may be compared with hydrographs of the Santa Clara spring and the Río Comandante (see Figure 4.2 for the relationships of the basins). Also shown is the rainfall at El Refugio, which is located against the western side of the El Abra range about half way between the Mante and the Santa Clara springs. For this period, the data avilable were the mean daily flows of Río Mante, but only occasional discharge measurements of the two canals (generally the flow of the canals totals 8-13 m^3/sec, but during major flood peaks the flow is often reduced to nil). The smooth curve represents the approximate general shape of the hydrograph, from which only small peaks and troughs would be missed. Examination of the Santa Clara hydrograph shows that the mean daily flows would give a reasonably good representation of its rainfall-flood events. Clearly, there is a significant difference between the flow pattern of the Mante and the other two. Large rainfalls on the supposed recharge area of the Mante spring in the El Abra range produced sharp responses and well-defined events at the Santa Clara spring; but at the Mante station, there occurred only a very broad flood wave which reached its peak more than a week after the heavy rains. Apparently, local surface runoff did not have a large effect on this Mante hydrograph. The discharge pattern shown here may have been caused by the time delays and dispersion of wave form that would be expected of an intermediate or regional flow system "pulse" of relatively shallow circulating type A ground water from potential source areas such as the

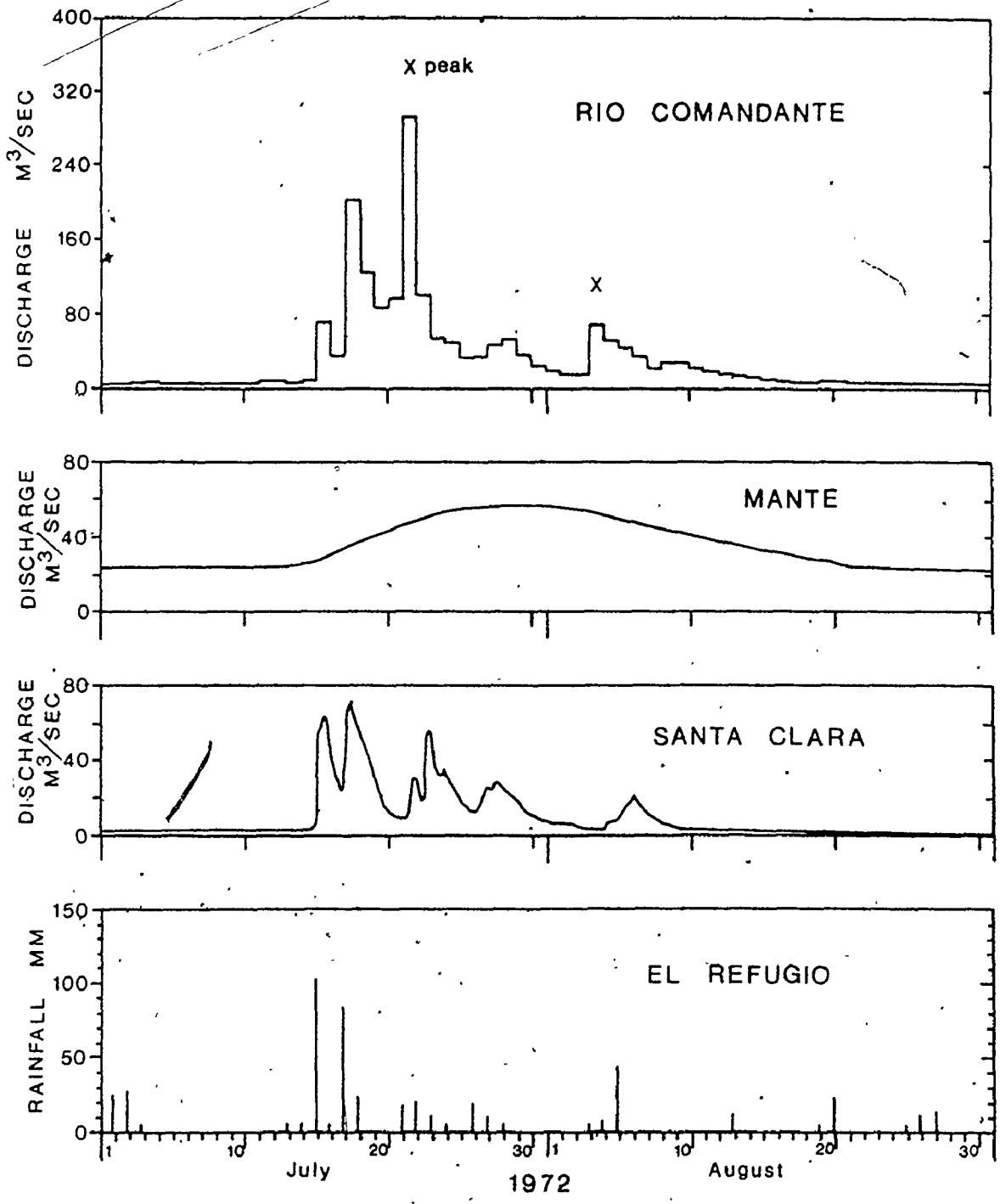

Figure 7.16 Comparison of Mante, Santa Clara, and Río Comandante hydrographs and precipitation for July-August, 1972.

northern Sierra Tamalave and other western ranges; or it may possibly have been caused by storms in the south-central part of the El Abra range (compare with the Choy hydrograph and rainfall for this period shown in Figure 4.7).

Thus, the true source areas of the Mante spring and to a certain extent the spring hydrograph (as opposed to that measured at the gauging station) remain uncertain. Contrary to Mitchell et al. (1977), the Choy spring probably responds more rapidly than the Mante spring, and is more peaked. Their contention that the Choy response lags a few days behind rainfall events was based on only one hydrograph for which they incorrectly reproduced S.R.H. discharge and rainfall data. About 70-80% of the Mante spring discharge may be considered as baseflow, whereas about 50% of the Choy discharge is produced by floods, and nearly all the discharge of the smaller springs is flood flow. In model "2", it is hypothesized that the Santa Clara and others such as the Tantoán rapidly drain away much of the local flood waters in the aquifer so that the Mante spring response is lessened. However, this explanation does not seem satisfactory for the hydrographs shown in Figure 7.16. It seems problematical to suggest that the principal recharge zone of the Mante spring lies south of the Santa Clara recharge zone.

Because nearly all of the caves having siphons thus far investigated in the Sierra de El Abra are believed to be perched, it has not been possible to map the top of the water-filled zone of the aquifer. The one potentially usable point is Sótano de Soyate, which gives a hydraulic gradient of 2.6 m/km. This compares with values of 1.0 m/km average for Florida

(2.3 m/km maximum) and the extraordinarily low gradient of 0.02 m/km for Yucatan (values from Back and Hanshaw, 1970). Palmer (in Miotke and Palmer, 1972) states that some of the major passages in Floyd Collins' Crystal Cave have gradients of less than 1 m/km and believes that they indicate the gradient of the water table. Considering the size of many of the passages observed in the Sierra de El Abra, the value calculated above for the Soyate lake seems rather large. A minimum gradient between the Mante (80 m) and the Choy (35 m) of 0.55 m/km may be determined by the difference in elevation and separation of the two springs. Between the normally stagnant Taninul "limestone" pool (see Section 5.3) and the Choy, there is a gradient of 0.46 m/km.

Several anomalies of fluid potential and flow exist in the El Abra range. Only 90 m from the Taninul "limestone" pool and 1.5 m higher lies the permanently flowing Taninul Sulfur Pool (thermal). However, the Sulfur Pool probably was raised artificially when it was made into a spa. Nevertheless, the flow systems are not connected. The two other thermal springs observed have very small flows, but are likely permanent. The Río Tampaón (28 m) and the Río Comandante (75 m at the east end of Canon Servilleta) provide the lowest possible ground-water discharge at the south and north ends of the range respectively (Figure 7.14). However, there is no dry season flow into the latter and probably very little into the former (no major boils or springs have been reported). Furthermore, as previously stated, in model "2", the Mante (80 m) receives more El Abra ground-water than the Choy (35 m). If correct, this has both hydrologic and geomorphic implications that should be carefully evaluated in future studies. Hydrologically, the above anomalies suggest that it takes a very

long time for ground-water conduit flow systems to adjust to changes in base level. The Río Comandante and Río Tampaón clearly have the elevation advantage, but the Mante and Choy springs have the advantages of well-developed hydraulically-efficient conduit systems and of position in the very elongated aquifer. From the morphology of the Choy cave (Section 6.2.1), it is clear that the Choy has been a spring for a long time. Presently, it is probably expanding its drainage area northward at the expense of the Mante spring. It also seems likely that after the initial exposure of the high central portion of the range, the principal outlets have slowly been migrating toward the ends of the range where the Río Comandante and Río Tampaón were established long ago (see Figures 7.12 and 7.16, and Section 3.3).

Wet season storms cause very dynamic conditions within the aquifer. In Section 4.4.2, some data and discussion of these transient situations are given. The Soyate lake hydrographs (stage) correlated very well with the Choy spring. Some minor discrepancies indicate that localized events occur which are not "felt" throughout the aquifer. Fluctuations well in excess of 10 m happen frequently. A maximum rise of about 30 m for extremely large floods is suggested. This upper bound is supported by the lack of mud on stalagmites and walls above that level in Soyate and by the presence of only two mud rings (layers) in a 10 cm diameter stalagmite 34 m above the January, 1972, water level (or 23 m above the stage recorder board). If this conclusion is correct, the mud rings indicate flood events that only happen once in thousands of years. A rise of 30 m would increase the fluid potential by only 128% -- to 5.75 m/km. It is anticipated that water level fluctuations in the aquifer will vary greatly from one conduit

to the next, depending on the capacity of each to transmit the quantity of water supplied to it. The swallet caves capture runoff from large areas of impermeable rocks; hence, they have very concentrated inputs to cave systems. The recorded pulses at Sótano de Jos are interpreted to be passing flood waves in a perched conduit. However, on some occasions, water rose above the level of the recorder; and Mitchell et al. (1977) report an observation of flood waters filling the entrance sink of Sótano del Arroyo to about half way up the entrance drop (water depth would probably be 5-8 m above the floor of the entrance passage). It is not certain whether water had backed up all the way from the phreatic zone or whether water had backed up behind passage constrictions or obstacles. In Jos, there are also many obstacles and constrictions that retard flow, and flood pulses coming from the surface basin are so sharp or peaked that the conduit may locally flood to the roof in this young swallet cave. In Arroyo, there are many examples of piles of breakdown, flowstone accumulation, and reduction of bedrock passage cross section which would affect flow (Section 6.4.5.2). At the Hotel Taninul, the springs behave in a very peculiar manner when it rains (see Section 5.3 for more details). The Taninul Sulfur Pool has two sources of water --one is a deep thermal-sulfurous source, the other is the El Abra range. When it rains, cool non-sulfurous El Abra waters dominate (Figure 5.11). Part of the flood waters flow overland into the normally stagnant "limestone" pool, which acts as a sink for some time (perhaps days) before the flow reverses and it becomes a spring, with a flow reaching at least 0.1 m^3/sec. The uncorrelated discharge pattern and anamolous flow in relation to the elevation of the springs indicates that the flow systems are discrete and that water levels

in the aquifer are very erratic under dynamic conditions.

In light of the information and interpretations given, a fourth model is suggested that will have to be considered along with the others in future work to better understand the hydrology. The fourth model suggests that: (a) nearly all of the base flow and a significant part of the flood flow of the Mante spring comes from regional ground-water sources outside the El Abra range; and (b) the Choy has the largest total discharge of Sierra de El Abra ground water, and is the principal base flow spring of the El Abra. In model "4", the Mante spring is considered to be the great regional flow outlet for the northern part of the Valles-San Luis Potosí Platform. The regional flow includes not only the high sulfate water of the hydrochemical model, but also some regional flow of type A water that may have a variable discharge. Flood waters at the Mante would then be a mixture of local water, regional type A water from sources such as the Sierra Tamalave, and the regional high-sulfate water. The model implies that the northern boundary of the Choy drainage area would extend considerably farther northward than in model "2". Furthermore, the potentiometric profile and the smaller springs between the Choy and the Mante could be lowered below that shown in Figure 7.14, possibly lower than the Mante spring. Thus, the elevations of the smaller springs, particularly the Santa Clara, may provide an important test of the models.

In this section, hydrologic data on the El Abra range have been summarized, and used to develop and to test four models that attempt to explain the observed and interpreted character of the aquifer. The models also focus attention on basic problems and uncertainties that remain.

None seem wholly satisfactory nor are the arguments against each totally convincing because insufficient data are available and more analysis is necessary in order to choose among them. Future work should include a lot of water tracing, discovery and survey of new caves, observation of water levels and water-level fluctuations in caves and specially drilled wells, measurement of the elevations of the smaller springs, pump tests, isotopic analysis of ground water, observation of the flow characteristics of the smaller springs, hydrochemical analysis of the smaller springs during flooding, more analysis of the Mante hydrograph, and attempts to determine the amount of storage in the aquifer as a function of the cross-sectional area of solution openings. Especially recommended are lycopodium spore tracing tests of sótanos Venadito, Yerbaniz and possibly Tigre, with nets placed in the Mante, the Choy, and all springs in between. Presently, only a small portion of the regional base flow is used for irrigation, and all of the flood waters escape unused. It is suggested that further studies could show how to use the El Abra aquifer as a natural reservoir so that its great water-supply potential can be developed for large-scale irrigation of the coastal plain.

7.4 Morphology and Origin of the Caves of the Sierra de El Abra

This section summarizes the morphologic features of the El Abra caves, and presents models of the hydrology of the caves and of their relationship to the surface geomorphology.

7.4.1 Character and Origin of the East Face Caves

The springs of the Sierra de El Abra discharge the integrated output of vast cavern systems within the range. The accessible portion of the active spring outlet caves is extremely short. No lengths greater than 100 m are known, and sometimes the outlet is completely flooded. This is because vertical circulation is so important in the El Abra range; water is discharged from the phreatic zone. At the Choy spring water rises at least 26.5 m from its source at the bottom of a lake (Figure 6.1) to flow onto the coastal plain. The Mante spring is accessible for about 30 m before becoming flooded, and it appears to discharge via a large horizontal conduit for at least this short distance. For most of the smaller springs, only the rise pool can be observed, the exception being the Nacimiento de Arroyo Seco on Rancho Peñon. At the latter site, there is a small upper cave, and a lower horizontal passage that is the water source. This spring is seasonal, which suggests that it is in a fluctuating water table zone, i.e., that it is a spill over of wet season higher water levels in the aquifer. The caves behind the presently active El Abra springs are clearly formed within the phreatic zone.

It is believed that all of the east face caves of the El Abra range that were observed were created entirely within the phreatic zone. Morphologic features that indicate this include broad and deep wall and ceiling pocketing, smooth blind domes and highly irregular ceilings formed by solution upward along joints (see the ceiling profile of Ventana Jabalí, Figure 6.8; El Choy; Cuates), highly irregular (ungraded) bedrock floors (El Choy, Ventana Jabalí, Ceiba, Taninul No. 2), spongework (Taninul No. 2),

bedrock natural bridges, and other manifestations of uniform solution under water-filled conditions. Furthermore, Taninul No. 1 and No. 2 are three-dimensional mazes or complexes that required development in the zone of saturation. The east face caves grew to their present size entirely within the phreatic zone, and have been only modestly altered by clastic sediment infilling, guano and stalagmite deposition, and ceiling collapse.

Bonet (1953a) believed the caves in the escarpment were formed in the nuclei of tabular reefs (not like modern coral reefs), but sometimes extended into adjacent peri-reef conglomerates. Although he stressed the importance of joints in the development of all the caves of the range, it seems implied that he believed reef porosity to be the controlling factor. The occurrence of the east face caves in reef nuclei as opposed to other facies of the reef zone has not been tested in this study. However, from observations in the caves, it appears that very large joints and bedding (facies) planes provided the openings for water flow through the reef zone, and therefore, became the loci of cave development. Some facies of the reef zone are probably more soluble than others, so that a passage may vary considerably in dimension when passing from one facies to the next. The caves are classified into two types: 1) short, vertical fissures or canyons having great height and controlled by a major joint or joints as El Choy, la Ceiba, and Cuates; and 2) relatively horizontal conduits that are longer, more equidimensional in cross section, and controlled by a facies plane in combination with smaller joints as exemplified by Quintero and Taninul No. 2. Ventana Jabalí is such a huge chamber (passage ?) that it is difficult to scrutinize. Many large joints were utilized by circulating water, but other factors may also have been important.

The relationships between the geology, the geomorphology, and the east face caves may be seen in Figure 7.17. The active spring caves all occur at the base of the scarp, albeit at various elevations along it. Basically, water spills from the phreatic zone of the range onto the impermeable coastal plain. As previously noted, there may be a considerable lift, as at El Choy, where the final portion of the ground-water flow system is up a large joint. A temporal sequence is envisioned in which the youngest spring sites occur at or a very short distance in front of the scarp (e.g. Santa Clara and a spring on Rancho Tampacuala), El Choy is an older although still active spring, and caves higher up the scarp are fossil spring sites that were active when the coastal plain stood at much higher levels. The phreatic morphology and height of the Choy cave clearly require it to have been an active spring for a very long time (Figures 6.1 and 7.17). Flat-topped hills in front of the cave are remnants of an older coastal plain level that probably correlates with Middle Entrance (or possibly a fossil exit at the present skylight); and prior to that time, water rose <u>up</u> the vertical pit at the back end of the cave to flow out the Upper Cave Entrance onto an even older coastal plain. The total phreatic lift was at least 120 m. The phreatic morphology of caves such as Ventana Jabalí requires ancient coastal plains to have reached the level of the highest of such features in the caves, and thus to the highest part of the El Abra range.

Models of east face caves and their relationship to the coastal plain are shown in Figure 7.18. The paleohydrology of the Choy cave has been discussed above. Where a major joint or group of joints exist over a large vertical range as at El Choy, a cave developed at that location

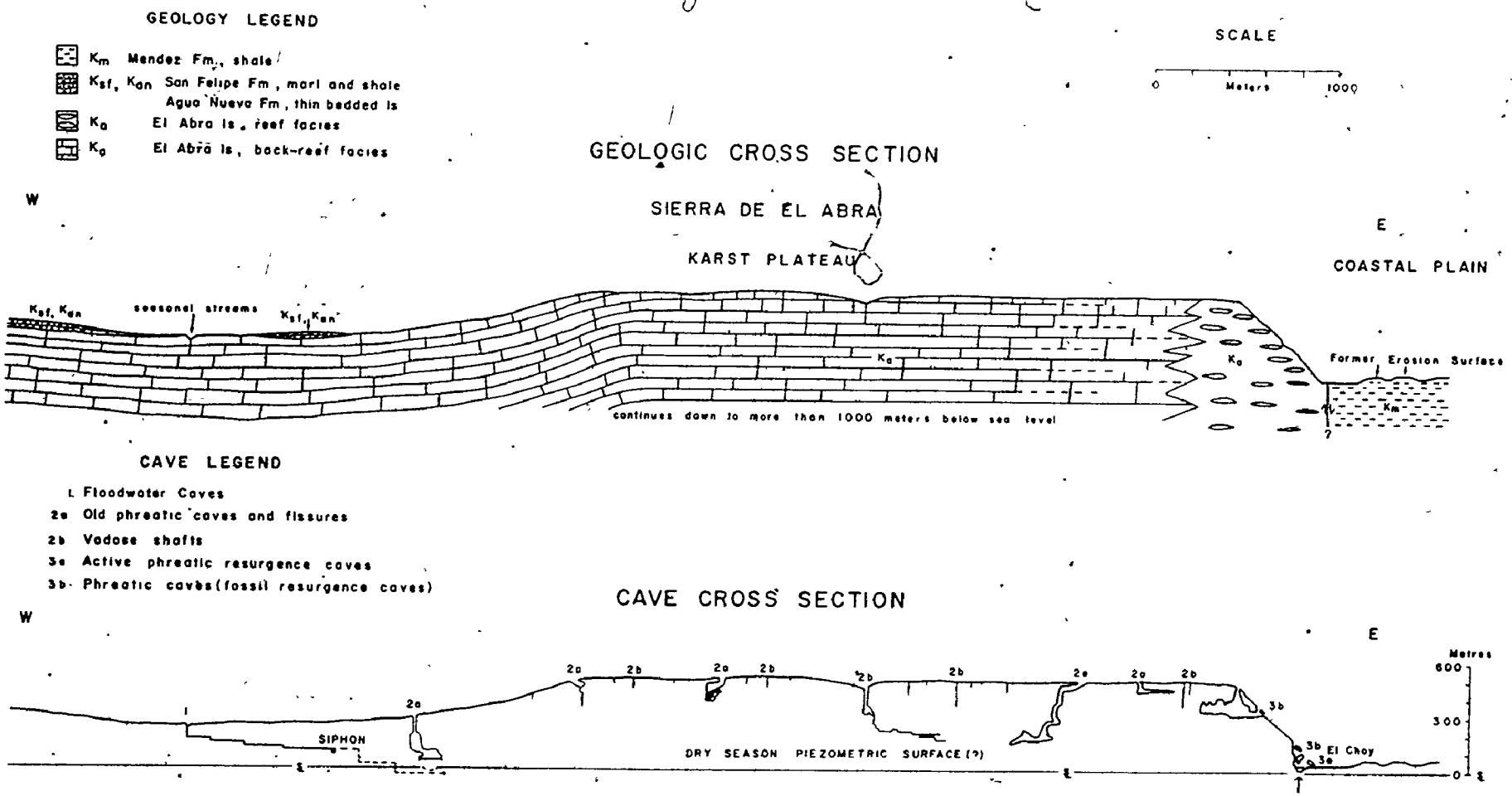

Figure 7.17 E - W cross section showing relationships of geology, hydrology, topography, and caves in the Sierra de El Abra

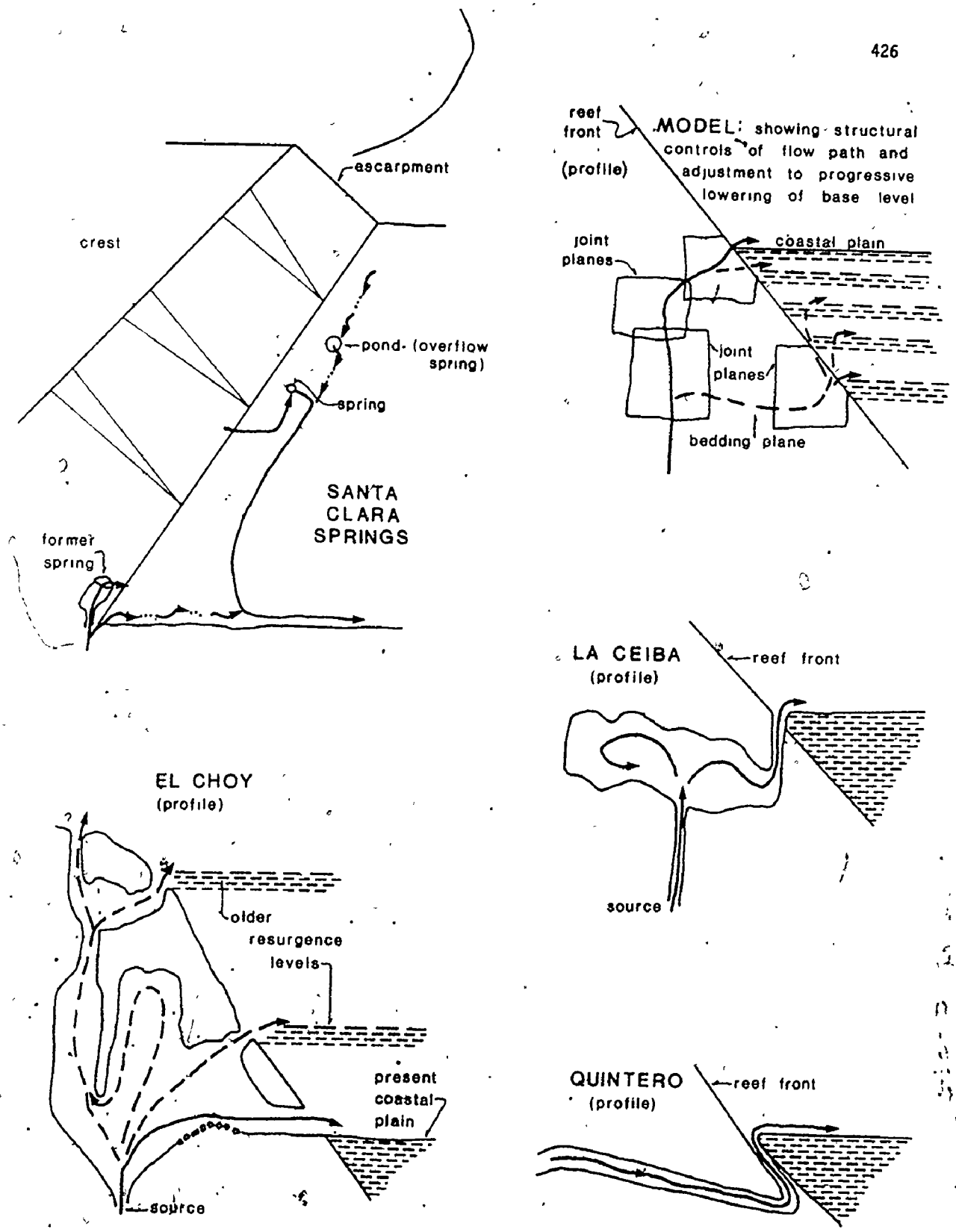

Figure 7.18 Models of the east face caves.

may function as a spring for a very long time. As the coastal plain is gradually lowered, new lower outlets from the reservoir are developed. Where the fossil spring caves are controlled by a reef facies plane as at Grutas de Quintero, there is less chance for continued use of the cave as the base level is lowered. Quintero must have had a simple rise shaft, now missing, in the El Abra limestone or coastal plain rocks. The Arroyo Seco spring cave on Rancho Peñon, which can be explored a few tens of meters, appears to be a horizontal conduit that is on the verge of being abandoned as a spring site. The cave above the spring shows that water from this same source conduit formerly flowed up east-dipping facies planes in the reef rock adjacent to the coastal plain, to resurge 15-20 m above the present level. Caves such as Ventana Jabalí and Cueva de La Ceiba are immense voids controlled by large vertical joints and perhaps by host rock that was especially favorable for solution. They also demonstrate great vertical range of circulation and probably had lifting shafts at their outlets as proposed for Quintero. The source(s) of water to Ventana Jabalí is probably buried beneath sediments. La Ceiba, however, has a central pit series having phreatic morphology that suggests it was the principal source for that cave. It would thus have had a flow system very similar to El Choy, and a phreatic lift of at least 190 m. Also shown in Figure 7.18 is a schematic model of the evolution of the discharge portion of an El Abra karst flow system. Water is discharged from the aquifer at some established favorable site, here shown as a series of interconnected or closely spaced joints. As the coastal plain is eroded away, the spring point lowers until the bottom of the joint is reached. After that time, water can no longer dissolve the conduit downward sufficiently rapidly;

hence, a new discharge site must be found. There is no sudden lowering of base level, or sudden draining of a phreatic system. Water gradually abandons the upper route. It may flow along a facies (bedding) plane and out, or perhaps intersect another joint and then rise upward along a joint chimney and through a small section of the coastal plain rocks (San Felipe?). In some instances, lower chambers may already have been created and the overlying materials may subside into it or be eroded away by flowing water. The Santa Clara spring may be an example of a diversion some hundreds of meters along the strike from a "hanging" site to a location at a more favorable elevation and structure.

The Coy spring and Coy caves in a smaller limestone mass separate from the Sierra de El Abra (Figure 6.26) beautifully illustrate the same kind of phreatic flow system, solutional morphology, and evolutionary characteristics described above. Above the present Coy spring are caves that were former water-filled discharge conduits, and in at least one of them it is possible to descend to part of the presently active flow system. Many of the other major springs in the region appear to have at least some phreatic lift. The most notable is the Media Luna, which discharges from three orifices at the bottom of a 75 m deep lake.

One type of cave not observed in this study that may occur along the east face is the vadose fissure or shaft. These may form where small concentrations of water running down the face are captured down a joint, or where a stream has in the past drained or presently drains from the top of the range and is pirated on the face. These caves will be very small compared with the spring caves of the El Abra.

7.4.2 Character and Origin of the Crest Caves

Before the thesis research was begun, virtually nothing was known about the caves on the crest of the El Abra range. This study and other recent exploration and survey work have greatly increased knowledge of the area. Because so much effort is often required to reach caves on the crest, the total number that have been explored is still relatively small; however, many important features of the caves are now known.

Caves on the crest of the range may be classified into two basic types: old phreatic caves or younger vadose systems. There is a third type that is considered to be a special case, and it will be discussed later. The phreatic caves are very short compared with the western margin swallet caves or those in many other regions of the world. However, what has been observed are merely short segments of much greater cavern systems. Some of the segments are horizontal and others are vertical or a combination of the two. To illustrate many common aspects of these caves and to indicate their importance, a detailed discussion of the history and hydrologic implications of La Hoya de Zimapán will be given next. A description of the cave with photographs and a map are contained in section 6.3.7.

In its formative period, Zimapán was a great phreatic tunnel, slowly transporting water in a very deep flow loop. That its development was entirely phreatic is shown by the round passage cross section, phreatic domes, and the smooth sculpturing and pocketing of the walls and ceiling. Water passed downward (probably) to a depth of more than 300 m, only to return nearly to the plateau surface and resurge from some fossil spring along the east face of the range, onto an ancient coastal plain (for example,

Ventana Jabalí or Cueva de la Ceiba; Figure 7.17). Thus, it is a very old cave, likely formed soon after or while the top of the El Abra range was being stripped of its impermeable cover, and while the coastal plain was approximately at the present crest of the range. It is entirely possible that water passed up the conduit instead of down. In either case, the cave is a segment of a karst flow system which demonstrates perhaps better than any other known cave that deep phreatic flow does occur. For that reason, it is considered the most important cave discovered in México so far.

Then over a period of time (presumably not instantly), the water supply was somehow cut off and the conduit ceased to function and grow. There may have been an intermediate period of vadose solution activity, but there are no bedrock solution features to suggest it. Since the flow ceased, erosion has lowered the coastal plain by 400-600 m. During this time, the cave will have resembled a well with a standing body of water. As the water gradually lowered, vadose seeps were able to reach progressively lower into the cave and stalagmite deposits began to accumulate. The massive stalagmite deposits in the entrance passage may be much older than those in the Zimapán Room.

How the Zimapán Room developed is a puzzle made difficult because its relationship to the passage or other passages (?) is hidden below the sediment floor. If the known cave is the only passage involved, it seems likely that the room grew to at least its present size in the phreatic zone, while the conduit was an active flow route. Some breakdown may have been dissolved or dispersed by a later vadose stream, but it is believed that this could not have had more than a minor effect. However, a junction

of passages below the present floor of the room could have been a significant factor in promoting its large size. This would be especially true if the lower passages continued to function long after the upper part of the cave ceased its hydrologic activity. No major fracture was observed in the Zimapán Room that would have been important in promoting exceptional rock solution or breakdown there. The lower 15-20 m of the walls (or roof) of the room are smoothly beveled and pocketed by solution (Plate 6.18); thus, if there has been significant wall retreat by collapse, the evidence is lost. The higher part of the roof has prominent steps left from upward stoping, but it also shows forms indicative of solution under water-filled conditions. These effects can be explained by a fluctuating water table or by intermittently ponded vadose water relatively late in the cave's history. The Zimapán Room now seems to be very stable because there are neither subsidence trenches in its floor, nor a significant accumulation of collapse boulders.

At some time a small vadose stream invaded Zimapán. This may have been the result of the collapse at the present entrance. It washed soil into the cave that has accumulated behind the stalagmite barriers in the entrance passage, at the base of the third drop, and probably as a thick deposit leveling the floor of the Zimapán Room. Breakdown and stalagmites may have trapped the fine-grained sediments, eventually making the room nearly watertight. Thus, when the vadose stream flowed, it would be ponded, causing re-solution of the stalagmites (Plates 6.19 and 6.20) and perhaps the solution of ceiling rock discussed above. This stream also was responsible for making the crawlway through the stalagmite barrier at the top of

the first drop, and possibly for the partial erosion of the flowstone in the pit series. These interpretations suggest that this ephemeral stream is a very late phenomenon in the cave's history, and mud in the gour pools and faint channel marks indicate that a stream still intermittently invades the cave although it is probably rather small. Vadose drips enter the cave at all levels, including the Zimapán Room where the whole floor is covered with gour pools that are active seasonally.

The discussion of Zimapán above illustrates many common morphologic features and processes that occur in the crest caves. Each cave was a segment of a much greater flow system that moved water from sources on the plateau surface to east face springs via flow loops in which depth was often an important dimension. After these great cavern systems ceased their hydrologic function, they were separated into small pieces by vadose zone processes such as collapse, stalagmite and flowstone deposition, clastic sediment infilling behind barriers and at the bottomss of flow loops, and guano deposition. Taninul No. 4 and Loros are horizontal segments of systems; the former is particularly interesting for its blind joint alcoves and domes, and its facies control. Tanchipa and Soyate are other examples of portions of deep phreatic flow loops. The Soyate loop must have been at least 234 m deep.

Access to nearly all of the phreatic caves is gained by entrances that are usually created by collapse of high phreatic domes (such as at Loros and Cueva Pinta). Although various types of cave sediment may accumulate before a collapse entrance forms, the rate of accumulation probably increase afterwards. Many of the caves are no more than large rooms

where access to the remainder of the system is blocked (Escalera, Pinta and many other examples not described). Where the original solution chamber is at considerable depth, and the amount of collapse is large, the chamber will probably be buried by collapse debris and other types of sediment. This creates the third type of cave (the special case referred to at the beginning of this section) where no part of the original solution cave can be reached. Escalera and Cuesta may be examples of this type. It is hypothesized that the "phreatic" re-solution features of stalagmites and wall rock seen in many of the caves are created by water temporarily ponded in chambers that have been made "water-tight" by sediment infilling. It appears that during storms, water from small peripheral areas flows into the caves. Hence, it is believed that the re-solution pocketing is not associated with fluctuating water tables, or with periods of higher water levels following periods of lower water levels that could be attributed to geomorphic or climatic events.

There are two fundamental problems concerning the phreatic crest caves that have not been solved. The first is the known passage segments are so short, that no knowledge of the interrelationships of passages have been gained. The second is that the sources of water or type of recharge that created the caves are not known. Of course, the two problems are not completely independent. Presently, within the phreatic zone, there ultimately must be considerable integration of passages because there are a great many more recharge points than there are springs, and the same condition is presumed for the past. However, there could be many instances where water becomes divided between two or more distributary channels, which later rejoin or integrate with other conduits. Thus, this

study has shown that very large caverns develop in the phreatic zone, that the flow loops can be very deep, and that structural and stratigraphic features control the locus of conduit development; but the pattern of the phreatic flow system remains unknown.

At La Hoya de Zimapán, there are no known tributary passages, although vadose drips and flows have obviously entered the cave at all levels. It would have taken a great quantity of water and a very long time to create the cave. There is a fossil surface arroyo perhaps 200 m long that drained into the doline at the cave's entrance. However, unlike the western-margin swallet caves which were created by pirated arroyos, it is suggested that this arroyo was not the progenitor of Zimapán or the entrance doline. Instead, the arroyo may have gradually evolved as a consequence of the cave collapse, and may have supplied the vadose stream which created the flowstone deposits in the pits and transported soil into the cave. The relationship of the surface geomorphology and hydrology to the caves during the period of removal of impermeable rocks from above the El Abra limestone during development of karstic permeability needs further study. The Zimapán entrance passage is nearly round (Plate 6.16) and 30 m+ in diameter. It was created wholly in the phreatic zone. Any reasonable discharge of water through its 700 m^2 cross-sectional area would have such a low velocity that there would have been considerable sediment accumulation. In fact, sediment would have collected long before the present passage size was reached. A passage which accumulates sediment cannot maintain a circular cross section as it enlarges. Hence, it is concluded that Zimapán was transporting sediment-free water, and that its source was not a sinking stream off a Méndez or a San Felipe catchment. The conduit must have inte-

grated the infiltration water from a vast number of small openings on a limestone pavement similar to the present surface.

Because the coastal plain of Méndez has been denuded much more rapidly than the Sierra de El Abrá, the topographic relief on the limestone has increased through time. The thickness of the vadose zone has grown concomitantly with the relief (Figure 7.17). In the high central portion of the range, the relief and the thickness of the vadose zone may reach 600 m. Solution and cave development in the vadose zone should be very important at the present time. However, on the limestone surface, the catchment area for the great majority of sink points is quite small. Consequently, only a small percentage of the openings are humanly explorable.

There are many vadose shafts which can be explored for some distance. Where larger basins are available, vadose caves such as Monos develop. Monos exhibits strong structural and stratigraphic controls; thus, it appears that those aspects are important for the vadose caves as well as the phreatic caves. There is some integration of flow in the vadose zone, but the bulk of it occurs within the present phreatic zone.

7.4.3 Character and Origin of the Western Flank and Western Margin Caves

On the western flank of the range, some caves believed to be of phreatic origin are known. Those observed in this study are Cueva de Los Sabinos, Cueva del Prieto, and Sótano de Soyate. It is not anticipated that the western flank phreatic caves will be significantly different from the crest phreatic caves -- Soyate was even included in the discussion

of depth of circulation in the previous section. The caves contain phreatic wall pocketing, blind solution domes, bedrock pillars, irregular ceiling profile, uniform solution of wall rock, and joint networks (in Los Sabinos). When more caves are discovered and studied, subtle differences in solution morphology and plan-profile characteristics as functions of structural attitude of strata and of lithology (and hence distance from the reef) may be found.

The interesting problems of the phreatic caves are their sources of water and their relationship to the surface geomorphology. All three of the aforementioned caves probably received recharge down joints at their present entrances. Prieto is located on top of a broad hill of El Abra limestone and is joint-controlled. At Cueva de los Sabinos, strike and dip measurements (see map, Figure 6.22) indicate that the entrance sink is situated on the crest of an anticline or a dome (crest or flank). Some time ago, the Río Sabinos or one of its tributaries passed very near or over the entrance sink of Los Sabinos, and probably lost water to the cave (the Río Sabinos is the name given to the ancestral river which was segmented and pirated underground at several places to form swallet caves; see Section 3.1.3 and Figure 3.2). Presently, there is a considerable difference in elevation between the coastal plain and the Río Sabinos valley (Figure 7.17). If the upper part (First Level) of Cueva de los Sabinos is truly a phreatic cave (rather than a floodwater cave), the geomorphic problem is to explain how such a cave could develop. For any reasonable discharge, a conduit the size of Los Sabinos will have a very low hydraulic gradient. This implies that the coastal plain (base level)

was perhaps 200 m higher when the cave formed and the difference in elevation between the Río Sabinos valley and the coastal plain was much less. Possibly, some water leaked through overlying San Felipe beds on the fold crest before the beds were completely eroded to expose the El Abra Formation.

The western margin swallet caves are the longest and most complex caves known in the El Abra range. They were initiated long after crest caves such as Zimapán ceased functioning, and in fact, they are still active. Streams flowing from impermeable catchments were pirated down the first major joints, typically 50-70 m deep, after passing onto the El Abra limestone. The basins are large, ranging up to 21.8 km^2, and the caves owe nearly all their growth to water supplied from them. The supply of water is sporadic. Occasional violent floods enter the caves during the rainy season, and small flows continue for some time after each flood; during the remaining time (most of the year), only vadose drips or flows enter the cave.

The swallet caves owe most of their characteristics to the combination of highly variable discharge of the source and strong structural and stratigraphic controls; they are here termed floodwater caves. Passages tend to be tunnels of relatively uniform cross section compared to the highly irregular profiles of phreatic caves such as Ventana Jabalí, El Choy, and Taninul No. 4 (where blind joint-controlled alcoves are also common). The floodwater caves exhibit quasi-phreatic solution features because the passages fill to the roof during floods. Blind domes have developed on joints and shallow semicircular or ovate domes are formed by solution upward during floods; they are excellently displayed in Sótano de la Tinaja

(see profile, Figure 6.25) and in all the other swallet caves. It is also clear that many of the joints permit percolating waters to enter so that mixing effects might occur, but the mixture-corrosion process (Bögli, 1965) should not be important because the flood waters should already be considerably undersaturated with respect to calcite. Pocketing of a sort occurs, but the form is not the same as nor nearly as large as the phreatic pocketing found in the east face or crest caves. Small scallops might be expected to develop, but are very rare. Vadose features include plunge pools, inlet domes or vertical shafts (Pohl, 1955; Brucker, Hess and White, 1972), floor channels, and possibly lateral encroachment on walls by streams perched on sediments.

Structural and stratigraphic features have played important roles in the development of the caves, and in their plan and profile characteristics. Large fractures initially captured the surface streams and in other places have served as "targets" for ground-water flow, as in Sótano del Arroyo. From sink to spring water must flow against a westerly (on the average) dip and descend several hundred meters of stratigraphic section. Joints up to 30 m in height, although normally less, provide the means of crossing or descending the section. For example, the Entrance Passage in Tinaja works against a 5° westerly dip, gradually descending via small joints along its 525 m length (projected) until it is physically 24 m below the entrance and about 65 m down-section. The initial profile was composed of bedding plane lifts up the dip between descents on joints, so that the overall appearance was somewhat similar to the teeth of an inverted saw raised at one end (the bedding plane segments were of course much longer than the joint segments). Much of the evidence of the original

profile has been obliterated, but at least one large example remains. From Third Room, water descended via a large joint, then flowed up the dip on a thin shale layer (2 cm thick) from 5-10 m vertically. Thus, another common characteristic of these floodwater caves is their irregular profile, i.e., one that is not continuously descending in the vadose zone. Floodwater first must fill the lows of the profile and then locally act as pressure conduits. Other examples are the Sandy Floored Passage where Lake Passage must flood to the roof to flow over a bedrock high in the middle of the Sandy Floored Passage, and the Wallows and Stricklands Bad Air Passage in Arroyo.

Various processes cause modifications of the passage shape and profile. Collapse of the roof, usually assisted by prominent fractures, creates domes not of solution origin, rooms, and boulder piles. Collapse debris occasionally restricts flow, and in all cases, ponds water, creating sediment traps for part of the huge quantity of mud and sand swept into the caves. The ponding probably enhances lateral and upward solution. In some instances, the flow is diverted against a wall so that lateral encroachment occurs, which further promotes breakdown and the development of a large room. In some instances, ponded water causes small distributary drains to form, which appear to divert water to unknown lower cave passages. The deposition of stalagmites and flowstone is quite prolific in places. Such deposits may also restrict flow, backing water up the passage during floods, and cause ponding. One such instance occurs in Neals Passage in Sótano del Arroyo where a large stalagmite or flowstone mass has almost totally blocked this major downstream passage. In some localities there may be a rough balance between the rate at which trickle

waters deposit calcite and the rate at which flood waters erode it. Sediment traps may also occur at low spots in irregular floor profiles, or behind bedrock barriers. The sediments found in the floodwater caves are clearly different than those observed in the crest caves (there the lower parts of the deposits have not been seen).

Most of the swallet caves have each been formed by only one source of water -- the sink of their respective surface arroyos. William H. Russell (see Russell and Raines, 1967) has previously advocated that the western margin swallet caves were formed in two stages: 1) development of large poorly-connected phreatic voids (rooms and tunnels) by slowly moving water, and 2) integration of the voids into large systems by invading swallet waters. It is believed that his model places too great an emphasis on the amount of phreatic cevelopment for these caves. Of the swallet caves studied in this work, only First Room in Tinaja has features suggesting that it may owe a significant part (perhaps most in this instance) of its size to prior phreatic solution. It is developed on a large joint (there has been considerable ceiling collapse) and water may have flowed down the joint while it was in the phreatic zone to create the broad solution pockets and other features high on the walls. Alternatively, these solution features might be quasi-phreatic manifestations of floodwater caves. These caves have a different solution morphology than the First Level in Cueva de los Sabinos, and phreatic caves on the crest or east face. Hence, it is believed that Arroyo, Tinaja, Japonés, Tigre, Jos and other swallet caves owe nearly all of their origin and development to the swallet waters.

Sótano de Japonés illustrates the potential that flood waters have to create maze caves (see detailed discussion, Section 6.4.3). As usual for the El Abra, water was initially pirated down a joint about 60-70 m deep. The characteristics of the strata at the base of the joint, in combination with the high local hydraulic gradient created by descending flood water, favored development of a maze from the base of the joint. Those rock characteristics must have been one or more of the following: 1) the nature of the bedding plane; 2) the jointing; 3) a resistant bed; or 4) stratal dip (formation of down-dip tubes). The water supply was much greater than the undeveloped aquifer could handle, so that water was distributed into a great many routes. The system is still relatively young and water may still back up during large floods. A second factor which further complicates the Japonés system is retrogressive piracy of the source and of flow within the cave. Sótano de Yerbaniz, a few kilometers north, apparently is also a multi-level maze system (Mitchell et al., 1977).

Despite the complexity of the Japonés cave, it is considered simpler in origin than Arroyo or Tinaja. Basically, Japonés formed in an isolated area in bedrock previously having no more than minor secondary permeability, when a perched stream forced water through many paths essentially radiating from one input point. Most of Arroyo's volume has been created by the sinking arroyo at the entrance of the cave, but it is clear that both Arroyo and Tinaja have numerous small inlets which have integrated with the systems (inlets occur in the Left Hand Passage, Tracy's Water Passage, and Steve's Surprise Passage (?) in Arroyo; and in Lake Passage, Sandy Floored Passage, Siphon Pit Series, and Water Passage in Tinaja -- see maps in Figures 6.23, 6.24). The sources of the inlets are bel[illegible] or

tration into the bed of the Río Sabinos dry valley (dry in at least some places) and other exposures of the El Abra limestone over the caves. Although the caves do not exhibit mazes like Japonés, Arroyo has many distributary channels, including some small ones in Main Passage that probably formed early in the cave's development. Arroyo diminishes in size as the flood waters are dispersed. Therefore, the Los Sabinos System (Arroyo + Tinaja + Los Sabinos) must be examined in terms of the principal sinks and their distributary systems, integrating inlets (which may be enlarged by backflooding), and possible phreatic voids or enlarged fissures which could act as targets for cave development. Sótano del Tigre, north of Arroyo, exhibits a tendency toward maze and distributary channel development near the entrance of the cave, but nearly all of its flood waters are carried by one major lower-level conduit.

The relationship of the swallet caves to geology, topography, and base level may be seen in Figure 7.17. The initial piracies took place at elevations between 200 m to 300 m (before entrenchment of the arroyos), although the southernmost occurred somewhat lower; this compares with the present elevation of the Choy rise pool of 35 m. A careful analysis needs to be made of the relationships between the ancient Río Sabinos, including the Soyate valley branch, the swallets, the geomorphology and profile of the South El Abra Pass, and the geomorphology of the coastal plain. The youngest swallets such as Jos, Yerbaniz, and Japonés undoubtedly correlate with the present Choy resurgence. The initiation of the oldest swallets, most likely Tinaja and Arroyo, might correlate with the Middle Entrance of El Choy and the 77 m coastal plain level, or at least with some higher

A sta on in ndv

Floored Passage was dated by the uranium-thorium method by Peter Thompson (1973), who estimated the base of the piece (above the true base of the stalagmite) to be 50,000 years old. This suggests that these caves may be at least a few hundreds of thousands of years old. Waters entering the swallets necessarily must enter the phreatic zone before they can be discharged at El Choy. However, the lowest point reached in Arroyo may be the only passage yet observed in these caves that might have formed below a fossil water table. Except for simple vadose zone piracies the caves are believed to have been created as a single phase of continuous growth; they have been controlled by rock structure, sediment infilling, and floodwater conditions -- not by one or more fossil water tables. This conclusion is easily accepted for the younger caves such as Japonés, but the origin of Steve's Surprise Passage (in Arroyo) and the Sandy Floored Passage pose some problems.

7.4.4 Discussion

In summary, most of the large caves found on the east face, the crest, and the western flank of the Sierra de El Abra were parts of great phreatic flow systems. The locus of flow (and thus of cavern development) was strongly controlled by bedding planes and large joints, a style of development advocated by Ford (1971) for other areas. The purity and massive bedding of the limestone, the large vertical range of joints, the lack of significant shale or other impermeable interbeds, and the great thickness of the limestone below base level have made depth an important dimension of the flow systems. La Hoya de Zimapán was part of one such system which

penetrated at least 300 m (possibly much more) below an ancient water table, thus demonstrating the existence of deep phreatic flow. The recharge of a large number of small sinks somehow integrated, to a considerable extent within the phreatic zone, to form large conduits that discharged their waters from fossil spring caves, such as Ventana Jabali, onto ancient and much higher coastal plains. Thus, these caves are equal in age to the time that has been required to erode up to as much as 600 m of the coastal plain. They are some millions of years old rather than post-Wisconsin as suggested by Harmon (1971).

Probably, the cave most similar to those developed in the El Abra is Carlsbad Caverns in the Guadalupe reef complex in New Mexico (Bretz, 1949). The El Abra caves could well serve as type examples of the deep phreatic solution features and pattern of circulation postulated by Davis (1930) and supported by Bretz (1942). Except locally, the location of flow bears no relationship to the water table (or potentiometric surface). In areas where the jointing is finer, the bedding usually thinner, and stratigraphic or lithologic controlling beds or partings more numerous, caves have often been attributed to water table control or shallow phreatic development. White (1969) has proposed conceptual models for flow systems developed in carbonate rocks having various hydrogeologic settings and flow properties; the models were for low to moderate relief terrains. His model for open, free flow karst systems having circulation below valley level emphasizes shallow phreatic development. The caves in the El Abra area indicate that another variable -- the structural-stratigraphic properties of the host rock -- needs to be included because, at least in some areas, deep phreatic

flow exists and is important.

The modern flow systems of the El Abra range proper have much thicker vadose zones than the ancient systems, but circulation within the phreas probably is still quite deep. Vadose zone caves on the range have not received much attention in this study because they generally are small, having only small catchments; however, further exploration may yield some significant vadose caves.

Swallet caves along the western margin belong to a special class of vadose caves called floodwater caves. The swallets generally lack entrenchment features, potholes and the continuously descending profile indicative of vadose caves which carry small to moderate discharges (in comparison with the capacity of the passage). Instead, the structural properties of the limestone and the extremely high discharges provided during floods create a host of features that are quasi-phreatic in character. Palmer (1972) distinguishes floodwater caves as an important class of cave and described several aspects of their morphology and hydraulics. The El Abra swallets belong to that class, and add variety to the passage plan and profile characteristics and the morphologic features that may be found in that class. The swallet entrances and passages, especially when primitive, are "overloaded" by the flood waters, and sometimes create a maze or a complex of distributary channels; they are excellent examples of some of the speleogenetic principles Ewers (Ph.D. thesis in preparation) has observed in his artificial modeling.

A few final points are:

1) Relief has not been an important variable in the El Abra caves; the nature of the ground-water circulation has not changed, although the relief and the thickness of the vadose zone have increased.

2) No major differences in the processes of cavern development have been found between caves in the El Abra and caves in other climatic regions, although the El Abra caves are larger than those in many other regions; there may be more subtle differences, such as large concentrations of organics washed into the caves and the growth of stalagmite barriers, which have their effects.

3) It is believed that a greater percentage of the dissolved load of the springs is obtained in the subsurface than in many (perhaps most) karst areas.

7.5 Summary and Conclusions

The region of interest is the Valles-San Luis Potosí Platform of Cretaceous age and in particular, the Sierra de El Abra along its eastern margin. A thick Lower Cretaceous deposit of gypsum and anhydrite occurs over a wide area in the interior of the Platform. More than 1200 m of the middle Cretaceous El Abra limestone with a basal dolomite was deposited over the entire Platform. Upper Cretaceous platform limestones are limited to the central area, and eventually, the whole Platform was covered with thin bedded limestones and a thick section of shale and sand. The area was folded and uplifted in the early Tertiary (possibly beginning in the latest Cretaceous).

The principal facts and conclusions of this study are summarized below.

1) Erosion of the Platform region began probably in the early Tertiary. Streams gradually removed the impermeable rocks from the crests and flanks of anticlines and the thrust-faulted Xilitla massif exposing the El Abra limestone to solutional attack.

2) A high relief karst has developed, but the largest features owe their size to structural relief of the limestone rather than to solution. A large part of the Platform is now a karst developed on the El Abra and Tamasopo Formations.

3) A very wide range of karst features are found, including areas with deep karren, large pinnacles, and mogotes or haystack hills that are commonly found in humid tropical karsts. Climate is probably the most important control on the types of karst features that develop in the region, but slope and various aspects of rock structure (in the geomorphic sense) are important also.

4) The Sierra de El Abra was formerly covered with impermeable rocks which have been stripped off. Traces of paleofluvial drainages exist on the flat crest (3 km wide), dry valleys are quite prominent on limestone on the western flank, and active drainages occur on impermeable rocks along the western margin; some of the latter are pirated underground to form large swallet caves. Karren, shallow solution dolines, and large collapse dolines occur on the crest, but none of the "typical" tropical karst forms are found. Soils are thin and discontinuous because the limestone is very pure; and where found contain

abundant vegetal matter.

5) The coastal plain formerly stood at least as high as the crest of the El Abra range. The eastern escarpment is partly formed by exhumation of a steep carbonate platform margin, and probably partly by structural relief from folding or faulting.

6) The El Abra Formation (plus the Tamasopo Formation and Lower Cretaceous platform limestones) forms a massive, continuous regional aquifer. Ground water passes through solutionally enlarged channels ranging in size from cracks to conduits (caves) perhaps as large as 30 m in diameter. All other rocks are relatively impermeable except thin sediment veneers in western valleys. Recharge to the El Abra limestone is believed to occur throughout most of the region, except where impermeable rocks remain. Nearly all of the recharge is by infiltration through a myriad of small sinks or cracks rather than by capture of large streams.

7) Rainfall is strongly spatially distributed into a wet eastern zone (800-2500 mm/year) and semiarid western zone (250-600 mm/year), and temporally distributed into a wet season (June-October) and a dry season (September-May).

8) Runoff from karstic and non-karstic basins on the Platform closely correlates with annual precipitation, with the season (wet or dry), and with individual precipitation events. The karst springs are extremely dynamic. Most have discharge variations (Q_{max}/Q_{min}) of 25-100 times in response to major precipitation events. This indicates well developed conduit flow systems and rapid discharge of infiltrating

flood waters. A response at springs usually occurs within a few hours after the initiation of major storms, and the crest is usually reached roughly 24 hours later.

9) The region has many large springs. At least 8, and perhaps twice that many are believed to have average flows greater than 3 m^3/sec (i.e., are first magnitude springs). The Coy (about 24 m^3/sec) and the Frío spring group (about 28 m^3/sec) are among the largest springs in the world. An even larger number of springs have peak flows greater than 100 m^3/sec (3530 c.f.s.).

10) Several lines of evidence incicate that a large part of the discharge of the springs has had a short residence time in the aquifer, ranging from one day to a few months. Some ground water has a longer residence time.

11) Cave waters sampled in the Sierra de El Abra were all of the calcium bicarbonate type, with high Ca/Mg ratios. Spring waters in the region were of three kinds: a) small to large springs having "normal" calcium bicarbonate type water (examples are Santa Clara, Huichihuayán, and Sabinas); b) large springs having very high concentrations of Ca, Mg, and SO_4 and approximately "normal" amounts of HCO_3 (examples are Choy, Coy, Mante, Media Luna); and c) thermal, sulfurous springs having variable chemistry, including one which has significant amounts of Na and Cl.

12) Measurement of the physical and chemical characteristics of spring waters through flood pulses provides a valuable means of studying the dynamics of karst aquifers. At the Choy and Coy springs, wet season

flood pulses cause their chemistries to diminish to calcium bicarbonate type waters similar to other nearby springs. For each spring, there was a strong correlation between Mg and SO_4, and between T (°C) and SO_4.

13) Based on the chemical compositions of the springs, the correlated behavior of Mg, SO_4, and T, and the distribution of minerals in the region, it is concluded that the high sulfate springs have two sources of water, whereas the calcium bicarbonate springs only have one source (local) of water. A geochemical model was developed in which water circulating at moderate depths within the El Abra limestone dissolves mostly calcite (type A water); and water circulating deeply in the central or western part of the region dissolves calcite, gypsum (Guaxcamá Formation), and the basal dolomite of the El Abra Formation (type B ground water), and is warmed by geothermal heat. Wherever type B water resurges, it mixes with type A water to form a mixed output.

14) The chemical data of the springs restricts the possible compositions of type B water. Solutions having $-0.3 \leq SI_g \leq 0$ and $0 \leq SI_c - SI_d \leq +0.12$ with $SI_c \leq +0.3$ are satisfactory compositions for type B ground water. The equilibrium model works well for El Choy, and has the highest possible total sulfate; other springs require type B water to have a small difference between SI_c and SI_d.

15) It is concluded that large regional ground-water flow systems exist based on: the spring water chemistries and the distribution of source minerals in the region; the thermal characteristics of the springs; the concentration of base flow at a few large low-elevation springs along the eastern margin; the occurrence at higher elevations of very-

large areas that have no surface runoff (particularly the whole northwestern quadrant -- about 37% -- of the Platform) and that are capable of recharge; the Coy spring which can only be supplied from distant sources; deep solution effects and permeability recorded in oil exploration wells; and the continuity of the supposed aquifer. The general correlation of parameters (which may be modified by local factors) is: a) springs that discharge only calcium bicarbonate type water have only local sources, lower base flows and the greatest variability of discharge, a higher elevation than nearby high sulfate springs, and a temperature reflecting the elevation of the local recharge area; and b) springs that have high Ca, Mg, SO_4 (mixed output) have local and regional sources, higher base flows and somewhat lower variability of discharge, lower elevation than nearby calcium bicarbonate type springs, and higher temperatures than nearby calcium bicarbonate type springs. The areal extent of the El Abra Formation (the same as the Valles-San Luis Potosí Platform) essentially delimits the region of active ground-water flow. The general direction of regional flow is easterly or southeasterly, and the flow path may be 100-200 km long. The coastal plain is a barrier to flow and acts as the spill point of the aquifer.

16) Mixing model calculations using a two-source dissolved load equation, and SO_4 and Mg as conservative parameters show that the total regional flow of type B water to the large eastern springs is 12-27 m^3/sec, depending on the chemical model selected, that the flow of type B water is approximately constant even during flooding of the springs (possibly varies slightly with seasonal hydraulic head), and that the

type A local flow is the dynamic component of spring discharge. It is possible that regional flow of type A water also exists, but it cannot be detected by the chemical mixing model. The Coy is the great regional outlet in the southern part of the region and the Mante is its northern, but lesser, counterpart.

17) Ground water storage in the Sierra de El Abra appears to lie mainly in the phreatic zone.

18) The lake in Sótano de Soyate is believed to lie at the water table. However, the calculated hydraulic gradient from Soyate to El Choy is somewhat larger than would be expected for the size of conduits that have been observed in the range (the late dry season level or decline is not yet known).

19) Hydrographs of the lake show that large fluctuations of the water table occur during storms. Hydrographs of the sump in Jos in conjunction with the geomorphic character of the swallet caves indicate that all their "terminal" siphons are perched, and that free-air passage lies on the other side.

20) The water budget and ground-water basins of the Sierra de El Abra are more complicated than previously envisioned. The two largest springs, the Mante and the Choy, receive a significant amount of water from sources outside the El Abra range (possibly more than 50% for the Mante spring). Furthermore, although the smaller springs have very small base flows, their flood flows are sufficient to form an important part of the total discharge from the range. Much more field work is required before the many problems can be resolved, and the aquifer

developed for water supply.

21) Most of the large explorable caves on the crest and east face of the El Abra range were parts of great deep phreatic flow systems. Circulation within the phreas reached at least 300 m (and perhaps much more) below ancient water tables.

22) These flow systems discharged through fossil spring caves on the east face of the El Abra onto ancient, much higher coastal plains. Thus, the caves are very old.

23) The locus of flow was structurally controlled. The factors which permitted deep circulation are believed to be joints of great vertical range, thickness of bedding and even greater distance between open bedding planes, lack of major and continuous perching layers, great depth of aquifer below base level, and possibly proximity to the reef.

24) The modern systems are probably similar to those of the past, except that the thickness of the vadose zone has increased.

25) The western margin swallet caves, the longest caves known in the El Abra, are floodwater caves. They owe their character to structural-stratigraphic control; to the extreme hydraulic gradients created, especially in the primitive stages when the developing conduits cannot transmit all the water supplied; and to a limited extent, to the large amount of sediment swept into the caves.

26) No major differences in the processes of cavern development have been found in the caves of the El Abra as compared with other regions.

APPENDIX I

ANALYTICAL METHODS AND SAMPLING PROCEDURES

Water samples for springs, cave lakes, and streams were collected (in duplicate) 10-15 cm below the surface in polyethylene bottles and sealed tightly before being removed. The spring samples were taken directly at the source except for two instances where that was not possible; the analyses of the latter were relegated to Table 5.1 b.

Water temperature was usually taken 5-10 cm below the surface using a laboratory thermometer graduated in 0.1°C intervals. The thermometer was checked against others. The pH of spring waters and surface streams was measured on site using a Metrohm portable meter. Care was taken to bring the electrode and buffer to the same temperature as the sample to eliminate drift. The readings were occasionally checked against other buffers. The 1971 samples usually have an accuracy of 0.05-0.1 pH units, but the 1972 and 1973 data are believed accurate to about ± 0.03 units. Except for two samples, the pH values of the cave lakes were measured at the field headquarters. Tests indicate that not much drift would normally occur if the samples were processed as soon as possible. Their values are believed accurate to 0.05-0.10 units. The pH of drip waters could be seriously in error, even though those listed were measured in the cave.

Alkalinity was determined by a potentiometric titration, using 0.0033N and 0.0098N HCl. Some samples were analyzed on location, but most

were taken in tightly sealed bottles to the field laboratory for analysis. The results were good when the sample was processed within a few hours. Considerable care was taken to avoid agitation when transporting and processing. The precision is probably ± 2% for the 1972 and 1973 samples, but somewhat less for 1971. Calcium and magnesium were determined using a commercially available Schwarzenbach titration kit with EDTA. Calcium was determined directly and magnesium was calculated as the difference from the total hardness. Duplicate analyses were made in 1972 and 1973, and if the results of the trials were significantly different, a third measurement was made. The precision of the data is considered to be better than ± 1% for calcium and ± 2% for magnesium for 1972 and 1973. Greater errors could occur for the 1971 data where samples were only tested once. Sulfate was determined at McMaster University by the visual thorin method (Rainwater and Thatcher, 1960). Samples were run twice and the results are accurate to ± 1% for high concentrations, but the error is larger for low concentrations. Sodium and potassium for a few samples were analyzed using a flame photometer. Chloride was determined by two methods: specific ion electrode for some samples, and a Hach field kit for rough values on the other samples. The sodium and potassium analyses were made by Jill Gleed.

APPENDIX II

CAVE MAP SYMBOLS

The symbols used on the cave maps in this thesis are shown below. They attempt to illustrate or "picture" the essential features of the caves without becoming lost in a multiplicity of fine detail. The maps were drawn over a period of years, and as new problems or needs were encountered, or a better method of presentation discovered, a few symbols were changed; thus, in some cases where two symbols are shown, the one on the left is now preferred. Bedrock walls are drawn with a heavier line than detail for contrast; this also distinguishes bedrock pillars from boulders. A few symbols not required here are included to make the legend of more general use. Lengths and depths on the maps drawn in this study are in meters; but the three maps provided by Neal Morris use feet.

Passage features:

surveyed passage

unsurveyed passage

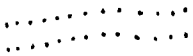

underlying passage

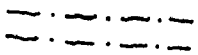

overlying passage

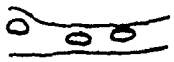

bedrock pillars (same line weight as walls)

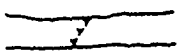

sharp change in ceiling height; hachures point toward low ceiling

dome, height above floor

pit with depth; ledge; when used for a skylight the word "skylight" should be used on the map

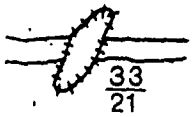

domepit, height over depth

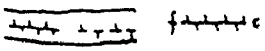

narrow slot or crevice in floor, in ceiling, and in both "f" and "c"

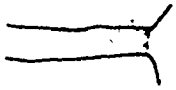

cave entrance, dripline

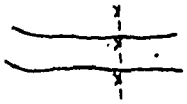

limit of daylight

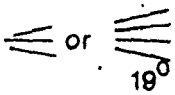

slope down in direction of splay; the angle may be indicated beside it

L 88 △

survey station and identifying number

0/0 △

datum (usually at entrance)

45	elevation above datum
45	elevation (depth) below datum
E 163	elevation above sea level
12 (12)	ceiling height
	cross section, tick points in direction of view; horizontal lines indicate what walls are shown on the map view
bushes	plants with notation as to type: trees, bushes, shrubs, mushrooms
3.5	scallops; average length in centimeters
65	joints, vertical and dipping
8	strike and dip of beds (dip in degrees)
	excavation, test pit

Hydrology:

	small stream or trickle, probably permanent
	intermittent flow
	inlet
	river
4	pool with depth
	intermittent pool and pool with high water line
	sump or siphon (cross hatched)

Clastic sediments:

fine-grained sediment; silt, clay, mud, dirt

sand

gravel, cobbles

rounded boulders

breakdown

chips, small breakdown

large mapped piece of breakdown

fallen stalagmite, stalactite or column

guano

crystalline sand, e.g., calcite or gypsum

vegetal debris

Chemical deposits:

stalactite

stalagmite

soda straws

column

flowstone on floor

large stalagmite

flowstone veneer on wall or flowstone cascade

gour pools, rimstone dams; use water symbol if active

flowstone on breakdown

hoar frost

ice

BIBLIOGRAPHY

Abbott, Patrick L., 1975, On the hydrology of the Edwards Limestone, south-central Texas. Jour. Hydrology, v. 24, p. 251-269.

Abbott, Patrick L., 1974, Calcitization of Edwards Group dolomites in the Balcones fault zone aquifer, south-central Texas. Geology, p. 359-362.

Ashton, K., 1967, The University of Leeds hydrological survey expedition to Jamaica 1963: Hydrology. Cave Res. Gp. of Great Britain, Trans., v. 9, no. 1, p. 36-45.

Ashton, K., 1966, The analysis of flow from karst drainage systems. Cave Res. Gp. of Great Britain, Trans., v. 7, no. 2., p. 161-203.

Atkinson, T.C., D.I. Smith, J.J. Lavis and R.J. Whitaker, 1973, Experiments in tracing underground waters in limestones. Jour. Hydrology, v. 19, p. 323-349.

Back, William and Bruce B. Hanshaw, 1974, Hydrogeochemistry of the northern Yucatan Peninsula, Mexico with a section on Mayan water practices. p. 45-77, in Field Seminar on Water and Carbonate Rocks of the Yucatan Peninsula, Mexico, ed. A.E. Weidie, New Orleans Geological Society for Field Trip 2, 1974 Annual Meeting, Miami, G.S.A., 274 p.

Back, William and Bruce B. Hanshaw, 1970, Comparison of chemical hydrogeology of the carbonate peninsulas of Florida and Yucatan. Jour. Hydrology, v. 10, p. 330-368.

Bassett, John, 1976, Hydrology and geochemistry of the Upper Lost River drainage basin, Indiana. Nat. Speleo. Soc. Bull., v. 38, no. 4, p. 79-87.

Bassett, John, 1971, Cueva de Ceiba. The Bloomington Indiana Grotto Newsletter, v. 10, no. 1, p. 14-16.

Bittinger, Steven and Don Broussard, personal communications. Austin, Texas, U.S.A.

Bögli, Alfred, 1965, The role of corrosion by mixed water in cave forming, p. 125-132. in Problems of the Speleological Research, ed. O. Stelcl, Proceedings of the International Speleological Conference held in Brno, June 29-July 4, 1964, Academia: Publishing House of the Czechoslovak Academy of Sciences, Prague, 220 p.

Bonet, Federico, 1963, Biostratigraphic notes on the Cretaceous of eastern Mexico. in Peregrina Canyon and Sierra de El Abra, Corpus Christi Geological Society Annual Field Trip, Corpus Christi, Texas, p. 36-48.

Bonet, Federico, 1953a, Datos sobre las cavernas y otras fenómenos erósivos de las calizas de la Sierra de El Abra. Mem. Cong. Cient. México, Cien. Fis., Mat., Geol., 5, p. 238-273.

Bonet, Federico, 1953b, Cuevas de la Sierra Madre Oriental en la región de Xilitla. Bol. Univ. Nac. Aut. Mex., Inst. Geol., v. 57, 96 p.

Bonet, Federico, 1952, La facies urgoniana del Cretacico Medio de la región de Tampico. Bol. Asoc. Mexicana Geólogos Petroleros, v. 4, no. 5-6, p. 153-262.

Boyd, Don R., 1963, Geology of the Golden Lane trend and related fields of the Tampico embayment. in Peregrina Canyon and Sierra de El Abra, Corpus Christi Geological Society Annual Field Trip, Corpus Christi, Texas, p. 49-56.

Boyd, D.R., J. Carrillo Bravo, E.K. Krause, R.B. Mixon, and G.E. Murray, 1963, Generalized Correlation Chart. in Geology of Peregrina Canyon and Sierra de El Abra, Guidebook for Eleventh Annual Field Trip, Corpus Christi Geological Soc.

Bretz, J.H., 1949, Carlsbad Caverns and other caves of the Guadalupe block, New Mexico. J. of Geology, v. 57, no. 5, p. 447-463.

Bretz, J.H., 1942, Vadose and phreatic features of limestone caverns. Jour. of Geology, v. 50 (L), no. 6, p. 675-811.

Brook, George, 1976, Geomorphology of the North Karst, South Nahanni River Region, Northwest Territories, Canada. Ph.D. thesis, Dept. of Geography, McMaster University, Hamilton, Ontario, 627 p.

Brown, Charles, 1970, Karst Geomorphology and Hydrology of the Lower Maligne Basin, Jasper, Alberta. Ph.D. thesis, Dept. of Geography, McMaster University, Hamilton, Ontario, 178 p.

Brown, M.C. and D.C. Ford, 1971, Quantitative tracer methods for investigation of karst hydrological systems. Trans. Cave Research Group of Great Britain, v. 13, p. 37-51.

Brucker, Roger W., John W. Hess and William B. White, 1972, Role of vertical shafts in the movement of ground water in carbonate aquifers. Ground Water, v. 10, no. 6, p. 5-13.

Burdon, David J. and Nicolas Papakis, 1963, Handbook of Karst Hydrogeology with Special Reference to the Carbonate Aquifers of the Mediterranean Region. F.A.O. of UNESCO, 276 p.

Burdon, David J. and Chafic Safadi, 1963, Ras-El-Ain: the great karst spring of Mesopotamia, a hydrogeological study. Jour. Hydrology, v. 1, p. 58-95.

Carrillo Bravo, José, 1971, La plataforma Valles-San Luis Potosí. Bol. Asoc. Mexicana Geólogos Petroleros, v. 23, no. 1-6, p. 1-113.

Carrillo Bravo, José, 1968, Exploracion geologica y posibilidades petroleros de la Plataforma Valles-San Luis Potosí (Sierra Madre Oriental-Altiplano Mexico). in Mesa Redonda no. 6, Problemas de Exploracion en Areas Posiblemente Petroliferas de la Republica Mexicana, paper no. 5, 20 p.

Carrillo Bravo, José, 1963, Geology of the Huizachal-Peregrina Anticlinorium northwest of Ciudad Victoria, Tamaulipas. in Peregrina Canyon and Sierra de El Abra, Corpus Christi Geological Society Annual Field Trip, Corpus Christi, Texas, p. 11-23.

Carrillo Bravo, José, personal communication. México City, Pemex.

Coogan, A.H., D.G. Bebout, and Carlos Maggio, 1972, Depositional environments and geologic history of Golden Lane and Poza Rica trend, Mexico, an alternative view. Am. Assoc. Petroleum Geologists Bull., v. 56, no. 8, p. 1419-1447.

Cowell, Daryl, 1976, Karst Geomorphology of the Bruce Peninsula, Ontario. M.A. Thesis, Dept. of Geography, McMaster University, Hamilton, Ontario.

Dalrymple, Tate, 1960, Flood-frequency analyses, manual of hydrology: Part 3. Flood-flow techniques. U.S. Geol. Survey Water-Supply Paper 1543-A, 80 p.

Davies, William E., 1960, Origin of caves in folded limestone. Nat. Speleo. Soc. Bull., v. 22, no. 1, p. 5-18.

Davis, W.M., 1930, Origin of limestone caverns. Geol. Soc. Am. Bull., v. 41, p. 475-628.

Deike III, George H., 1960, Origin and geologic relations of Breathing Cave, Virginia. Nat. Speleo. Soc. Bull., v. 22, no. 1, p. 30-42.

Drake, J. John, 1974, Hydrology and Karst Solution in the Southern Canadian Rockies. Ph.D. thesis, Dept. of Geography, McMaster University, Hamilton, Ontario, 222 p.

Drew, D.P., 1966, The water table concept in limestones. British Speleological Association Proc. 4, p. 57-68.

Drew, David P. and David I. Smith, 1969, Techniques for the tracing of subterranean drainage. Tech. Bull. No. 2, British Geomorphological Research Group, 36 p.

Eakin, Thomas E., 1966, A regional interbasin groundwater system in the White River area, southeastern Nevada. Water Resour. Res., v. 2, no. 2, p. 251-271.

Elliott, William R., 1970, El Sótano de Soyate. The Texas Caver, v. XV, p. 63-66.

Enjalbert, H., 1964, Phenomenes karstiques Mexique et au Guatemala. Bull. Assn. Geog. Francais, 324-325, p. 30-58.

Enos, Paul, 1974, Reefs, platforms, and basins of middle Cretaceous in northeast Mexico. Am. Assoc. Petroleum Geologists Bull., v. 58, p. 800-809.

Ewers, Ralph O., Ph.D. thesis in preparation. Dept. of Geography, McMaster University, Hamilton, Ontario.

Faulkner, Glen L., 1976, Flow analysis of karst systems with well developed underground circulation. in Karst Hydrology and Water Resources, ed. Vujica Yevjevich, v. 1, p. 137-164, from Proceedings of the U.S.-Yugoslavian Symposium, Dubrovnik, June 2-7, 1975. Water Resources Publications, Fort Collins, Coloradao, U.S.A.

Ferguson, G.E., C.W. Lingham, S.K. Love, and R.O. Vernon, 1947, Springs of Florida. Florida Geol. Survey Bull. 31, 196 p.

Fish, John E., 1977, The Circum-Gulf Karst Belt. in Karst Hydrogeology, Proc. Twelfth Int. Congress of Int. Assoc. Hydrogeologists, 1975, eds. J.S. Tolson and F.L. Doyle, Alabama Geol. Survey, 578 p.

Fish, John, 1974, La Sistema de Los Sabinos, Mexico's longest cave. Canadian Caver, v. 6, no. 1, p. 3-20.

Fish, John E., 1968, Cave description and speleogenesis. p. 3-5, in Sótano de las Golondrinas, Bull. 2 of the Assoc. for Mexican Cave Studies, ed. T.W. Raines, 20 p.

Fish, John and D.C. Ford, 1973, Karst geomorphology and hydrology of the Sierra de El Abra, S.L.P. and Tamps., Mexico. Proc. 6th Int. Congress of Speleology, Olomouc, CSSR, v. II, sub-section Ba, p. 151-156.

Fish, John and William Russell, 1972, "Preliminary results on the ground water geochemistry of the Sierra de El Abra region, north central Mexico", discussion. Nat. Speleo. Soc. Bull. v. 34, no. 3, p. 111-112.

Ford, Derek C., 1971, Geologic structure and a new explanation of limestone cavern genesis. Cave Res. Gp. of Great Britain, Trans., v. 13, no. 2, p. 81-94.

Ford, Derek C., 1968, Features of cavern development in Central Mendip. Cave Res. Gp. of Great Britain, Trans., v. 10, no. 1, p. 11-25.

Ford, Derek C., 1965, The origin of limestone caverns: a model from the Central Mendip Hills, England. Nat. Speleo. Soc. Bull., v. 27, no. 4, p. 109-132.

Ford, Prof. D.C., personal communication. Dept. of Geography, McMaster Univ., Hamilton, Ontario, Canada.

Freeze, R. Allan and P.A. Witherspoon, 1967, Theoretical analysis of regional groundwater flow: 2. Effect of water-table configuration and subsurface permeability variation. Water Resour. Res., v. 3, no. 2, p. 623-634.

Freeze, R. Allan and P.A. Witherspoon, 1966, Theoretical analysis of regional groundwater flow: 1. Analytical and numerical solutions to the mathematical model. Water Resour. Res., v. 2, no. 4, p. 641-656.

Garrels, Robert M. and Charles L. Christ, 1965, Solutions, Minerals, and Equilibria. Harper & Row, New York, N.Y., 450 p.

Griffith, L.S., Max G. Pitcher, and G. Wesley Rice, 1969, Quantitative environmental analysis of a Lower Cretaceous reef complex. in Depositional Environments in Carbonate Rocks, A Symposium, G.M. Friedman ed., Soc. Econ. Paleontologists and Mineralogists, Spec. Pub. no. 14, p. 120-138.

Gunnerson, C.G., 1967, Stream flow and quality in the Columbia River basin. J. Sanitary Eng. Div., Amer. Soc. Civil Eng., v. 93 (SA6) p. 1-16.

Hall, Francis R., 1970, Dissolved solids-discharge relationships, 1. Mixing models. Water Resour. Res., v. 6, no. 3, p. 845-850.

Hall, Francis R., 1971, Dissolved solids-discharge relationships, 2. Applications to field data. Water Resour. Res., v. 7, no. 3, p. 591-601.

Harmon, Russell S., 1971, Preliminary results on the ground-water geochemistry of the Sierra de El Abra region, North Central Mexico. Nat. Speleo. Soc. Bull., v. 33, no. 2, p. 73-86.

Harmon, Russell S., William B. White, John J. Drake, and John W. Hess, 1975, Regional hydrochemistry of North American carbonate terrains. Water Resour. Res., v. 11, no. 6, p. 963-967.

Harmon, R.S., J.J. Drake, J.W. Hess, R.L. Jacobson, D.C. Ford, W.B. White, J. Fish, J. Coward, R. Ewers, and J. Quinlan, 1973 (in press), Geochemistry of karst waters in North America. Paper presented at 6th International Congress of Speleology, Olomouc, CSSR.

Harmon, R.S., J.W. Hess, R.W. Jacobson, E.T. Shuster, C. Haygood, and W.B. White, 1972, Chemistry of carbonate denudation in North America. Cave Res. Gp. of Great Britain, Trans., v. 14, no. 2, p. 96-103.

Heim, A., 1940, The front ranges of the Sierra Madre Oriental, Mexico, from Ciudad Victoria to Tamazunchale. Eclogae Geol. Helvetiae, v. 20, no. 2, p. 313-352.

Hem, John D., 1970, Study and interpretation of the chemical characteristics of natural water. U.S. Geol. Survey Water-Supply Paper 1473, 363 p.

Hendrickson, G.E., and Krieger, R.A., 1964, Geochemistry of natural waters of the Blue Grass Region, Kentucky. U.S. Geol. Survey Water-Supply Paper 1700, 135 p.

Hostetler, P.B., 1963, Complexing of magnesium with bicarbonate. Jour. Phys. Chem., v. 67, p. 720-721.

Hubbert, M.K., 1940, The theory of groundwater motion. J. of Geology, v. 48, p. 785-944.

Jennings, Joseph N., 1971, Karst. The M.I.T. Press, Cambridge, Mass., 252 p.

Lange, Arthur L., 1960, Geometrical basis for cave interpretation. Nat. Speleo. Soc. Bull., v. 22, no. 1, p. 77-83.

Langmuir, Donald, 1971, The geochemistry of some carbonate ground waters in central Pennsylvania. Geochimica et Cosmochimica Acta, v. 35, p. 1023-1045.

Le Grand, Harry and V.T. Stringfield, 1971, Water levels in carbonate rock terranes. Ground Water, v. 9, no. 3, p. 4-10.

Lesser, Juan Manuel, c. 1973, Interpretación geoquímica del agua subterránea del valle de Ríoverde, San Luis Potosí. unpublished report of the Sectretaría de Recursos Hidráulicos, 23 p.

Lesser-Jones, H., 1967, Confined fresh water aquifers in limestone, exploited in the north of Mexico with deep wells below sea level. in Hydrology of Fractured Rocks, v. II, Proc. of Dubrovnik Symposium, 1965, UNESCO and Int. Assoc. Sci. Hydrology, p. 526-539.

Lucia, F.J., 1961, Dedolomitization in the Tansill (Permian) Formation. Geol. Soc. Am. Bull., v. 72, p. 1107-1110.

Martin, P.S., 1958, A biogeography of reptiles and amphibians in the Gómez Farías Region, Tamaulipas, México. Mus. Zod., Univ. Michigan, Misc., Publ., 101, 102 p.

Maxey, George, 1968, Hydrogeology of desert basins. Ground Water, v. 6, no. 5, p. 10-22.

Maxey, George B., 1964, Hydrostratigraphic units. Jour. Hydrology, v. 2, p. 124-129.

Maxey, George B. and Martin D. Mifflin, 1966, Occurrence and movement of ground water in carbonate rocks of Nevada. Nat. Speleo. Soc. Bull., v. 28, no. 3, p. 141-157.

Mercado A. and G.K. Billings, 1975, The kinetics of mineral dissolution in carbonate aquifers as a tool for hydrological investigations, I. Concentration-time relationships. Jour. Hydrology, v. 24, p. 303-331.

Mifflin, M.D., 1968, Delineation of Ground-Water Flow Systems in Nevada. Hyd. and Water Res. Pub. No. 4, Cen. Wat. Res. Research, Desert Research Inst., Univ. Nevada System, Reno, 111 p.

Mitchell, Robert W., William H. Russell, and William R. Elliott, 1977, Mexican Eyeless Characin Fishes, Genus Astyanax: Environment, Distribution, and Evolution. The Museum, Texas Tech. Univ. Special Publications, no. 12, 89 p.

Mixon, Robert B., 1963, Geology of the Huizachal Redbeds Ciudad Victoria area, southwestern Tamaulipas. in Peregrina Canyon and Sierra de El Abra, Corpus Christi Geological Society Annual Field Trip, Corpus Christi, Texas, p. 24-35.

Morris, Neal, 1976, The Otates Mine Area Sierra de El Abra, Tamaulipas, Mexico. Assoc. for Mexican Cave Studies, Activities Letter No. 4, p. 17-22.

Morris, Neal, personal communication. Austin, Texas, U.S.A.

Muir, J.M., 1936, Geology of the Tampico Region. Memoir, Amer. Assoc. Petroleum Geologists, Tulsa, Oklahoma, 280 p.

Nigra, J.O., 1951, El Cretacico Medio de México, con especial referencia a la facies de caliza arrecifal del Albiano-Cenomaniano en la Ceno-bahia de Tampico-Tuxpan. Bol. Asoc. Mexicana Geólogos Petroleros, v. 3, nos. 3-4, p. 107-175.

Palmer, Arthur N., 1975, The origin of maze caves. Nat. Speleo. Soc. Bull., v. 37, no. 3, p. 56-76.

Palmer, Arthur N., 1972, Dynamics of a sinking stream system: Onesquethaw Cave. Nat. Speleo. Soc. Bull., v. 34, no. 3, p. 89-110.

Palmer, A.N., 1972, Origin of cave levels in Mammoth Cave National Park. in Miotke, F.D. and A.N. Palmer, Genetic Relationship Between Caves and Landforms in the Mammoth Cave National Park Area. Technischen Universität Hannover, Hannover, W. Germany, 69 p.

Palmer, Arthur N., 1969, A Hydrologic Study of the Indiana Karst. Ph.D. thesis, Dept. of Geology, Indiana University, Bloomington, Indiana.

Pinder, George F. and John F. Jones, 1969, Determination of the ground-water component of peak discharge from the chemistry of total runoff. Water Resour. Res., v. 5, no. 2, p. 438-445.

Plummer, L.N., Jr., 1972, Rates of Mineral-Aqueous Solution Reactions. Unpubl. Ph.D. thesis, Northwestern University, Illinois.

Pohl, E.R., 1955, Vertical shafts in limestone caves. Nat. Speleo. Soc., Occ. Pap., no. 2, 24 p.

Raines, Terry W. (ed.), 1968, Sótano de las Golondrinas. Assoc. for Mexican Cave Studies, Bull. 2, 20 p.

Rainwater, F.H., and L.L. Thatcher, 1960, Methods for collection and analysis of water samples. U.S. Geol. Survey Water-Supply Paper 1454, 301 p.

Roglić, J., 1972, Historical review of morphologic concepts. p. 1-18., in Karst: Important Karst Regions of the Northern Hemisphere, ed. M. Herak and V.T. Stringfield, Elsevier Publishing Company, Amsterdam, 551 p.

Rose, Peter R., 1963, Comparison of type El Abra of Mexico with "Edwards Reef Trend" of south-central Texas. in Peregrina Canyon and Sierra de El Abra, Corpus Christi Geological Society Annual Field Trip, Corpus Christi, Texas, p. 57-64.

Russell, William H., 1972, Alphabetical listing of caves of the Sierra de El Abra: El Abra list number one, July 1, 1972. Assoc. for Mexican Cave Studies, Newsletter, v. III, no. 6, p. 129-132.

Russell, William, 1968, Regional Geology. p. 6-15, in Sótano de las Golondrinas, Assoc. for Mexican Cave Studies, Bull. 2, ed. T.W. Raines, 20 p.

Russell, William H., personal communication. 1300 Kirkwood, Austin, Texas, U.S.A.

Russell, William H., and Terry W. Raines, 1967, Caves of the Inter-American Highway, Nuevo Laredo, Tamaulipas to Tamazunchale, San Luis Potosí. Assoc. Mexican Cave Studies, Bull. 1, 126 p.

Searcy, James K., 1959, Flow-duration curves, manual of hydrology: Part 2. Low-Flow techniques. U.S. Geol. Survey Water-Supply Ppaer 1542-A, 33 p.

Sectretaría de Recursos Hidráulicos, (no date), Datos Hidrometricos Cuenca del Río Panuco. Bol. Hidrológico No. 32, Tomos I & II, (data through Dec., 1968).

Secretaría de Recursos Hidráulicos, 1962, Datos de la Región del Bajo Panuco. Bol. Hidrológico No. 19, 288 p.

Segerstrom, Kenneth, 1962, Geology of south-central Hidalgo and northeastern México, México. U.S. Geol. Survey Bull. 1104-C, 162 p.

Segerstrom, Kenneth, 1961, Geology of the Bernal-Jalpan Area Estado de Querétaro, México. U.S. Geol. Survey Bull. 1104-B, p. 19-86.

Shuster, Evan T. and William B. White, 1971, Seasonal fluctuations in the chemistry of limestone springs: a possible means for characterizing carbonate aquifers. Jour. Hydrology, v. 14, p. 93-128.

Sprouse, Peter, personal communication. 1006-½ E. 15th St., Austin, Texas, U.S.A.

Stephens, John Lloyd, 1842, Incidents of Travel in Yucatán V: I & II. ed. V.W. von Hagen, University of Oklahoma Press, Norman, 349 & 347 p.

Stumm, Werner and James J. Morgan, 1970, Aquatic Chemistry: An Introduction Emphasizing Chemical Equilibria in Natural Waters. Wiley-Interscience, New York, N.Y., 583 p.

Thompson, Peter, 1973, Speleochronology and Late Pleistocene Climates Inferred from O, C, H, U and Th Isotopic Abundances in Speleothems. Ph.D. Thesis, Dept. of Geology, McMaster University, Hamilton, Ontario, 352 p.

Thrailkill, John, 1972, Carbonate chemistry of aquifer and stream water in Kentucky. Jour. Hydrology, v. 16, p. 93-104.

Thrailkill, John, 1968, Chemical and hydrologic factors in the excavation of limestone caves. Geol. Soc. Am. Bull., v. 79, p. 19-46.

Tóth, J., 1972, Properties and manifestations of regional groundwater movement. 24th International Geological Congress, Section II, Hydrogeology, p. 153-163.

Tóth, J., 1963, A theoretical analysis of groundwater flow in small drainage basins. Jour. Geoph. Res., v. 68, no. 16, p. 4795-4812.

Trainer, Frank W. and Ralph C. Heath, 1976, Bicarbonate content of groundwater in carbonate rock in eastern North America. Jour. Hydrology, v. 31, p. 37-55.

Viniegra, O.F. and C. Castillo-Tejero, 1970, Golden Lane fields, Veracruz, México. in Geology of Giant Petroleum Fields, M.T. Halbouty, ed., Am. Assoc. Petroleum Geologists Mem. 14, p. 309-325.

Walsh, M., 1972, Mexican Caving, 1966-1971. Southwest Texas Grotto, San Marcos, Texas, 146 p.

Waring, Gerald A. (revised by Reginald R. Blankenship and Ray Bentall), 1965, Thermal Springs of the United States and Other Countries of the World-A Summary. U.S. Geol. Survey Prof. Paper 492, 383 p.

White, W.B., 1969, Conceptual models for carbonate aquifers. Ground Water, v. 7, p. 15-21.

White, William B., personal communication. 210 Materials Research Lab., Penn. St. Univ., University Park, Pa., U.S.A.

White, W.B. and J. Longyear, 1962, Some limitations on speleo-genetic speculation imposed by the hydraulics of groundwater flow in limestone. Nittany Grotto Newsletter, v. 10, no. 9, p. 155-167.

Wigley, T.M.L., 1973, Chemical evolution of the system Calcite-Gypsum-Water. Can. J. Earth Science, v. 10, no. 2, p. 306-315.

Wigley, T.M.L.,1972, A computer programme for water quality analysis. Tech. Note 15, Dept. of Mech. Eng., Univ. of Waterloo.

Wilford, G.E., 1964, The Geology of Sarawak and Sabah Caves. Bull. 6, Geological Survey, Borneo Region, Malaysia, 181 p.